frontiers

RESEARCH TOPICS

Ca^{2+} AND Ca^{2+}-INTERLOCKED MEMBRANE GUANYLATE CYCLASE MODULATION OF NEURONAL AND CARDIOVASCULAR SIGNAL TRANSDUCTION

Topic Editors

Rameshwar K. Sharma, Wolfgang Baehr, Clint L. Makino and Teresa Duda

frontiers in MOLECULAR NEUROSCIENCE

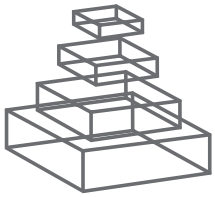

frontiers

ISSN 1664-8714
ISBN 978-2-88919-506-0
DOI 10.3389/978-2-88919-506-0

ABOUT FRONTIERS

Frontiers is more than just an open-access publisher of scholarly articles: it is a pioneering approach to the world of academia, radically improving the way scholarly research is managed. The grand vision of Frontiers is a world where all people have an equal opportunity to seek, share and generate knowledge. Frontiers provides immediate and permanent online open access to all its publications, but this alone is not enough to realize our grand goals.

FRONTIERS JOURNAL SERIES

The Frontiers Journal Series is a multi-tier and interdisciplinary set of open-access, online journals, promising a paradigm shift from the current review, selection and dissemination processes in academic publishing.
All Frontiers journals are driven by researchers for researchers; therefore, they constitute a service to the scholarly community. At the same time, the Frontiers Journal Series operates on a revolutionary invention, the tiered publishing system, initially addressing specific communities of scholars, and gradually climbing up to broader public understanding, thus serving the interests of the lay society, too.

DEDICATION TO QUALITY

Each Frontiers article is a landmark of the highest quality, thanks to genuinely collaborative interactions between authors and review editors, who include some of the world's best academicians. Research must be certified by peers before entering a stream of knowledge that may eventually reach the public - and shape society; therefore, Frontiers only applies the most rigorous and unbiased reviews.
Frontiers revolutionizes research publishing by freely delivering the most outstanding research, evaluated with no bias from both the academic and social point of view.
By applying the most advanced information technologies, Frontiers is catapulting scholarly publishing into a new generation.

WHAT ARE FRONTIERS RESEARCH TOPICS?

Frontiers Research Topics are very popular trademarks of the Frontiers Journals Series: they are collections of at least ten articles, all centered on a particular subject. With their unique mix of varied contributions from Original Research to Review Articles, Frontiers Research Topics unify the most influential researchers, the latest key findings and historical advances in a hot research area!
Find out more on how to host your own Frontiers Research Topic or contribute to one as an author by contacting the Frontiers Editorial Office: researchtopics@frontiersin.org

Ca^{2+} AND Ca^{2+}-INTERLOCKED MEMBRANE GUANYLATE CYCLASE MODULATION OF NEURONAL AND CARDIOVASCULAR SIGNAL TRANSDUCTION

Topic Editors:
Rameshwar K. Sharma, Salus University, USA
Wolfgang Baehr, University of Utah, USA
Clint L. Makino, Massachusetts Eye and Ear Infirmary and Harvard Medical School, USA
Teresa Duda, Salus University, USA

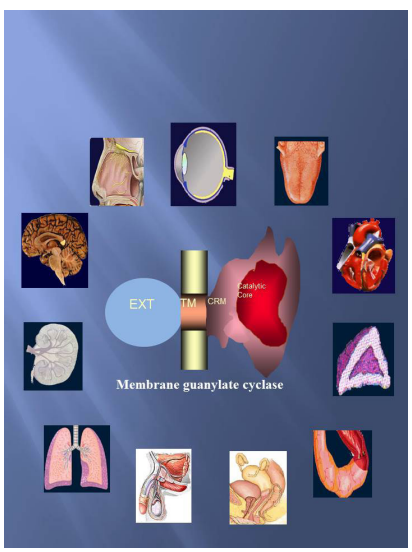

Image property of the Sharma lab

The tale of cyclic GMP has been astonishing. Having overcome an initial disbelief, cyclic GMP has risen to its present eminence as a premium cellular signal transduction messenger of not only hormonal extracellular but also of the intracellular signals. This research topic focuses on the pathways and functions of membrane guanylate cyclases in different tissues of the body and their interplay with intracellular sensory signals where in many cases, cyclic GMP along with Ca^{2+} have taken on roles as synarchic co-messengers.

Table 1. Nomenclature: Membrane Guanylate cyclases; Extracellular Ligands; Ca^{2+} Binding Protein Subunit/s

Guanylate Cyclase	Other Names	Extracellular Ligands	Ca^{2+} Binding Protein Subunit/s
ANF-RGC	GC-A, NPR-A	ANF, BNP	Neurocalcin δ
CNP-RGC	GC-B, NPR-B	CNP	
Sta-RGC	GC-C	Enterotoxin, guanylin, uroguanylin	
ONE-GC	GC-D	Guanylin, uroguanylin	GCAP1, Neurocalcin δ, Hippocalcin
ROS-GC1	GC-E, retGCl		GCAPs, S100B, GCIP, Neurocalcin δ
ROS-GC2	GC-F, retGC2		GCAPs, GCIP
GC-G			

Hippocalcin and GCIP are not specifically covered in this Topic. Future research is needed to revise this Table and eliminate any errors of omission. ANP, atrial natriuretic peptide (also known as ANF, atrial natriuretic factor); ANF-RGC, atrial natriuretic factor receptor guanylate cyclase; BNP, B-type natriuretic peptide; CNP, C-type natriuretic peptide; CNP-RGC, CNP receptor guanylate cyclase; GCAP, guanylate cyclase activating protein; ONE-GC, olfactory neuroepithelium guanylate cyclase; ROS-GC, rod outer segment guanylate cyclase; GCIP, guanylate cyclase inhibitory protein.

Table of Contents

frontiers in Molecular Neuroscience

EDITORIAL
published: 06 March 2015
doi: 10.3389/fnmol.2015.00007

Ca^{2+} and Ca^{2+}-interlocked membrane guanylate cyclase signal modulation of neuronal and cardiovascular signal transduction

Rameshwar K. Sharma[1], Wolfgang Baehr[2], Clint L. Makino[3] and Teresa Duda[1]*

[1] Research Divisions of Biochemistry and Molecular Biology, The Unit of Regulatory and Molecular Biology, Salus University, Elkins Park, PA, USA, [2] School of Medicine, Department of Ophthalmology and Visual Sciences, University of Utah, Salt Lake City, UT, USA, [3] Massachusetts Eye and Ear Infirmary and Harvard Medical School, Boston, MA, USA

Keywords: cyclic GMP, Ca^{2+}, membrane guanylate cyclase, multiple transduction modes, signal transduction

The papers in this research topic are focused on the extraordinary tale of cyclic GMP: its recognition as a hormonal second messenger and its subsequent interplay with intracellular calcium where the two together become co-messengers in cellular signal transduction processes. In this emerging theme membrane guanylate cyclases sense intracellular as well as extracellular signals. Four original research and 12 review articles sample the extraordinary progress that has been made in the field.

The topic introduces the present status of the field with a figure illustrating that cyclic GMP is generated by two structurally different guanylate cyclases, soluble and the membrane form (Figure 1: Sharma and Duda, 2014). The synthetic machinery and the modes of their operation by which they generate cyclic GMP are entirely different, and so are their physiologically regulated processes. Since many of the membrane guanylate cyclases carry multiple names and all names remain in use, the review also provides a guide to the current nomenclature of the membrane guanylate cyclases (Introductory text Table 1). Then it moves on with a lively historical perspective, replete with unexpected twists and turns. Current research suggests that new developments will continue to follow a tortuous but always exciting path! Guanylate cyclase activating proteins or GCAPs are neuronal calcium sensing proteins that serve as subunits in the ROS-GC complex. The review article by Lim et al. (2014) delves into the molecular mechanism by which GCAPs inhibit GC activity when $[Ca^{2+}]_i$ is high and stimulate it when $[Ca^{2+}]_i$ is low. As it turns out, GCAP1 has a more subtle use for its myristoyl tail, compared to other, related neuronal calcium sensors. Besides the additional forms of GCAPs that are being discovered (cf. Wen et al., 2014), ROS-GC1 is subject to modulation by other Ca^{2+} binding proteins: S100B in retinal cones (reviewed by Sharma et al., 2014) and S100B and neurocalcin δ (NCδ) in spermatozoa (Jankowska et al., 2014). Unlike GCAPs, S100B and NCδ stimulate ROS-GC1 at high $[Ca^{2+}]_i$. Co-expression of S100B and GCAPs with ROS-GC1 in the same cells empowers ROS-GC1 with the ability to operate as a novel, bimodal Ca^{2+} switch wherein guanylate cyclase activity is elevated at very high and at very low $[Ca^{2+}]_i$. Transduction of Ca^{2+} signals is not restricted to ROS-GCs; NCδ serves as a subunit for the transduction of the ANF signal by ANF-RGC (Duda et al., 2014). Thus, NCδ, in addition to being a "neuronal" calcium sensor, takes on responsibilities outside of neurons. If other guanylate cyclases possess the proper sequences for NCδ, S100B and/or GCAPs interactions, their calcium sensing paradigms will unfold in the future.

Interestingly, GCAP2 has an alternate binding partner that is not a guanylate cyclase. At the photoreceptor synapse, it interacts with RIBEYE to control ribbon size (reviewed by Schmitz, 2014). Recent work on a new ROS-GC binding partner, RD3, (reviewed by Molday et al., 2014) reveals that it is necessary for the intracellular transport of ROS-GC. It also inhibits ROS-GC possibly as a means of suppressing unwanted activity until the cyclase arrives at the proper cellular location.

OPEN ACCESS

Edited and reviewed by:
Robert J. Harvey, UCL School of Pharmacy, UK

****Correspondence:***
Rameshwar K. Sharma, rsharma@salus.edu

Received: *02 December 2014*
Accepted: *16 February 2015*
Published: *06 March 2015*

Citation:
Sharma RK, Baehr W, Makino CL and Duda T (2015) Ca^{2+} and Ca^{2+}-interlocked membrane guanylate cyclase signal modulation of neuronal and cardiovascular signal transduction. Front. Mol. Neurosci. 8:7. doi: 10.3389/fnmol.2015.00007

In retinal rods and cones, cyclic GMP produced by ROS-GCs opens cyclic nucleotide gated cation channels in readiness for visual transduction. Wen et al. (2014) describe the rationale for expressing multiple forms of guanylate cyclases and GCAPs in order to adjust photon response amplitude and quicken photoresponse kinetics according to the requirements of the individual photoreceptor. Besides photoreceptors, there are cyclic GMP pathways in place elsewhere in the retina. Dhingra et al. (2014) have begun to probe the function of these pathways in PDE9A knockout mice by ERG recording.

Downstream signaling pathways for natriuretic peptide receptor GCs are more complex and have not yet been so well characterized (reviewed by Pandey, 2014). In different systems, cyclic GMP synthesis by natriuretic peptide receptor guanylate cyclases decreases cyclic AMP, Ca^{2+}, and inositol triphosphate, and downregulates PKC (protein kinase C) and mitogen-activated protein kinases. Barmashenko et al. (2014) present intriguing experiments in rats with reduced expression of C-type natriuretic peptide receptor guanylate cyclase, CNP-RGC. In neuronal recordings from hippocampus, long term potentiation was enhanced while long term depression was reduced. The changes in neuronal excitability were accompanied by increased exploratory behavior and improved object recognition.

Failure to synthesize cyclic GMP properly can cause severe forms of blindness in early childhood. Disruptions in RD3 cause Leber congenital amaurosis (Molday et al., 2014). In a research article, Zägel and Koch (2014) explain how three separate point mutations that cause another form of Leber congenital amaurosis, progressive cone degeneration, and juvenile retinitis pigmentosa, respectively, alter ROS-GC1 biochemistry. Boye (2014) summarizes promising results of experiments in which gene replacement therapy was used to correct faulty ROS-GC1 function in animal models with recessive retinal disease. Prospects for clinical trials are discussed. Dominant forms of retinal degeneration call for a different approach. The application of RNA interference to attenuate faulty ROS-GC activity caused by mutations in GCAP1 suggests that it may be a viable option (reviewed by Jiang et al., 2014). Glaucoma is yet another major cause of blindness, in this case, due to compromise of retinal ganglion cell function. Buys et al. (2014) examine studies on a major risk factor, elevated intraocular pressure, and the link to cyclic GMP synthesis by both soluble and membrane guanylate cyclases. We conclude the topic with a review by Hannig et al. (2014), that outlines the involvement of STa-RGC in the sensation of visceral pain and how a synthetic peptide may provide relief to patients suffering from abdominal pain.

References

Barmashenko, G., Buttgereit, J., Özcelik, C., Herring, N., Bader, M., Manahan-Vaughan, D., et al. (2014). Regulation of hippocampal synaptic plasticity thresholds and changes in exploratory and learning behavior in dominant negative NPR-B mutant rats. *Front. Mol. Neurosci.* 7:95. doi: 10.3389/fnmol.2014.00095

Boye, S. E. (2014). Insights gained from gene therapy in animal models of retGC1 deficiency. *Front. Mol. Neurosci.* 7:43. doi: 10.3389/fnmol.2014.00043

Buys, E. S., Potter, L. R., Pasquale, L. R., and Ksander, B. R. (2014). Regulation of intraocular pressure by soluble and membrane guanylate cyclases and their role in glaucoma. *Front. Mol. Neurosci.* 7:38. doi: 10.3389/fnmol.2014.00038

Dhingra, A., Tummala, S. R., Lyubarsky, A., and Vardi, N. (2014). PDE9A is expressed in the inner retina and contributes to the normal shape of the photopic ERG waveform. *Front. Mol. Neurosci.* 7:60. doi: 10.3389/fnmol.2014.00060

Duda, T., Pertzev, A., and Sharma, R. K. (2014). Atrial natriuretic factor receptor guanylate cyclase, ANF-RGC, transduces two independent signals, ANF and Ca^{2+}. *Front. Mol. Neurosci.* 7:17. doi: 10.3389/fnmol.2014.00017

Hannig, G., Tchernychev, B., Kurtz, C. B., Bryant, A. P., Currie, M. G., and Silos-Santiago, I. (2014). Guanylate cyclase-C/cGMP: an emerging pathway in the regulation of visceral pain. *Front. Mol. Neurosci.* 7:31. doi: 10.3389/fnmol.2014.00031

Jankowska, A., Sharma, R. K., and Duda, T. (2014). Ca^{2+}-modulated ROS-GC1 transduction system in testes and its presence in the spermatogenic cells. *Front. Mol. Neurosci.* 7:34. doi: 10.3389/fnmol.2014.00034

Jiang, L., Frederick, J. M., and Baehr, W. (2014). RNA interference gene therapy in dominant retinitis pigmentosa and cone-rod dystrophy mouse models caused by GCAP1 mutations. *Front. Mol. Neurosci.* 7:25. doi: 10.3389/fnmol.2014.00025

Lim, S., Dizhoor, A., and Ames, J. B. (2014). Structural diversity of neuronal calcium sensor proteins and insights for activation of retinal guanylyl cyclase by GCAP1. *Front. Mol. Neurosci.* 7:19. doi: 10.3389/fnmol.2014.00019

Molday, L. L., Jefferies, T., and Molday, R. S. (2014). Insights into the role of RD3 in guanylate cyclase trafficking, photoreceptor degeneration, and Leber congenital amaurosis. *Front. Mol. Neurosci.* 7:44. doi: 10.3389/fnmol.2014.00044

Pandey, K. N. (2014). Guanylyl cyclase/natriuretic peptides receptor-A signaling antagonizes phosphoinositide hydrolysis, Ca^{2+} release, and activation of protein kinase C. *Front. Mol. Neurosci.* 7:75. doi: 10.3389/fnmol.2014.00075

Schmitz, F. (2014). Presynaptic [Ca^{2+}] and GCAPs: aspects on the structure and function of photoreceptor ribbon synapses. *Front. Mol. Neurosci.* 7:3. doi: 10.3389/fnmol.2014.00003

Sharma, R. K., and Duda, T. (2014). Membrane guanylate cyclase, a multimodal transduction machine: history, present, and future directions. *Front. Mol. Neurosci.* 7:56. doi: 10.3389/fnmol.2014.00056

Sharma, R. K., Makino, C. L., Hicks, D., and Duda, T. (2014). ROS-GC interlocked Ca^{2+}-sensor S100B protein signaling in cone photoreceptors: review. *Front. Mol. Neurosci.* 7:21. doi: 10.3389/fnmol.2014.00021

Wen, X.-H., Dizhoor, A. M., and Makino, C. L. (2014). Membrane guanylyl cyclase complexes shape the photoresponses of retinal rods and cones. *Front. Mol. Neurosci.* 7:45. doi: 10.3389/fnmol.2014.00045

Zägel, P., and Koch, K.-W. (2014). Dysfunction of outer segment guanylate cyclase caused by retinal disease related mutations. *Front. Mol. Neurosci.* 7:4. doi: 10.3389/fnmol.2014.00004

Conflict of Interest Statement: The authors declare that the research was conducted in the absence of any commercial or financial relationships that could be construed as a potential conflict of interest.

frontiers in
MOLECULAR NEUROSCIENCE

REVIEW ARTICLE
published: 02 July 2014
doi: 10.3389/fnmol.2014.00056

Membrane guanylate cyclase, a multimodal transduction machine: history, present, and future directions

Rameshwar K. Sharma* and Teresa Duda*

Research Divisions of Biochemistry and Molecular Biology, The Unit of Regulatory and Molecular Biology, Salus University, Elkins Park, PA, USA

Edited by:
Clint Lawrence Makino, Massachusetts Eye and Ear Infirmary and Harvard Medical School, USA

Reviewed by:
Kailash N. Pandey, Tulane University Health Sciences Center, USA
Alexander Scholten, University of Oldenburg, Germany

****Correspondence:***
Distinguished Professor Rameshwar K. Sharma, Research Divisions of Biochemistry and Molecular Biology, The Unit of Regulatory and Molecular Biology, Salus University, 8360 Old York Road, Elkins Park, PA 19027, USA
e-mail: rsharma@salus.edu;
Teresa Duda, Research Divisions of Biochemistry and Molecular Biology, The Unit of Regulatory and Molecular Biology, Salus University, 8360 Old York Road, Elkins Park, PA 19027, USA
e-mail: tduda@salus.edu

A sequel to these authors' earlier comprehensive reviews which covered the field of mammalian membrane guanylate cyclase (MGC) from its origin to the year 2010, this article contains 13 sections. The first is historical and covers MGC from the year 1963–1987, summarizing its colorful developmental stages from its passionate pursuit to its consolidation. The second deals with the establishment of its biochemical identity. MGC becomes the transducer of a hormonal signal and founder of the peptide hormone receptor family, and creates the notion that hormone signal transduction is its sole physiological function. The third defines its expansion. The discovery of ROS-GC subfamily is made and it links ROS-GC with the physiology of phototransduction. Sections ROS-GC, a Ca^{2+}-Modulated Two Component Transduction System to Migration Patterns and Translations of the GCAP Signals Into Production of Cyclic GMP are Different cover its biochemistry and physiology. The noteworthy events are that augmented by GCAPs, ROS-GC proves to be a transducer of the free Ca^{2+} signals generated within neurons; ROS-GC becomes a two-component transduction system and establishes itself as a source of cyclic GMP, the second messenger of phototransduction. Section ROS-GC1 Gene Linked Retinal Dystrophies demonstrates how this knowledge begins to be translated into the diagnosis and providing the molecular definition of retinal dystrophies. Section Controlled By Low and High Levels of $[Ca^{2+}]_i$, ROS-GC1 is a Bimodal Transduction Switch discusses a striking property of ROS-GC where it becomes a "$[Ca^{2+}]_i$ bimodal switch" and transcends its signaling role in other neural processes. In this course, discovery of the first CD-GCAP (Ca^{2+}-dependent guanylate cyclase activator), the S100B protein, is made. It extends the role of the ROS-GC transduction system beyond the phototransduction to the signaling processes in the synapse region between photoreceptor and cone ON-bipolar cells; in section Ca^{2+}-Modulated Neurocalcin δ ROS-GC1 Transduction System Exists in the Inner Plexiform Layer (IPL) of the Retinal Neurons, discovery of another CD-GCAP, NCδ, is made and its linkage with signaling of the inner plexiform layer neurons is established. Section ROS-GC Linkage With Other Than Vision-Linked Neurons discusses linkage of the ROS-GC transduction system with other sensory transduction processes: Pineal gland, Olfaction and Gustation. In the next, section Evolution of a General Ca^{2+}-Interlocked ROS-GC Signal Transduction Concept in Sensory and Sensory-Linked Neurons, a theoretical concept is proposed where "Ca^{2+}-interlocked ROS-GC signal transduction" machinery becomes a common signaling component of the sensory and sensory-linked neurons. Closure to the review is brought by the conclusion and future directions.

Keywords: membrane guanylate cyclase, cyclic GMP, multiple transduction modes

INTRODUCTION

In addition to cyclic AMP and inositol triphosphate (IP_3), cyclic GMP is an omnipresent intracellular second messenger of prokaryotes and eukaryotes. It plays a critical role in the control of physiological processes of cardiac vasculature, smooth muscle relaxation, blood pressure, blood volume, cellular growth, sensory transduction, neural plasticity, learning, and memory. Unique to itself, this second messenger system is generated by the catalysis of GTP by two structurally different guanylate cyclases, soluble and the membrane form (**Figure 1**). The synthetic machinery and the modes of their operation by which they generate cyclic GMP are entirely different, and so are their physiologically regulated processes. This review is focused on the mammalian membrane guanylate cyclase transduction field, a principal area of research by the authors for several decades. It begins with its historical development. Briefly

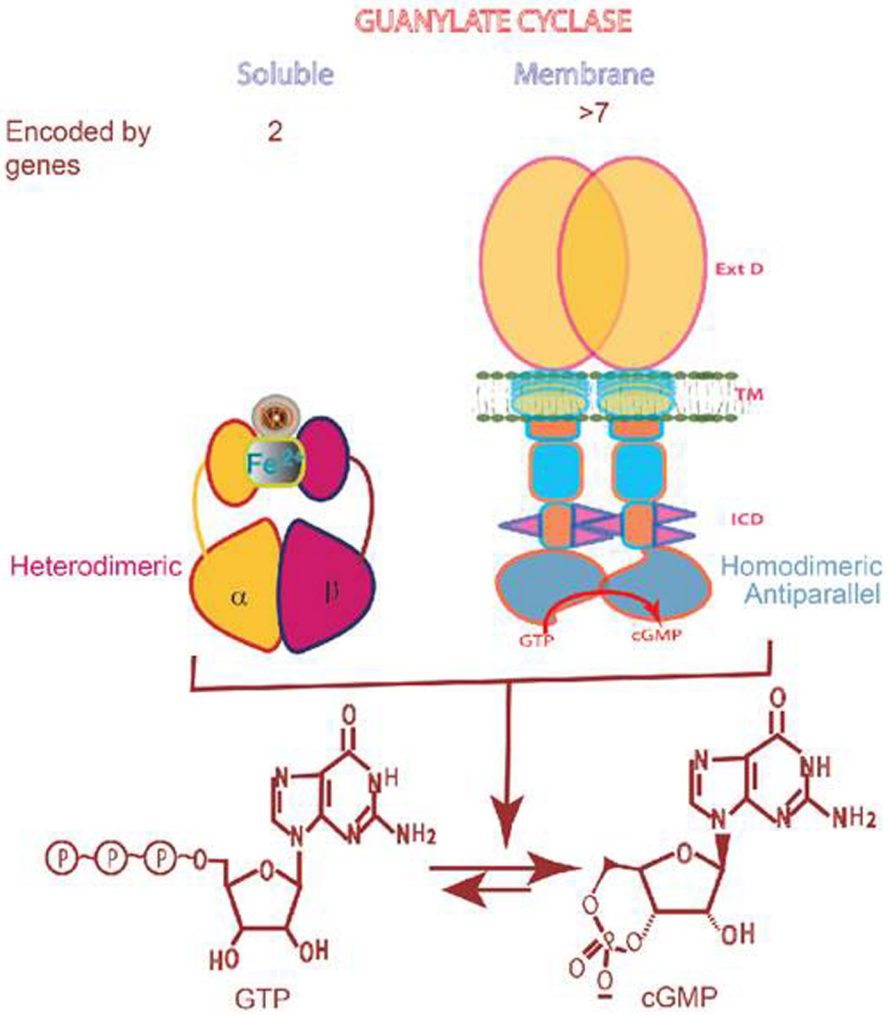

FIGURE 1 | Soluble vs membrane guanylate cyclase. Upper panel: Graphical representation of soluble and membrane guanylate cyclases. The soluble form is encoded by two genes; it is heterodimeric (subunits α and β) and requires heme for its activity. Both monomers contribute to the catalytic center, but their orientation is unknown yet (Allerston et al., 2013). The membrane guanylate cyclase is encoded by 7 genes. It is a single transmembrane spanning protein. The extracelular domain (Ext) is located outside the cell; the transmembrane domain (TM) spans the plasma membrane; and the intracellular domain (ICD) is located inside the cell. The active form is homodimeric. The cyclase catalytic domain is located at the C-terminus of the protein. Both monomers in antiparallel orientation contribute to the catalytic center (Duda et al., 2012). **Lower panel:** Both cyclases are lyases (EC4.6.1.2) and catalyze synthesis of cyclic GMP from GTP.

narrates the efforts involved building on small projects, brick by brick, and emerged from the chasm of disbelief, through steady, continuous work. It then moves on to its present status. To make the presentation simple and chronologically continuous, the subject matters of the earlier reviews (Sharma et al., 1997; Pugh et al., 1997; Sharma, 2002; Duda et al., 2005b; Sharma, 2010; Sharma and Duda, 2012) and publication of these authors have been freely borrowed with appropriate citations.

HISTORY: YEAR 1963–1987

BACKGROUND

The present day usage of the term "signal transduction" is rooted in the original discovery of cyclic AMP (Sutherland and Rall, 1958; reviewed in: Sutherland and Rall, 1960) for which Earl Wilbur Sutherland, Jr. won a Nobel Prize in physiology/medicine in 1971. Based on the studies with glycogen metabolism in skeletal muscle, Sutherland's group proposed the "second messenger" role of cyclic AMP in the hormone actions of epinephrine and glucagon (reviewed in Sharma et al., 1997). This "second messenger" concept was revolutionary because the consensus at the time was that the hormones acted directly on their target tissues, and, thus the hormonal pathway could only be studied in intact cells. Sutherland's studies demonstrated that it was possible to study the cell-free systems and monitor the generation of cyclic AMP indicative of the parent hormone action. Conceptually, the hormone action occurred in the particulate fraction of the cell in two stages; first, the hormone interacted with the particulate

fraction of a cell and second, generated its second messenger, cyclic AMP.

In this concept, the hormone was the first messenger whose interaction with its receptor resulted in a stimulus that caused the production of the second messenger "cyclic AMP," which then acted as the hormone messenger in eliciting the intracellular response (reviewed in Sharma et al., 1997). Thus, the term "second messenger" was coined. Reflective of the time, the biochemical nature of the receptor was not known, because none had been purified. It was not clear whether the enzyme, termed adenylate cyclase, catalyzing the formation of cyclic AMP, was a separate molecule or part, as a subunit, of the receptor. However, it was envisioned that interaction between the receptor and adenylate cyclase generates the second messenger. So enticing was the concept that it was viewed to be applicable to all hormonal systems, i.e., that cyclic AMP is the universal second messenger of all hormones (Robison et al., 1967). Hence, the general concept evolved in which hormone, the first messenger, transmits the extracellular (biological) information to the interior of the cellular machinery through the adenylate cyclase system, and the concept supposed that the receptor was a part of the adenylate cyclase system. The receptor was conceptualized, as defined by the studies in 1930s, as a part of the cell where hormone, the stimulus, interacts (Clark, 1937; Ariëns and Simonis, 1966). The term "stimulus" was equivalent to the presently used term "signal," which, then, according to the "second messenger" concept meant that adenylate cyclase was the means to convert the extracellular ligand binding signal, into the production of the intracellular messenger cyclic AMP. Implicit in this concept was the understanding that the events leading to the transformation of the hormonal binding signal into the production of the second messenger occurred in the cell's plasma membrane.

The "cyclic AMP second messenger concept" was brought to the molecular level by the discoveries of Martin Rodbell and Alfred G. Gilman for which in 1994 they shared the Nobel Prize in physiology/medicine. They demonstrated that G-protein signaling bridged the gap between the hormonal signal and activation of the adenylate cyclase. Rodbell's group argued that the cellular system that processes the hormonal signal was made up of three separate molecular entities: (1) Discriminator (RECEPTOR); (2) Transducer (G-Protein); (3) Amplifier, which as we understand now is the adenylate cyclase. The surface receptor receives information from the exterior of the cell; the G-protein (transducer) transmigrates the information across the cell membrane; and the amplifier (adenylate cyclase) strengthens it to initiate reactions within the cell or to communicate with other cells. In formulating this "G-Protein hormonal hypothesis" the group demonstrated that GTP was obligatory for the hormonal action of glucagon in liver membranes. The term TRANSDUCTION was introduced to indicate this GTP-dependent transformation step. And usage of the term SIGNAL TRANSDUCTION entered the field of cellular signaling (these early studies are reviewed in Rodbell, 1978). The Gilman's and then Birnbaumer's group defined the sequence of these signal transduction steps (Hepler and Gilman, 1992; Birnbaumer and Birnbaumer, 1995). Two types of G proteins, one stimulatory, termed G_s, and the other inhibitory, G_i, were purified and characterized; G_s mediated the stimulatory and G_i the inhibitory transduction. The nature of the receptor defined the specificity of the hormone. The cyclic AMP signaling system therefore comprised of three distinct proteins—receptor, G-protein, and adenylate cyclase (**Figure 2**).

Following the three-component signaling template of cyclic AMP, phosphatidylinositol (IP_3) cellular signaling pathway evolved. Here, the surface receptor responded to an extracellular hormonal signal and converted phosphatidyl-4,5-bisphosphate (PIP_2) in two separate second messengers, diacylglycerol and inositol trisphosphate (IP_3). IP_3 signal transduction splits into two: (1) mobilizes the intracellular calcium and (2) results in the activation of protein kinase C (Early studies respectively reviewed in Nishizuka, 1988; Berridge and Irvine, 1989).

In this manner, these, and complimentary studies from other laboratories (reviewed in Strader et al., 1994) established the presence of two major G-proteins linked with three-component cellular signal transduction pathways—cyclic AMP and phosphatidylinositol—providing the means by which the extracellular hormonal signal is translated into the production of the intracellular second messengers. These second messengers, in turn, initiate a cascade of chemical reactions which ultimately translate the hormonal signal into a biological response.

CYCLIC GMP SIGNALING PATHWAY

Pursuit

Besides cyclic AMP, could another cyclic nucleotide be an alternative hormonal second messenger in cellular signaling?

Cyclic GMP was first identified in rat urine (Ashman et al., 1963). Six years later, cyclic GMP and the enzyme membrane guanylate cyclase catalyzing its synthesis from GTP were detected in all tested animal tissues (Goldberg et al., 1969, 1973; Ishikawa et al., 1969). A groundbreaking "Ying Yang" hypothesis was proposed where both cyclic AMP and cyclic GMP served as hormonal second messengers. They were intertwined and exhibited opposing biological activities of the cellular regulation (Goldberg et al., 1975).

Denial

The celebration was short lived, however. The original proponents failed to consistently demonstrate a hormonally dependent guanylate cyclase in their tested systems (Goldberg and Haddox, 1977). They observed that a variety of non-hormonal ligands like polyunsaturated fatty acids, peroxides, hydroperoxides, free radicals, ascorbic acid, sodium nitroprusside, cigarette smoke also stimulated membrane guanylate cyclase activity. Thus, the membrane guanylate cyclase was a non-specific enzyme and underwent regulation *via* the oxidation-reduction potential of the biochemical reactions (Murad et al., 1979). Also, at the time, the only known cyclic GMP-dependent cellular component was cyclic GMP-dependent protein kinase but not one of its specific, distinct from that of the cyclic AMP-dependent protein kinase, substrate was known. Hence, the revised consensus was that the cyclic GMP-dependent system lacked specificity and acted as a sub-servant to the cyclic AMP system. Therefore, no distinct hormonally dependent membrane guanylate cyclase or cyclic GMP-related specific signaling system existed in any of the biological systems and cyclic GMP had no second messenger role in cellular signaling (Gill and McCune, 1979).

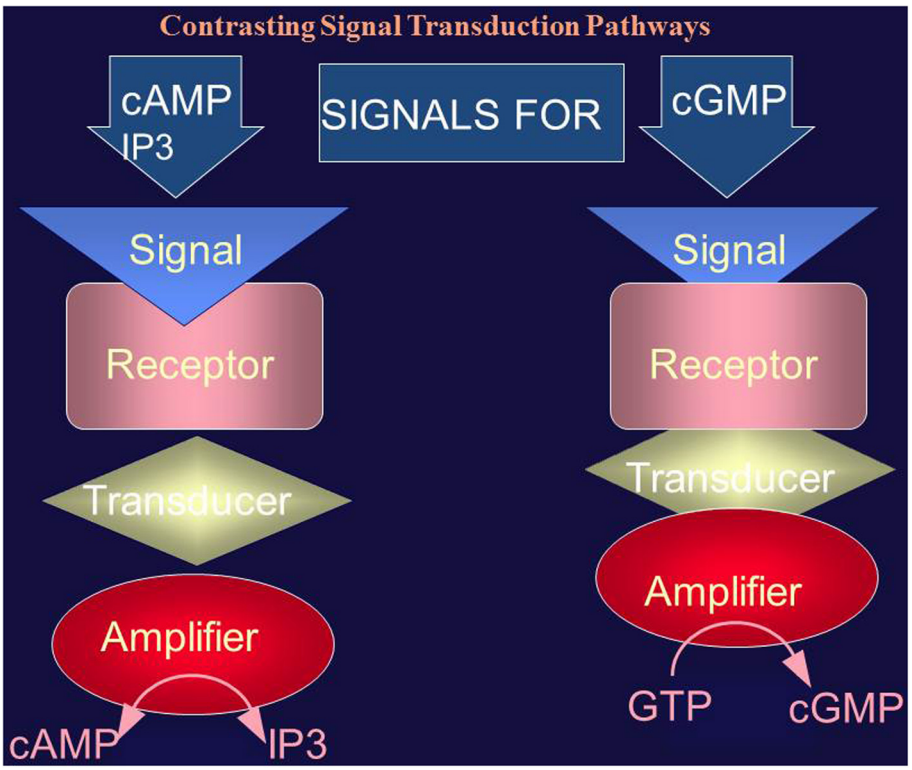

FIGURE 2 | Comparison of the cyclic AMP (and IP3) and cyclic GMP signaling systems. The cyclic AMP (and IP3) signaling system consists of three separate components: hormone receptor, transducer (G protein) and amplifier (adenylate cyclase). The cyclic GMP signaling system consists of a single protein. The hormonal signal is recognized by the extracellular receptor domain; the signal is potentiated at the ATP-modulated ARM domain located next to the transmembrane domain in the intracellular portion of the protein (transducer) and the signal is amplified by the cyclase catalytic domain located at the C-terminus of the protein.

With a new twist, this view was strengthened as the presence of a soluble form of guanylate cyclase activity was found in the originally tested systems (Murad et al., 1979). This form was stimulated by polyunsaturated fatty acids, peroxides, hydroperoxides, free radicals and other agents. Impacted by these new findings and a passion to pursue this new field of soluble guanylate cyclase, the role of cyclic GMP in hormonal signal transduction was totally discarded (Goldberg and Haddox, 1977; Murad et al., 1979). These views are summed up in two of many high-impact reviews:

"While the metabolism of cyclic GMP has many parallelism to that of cyclic AMP, it is becoming quite clear that the two systems have distinct differences and that the functions of one system may not necessarily provide clues to the function of the other. In retrospect, the apparent parallelisms of the two systems hindered the originality of approaches to the cyclic GMP system and may, in fact, have impeded some of the developments in the area. Certainly, many early experiments with guanylate cyclase and cyclic GMP conducted in this laboratory and others were done based on previous experience and biases with the cyclic AMP system …, the properties of the soluble and particulate activities in tissues are quite different …. Minor differences have also been noted between particulate activities and in plasma and endoplasmic reticulum preparations. In spite of these significant physical and/or kinetic differences that suggest two or more forms of guanylate cyclase may exist in tissues, it is not yet known whether or not the proteins or their subunits are different. The apparent differences may be attributable to assay conditions, other constituents in crude preparations, or possibly other factors" (Murad et al., 1979).

"Considerable effort has been put forth to demonstrate an activation of the enzyme by hormonal or other physiological agents that promote the accumulation of cGMP in intact cells. To date, no specific direct effect of such an agent on guanylate cyclase activity *in vitro* has been convincingly demonstrated. This is a characteristic of the cGMP system that contrasts sharply with its cAMP counterpart; adenylate cyclase from disrupted cells as a general rule can be activated by the agents that stimulate cellular cAMP accumulation ….It is becoming evident that the greatest dissimilarity between guanylate cyclase and adenylate cyclase may be that the activity of the former is modulated indirectly with respect to the cellular action of hormones (and other cell stimuli) compared with the direct effect that hormones seem to have on the activity of adenylate cyclase" (Goldberg and Haddox, 1977).

Consolidation, parallel competing concept

The above intimidating concept, lasting to the mid-1980s, was challenged mainly by the competing concept of our group. It favored the hormonal second messenger role of cyclic GMP

(reviewed in Sharma, 2010). Studies with the model systems of the isolated adrenal fasciculata and the adrenocortical carcinoma cells established a membrane guanylate cyclase to be the direct and specific transducer of the adrenocorticotropic hormone (ACTH). Notably, ACTH had no effect on the activity of the soluble guanylate cyclase (reviewed in Sharma, 2002). Thus, the guanylate cyclase existed in two forms, membrane and soluble; and the membrane form was hormone-dependent. These studies are briefly outlined below.

The models of the isolated adrenal fasciculata and the adrenocortical carcinoma cells were tailored to have no phosphodiesterase activity (Kitabchi and Sharma, 1971), and they were used to investigate the second messenger roles of cyclic AMP and cyclic GMP in steroidogenesis. The tailoring created a heightened membrane response to ACTH and it was direct, reflective of membrane-specific guanylate cyclase activity. The tailored PDE-deleted isolated fasciculata cells were sensitive to as little as 0.5–10 μU ACTH in stimulating corticosterone synthesis (Sharma et al., 1974, 1976; Perchellet et al., 1978). These concentrations of ACTH did not raise the level of cyclic AMP, yet they stimulated steroidogenesis (Sharma et al., 1974, 1976; Perchellet et al., 1978). The rise in cyclic AMP level was observed only at ACTH concentrations beyond their maximal steroidogenic capacity (Sharma et al., 1974). Thus, cyclic AMP was not the physiological second messenger of ACTH.

The physiological levels of ACTH in these cells also generated an excellent temporal correlation between the sequential production of cyclic GMP, phosphorylation, and the concomitant synthesis of corticosterone, indicating that the hormone caused the production of cyclic GMP, this, in turn, led to phosphorylation, and finally to corticosterone synthesis (Sharma et al., 1976, 1977). On similar lines, addition of cyclic GMP to these cells stimulated the protein kinase activity which was followed by a rise in their steroidogenic activity (Sharma et al., 1976); and, importantly, this added cyclic GMP mimicked the exogenously supplied ACTH action in stimulating the direct transformation of cholesterol to corticosterone (Sharma et al., 1972). Consistent with the earlier findings these studies also supported the obligatory role of Ca^{2+} in the ACTH-induced steroidogenesis (Perchellet and Sharma, 1979). The conclusions were that cyclic GMP and Ca^{2+} were the two complementary physiological second messengers of the hormone.

The stage was set to directly demonstrate the ACTH-dependent membrane guanylate cyclase in the adrenal cell membranes and also the presence of its companion cyclic GMP system, protein kinase in the bovine adrenal cortex, to strengthen the cyclic GMP second messenger concept.

The cyclic GMP-dependent protein kinase was purified from the bovine adrenal cortex. Its important distinctive characteristic that set it apart from the cyclic AMP signaling system was that its most effective effector molecule was 8-bromo cyclic GMP (Ahrens et al., 1982). Compared to its dibutyryl analog, it was 10,000-fold more active in stimulating the protein kinase activity. This feature established its unique functional identity because the dibutyryl cyclic AMP was more potent than cyclic AMP in stimulating cyclic AMP-dependent protein kinase. Finally, the molecular structure of the cyclic GMP-dependent protein kinase was entirely different from that of the cyclic AMP-dependent protein kinase. The single subunit of the former protein contained both the non-dissociable regulatory and catalytic domains, opposite was the case with the latter protein (Ahrens et al., 1982). Besides providing clarity of the molecular elements of the cyclic GMP signaling system, these unique characteristics of these proteins helped to resolve an earlier argument that cyclic GMP signaling system was the "subservant" of the cyclic AMP signaling system *(vide supra)*. Clearly, it was not the case.

Analysis of the adrenal cortex and the adrenocortical carcinoma tissues demonstrated the direct presence of the ACTH/Ca^{2+}-dependent membrane guanylate cyclase (Nambi and Sharma, 1981a,b; Nambi et al., 1982). In addition, the distinct features of the membrane and the soluble form of guanylate cyclases were established (Table 1 of Nambi et al., 1982). Most fundamentally, the membrane guanylate cyclase activity was not dependent on the free radical and nitric-oxide-generating agents, including hemin.

These conclusions were supported by the findings of other investigators. ACTH stimulated membrane guanylate cyclase activity in the cultured neurons (Anglard et al., 1985), and ANF peptide hormone stimulated membrane guanylate cyclase activity of several rat tissues (Hamet et al., 1984; Waldman et al., 1984). Ironically, these were the same tissues, in the hands of the same investigators, in which earlier the membrane guanylate cyclase activity was not observed (Goldberg and Haddox, 1977; Murad et al., 1979).

The issue was thus resolved. A hormonally-dependent membrane guanylate cyclase existed in the mammalian cells; it was a transducer of specific hormonal signals and cyclic GMP was their second messenger. In addition, the membrane guanylate cyclase was functionally and kinetically distinct from the soluble form. At this moment, the task at hand was to define the cyclase's molecular nature and to elucidate the mechanism of the hormonal signal transduction.

BIOCHEMICAL IDENTITY: ATRIAL NATRIURETIC FACTOR RECEPTOR, THE PROTOTYPE MEMBER OF THE MEMBRANE GUANYLATE CYCLASE FAMILY

A plasma membrane guanylate cyclase was purified from the rat adrenocortical carcinoma and its absolute purity was established by these criteria: (1) protein staining: SDS-PAGE showed a single Coomassie blue- and silver-stained band; (2) isoelectric focusing, native protein and its iodinated form yielded a symmetrical protein peak, which superimposed over the guanylate cyclase activity peak; (3) Western blot analysis using a monospecific polyclonal antibody raised against the native protein yielded a single immunoreactive band which co-migrated with that of the purified protein; (4) the antibody raised against the native protein blocked almost all of its membrane guanylate cyclase activity; and (5) the protein bound ANF peptide hormone in a stoichiometric fashion (Paul, 1986; Paul et al., 1987).

Thus, the protein was pure, it was a membrane guanylate cyclase, and possessed a remarkable characteristic of being also the ANF hormonal receptor. Accordingly, it was named ANF-RGC (ANF RECEPTOR GUANYLATE CYCLASE) also known as GC-A or NPR-A.

The properties of ANF-RGC also resolved the earlier erroneous conclusions on the nature of the membrane guanylate cyclase (Goldberg and Haddox, 1977; Murad et al., 1979). The membrane guanylate cyclase activity was independent of the nitric-oxide-generating agents—catalase, hemin, dithiothreitol, arachidonic acid, and tuftsin, including cigarette smoke. These non-specific activities apparently belonged to the soluble form of the guanylate cyclase whose constituent, critical for the functional operation, was heme (**Figure 1**).

A parallel report described the purification of a protein from the rat lung and claimed that "ANF-binding and guanylate cyclase activity resided on a single protein" (Kuno et al., 1986). These authors demanded priority on their finding and challenged the priority on the original discovery of ANF-RGC. This issue was settled in a commentary (Sharma, 1988), which revealed that in contrast to the criteria of the absolute purity established for the adrenocortical carcinoma ANF-RGC guanylate cyclase (Paul et al., 1987), the lung guanylate cyclase preparation was crude (Kuno et al., 1986)—in addition to the main and major 120-kD protein it contained at least 13 other minor bands and the authors themselves stated "that it was about 95% pure" (Kuno et al., 1986). The possibility existed that the 5% contaminant contained the separate ligand-binding or the cyclase activity. There were two other serious problems with the claim that the lung guanylate cyclase was also the ANF receptor: (1) it bound only 14.5% of ANF at the noted theoretical value; (2) the lung enzyme was stimulated by hemin, a characteristic of the soluble guanylate cyclase, not possessed by the membrane guanylate cyclase (Kuno et al., 1986). To this date, these deficiencies in the lung enzyme to categorize it as a genuine ANF-RGC have not been resolved.

With two subsequent reports on ANF-RGC purification from the adrenal cortex and its characterization (Takayanagi et al., 1987; Meloche et al., 1988), the concept that this membrane guanylate cyclase is also a surface receptor of the ANF hormone was established. And a new field of the hormone receptor membrane guanylate cyclases was borne.

This happening had a powerful impact on the cellular signal transduction field, as it was a ground-breaker. It demonstrated that the hormonally modulated membrane guanylate cyclase transduction system was radically different from the two existing cyclic AMP and IP_3 signaling pathways, quoting in the original publication "coexistence of the ANF receptor and guanylate cyclase activities on a single polypeptide chain indicates that the mechanism of transmembrane signal transduction involving mediation by second messenger, cyclic GMP, is different from the well-established adenylate cyclase system. In the hormone-dependent adenylate cyclase, there is an assemblage of individual components—receptor, GTP-binding protein, and catalytic moiety—for signal transduction. In contrast, the presence of dual activities—receptor-binding and enzymic—on a single polypeptide chain indicates that this transmembrane protein contains both the information for signal recognition and its translation into a second messenger" (Paul et al., 1987) (**Figure 2**).

In the proposed model, ANF-RGC is depicted as a single transmembrane-spanning protein; the ANF-receptor domain resided on the outside, the catalytic domain protruded inside the cell and a transmembrane segment separated its two portions (Sharma et al., 1988; Sharma, 2002; modified version of Figure 1 in Sharma, 2002). Mechanistically, ANF will bind to its receptor which resided in the extracellular domain of ANF-RGC. It will generate a cascade of structural changes, they will be carried over the transmembrane domain of ANF-RGC and finally stimulate its catalytic domain residing in the interior of the cell. The cyclic GMP will be produced and serve as a second messenger of the hormonal ANF signal.

ANF-RGC FAMILY

Almost 3 years after its purification, ANF-RGC mRNA was cloned from the human and rat brain (Chinkers et al., 1989; Lowe et al., 1989), adrenal gland (Duda et al., 1991) and the mouse Leydig tumor cells (Pandey and Singh, 1990). In all cases the deduced protein structure validated the original theoretical prediction (Paul et al., 1987) that ANF-RGC was a single-transmembrane-spanning protein. The transmembrane region divides it in two roughly equal portions: extracellular and intracellular (please note: a more detailed description of a representative membrane guanylate cyclase modular structure is provided in **Figure 4**).

Analysis of the two additional cloned membrane guanylate cyclases demonstrated that they were the surface receptors of the respective hormones, CNP (Chang et al., 1989; Schulz et al., 1989; Duda et al., 1993) and enterotoxin (de Sauvage et al., 1991; Singh et al., 1991); and they have the identical structural topography as ANF-RGC. According to their function, they were named CNP-RGC (CNP receptor guanylate cyclase also known as GC-B or NPR-B) and STa-RGC (enterotoxin receptor guanylate cyclase also known as GC-C). These findings established a three-member surface receptor family of membrane guanylate cyclases, which remains the case to date (reviewed in Sharma, 2010).

HORMONE SIGNALING SITE RESIDES IN THE EXTRACELLULAR DOMAIN OF RECEPTOR GUANYLATE CYCLASES

With the model system of the variant form of ANF-RGC, GCα, cloned from the adrenal cortex, the original study of Duda et al. (1991) demonstrated that the ANF binding site in ANF-RGC resides in the extracellular domain. Compared to ANF-GC, GCα in its structure had only two amino acid substitutions, Gln^{338}His and Leu^{364}Pro, but it did not bind ANF. Importantly, it did retain basal cyclase catalytic activity. Reconstitution of the native ANF-RGC residues restored the mutant's ANF-binding and ANF-dependent catalytic activities (Duda et al., 1991). Thus, the ANF ligand-binding domain resided in the extracellular domain of ANF-RGC; and one, or both of the residues—Gln^{338}, Leu^{364}—controlled its ANF-binding and ANF-dependent catalytic activities. Refined point mutation analysis demonstrated that both of these controls resided in Leu^{364} (Duda et al., 1991). Thus, the hypothesis for the ANF signal transduction mechanism evolved. It involved the ANF binding to its extracellular domain in ANF-RGC; the binding initiated a cascade of structural changes in ANF-RGC; these changes, in turn, stimulated its catalytic domain, which resided at the opposite end on the intracellular domain

of the cyclase. The generated cyclic GMP served as the second messenger of ANF signal.

This signal transduction mechanistic template was applied to CNP-RGC cloned from the human retina (Duda et al., 1993). CNP-RGC is a homologous protein to ANF-RGC, with 59% structural identity. It was found that Glu^{332} residue of CNP-RGC was critical for the CNP binding and the CNP-dependent catalytic activity of CNP-RGC (Duda et al., 1994). Like ANF-RGC, the site had no influence on the basal guanylate cyclase activity. These studies were extended to compare the identities of the folding patterns of the external domains of these membrane guanylate cyclases (Duda et al., 1994). They were found to be almost identical (Duda et al., 1994). The counterpart of CNP-RGC-Glu^{332} residue is the Gln^{338} residue of ANF-RGC, and that of ANF-RGC-Leu^{364} residue is Val^{358} of CNP-RGC. Conversion of the ANF-RGC residue Gln^{338} to Glu resulted in a change from none to significant CNP signal transduction activity. And, the conversion of Val^{358} to Leu generated significant ANF signal transduction activity in CNP-RGC (Duda et al., 1994). These studies validated that the ligand-binding domain resides in the extracellular domain of ANF-RGC and CNP-RGC, provided identity of the residues that are critical in defining the ligand-binding domains and showed that the folding patterns of these domains in two guanylate cyclases are very similar.

The subsequent crystallization studies on the isolated extracellular domains of ANF-RGC and CNP-RGC validated the conclusions that the hormone-binding site, indeed, resides in the external domain of the guanylate cyclase and Leu^{364} of ANF-RGC and Val^{358} of CNP-RGC constitute critical hydrophobic sites essential for the ANF or CNP signaling but the sites are not the direct hormone-binding sites (Ogawa et al., 2004; He et al., 2001).

ATP IS OBLIGATORY FOR ANF AND CNP HORMONAL SIGNALING

Prior to the molecular characterization of ANF-RGC, two studies with crude membrane preparations proposed that ATP accelerates ANF-dependent ANF-RGC activity (Kurose et al., 1987; Chang et al., 1990). Two different mechanisms for the acceleration were proposed; direct (Kurose et al., 1987) and indirect *via* an accessory protein (Chang et al., 1990). Because the preparations were crude and the guanylate cyclase was uncharacterized, the issue as to which mechanism was correct could not be resolved.

Subsequently, in parallel two independent groups established that ATP is obligatory for the ANF-dependent ANF-RGC transduction activity (Marala et al., 1991; Chinkers et al., 1991). Neither ANF, nor ATP alone, is able to stimulate ANF-RGC catalytic activity. Only when these two are together they are able to stimulate the cyclase. Because the non-hydrolyzable analogs, ATPγS and AMP-PNP, mimicked the ATP effect, both groups proposed that ATP acts directly by allosteric regulation of ANF-RGC (Marala et al., 1991; Chinkers et al., 1991). Later study with CNP-RGC demonstrated that ATP is also obligatory for its CNP-dependent activity (Duda et al., 1993).

The mechanistic models proposed for the ATP effect by these two groups were different, however. Which one is valid, was debated for over two decades. MODEL 1 proposed by the Garbers'group stated "…binding of ANP [ANF] to the extracellular domain of its receptor initiates a conformational change in the protein kinase-like domain (KHD), resulting in derepression of guanylate cyclase activity" (Chinkers and Garbers, 1989). Its central idea was that "KHD in native ANF-RGC suppresses its catalytic module activity; ANF functions by relieving this suppression." Sharma's group challenged this model on the grounds of their findings that partial or complete deletion of the KHD did not cause any significant elevation in the basal activity of the guanylate cyclase; therefore, ANF signaling did not involve overcoming the KHD suppression of the guanylate cyclase activity, contradicting the central theme of MODEL 1. (Goraczniak et al., 1992; reviewed in Duda et al., 2005b). They proposed an alternate MODEL 2. In it the repressor of the core catalytic domain (CCD) of the guanylate cyclase was the disulfide structural motif of ANF-RGC (Duda and Sharma, 2005). This motif was juxtaposed to the N-terminus of the TM (transmembrane of the domain). The motif repressed the ARM (ATP REGULATED MODULE) domain, which, in turn, inhibited the CCD. ATP-modulated ANF signal overcame the disulfide structural motif-dependent inhibition of ARM resulting in activation of the CCD of ANF-RGC.

The MODEL 2 has been defined in molecular terms by simulating structure of the ARM domain in 3D-terms, experimentally validating the biochemistry of the structure and its physiology through the mouse molecular genetic models (Duda et al., 2001c, 2009, 2013). The definition has been arrived at through biochemical experiments involving point mutation, time-resolved tryptophan fluorescence, Forster Resonance Energy Transfer (FRET), reconstitution, recombinant constructs, molecular modeling, immunohistochemistry and recently mouse molecular genetics (these studies are comprehensively reviewed in Duda et al., 2014).

LINKAGE WITH SENSORY TRANSDUCTION SIGNALS EXPANDS THE FAMILY

Because the property of being a hormonal receptor, transducer and signal amplifier was common in all known members of the membrane guanylate cyclase family (ANF-RGC, CNP-RGC and STa-RGC), the notion was that the cyclic GMP signaling pathway operated solely in the hormonal signaling pathways and was designed to transduce only the signals generated outside the cell. However, it was not the case.

The membrane guanylate cyclase signal transduction paradigm changed with the landmark discovery of the photoreceptor ROS-GC guanylate cyclase. Here the signal initiation occurred inside the cell and the signal transduction system was composed of two separate elements, Signal receiver and the Transducer (detailed reviews Sharma and Duda, 2012; Koch et al., 2010; Pugh et al., 1997).

It was known that in phototransduction, which is the transformation of the light signal into an electrical signal, both $[Ca^{2+}]_i$ and cyclic GMP are the critical cytosolic regulatory effectors of the photon signal in the vertebrate photoreceptors. Which one of these is the second messenger of the LIGHT signal; how these signals are generated; how they interact with each other; and what was the source of the cyclic GMP was not known, however

(early reviews Pugh and Cobbs, 1986; Stryer, 1986; Lamb et al., 1986). Early reports on the successful identification of photoreceptor ROS-GC contradicted each other, and created chaos. They ranged from the guanylate cyclase being a 67 kDa subunit (Horio and Murad, 1991a,b), consisting of "separate regulatory and catalytic subunits" (Stryer, 1991) and of its molecular from of retGC (Shyjan et al., 1992).

The breakthrough came with the seminal observation that a soluble bovine rod outer segment (ROS) fraction stimulated the catalytic activity of a particulate photoreceptor guanylate cyclase in the absence of Ca^{2+} (Koch and Stryer, 1988). This hinted that the guanylate cyclase was of the membrane form; the soluble ROS fraction was Ca^{2+} sensitive and the two components together constituted the phototransduction-linked guanylate cyclase transduction element. However, the conceived structure of this guanylate cyclase was erroneous, believed to be composed of "separate regulatory and catalytic subunits" (Stryer, 1991).

The true identity of the photoreceptor ROS-guanylate cyclase (ROS-GC also known as GC-E) was resolved by establishing its direct purification from the bovine outer segments (OS) (Margulis et al., 1993), the site of phototransduction; and its protein-sequence-based molecular cloning, structure, and function (Goraczniak et al., 1994). ROS-GC had a theoretical molecular mass of 120,360 Da; a value similar to that reported earlier for a bovine (Koch, 1991) and a toad photoreceptor guanylate cyclase (Hayashi and Yamazaki, 1991). Unlike the other known membrane guanylate cyclases, atrial natriuretic factor receptor guanylate cyclase ANF-RGC (Paul et al., 1987; Sharma, 1988; Chinkers et al., 1989; Duda et al., 1991) and type C natriuretic peptide CNP-RGC guanylate cyclase (Chang et al., 1989; Duda et al., 1993), ROS-GC was not hormonally-responsive (Goraczniak et al., 1994). And also ROS-GC was not composed of "separate regulatory and catalytic subunits"; it was not nitric oxide sensitive nor was its structure identical to retGC (Shyjan et al., 1992), which apparently was a cloning artifact whose primary structure was eventually revised to match that of bovine ROS-GC (Accession number M92432).

Hydropathy analysis of its deduced amino acid sequence revealed that topography of this protein was similar to the other three peptide hormone receptor guanylate cyclase members (Goraczniak et al., 1994), i.e., (1) it was a single transmembrane spanning protein; (2) the TM domain divided the protein into roughly two equal segments, extracellular and intracellular; (3) it showed a significant overall homology with the other peptide hormone receptor guanylate cyclases: 27% identity with STa-RGC, 30% with ANF-RGC, 31% with CNP-RGC. The level of identity rose to 37, 40, and 41% in their intracellular regions, and there were respective identities of 25, 32, and 32% between their kinase like domains. The least identity with peptide hormone receptor guanylate cyclase existed in their extracellular domains: 14% with STa-RGC, 17% with ANF-RGC and 18% with CNP-RGC. Despite these similarities, there were two significant structural variances. The signature ATP-modulated domain Gly-X-X-X-Gly present in ANF-RGC and CNP-RGC was absent in ROS-GC. And the ROS-GC protein beyond the catalytic domain contained a C-terminal extension tail of 90 amino acids, Y^{965}-K^{1054}, this tail was absent in ANF-RGC and CNP-RGC. On these grounds the discovery of ROS-GC represented expansion and the generation of a new subfamily of the membrane guanylate cyclases.

It is noteworthy that in the membrane guanylate cyclase family ROS-GC is the only one whose molecular identity has been established on the basis of its protein sequence. This strategy has provided an experimental proof for the position of the N-terminus amino acid of the mature protein and demonstrated that the mature protein contains a 56 amino acid N-terminus hydrophobic signal peptide. The theoretical molecular mass of the protein with its signal peptide is 120,361 Da and without it is 114,360 Da. (Goraczniak et al., 1994).

ROS-GC, A CA^{2+}-MODULATED TWO COMPONENT TRANSDUCTION SYSTEM

Following the functional description by Koch and Stryer (1988), almost contemporaneously, two independent groups discovered two structurally dissimilar guanylate cyclase activating proteins (GCAPs), GCAP1 (Palczewski et al., 1994; Subbaraya et al., 1994; Gorczyca et al., 1994; Frins et al., 1996) and GCAP2 (Dizhoor et al., 1995). In the presence of free Ca^{2+}, did these GCAPs inhibit catalytic activity of the photoreceptor ROS-GC?

Availability of the recombinant (r)ROS-GC made it possible to answer this question. Expressed in the heterologous system of COS cells, ROS-GC was responsive at 10 nM $[Ca^{2+}]_i$ to the GCAP1 stimulation in a dose dependent manner. The stimulation was inhibited cooperatively by free Ca^{2+} with a $K_{1/2}$ of 100 nM. Under identical conditions, GCAP1 had no effect on the catalytic activity of the recombinant peptide hormone ANF-RGC (Duda et al., 1996b). An important characteristic of the transduction system was that GCAP1 remained bound to ROS-GC at the low and high Ca^{2+} levels, consistent with physiological observations (Koutalos et al., 1995). Similar reconstitution studies established GCAP2 as another Ca^{2+}-sensor of ROS-GC signaling. With the subsequent discovery of a second ROS-GC, termed ROS-GC2, or GC-F (Lowe et al., 1995) to distinguish it from the original ROS-GC which was renamed as ROS-GC1 (GC-E), it became clear that a Ca^{2+}-modulated system composed of a pair of ROS-GCs and a pair of GCAPs sub-serve phototransduction in the outer segments of photoreceptors. Which of the two ROS-GCs is physiologically linked with phototransduction?

This problem has not yet been solved for ROS-GC2, but by all criteria ROS-GC1 is a vital component of the phototransduction machinery. (1) It is the only one purified directly from the ROS, the site of phototransduction. (2) Direct quantitative estimation of the two isozyme guanylate cyclases in the bovine ROS demonstrates that their ratios are 96% ROS-GC1 and 4% ROS-GC2, suggesting ROS-GC2 presence is minor (Helten et al., 2007). The latest estimation in the mouse shows the same pattern, 76 vs. 24% (Peshenko et al., 2011). Notably, in contrast to the bovine, the mouse study was made with the total OS instead of the isolated membrane fractions. (3) The multiple cone rod dystrophies in humans have only been linked with the ROS-GC1 mutations, none so far with ROS-GC2 (reviewed in Hunt et al., 2010). Finally, (4) it has been demonstrated that the ROS-GC1 gene deletion results sequentially in the cone and then the rod

degenerations, indicating that the guanylate cyclase is directly linked with the vitality and the function of photoreceptors (Yang et al., 1999).

GCAPS INTERLACE CA^{2+} AND ROS-GC

Together with recoverin (Dizhoor et al., 1991; Hurley et al., 1993), GCAPs are the prototype members of the NCS (neuronal Ca^{2+} sensor) proteins family (reviewed in Sharma and Duda, 2012; Koch et al., 2010). Except for S100B, which has two, a general characteristic of this family is that its members have four Ca^{2+}-specific structural motifs, termed EF hands. They define the general Ca^{2+} sensor property of the family. While the teleost fish expresses up to 8 forms, the mammals express 2-3 GCAPs (reviewed in: Rätscho et al., 2010).

GCAP1 and GCAP2 are expressed in the same concentration of 3 μM in the bovine ROS (Hwang et al., 2003). Their quantitative, relative, and cellular concentrations in the cones are not known. Yet immunocytochemical studies show that both GCAPs are present in the outer and inner segments of the rods and cones (Gorczyca et al., 1994; Frins et al., 1996). In mouse cones, the expression of GCAP1 exceeds significantly the expression of GCAP2 (Wen et al., 2014). Notably, GCAP1 presence in the cone synaptic pedicles can be clearly defined (Venkataraman et al., 2003).

True to the NCS family trait, GCAPs harbor four EF-hand Ca^{2+}-binding motifs, yet only three are functional (reviewed in Koch et al., 2010; Sharma and Duda, 2012). They are second, third and fourth. They sense Ca^{2+} in the range of tens to hundreds nanomoles and are the Ca^{2+}-sensor elements of the ROS-GC linked phototransduction machinery.

The knowledge on the $[Ca^{2+}]_i$ sensing properties of GCAP1 is more advanced than that of GCAP2. In a recent proposal, the transition from the DARK State to the illuminated state of the photoreceptors occurs by the substitution of bound Ca^{2+} with the bound Mg^{2+} to ROS-GC1 (Peshenko and Dizhoor, 2006, 2007). Ca^{2+} associates with GCAP1 with a rate of $\sim 2 \times 10^8$ M^{-1} s^{-1} (k_{on}) which is close to the diffusion limit (Sokal et al., 1999). The apparent dissociation constants of each EF-hand for Ca^{2+} are between 0.08 and 0.9 μM and between 0.1 and 1.6 μM in the absence and in the presence of 2 mM Mg^{2+}, respectively (Lim et al., 2009). Thus, these nanomolar affinities result in fast dissociation rates (for example, $k_{off} = k_{on} \times K_D = 2 \times 10^8$ M^{-1} s^{-1} $\times 0.2 \times 10^{-6}$ $M = 40s^{-1}$; $1/k_{off} = 25$ ms), consistent with the kinetics of the photoresponse.

GCAP2 senses Ca^{2+} signals differently through its second, third, and fourth EF-hands. They display an apparent K_D of 300 nM (Ames et al., 1999), but no specific assignment for the affinity of each EF-hand has been made so far. It appears, however, that EF hands two and four influence Ca^{2+} sensitivity of GCAP2 more than EF-hand three (Dizhoor and Hurley, 1996). Cysteine accessibility study with GCAP2 mutants shows its restricted reactivity toward Cys^{111} at sub-micromolar Ca^{2+}-concentrations, indicating that within the Ca^{2+} concentration range where ROS-GCs are regulated, Ca^{2+}-induces conformational changes in GCAP2 (Helten and Koch, 2007). Thus, these fluctuations in the free Ca^{2+} concentrations of the rods and cones control and signal GCAPs to transmit their messages to the bound ROS-GC and be transduced in the generation of cyclic GMP, the second messenger of phototransduction.

DIFFERENTIAL ROS-GC1 MODULATION BY GCAPS

In a significant conceptual advancement, the original study of Krishnan et al. (1998) proposed and demonstrated that "the intracellular region of ROS-GC1 is composed of multiple modules, each designed to mediate a specific Ca^{2+} signaling pathway." This meant that the sensing mechanisms of $[Ca^{2+}]_i$ by the ROS-GC1 modules are more than one. This concept was arrived at through the use of ROS-GC1 deletion and ANF-RGC/ROS-GC1 hybrid mutants which retained only the catalytic domain of ROS-GC1. The GCAP1- and GCAP2- modulated domains in ROS-GC1 were separate and they resided on the opposing ends of the catalytic domain of ROS-GC1, GCAP2 at the C-terminal side and the GCAP1 at the N-terminal.

This concept was fine-tuned by mapping the GCAP1- and GCAP2-modulated sites of ROS-GC1 by the use of a comprehensive technology involving soluble constructs of ROS-GC1, direct binding measurements by surface plasmon resonance (SPR) spectroscopy, coimmunoprecipitation and functional reconstitution utilizing progressive deletion constructs and peptide competition studies. The GCAP1 site is composed of two subdomains: transduction, M^{445}-L^{456} and binding, L^{503}-I^{522} (Lange et al., 1999), and the GCAP2 of one continuous domain, Y^{965}-N^{981}, containing both the transduction and the binding site (Duda et al., 2005a).

These two GCAP sites have different sensitivities to capture $[Ca^{2+}]_i$ signals and activate ROS-GC1. The $[Ca^{2+}]$ $K_{1/2}$ for GCAP1 is 707 nM and for GCAP2, 100 nM (Hwang et al., 2003). Thus, the latter is about one-order of magnitude more sensitive to $[Ca^{2+}]_i$ in signaling ROS-GC1 activation.

At a secondary structural level, there also exists a striking difference between the activities of the two GCAPs. The indication is that dimerization of GCAP2 is a necessary requisite to activate the ROS-GC (Olshevskaya et al., 1999). In contrast, the dimeric form of GCAP1 is inactive and does not result in activation of the ROS-GC (Hwang et al., 2004).

GCAP-MODULATED ROS-GC1 PHOTOTRANSDUCTION MODEL (FIGURE 3)

The biochemical process by which the rods and cones convert the incoming LIGHT signal into the generation of the electrical signal is termed photo-transduction. Educated by the ROS specific photoreceptor features of the interlocked GCAP/ROS-GC transduction system, a model for its role in operation of the photo-transduction machinery is proposed (**Figure 3**). This model explains two principal characteristics of photo-transduction machinery, recovery and its variable luminosity dependent operation; the latter characteristic adds an advanced feature to the previous models (Pugh et al., 1999; Burns and Baylor, 2001; Koch et al., 2002, 2010; Sharma, 2002; Luo et al., 2008; Stephen et al., 2008; Wensel, 2008) and depicts the differential involvement of GCAPs in its operation. The luminosity-dependent phototransduction principles of the present model incorporate a core theme of the previously proposed "Ca^{2+}-relay model" (Koch, 2006; reviewed in Koch et al., 2010; Sharma, 2010), which explained the results of a transgenic GCAPs null mice study where

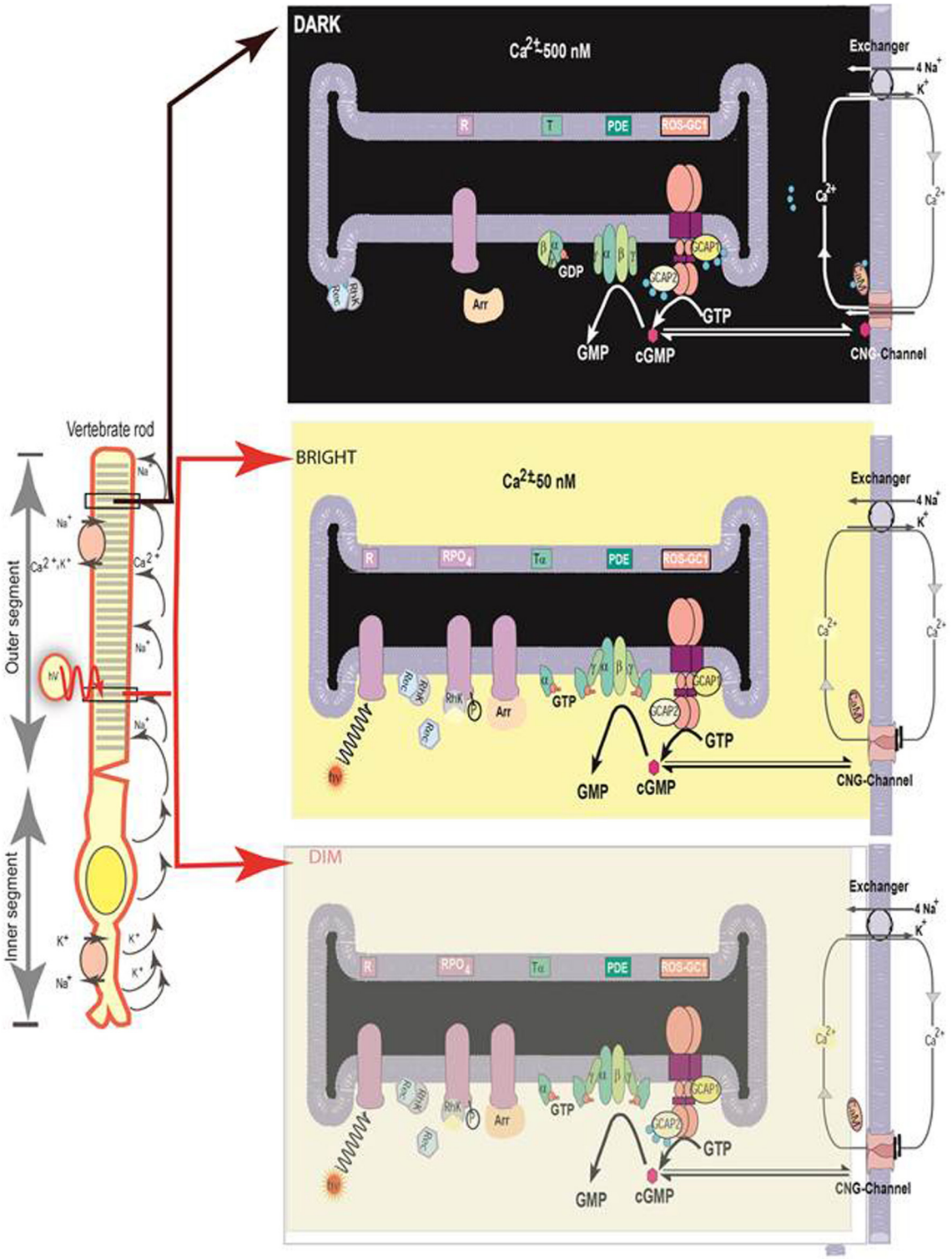

FIGURE 3 | Schematic representation of the luminosity-dependent operation of the ROS-GC-GCAP transduction system. Left panel. An illustration of a typical vertebrate rod. In the DARK a circulating current (arrows) is present. It is outward in the inner segment and carried primarily by K^+; in the outer segment the net charge is inward, with about 90% of the inward flow carried by the Na^+ and 10% by Ca^{2+} ions. Na^+/K^+ exchange pumps in the inner segment membrane and Na^+/K^+-Ca^{2+} exchangers in the outer segment membrane (see also right panels) maintain the overall ionic gradients against the dark flows. The capture of a photon (hν) by a rhodopsin molecule in one of the disc membranes of the outer segment initiates the photo-transduction cascade. **Right upper panel. DARK.** The components of the Photo-Transduction cascade are shown in the dark/resting steady-state. Cytoplasmic cyclic GMP, generated by the basal catalytic activity of ROS-GC,

(Continued)

FIGURE 3 | Continued
keeps a fraction of CNG channels in the plasma membrane open. ROS-GC1 via its ^{415}M-L^{456} segment is GCAP1- and via ^{965}Y-N^{981} is GCAP2-bound. Ca^{2+} ions enter the cell via the CNG-channel and are extruded via the Na^+/K^+, Ca^{2+}-exchanger. Synthesis and hydrolysis of cyclic GMP by ROS-GC and PDE, respectively, occur at a low rate. The heterotrimeric G protein transducin is in its GDP-bound state and is inactive. The Ca^{2+} binding proteins calmodulin (CaM), recoverin (Rec) are bound to their target proteins, the CNG-channel, rhodopsin kinase (Rhk), respectively. **Right middle panel.** Absorption of **BRIHT LIGHT** by the visual pigment rhodopsin leads to the activation of the transduction cascade: the GTP-bound α-subunit of transducin activates PDE that rapidly hydrolyzes cGMP. Subsequently the CNG-channels close and the Ca^{2+}-concentration falls. The fall in cytoplasmic $[Ca^{2+}]_i$ is sensed by Ca^{2+}-binding proteins: CaM dissociates from the CNG-channel what leads to an increase in cyclic GMP sensitivity of the channel; recoverin stops inhibiting rhodopsin kinase; rhodopsin becomes phosphorylated. Both Ca^{2+}-free GCAPs in their changed configurations activate ROS-GC and synthesis of cyclic GMP increases. Arrestin (Arr) binds to phosphorylated rhodopsin and interferes with the binding and further activation of transducin. Enhancement of cyclic GMP synthesis brings it to its original DARK state level and termination of the cascade, which leads to reopening of CNG channels. **Right bottom panel, DIM LIGHT**. The initial fall of $[Ca^{2+}]_i$ is selectively detected only by GCAP1. In its Ca^{2+}-free state GCAP1 attains the activated mode and stimulates ROS-GC activity. GCAP2 remains Ca^{2+}-bound and in its inhibitory mode.

the role of GCAP2 was questioned (Howes et al., 2002; Wen et al., 2014).

MIGRATION PATTERNS AND TRANSLATIONS OF THE GCAP SIGNALS INTO PRODUCTION OF CYCLIC GMP ARE DIFFERENT

After settling the issue that the biochemical modes of two GCAPs in Ca^{2+} signaling of the photoreceptor ROS-GC1 are different and autonomous of each other, the next task was to analyze their migratory pathways at the structural levels, determine the mechanisms involved in transmission and translation of the signals at the CCD of ROS-GC1 into the production of cyclic GMP.

To comprehend these issues and their resolutions, **Figure 4** is presented and the parts of the discussion are excerpted (Duda et al., 2012) and briefly recounted. The study involved a programmed domain deletion, expression, *in vivo* fluorescence spectroscopy, and *in vitro* reconstitution experiments. The findings validated (1) in structural terms that operational modes of two GCAPs in signaling of ROS-GC1 activity are different. GCAP1 signal transduction occurs through M^{445}-L^{456} and L^{503}-I^{522} subdomains of JMD and of GCAP2 signal transduction via the Y^{965}-N^{981} subdomain of CTE. These subdomains are at the opposite ends of CCD and they are the sites where the signal of the respective GCAPs originates.

(2) In living cells, both GCAPs by themselves are soluble proteins. Only when they are present with ROS-GC do they become membrane bound through their specific target sites on the ROS-GC1. Thus, ROS-GC1 is the one that bestows on them the property of being membrane bound; the anchoring sites are M^{445}-L^{456} and L^{503}-I^{522} for GCAP1 and Y^{965}-N^{981} for GCAP2. In accordance with these conclusions, disruption of the GCAP1 anchoring site on ROS-GC1 through mutagenesis, results in GCAP1 being a soluble protein. In contrast, GCAP2 remains bound to this ROS-GC1 as its activator. These results prove that the two GCAPs signal ROS-GC1 activation through different modes and the differences reside in the spatial characteristics of ROS-GC1; and because orientations of the two domains of their signal origins are different, their migration pathways are different: GCAP1 downstream from M^{445}-L^{456} and L^{503}-I^{522} to the P^{808}-K^{1054}. This assumption was validated through the studies with the SHD-deleted ROS-GC1 mutant. Being downstream from the JMD, the site of the GCAP1 signal, and being a component of the GCAP1 signal trajectory, deletion of the SHD disrupted the GCAP1 signaling of ROS-GC1. But the GCAP2 signaling of the ROS-GC remained intact.

Strikingly, these results also revealed the existence of an in intriguing signaling pathway, never observed before for the membrane guanylate cyclase family. This pathway is unique to GCAP2 and runs opposite to that of GCAP1, upstream from the Y^{965}-N^{981} site in CTE to the CCD for translation of the signal into the production of cyclic GMP (**Figure 4**).

(3) The CCD is a common and conserved translation site for the GCAP1, GCAP2 and all other signals generated by the ligands of the membrane guanylate cyclase family. The current model, based on biochemical analysis, is one in which CCD has intrinsic basal catalytic activity and in its isolated form exists as a homodimer (Venkataraman et al., 2008). Through molecular modeling, this secondary structure has been advanced to its 3D-form, which reveals that its two subunits are in antiparallel conformation (Liu et al., 1997; Venkataraman et al., 2008). Is this model applicable in depicting the 3D structure of CCD in a living cell?

It is. The studies using the bimolecular fluorescence complementation (BiFC) technique demonstrated for the first time that in living cells, the CCD is present in its homodimeric form; and the two subunits are fused in the antiparallel orientations (Duda et al., 2012).

ROS-GC1 GENE LINKED RETINAL DYSTROPHIES

The disclosure of true identity, complete structure and organization of the ROS-GC1 gene (Duda et al., 1998) and the mechanism by which Ca^{2+} signal modulates its encoded ROS-GC1 enzyme activity made it possible to investigate its role in the human retinal diseases at the genetic levels and explain their biochemistry in molecular terms. For recent comprehensive reviews on this topic the reader is referred to (Hunt et al., 2010; Karan et al., 2010; Sharma, 2010; earlier findings to the year 2002 are covered in Duda and Koch, 2002; Newbold et al., 2002).

In their original study Perrault et al. (1996) demonstrated that there is a point mutation in the human ROS-GC1 gene, F^{565}S. Patients inheriting this mutation are inflicted with Leber's congetinal amauresis type 1 (LCA1); they are born blind or become blind soon after birth. Identity of the GCAP1 regulatory regions in bovine ROS-GC1 provided an opportunity to define this dystrophy in molecular terms (Lange et al., 1999). The human F^{565}S residue corresponds to the bovine F^{514}S residue. This residue is located in the mapped L^{503}-I^{522} ROS-GC1 binding region for GCAP1. Biochemical analysis on the heterologusly expressed LCA1-linked ROS-GC1 mutant in COS cells demonstrated that the point mutation causes almost complete loss (84%) of the basal

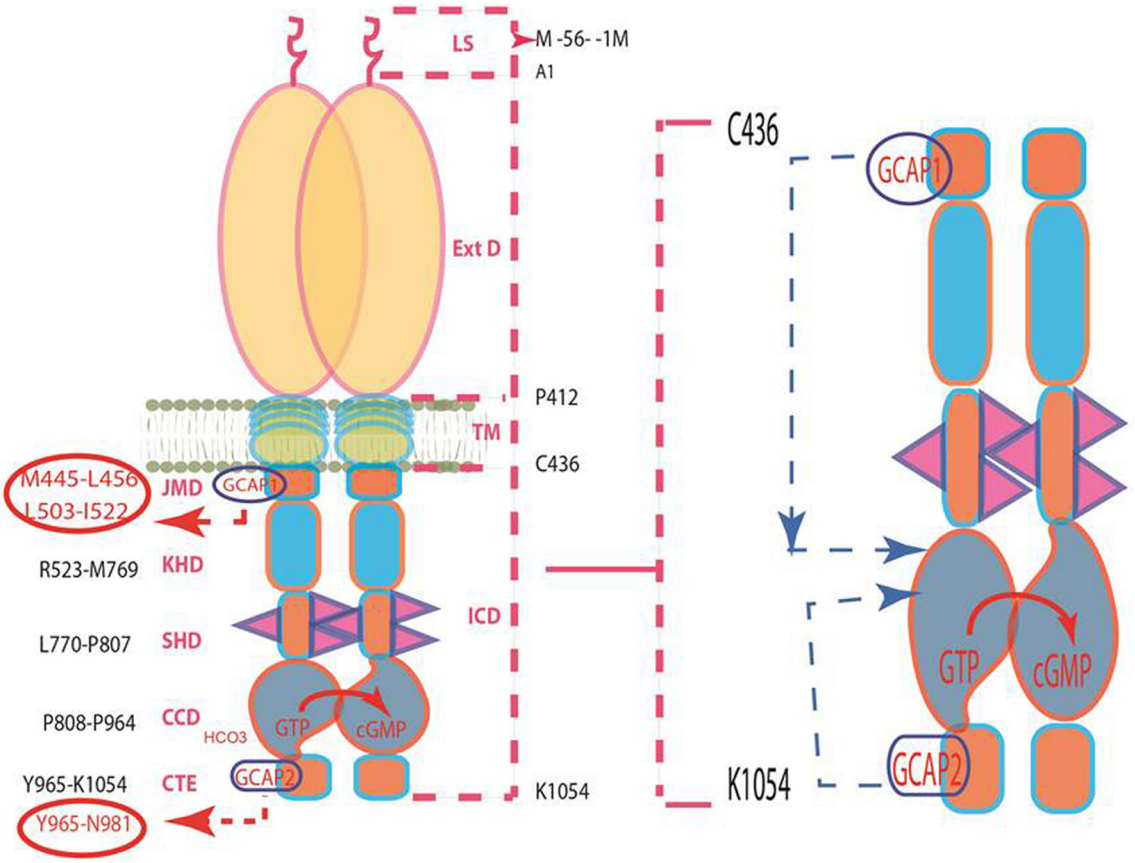

FIGURE 4 | Pathways of GCAPs signaling of ROS-GC1 activity. Left panel: Schematic representation of the structural topography of ROS-GC1. It is a single transmembrane homodimer protein. The dashed lines on the right show the defined boundaries of its segments: LS, leader sequence; ExtD, extracellular domain; TM, transmembrane domain; ICD, intracellular domain. All its functional domains are housed in ICD; their designated names and the amino acid residues constituting their boundaries are indicated at the left: JMD, juxtamembrane domain housing the indicated GCAP1-targeted domain; KHD, kinase homology domain; SHD-signaling helix domain; CCD-core catalytic domain; CTE-C-terminal extension housing the GCAP2-targeted domain. It is noteworthy, that the sites targeted by the two GCAPs (encircled) are at the opposite ends of CCD. **Right panel:** The two GCAP pathways run in opposite directions. The trajectory of the GCAP1 pathway shown in blue dashed arrow is downstream. From its origin in the JMD, it passes through the structural domains of KHD and SHD in its course to CCD. In contrast, the trajectory of the GCAP2 pathway (shown in pink dashed arrow) is upstream. From its origin in the CTE, it directly flows to CCD. The CCD exists as an antiparallel homodimer. Both GCAP signals are translated at the CCD into the production of cyclic GMP, which serves the second messenger of the LIGHT signals.

catalytic activity of ROS-GC1 and also of its Ca^{2+} sensitivity to modulation by GCAP1 (Duda et al., 1999b). Thus, the basic structural integrity of ROS-GC1 has been deranged by the mutation and this has also incapacitated GCAP1-modulated Ca^{2+} signaling mechanism of the guanylate cyclase.

Following this lead, similar approach has been used to investigate the second type of retinal disease that correlates with mutations of the ROS-GC1 gene. Named cone-rod dystrophy type 6 (CORD 6), patients suffering with this disease carry one or several point mutations in the dimerization domain of ROS-GC1 (Kelsell et al., 1998). One example is ROS-GC1-E^{786}D, R^{787}C, T^{788}M mutation. The mutation deranges the dimer formation of the guanylate cyclase and reduces the basal catalytic activity of the ROS-GC (Duda et al., 1999a, 2000; Tucker et al., 1999). This basic structural derangement in the guanylate cyclase, intriguingly, increases its sensitivity to GCAP1 and GCAP2. Physiological consequences are that there is a change in the trigger of the Ca^{2+}-feedback causing a shift in the response-intensity curve to lower light intensities. These effects explain the photophobia often reported by CORD 6 patients and the accumulating light damage of the retina leading to loss of cone and rod vision over a time period of decades.

CONTROLLED BY LOW AND HIGH LEVELS OF $[CA^{2+}]_I$, ROS-GC1 IS A BIMODAL TRANSDUCTION SWITCH

Discovered contemporaneously with GCAPs, CD-GCAP (Ca^{2+}-dependent guanylate cyclase activator) is the conformational isomer of S100B protein (Pozdnyakov et al., 1995, 1997; Margulis et al., 1996; Duda et al., 1996a, 2002; Wen et al., 2012). In contrast to the commercial S100B that is apparently Zn^{2+}-bound, CD-GCAP native to the retinal neurons is Zn^{2+}-free (Pozdnyakov et al., 1997).

S100B possesses a striking property toward ROS-GC1 stimulation that is opposite to that of GCAPs. This finding started a new paradigm of Ca^{2+} signaling to the cyclic GMP pathway. Recombinant ROS-GC1 expressed in a heterologous system of

COS cells responds at 10 nM $[Ca^{2+}]_i$ to GCAP1 stimulation in a dose dependent manner. Free Ca^{2+} inhibits this stimulation with a $K_{1/2}$ of 100 nM (Duda et al., 1996a). Zn^{2+}-free S100B, however, stimulates native and recombinant ROS-GC1 with a $[Ca^{2+}]$ $K_{1/2}$ of 400 nM. Presence and ability of the ROS-GC to couple to GCAPs and/or to S100B places a neuronal cell under stringent $[Ca^{2+}]_i$ modulation. The cell can accelerate or de-accelerate the generation of cyclic GMP; and in this manner can operate as a Ca^{2+} bimodal switch. In this hypothetical scheme, the bimodal Ca^{2+} ROS-GC transduction switch would be an elegant general mechanism for neural transmissions.

This hypothesis was put to test (Duda et al., 2002). Direct interaction between ROS-GC1 and S100B was demonstrated by cross-linking studies utilizing bis-(sulfosuccinimidyl)suberate. A cross-linked product between ROS-GC1 dimer and S100B occurred. Studies with ROS-GC1 deletion constructs confined an interaction of S100B with the C-terminus of ROS-GC1, aa731–1054. An EC_{50} of 395 nM, calculated using SPR spectroscopy, was comparable to the EC_{50} of 800 nM for stimulation of ROS-GC1 by S100B. Refined analysis revealed that aa952–991 segment of ROS-GC1 defines the S100B binding site with half maximal binding at 198 nM. The site contained a ^{966}RIHVNS^{972} motif that was obligatory for binding and a flanking cluster of four aa residues, ^{1039}RRQK^{1042} forming a transduction site. This transduction site did not contribute to S100B binding but promoted maximal activation of ROS-GC1.

These interactive physical parameters between S100B and ROS-GC1 were brought to the functional level in the synaptic layers of the retina where the co-presence of ROS-GC1, GCAP1 and S100B existed (Liu et al., 1994; Cooper et al., 1995; Duda et al., 2002). Below 200 nM, Ca^{2+} elicited a dose-dependent decrease in guanylate cyclase activity with an IC_{50} for Ca^{2+} of 100 nM. In contrast, at higher concentrations, ROS-GC activity began to climb with an EC_{50} of 0.8 μM. That GCAP1 is involved in the inhibitory phase of ROS-GC1 activity was confirmed by peptide competition experiments. A sequence motif L^{503}-I^{522} in ROS-GC1 is critical and specific for the cyclase activation by GCAP1 (Lange et al., 1999). The core motif within this domain consists of D^{507}-R^{518}.

Thus, in the synapse ROS-GC1 acts as a bimodal Ca^{2+} transduction switch. GCAP1 has the higher affinity for Ca^{2+} and upon binding, lowers ROS-GC1 activity. S100B captures the high Ca^{2+} signal and upon binding, stimulates ROS-GC1. This ROS-GC1 signal transduction model is schematically diagrammed in (Wen et al., 2012) (**Figure 4**: Sharma et al., 2014).

RECENT FINDINGS

ERG recordings on the retinas of the mouse $S100B^{-/-}$ model suggest that S100B up-regulates ROS-GC1 Ca^{2+}-dependent catalytic activity and modulates the transmission of neural signals to cone ON-bipolar cells (Wen et al., 2012).

CA^{2+}-MODULATED NEUROCALCIN δ ROS-GC1 TRANSDUCTION SYSTEM EXISTS IN THE INNER PLEXIFORM LAYER (IPL) OF THE RETINA

Besides S100B, a NCS family member, neurocalcin δ (NCδ), is present in bovine IPL (Krishnan et al., 2004; details reviewed in Sharma and Duda, 2012). Co-expressed with ROS-GC1 in the heterologous system of COS cells, NCδ stimulates ROS-GC1 in a Ca^{2+}-dependent manner with a $K_{1/2}$ of 0.8 μM. Its target site in the ROS-GC is V^{837}-L^{858} (Venkataraman et al., 2008). In accordance with their mutual physiological interaction, NCδ and ROS-GC1 are present together in IPL; added presence of $[Ca^{2+}]_i$ stimulates native IPL ROS-GC1 activity and nM range of Ca^{2+} keeps NCδ ROS-GC1 bound. The Ca^{2+}-dependent NCδ interactive ROS-GC1 kinetic parameters are: without Ca^{2+}, NCδ has no affinity for ROS-GC1; in the presence of Ca^{2+}, it binds ROS-GC1 with a K_A of 2.3×10^6 M^{-1} and a K_D of 4.6×10^{-7} M.

These analyses reveal that the steps of NCδ binding to and dissociation from ROS-GC1 are Ca^{2+}-dependent, they occur within the physiological levels of Ca^{2+}, they are direct and of moderate affinity; and they occur within the time span of the visual transduction steps. And significantly, the target site of NCδ for ROS-GC1 is unique to itself; it does not overlap with that of S100B or the GCAPs.

An extraordinary characteristic about the NCδ binding domain in ROS-GC is that it resides directly within the CCD (Venkataraman et al., 2008). This finding demonstrated that NCδ-modulated Ca^{2+} signaling of ROS-GC1 occurs through a new model, its principles are (1) NCδ directly interacts with CCD; (2) it does not require the adjacent N-terminally located α-helical dimerization domain structural element for its interaction; (3) the CCD module, housing the site, is intrinsically active, i.e., it has basal guanylate cyclase activity. (4) The CCD module by itself is dimeric; it does not require the dimerization domain structural element for being so; and (5) the core dimeric form of the catalytic module is directly regulated by the Ca^{2+}-bound NCδ; Ca^{2+}-unbound NCδ is ineffective (Venkataraman et al., 2008).

ROS-GC LINKAGE WITH OTHER THAN VISION-LINKED NEURONS

The very brief following sections are meant to demonstrate that the interlocked elements of the Ca^{2+} sensors and ROS-GC family are not unique to just the visual transduction processes they expand their signaling roles to many other sensory and sensory-linked transduction processes.

PINEAL GLAND

The bovine pineal gland embodies the Ca^{2+}-modulated GCAP1- and S100B-modulated ROS-GC1 transduction systems. They exist in two separate sets of pinealocytes. In one set, in the GCAP1 mode, the ROS-GC catalytic activity is modulated by free $[Ca^{2+}]_i$ $K_{1/2}$ of 100 nM. The second set is in the S100B mode, the ROS-GC activity is modulated by $[Ca^{2+}]_i$ with $K_{1/2}$ of about 0.5 μM. It has been proposed that these two processes may be involved in the dark and light states of the two types of pinealocytes (Venkataraman et al., 1998, 2000).

OLFACTION

Following the lead observation of Duda et al. (2001b) that GCAP1-modulated Ca^{2+}- signaling of ROS-GC1 transduction system is expressed in the rat olfactory bulb, its presence and a role in odorant transduction was investigated (Duda et al., 2001a). Prior to these studies role of the membrane guanylate

cyclase transduction system was denied in the odorant transduction and the system was exclusively believed to be "involved in behavioral responses induced by hormones or pheromones, possibly related to reproduction, rather than a response to specific odorants" (Juilfs et al., 1997; Meyer et al., 2000). Yet, these studies revealed the presence of selected components of the membrane guanylate cyclase in the ONE-GC (GC-D) neurons. These neurons were segregated from the dominant odorant linked cyclic AMP signaling neurons.

Odorant Transduction Model (Duda and Sharma, 2009, Figure 4)

A small population of the olfactory receptor neurons (ORN) contains a cyclic GMP signal transduction pathway (Juilfs et al., 1997; Leinders-Zufall et al., 2007; Duda and Sharma, 2008; Pertzev et al., 2010). This pathway resides at the apical region of the cilia. Present in this region is ONE-GC. Its outer domain is a receptor for uroguanylin (Duda and Sharma, 2008). In its inner domain, at the C-terminus, resides the catalytic domain (Duda and Sharma, 2008). The M^{880}-L^{921} segment of this domain is bound to Ca^{2+} sensor component NCδ. In the resting state, the ORN is in a 60–100 nM range of $[Ca^{2+}]_i$ and ONE-GC is in its basal state. The uroguanylin odorant signal starts by its interaction with the receptor domain of ONE-GC (Duda and Sharma, 2008). It is processed through two sequential steps. In step one, ONE-GC is primed and activated minimally. In step 2, $[Ca^{2+}]_i$ rises. With a $K_{1/2}$ of 0.3–0.8 μM, Ca^{2+} binds NCδ facilitating its interaction with the ONE-GC's segment M^{880}-L^{921} (Duda and Sharma, 2008; Duda et al., 2004); Ca^{2+}-bound NCδ than signals full activation of ONE-GC and maximal synthesis of cyclic GMP (reviewed in Sharma and Duda, 2010a,b; Zufall and Munger, 2010).

It is envisioned that the operation of step 2 starts with the generation of a small amount of cyclic GMP in step 1. This pool of cyclic GMP opens a limited number of the cyclic GMP-gated channels causing influx of Ca^{2+} in the ORN. Ca^{2+} binds NCδ, which then fully activates ONE-GC.

SPECIAL NOTE

There are clues that, besides NCδ, two additional Ca^{2+} sensors of ONE-GC are involved in the odorant transduction. One is hippocalcin (Hpca) (Krishnan et al., 2009) and the other is GCAP1 (Pertzev et al., 2010). The studies with the $Hpca^{-/-}$ mouse model and with the GCAP1-specific antibodies demonstrate that both Ca^{2+} sensors are physically linked with ONE-GC and are present in the rat and the mouse olfactory neuroepithelium region. In addition, 35% of the total ONE-GC transduction activity is controlled by GCAP1, 27% by NCδ, and 38% by Hpca (reviewed in: Sharma and Duda, 2010a).

GUSTATION

Similar to olfaction, gustation (taste) belongs to chemical senses. In response to the sweet, sour, salty, bitter, and umami, taste receptor cells generate electric signal in a process called gustatory transduction (Avenet and Lindemann, 1989; Gilbertson et al., 2000, 2001; Herness, 2000; Lindemann, 1996). The molecular steps in this transduction process are ill defined. Yet in a general scheme Ca^{2+} is pivotal for the process; it depolarizes plasma membrane of the given taste cell, releases the transmitter release and functions through the CNG-gated channels, cyclic AMP and cyclic GMP (Kolesnikov and Margolskee, 1995).

The expression of a Ca^{2+} signaling ROS-GC1 transduction system in the anterior portion of the bovine gustatory epithelium has been demonstrated at the biochemical, molecular and functional levels (Duda and Sharma, 2004). The system is composed of two components: the Ca^{2+}-sensor protein, S100B and the transducer, ROS-GC1. Co-immunoprecipitation experiments reveal that ROS-GC1 and S100B physically interact with each other. The precise operational mechanism of this signal transduction mechanism and its physiology has yet not been decoded (reviewed in Sharma and Duda, 2010b).

EVOLUTION OF A GENERAL CA^{2+}-INTERLOCKED ROS-GC SIGNAL TRANSDUCTION CONCEPT IN SENSORY AND SENSORY-LINKED NEURONS

Extraordinary feature of the ROS-GC signal transduction system is that it is an extremely delicate Ca^{2+}-modulated machinery. It is crafted impressively to do so. In a range of nM, $[Ca^{2+}]_i$ signals produce the ROS-GC activity to its peak level and then they decline it with a $[Ca^{2+}]_i$ $K_{1/2}$ of 100 nM. In a bimodal fashion, the signals then accelerate it with a Ca^{2+} $K_{1/2}$ of 500 nM to 800 nM. The ROS-GC accomplishes the former mode through its Ca^{2+} sensor partners, GCAPs and the latter function through its CD-GCAP partners. This mechanism of bimodal regulation enables ROS-GC to generate the Ca^{2+}-dependent pulsated levels of cyclic GMP, which functions as a second messenger of the sensory and sensory-linked Ca^{2+} transduction mechanisms. Presented illustrations are: (1) LIGHT signal induced GCAP-modulated ROS-GC transduction mode in the photoreceptor cells; (2) bimodal GCAP1 and S100B modes in the photoreceptor-cone synapse; (3) the odorant signal–GCAP1, S100B and Hpca–regulated modes in ONE-GC neurons and (4) not yet well-understood processes of the pineal gland and gustation. Bestowed with this design and clues of its linkage with physiology of the various sensory neurons, these investigators have proposed that "Ca^{2+}-modulated ROS-GC" machinery is a central signal transduction component of all the sensory and/or sensory-linked secondary neurons. Accompanied by a nearby CNG channel, the machinery is empowered to de-or hyper-polarize neurons, thereby affecting the generation of action potentials (model in Figure 4 of Sharma, 2010). It becomes an elegant theoretical general mechanism for neural transmissions.

CONCLUSION AND FUTURE DIRECTIONS

This review has briefly chronicled the events that have resulted in the step-by-step development of the field of membrane guanylate cyclase. Its foundation rests on the initial seminal finding made five decades ago (1963) that cyclic GMP exists in rat urine. Based on the conceptual framework of the cyclic AMP second messenger, it implied the existence of a hormonally-dependent membrane guanylate cyclase transduction system that generates cyclic GMP in the mammalian cells. For about a decade, this concept underwent a tortuous evolution; first, the euphoria and then a chaos. Barring ours, and few others, most of the fashionable groups denied existence of this transduction system. The field rekindled with the first purification and characterization of

a membrane guanylate cyclase, ANF-RGC. Surprisingly, besides being a guanylate cyclase, it was also a hormone receptor. And, the field of membrane guanylate cyclase was born. Yet, the notion evolved that the membrane guanylate cyclase family is solely represented by its hormone-receptors. The field expanded and changed with the discovery of a Ca^{2+}-modulated ROS-GC transduction system. Yet it remained restrictive, believed to be linked with the single physiological function of phototransduction in the photoreceptor cells. This belief also changed with the discovery that besides GCAPs, which are selectively linked with phototransduction, other Ca^{2+} sensors coupled with ROS-GC exist beyond the photoreceptor cells. Consistent with its broader role, Ca^{2+}-sensor S100B modulated ROS-GC transduction system is linked with the photoreceptor-bipolar neural transmissions. In addition, the system is also present in the pinealocytes and a ROS-GC-variant (ONE-GC) transduction system is expressed in the rodent olfactory systems.

Exponential expansion of the field has generated new problems which have to be solved. Some of them are briefly outlined below.

The first at hand deals with the modes of guanylate cyclases modulation. Have all the modulators of each cyclase been discovered? Recent studies suggest that it may not be the case as exemplified by ONE-GC. For over a decade this cyclase was considered by some groups an orphan receptor (Fulle et al., 1995; Juilfs et al., 1997) but it is now known that it is the receptor for odorant uroguanylin/guanylin (Leinders-Zufall et al., 2007; Duda and Sharma, 2008; Zufall and Munger, 2010). In this new paradigm, the extracellularly-generated odorant signal needs to be further processed in the intracellular domain of the cyclase in a Ca^{2+}-dependent manner (Duda and Sharma, 2009). Thus, ONE-GC becomes the first cross-over functional guanylate cyclase, being modulated by both odorant peptide receptor domain and the Ca^{2+}-modulated domain. How many other guanylate cyclases possess this feature and what is the molecular mechanism underlying the process of dual regulation?

Second, a new model of ANF-RGC signal transduction has evolved (Duda et al., 2012). ANF-RGC is the bimodal switch; one switch is the traditional ANF hormone and the other, $[Ca^{2+}]_i$. $[Ca^{2+}]_i$ signal targets directly the CCD of ANF-RGC and increases the production of cyclic GMP. What is its mechanism of operation? Are other hormone receptor guanylate cyclases also bimodal switches?

Third, the ANF-RGC receptor subfamily is multifunctional. Besides controlling the well-known processes linked with cardiac vasculature—diuresis, fluid secretion, smooth muscle relaxation, it also influences the processes involved in metabolic syndrome and obesity control (Martel et al., 2010). Similarly, CNP-RGC triggered by its hormonal CNP signal affects such diverse processes as bone growth (Bartels et al., 2004) and axonal sprouting in neurons (Schmidt et al., 2007, 2009). How does it achieve this characteristic?

Transcending to the ROS-GC subfamily, it is also multifunctional; linked with the physiology of visual transduction in the retina, photoentrainment in the pineal gland, as well as odorant- and gustatory transduction. Except for phototransduction, the underlying molecular principles of its linkage with the other sensory processes are lacking.

Fourth, a new model of ROS-GC1 signaling specific to cone photoreceptors has emerged. Its key molecule is the S100B protein. Molecular principles of this model need to be deciphered.

Fifth, ill-defined information suggests that GC-G is linked with the processes of capacitation (Kuhn et al., 2004), atmospheric CO_2 detection (Chao et al., 2010) and is also modulated by cool ambient temperature (Mamasuew et al., 2008). The molecular explanations for these processes are not available.

Sixth, a common trait of the membrane guanylate cyclase family is that it is a multi-modular protein. Experimentally validated evidence indicates that each of its modular domains is precisely crafted to control the cyclase's functional specificity (Sharma and Duda, 1997). Complete function of each domain is lacking, however. Consequently, none of the intact membrane guanylate cyclase structures have been solved by X-ray crystallography.

Seventh, and final, the basic knowledge gained by the preceding studies will be invaluable in defining the physiology of each of the guanylate cyclases, linking them with respective pathological states, and in the long run, in designing targeted therapies against these pathologies.

ACKNOWLEDGMENTS

RKS gratefully acknowledges the continuous support for the past 35 years by the numerous USPHS awards from the National Institutes of Health, the beginning awards from the National Science Foundation and the Damon Runyon Walter Winchell Cancer Fund. TD acknowledges National Heart, Blood and Lung Institute grant HL084584. The authors are thankful to Ms Sanya Sharma for editorial assistance.

REFERENCES

Ahrens, H., Paul, A. K., Kuroda, Y., and Sharma, R. K. (1982). Adrenocortical cyclic GMP-dependent protein kinase: purification, characterization, and modification of its activity by calmodulin, and its relationship with steroidogenesis. *Arch. Biochem. Biophys.* 215, 597–609. doi: 10.1016/0003-9861(82)90121-7

Allerston, C. K., von Delf, T. F., and Gileadi, O. (2013). Crystal structures of the catalytic domain of human soluble guanylate cyclase. *PLoS ONE* 8:e57644. doi: 10.1371/journal.pone.0057644

Ames, J. B., Dizhoor, A. M., Ikura, M., Palczewski, K., and Stryer, L. (1999). Three-dimensional structure of guanylyl cyclase activating protein-2, a calcium-sensitive modulator of photoreceptor guanylyl cyclases. *J. Biol. Chem.* 274, 19329–19337. doi: 10.1074/jbc.274.27.19329

Anglard, P., Zwiller, J., Vincendon, G., and Louis, J. C. (1985). Regulation of cyclic AMP and cyclic GMP levels by adrenocorticotropic hormone in cultured neurons. *Biochem. Biophys. Res. Commun.* 133, 286–292. doi: 10.1016/0006-291X(85)91873-X

Ariëns, E. J., and Simonis, A. M. (1966). Aspects of molecular pharmacology. II. Theories of receptors and structure-action relationship. *Farmaco. Sci.* 21, 581–608.

Ashman, D. F., Lipton, R., Melicow, M. M., and Price, T. D. (1963). Isolation of adenosine 3′, 5′-monophosphate and guanosine 3′, 5′-monophosphate from rat urine. *Biochem. Biophys. Res. Commun.* 11, 330–334. doi: 10.1016/0006-291X(63)90566-7

Avenet, P., and Lindemann, B. (1989). Perspectives of taste reception. *J. Membr. Biol.* 112, 1–8. doi: 10.1007/BF01871158

Bartels, C. F., Bükülmez, H., Padayatti, P., Rhee, D. K., van Ravenswaaij-Arts, C., Pauli, R. M., et al. (2004). Mutations in the transmembrane natriuretic peptide receptor NPR-B impair skeletal growth and cause acromesomelic dysplasia, type Maroteaux. *Am. J. Hum. Genet.* 75, 27–34. doi: 10.1086/422013

Berridge, M. J., and Irvine, R. F. (1989). Inositol phosphates and cell signalling. *Nature* 341, 197–205. doi: 10.1038/341197a0

Birnbaumer, L., and Birnbaumer, M. (1995). Signal transduction by G proteins: 1994 edition. *J. Recept. Signal Transduct. Res.* 15, 213–252. doi: 10.3109/10799899509045218

Burns, M. E., and Baylor, D. A. (2001). Activation, deactivation, and adaptation in vertebrate photoreceptor cells. *Annu. Rev. Neurosci.* 24, 779–805. doi: 10.1146/annurev.neuro.24.1.779

Chang, C. H., Kohse, K. P., Chang, B., Hirata, M., Jiang, B., Douglas, J. E., et al. (1990). Characterization of ATP-stimulated guanylate cyclase activation in rat lung membranes. *Biochim. Biophys. Acta* 1052, 159–165. doi: 10.1016/0167-4889(90)90071-K

Chang, M. S., Lowe, D. G., Lewis, M., Hellmis, R., Chen, E., and Goeddel, D. V. (1989). Differential activation by atrial and brain natriuretic peptides of two different receptor guanylate cyclases. *Nature* 341, 68–72. doi: 10.1038/341068a0

Chao, Y.-C., Cheng, C.-J., Hsieh, H.-T., Lin, C.-C., Chen, C.-C., and Yang, R.-B. (2010). Guanylate cyclase-G, expressed in the Grueneberg ganglion olfactory subsystem, is activated by bicarbonate. *Biochem. J.* 432, 267–273. doi: 10.1042/BJ20100617

Chinkers, M., and Garbers, D. L. (1989). The protein kinase domain of the ANP receptor is required for signaling. *Science* 245, 1392–1394. doi: 10.1126/science.2571188

Chinkers, M., Garbers, D. L., Chang, M. S., Lowe, D. G., Chin, H. M., Goeddel, D. V., et al. (1989). A membrane form of guanylate cyclase is an atrial natriuretic peptide receptor. *Nature* 338, 78–83. doi: 10.1038/338078a0

Chinkers, M., Singh, S., and Garbers, D. L. (1991). Adenine nucleotides are required for activation of rat atrial natriuretic peptide receptor/guanylyl cyclase expressed in a baculovirus system. *J. Biol. Chem.* 266, 4088–4093.

Clark, A. (1937). "The cell as a physico-chemical system," in *General Pharmacology*, ed A. Heffter. Handbuch der Experimentellen Pharmakologie series, eds W. Heubner and J. Schuller (Berlin: Springer), 10–17.

Cooper, N., Liu, L., Yoshida, A., Pozdnyakov, N., Margulis, A., and Sitaramayya, A. (1995). The bovine rod outer segment guanylate cyclase, ROS-GC, is present in both outer segment and synaptic layers of the retina. *J. Mol. Neurosci.* 6, 211–222. doi: 10.1007/BF02736766

de Sauvage, F. J., Camerato, T. R., and Goeddel, D. V. (1991). Primary structure and functional expression of the human receptor for *Escherichia coli* heat-stable enterotoxin. *J. Biol. Chem.* 266, 17912–17918.

Dizhoor, A. M., and Hurley, J. B. (1996). Inactivation of EF-hands makes GCAP-2 (p24) a constitutive activator of photoreceptor guanylyl cyclase by preventing a Ca2+-induced "activator-to-inhibitor" transition. *J. Biol. Chem.* 271, 19346–19350. doi: 10.1074/jbc.271.32.19346

Dizhoor, A. M., Olshevskaya, E. V., Henzel, W. J., Wong, S. C., Stults, J. T., Ankoudinova, I., et al. (1995). Cloning, sequencing, and expression of a 24-kDa Ca2+-binding protein activating photoreceptor guanylyl cyclase. *J. Biol. Chem.* 270, 25200–22520. doi: 10.1074/jbc.270.42.25200

Dizhoor, A. M., Ray, S., Kumar, S., Niemi, G., Spencer, M., Brolley, D., et al. (1991). Recoverin: a calcium sensitive activator of retinal rod guanylate cyclase. *Science* 251, 915–918. doi: 10.1126/science.1672047

Duda, T., Bharill, S., Wojtas, I., Yadav, P., Gryczynski, I., Gryczynski, Z., et al. (2009). Atrial natriuretic factor receptor guanylate cyclase signaling: new ATP-regulated transduction motif. *Mol. Cell. Biochem.* 324, 39–53. doi: 10.1007/s11010-008-9983-2

Duda, T., Fik-Rymarkiewicz, E., Venkataraman, V., Krishnan, R., Koch, K.-W., and Sharma R.K. (2005a). The calcium-sensor guanylate cyclase activating protein type 2 specific site in rod outer segment membrane guanylate cyclase type 1. *Biochemistry* 44, 7336–7345. doi: 10.1021/bi050068x

Duda, T., Fik-Rymarkiewicz, E., Venkataraman, V., Krishnan, A., and Sharma, R. K. (2004). Calcium-modulated ciliary membrane guanylate cyclase transduction machinery: constitution and operational principles. *Mol. Cell. Biochem.* 267, 107–122. doi: 10.1023/B:MCBI.0000049372.33965.4f

Duda, T., Goraczniak, R. M., and Sharma, R. K. (1991). Site-directed mutational analysis of a membrane guanylate cyclase cDNA reveals the atrial natriuretic factor signaling site. *Proc. Natl. Acad. Sci. U.S.A.* 88, 7882–7886. doi: 10.1073/pnas.88.17.7882

Duda, T., Goraczniak, R. M., and Sharma, R. K. (1994). Glutamic acid-332 residue of the type C natriuretic peptide receptor guanylate cyclase is important for signaling. *Biochemistry* 33, 7430–3743. doi: 10.1021/bi00189a050

Duda, T., Goraczniak, R. M., and Sharma, R. K. (1996a). Molecular characterization of S100A1-S100B protein in retina and its activation mechanism of bovine photoreceptor guanylate cyclase. *Biochemistry* 35, 6263–6266. doi: 10.1021/bi960007m

Duda, T., Goraczniak, R. M., Sitaramayya, A., and Sharma, R. K. (1993). Cloning and expression of an ATP-regulated human retina C-type natriuretic factor receptor guanylate cyclase. *Biochemistry* 32, 1391–1395. doi: 10.1021/bi00057a001

Duda, T., Goraczniak, R., Surgucheva, I., Rudnicka-Nawrot, M., Gorczyca, W. A., Palczewski, K., et al. (1996b). Calcium modulation of bovine photoreceptor guanylate cyclase. *Biochemistry* 35, 8478–8482. doi: 10.1021/bi960752z

Duda, T., Jankowska, A., Venkataraman, V., Nagele, R. G., and Sharma, R. K. (2001a). A novel calcium-regulated membrane guanylate cyclase transduction system in the olfactory neuroepithelium. *Biochemistry* 40, 12067–12077. doi: 10.1021/bi0108406

Duda, T., and Koch, K.-W. (2002). Retinal diseases linked with photoreceptor guanylate cyclase. *Mol. Cell. Biochem.* 230, 129–138. doi: 10.1023/A:1014296124514

Duda, T., Koch, K.-W., Venkataraman, V., Lange, C., Beyermann, M., and Sharma, R. K. (2002). Ca2+ sensor S100beta-modulated sites of membrane guanylate cyclase in the photoreceptor-bipolar synapse. *EMBO J.* 21, 2547–2556. doi: 10.1093/emboj/21.11.2547

Duda, T., Krishnan, A., Venkataraman, V., Lange, C., Koch, K.-W., and Sharma, R. K. (1999a). Mutations in the rod outer segment membrane guanylate cyclase in a cone-rod dystrophy cause defects in calcium signaling. *Biochemistry* 38, 13912–13919. doi: 10.1021/bi9915972

Duda, T., Pertzev, A., and Sharma, R. K. (2012). Differential Ca2+ sensor guanylate cyclase activating protein modes of photoreceptor rod outer segment membrane guanylate cyclase signaling. *Biochemistry* 51, 4650–4657. doi: 10.1021/bi300572w

Duda, T., Pertzev, A., and Sharma, R. K. (2013). The ANF-RGC gene motif 669WTAPELL675 is vital for blood pressure regulation: biochemical mechanism. *Biochemistry* 52, 2337–2334. doi: 10.1021/bi400175d

Duda, T., Pertzev, A., and Sharma, R. K. (2014). Atrial natriuretic factor receptor guanylate cyclase, ANF-RGC, transduces two independent signals, ANF and Ca2+. *Front. Mol. Neurosci.* 7:17. doi: 10.3389/fnmol.2014.00017

Duda, T., and Sharma, R. K. (2004). S100B-modulated Ca2+-dependent ROS-GC1 transduction machinery in the gustatory epithelium: a new mechanism in gustatory transduction. *FEBS Lett.* 577, 393–398. doi: 10.1016/j.febslet.2004.09.089

Duda, T., and Sharma, R. K. (2005). Two membrane juxtaposed signaling modules in ANF-RGC are interlocked. *Biochem. Biophys. Res. Commun.* 332, 149–156. doi: 10.1016/j.bbrc.2005.04.102

Duda, T., and Sharma, R. K. (2008). ONE-GC membrane guanylate cyclase, a trimodal odorant signal transducer. *Biochem. Biophys. Res. Commun.* 367, 440–444. doi: 10.1016/j.bbrc.2007.12.153

Duda, T., and Sharma, R. K. (2009). Ca2+-modulated ONE-GC odorant signal transduction. *FEBS Lett.* 583, 1327–1330. doi: 10.1016/j.febslet.2009.03.036

Duda, T., Venkataraman, V., Goraczniak, R., Lange, C., Koch, K.-W., and Sharma, R. K. (1999b). Functional consequences of a rod outer segment membrane guanylate cyclase (ROS-GC1) gene mutation linked with Leber's congenital amaurosis. *Biochemistry* 38, 509–515. doi: 10.1021/bi9824137

Duda, T., Venkataraman, V., Jankowska, A., Lange, C., Koch, K.-W., and Sharma, R. K. (2000). Impairment of the rod outer segment membrane guanylate cyclase dimerization in a cone-rod dystrophy results in defective calcium signaling. *Biochemistry* 39, 12522–12533. doi: 10.1021/bi001514d

Duda, T., Venkataraman, V., Krishnan, A., Nagele, R. G., and Sharma, R. K. (2001b). Negatively calcium-modulated membrane guanylate cyclase signaling system in the rat olfactory bulb. *Biochemistry* 40, 4654–4662. doi: 10.1021/bi0027985

Duda, T., Venkataraman, V., Krishnan, A., and Sharma, R. K. (1998). Rod outer segment membrane guanylate cyclase type 1 (ROS-GC1) gene: structure, organization and regulation by phorbol ester, a protein kinase C activator. *Mol. Cell. Biochem.* 189, 63–70. doi: 10.1023/A:1006944629935

Duda, T., Venkataraman, V., Ravichandran, S., and Sharma, R. K. (2005b). ATP-regulated module (ARM) of the atrial natriuretic factor receptor guanylate cyclase. *Peptides* 26, 969–984. doi: 10.1016/j.peptides.2004.08.032

Duda, T., Yadav, P., Jankowska, A., Venkataraman, V., and Sharma, R. K. (2001c). Three dimensional atomic model and experimental validation for the ATP-Regulated Module (ARM) of the atrial natriuretic factor receptor guanylate cyclase. *Mol. Cell. Biochem.* 217, 165–172. doi: 10.1023/A:1007236917061

Frins, S., Bönigk, W., Müller, F., Kellner, R., and Koch, K.-W. (1996). Functional characterization of a guanylyl cyclase-activating protein from vertebrate rods. Cloning, heterologous expression, and localization. *J. Biol. Chem*. 271, 8022–8027. doi: 10.1074/jbc.271.14.8022

Fulle, H. J., Vassar, R., Foster, D. C., Yang, R. B., Axel, R., and Garbers, D. L. (1995). A receptor guanylyl cyclase expressed specifically in olfactory sensory neurons. *Proc. Natl. Acad. Sci. U.S.A*. 92, 3571–3575. doi: 10.1073/pnas.92.8.3571

Gilbertson, T. A., Boughter, J. D. Jr, Zhang, H., and Smith, D. V. (2001). Distribution of gustatory sensitivities in rat taste cells: whole-cell responses to apical chemical stimulation. *J. Neurosci.* 21, 4931–4941.

Gilbertson, T. A., Damak, S., and Margolskee, R. F. (2000). The molecular physiology of taste transduction. *Curr. Opin. Neurobiol*. 10, 519–527. doi: 10.1016/S0959-4388(00)00118-5

Gill, G. N., and McCune, R. W. (1979). Guanosine 3′,5′-monophosphate-dependent protein kinase. *Curr. Top. Cell. Regul*. 15, 1–45.

Goldberg, N. D., Dietz, S. B., and O'Toole, A. G. (1969). Cyclic guanosine 3′,5′-monophosphate in mammalian tissues and urine. *J. Biol. Chem*. 244, 4458–4466.

Goldberg, N. D., and Haddox, M. K. (1977). Cyclic GMP metabolism and involvement in biological regulation. *Annu. Rev. Biochem*. 46, 823–896. doi: 10.1146/annurev.bi.46.070177.004135

Goldberg, N. D., Haddox, M. K., Nicol, S. E., Glass, D. B., Sanford, C. H., Kuehl, F. A. Jr., et al. (1975). Biologic regulation through opposing influences of cyclic GMP and cyclic AMP: the Yin Yang hypothesis. *Adv. Cyclic Nucleotide Res*. 5, 307–330.

Goldberg, N. D., O'Dea, R. F., and Haddox, M. K. (1973). Cyclic GMP. *Adv. Cyclic Nucleotide Res*. 3,155–223.

Goraczniak, R. M., Duda, T., and Sharma, R. K. (1992). A structural motif that defines the ATP-regulatory module of guanylate cyclase in atrial natriuretic factor signalling. *Biochem. J*. 282, 533–537.

Goraczniak, R. M., Duda, T., Sitaramayya, A., and Sharma, R. K. (1994). Structural and functional characterization of the rod outer segment membrane guanylate cyclase. *Biochem. J*. 302, 455–461.

Gorczyca, W. A., Gray-Keller, M. P., Detwiler, P. B., and Palczewski, K. (1994). Purification and physiological evaluation of a guanylate cyclase activating protein from retinal rods. *Proc. Natl. Acad. Sci. U.S.A*. 91, 4014–4018. doi: 10.1073/pnas.91.9.4014

Hamet, P., Tremblay, J., Pang, S. C., Garcia, R., Thibault, G., Gutkowska, J., et al. (1984). Effect of native and synthetic atrial natriuretic factor on cyclic GMP. *Biochem. Biophys. Res. Commun*. 123, 515–527. doi: 10.1016/0006-291X(84)90260-2

Hayashi, F., and Yamazaki, A. (1991). polymorphism in purified guanylate cyclase from vertebrate rod photoreceptors. *Proc. Natl. Acad. Sci. U.S.A*. 88, 4746–4750. doi: 10.1073/pnas.88.11.4746

He, X. L., Chow, D. C., Martick, M. M., and Garcia, K. C. (2001). Allosteric activation of a spring-loaded natriuretic peptide receptor dimer by hormone. *Science* 293, 1657–1662. doi: 10.1126/science.1062246

Helten, A., Säftel, W., and Koch, K. W. (2007). Expression level and activity profile of membrane bound guanylate cyclase type 2 in rod outer segments. *J. Neurochem*. 103, 1439–1446. doi: 10.1111/j.1471-4159.2007.04923.x

Helten, A., and Koch, K. W. (2007). Calcium-dependent conformational changes in guanylate cyclase-activating protein 2 monitored by cysteine accessibility. *Biochem. Biophys. Res. Commun*. 356, 687–692. doi: 10.1016/j.bbrc.2007.03.023

Hepler, J. R., and Gilman, A. G. (1992). G proteins. *Trends Biochem. Sci*. 17, 383–387. doi: 10.1016/0968-0004(92)90005-T

Herness, S. (2000). Coding in taste receptor cells. The early years of intracellular recordings. *Physiol. Behav*. 69, 17–27. doi: 10.1016/S0031-9384(00)00186-4

Horio, Y., and Murad, F. (1991a). Solubilization of guanylyl cyclase from bovine rod outer segments and effects of lowering Ca2+ and nitro compounds. *J. Biol. Chem*. 266, 3411–3415.

Horio, Y., and Murad, F. (1991b). Purification of guanylyl cyclase from rod outer segments. *Biochim. Biophys. Acta* 1133, 81–88. doi: 10.1016/0167-4889(91)90244-R

Howes, K. A., Pennesi, M. E., Sokal, I., Church-Kopish, J., Schmidt, B., Margolis, D., et al. (2002). GCAP1 rescues rod photoreceptor response in GCAP1/GCAP2 knockout mice. *EMBO J*. 21, 1545–1554. doi: 10.1093/emboj/21.7.1545

Hunt, D. M., Buch, P., and Michaelides, M. (2010). Guanylate cyclases and associated activator proteins in retinal disease. *Mol. Cell. Biochem*. 334, 157–168. doi: 10.1007/s11010-009-0331-y

Hurley, J. B., Dizhoor, A. M., Ray, S., and Stryer, L. (1993). Recoverin's role: conclusion withdrawn. *Science* 260:740. doi: 10.1126/science.8097896

Hwang, J. Y., Lange, C., Helten, A., Höppner-Heitmann, D., Duda, T., Sharma, R. K., et al. (2003). Regulatory modes of rod outer segment membrane guanylate cyclase differ in catalytic efficiency and Ca2+-sensitivity. *Eur. J. Biochem*. 270, 3814–3821. doi: 10.1046/j.1432-1033.2003.03770.x

Hwang, J. Y., Schlesinger, R., and Koch, K-W. (2004). Irregular dimerization of guanylate cyclase-activating protein 1 mutants causes loss of target activation. *Eur. J. Biochem*. 271, 3785–3793. doi: 10.1111/j.1432-1033.2004.04320.x

Ishikawa, E., Ishikawa, S., Davis, J. W., and Sutherland, E. W. (1969). Determination of guanosine 3′,5′-monophosphate in tissues and of guanyl cyclase in rat intestine. *J. Biol. Chem*. 244, 6371–6376.

Juilfs, D. M., Fülle, H. J., Zhao, A. Z., Houslay, M. D., Garbers, D. L., and Beavo, J. A. (1997). A subset of olfactory neurons that selectively express cGMP-stimulated phosphodiesterase (PDE2) and guanylyl cyclase-D define a unique olfactory signal transduction pathway. *Proc. Natl. Acad. Sci. U.S.A*. 94, 3388–3395. doi: 10.1073/pnas.94.7.3388

Karan, S., Frederick, J. M., and Baehr, W. (2010). Novel functions of photoreceptor guanylate cyclases revealed by targeted deletion. *Mol. Cell. Biochem*. 334, 141–155. doi: 10.1007/s11010-009-0322-z

Kelsell, R. E., Gregory-Evans, K., Payne, A. M., Perrault, I., Kaplan, J., Yang, R. B., et al. (1998). Mutations in the retinal guanylate cyclase (RETGC-1) gene in dominant cone-rod dystrophy. *Hum. Mol. Genet*. 7, 1179–1184. doi: 10.1093/hmg/7.7.1179

Kitabchi, A. E., and Sharma, R. K. (1971). Corticosteroidogenesis in isolated adrenal cells of rats. I. Effect of corticotropins and 3′,5′-cyclic nucleotides on corticosterone production. *Endocrinology* 88, 1109–1116. doi: 10.1210/endo-88-5-1109

Koch, K.-W. (1991). Purification and identification of photoreceptor guanylate cyclase. *J. Biol. Chem*. 266, 8634–8637.

Koch, K.-W. (2006). GCAPs, the classical neuronal calcium sensors in the retina – a Ca2+-relay model of guanylate cyclase activation. *Calcium Binding Proteins* 1, 3–6.

Koch, K.-W., Duda, T., and Sharma, R. K. (2002). Photoreceptor specific guanylate cyclases in vertebrate phototransduction. *Mol. Cell. Biochem*. 230, 97–106. doi: 10.1023/A:1014209711793

Koch, K.-W., Duda, T., and Sharma, R. K. (2010). Ca2+-modulated vision-linked ROS-GC guanylate cyclase transduction machinery. *Mol. Cell. Biochem*. 334, 105–115. doi: 10.1007/s11010-009-0330-z

Koch, K.-W., and Stryer, L. (1988). Highly cooperative feedback control of retinal rod guanylate cyclase by calcium ions. *Nature* 334, 64–66. doi: 10.1038/334064a0

Kolesnikov, S. S., and Margolskee, R. F. (1995). A cyclic-nucleotide-suppressible conductance activated by transducin in taste cells. *Nature* 376, 85–88. doi: 10.1038/376085a0

Koutalos, Y., Nakatani, K., Tamura, T., and Yau, K. W. (1995). Characterization of guanylate cyclase activity in single retinal rod outer segments. *J. Gen. Physiol*. 106, 863–890. doi: 10.1085/jgp.106.5.863

Krishnan, A., Duda, T., Pertzev, A., Kobayashi, M., Takamatsu, K., and Sharma, R. K. (2009). Hippocalcin, new Ca2± sensor of a ROS-GC subfamily member, ONE-GC, membrane guanylate cyclase transduction system. *Mol. Cell. Biochem*. 325, 1–14. doi: 10.1007/s11010-008-0015-z

Krishnan, A., Goraczniak, R. M., Duda, T., and Sharma, R. K. (1998). Third calcium-modulated rod outer segment membrane guanylate cyclase transduction mechanism. *Mol. Cell. Biochem*. 178, 251–259. doi: 10.1023/A:1006860018300

Krishnan, A., Venkataraman, V., Fik-Rymarkiewicz, E., Duda, T., and Sharma, R. K. (2004). Structural, biochemical, and functional characterization of the calcium sensor neurocalcin delta in the inner retinal neurons and its linkage with the rod outer segment membrane guanylate cyclase transduction system. *Biochemistry* 43, 2708–2723. doi: 10.1021/bi035631v

Kuhn, M., Ng, C. K., Su, Y. H., Kilić, A., Mitko, D., Bien-Ly, N., et al. (2004). Identification of an orphan guanylate cyclase receptor selectively expressed in mouse testis. *Biochem. J*. 379, 385–393. doi: 10.1042/BJ20031624

Kuno, T., Andresen, J. W., Kamisaki, Y., Waldman, S. A., Chang, L. Y., Saheki, S., et al. (1986). Co-purification of an atrial natriuretic factor receptor and particulate guanylate cyclase from rat lung. *J. Biol. Chem*. 261, 5817–5823.

Kurose, H., Inagami, T., and Ui, M. (1987). Participation of adenosine 5′-triphosphate in the activation of membrane-bound guanylate cyclase by

the atrial natriuretic factor. *FEBS Lett*. 219, 375–379. doi: 10.1016/0014-5793(87)80256-9

Lamb, T. D., Matthews, H. R., and Torre, V. (1986). Incorporation of calcium buffers into salamander retinal rods: a rejection of the calcium hypothesis of phototransduction. *J. Physiol*. 372, 315–349.

Lange, C., Duda, T., Beyermann, M., Sharma, R. K., and Koch, K.-W. (1999). Regions in vertebrate photoreceptor guanylyl cyclase ROS-GC1 involved in Ca2+-dependent regulation by guanylyl cyclase-activating protein GCAP-1. *FEBS Lett*. 460, 27–31. doi: 10.1016/S0014-5793(99)01312-5

Leinders-Zufall, T., Cockerham, R. E., Michalakis, S., Biel, M., Garbers, D. L., Reed, R. R., et al. (2007). Contribution of the receptor guanylyl cyclase GC-D to chemosensory function in the olfactory epithelium. *Proc. Natl. Acad. Sci. U.S.A*. 104, 14507–14512. doi: 10.1073/pnas.0704965104

Lim, S., Peshenko, I., Dizhoor, A., and Ames, J. B. (2009). Effects of Ca2+, Mg2+, and myristoylation on guanylyl cyclase activating protein 1 structure and stability. *Biochemistry* 48, 850–862. doi: 10.1021/bi801897p

Lindemann, B. (1996). Chemoreception: tasting the sweet and the bitter. *Curr. Biol*. 6, 1234–1237. doi: 10.1016/S0960-9822(96)00704-X

Liu, X., Seno, K., Nishizawa, Y., Hayashi, F., Yamazaki, A., Matsumoto, H., et al. (1994). Ultrastructural localization of retinal guanylate cyclase in human and monkey retinas. *Exp. Eye Res*. 59, 761–768. doi: 10.1006/exer.1994.1162

Liu, Y., Ruoho, A. E., Rao, V. D., and Hurley, J. H. (1997). Catalytic mechanism of the adenylyl and guanylyl cyclases: modeling and mutational analysis. *Proc. Natl. Acad. Sci. U.S.A*. 94, 13414–13419. doi: 10.1073/pnas.94.25.13414

Lowe, D. G., Chang, M. S., Hellmiss, R., Chen, E., Singh, S., Garbers, D. L., et al. (1989). Human atrial natriuretic peptide receptor defines a new paradigm for second messenger signal transduction. *EMBO J*. 8, 1377–1384.

Lowe, D. G., Dizhoor, A. M., Liu, K., Gu, Q., Spencer, M., Laura, R., et al. (1995). Cloning and expression of a second photoreceptor-specific membrane retina guanylyl cyclase (RetGC), RetGC-2. *Proc. Natl. Acad. Sci. U.S.A*. 92, 5535–5539. doi: 10.1073/pnas.92.12.5535

Luo, D. G., Xue, T., and Yau, K. W. (2008). How vision begins: an odyssey. *Proc. Natl. Acad. Sci. U.S.A*. 105, 9855–9862. doi: 10.1073/pnas.0708405105

Mamasuew, K., Breer, H., and Fleischer, J. (2008). Gruenberg ganglion neurons respond to cool ambient temperatures. *Eur. J. Neurosci*. 28, 1775–1785. doi: 10.1111/j.1460-9568.2008.06465.x

Marala, R. B., Sitaramayya, A., and Sharma, R. K. (1991). Dual regulation of atrial natriuretic factor-dependent guanylate cyclase activity by ATP. *FEBS Lett*. 281, 73–76. doi: 10.1016/0014-5793(91)80361-6

Margulis, A., Goraczniak, R. M., Duda, T., Sharma, R. K., and Sitaramayya, A. (1993). Structural and biochemical identity of retinal rod outer segment membrane guanylate cyclase. *Biochem. Biophys. Res. Commun*. 194, 855–861. doi: 10.1006/bbrc.1993.1900

Margulis, A., Pozdnyakov, N., and Sitaramayya, A. (1996). Activation of bovine photoreceptor guanylate cyclase by S100 proteins. *Biochem. Biophys. Res. Commun*. 218, 243–247. doi: 10.1006/bbrc.1996.0043

Martel, G., Hamet, P., and Tremblay, J. (2010). Central role of guanylyl cyclase in natriuretic peptide signaling in hypertension and metabolic syndrome. *Mol. Cell. Biochem*. 334, 53–65. doi: 10.1007/s11010-009-0326-8

Meloche, S., McNicoll, N., Liu, B., Ong, H., and De Léan, A. (1988). Atrial natriuretic factor R1 receptor from bovine adrenal zona glomerulosa: purification, characterization, and modulation by amyloidal. *Biochemistry* 27, 8151–8158. doi: 10.1021/bi00421a025

Meyer, M. R., Angele, A., Kremmer, E., Kaupp, U. B., and Muller, F. (2000). A cGMP-signaling pathway in a subset of olfactory sensory neurons. *Proc. Natl. Acad. Sci. U.S.A*. 97, 10595–10600. doi: 10.1073/pnas.97.19.10595

Murad, F., Arnold, W. P., Mittal, C. K., and Braughler, J. M. (1979). Properties and regulation of guanylate cyclase and some proposed functions for cyclic GMP. *Adv. Cyclic Nucleotide Res*. 11, 175–204.

Nambi, P., Aiyar, N. V., and Sharma, R. K. (1982). Adrenocorticotropin-dependent particulate guanylate cyclase in rat adrenal and adrenocortical carcinoma: comparison of its properties with soluble guanylate cyclas and its relationship with ACTH-induced steroidogenesis. *Arch. Biochem. Biophys*. 217, 638–646. doi: 10.1016/0003-9861(82)90545-8

Nambi, P., and Sharma, R. K. (1981a). Adrenocorticotropic hormone-responsive guanylate cyclase in the particulate fraction of rat adrenal glands. *Endocrinology* 108, 2025–2027. doi: 10.1210/endo-108-5-2025

Nambi, P., and Sharma, R. K. (1981b). Demonstration of ACTH-sensitive particulate guanylate cyclase in adrenocortical carcinoma. *Biochem. Biophys. Res. Commun*. 100, 508–514. doi: 10.1016/S0006-291X(81)80206-9

Newbold, R. J., Deery, E. C., Payne, A. M., Wilkie, S. E., Hunt, D. M., and Warren, M. J. (2002). Guanylate cyclase activating proteins, guanylate cyclase and disease. *Adv. Exp. Med. Biol*. 514, 411–438. doi: 10.1007/978-1-4615-0121-3_25

Nishizuka, Y. (1988). The molecular heterogeneity of protein kinase C and its implications for cellular regulation. *Nature* 334, 661–665. doi: 10.1038/334661a0

Ogawa, H., Qiu, Y., Ogata, C. M., and Misono, K. S. (2004). Crystal structure of hormone-bound atrial natriuretic peptide receptor extracellular domain: rotation mechanism for transmembrane signal transduction. *J. Biol. Chem*. 279, 28625–28631. doi: 10.1074/jbc.M313222200

Olshevskaya, E. V., Ermilov, A. N., and Dizhoor, A. M. (1999). Dimerization of guanylyl cyclase-activating protein and a mechanism of photoreceptor guanylyl cyclase activation. *J. Biol. Chem*. 274, 25583–25587. doi: 10.1074/jbc.274.36.25583

Palczewski, K., Subbaraya, I., Gorczyca, W. A., Helekar, B. S., Ruiz, C. C., Ohguro, H., et al. (1994). Molecular cloning and characterization of retinal photoreceptor guanylyl cyclase-activating protein. *Neuron* 13, 395–404. doi: 10.1016/0896-6273(94)90355-7

Pandey, K. N., and Singh, S. (1990). Molecular cloning and expression of murine guanylate cyclase/atrial natriuretic factor receptor cDNA. *J. Biol. Chem*. 265, 12342–12348.

Paul, A. K. (1986). *Particulate Guanylate Cyclase from Adrenocortical Carcinoma 494. Purification, Biochemical and Immunological Characterization*. Doctoral Thesis, University of Tennessee.

Paul, A. K., Marala, R. B., Jaiswal, R. K., and Sharma, R. K. (1987). Coexistence of guanylate cyclase and atrial natriuretic factor receptor in a 180-kD protein. *Science* 235, 1224–1226. doi: 10.1126/science.2881352

Perchellet, J. P., Shanker, G., and Sharma, R. (1978). Regulatory role of guanosine 3′,5′-monophosphate in adrenocorticotropin hormone-induced steroidogenesis. *Science* 199, 311–312. doi: 10.1126/science.202028

Perchellet, J. P., and Sharma, R. K. (1979). Mediatory role of calcium and guanosine 3′, 5′-monophosphate in adrenocorticotropin-induced steroidogenesis by adrenal cells. *Science* 203, 1259–1261. doi: 10.1126/science.34216

Perrault, I., Rozet, J. M., Calvas, P., Gerber, S., Camuzat, A., Dollfus, H., et al. (1996). Retinal-specific guanylate cyclase gene mutations in Leber's congenital amaurosis. *Nat. Genet*. 14, 461–464. doi: 10.1038/ng1296-461

Pertzev, A., Duda, T., and Sharma, R. K. (2010). Ca2+ sensor GCAP1: a constitutive element of the ONE-GC-modulated odorant signal transduction pathway. *Biochemistry* 49, 7303–7313. doi: 10.1021/bi101001v

Peshenko, I. V., and Dizhoor, A. M. (2006). Ca2+ and Mg2+ binding properties of GCAP-1. Evidence that Mg2+-bound form is the physiological activator of photoreceptor guanylyl cyclase. *J. Biol. Chem*. 281, 23830–23841. doi: 10.1074/jbc.M600257200

Peshenko, I. V., and Dizhoor, A. M. (2007). Activation and inhibition of photoreceptor guanylyl cyclase by guanylyl cyclase activating protein 1 (GCAP-1): the functional role of Mg2+/Ca2+ exchange in EF-hand domains. *J. Biol. Chem*. 282, 21645–21652. doi: 10.1074/jbc.M702368200

Peshenko, I. V., Olshevskaya, E. V., Savchenko, A. B., Karan, S., Palczewski, K., Baehr, W., et al. (2011). Enzymatic properties and regulation of the native isozymes of retinal membrane guanylyl cyclase (RetGC) from mouse photoreceptors. *Biochemistry* 50, 5590–5600. doi: 10.1021/bi200491b

Pozdnyakov, N., Goraczniak, R., Margulis, A., Duda, T., Sharma, R. K., Yoshida, A., et al. (1997). Structural and functional characterization of retinal calcium-dependent guanylate cyclase activator protein (CD-GCAP): identity with S100beta protein. *Biochemistry* 36, 14159–14166. doi: 10.1021/bi971792l

Pozdnyakov, N., Yoshida, A., Cooper, N. G., Margulis, A., Duda, T., Sharma, R. K., et al. (1995). A novel calcium-dependent activator of retinal rod outer segment membrane guanylate cyclase. *Biochemistry* 34, 14279–14283. doi: 10.1021/bi00044a002

Pugh, E. N. J.r, and Cobbs, W. H. (1986). Visual transduction in vertebrate rods and cones: a tale of two transmitters, calcium and cyclic GMP. *Vision Res*. 26, 1613–1643. doi: 10.1016/0042-6989(86)90051-9

Pugh, E. N. Jr., Duda, T., Sitaramayya, A., and Sharma, R. K. (1997). Photoreceptor guanylate cyclases: a review. *Biosci. Rep*. 17, 429–473. doi: 10.1023/A:1027365520442

Pugh, E. N. Jr., Nikonov, S., and Lamb, T. D. (1999). Molecular mechanisms of vertebrate photoreceptor light adaptation. *Curr. Opin. Neurobiol*. 9, 410–418. doi: 10.1016/S0959-4388(99)80062-2

Rätscho, N., Scholten, A., and Koch, K.-W. (2010). Diversity of sensory guanylate cyclases in teleost fishes. *Mol. Cell. Biochem*. 334, 207–214. doi: 10.1007/s11010-009-0320-1

Robison, G. A., Butcher, R. W., and Sutherland, E. W. (1967). Adenyl cyclase as an adrenergic receptor. *Ann. N.Y. Acad. Sci*. 139, 703–723. doi: 10.1111/j.1749-6632.1967.tb41239.x

Rodbell, M. (1978). "The role of nucleotide regulatory components in the coupling of hormone receptors and adenylate cyclase," in *Molecular Biology and Pharmacology of Cyclic Nucleotides*, eds G. Folco and R. Paoletti (Amsterdam: Elsevier), 1–12.

Schmidt, H., Stonkute, A., Jüttner, R., Koesling, D., Friebe, A., and Rathjen, F. G. (2009). C-type natriuretic peptide (CNP) is a bifurcation factor for sensory neurons. *Proc. Natl. Acad. Sci. U.S.A*. 106, 16847–16852. doi: 10.1073/pnas.0906571106

Schmidt, H., Stonkute, A., Jüttner, R., Schäffer, S., Buttgereit, J., Feil, R., et al. (2007). The receptor guanylyl cyclase Npr2 is essential for sensory axon bifurcation within the spinal cord. *J. Cell Biol*. 179, 331–340. doi: 10.1083/jcb.200707176

Schulz, S., Singh, S., Bellet, R. A., Singh, G., Tubb, D. J., Chin, H., et al. (1989). The primary structure of a plasma membrane guanylate cyclase demonstrates diversity within this new receptor family. *Cell* 58, 1155–1162. doi: 10.1016/0092-8674(89)90513-8

Sharma, R. K. (1988). Guanylate cyclase and the atrial natriuretic factor receptor. Response to Waldman, S.A., Leitman, D.C., Anderson,J., and Murad, F. *Science* 240, 805–806. doi: 10.1126/science.240.4853.805-a

Sharma, R. K. (2002). Evolution of the membrane guanylate cyclase transduction system. *Mol. Cell. Biochem*. 230, 3–30. doi: 10.1023/A:1014280410459

Sharma, R. K. (2010). Membrane guanylate cyclase is a beautiful signal transduction machine: overview. *Mol.Cell. Biochem*. 334, 3–36. doi: 10.1007/s11010-009-0336-6

Sharma, R. K., Ahmed, N. K., and Shanker, G. (1976). Metabolic regulation of steroidogenesis in isolated adrenal cells of rat. Relationship of adrenocorticotropin-, adenosine 3′:5′-monophosphate-and guanosine 3′:5′-monophosphate-stimulated steroidogenesis with the activation of protein kinase. *Eur. J. Biochem*. 70, 427–433. doi: 10.1111/j.1432-1033.1976.tb11033.x

Sharma, R. K., Ahmed, N. K., Sutliff, L. S., and Brush, J. S. (1974). Metabolic regulation of steroidogenesis in isolated adrenal cells of the rat. ACTH regulation of cGMP and cAMP levels and steroidogenesis. *FEBS Lett* 45, 107–110. doi: 10.1016/0014-5793(74)80822-7

Sharma, R. K., and Duda, T. (1997). Plasma membrane guanylate cyclase. A multimodule transduction system. *Adv. Exp. Med. Biol*. 407, 271–279. doi: 10.1007/978-1-4899-1813-0_41

Sharma, R. K., and Duda, T. (2010a). Odorant-linked ROS-GC subfamily membrane guanylate cyclase transduction system. *Mol. Cell. Biochem*. 334, 181–189. doi: 10.1007/s11010-009-0333-9

Sharma, R. K., and Duda, T. (2010b). ROS-GC1 subfamily guanylate cyclase-linked transduction systems: taste, pineal gland and hippocampus. *Mol. Cell. Biochem*. 334, 199–206. doi: 10.1007/s11010-009-0334-8

Sharma, R. K., and Duda, T. (2012). Ca2±-sensors and ROS-GC: interlocked sensory transduction elements: a review. *Front. Mol. Neurosci*. 5:42. doi: 10.3389/fnmol.2012.00042

Sharma, R. K., Duda, T., Goraczniak, R., and Sitaramayya, A. (1997). Membrane guanylate cyclase signal transduction system. *Indian J. Biochem. Biophys*. 34, 40–49. doi: 10.1006/abbi.1996.9837

Sharma, R. K., Hashimoto, K., and Kitabchi, A. E. (1972). Steroidogenesis in isolated adrenal cells of rat. 3. Morphological and biochemical correlation of cholesterol and cholesterol ester content in ACTH and N6-2′-O-dibutyryl-adenosine-3′,5′-monophosphate activated adrenal cells. *Endocrinology* 91, 994–1003. doi: 10.1210/endo-91-4-994

Sharma, R. K., Jaiswal, R. K., and Duda, T. (1988). "Second messenger role of cyclic GMP in atrial natriuretic factor receptor mediated signal transduction: 180-kDa membrane guanylate cyclase, its coupling with atrial natriuretic factor receptor and its regulation by protein kinase C," in *Biological and Molecular Aspects of Atrial Factors*. New Series, UCLA Symposia on Molecular and Cellular Biology, ed P. Needleman, Vol. 81 (New York, NY: Alan R. Liss, Inc.), 77–96.

Sharma, R. K., Makino, C. L., Hicks, D., and Duda, T. (2014). ROS-GC interlocked Ca^{2+}-sensor S100B protein signaling in cone photoreceptors: review. *Front. Mol. Neurosci.* 7:21. doi: 10.3389/fnmol.2014.00021

Sharma, R. K., Shanker, G., and Ahmed, N. K. (1977). Metabolic regulation and relationship of endogenous protein kinase activity and steroidogenesis in isolated adrenocortical carcinoma cells of the rat. *Cancer Res*. 37, 472–475.

Shyjan, A. W., de Sauvage, F. J., Gillett, N. A., Goeddel, D. V., and Lowe, D. G. (1992). Molecular cloning of a retina-specific membrane guanylyl cyclase. *Neuron* 9, 727–723. doi: 10.1016/0896-6273(92)90035-C

Singh, S., Singh, G., Heim, J. M., and Gerzer, R. (1991). Isolation and expression of a guanylate cyclase-coupled heat stable enterotoxin receptor cDNA from a human colonic cell line. *Biochem. Biophys. Res. Commun*. 179, 1455–1463. doi: 10.1016/0006-291X(91)91736-V

Sokal, I., Otto-Bruc, A. E., Surgucheva, I., Verlinde, C. L., Wang, C. K., Baehr, W., et al. (1999). Conformational changes in guanylyl cyclase-activating protein 1 (GCAP1) and its tryptophan mutants as a function of calcium concentration. *J. Biol. Chem*. 274, 19829–19837. doi: 10.1074/jbc.274.28.19829

Stephen, R., Filipek, S., Palczewski, K., and Sousa, M. C. (2008). Ca2+ -dependent regulation of phototransduction. *Photochem. Photobiol*. 84, 903–910. doi: 10.1111/j.1751-1097.2008.00323.x

Strader, C. D., Fong, T. M., Tota, M. R., Underwood, D., and Dixon, R. A. (1994). Structure and function of G protein-coupled receptors. *Annu. Rev. Biochem*. 63, 101–132. doi: 10.1146/annurev.bi.63.070194.000533

Stryer, L. (1986). Cyclic GMP cascade of vision. *Annu. Rev. Neurosci*. 9, 87–119. doi: 10.1146/annurev.ne.09.030186.000511

Stryer, L. (1991). Visual excitation and recovery. *J. Biol. Chem*. 266, 10711–10714.

Subbaraya, I., Ruiz, C. C., Helekar, B. S., Zhao, X., Gorczyca, W. A., Pettenati, M. J., et al. (1994). Molecular characterization of human and mouse photoreceptor guanylate cyclase-activating protein (GCAP) and chromosomal localization of the human gene. *J. Biol. Chem*. 269, 31080–31089.

Sutherland, E. W., and Rall, T. W. (1958). Fractionation and characterization of a cyclic adenine ribonucleotide formed by tissue particles. *J. Biol. Chem*. 232,1077–1091.

Sutherland, E. W., and Rall, T. W. (1960). Formation of adenosine-3,5-phosphate (cyclic adenylate) and its relation to the action of several neurohormones or hormones. *Acta Endocrinol.* 34(Suppl. 50), 171–174.

Takayanagi, R., Inagami, T., Snajdar, R. M., Imada, T., Tamura, M., and Misono, K. S. (1987). Two distinct forms of receptors for atrial natriuretic factor in bovine adrenocortical cells. Purification, ligand binding, and peptide mapping. *J. Biol. Chem*. 262, 12104–12113.

Tucker, C. L., Woodcock, S. C., Kelsell, R. E., Ramamurthy, V., Hunt, D. M., and Hurley, J. B. (1999). Biochemical analysis of a dimerization domain mutation in RetGC-1 associated with dominant cone-rod dystrophy. *Proc. Natl. Acad. Sci. U.S.A*. 96, 9039–9044. doi: 10.1073/pnas.96.16.9039

Venkataraman, V., Duda, T., Ravichandran, S., and Sharma, R. K. (2008). Neurocalcin delta modulation of ROS-GC1, a new model of Ca2+ signaling. *Biochemistry* 47, 6590–6601. doi: 10.1021/bi800394s

Venkataraman, V., Duda, T., and Sharma, R. K. (1998). The alpha2D/A-adrenergic receptor-linked membrane guanylate cyclase: a new signal transduction system in the pineal gland. *FEBS Lett*. 427, 69–73. doi: 10.1016/S0014-5793(98)00396-2

Venkataraman, V., Duda, T., Vardi, N., Koch, K.-W., and Sharma, R. K. (2003). Calcium-modulated guanylate cyclase transduction machinery in the photoreceptor–bipolar synaptic region. *Biochemistry* 42, 5640–5648. doi: 10.1021/bi034025x

Venkataraman, V., Nagele, R., Duda, T., and Sharma, R. K. (2000). Rod outer segment membrane guanylate cyclase type 1-linked stimulatory and inhibitory calcium signaling systems in the pineal gland: biochemical, molecular, and immunohistochemical evidence. *Biochemistry* 39, 6042–6052. doi: 10.1021/bi9929960

Waldman, S. A., Rapoport, R. M., and Murad, F. (1984). Atrial natriuretic factor selectively activates particulate guanylate cyclase and elevates cyclic GMP in rat tissues. *J. Biol. Chem*. 259, 14332–14334.

Wen, X. H., Dizhoor, A. M., and Makino, C. L. (2014). Membrane guanylyl cyclase complexes shape the photoresponses of retinal rods and cones. *Front. Mol. Neurosci.* 7:45. doi: 10.3389/fnmol.2014.00045

Wen, X. H., Duda, T., Pertzev, A., Venkataraman, V., Makino, C. L., and Sharma, R. K. (2012). S100B serves as a Ca2+ sensor for ROS-GC1 guanylate cyclase in cones but not in rods of the murine retina. *Cell. Physiol. Biochem*. 29, 417–430. doi: 10.1159/000338496

Wensel, T. G. (2008). Signal transducing membrane complexes of photoreceptor outer segments. *Vision Res*. 48, 2052–2061. doi: 10.1016/j.visres.2008.03.010

Yang, R. B., Robinson, S. W., Xiong, W. H., Yau, K. W., Birch, D. G., and Garbers, D. L. (1999). Disruption of a retinal guanylyl cyclase gene leads to cone-specific dystrophy and paradoxical rod behavior. *J. Neurosci.* 19, 5889–5897.

Zufall, F., and Munger, S. D. (2010). Receptor guanylyl cyclases in mammalian olfactory function. *Mol Cell Biochem.* 334, 191–197. doi: 10.1007/s11010-009-0325-9

Conflict of Interest Statement: The authors declare that the research was conducted in the absence of any commercial or financial relationships that could be construed as a potential conflict of interest.

Received: 14 March 2014; accepted: 30 May 2014; published online: 02 July 2014.
*Citation: Sharma RK and Duda T (2014) Membrane guanylate cyclase, a multimodal transduction machine: history, present, and future directions. Front. Mol. Neurosci. **7**:56. doi: 10.3389/fnmol.2014.00056*
This article was submitted to the journal Frontiers in Molecular Neuroscience.

frontiers in
MOLECULAR NEUROSCIENCE

REVIEW ARTICLE
published: 17 March 2014
doi: 10.3389/fnmol.2014.00019

Structural diversity of neuronal calcium sensor proteins and insights for activation of retinal guanylyl cyclase by GCAP1

***Sunghyuk Lim*[1], *Alexander M. Dizhoor*[2] *and James B. Ames*[1]*

[1] *Department of Chemistry, University of California at Davis, Davis, CA, USA*
[2] *Basic Sciences, Pennsylvania College of Optometry, Salus University, Elkins Park, PA, USA*

Edited by:
Rameshwar K. Sharma, Salus University, USA

Reviewed by:
Baojin Ding, University of Massachusetts Medical School, USA
Frank Schmitz, Saarland University, Germany

****Correspondence:***
James B. Ames, Department of Chemistry, University of California at Davis, One Shields Avenue, Davis, CA 95616, USA
e-mail: jbames@ucdavis.edu

Neuronal calcium sensor (NCS) proteins, a sub-branch of the calmodulin superfamily, are expressed in the brain and retina where they transduce calcium signals and are genetically linked to degenerative diseases. The amino acid sequences of NCS proteins are highly conserved but their physiological functions are quite different. Retinal recoverin controls Ca^{2+}-dependent inactivation of light-excited rhodopsin during phototransduction, guanylyl cyclase activating proteins 1 and 2 (GCAP1 and GCAP2) promote Ca^{2+}-dependent activation of retinal guanylyl cyclases, and neuronal frequenin (NCS-1) modulates synaptic activity and neuronal secretion. Here we review the molecular structures of myristoylated forms of NCS-1, recoverin, and GCAP1 that all look very different, suggesting that the attached myristoyl group helps to refold these highly homologous proteins into different three-dimensional folds. Ca^{2+}-binding to both recoverin and NCS-1 cause large protein conformational changes that ejects the covalently attached myristoyl group into the solvent exterior and promotes membrane targeting (Ca^{2+}-myristoyl switch). The GCAP proteins undergo much smaller Ca^{2+}-induced conformational changes and do not possess a Ca^{2+}-myristoyl switch. Recent structures of GCAP1 in both its activator and Ca^{2+}-bound inhibitory states will be discussed to understand structural determinants that control their Ca^{2+}-dependent activation of retinal guanylyl cyclases.

Keywords: calcium, EF-hand, Ca^{2+}-myristoyl switch, NCS-1, recoverin, GCAP1, NCS protein, NMR

INTRODUCTION

Intracellular calcium ions (Ca^{2+}) regulate neuronal signaling in the central nervous system (Berridge et al., 2000; Augustine et al., 2003). Neuronal Ca^{2+} signals are detected by a family of neuronal calcium sensor (NCS) proteins (Ames et al., 1996, 2012; Braunewell and Gundelfinger, 1999; Burgoyne and Weiss, 2001; Burgoyne et al., 2004; Weiss et al., 2010) that contain EF-hand motifs (Moncrief et al., 1990; Ikura, 1996; Ikura and Ames, 2006) as well as by a family of C_2-domain containing proteins (synaptotagmin and protein kinase C isoforms; Nalefski and Falke, 1996; Corbalan and Gomez, 2014). At least sixteen different NCS proteins are known (Weiss and Burgoyne, 2002; Burgoyne and Haynes, 2012) and are conserved from yeast to humans (**Figure 1**). Recoverin (Dizhoor et al., 1991) and guanylyl cyclase activating proteins 1 and 2 (GCAP1 and GCAP2; Dizhoor et al., 1994; Palczewski et al., 1994) are expressed in the retina, where they regulate phototransduction in photoreceptor cells (Palczewski et al., 2000; Ames and Ikura, 2002; Stephen et al., 2008; Ames et al., 2012). NCS proteins are also expressed in the brain such as neurocalcin (Hidaka and Okazaki, 1993), frequenin (NCS-1; Pongs et al., 1993; McFerran et al., 1998), visinin-like proteins (VILIPs; Bernstein et al., 1999; Braunewell and Klein-Szanto, 2009), K^+ channel interacting proteins (KChIPs; An et al., 2000), calsenilin/DREAM (Buxbaum et al., 1998; Carrion et al., 1999), and hippocalcin (Kobayashi et al., 1992, 1993; Tzingounis et al., 2007).

Recoverin also called S-modulin (Dizhoor et al., 1991; Kawamura and Murakami, 1991), the first NCS protein to be discovered, controls the lifetime of photo-excited rhodopsin (Kawamura, 1993; Erickson et al., 1998; Makino et al., 2004) by regulating rhodopsin kinase (Calvert et al., 1995; Chen et al., 1995; Klenchin et al., 1995; Komolov et al., 2009). Recoverin decreases the lifetime of rhodopsin at low Ca^{2+} levels to control visual recovery and promote photoreceptor adaptation to background light. More recent evidence indicates that recoverin can also modulate the decay of the light-activated phsophodiesterase activity. Such modulation may help accelerate visual recovery in the presence of background light (Chen et al., 2012). Recoverin is also located in the rod inner segment (Strissel et al., 2005) and is associated with cancer-associated retinopathy (Polans et al., 1991; Subramanian and Polans, 2004).

Guanylyl cyclase activating proteins 1 and 2 are also expressed in photoreceptor cells where they activate retinal guanylyl cyclase at low cytosolic Ca^{2+} levels upon light activation (Dizhoor et al., 1994; Palczewski et al., 1994, 2004). The EF-hand motifs in GCAPs can bind both Mg^{2+} and Ca^{2+} (Peshenko and Dizhoor, 2004, 2006). Mg^{2+} binding stabilizes a structural form of GCAPs that activates cyclase activity (Peshenko and Dizhoor, 2006; Lim et al., 2009), whereas Ca^{2+}-bound GCAPs inhibit the cyclase (Dizhoor and Hurley, 1996; Dizhoor et al., 1998). GCAPs are important for regulating the recovery phase of visual excitation and particular mutants are linked to various forms of retinal degeneration (Semple-Rowland et al., 1996; Sokal et al., 1998; Baehr and Palczewski, 2007; Bondarenko et al., 2010; Jiang and Baehr, 2010).

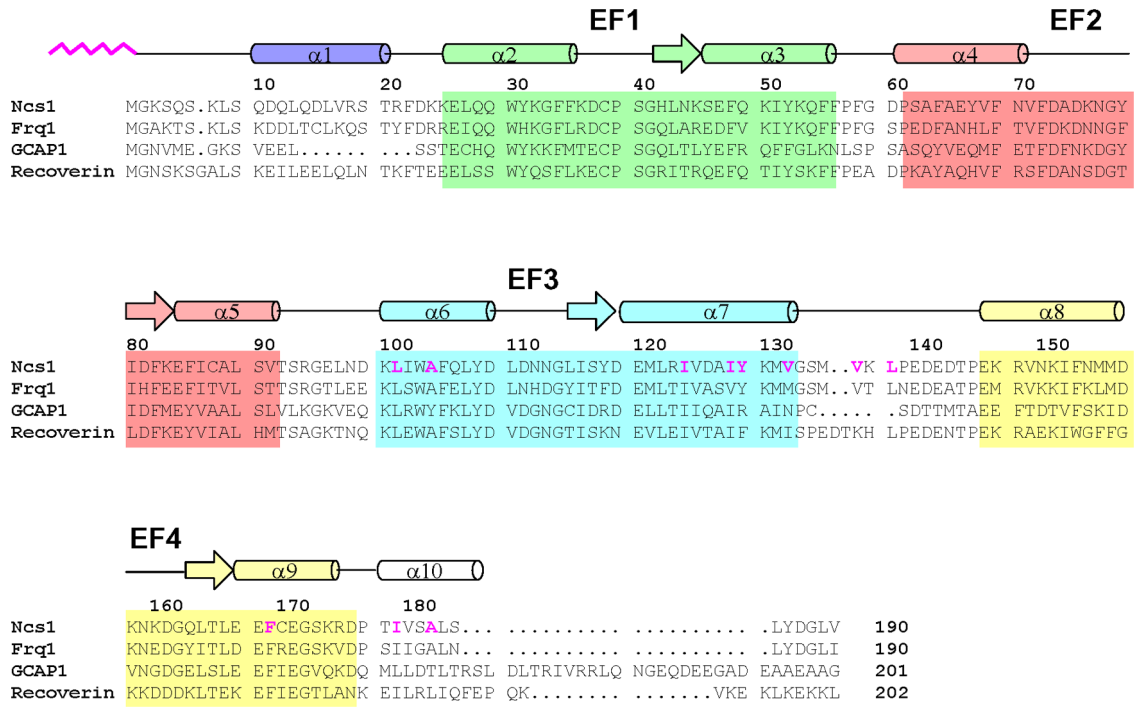

FIGURE 1 | Amino acid sequence alignment of selected NCS proteins (sequence numbering is for *S.* pombe NCS-1). Secondary structure elements (helices and strands), EF-hand motifs (EF1 green, EF2 red, EF3 cyan, and EF4 yellow), and residues that interact with the myristoyl group (highlighted magenta) are indicated. Swiss Protein Database accession numbers are Q09711 (*S. pombe* NCS-1), Q06389 (*S. cerevisiae* Frq1), P21457 (bovine recoverin), and P43080 (human GCAP1).

Neuronal calcium sensor proteins (frequenin or NCS-1) are expressed in other tissues beside the brain (Kapp et al., 2003) and in lower organisms including flies (Pongs et al., 1993), worms (Gomez et al., 2001), and yeast (Frq1; Hendricks et al., 1999; Huttner et al., 2003; Hamasaki et al., 2004). Yeast NCS homologs (called Frq1) activate a phosphatidyl inositol 4-OH kinase isoform (Pik1; Hendricks et al., 1999; Kapp et al., 2003; Strahl et al., 2003, 2007) required for vesicle trafficking and secretion (Hama et al., 1999; Walch-Solimena and Novick, 1999). Mammalian NCS-1 interacts with voltage-gated Ca^{2+} and K^+ channels (Weiss et al., 2000; Nakamura et al., 2001) and activates inositol trisphosphate receptors (Boehmerle et al., 2006).

NCS proteins typically contain about 200 amino acid residues in chain length with four EF-hand motifs, a first EF-hand that does not bind Ca^{2+}, and a myristoylation consensus sequence at the N-terminus. NCS proteins have similar sequences, ranging from 35 to 60% identity (**Figure 1**). EF-hand residues are the most highly conserved, particularly in the Ca^{2+} binding loops. The fourth EF-hand sequence is variable, and Ca^{2+} is able to bind to EF4 in frequenin (Cox et al., 1994; Ames et al., 2000) and GCAPs (Peshenko and Dizhoor, 2007; Stephen et al., 2007) but Ca^{2+} does not bind to EF4 in recoverin (Ames et al., 1995a) and VILIPs (Cox et al., 1994; Li et al., 2011). Ca^{2+}-binding to EF4 in GCAP1 controls whether GCAP1 can activate or inhibit guanylyl cyclase (Peshenko and Dizhoor, 2007). The residues near the C-terminus and linker between EF3 and EF4 are non-conserved, suggesting that these regions may play a role in target specificity for recoverin but not for GCAPs.

Retinal recoverin and most other NCS proteins are myristoylated at the amino terminus (Dizhoor et al., 1992; Kobayashi et al., 1993; Ladant, 1995). Recoverin and GCAPs contain a saturated myristoyl (14:0) or related fatty acyl group (12:0, 14:1, 14:2), because N-myristoyl transferase (Gordon et al., 1991) can efficiently utilize C12 and/or C14 acetyl-CoA as fatty acyl donors in the retina. In tissues other than the retina, myristoylation is the predominant modification. Myristoylated recoverin binds to cell membranes only at high Ca^{2+} levels (Zozulya and Stryer, 1992; Dizhoor et al., 1993), whereas unmyristoylated recoverin does not bind to membranes. Likewise, bovine neurocalcin (Ladant, 1995) and hippocalcin (Kobayashi et al., 1993) both are myristoylated and exhibit Ca^{2+}-induced localization at the plasma membrane in response to neuronal stimulation. Ca^{2+}-induced membrane targeting by NCS proteins has been termed, Ca^{2+}-myristoyl switch. The attached fatty acyl group is buried inside the protein structure of Ca^{2+}-free recoverin (Tanaka et al., 1995). Ca^{2+} binding to recoverin causes extrusion of the fatty acid, enabling it to interact with lipid bilayer membranes. Recoverin's Ca^{2+}-myristoyl switch may control its light-induced movement into the rod inner segment (Strissel et al., 2005). GCAP proteins are also myristoylated (Palczewski et al., 1994; Frins et al., 1996; Olshevskaya et al., 1997). However, unlike recoverin, GCAPs do not possess a functional Ca^{2+}-myristoyl switch (Olshevskaya et al., 1997; Hwang and Koch, 2002). Instead the N-terminal myristoyl group remains

sequestered inside GCAP1 in both Ca^{2+}-free and Ca^{2+}-bound states (Hughes et al., 1998; Lim et al., 2009). Indeed, the crystal structure of Ca^{2+}-bound GCAP1 shows the myristoyl group surrounded by the protein (Stephen et al., 2007), and a recent nuclear magnetic resonance (NMR) structural analysis reveals that the activator state of GCAP1 has an overall structure similar to that of Ca^{2+}-bound inhibitory state in which the N-terminal myristoyl group is buried in both the Ca^{2+}-free and Ca^{2+}-bound states (Lim et al., 2013).

Atomic-resolution structures are known for myristoylated forms of recoverin (Ames et al., 1997), GCAP1 (Stephen et al., 2007), and NCS-1 (Lim et al., 2011) that each fold differently around the attached myristoyl group (**Figure 2**). For NCS-1, the attached myristoyl group is located in a protein crevice formed by helices from EF3 and EF4 near the C-terminus (**Figure 2A**). The covalently attached fatty acyl group in NCS-1 protrudes in a parallel fashion between four helices from EF3 and EF4 (**Figure 2B**). The C-terminal location of the myristoyl binding site in NCS-1 is quite different from that of recoverin in which the myristate is positioned inside a cavity near the N-terminus (**Figure 2C**). The attached fatty acyl chain in recoverin is wedged between the helices of EF1 and EF2 in a perpendicular fashion (**Figure 2D**), which contrasts with the parallel arrangement of the fatty acyl chain in NCS-1 (**Figure 2B**). For GCAP1, the myristoyl group is sequestered in a cavity formed by the N-terminal domain with participation of a C-terminal helix (**Figure 2E**). The myristoyl group in GCAP1 bridges the N-terminal and C-terminal ends of the protein by contacting helices at each end (**Figure 2F**). In short, the protein structural environment around the myristoyl group is quite different in recoverin, GCAP1 and NCS-1 (**Figure 2**). This suggests that each NCS protein folds differently around the N-terminal myristoyl group by contacting non-conserved patches of hydrophobic residues that are unique to each NCS protein. However, myristoylation of GCAP2 is not essential for its ability to activate its target (retinal guanylyl cyclase), because unmyristoylated GCAP2 can activate cyclase activity nearly as well as myristoylated GCAP2 (Olshevskaya et al., 1997).

In this review, we discuss recent structures of GCAP1 in both Ca^{2+}-free activator and Ca^{2+}-bound inhibitor states to understand structural determinants that control Ca^{2+}-dependent activation of retinal guanylyl cyclases.

Ca^{2+}-DEPENDENT ACTIVATION OF RETINAL GUANYLYL CYCLASE

GUANYLYL CYCLASE ACTIVATION AND PHOTORECEPTOR RECOVERY

In vertebrate rods and cones, photon absorption by rhodopsin or cone visual pigments triggers a phototransduction cascade that hydrolyzes cGMP, resulting in the closure of cGMP-gated cation channels on the plasma membrane that causes membrane hyperpolarization [see reviews (Pugh et al., 1997, 1999)]. To reset the resting dark-state of retinal rods (known as visual recovery), cGMP levels are replenished very quickly (Burns and Baylor, 2002) by retina-specific guanylyl cyclases (RetGCs), a membrane enzyme present in rod and cone outer segments (Dizhoor et al., 1994; Lowe et al., 1995). RetGC is a Ca^{2+}-regulated enzyme (Koch and Stryer, 1988; Koutalos and Yau, 1996) whose activity is controlled by intracellular domains (Laura et al., 1996; Duda et al., 2005) that interact with soluble EF-hand Ca^{2+} sensor proteins, called guanylyl cyclase activating proteins (GCAPs: GCAP1 and GCAP2; Dizhoor et al., 1994, 1995; Gorczyca et al., 1994, 1995; Koutalos et al., 1995).

Light-induced channel closure in photoreceptor cells causes a decrease in the cytosolic free Ca^{2+} concentration (Gray-Keller and Detwiler, 1994), in mammals from 250 nM in the dark to 25 nM in the light (Woodruff et al., 2002). The catalytic activity of RetGC in the dark is negatively controlled by Ca^{2+}-bound GCAPs (Dizhoor and Hurley, 1996; Dizhoor et al., 1998; Burns and Baylor, 2002), whereas the release of Ca^{2+} from GCAPs at low Ca^{2+} levels in light-activated photoreceptors causes activation of RetGC (Dizhoor et al., 1994, 1995; Gorczyca et al., 1994, 1995; Dizhoor and Hurley, 1996; Mendez et al., 2001). Light stimulation of the rod cell causes a more than 10-fold increase in cGMP production due to the activation of RetGC by GCAPs (Hodgkin and Nunn, 1988; Burns and Baylor, 2002) and is a critical step for controlling the recovery rate of a single-photon response (Pugh et al., 1999; Burns and Baylor, 2002) as well as the cone response to stronger light stimuli (Sakurai et al., 2011). In mouse rods, GCAPs have been demonstrated to have different Ca^{2+} sensitivities (Dizhoor et al., 1998; Hwang et al., 2003) and therefore contribute to the recovery by activating guanylyl cyclase at different steps of excitation and recovery, thus imparting proper recovery kinetics to the rod response (Mendez et al., 2001; Makino et al., 2008, 2012).

Mg^{2+} AND Ca^{2+} BINDING TO GCAPs RECIPROCALLY CONTROL CYCLASE ACTIVATION

Guanylyl cyclase activating proteins activate RetGC at low Ca^{2+} levels (less than 50 nM) and only in the presence of physiological Mg^{2+} levels (Peshenko and Dizhoor, 2004, 2006, 2007; Dizhoor et al., 2010). This Mg^{2+} requirement for RetGC activation by GCAPs initially suggested that Mg^{2+} binding to GCAPs might be important for their activation of RetGC. Indeed, Mg^{2+} was shown to bind directly to at least two of the EF-hands in GCAP1 (Lim et al., 2009), and NMR studies showed that Mg^{2+} binding to GCAP1 at EF2 and EF3 was needed to stabilize the overall tertiary fold of the protein (Lim et al., 2009). By contrast, the Ca^{2+}-free/Mg^{2+}-free GCAP1 (apo-state) forms a molten globule-like structure, that contains regular secondary structure (Dell'Orco et al., 2010) but does not form a stable tertiary fold (Peshenko and Dizhoor, 2004; Lim et al., 2009). The flexible and unstructured molten-globule apo-protein could explain in part why GCAPs do not activate RetGC in the absence of Mg^{2+} (Dizhoor et al., 2010). Thus, Mg^{2+} binding to GCAP1 stablizes its protein structure in order to bind and activate RetGC (Dizhoor et al., 1994; Peshenko and Dizhoor, 2004), whereas Ca^{2+} binding to GCAP1 stabilizes a distinct structure important for the inhibition of RetGC (Dizhoor et al., 1998).

The four EF-hands in the GCAPs have quite distinct divalent metal binding properties that control whether GCAPs can activate or inhibit RetGC. The first EF-hand (EF1) does not bind to either Ca^{2+} or Mg^{2+} because the residue at the 3-position in the EF-hand binding loop (Cys29 in GCAP1, see **Figure 1**) is not suitable for ligating either Ca^{2+} or Mg^{2+}. Ca^{2+} binds to GCAP1 at the other three EF-hands (EF2, EF3, and EF4) in an independent fashion

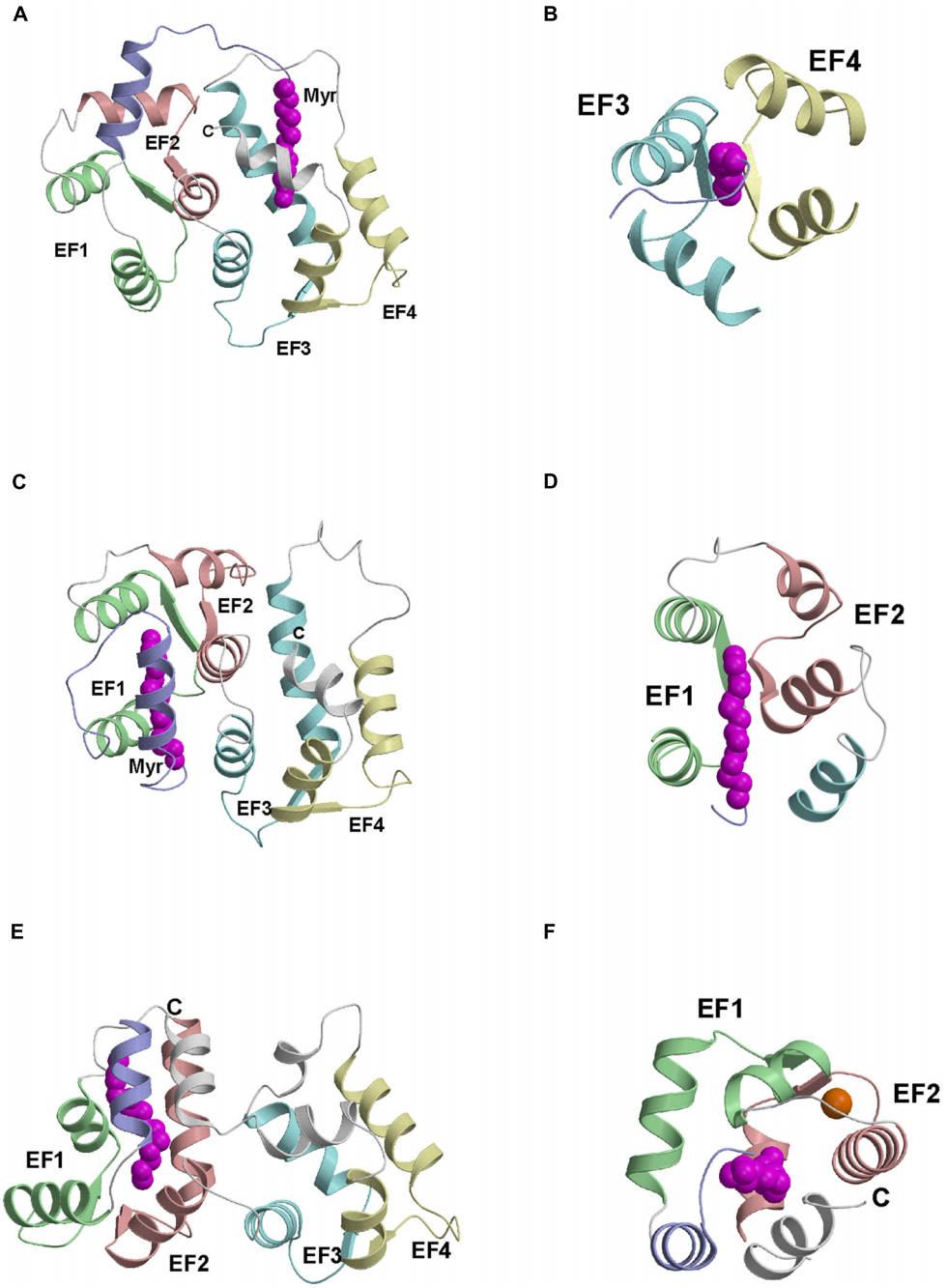

FIGURE 2 | Main chain structures of Ca^{2+}-free myrisoylated NCS-1 (PDB ID: 212e) (A), recoverin (PDB ID: 1iku) (C), and GCAP1 (PDB ID: 2r2i) (E). Close-up views of the myristate binding pocket in NCS-1 **(B)**, recoverin **(D)** and GCAP1 **(F)**. EF-hands and myristoyl group (magenta) are colored as defined in **Figure 1**. Adapted from and originally published by Lim et al. (2011).

(Lim et al., 2009) in contrast to the cooperative binding of two Ca^{2+} to recoverin (Ames et al., 1995a). The apparent dissociation constant for Ca^{2+} binding to GCAPs is in the submicromolar range (Lim et al., 2009; Dizhoor et al., 2010), whereas Mg^{2+} binds with ~1000-fold lower affinity (Gifford et al., 2007) in the sub-millimolar range (Peshenko and Dizhoor, 2004, 2007; Lim et al., 2009). These binding affinities imply that three Ca^{2+} bind per mole of GCAP1 in dark-adapted rod cells, which have relatively high cytosolic Ca^{2+} levels $[Ca^{2+}]_{free} = 250–500$ nM [(Woodruff et al., 2002; Matthews and Fain, 2003) and $[Mg^{2+}] \sim 1$ mM (Chen et al., 2003)]. Light-activation of the rod cell causes a dramatic lowering of the cytosolic Ca^{2+} level $[Ca^{2+}]_{free} = 5–50$ nM (Gray-Keller and Detwiler, 1994; Sampath et al., 1998; Woodruff et al., 2002) while the Mg^{2+} level remains fixed at $[Mg^{2+}]_{free} \sim 1$ mM

(Chen et al., 2003). Therefore in light-adapted rods, GCAPs do not bind Ca^{2+} but instead bind to at least two Mg^{2+}. Thus, Ca^{2+}-free/Mg^{2+}-bound GCAPs activate RetGC in light exposed rods (Dizhoor et al., 1994, 1995; Gorczyca et al., 1995), whereas Ca^{2+}-bound GCAPs (with Ca^{2+} bound at EF2, EF3, and EF4) inhibit RetGC in dark-adapted rods (Dizhoor and Hurley, 1996; Dizhoor et al., 1998).

CONSTITUTIVELY ACTIVE MUTANTS OF GCAP1 CAUSE RETINAL DISEASE

Various point mutations in the EF-hand motifs of GCAP1 that weaken Ca^{2+} binding (but do not affect Mg^{2+} binding) cause GCAP1 to constitutively activate RetGC in rods and cones, which is genetically linked to various retinal diseases (Jiang and Baehr, 2010). These mutations in the EF-hand motifs [Y99C (Dizhoor et al., 1998; Payne et al., 1998) and E155G (Wilkie et al., 2000, 2001)] weaken the Ca^{2+} binding affinity beyond the photoreceptor Ca^{2+} concentration and cause the Ca^{2+}-free/Mg^{2+}-bound GCAP1 activator state to persist even at high Ca^{2+} levels in dark-adapted rods, which causes persistent activation of RetGC (Sokal et al., 1998; Olshevskaya et al., 2004). The GCAP mutants that constitutively activate RetGC then cause elevated cGMP levels in photoreceptor cells that promotes apoptosis and disease (Olshevskaya et al., 2004, 2012; Woodruff et al., 2007).

Mutagenesis studies of the individual EF-hands in GCAP1 have revealed that Ca^{2+}-binding to EF4 is critical for controlling Ca^{2+}-dependent activation of RetGC (Peshenko and Dizhoor, 2007). Mutants of GCAP1 that weaken or abolish Ca^{2+} binding to EF4 but retain Ca^{2+} binding at EF2 and EF3 [D144N/D148G (Peshenko and Dizhoor, 2007 and E155G Wilkie et al., 2000, 2001)] are constitutively active even in the presence of high Ca^{2+} levels in dark-adapted photoreceptors. Furthermore, these mutants that disable Ca^{2+} binding to EF4 (but not EF2 and EF3) are unable to inhibit RetGC at high Ca^{2+} levels in the dark (Peshenko and Dizhoor, 2007). In summary, GCAP1 can activate RetGC even if Ca^{2+} is bound to EF2 and EF3 (but not bound to EF4). Also, Ca^{2+} binding to EF4 is essential for having Ca^{2+}-induced inhibition of RetGC. Therefore, Ca^{2+} binding to EF4 is critical for controlling whether GCAP1 can activate or inhibit RetGC.

GCAPs DO NOT POSSESS A Ca^{2+}-MYRISTOYL SWITCH

Ca^{2+} binding to GCAP1 and GCAP2 does not cause ejection of the covalently attached myristoyl group (Hughes et al., 1998; Lim et al., 2009, 2013) and Ca^{2+} binding to GCAPs do not promote their membrane targeting (Olshevskaya et al., 1997; Hwang and Koch, 2002). This is in stark contrast to the Ca^{2+}-induced exposure of the N-terminal myristoyl group [termed Ca^{2+}-myristoyl switch (Zozulya and Stryer, 1992; Dizhoor et al., 1993)] that promotes membrane targeting of recoverin (Zozulya and Stryer, 1992; Dizhoor et al., 1993; Valentine et al., 2003), neurocalcin (Ladant, 1995), hippocalcin (O'Callaghan et al., 2003), VILIPs (Spilker et al., 1997, 2002), and NCS-1 (Hamasaki et al., 2004). Instead, the covalently attached myristoyl group of GCAP1 remains sequestered inside the protein hydrophobic core in both Ca^{2+}-free and Ca^{2+}-bound forms of GCAP1 (Lim et al., 2009, 2013). NMR studies on the myristate attached to recoverin (Ames et al., 1995b, 1997; Hughes et al., 1995), VILIP1 (Li et al., 2011), and NCS-1 (Lim et al., 2011) reveal that the covalently attached myristoyl group is buried inside these proteins only in the Ca^{2+}-free state. Ca^{2+}-binding causes protein conformational changes that lead to exposure of the fatty acyl chain in recoverin (Ames et al., 1997), VILIP1 (Li et al., 2011), and NCS-1 (Lim et al., 2011). By stark contrast, NMR studies on GCAP1 indicate that the covalently attached myristoyl group is buried inside both Ca^{2+}-free and Ca^{2+}-bound GCAP1 (Lim et al., 2009, 2013). Further evidence that GCAP1 lacks a Ca^{2+}-myristoyl switch comes from SPR studies that show myristoylation of GCAP1 has little effect on membrane binding (Hwang and Koch, 2002). Finally, the recent atomic level structures of GCAP1 directly demonstrated that the myristoyl group is buried inside the protein in a similar environment in both the Ca^{2+}-free activator (Lim et al., 2013) and Ca^{2+}-bound inhibitor states (Stephen et al., 2007).

Solid-state NMR and other spectroscopic studies on GCAP2 have suggested that Ca^{2+}-free GCAP2 might be targeted to cell membranes by a reversed Ca^{2+}-myristoyl switch (Theisgen et al., 2010, 2011). The covalently attached fatty acyl group has been suggested to become exposed in Ca^{2+}-free GCAP2 in the presence of lipid bilayer membranes (Theisgen et al., 2011), in contrast to having the myristoyl group sequestered inside Ca^{2+}-bound GCAP2 (Schroder et al., 2011). However, other studies on GCAP2 indicate that the myristoyl group remains sequestered inside the protein environment in both Ca^{2+}-free and Ca^{2+}-bound GCAP2 (Hughes et al., 1998). Also, unmyristoylated GCAP2 activates RetGC with nearly the same potency as that of myristoylated GCAP2, and myristoylation of GCAP2 is not essential for its targeting to the membrane-bound cyclase (Olshevskaya et al., 1997; Hwang and Koch, 2002).

Ca^{2+}-INDUCED PROTEIN CONFORMATIONAL CHANGES IN GCAPs

Atomic level structures are known for Ca^{2+}-bound forms of GCAP1 (Stephen et al., 2007) and GCAP2 (Ames et al., 1999). The four EF-hands in GCAP1 (**Figures 1** and **3**) are grouped into two globular domains: N-domain includes EF1 and EF2 (residues 18–83) and C-domain contains EF3 and EF4 (residues 88–161). Ca^{2+} is bound to GCAP1 at EF2, EF3 and EF4, and the structure of each Ca^{2+}-bound EF-hand in GCAP1 (**Figure 3B**) adopts the familiar open conformation of EF-hands as seen in calmodulin and other Ca^{2+}-bound EF-hand proteins (Ikura, 1996). Indeed, the interhelical angles for each Ca^{2+}-bound EF-hand in GCAP1 are similar to those of recoverin (Ames et al., 1997) and NCS-1 (Bourne et al., 2001). Although the internal structure of each EF-hand in GCAP1 is similar to that of recoverin, the overall three-dimensional packing arrangement and spatial organization of the four EF-hands is very different for GCAP1 vs. recoverin. Indeed, the overall root-mean-squared deviation of main chain atoms is 3.4 Å when comparing the structures of GCAP1 and recoverin (**Figure 2**). A unique structural feature of GCAP1 is that the N-terminal α-helix (residues 5–15) upstream of EF1 and C-terminal helix (residues 175–183) downstream of EF4 are held closely together by their mutual interaction with the N-terminal myristoyl group (**Figure 2F**). Thus, the covalently

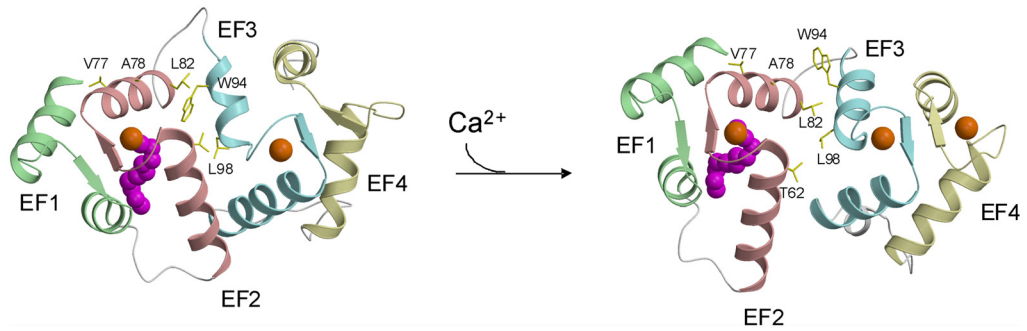

FIGURE 3 | Structures of activator (A) vs. inhibitor forms (B) of GCAP1 adapted from and originally published by Lim et al. (2013).

attached myristoyl group in GCAP1 is sequestered within a unique environment inside the Ca^{2+}-bound protein, which is quite different from that of recoverin as described above in **Figure 2**. The myristoyl group attached to GCAP1 makes contacts with N-terminal residues (V9, L12, and F42) and the C-terminal helix (L174, V178 and I181; **Figure 2F**). In essence, the myristoyl group serves to bridge both the N-terminal and C-terminal ends of the protein, which explains how Ca^{2+}-induced conformational changes in the C-terminal domain (particularly in EF4) might be transmitted to a possible target binding site in EF1. A Ca^{2+}-myristoyl tug mechanism (Peshenko et al., 2012) has been proposed to explain how Ca^{2+}-induced conformational changes in EF4 serve to "tug" on the adjacent C-terminal helix that connects structurally to the myristoyl group and EF1. This tug mechanism helps explain how Ca^{2+}-induced structural changes in EF4 might be relayed to the cyclase binding region in EF1 (Lim et al., 2013). The Ca^{2+}-induced structural changes involving the C-terminal helix might also be related to Ca^{2+}-dependent phosphorylation of S201 in GCAP2 (Peshenko et al., 2004).

The atomic level structure of Ca^{2+}-free/Mg^{2+}-bound activator form of GCAP1 or GCAP2 is currently not known. The main difficulty is that Ca^{2+}-free/Mg^{2+}-bound GCAP proteins form dimers and higher order protein oligomers that causes considerable sample heterogeneity at high protein concentrations needed for NMR or to make crystals for X-ray crystallography (Ames et al., 1999; Lim et al., 2009, 2013). Ca^{2+}-dependent dimerization of GCAP2 has been suggested to be important for activating the cyclase (Olshevskaya et al., 1999b; Ermilov et al., 2001). Protein dimerization was also reported for GCAP1, and a GCAP1 mutant (V77E) that prevents protein dimerization also abolishes its ability to activate RetGC, suggesting that dimerization of Ca^{2+}-free/Mg^{2+}-bound activator state might be important for activating RetGC (Lim et al., 2013). However, protein dimerization of GCAP1 is not Ca^{2+} dependent and only occurs at relatively high protein concentrations above 100 μM (Lim et al., 2013). Future studies are needed to investigate whether GCAPs might form a functional dimer upon binding to the dimeric RetGC to form a 2:2 complex (Ramamurthy et al., 2001; Peshenko et al., 2010), and whether the dimeric quaternary structure may play a regulatory role.

A GCAP1 mutant, D144N/D148G called EF4mut, (Lim et al., 2013) that binds Ca2+ at EF2 and EF3 (and does not bind Ca^{2+} at EF4) can activate RetGC at high Ca^{2+} concentrations (Peshenko and Dizhoor, 2007). Therefore, EF4mut (with Ca^{2+} bound at EF2 and EF3) serves as a model of the Ca^{2+}-free/Mg^{2+}-bound activator state. The EF4mut protein is more soluble and stable than Ca^{2+}-free/Mg^{2+}-bound wild type, and EF4mut exhibits NMR spectra with much higher resolution and sensitivity compared to that of Ca^{2+}-free/Mg^{2+}-bound wild type (Lim et al., 2009, 2013). NMR structural studies on EF4mut provide some insights for a structural model of the GCAP1 activator state (**Figure 3A**). The overall structure of EF4mut is similar to the crystal structure of Ca^{2+}-bound GCAP1 (root mean squared deviation of main chain atoms is 1.3 Å when comparing the two structures). However, residues at the domain interface (between EF2 and EF3) are structured somewhat differently in EF4mut compared to the crystal structure of Ca^{2+}-bound GCAP1. Many of the GCAP1 residues at the domain interface have quite broad NMR resonances, suggesting that these residues are conformationally dynamic (Lim et al., 2013). The corresponding residues in recoverin (**Figure 1**) also exhibited broad NMR resonances and ^{15}N NMR relaxation dispersion studies reveal that these domain interface residues exhibit millisecond exchange kinetics (Xu et al., 2011). Ca^{2+}-induced rearrangement of residues at the domain interface in recoverin gives rise to a 45° swiveling of the two domains (Ames et al., 1997). A structural comparison between EF4mut and Ca^{2+}-bound GCAP1 suggests a related but much smaller Ca^{2+}-induced structural change at the domain interface in GCAP1 (**Figure 3**). The most noteworthy Ca^{2+}-induced structural difference in GCAP1 can be seen in the entering helix of EF3 that unravels a half turn in EF4mut, which causes a repositioning of the W94 side-chain at the domain interface. A Ca^{2+}-induced change in the structural environment around W94 is consistent with previous tryptophan fluorescence and electron paramagnetic resonance studies of GCAP1 (Sokal et al., 2001; Peshenko and Dizhoor, 2006, 2007). We suggest that Ca^{2+}-induced rearrangement of residues at the domain interface (V77, A78, L82, K85, and

W94) plays a role in modulating Ca^{2+}-dependent contacts with RetGC1.

ACTIVATION MECHANISM FOR RetGC BY GCAPs

The structural information for the GCAPs above provides insights into the activation mechanism of RetGC (**Figure 4**). GCAP1 residues in EF1 (Krylov et al., 1999; Olshevskaya et al., 1999a,b; Ermilov et al., 2001) and at the domain interface (Krylov et al., 1999; Lim et al., 2013; Peshenko et al., 2014) are suggested to make direct contact with RetGC (see labeled residues in **Figure 4**). In our model (**Figure 4**), Ca^{2+}-induced conformational changes in EF4 (Lim et al., 2013) are transmitted to the cyclase binding site (see labeled residues in EF1, EF2, and EF3, **Figure 4**) by a Ca^{2+}-myristoyl tug mechanism as described by (Peshenko et al., 2012). In the GCAP1 activator state under physiological conditions (**Figure 4**, left panel), EF2 and EF3 are bound to Mg^{2+} (blue circles in **Figure 4**) with EF1 and EF4 unoccupied. The Ca^{2+}-free state of EF4 forms a loose and dynamic structure (Lim et al., 2013), which allows the adjacent C-terminal helix to reach all the way to the N-terminal myristoyl group (magenta in **Figure 4**) and thus indirectly form hydrophobic contacts with residues in EF1 and EF2. In essence, the myristoyl group forms a bridge between Ca^{2+}-induced conformational changes in the C-terminal domain and the cyclase binding site in the N-terminal domain. In the GCAP1 activator state, residues in the cyclase binding site [see **Figure 4**, labeled residues in EF1, EF2 and EF3 (Peshenko et al., 2014)] are spatially close together and form particular contacts with RetGC that require close proximity between W94 and V77 (see arrow in **Figure 4**). In the Ca^{2+}-bound GCAP1 inhibitor state (**Figure 4**, right panel), Ca^{2+} is bound to EF2, EF3, and EF4 (orange circles in **Figure 4**). Ca^{2+}-binding to EF4 causes local conformational changes that in turn "tug" on the C-terminal helix which causes a slight reorientation of the N-terminal domain (EF1 and EF2) with respect to the C-terminal domain (EF3 and EF4). This domain swiveling causes key residues in EF3 at the domain interface (K85, W94, and K97) to move farther away from cyclase binding site residues in EF2 [F73, V77, and A78 (Peshenko et al., 2014)], which disrupts key contacts to RetGC that we suggest may be important for regulating cyclase activation.

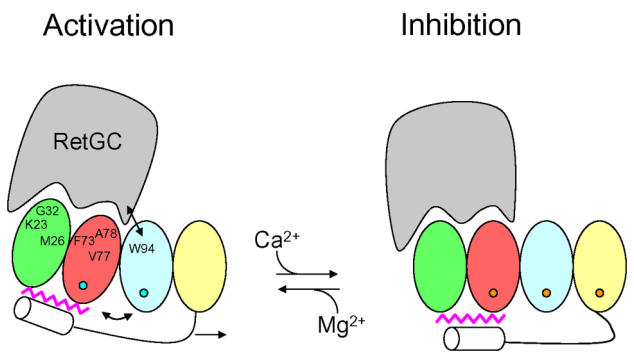

FIGURE 4 | Schematic diagram of retinal guanylyl cyclase activation by GCAP1. RetGC is shown in gray. The four EF-hands in GCAP1 are colored coded as defined in **Figure 1**, bound Mg^{2+} are depicted by blue circles, bound Ca^{2+} are orange circles, the C-terminal helix is white, and N-terminal myristoyl group is magenta. The labeled GCAP1 residues (K23, M26, G32, F73, V77, A78, and W94) have been implicated in the RetGC binding site (Lim et al., 2013; Peshenko et al., 2014). The binding of Ca^{2+} at EF4 causes conformational changes that are transmitted to the RetGC binding site by a Ca^{2+}-myristoyl tug mechanism (see arrows) modified from Peshenko et al. (2012).

CONCLUSION

N-terminal myristoylation serves to remodel the structure of NCS proteins as seen for recoverin, GCAP1 and NCS-1. Each NCS protein folds differently around the attached myristoyl group, which causes each NCS protein to adopt a unique structure. Most NCS proteins possess a functional Ca^{2+}-myristoyl switch that promotes their Ca^{2+}-induced membrane targeting. By contrast, GCAP1 contains a sequestered myristoyl group in both its Ca^{2+}-free and Ca^{2+}-bound states and undergoes rather small Ca^{2+}-induced protein conformational changes. Ca^{2+} binding to the fourth EF-hand in GCAP1 triggers conformational changes in the N-terminal domain via a Ca^{2+}-myristoyl tug mechanism that controls the exposure of residues in EF1 and EF2 that we propose may serve as a target binding site for guanylyl cyclase.

ACKNOWLEDGMENTS

This work was supported by grants to James B. Ames (EY012347) and Alexander M. Dizhoor (EY11522) from the National Institutes of Health.

REFERENCES

Ames, J. B., and Ikura, M. (2002). Structure and membrane-targeting mechanism of retinal Ca^{2+}-binding proteins, recoverin and GCAP-2. *Adv. Exp. Med. Biol.* 514, 333–348. doi: 10.1007/978-1-4615-0121-3_20

Ames, J. B., Dizhoor, A. M., Ikura, M., Palczewski, K., and Stryer, L. (1999). Three-dimensional structure of guanylyl cyclase activating protein-2, a calcium-sensitive modulator of photoreceptor guanylyl cyclases. *J. Biol. Chem.* 274, 19329–19337. doi: 10.1074/jbc.274.27.19329

Ames, J. B., Hendricks, K. B., Strahl, T., Huttner, I. G., Hamasaki, N., and Thorner, J. (2000). Structure and calcium-binding properties of Frq1, a novel calcium sensor in the yeast *Saccharomyces cerevisiae*. *Biochemistry* 39, 12149–12161. doi: 10.1021/bi0012890

Ames, J. B., Ishima, R., Tanaka, T., Gordon, J. I., Stryer, L., and Ikura, M. (1997). Molecular mechanics of calcium-myristoyl switches. *Nature* 389, 198–202. doi: 10.1038/38310

Ames, J. B., Lim, S., and Ikura, M. (2012). Molecular structure and target recognition of neuronal calcium sensor proteins. *Front. Mol. Neurosci.* 5:10. doi: 10.3389/fnmol.2012.00010

Ames, J. B., Porumb, T., Tanaka, T., Ikura, M., and Stryer, L. (1995a). Amino-terminal myristoylation induces cooperative calcium binding to recoverin. *J. Biol. Chem.* 270, 4526–4533. doi: 10.1074/jbc.270.9.4526

Ames, J. B., Tanaka, T., Ikura, M., and Stryer, L. (1995b). Nuclear magnetic resonance evidence for Ca(2+)-induced extrusion of the myristoyl group of recoverin. *J. Biol. Chem.* 270, 30909–30913. doi: 10.1074/jbc.270.52.30909

Ames, J. B., Tanaka, T., Stryer, L., and Ikura, M. (1996). Portrait of a myristoyl switch protein. *Curr. Opin. Struct. Biol.* 6, 432–438. doi: 10.1016/S0959-440X(96)80106-0

An, W. F., Bowlby, M. R., Betty, M., Cao, J., Ling, H. P., Mendoza, G., et al. (2000). Modulation of A-type potassium channels by a family of calcium sensors. *Nature* 403, 553–556. doi: 10.1038/35000592

Augustine, G. J., Santamaria, F., and Tanaka, K. (2003). Local calcium signaling in neurons. *Neuron* 40, 331–346. doi: 10.1016/S0896-6273(03)00639-1

Baehr, W., and Palczewski, K. (2007). Guanylate cyclase-activating proteins and retina disease. *Subcell. Biochem.* 45, 71–91. doi: 10.1007/978-1-4020-6191-2_4

Bernstein, H. G., Baumann, B., Danos, P., Diekmann, S., Bogerts, B., Gundelfinger, E. D., et al. (1999). Regional and cellular distribution of neural visinin-like protein

immunoreactivities (VILIP-1 and VILIP-3) in human brain. *J. Neurocytol.* 28, 655–662. doi: 10.1023/A:1007056731551

Berridge, M. J., Lipp, P., and Bootman, M. D. (2000). The versatility and universality of calcium signalling. *Nat. Rev. Mol. Cell Biol.* 1, 11–21. doi: 10.1038/35036035

Boehmerle, W., Splittgerber, U., Lazarus, M. B., McKenzie, K. M., Johnston, D. G., Austin, D. J., et al. (2006). Paclitaxel induces calcium oscillations via an inositol 1,4,5-trisphosphate receptor and neuronal calcium sensor 1-dependent mechanism. *Proc. Natl. Acad. Sci. U.S.A.* 103, 18356–18361. doi: 10.1073/pnas.0607240103

Bondarenko, V. A., Hayashi, F., Usukura, J., and Yamazaki, A. (2010). Involvement of rhodopsin and ATP in the activation of membranous guanylate cyclase in retinal photoreceptor outer segments (ROS-GC) by GC-activating proteins (GCAPs): a new model for ROS-GC activation and its link to retinal diseases. *Mol. Cell. Biochem.* 334, 125–139. doi: 10.1007/s11010-009-0323-y

Bourne, Y., Dannenberg, J., Pollmann, V. V., Marchot, P., and Pongs, O. (2001). Immunocytochemical localization and crystal structure of human frequenin (neuronal calcium sensor1). *J. Biol. Chem.* 276, 11949–11955. doi: 10.1074/jbc.M009373200

Braunewell, K. H., and Gundelfinger, E. D. (1999). Intracellular neuronal calcium sensor proteins: a family of EF-hand calcium-binding proteins in search of a function. *Cell Tissue Res.* 295, 1–12. doi: 10.1007/s004410051207

Braunewell, K. H., and Klein-Szanto, A. J. (2009). Visinin-like proteins (VSNLs): interaction partners and emerging functions in signal transduction of a subfamily of neuronal Ca^{2+} -sensor proteins. *Cell Tissue Res.* 335, 301–316. doi: 10.1007/s00441-008-0716-3

Burgoyne, R. D., and Haynes, L. P. (2012). Understanding the physiological roles of the neuronal calcium sensor proteins. *Mol. Brain* 5, 2. doi: 10.1186/1756-6606-5-2

Burgoyne, R. D., O'Callaghan, D. W., Hasdemir, B., Haynes, L. P., and Tepikin, A. V. (2004). Neuronal Ca^{2+}-sensor proteins: multitalented regulators of neuronal function. *Trends Neurosci.* 27, 203–209. doi: 10.1016/j.tins.2004.01.010

Burgoyne, R. D., and Weiss, J. L. (2001). The neuronal calcium sensor family of Ca^{2+}-binding proteins. *Biochem. J.* 353, 1–12. doi: 10.1042/0264-6021:3530001

Burns, M. E., and Baylor, D. A. (2002). Activation, deactivation, and adaptation in vertebrate photoreceptor cells. *Annu. Rev. Neurosci.* 24, 779–805. doi: 10.1146/annurev.neuro.24.1.779

Buxbaum, J. D., Choi, E. K., Luo, Y., Lilliehook, C., Crowley, A. C., Merriam, D. E., et al. (1998). Calsenilin: a calcium-binding protein that interacts with the presenilins and regulates the levels of a presenilin fragment. *Nat. Med.* 4, 1177–1181. doi: 10.1038/2673

Calvert, P. D., Klenchin, V. A., and Bownds, M. D. (1995). Rhodopsin kinase inhibition by recoverin. Function of recoverin myristoylation. *J. Biol. Chem.* 270, 24127–24129. doi: 10.1074/jbc.270.27.16147

Carrion, A. M., Link, W. A., Ledo, F., Mellstrom, B., and Naranjo, J. R. (1999). DREAM is a Ca^{2+}-regulated transcriptional repressor. *Nature* 398, 80–84. doi: 10.1038/18044

Chen, C. K., Inglese, J., Lefkowitz, R. J., and Hurley, J. B. (1995). Ca(2+)-dependent interaction of recoverin with rhodopsin kinase. *J. Biol. Chem.* 270, 18060–18066. doi: 10.1074/jbc.270.30.18060

Chen, C. K., Woodruff, M. L., Chen, F. S., Chen, Y., Cilluffo, M. C., Tranchina, D., et al. (2012). Modulation of mouse rod response decay by rhodopsin kinase and recoverin. *J. Neurosci.* 32, 15998–16006. doi: 10.1523/JNEUROSCI.1639-12.2012

Chen, C., Nakatani, K., and Koutalos, Y. (2003). Free magnesium concentration in salamander photoreceptor outer segments. *J. Physiol.* 553, 125–135. doi: 10.1113/jphysiol.2003.053280

Corbalan, S., and Gomez, J. C. (2014). Signaling through C2 domains: more than one lipid target. *Biochim. Biophys. Acta* doi: 10.1016/j.bbamem.2014.01.008 [Epub ahead of print].

Cox, J. A., Durussel, I., Comte, M., Nef, S., Nef, P., Lenz, S. E., et al. (1994). Cation binding and conformational changes in VILIP and NCS-1, two neuron-specific calcium-binding proteins. *J. Biol. Chem.* 269, 32807–32813.

Dell'Orco, D., Behnen, P., Linse, S., and Koch, K. W. (2010). Calcium binding, structural stability and guanylate cyclase activation in GCAP1 variants associated with human cone dystrophy. *Cell. Mol. Life Sci.* 67, 973–984. doi: 10.1007/s00018-009-0243-8

Dizhoor, A. M., Boikov, S. G., and Olshevskaya, E. V. (1998). Constitutive activation of photoreceptor guanylate cyclase by Y99C mutant of GCAP-1. Possible role in causing human autosomal dominant cone degeneration. *J. Biol. Chem.* 273, 17311–17314. doi: 10.1074/jbc.273.28.17311

Dizhoor, A. M., Chen, C. K., Olshevskaya, E., Sinelnikova, V. V., Phillipov, P., and Hurley, J. B. (1993). Role of the acylated amino terminus of recoverin in Ca(2+)-dependent membrane interaction. *Science* 259, 829–832. doi: 10.1126/science.8430337

Dizhoor, A. M., Ericsson, L. H., Johnson, R. S., Kumar, S., Olshevskaya, E., Zozulya, S., et al. (1992). The NH2 terminus of retinal recoverin is acylated by a small family of fatty acids. *J. Biol. Chem.* 267, 16033–16036.

Dizhoor, A. M., and Hurley, J. B. (1996). Inactivation of EF-hands makes GCAP-2 (p24) a constitutive activator of photoreceptor guanylyl cyclase by preventing a Ca^{2+}-induced "activator-to-inhibitor" transition. *J. Biol. Chem.* 271, 19346–19350. doi: 10.1074/jbc.271.32.19346

Dizhoor, A. M., Lowe, D. G., Olsevskaya, E. V., Laura, R. P., and Hurley, J. B. (1994). The human photoreceptor membrane guanylyl cyclase, RetGC, is present in outer segments and is regulated by calcium and a soluble activator. *Neuron* 12, 1345–1352. doi: 10.1016/0896-6273(94)90449-9

Dizhoor, A. M., Olshevskaya, E. V., and Peshenko, I. V. (2010). Mg^{2+}/Ca^{2+} cation binding cycle of guanylyl cyclase activating proteins (GCAPs): role in regulation of photoreceptor guanylyl cyclase. *Mol. Cell. Biochem.* 334, 117–124. doi: 10.1007/s11010-009-0328-6

Dizhoor, A. M., Olshevskaya, E. V., Henzel, W. J., Wong, S. C., Stults, J. T., Ankoudinova, I., et al. (1995). Cloning, sequencing and expression of a 24-kDa Ca^{2+}-binding protein activating photoreceptor guanylyl cyclase. *J. Biol. Chem.* 270, 25200–25206. doi: 10.1074/jbc.270.42.25200

Dizhoor, A. M., Ray, S., Kumar, S., Niemi, G., Spencer, M., Rrolley, D., et al. (1991). Recoverin: a calcium sensitive activator of retinal rod guanylate cyclase. *Science* 251, 915–918. doi: 10.1126/science.1672047

Duda, T., Fik, E., Venkataraman, V., Krishnan, R., Koch, K. W., and Sharma, R. K. (2005). The calcium-sensor guanylate cyclase activating protein type 2 specific site in rod outer segment membrane guanylate cyclase type 1. *Biochemistry* 44, 7336–7345. doi: 10.1021/bi050068x

Erickson, M. A., Lagnado, L., Zozulya, S., Neubert, T. A., Stryer, L., and Baylor, D. A. (1998). The effect of recombinant recoverin on the photoresponse of truncated rod photoreceptors. *Proc. Natl. Acad. Sci. U.S.A.* 95, 6474–6479. doi: 10.1073/pnas.95.11.6474

Ermilov, A. N., Olshevskaya, E. V., and Dizhoor, A. M. (2001). Instead of binding calcium, one of the EF-hand structures in guanylyl cyclase activating protein-2 is required for targeting photoreceptor guanylyl cyclase. *J. Biol. Chem.* 276, 48143–48148. doi: 10.1074/jbc.M107539200

Frins, S., Bonigk, W., Muller, F., Kellner, R., and Koch, K. W. (1996). Functional characterization of a guanylyl cyclase activating protein from vertebrate rods. Cloning, heterologous expression, and localization. *J. Biol. Chem.* 271, 8022–8027. doi: 10.1074/jbc.271.14.8022

Gifford, J. L., Walsh, M. P., and Vogel, H. J. (2007). Structures and metal-ion-binding properties of the Ca^{2+}-binding helix-loop-helix EF-hand motifs. *Biochem. J.* 405, 199–221. doi: 10.1042/BJ20070255

Gomez, M., De Castro, E., Guarin, E., Sasakura, H., Kuhara, A., Mori, I., et al. (2001). Ca^{2+} signaling via the neuronal calcium sensor-1 regulates associative learning and memory in *C. elegans. Neuron* 30, 241–248. doi: 10.1016/S0896-6273(01)00276-8

Gorczyca, W. A., Polans, A. S., Surgucheva, I. G., Subbaraya, I., Baehr, W., and Palczewski, K. (1995). Guanylyl cyclase activating protein. A calcium-sensitive regulator of phototransduction. *J. Biol. Chem.* 270, 22029–22036. doi: 10.1074/jbc.270.37.22029

Gorczyca, W. A., Van Hooser, J. P., and Palczewski, K. (1994). Nucleotide inhibitors and activators of retinal guanylyl cyclase. *Biochemistry* 33, 3217–3222. doi: 10.1021/bi00177a011

Gordon, J. I., Duronio, R. J., Rudnick, D. A., Adams, S. P., and Gokel, G. W. (1991). Protein myristoylation. *J. Biol. Chem.* 266, 8647–8650.

Gray-Keller, M. P., and Detwiler, P. B. (1994). The calcium feedback signal in the phototransduction cascade of vertebrate rods. *Neuron* 13, 849–861. doi: 10.1016/0896-6273(94)90251-8

Hama, H., Schnieders, E. A., Thorner, J., Takemoto, J. Y., and DeWald, D. B. (1999). Direct involvement of phosphatidylinositol 4-phosphate in secretion

in the yeast *Saccharomyces cerevisiae*. *J. Biol. Chem.* 274, 34294–34300. doi: 10.1074/jbc.274.48.34294

Hamasaki, N., Molchanova, T., Takeda, K., and Ames, J. B. (2004). Fission yeast homolog of neuronal calcium sensor-1 (Ncs1p) regulates sporulation and confers calcium tolerance. *J. Biol. Chem.* 279, 12744–12754. doi: 10.1074/jbc.M311895200

Hendricks, K. B., Wang, B. Q., Schnieders, E. A., and Thorner, J. (1999). Yeast homologue of neuronal frequenin is a regulator of phosphatidylinositol-4-OH kinase. *Nat. Cell Biol.* 1, 234–241. doi: 10.1038/12058

Hidaka, H., and Okazaki, K. (1993). Neurocalcin family: a novel calcium-binding protein abundant in bovine central nervous system. *Neurosci. Res.* 16, 73–77. doi: 10.1016/0168-0102(93)90074-Z

Hodgkin, A. L., and Nunn, B. J. (1988). Control of light-sensitive current in salamander rods. *J. Physiol.* 403, 439–471.

Hughes, R. E., Brzovic, P. S., Dizhoor, A. M., Klevit, R. E., and Hurley, J. B. (1998). Ca^{2+}-dependent conformational changes in bovine GCAP-2. *Protein Sci.* 7, 2675–2680. doi: 10.1002/pro.5560071222

Hughes, R. E., Brzovic, P. S., Klevit, R. E., and Hurley, J. B. (1995). Calcium-dependent solvation of the myristoyl group of recoverin. *Biochemistry* 34, 11410–11416. doi: 10.1021/bi00036a013

Huttner, I. G., Strahl, T., Osawa, M., King, D. S., Ames, J. B., and Thorner, J. (2003). Molecular interactions of yeast frequenin with Pik1. *J. Biol. Chem.* 278, 4862–4874. doi: 10.1074/jbc.M207920200

Hwang, J. Y., and Koch, K. W. (2002). Calcium- and myristoyl-dependent properties of guanylate cyclase-activating protein-1 and protein-2. *Biochemistry* 41, 13021–13028. doi: 10.1021/bi026618y

Hwang, J. Y., Lange, C., Helten, A., Hoppner-Heitmann, D., Duda, T., Sharma, R. K., et al. (2003). Regulatory modes of rod outer segment membrane guanylate cyclase differ in catalytic efficiency and Ca(2+)-sensitivity. *Eur. J. Biochem.* 270, 3814–3821. doi: 10.1046/j.1432-1033.2003.03770.x

Ikura, M. (1996). Calcium binding and conformational response in EF-hand proteins. *Trends Biochem. Sci.* 21, 14–17. doi: 10.1016/0968-0004(96)80879-6

Ikura, M., and Ames, J. B. (2006). Genetic polymorphism and protein conformational plasticity in the calmodulin superfamily: two ways to promote multifunctionality. *Proc. Natl. Acad. Sci. U.S.A.* 103, 1159–1164. doi: 10.1073/pnas.0508640103

Jiang, L., and Baehr, W. (2010). GCAP1 mutations associated with autosomal dominant cone dystrophy. *Adv. Exp. Med. Biol.* 664, 273–282. doi: 10.1007/978-1-4419-1399-9_31

Kapp, Y., Melnikov, S., Shefler, A., Jeromin, A., and Sagi, R. (2003). NCS-1 and phosphatidylinositol 4-kinase regulate IgE receptor-triggered exocytosis in cultured mast cells. *J. Immunol.* 171, 5320–5327.

Kawamura, S. (1993). Rhodopsin phosphorylation as a mechanism of cyclic GMP phosphodiesterase regulation by S-modulin. *Nature* 362, 855–857. doi: 10.1038/362855a0

Kawamura, S., and Murakami, M. (1991). Calcium-dependent regulation of cyclic GMP phosphodiesterase by a protein from frog retinal rods. *Nature* 349, 420–423. doi: 10.1038/349420a0

Klenchin, V. A., Calvert, P. D., and Bownds, M. D. (1995). Inhibition of rhodopsin kinase by recoverin. Further evidence for a negative feedback system in phototransduction. *J. Biol. Chem.* 270, 16147–16152. doi: 10.1074/jbc.270.41.24127

Kobayashi, M., Takamatsu, K., Saitoh, S., Miura, M., and Noguchi, T. (1992). Molecular cloning of hippocalcin, a novel calcium-binding protein of the recoverin family exclusively expressed in hippocampus [published erratum appears in *Biochem. Biophys. Res. Commun.* (1993). 196, 1017]. *Biochem. Biophys. Res. Commun.* 189, 511–517. doi: 10.1016/0006-291X(92)91587-G

Kobayashi, M., Takamatsu, K., Saitoh, S., and Noguchi, T. (1993). Myristoylation of hippocalcin is linked to its calcium-dependent membrane association properties. *J. Biol. Chem.* 268, 18898–18904.

Koch, K. W., and Stryer, L. (1988). Highly cooperative feedback control of retinal rod guanylate cyclase by calcium ions. *Nature* 334, 64–66. doi: 10.1038/334064a0

Komolov, K. E., Senin, I. I., Kovaleva, N. A., Christoph, M. P., Churumova, V. A., Grigoriev, I. I., et al. (2009). Mechanism of rhodopsin kinase regulation by recoverin. *J. Neurochem.* 110, 72–79. doi: 10.1111/j.1471-4159.2009.06118.x

Koutalos, Y., Nakatani, K., Tamura, T., and Yau, K. W. (1995). Characterization of guanylate cyclase activity in single retinal rod outer segments. *J. Gen. Physiol.* 106, 863–890. doi: 10.1085/jgp.106.5.863

Koutalos, Y., and Yau, K. W. (1996). Regulation of sensitivity in vertebrate rod photoreceptors by calcium. *Trends Neurosci.* 19, 73–81. doi: 10.1016/0166-2236(96)89624-X

Krylov, D. M., Niemi, G. A., Dizhoor, A. M., and Hurley, J. B. (1999). Mapping sites in guanylyl cyclase activating protein-1 required for regulation of photoreceptor membrane guanylyl cyclases. *J. Biol. Chem.* 274, 10833–10839. doi: 10.1074/jbc.274.16.10833

Ladant, D. (1995). Calcium and membrane binding properties of bovine neurocalcin expressed in *Escherichia coli*. *J. Biol. Chem.* 270, 3179–3185.

Laura, R. P., Dizhoor, A. M., and Hurley, J. B. (1996). The membrane guanylyl cyclase, retinal guanylyl cyclase-1, is activated through its intracellular domain. *J. Biol. Chem.* 271, 11646–11651. doi: 10.1074/jbc.271.20.11646

Li, C., Pan, W., Braunewell, K. H., and Ames, J. B. (2011). Structural analysis of Mg^{2+} and Ca^{2+} binding, myristoylation, and dimerization of the neuronal calcium sensor and visinin-like protein 1 (VILIP-1). *J. Biol. Chem.* 286, 6354–6366. doi: 10.1074/jbc.M110.173724

Lim, S., Peshenko, I. V., Dizhoor, A. M., and Ames, J. B. (2009). Effects of Ca^{2+}, Mg^{2+}, and myristoylation on guanylyl cyclase activating protein 1 structure and stability. *Biochemistry* 48, 850–862. doi: 10.1021/bi801897p

Lim, S., Peshenko, I. V., Dizhoor, A. M., and Ames, J. B. (2013). Structural insights for activation of retinal guanylate cyclase by GCAP1. *PLoS ONE* 8:e81822. doi: 10.1371/journal.pone.0081822

Lim, S., Strahl, T., Thorner, J., and Ames, J. B. (2011). Structure of a Ca^{2+}- myristoyl switch protein that controls activation of a phosphatidylinositol 4-kinase in fission yeast. *J. Biol. Chem.* 286, 12565–12577. doi: 10.1074/jbc.M110.208868

Lowe, D. G., Dizhoor, A. M., Liu, K., Gu, Q., Spencer, M., Laura, R., et al. (1995). Cloning and expression of a second photoreceptor-specific membrane retina guanylyl cyclase (RetGC), RetGC-2. *Proc. Natl. Acad. Sci. U.S.A.* 6, 5535–5539. doi: 10.1073/pnas.92.12.5535

Makino, C. L., Dodd, R. L., Chen, J., Burns, M. E., Roca, A., Simon, M. I., et al. (2004). Recoverin regulates light-dependent phosphodiesterase activity in retinal rods. *J. Gen. Physiol.* 123, 729–741. doi: 10.1085/jgp.200308994

Makino, C. L., Peshenko, I. V., Wen, X. H., Olshevskaya, E. V., Barrett, R., and Dizhoor, A. M. (2008). A role for GCAP2 in regulating the photoresponse. Guanylyl cyclase activation and rod electrophysiology in GUCA1B knock-out mice. *J. Biol. Chem.* 283, 29135–29143. doi: 10.1074/jbc.M804445200

Makino, C. L., Wen, X. H., Olshevskaya, E. V., Peshenko, I. V., Savchenko, A. B., and Dizhoor, A. M. (2012). A role for GCAP2 in regulating the photoresponse. Guanylyl cyclase activation and rod electrophysiology in GUCA1B knock-out mice. *PLoS ONE* 7:e47637. doi: 10.1371/journal.pone.0047637

Matthews, H. R., and Fain, G. L. (2003). The effect of light on outer segment calcium in salamander rods. *J. Physiol.* 552, 763–776. doi: 10.1113/jphysiol.2003.050724

McFerran, B. W., Graham, M. E., and Burgoyne, R. D. (1998). Neuronal Ca^{2+} sensor 1, the mammalian homologue of frequenin, is expressed in chromaffin and PC12 cells and regulates neurosecretion from dense-core granules. *J. Biol. Chem.* 273, 22768–22772. doi: 10.1074/jbc.273.35.22768

Mendez, A., Burns, M. E., Izabela, S., Dizhoor, A. M., Baehr, W., Palczewski, K., et al. (2001). Role of guanylate cyclase-activating proteins (GCAPs) in setting the flash sensitivity of rod photoreceptors. *Proc. Natl. Acad. Sci. U.S.A.* 98, 9948–9953. doi: 10.1073/pnas.171308998

Moncrief, N. D., Kretsinger, R. H., and Goodman, M. (1990). Evolution of EF-hand calcium-modulated proteins. *J. Mol. Evol.* 30, 522–562. doi: 10.1007/BF02101108

Nakamura, T. Y., Pountney, D. J., Ozaita, A., Nandi, S., Ueda, S., Rudy, B., et al. (2001). A role for frequenin, a Ca^{2+}-binding protein, as a regulator of Kv4 K^{+}-currents. *Proc. Natl. Acad. Sci. U.S.A.* 98, 12808–12813. doi: 10.1073/pnas.221168498

Nalefski, E. A., and Falke, J. J. (1996). The C2 domain calcium-binding motif: structural and functional diversity. *Protein Sci.* 5, 2375–2390. doi: 10.1002/pro.5560051201

O'Callaghan, D. W., Tepikin, A. V., and Burgoyne, R. D. (2003). Dynamics and calcium sensitivity of the Ca^{2+}/myristoyl switch protein hippocalcin in living cells. *J. Cell Biol.* 163, 715–721. doi: 10.1083/jcb.200306042

Olshevskaya, E. V., Boikov, S., Ermilov, A., Krylov, D., Hurley, J. B., and Dizhoor, A. M. (1999a). Mapping functional domains of the guanylate cyclase regulator protein, GCAP-2. *J. Biol. Chem.* 274, 10823–10832. doi: 10.1074/jbc.274.16.10823

Olshevskaya, E. V., Ermilov, A. N., and Dizhoor, A. M. (1999b). Dimerization of guanylyl cyclase-activating protein. *J. Biol. Chem.* 274, 25583–25587. doi: 10.1074/jbc.274.36.25583

Olshevskaya, E. V., Calvert, P. D., Woodruff, M. L., Peshenko, I. V., Savchenko, A. B., Makino, C. L., et al. (2004). The Y99C mutation in guanylyl cyclase-activating protein 1 increases intracellular Ca^{2+} and causes photoreceptor degeneration in transgenic mice. *J. Neurosci.* 24, 6078–6085. doi: 10.1523/JNEUROSCI.0963-04.2004

Olshevskaya, E. V., Hughes, R. E., Hurley, J. B., and Dizhoor, A. M. (1997). Calcium binding, but not a calcium-myristoyl switch, controls the ability of guanylyl cyclase-activating protein GCAP-2 to regulate photoreceptor guanylyl cyclase. *J. Biol. Chem.* 272, 14327–14333. doi: 10.1074/jbc.272.22.14327

Olshevskaya, E. V., Peshenko, I. V., Savchenko, A. B., and Dizhoor, A. M. (2012). Retinal guanylyl cyclase isozyme 1 is the preferential in vivo target for constitutively active GCAP1 mutants causing congenital degeneration of photoreceptors. *J. Neurosci.* 32, 7208–7217. doi: 10.1523/JNEUROSCI.0976-12.2012

Palczewski, K., Polans, A. S., Baehr, W., and Ames, J. B. (2000). Ca(2+)-binding proteins in the retina: structure, function, and the etiology of human visual diseases. *Bioessays* 22, 337–350. doi: 10.1002/(SICI)1521-1878(200004)22:4<337::AID-BIES4>3.0.CO;2-Z

Palczewski, K., Sokal, I., and Baehr, W. (2004). Guanylate cyclase-activating proteins: structure, function, and diversity. *Biochem. Biophys. Res. Commun.* 322, 1123–1130. doi: 10.1016/j.bbrc.2004.07.122

Palczewski, K., Subbaraya, I., Gorczyca, W. A., Helekar, B. S., Ruiz, C. C., Ohguro, H., et al. (1994). Molecular cloning and characterization of retinal photoreceptor guanylyl cyclase-activating protein. *Neuron* 13, 395–404. doi: 10.1016/0896-6273(94)90355-7

Payne, A. M., Downes, S. M., Bessant, D. A., Taylor, R., Holder, G. E., Warren, M. J., et al. (1998). A mutation in guanylate cyclase activator 1A (GUCA1A) in an autosomal dominant cone dystrophy pedigree mapping to a new locus on chromosome 6p21.1. *Hum. Mol. Genet.* 7, 273–277. doi: 10.1093/hmg/7.2.273

Peshenko, I. V., and Dizhoor, A. M. (2004). Guanylyl cyclase-activating proteins (GCAPs) are Ca^{2+}/Mg^{2+} sensors: implications for photoreceptor guanylyl cyclase (RetGC) regulation in mammalian photoreceptors. *J. Biol. Chem.* 279, 16903–16906. doi: 10.1074/jbc.C400065200

Peshenko, I. V., and Dizhoor, A. M. (2006). Ca^{2+} and Mg^{2+} binding properties of GCAP-1. Evidence that Mg^{2+}-bound form is the physiological activator of photoreceptor guanylyl cyclase. *J. Biol. Chem.* 281, 23830–23841. doi: 10.1074/jbc.M600257200

Peshenko, I. V., and Dizhoor, A. M. (2007). Activation and inhibition of photoreceptor guanylyl cyclase by guanylyl cyclase activating protein 1 (GCAP-1): the functional role of Mg^{2+}/Ca^{2+} exchange in EF-hand domains. *J. Biol. Chem.* 282, 21645–21652. doi: 10.1074/jbc.M702368200

Peshenko, I. V., Olshevskaya, E. V., and Dizhoor, A. M. (2004). Ca(2+)-dependent conformational changes in guanylyl cyclase-activating protein 2 (GCAP-2) revealed by site-specific phosphorylation and partial proteolysis. *J. Biol. Chem.* 279, 50342–50349. doi: 10.1074/jbc.M408683200

Peshenko, I. V., Olshevskaya, E. V., Lim, S., Ames, J. B., and Dizhoor, A. M. (2012). Calcium-myristoyl Tug is a new mechanism for intramolecular tuning of calcium sensitivity and target enzyme interaction for guanylyl cyclase-activating protein 1: dynamic connection between N-fatty acyl group and EF-hand controls calcium sensitivity. *J. Biol. Chem.* 287, 13972–13984. doi: 10.1074/jbc.M112.341883

Peshenko, I. V., Olshevskaya, E. V., Lim, S., Ames, J. B., and Dizhoor, A. M. (2014). Identification of target binding site in photoreceptor guanylyl cyclase activating protein 1 (GCAP1). *J. Biol. Chem.* 289. doi: 10.1074/jbc.M113.540716 [Epub ahead of print].

Peshenko, I. V., Olshevskaya, E. V., Yao, S., Ezzeldin, H. H., Pittler, S. J., and Dizhoor, A. M. (2010). Activation of retinal guanylyl cyclase RetGC1 by GCAP1: stoichiometry of binding and effect of new LCA-related mutations. *Biochemistry* 49, 709–717. doi: 10.1021/bi901495y

Polans, A. S., Buczylko, J., Crabb, J., and Palczewski, K. (1991). A photoreceptor calcium binding protein is recognized by autoantibodies obtained from patients with cancer-associated retinopathy. *J. Cell Biol.* 112, 981–989. doi: 10.1083/jcb.112.5.981

Pongs, O., Lindemeier, J., Zhu, X. R., Theil, T., Engelkamp, D., Krah-Jentgens, I., et al. (1993). Frequenin-a novel calcium-binding protein that modulates synaptic efficacy. *Neuron* 11, 15–28. doi: 10.1016/0896-6273(93)90267-U

Pugh, E. N., Duda, T., Sitaramayya, A., and Sharma, R. K. (1997). Photoreceptor guanylate cyclases: a review. *Biosci. Rep.* 17, 429–473. doi: 10.1023/A:1027365520442

Pugh, E. N., Nikonov, S., and Lamb, T. D. (1999). Molecular mechanisms of vertebrate photoreceptor light adaptation. *Curr. Opin. Neurobiol.* 9, 410–418. doi: 10.1016/S0959-4388(99)80062-2

Ramamurthy, V., Tucker, C., Wilkie, S. E., Daggett, V., Hunt, D. M., and Hurley, J. B. (2001). Interactions within the coiled-coil domain of RetGC-1 guanylyl cyclase are optimized for regulation rather than for high affinity. *J. Biol. Chem.* 276, 26218–26229. doi: 10.1074/jbc.M010495200

Sakurai, K., Chen, J., and Kefalov, V. J. (2011). Role of guanylyl cyclase modulation in mouse cone phototransduction. *J. Neurosci.* 31, 7991–8000. doi: 10.1523/JNEUROSCI.6650-10.2011

Sampath, A. P., Matthews, H. R., Cornwall, M. C., and Fain, G. L. (1998). Bleached pigment produces a maintained decrease in outer segment Ca^{2+} in salamander rods. *J. Gen. Physiol.* 111, 53–64. doi: 10.1085/jgp.111.1.53

Schroder, T., Lilie, H., and Lange, C. (2011). The myristoylation of guanylate cyclase-activating protein-2 causes an increase in thermodynamic stability in the presence but not in the absence of Ca^{2+}. *Protein Sci.* 20, 1155–1165. doi: 10.1002/pro.643

Semple-Rowland, S. L., Gorczyca, W. A., Buczylko, J., Helekar, B. S., Ruiz, C. C., Subbaraya, I., et al. (1996). Expression of GCAP1 and GCAP2 in the retinal degeneration (rd) mutant chicken retina. *FEBS Lett.* 385, 47–52. doi: 10.1016/0014-5793(96)00345-6

Sokal, I., Li, N., Klug, C. S., Filipek, S., Hubbell, W. L., Baehr, W., et al. (2001). Calcium-sensitive regions of GCAP1 as observed by chemical modifications, fluorescence, and EPR spectroscopies. *J. Biol. Chem.,* 276, 43361–43373. doi: 10.1074/jbc.M103614200

Sokal, I., Li, N., Surgucheva, I., Warren, M. J., Payne, A. M., Bhattacharya, S. S., et al. (1998). GCAP1 (Y99C) mutant is constitutively active in autosomal dominant cone dystrophy. *Mol. Cell* 2, 129–133. doi: 10.1016/S1097-2765(00)80121-5

Spilker, C., Dresbach, T., and Braunewell, K. H. (2002). Reversible translocation and activity-dependent localization of the calcium-myristoyl switch protein VILIP-1 to different membrane compartments in living hippocampal neurons. *J. Neurosci.* 22, 7331–7339.

Spilker, C., Gundelfinger, E. D., and Braunewell, K. H. (1997). Calcium- and myristoyl-dependent subcellular localization of the neuronal calcium-binding protein VILIP in transfected PC12 cells. *Neurosci. Lett.* 225, 126–128. doi: 10.1016/S0304-3940(97)00201-2

Stephen, R., Bereta, G., Golczak, M., Palczewski, K., and Sousa, M. C. (2007). Stabilizing function for myristoyl group revealed by the crystal structure of a neuronal calcium sensor, guanylate cyclase-activating protein 1. *Structure* 15, 1392–1402. doi: 10.1016/j.str.2007.09.013

Stephen, R., Filipek, S., Palczewski, K., and Sousa, M. C. (2008). Ca^{2+} -dependent regulation of phototransduction. *Photochem. Photobiol.* 84, 903–910. doi: 10.1111/j.1751-1097.2008.00323.x

Strahl, T., Grafelmann, B., Dannenberg, J., Thorner, J., and Pongs, O. (2003). Conservation of regulatory function in calcium-binding proteins: human frequenin (neuronal calcium sensor-1) associates productively with yeast phosphatidylinositol 4-kinase isoform, Pik1. *J. Biol. Chem.* 278, 49589–49599. doi: 10.1074/jbc.M309017200

Strahl, T., Huttner, I. G., Lusin, J. D., Osawa, M., King, D., Thorner, J., et al. (2007). Structural insights into activation of phosphatidylinositol 4-kinase (Pik1) by yeast frequenin (Frq1). *J. Biol. Chem.* 282, 30949–30959. doi: 10.1074/jbc.M705499200

Strissel, K. J., Lishko, P. V., Trieu, L. H., Kennedy, M. J., Hurley, J. B., and Arshavsky, V. Y. (2005). Recoverin undergoes light-dependent intracellular translocation in rod photoreceptors. *J. Biol. Chem.* 280, 29250–29255. doi: 10.1074/jbc.M501789200

Subramanian, L., and Polans, A. S. (2004). Cancer-related diseases of the eye: the role of calcium and calcium-binding proteins. *Biochem. Biophys. Res. Commun.* 322, 1153–1165. doi: 10.1016/j.bbrc.2004.07.109

Tanaka, T., Ames, J. B., Harvey, T. S., Stryer, L., and Ikura, M. (1995). Sequestration of the membrane-targeting myristoyl group of recoverin in the calcium-free state. *Nature* 376, 444–447. doi: 10.1038/376444a0

Theisgen, S., Scheidt, H. A., Magalhaes, A., Bonagamba, T. J., and Huster, D. (2010). A solid-state NMR study of the structure and dynamics of the myristoylated N-terminus of the guanylate cyclase-activating protein-2. *Biochim. Biophys. Acta* 1798, 266–274. doi: 10.1016/j.bbamem.2009.06.028

Theisgen, S., Thomas, L., Schroder, T., Lange, C., Kovermann, M., Balbach, J., et al. (2011). The presence of membranes or micelles induces structural changes of the

myristoylated guanylate-cyclase activating protein-2. *Eur. Biophys. J.* 40, 565–576. doi: 10.1007/s00249-011-0680-9

Tzingounis, A. V., Kobayashi, M., Takamatsu, K., and Nicoll, R. A. (2007). Hippocalcin gates the calcium activation of the slow after hyperpolarization in hippocampal pyramidal cells. *Neuron* 53, 487–493. doi: 10.1016/j.neuron.2007.01.011

Valentine, K. G., Mesleh, M. F., Opella, S. J., Ikura, M., and Ames, J. B. (2003). Structure, topology, and dynamics of myristoylated recoverin bound to phospholipid bilayers. *Biochemistry* 42, 6333–6340. doi: 10.1021/bi0206816

Walch-Solimena, C., and Novick, P. (1999). The yeast phosphatidylinositol-4-OH kinase Pik1 regulates secretion at the Golgi. *Nat. Cell Biol.* 1, 523–525. doi: 10.1038/70319

Weiss, J. L., Archer, D. A., and Burgoyne, R. D. (2000). Neuronal Ca^{2+} sensor-1/frequenin functions in an autocrine pathway regulating Ca^{2+} channels in bovine adrenal chromaffin cells. *J. Biol. Chem.* 275, 40082–40087. doi: 10.1074/jbc.M008603200

Weiss, J. L., and Burgoyne, R. D. (2002). "Neuronal calcium sensor proteins," in *Handbook of Cell Signaling*, Vol. 2, ed. R. Bradshaw (San Diego: Academic Press), 79–82.

Weiss, J. L., Hui, H., and Burgoyne, R. D. (2010). Neuronal calcium sensor-1 regulation of calcium channels, secretion, and neuronal outgrowth. *Cell. Mol. Neurobiol.* 30, 1283–1292. doi: 10.1007/s10571-010-9588-7

Wilkie, S. E., Li, Y., Deery, E. C., Newbold, R. J., Garibaldi, D., Bateman, J. B., et al. (2001). Identification and functional consequences of a new mutation (E155G) in the gene for GCAP1 that causes autosomal dominant cone dystrophy. *Am. J. Hum. Genet.* 69, 471–480. doi: 10.1086/323265

Wilkie, S. E., Newbold, R. J., Deery, E., Walker, C. E., Stinton, I., Ramamurthy, V., et al. (2000). Functional characterization of missense mutations at codon 838 in retinal guanylate cyclase correlates with disease severity in patients with autosomal dominant cone-rod dystrophy. *Hum. Mol. Genet.* 9, 3065–3073. doi: 10.1093/hmg/9.20.3065

Woodruff, M. L., Olshevskaya, E. V., Savchenko, A. B., Peshenko, I. V., Barrett, R., Bush, R. A., et al. (2007). Constitutive excitation by Gly90Asp rhodopsin rescues rods from degeneration caused by elevated production of cGMP in the dark. *J. Neurosci.* 27, 8805–8815. doi: 10.1523/JNEUROSCI.2751-07.2007

Woodruff, M. L., Sampath, A. P., Mathews, H. R., Krasnoperova, N. V., Lem, J., and Fain, G. L. (2002). Measurement of cytoplasmic calcium concentration in the rods of wild-type and transducin knock-out mice. *J. Physiol.* 542, 843–854. doi: 10.1113/jphysiol.2001.013987

Xu, X., Ishima, R., and Ames, J. B. (2011). Conformational dynamics of recoverin's Ca^{2+}-myristoyl switch probed by 15N NMR relaxation dispersion and chemical shift analysis. *Proteins* 79, 1910–1922. doi: 10.1002/prot.23014

Zozulya, S., and Stryer, L. (1992). Calcium-myristoyl protein switch. *Proc. Natl. Acad. Sci. U.S.A.* 89, 11569–11573. doi: 10.1073/pnas.89.23.11569

Conflict of Interest Statement: The authors declare that the research was conducted in the absence of any commercial or financial relationships that could be construed as a potential conflict of interest.

Received: 27 January 2014; paper pending published: 17 February 2014; accepted: 27 February 2014; published online: 17 March 2014.

Citation: Lim S, Dizhoor AM and Ames JB (2014) Structural diversity of neuronal calcium sensor proteins and insights for activation of retinal guanylyl cyclase by GCAP1. Front. Mol. Neurosci. 7:19. doi: 10.3389/fnmol.2014.00019

This article was submitted to the journal Frontiers in Molecular Neuroscience.

frontiers in
MOLECULAR NEUROSCIENCE

REVIEW ARTICLE
published: 26 March 2014
doi: 10.3389/fnmol.2014.00021

ROS-GC interlocked Ca^{2+}-sensor S100B protein signaling in cone photoreceptors: review

Rameshwar K. Sharma[1]*, Clint L. Makino[2]*, David Hicks[3] and Teresa Duda[1]*

[1] *Research Divisions of Biochemistry and Molecular Biology, The Unit of Regulatory and Molecular Biology, Salus University, Elkins Park, PA, USA*
[2] *Department of Ophthalmology, Massachusetts Eye and Ear Infirmary, Harvard Medical School, Boston, MA, USA*
[3] *Department of Neurobiology of Rhythms, Institute for Cellular and Integrative Neuroscience, CNRS UPR 3212, Strasbourg, France*

Edited by:
Wolfgang Baehr, University of Utah, USA

Reviewed by:
Karl-Wilhelm Koch, Carl von Ossietzky University Oldenburg, Germany
Wolfgang Baehr, University of Utah, USA

****Correspondence:***
Rameshwar K. Sharma and Teresa Duda, Research Divisions of Biochemistry and Molecular Biology, The Unit of Regulatory and Molecular Biology, Salus University, 8360 Old York Road, Elkins Park, PA 19027, USA
e-mail: rsharma@salus.edu; tduda@salus.edu;
Clint L. Makino, Department of Ophthalmology, Massachusetts Eye and Ear Infirmary, Harvard Medical School, 234 Charles Street, Boston, MA 02114, USA
e-mail: Clint_Makino@meei.harvard.edu

Photoreceptor rod outer segment membrane guanylate cyclase (ROS-GC) is central to visual transduction; it generates cyclic GMP, the second messenger of the photon signal. Photoexcited rhodopsin initiates a biochemical cascade that leads to a drop in the intracellular level of cyclic GMP and closure of cyclic nucleotide gated ion channels. Recovery of the photoresponse requires resynthesis of cyclic GMP, typically by a pair of ROS-GCs, 1 and 2. In rods, ROS-GCs exist as complexes with guanylate cyclase activating proteins (GCAPs), which are Ca^{2+}-sensing elements. There is a light-induced fall in intracellular Ca^{2+}. As Ca^{2+} dissociates from GCAPs in the 20–200 nM range, ROS-GC activity rises to quicken the photoresponse recovery. GCAPs then progressively turn down ROS-GC activity as Ca^{2+} and cyclic GMP levels return to baseline. To date, GCAPs mediate the only known mechanism of ROS-GC regulation in the photoreceptors. However, in mammalian cone outer segments, cone synapses and ON bipolar cells, another Ca^{2+} sensor protein, S100B, complexes with ROS-GC1 and senses the Ca^{2+} signal with a $K_{1/2}$ of 400 nM. Unlike GCAPs, S100B stimulates ROS-GC activity when Ca^{2+} is bound. Thus, the ROS-GC system in cones functions as a Ca^{2+} bimodal switch; with rising intracellular Ca^{2+}, its activity is first turned down by GCAPs and then turned up by S100B. This presentation provides a historical perspective on the role of S100B in the photoreceptors, offers a pictorial model for the "bimodal" operation of the ROS-GC switch and projects future tasks that are needed to understand its operation. Some accounts of this review have been adopted from the original publications of these authors.

Keywords: ROS-GC guanylate cyclase, cyclic GMP, phototransduction, cones, S100B

INTRODUCTION

A seminal observation in the field of visual transduction was that a soluble bovine rod outer segment (ROS) fraction kicked the catalytic activity of a photoreceptor guanylate cyclase into high gear in the absence of Ca^{2+} (Koch and Stryer, 1988). The structure of this guanylate cyclase was believed to be composed of "separate regulatory and catalytic subunits" (Stryer, 1991); however, elucidating the molecular identity of the guanylate cyclase and its regulator turned out to be quite complicated. There were reports that guanylate cyclase possessed a molecular mass of 67 kDa and was nitric oxide sensitive (Horio and Murad, 1991a,b). Yet another report claimed to have solved the molecular structure of the photoreceptor retGC, the human retinal guanylate cyclase (Shyjan et al., 1992).

Later, the true photoreceptor ROS-guanylate cyclase (ROS-GC) was purified directly from bovine outer segments (Margulis et al., 1993) and its protein-sequence-based molecular cloning, structure, and function were established (Goraczniak et al., 1994). ROS-GC had a calculated molecular mass of 120,360 Da, a value similar to 112,000 Da reported earlier for a bovine (Koch, 1991) and 110,000–115,000 Da for toad photoreceptor guanylate cyclase (Hayashi and Yamazaki, 1991). Unlike the other known membrane guanylate cyclases, atrial natriuretic factor receptor guanylate cyclase (ANF-RGC; Paul et al., 1987; Sharma, 1988; Chinkers et al., 1989; Duda et al., 1991) and type C natriuretic peptide CNP-RGC guanylate cyclase (Koller et al., 1991; Duda et al., 1993), ROS-GC was not hormonally responsive (Goraczniak et al., 1994). It thus represented a new subfamily of the membrane guanylate cyclases. Further study revealed that ROS-GC was not composed of "separate regulatory and catalytic subunits", it was not nitric oxide sensitive nor was its structure identical to retGC. The RetGC structure was eventually revised to match that of bovine ROS-GC (Accession number M92432).

Meanwhile, groups from the U.S. and the former Soviet Union joined forces to describe a newly purified Ca^{2+} binding protein, recoverin, that appeared to regulate guanylate cyclase activity (Dizhoor et al., 1991) and adhere to the functional description of Koch and Stryer (Koch and Stryer, 1988). It was therefore considered a Ca^{2+} modulator of ROS-GC; hence, named recoverin "because it promotes recovery of the dark state" (Dizhoor et al., 1991). However, ever purer preparations of recoverin showed a disturbing decline in guanylate cyclase stimulation. It became evident that recoverin was not the sought after regulator of guanylate cyclase activity and the initial conclusion was withdrawn (Hurley et al., 1993). Instead, recoverin exerted Ca^{2+}-dependent control over the phosphorylation of photoexcited rhodopsin by rhodopsin

kinase (Chen et al., 1995; Klenchin et al., 1995; Kawamura, 1999). At almost the same time, two separate groups discovered similar but distinct guanylate cyclase activating proteins (GCAPs), GCAP1 (Palczewski et al., 1994; Subbaraya et al., 1994; Gorczyca et al., 1995; Frins et al., 1996) and GCAP2 (Dizhoor et al., 1995). These GCAPs did indeed stimulate ROS-GC activity as described by Koch and Stryer (1988).

Recombinant ROS-GC expressed in a heterologous system of COS cells responded at 10 nM $[Ca^{2+}]_i$ to GCAP1 stimulation in a dose-dependent manner (Duda et al., 1996b). The stimulation was inhibited cooperatively by free Ca^{2+} with a $K_{1/2}$ of 100 nM. Under identical conditions, GCAP1 had no effect on recombinant ANF-RGC, the peptide hormone receptor guanylate cyclase. An important characteristic of the transduction system was that GCAP remained bound to ROS-GC at low and high Ca^{2+} levels, consistent with physiological observations (Koutalos et al., 1995). Similar reconstitution studies established GCAP2 as another Ca^{2+}-sensing subunit of ROS-GC (Dizhoor et al., 1995; Gorczyca et al., 1995). When a second ROS-GC was subsequently discovered in the bovine retina, termed Ret-GC2 in human retina (Lowe et al., 1995), it was named ROS-GC2 to distinguish it from the original ROS-GC which was renamed as ROS-GC1 (Goraczniak et al., 1997). It became clear that a Ca^{2+}-modulated system, composed of a pair of ROS-GCs and a pair of GCAPs, subserves phototransduction in the outer segments of photoreceptors. This conclusion was supported at the physiological level by the studies with the double knockout ROS-GC1/ROS-GC2 mouse model (Baehr et al., 2007). Rods and cones were non-functional, excluding the presence of a third guanylate cyclase linked with phototransduction.

Thus ROS-GCs are related to peptide hormone receptor guanylate cyclases but they do not respond to extracellular ligands. Instead, they exist in stable complexes with GCAPs that sense changes in internal $[Ca^{2+}]$. The feature that incrementing $[Ca^{2+}]_i$ progressively reduces ROS-GC1 catalytic activity was academically challenging because such a mechanism had never been observed before for any of the members of the guanylate cyclase family. All other members were solely stimulated by their effector ligands, natriuretic peptide hormones, at their extracellular domains. The molecular properties of this remarkable system and the role that the system plays in phototransduction are described in greater depth in Pugh et al. (1997), Sharma and Duda (2012).

DISCOVERY OF CD-GCAP MEANT THAT ROS-GC1 COULD OPERATE AS A Ca^{2+} BIMODAL TRANSDUCTION SWITCH

Contemporaneous with the discovery of GCAPs that stimulated ROS-GC1 at low Ca^{2+}, a post-mitochondrial 100,000 *g* supernatant fraction from retina was found to stimulate recombinant ROS-GC at high Ca^{2+} by as much as 25-fold (Pozdnyakov et al., 1995). The new factor was a peptide with an apparent molecular weight of 6–7 kDa protein that oligomerized to a functional size of 40 kDa. It stimulated native and recombinant ROS-GC with a $K_{1/2}$ for Ca^{2+} of 2 μM with biochemical characteristics typical of a Ca^{2+}-binding protein. To distinguish it from the just-discovered GCAPs, the new factor was named CD-GCAP (Ca^{2+}-dependent guanylate cyclase activator protein; Pozdnyakov et al., 1995).

The capacity for ROS-GC to couple to GCAPs or to CD-GCAP allows for a cell to sculpt its response to Ca^{2+}. Depending upon the cell's specific needs, it could express either GCAP or CD-GCAP to stimulate cyclic GMP synthesis at low (tens of nanomolar) or at high (sub-micromolar) ranges of $[Ca^{2+}]$. An even more exciting possibility exists for the simultaneous expression of both Ca^{2+}-regulatory subunits in the same cell. ROS-GC could then operate as a Ca^{2+}-bimodal transduction switch, stimulated at low and at high free $[Ca^{2+}]$ by Ca^{2+} -free GCAPs and by Ca^{2+}-bound S100B, respectively. A theoretical Ca^{2+}-BIMODAL ROS-GC transduction model embodying these features was proposed (**Figure 1**). Bimodal Ca^{2+} sensing could be an elegant general mechanism for neural transmission.

CD-GCAP IS AN S100 PROTEIN

The first indication that CD-GCAP might be related to S100 proteins was that it appeared as a 6–7 kDA Ca^{2+}-binding protein on SDS-PAGE (Pozdnyakov et al., 1995). S100 proteins are known to run anomalously as 6–7 kDa proteins in SDS-PAGE even though their subunit molecular weight, calculated from amino acid (aa) sequence, is about 10.5 kDa (Kligman and Marshak, 1985). Additional evidence for the structural similarity of CD-GCAP to S100 emerged from mass spectrometry analysis (Pozdnyakov et al., 1997). The fragmented molecular masses of 10,580 Da for CD-GCAP and 10,582 Da for S100B were essentially the same. Tryptic digests also yielded indistinguishable fragmentation patterns. Finally, bovine CD-GCAP and bovine S100B

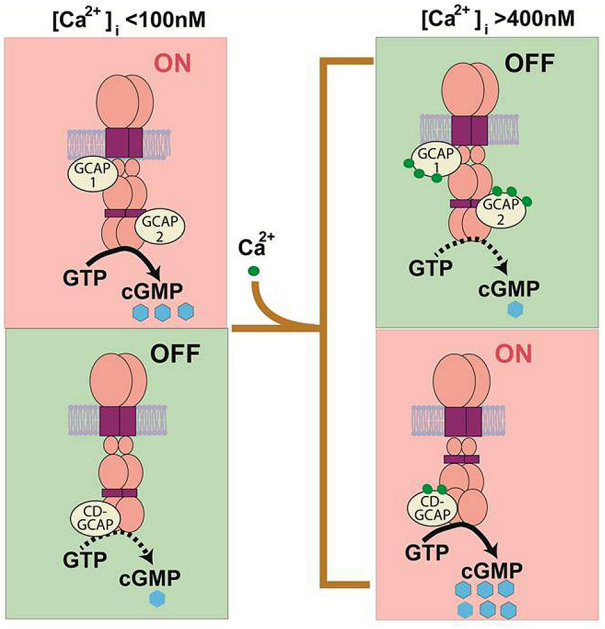

FIGURE 1 | Original theoretical Ca^{2+} bimodal ROS-GC transduction model. In the absence of bound Ca^{2+}, GCAPs 1 and 2 boost ROS-GC1 catalytic activity. In contrast, S100B boosts ROS-GC1 activity in the Ca^{2+}-bound state. GCAPs sense $[Ca^{2+}]_i$ < 200 nM while S100B senses $[Ca^{2+}]_i$ > 200 nM. Thus in the GCAPs operational mode the S100B switch is "OFF" and in the S100B operational mode the GCAP switch is "OFF" (Upgraded with permission from Sharma, 2010; Sharma and Duda, 2012).

were cloned and their predicted primary protein structures were identical (Pozdnyakov et al., 1997).

Despite being structurally identical proteins, biochemical analyses revealed two surprising functional discrepancies. As expected, S100A1–S100B and S100ββ dimer (S100B) from commercial sources stimulated cloned recombinant and wt-photoreceptor ROS-GC (Duda et al., 1996a; Margulis et al., 1996). But the V_{max} of ROS-GC was about 50% higher when activated by CD-GCAP than when activated by commercially obtained S100B. In addition, the commercial S100B required about 20-times more calcium (3.2×10^{-5} M vs. 1.5×10^{-6} M for CD-GCAP) for half-maximal stimulation of guanylate cyclase. Clearly, CD-GCAP was not quite the same as the commercially obtained S100B.

In the search for the explanation for these functional differences, the proteins were analyzed for post-translational modifications and higher order structures (Pozdnyakov et al., 1997). After treating both proteins with hydroxylamine, a deacylating agent, CD-GCAP no longer activated guanylate cyclase while S100B activation retained its ability to do so. Furthermore, hydroxylamine fragmented CD-GCAP while S100B was unaffected. These results indicated that the conformations of the two proteins were different. Such a difference could have arisen from variations in the procedures for purifying the two proteins: CD-GCAP purification entailed heating at 75°C in 5 mM Ca^{2+}, while S100B purification included zinc affinity chromatography (commercial sources refused to provide these details but their references indicated so). To investigate, CD-GCAP was subjected to zinc affinity chromatography (CD-GCAP-to-S100B) and S100B was heated to 75°C in Ca^{2+} (S100B-to-CD-GCAP). Guanylate cyclase activation, calcium–sensitivity, and hydroxylamine lability measurements demonstrated that CD-GCAP-to-S100B was identical to S100B and that S100B-to-CD-GCAP was identical to CD-GCAP. Apparently zinc inhibits the native S100B potency toward stimulation of ROS-GC. An additional finding was that S100B monomer is about twice as effective as the dimer in activating the ROS-GC catalytic activity. Hence, CD-GCAP and commercially obtained S100B are conformational isomers. The native form of S100B present in the retinal neurons is CD-GCAP.

CHARACTERIZATION OF THE S100B BINDING SITE OF ROS-GC1

Direct interaction between ROS-GC1 and S100B was verified by cross-linking experiments with bis-(sulfosuccinimidyl)suberate. A cross-linked complex, consisting of ROS-GC1 dimer and S100B, was detected by both ROS-GC1 and S100B antibodies on Western blots (Duda et al., 2002). Biochemical experiments with ROS-GC1 deletion constructs localized an interaction of S100B with the C-terminus of ROS-GC1, aa 731–1054 (Duda et al., 1996a). An EC_{50} of 395 nM, measured using surface plasmon spectroscopy, was comparable to the EC_{50} of 800 nM for stimulation of ROS-GC1 by S100B in a biochemical assay (Duda et al., 2002).

Since the aa 733–964 segment containing the putative dimerization and catalytic domains is highly conserved, the less conserved aa 965–1054 segment was subjected to further analyses. First, three ROS-GC1 deletion mutants: Δ965–1054, Δ972–1054, and Δ1016–1054 were analyzed for their responses to S100B. The first mutant was totally unresponsive, the response of the second mutant was only ∼25% and that of the third mutant ∼50% of the wild-type ROS-GC1 response to S100B. Therefore the entire region aa 965–1054 of ROS-GC1 is important for Ca^{2+}-dependent stimulation by S100B, but the region aa 965–1016 appears to be the most critical (Duda et al., 2002). Second, overlapping peptides encompassing this region were screened for their effects on S100B-dependent stimulation of ROS-GC1 at high Ca^{2+}. Two peptides covering aa regions 952–991 and 1029–1040 prevented ROS-GC1 stimulation by S100B. Finer analysis revealed that aa 962–981 formed the critical binding site of ROS-GC1 with half-maximal binding at 198 nM. A ^{966}RIHVNRS^{972} motif was obligatory, however, a flanking cluster of four aa residues, R^{1039}RQK^{1042} formed a low affinity binding site. While not absolutely required for binding, the secondary site was an S100B-modulated transduction site that conferred a twofold increase in maximal activation of ROS-GC1 (Duda et al., 2002).

These studies validated the unique ability of ROS-GC1 to respond not only to low Ca^{2+} signals mediated by GCAPs but also to high Ca^{2+} signals mediated by S100B. To analyze the possible interplay of these signals, the aforementioned ROS-GC1 deletion mutants were analyzed for their responses to GCAP1 (Duda et al., 2002) and GCAP2 (Duda et al., 2005). At 10 nM Ca^{2+}, activation of all mutants was identical to that of wild-type ROS-GC1. Thus, the S100B and GCAP1 regulatory sites of ROS-GC1 are distinct and do not interfere with one other. This result was not surprising because the binding site for GCAP1 was previously mapped to the N-terminal part of the ROS-GC1 cytoplasmic domain (Duda et al., 1999; Lange et al., 1999).

The case for GCAP2 was not so clear. Initial mapping had localized the GCAP2 binding site closer to the C-terminus of ROS-GC1 (Krishnan et al., 1998). In reconstitution experiments with the ROS-GC1 deletion mutants (the same as used for mapping the S100B site: *vide supra*), the Δ965–1054 mutant failed to respond to GCAP2, the Δ972–1045 responded with V_{max} of ∼50% of that of the wild-type ROS-GC1, and the response of the Δ1016–1054 mutant matched that of the wild-type cyclase, indicating that the functional GCAP2-modulated domain resided within aa 965–1016. Detailed peptide competition assays narrowed down the GCAP2-modulated site to the sequence motif Y^{965}-N^{981} (Duda et al., 2005). As expected, this site is distinct from the GCAP1 site. It, however, partially overlaps with the S100B-regulatory site. These results provide a hint that, when GCAP1 and S100B are co-expressed, a single ROS-GC1 complex could operate as a bimodal Ca^{2+} switch. On the other hand, when GCAP2 and S100B are co-expressed, the switch might involve separate populations of ROS-GC1 complexes. Furthermore, identification of the binding sites for the Ca^{2+} sensors disclosed an intriguing topographical feature of ROS-GC1; GCAP2 and S100B transmit the Ca^{2+} signals to the catalytic domain of ROS-GC1 from the C-terminal side while GCAP1 does so from a more distant location on the N-terminal side. These intramolecular mechanics are specific to ROS-GC1 and are different from the peptide hormone receptor subfamily, where the signal to the catalytic site migrates solely downstream from a site on the N-terminus located on the opposite side of

the membrane. A schematic model of the system is depicted in **Figure 2**.

ROS-GC2 has an ~8x lower affinity for S100B and with S100B bound at high Ca^{2+}, its maximal activation is twofold lower than that of ROS-GC1. Substitution of aa 731–1053 of ROS-GC1 into the corresponding region of ROS-GC2 and vice versa reversed the selectivity (Duda et al., 1998). These results suggest that ROS-GC2 may be an S100B partner of lesser importance than ROS-GC1.

S100B IS EXPRESSED IN CONES BUT NOT IN RODS

Guided by the knowledge that ROS-GC and GCAPs are present in photoreceptors, including their outer segments where they serve as critical components of phototransduction (Cuenca et al., 1998; Kachi et al., 1999; reviewed in Pugh et al., 1997; Koch et al., 2010; Sharma and Duda, 2012), and that S100B is also present in photoreceptors (Rambotti et al., 1999; reviewed in: Rambotti et al., 2002), questions were raised as to whether a ROS-GC1 bimodal Ca^{2+} -regulated system operates in visual transduction and whether it is present in both rods and cones. These issues are being addressed in mouse (e.g., Wen et al., 2012), for which there exist useful knockouts including $S100B^{-/-}$, $GCAP1^{-/-}$, $GCAP2^{-/-}$, $GCAP1/GCAP2^{-/-}$, $ROS\text{-}GC1^{-/-}$.

Affinity purified S100B antibody recognized on Western blots of mouse photoreceptors, a protein of molecular weight corresponding to S100B. In biochemical assays, guanylate cyclase activity of mouse ROS membranes exhibited bimodal Ca^{2+} switch behavior; activity decreased as $[Ca^{2+}]$ rose from 10 to 300 nM and then increased as $[Ca^{2+}]$ began to exceed 300 nM. The "inhibitory" phase of the guanylate cyclase activity was consistent with the loss of ROS-GC1 activation by GCAPs upon Ca^{2+} binding to the latter and the stimulatory phase with Ca^{2+}-induced activation of ROS-GC1 activity by S100B. The increase in ROS-GC activity at low $[Ca^{2+}]$ disappeared in ROS membranes from $GCAP1/GCAP2^{-/-}$ mice, whereas the increase in ROS-GC activity at high $[Ca^{2+}]$ was missing in ROS membranes from $S100B^{-/-}$ mice and from $ROS\text{-}GC1^{-/-}$ mice. The significance of the result from $ROS\text{-}GC1^{-/-}$ mice will be revealed below. Yet, regulation of ROS-GC1 by S100B was not functionally linked to phototransduction in rods because flash responses from wild-type and S100B-KO rods were indistinguishable (Wen et al., 2012). The possibility that S100B might

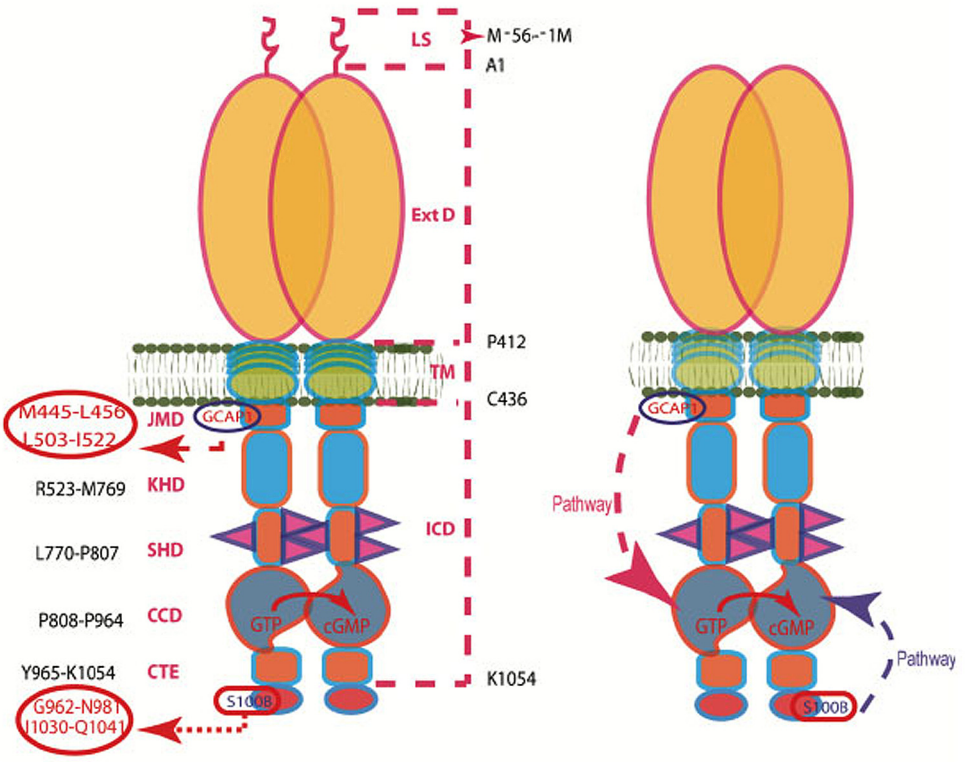

FIGURE 2 | The modular nature of ROS-GC1. *Left Panel.* The dashed lines on the right show the domain boundaries: LS, leader sequence (note: the leader sequence is absent from the mature protein shown in the right panel); ExtD, extracellular domain; TM, transmembrane domain; ICD, intracellular domain. The designated names and the amino acid residues constituting their boundaries are indicated on the left: JMD, juxtamembrane domain housing the indicated GCAP1-binding site; KHD, kinase homology domain; SHD, signaling helix domain; CCD, core catalytic domain; CTE, C-terminal extension housing the S100B-binding site. It is noteworthy that the ICD contains all of the functional domains and that GCAP1 and S100B target sites on opposite sides of the CCD. *Right panel.* The GCAP1 and S100B signaling pathways within ROS-GC propagate in opposite directions. The trajectory of the GCAP1 pathway is shown with the red dashed arrow. From its origin in the JMD, it passes "downstream" through the structural KHD and SHD in its course to the CCD. The trajectory of the S100B pathway shown with the blue dashed arrow. Originating in the CTE, it directly flows "upstream" to the CCD. The CCD exists as an antiparallel homodimer. Both GCAP1 and S100B signals are translated at the CCD into faster production of cyclic GMP (Modified from Duda et al., 2012).

contribute to the rod photoresponse at high free $[Ca^{2+}]$ outside the normal physiological range was tested and not found.

Detailed histochemical analysis of S100B expression in the mouse retina brought all these observations into accord (**Figure 3**). As expected, the S100B-KO retina showed no S100B immunoreactivity (Wen et al., 2012), affirming the specificity of the S100B antibody, because photoreceptor outer segments also express S100A1, another member of the S100 family (Rambotti et al., 1999). S100B immunoreactivity was present in wild-type photoreceptors, however, it was not present in all of them. The scattered S100B staining corresponded to that for cone-specific arrestin. On the other hand, in retinas of $Nrl^{-/-}$ mice, all outer segments labeled for S100B as well as for cone arrestin. Because $Nrl^{-/-}$ retina is rod-less and populated exclusively with cone photoreceptors (Mears et al., 2001) these results strongly indicate that among photoreceptors, S100B expression is restricted to cones. Unimodal switch behavior in ROS-$GC1^{-/-}$ outer segments (above) is now easy to understand. In ROS-$GC1^{-/-}$ retinas, cones degenerate but the rods remain intact (Yang et al., 1999). Rods however, do not express S100B, so the only Ca^{2+}-regulated guanylate cyclase activity in ROS-$GC1^{-/-}$ retinas is the GCAPs modulated ROS-GC2 activity.

Our ongoing immunohistochemical studies with the Nile Rat (*Arvicanthis ansorgei*) retina in which 33% of the photoreceptors are cones, in contrast to the 3% cone population in the mouse (Bobu et al., 2006) appear to corroborate the conclusion derived from analyses of murine retinas that S100B co-exists with ROS-GC1 exclusively in the cone outer segments.

At present, the question about the role of the ROS-GC1 bimodal switch in cone phototransduction is still unanswered because cones from $S100B^{-/-}$ mice have yet to be recorded. A model illustrating some of the difficulties in understanding the operation of the bimodal switch is shown in **Figure 4**. One issue is that in darkness (DARK), Ca^{2+} will not bind to S100B and activate the switch if $[Ca^{2+}]_i$ never exceeds 250 nM. However, the value of 250 nM for $[Ca^{2+}]_i$ in darkness was taken from mouse rods (Woodruff et al., 2002) because measurements from mouse cones have not yet been made. Thus the true $[Ca^{2+}]_i$ for cones in darkness may be higher. A second issue is that without proper restraint, operation of the bimodal switch at high $[Ca^{2+}]_i$ would ignite an explosive positive feedback: increased cyclic GMP production, followed by opening of more cyclic GMP-gated channels, which then allow a greater influx of Ca^{2+}, etc. Cones could accumulate lethal levels of Ca^{2+} or experience a collapse in ion gradients (DEPOLARIZATION-S100B Mode). Indeed, genetic mutations that result in a hyperactive ROS-GC complex cause the photoreceptors to degenerate (Olshevskaya et al., 2002; Zägel and Koch, 2014).

THE BIMODAL SWITCH EXISTS AT THE PHOTORECEPTOR-BIPOLAR CELL SYNAPSE

Immunohistochemical studies also place ROS-GC1, GCAP1 and S100B in the synaptic layers of the retina (Liu et al., 1994; Cooper et al., 1995; Duda et al., 2002; Venkataraman et al., 2003). To test whether the ROS-GC1 transduction system utilizes a Ca^{2+} bimodal switch at the photoreceptor-bipolar cell synapse (presumably the cone to bipolar synapse, see **Figure 3**), bovine retinal synaptosomes (P1) were prepared and analyzed. Purity of the preparation was ascertained by Western blotting with rhodopsin kinase antibody. No immunoreactivity for rhodopsin kinase was detected, assuring that the preparation was not contaminated with ROSs, the original residential site of the ROS-GC1. Western blots were positive for ROS-GC1, GCAP1 and S100B demonstrating that indeed the synaptosomal fraction contained all the components

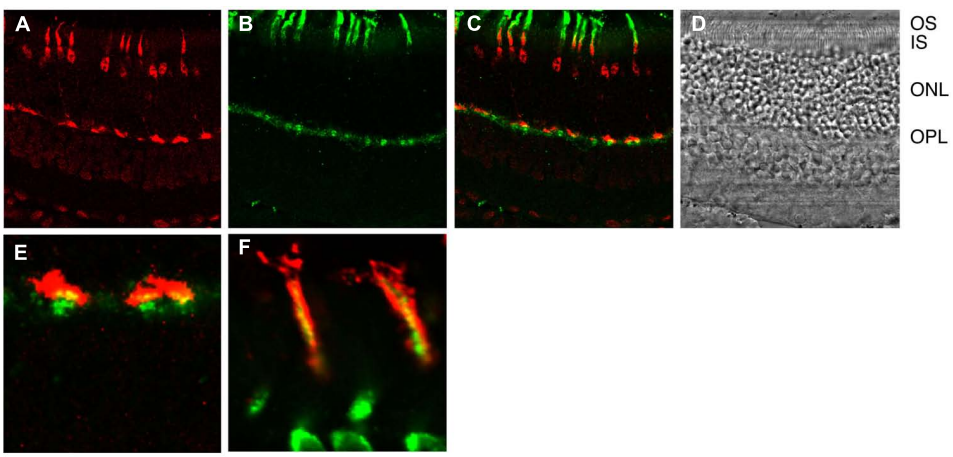

FIGURE 3 | Immunhistochemical localization of S100B to cones in the murine retina. (A) Cone arrestin in red. Cone outer segment labeling is overshadowed with by strong labeling of the synapse, nucleus and inner segment. **(B)** S100B in green. Selected outer segments are labeled intensely. Inner segments and synapses are also labeled. **(C)** Composite showing that cone arrestin and S100B labeling are restricted to cones. **(D)** Bright field. OS, outer segments; IS, inner segments; ONL, outer nuclear layer containing nuclei of rods and cones; OPL, outer plexiform layer containing synapses of rods and cones. **(E)** Composite showing cone synapses at higher magnification. Overlap (yellow) between arrestin and S100B is not perfect because the former is a soluble protein whereas the latter is membrane bound. **(F)** Section from a different retina that was doubly labeled for cone arrestin in green and S100B in red at high magnification. Conditions were adjusted to optimize the detection of outer segment labeling Courtesy of A. Pertzev, Salus University.

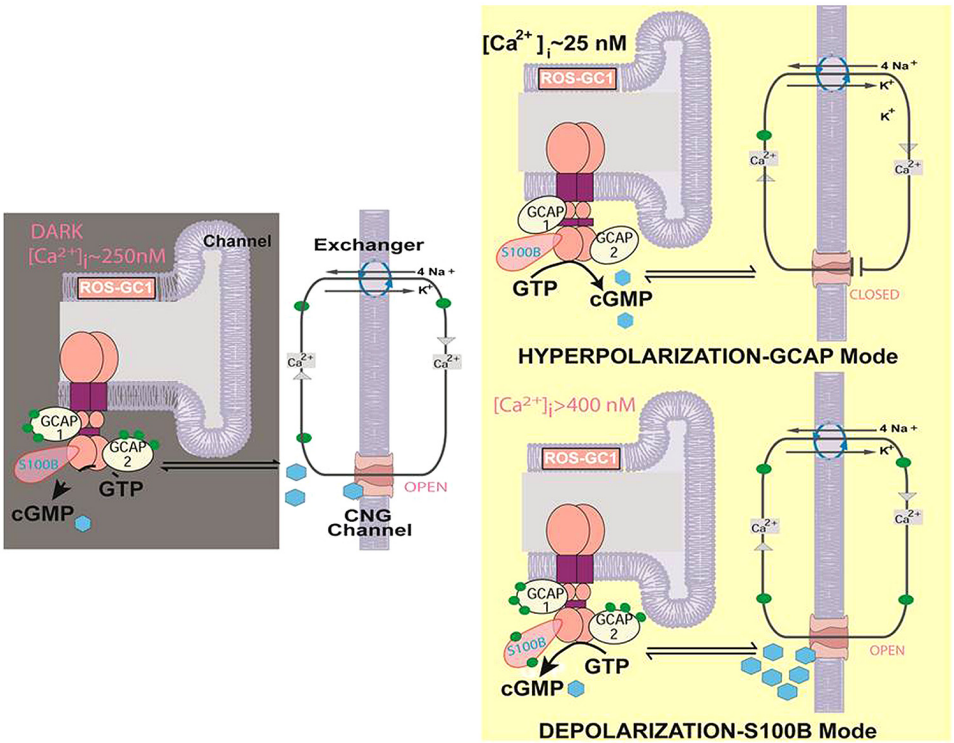

FIGURE 4 | Two modes of ROS-GC1 modulation by $[Ca^{2+}]_i$ in cones. *Dark state [left].* At $[Ca^{2+}]_i$ ~250 nM Ca^{2+} sensors: GCAP1, GCAP2, S100B are ROS-GC1 bound; GCAP1 and GCAP2 are $[Ca^{2+}]_i$ bound; ROS-GC1 is in the basal state. Cyclic GMP generated keeps a fraction of CNG channels open allowing an influx of Na^+ and Ca^{2+}. In this graphical simplification, GCAP2 and S100B are shown bound to the same ROS-GC dimer but it is more likely that these two Ca^{2+} sensors bind separate dimers. *Hyperpolarization-GCAP mode [Top right].* LIGHT triggers activation of phosphodiesterase and hydrolysis of cyclic GMP. The decrease in cyclic GMP causes CNG channels to close, preventing influx of Na^+ and Ca^{2+} and hyperpolarizing the outer segment plasma membrane. Extrusion of Ca^{2+} by the Na^+/Ca^{2+}, K^+ exchanger lowers $[Ca^{2+}]_i$ from ~250 nM to about 25 nM. The decline causes GCAPs to stimulate ROS-GC1. *Depolarization-S100B mode [Bottom right].* $[Ca^{2+}]_i$ levels rise when CNG channels open. With $K_{1/2}$ of 400 nM, S100B captures Ca^{2+}, triggering activation of ROS-GC1. Cyclic GMP formed could open many more CNG channels, greatly increasing the influx of Na^+ and Ca^{2+}. $[Ca^{2+}]_i$ levels rise still further because extrusion of Ca^{2+} through Na^+/Ca^{2+}, K^+ exchanger slows as the ion gradients collapse. The cone outer segment may lose the ability to maintain a membrane potential (Modified from Wen et al., 2012).

of the ROS-GC1 bimodal system and was suitable for functional analyses.

To be physiologically relevant, the components of the ROS-GC1 bimodal system, ROS-GC1, GCAP1 and S100B must reside in proximity and not, e.g., in different populations of synaptosomes. Because the Western analyses described above did not provide information about the proximity of ROS-GC1, GCAP1 and S100B molecules, immunohistochemical analyses (Duda et al., 2002; Venkataraman et al., 2003) and cross-linking experiments were performed.

Cryosections of bovine retina were doubly labeled with antibodies against GCAP1 or ROS-GC1 and SV2, a synaptic vesicle protein that strongly stains photoreceptor termini (Buckley and Kelly, 1985). The results revealed co-expression of ROS-GC1 and GCAP1 in cone synaptic termini (Venkataraman et al., 2003). Similarly, co-localization of ROS-GC1 and S100B was shown (Duda et al., 2002).

Cross-linking experiments with a non-cleavable imidoester confirmed the proximity of ROS-GC1 and GCAP1 in the synaptosomal fraction (Venkataraman et al., 2003). Without the cross-linker, the ROS-GC1 and GCAP1 antibodies identified separate bands at ~120 kDa and ~21 kDa, respectively, corresponding to the appropriate monomers. But in presence of the cross-linker, both GCAP1 and ROS-GC1 antibodies identified a common immunoreactive band at ~250 kDa, the approximate size for a ROS-GC1 dimer-GCAP1 complex. The results demonstrated that ROS-GC1 and GCAP1, indeed, resided in proximity. Because ROS-GC1 resides with GCAP1 in cone synaptic terminals and ROS-GC1 also resides with S100B, it was inferred that all three components of the bimodal system co-reside in the photoreceptor synaptic terminals, specifically cone synaptic terminals.

Functionality of the ROS-GC1 bimodal switch in the P1 fraction was determined by measuring guanylate cyclase activity at Ca^{2+} concentrations ranging from 10 nM to 10 μM. Below 200 nM, Ca^{2+} elicited a dose-dependent decrease in guanylate cyclase activity with an "inhibitory" value (IC_{50}) for Ca^{2+} of 100 nM. But at higher concentrations, ROS-GC activity began to climb with an EC_{50} of 0.8 μM. Side by side analysis of photoreceptor outer segment and P1 membranes demonstrated that the cyclic GMP synthetic activities were inhibited identically by free Ca^{2+} with an IC_{50} of 100 nM.

That GCAP1 was involved in the "inhibitory" phase of ROS-GC1 activity was confirmed by peptide competition experiments. A sequence motif L^{503}–I^{522} in ROS-GC1 is critical and specific for the cyclase activation by GCAP1 (Lange et al., 1999). The core motif within this domain consists of D^{507}–R^{518}. Analysis of the P1 and photoreceptor outer segments membranes in parallel demonstrated that the incremental concentrations of the L^{503}–I^{522} and D^{507}–R^{518} peptides at 10 nM Ca^{2+} inhibited their guanylate cyclase activities with the same dose-dependence. A control peptide of L^{503}–I^{522} with a scrambled sequence had no effect on GCAP-dependent ROS–GC1 activity. Both fractions showed a reversal of the peptide (D^{507}–R^{518})-dependent inhibition upon the addition of an excess of GCAP1 (Venkataraman et al., 2003). Thus Ca^{2+} signaling in the synapse region is modulated by GCAP1 and S100B. GCAP1 has the higher affinity for Ca^{2+} and upon binding, lowers ROS-GC1 activity. S100B captures the high Ca^{2+} signal and upon binding, stimulates ROS-GC1.

A ROLE IN SIGNAL PROCESSING IN THE RETINA?

ERG recordings from wild-type and $S100B^{-/-}$ mice provided the first clues as to the physiological significance of S100B in retinal function (Wen et al., 2012). The ERG is a field potential across the retina generated by the electrical activity of all cells, including that of rods and cones (reviewed in: Peachey and Ball, 2003; Weymouth and Vingrys, 2008). The corneal negative a-wave, which sums the photocurrent responses of rods, is normal in the S100B-KO mice because S100B is not present in rods. The corneal positive b-wave, generated mainly by ON-bipolar cells, displays slower kinetics in $S100B^{-/-}$ mice; it peaks later and takes longer to recover. Oscillatory potentials that arise from the activity of inner retinal neurons are smaller and there are disturbances in their timing. Gaps in our knowledge about what S100B is doing in the cone outer segment, the cone synapses and for that matter, in other retinal neurons preclude any attempt to interpret the changes in the ERG at this time.

FUTURE DIRECTIONS

The composition and the operational principles of cones and rods differ in ways that support their specialized visual functions: extremely high sensitivity in rods, rapid responsiveness over a wide dynamic range in cones. In addition to the GCAPs, S100B serves as an additional Ca^{2+} sensor component of ROS-GC1 in cones. Future tasks will be to decode this signal transduction system at the molecular and physiological levels, to link it with cone-related dystrophies and to design therapeutic options. Progress would be facilitated if several important objectives were to be met. (1) A suitable mammalian model with abundant cones needs to be selected. No such mouse model is available at present. Through genetic manipulation, development of the rods has been suppressed in $Nrl^{-/-}$ mice and their retinas are cone-exclusive. But these cones may not be exact copies of the natural, although biochemically and physiologically, they appear to be very close (Nikonov et al., 2005, 2006). One alternative is the Nile rat (*A. ansorgei*), whose retina contains about 30% cones in contrast to the 3% population in the mouse (Bobu et al., 2006). (2) The molecular architecture of the ROS-GC complex needs to be understood. Which combinations of Ca^{2+} sensor proteins are possible in the complex? Which actually occur? How are their relative levels within different cell types regulated? (3) Ca^{2+}-modulated signal transduction by the ROS-GC complex needs to be defined at a molecular level. For the S100B native to cones, what are the kinetic parameters of the S100B transduction switch? By what mechanism does S100B sense Ca^{2+} and how does it effect a change in the catalytic domain of ROS-GC? (4) The physiological role of S100B in the cone photoresponse needs to be assessed. Does it accelerate the recovery of cone response and increase the dark current? What limits S100B stimulated ROS-GC activity at high Ca^{2+}? Does S100B increase the rate of vesicular release of neurotransmitter at the synapse? S100A1 is also expressed in outer segments, what is its function? (5) S100B is expressed in inner retinal neurons but nothing is known about what it does there. (6) S100B protein does not fit in the presently classified NCS protein family, sharing only 15% sequence identity and containing only two EF-hands. Therefore, the NCS family needs to be expanded to include S100B as a branch.

ACKNOWLEDGMENTS

The authors gratefully acknowledge the continuous past support by the numerous USPHS award from the National Institutes of Health, the beginning award from the National Science Foundation and the Damon Runyon Walter Winchell Cancer Fund and the Howe Laboratory Endowment of the Massachusetts Eye and Ear Infirmary.

REFERENCES

Baehr, W., Karan, S., Maeda, T., Luo, D. G., Li, S., Bronson, J. D., et al. (2007). The function of guanylate cyclase 1 and guanylate cyclase 2 in rod and cone photoreceptors. *J. Biol. Chem.* 282, 8837–8847. doi: 10.1074/jbc.M610369200

Bobu, C., Craft, C. M., Masson-Pevet, M., and Hicks, D. (2006). Photoreceptor organization and rhythmic phagocytosis in the nile rat *Arvicanthis ansorgei*: a novel diurnal rodent model for the study of cone pathophysiology. *Invest. Ophthalmol. Vis. Sci.* 47, 3109–3118. doi: 10.1167/iovs.05-1397

Buckley, K., and Kelly, R. B. (1985). Identification of a transmembrane glycoprotein specific for secretory vesicles of neural and endocrine cells. *J. Cell Biol.* 100, 1284–1294. doi: 10.1083/jcb.100.4.1284

Chen, C. K., Inglese, J., Lefkowitz, R. J., and Hurley, J. B. (1995). Ca(2+)-dependent interaction of recoverin with rhodopsin kinase. *J. Biol. Chem.* 270, 18060–18066. doi: 10.1074/jbc.270.30.18060

Chinkers, M., Garbers, D. L., Chang, M. S., Lowe, D. G., Chin, H. M., Goeddel, D. V., et al. (1989). A membrane form of guanylate cyclase is an atrial natriuretic peptide receptor. *Nature* 338, 78–83. doi: 10.1038/338078a0

Cooper, N., Liu, L., Yoshida, A., Pozdnyakov, N., Margulis, A., and Sitaramayya A. (1995). The bovine rod outer segment guanylate cyclase, ROS-GC, is present in both outer segment and synaptic layers of the retina. *J. Mol. Neurosci.* 6, 211–222. doi: 10.1007/BF02736766

Cuenca, N., Lopez, S., Howes, K., and Kolb, H. (1998). The localization of guanylyl cyclase-activating proteins in the mammalian retina. *Invest. Ophthalmol. Vis. Sci.* 39, 1243–1250.

Dizhoor, A. M., Olshevskaya, E. V., Henzel, W. J., Wong, S. C., Stults, J. T., Ankoudinova, I., et al. (1995). Cloning, sequencing, and expression of a 24-kDa Ca(2+)-binding protein activating photoreceptor guanylyl cyclase. *J. Biol. Chem.* 270, 25200–25206. doi: 10.1074/jbc.270.42.25200

Dizhoor, A. M., Ray, S., Kumar, S., Niemi, G., Spencer, M., Brolley, D., et al. (1991). Recoverin: a calcium sensitive activator of retinal rod guanylate cyclase. *Science* 251, 915–918. doi: 10.1126/science.1672047

Duda, T., Fik-Rymarkiewicz, E., Venkataraman, V., Krishnan, R., Koch, K. W., and Sharma, R. K. (2005). The calcium-sensor guanylate cyclase activating protein type 2 specific site in rod outer segment membrane guanylate cyclase type 1. *Biochemistry* 44, 7336–7345. doi: 10.1021/bi050068x

Duda, T., Goraczniak, R. M., and Sharma, R. K. (1996a). Molecular characterization of S100A1-S100B protein in retina and its activation mechanism of bovine photoreceptor guanylate cyclase. *Biochemistry* 35, 6263–6266. doi: 10.1021/bi960007m

Duda, T., Goraczniak, R., Surgucheva, I., Rudnicka-Nawrot, M., Gorczyca, W. A., Palczewski, K., et al. (1996b). Calcium modulation of bovine photoreceptor guanylate cyclase. *Biochemistry* 35, 8478–8482. doi: 10.1021/bi960752z

Duda, T., Goraczniak, R. M., Pozdnyakov, N., Sitaramayya, A., and Sharma, R. K. (1998). Differential activation of rod outer segment membrane guanylate cyclases, ROS-C1 and ROS-GC2, by CD-GCAP and indentification of signaling domain. *Biochem. Biophys. Res. Commun.* 242, 118–122. doi: 10.1006/bbrc.1997.7921

Duda, T., Goraczniak, R. M., and Sharma, R. K. (1991). Site-directed mutational analysis of a membrane guanylate cyclase cDNA reveals the atrial natriuretic factor signaling site. *Proc. Natl. Acad. Sci. U.S.A.* 88, 7882–7886. doi: 10.1073/pnas.88.17.7882

Duda, T., Goraczniak, R. M., Sitaramayya, A., and Sharma, R. K. (1993). Cloning and expression of an ATP-regulated human retina C-type natriuretic factor receptor guanylate cyclase. *Biochemistry* 32, 1391–1395. doi: 10.1021/bi00057a001

Duda, T., Koch, K. W., Venkataraman, V., Lange, C., Beyermann, M., and Sharma, R. K. (2002). Ca^{2+} sensor S100beta-modulated sites of membrane guanylate cyclase in the photoreceptor-bipolar synapse. *EMBO J.* 21, 2547–2556. doi: 10.1093/emboj/21.11.2547

Duda, T., Pertzev, A., and Sharma, R. K. (2012). Differential Ca2+ sensor guanylate cyclase activating protein modes of photoreceptor rod outer segment membrane guanylate cyclase signaling. *Biochemistry* 51, 4650–4657. doi: 10.1021/bi300572w

Duda, T., Venkataraman, V., Goraczniak, R., Lange, C., Koch, K. W., and Sharma, R. K. (1999). Functional consequences of a rod outer segment membrane guanylate cyclase (ROS-GC1) gene mutation linked with Leber's congenital amaurosis. *Biochemistry* 38, 509–515. doi: 10.1021/bi9824137

Frins, S., Bönigk, W., Müller, F., Kellner, R., and Koch, K. W. (1996). Functional characterization of a guanylyl cyclase-activating protein from vertebrate rods. Cloning, heterologous expression, and localization. *J. Biol. Chem.* 271, 8022–8027. doi: 10.1074/jbc.271.14.8022

Goraczniak, R. M., Duda, T., and Sharma, R. K. (1997). Structural and functional characterization of a second subfamily member of the calcium-modulated bovine rod outer segment membrane guanylate cyclase, ROS-GC2. *Biochem. Biophys. Res. Commun.* 234, 666–670. doi: 10.1006/bbrc.1997.6579

Goraczniak, R. M., Duda, T., Sitaramayya, A., and Sharma, R. K. (1994). Structural and functional characterization of the rod outer segment membrane guanylate cyclase. *Biochem. J.* 302, 455–461.

Gorczyca, W. A., Polans, A. S., Surgucheva, I. G., Subbaraya, I., Baehr, W., and Palczewski, K. (1995). Guanylyl cyclase activating protein. A calcium-sensitive regulator of phototransduction. *J. Biol. Chem.* 270, 22029–22036. doi: 10.1074/jbc.270.37.22029

Hayashi, F., and Yamazaki, A. (1991). Polymorphism in purified guanylate cyclase from vertebrate rod photoreceptors. *Proc. Natl. Acad. Sci. U.S.A.* 88, 4746–4750. doi: 10.1073/pnas.88.11.4746

Horio, Y., and Murad, F. (1991a). Solubilization of guanylyl cyclase from bovine rod outer segments and effects of lowering Ca^{2+} and nitro compounds. *J. Biol. Chem.* 266, 3411–3415.

Horio, Y., and Murad, F. (1991b). Purification of guanylyl cyclase from rod outer segments. *Biochim. Biophys. Acta* 1133, 81–88. doi: 10.1016/0167-4889(91)90244-R

Hurley, J. B., Dizhoor, A. M., Ray, S., and Stryer, L. (1993). Recoverin's role: conclusion withdrawn. *Science* 260, 740. doi: 10.1126/science.8097896

Kachi, S., Nishizawa, Y., Olshevskaya, E., Yamazaki, A., Miyake, Y., Wakabayashi, T., et al. (1999). Detailed localization of photoreceptor guanylate cyclase activating protein-1 and -2 in mammalian retinas using light and electron microscopy. *Exp. Eye Res.* 68, 465–473. doi: 10.1006/exer.1998.0629

Kawamura, S. (1999). Calcium-dependent regulation of rhodopsin phosphorylation. *Novartis Found. Symp.* 224, 208–218; discussion 218–224.

Klenchin, V. A., Calvert, P. D., and Bownds, M. D. (1995). Inhibition of rhodopsin kinase by recoverin. Further evidence for a negative feedback system in phototransduction. *J. Biol. Chem.* 270, 16147–16152. doi: 10.1074/jbc.270.41.24127

Kligman, D., and Marshak, D. R. (1985). Purification and characterization of a neurite extension factor from bovine brain. *Proc. Natl. Acad. Sci. U.S.A.* 82, 7136–7139. doi: 10.1073/pnas.82.20.7136

Koch, K.-W. (1991). Purification and identification of photoreceptor guanylate cyclase. *J. Biol. Chem.* 266, 8634–8637.

Koch, K. W., Duda, T., and Sharma, R. K. (2010). Ca^{2+}-modulated vision-linked ROS-GC guanylate cyclase transduction machinery. *Mol. Cell. Biochem.* 334, 105–115. doi: 10.1007/s11010-009-0330-z

Koch, K. W., and Stryer, L. (1988). Highly cooperative feedback control of retinal rod guanylate cyclase by calcium ions. *Nature* 334, 64–66. doi: 10.1038/334064a0

Koller, K. J., Lowe, D. G., Bennett, G. L., Minamino, N., Kangawa, K., Matsuo, H., et al. (1991). Selective activation of the B natriuretic peptide receptor by C-type natriuretic peptide (CNP). *Science* 252, 120–123. doi: 10.1126/science.1672777

Koutalos, Y., Nakatani, K., Tamura, T., and Yau, K. W. (1995). Characterization of guanylate cyclase activity in single retinal rod outer segments. *J. Gen. Physiol.* 106, 863–890. doi: 10.1085/jgp.106.5.863

Krishnan, A., Goraczniak, R. M., Duda, T., and Sharma, R. K. (1998). Third calcium-modulated rod outer segment membrane guanylate cyclase transduction mechanism. *Mol. Cell. Biochem.* 178, 251–259. doi: 10.1023/A:1006860018300

Lange, C., Duda, T., Beyermann, M., Sharma, R. K., and Koch, K. W. (1999). Regions in vertebrate photoreceptor guanylyl cyclase ROS-GC1 involved in Ca(2+)-dependent regulation by guanylyl cyclase-activating protein GCAP-1. *FEBS Lett.* 460, 27–31. doi: 10.1016/S0014-5793(99)01312-5

Liu, X., Seno, K., Nishizawa, Y., Hayashi, F., Yamazaki, A., Matsumoto, H., et al. (1994). Ultrastructural localization of retinal guanylate cyclase in human and monkey retinas. *Exp. Eye Res.* 59, 761–768. doi: 10.1006/exer.1994.1162

Lowe, D. G., Dizhoor, A. M., Liu, K., Gu, Q., Spencer, M., Laura, R., et al. (1995). Cloning and expression of a second photoreceptor-specific membrane retina guanylyl cyclase (RetGC), RetGC-2. *Proc. Natl. Acad. Sci. U.S.A.* 92, 5535–5539.

Margulis, A., Goraczniak, R. M., Duda, T., Sharma, R. K., and Sitaramayya, A. (1993). Structural and biochemical identity of retinal rod outer segment membrane guanylate cyclase. *Biochem. Biophys. Res. Commun.* 194, 855–861. doi: 10.1006/bbrc.1993.1900

Margulis, A., Pozdnyakov, N., and Sitaramayya, A. (1996). Activation of bovine photoreceptor guanylate cyclase by S100 proteins. *Biochem. Biophys. Res. Commun.* 218, 243–247. doi: 10.1006/bbrc.1996.0043

Mears, A. J., Kondo, M., Swain, P. K., Takada, Y., Bush, R. A., Saunders, T. L., et al. (2001). Nrl is required for rod photoreceptor development. *Nat. Genet.* 29, 447–452. doi: 10.1038/ng774

Nikonov, S. S., Daniele, L. L., Zhu, X., Craft, C. M., Swaroop, A., and Pugh, E. N. Jr. (2005). Photoreceptors of Nrl-/- mice coexpress functional S- and M-cone opsins having distinct inactivation mechanisms. *J. Gen. Physiol.* 125, 287–304. doi: 10.1085/jgp.200409208

Nikonov, S. S., Kholodenko, R., Lem, J., and Pugh, E. N. Jr. (2006). Physiological features of the S- and M-cone photoreceptors of wild-type mice from single-cell recordings. *J. Gen. Physiol.* 127, 359–374. doi: 10.1085/jgp.200609490

Olshevskaya, E. V., Ermilov, A. N., and Dizhoor, A. M. (2002). Factors that affect regulation of cGMP synthesis in vertebrate photoreceptors and their genetic link to human retinal degeneration. *Mol. Cell. Biochem.* 230, 139–147. doi: 10.1023/A:1014248208584

Palczewski, K., Subbaraya, I., Gorczyca, W. A., Helekar, B. S., Ruiz, C. C., Ohguro, H., et al. (1994). Molecular cloning and characterization of retinal photoreceptor guanylyl cyclase-activating protein. *Neuron* 13, 395–404. doi: 10.1016/0896-6273(94)90355-7

Paul, A. K., Marala, R. B., Jaiswal, R. K., and Sharma, R. K. (1987). Coexistence of guanylate cyclase and atrial natriuretic factor receptor in a 180-kD protein. *Science* 235, 1224–1226. doi: 10.1126/science.2881352

Peachey, N. S., and Ball, S. L. (2003). Electrophysiological analysis of visual function in mutant mice. *Doc. Ophthalmol.* 107, 13–36. doi: 10.1023/A:1024448314608

Pozdnyakov, N., Goraczniak, R., Margulis, A., Duda, T., Sharma, R. K., Yoshida, A., et al. (1997). Structural and functional characterization of retinal calcium-dependent guanylate cyclase activator protein (CD-GCAP): identity with S100beta protein. *Biochemistry* 36, 14159–14166. doi: 10.1021/bi971792l

Pozdnyakov, N., Yoshida, A., Cooper, N. G., Margulis, A., Duda, T., Sharma, R. K., et al. (1995). A novel calcium-dependent activator of retinal rod outer segment membrane guanylate cyclase. *Biochemistry* 34, 14279–14283. doi: 10.1021/bi00044a002

Pugh, E. N. Jr., Duda, T., Sitaramayya, A., and Sharma, R. K. (1997). Photoreceptor guanylate cyclases: a review. *Biosci. Rep.* 17, 429–473. doi: 10.1023/A:1027365520442

Rambotti, M. G., Giambanco, I., Spreca, A., and Donato, R. (1999). S100B and S100A1 proteins in bovine retina:their calcium-dependent stimulation of a membrane-bound guanylate cyclase activity as investigated by ultracytochemistry. *Neuroscience* 92, 1089–1101. doi: 10.1016/S0306-4522(99)00074-3

Rambotti, M. G., Spreca, A., Giambanco, I., Sorci, G., and Donato, R. (2002). Ultracytochemistry as a tool for the study of the cellular and subcellular localization of membrane-bound guanylate cyclase (GC) activity. Applicability to both receptor-activated and receptor-independent GC activity. *Mol. Cell. Biochem.* 230, 85–96. doi: 10.1023/A:1014275520879

Sharma, R. K. (1988). Guanylate cyclase and the atrial natriuretic factor receptor. Response to Waldman, S. A., Leitman, D. C., Anderson, J., and Murad, F. *Science* 240, 805–806. doi: 10.1126/science.240.4853.805-a

Sharma, R. K. (2010). Membrane guanylate cyclase is a beautiful signal transduction machine: overview. *Mol.Cell. Biochem.* 334, 3–36. doi: 10.1007/s11010-009-0336-6

Sharma, R. K., and Duda, T. (2012). Ca(2+)-sensors and ROS-GC: interlocked sensory transduction elements: a review. *Front. Mol. Neurosci.* 5:42. doi: 10.3389/fnmol.2012.00042

Shyjan, A. W., de Sauvage, F. J., Gillett, N. A., Goeddel, D. V., and Lowe, D. G. (1992). Molecular cloning of a retina-specific membrane guanylyl cyclase. *Neuron* 9, 727–737. doi: 10.1016/0896-6273(92)90035-C

Stryer, L. (1991). Visual excitation and recovery. *J. Biol. Chem.* 266, 10711–10714.

Subbaraya, I., Ruiz, C. C., Helekar, B. S., Zhao, X., Gorczyca, W. A., Pettenati, M. J., et al. (1994). Molecular characterization of human and mouse photoreceptor guanylate cyclase-activating protein (GCAP) and chromosomal localization of the human gene. *J. Biol. Chem.* 269, 31080–31089.

Venkataraman, V., Duda, T., Vardi, N., Koch, K. W., and Sharma, R. K. (2003). Calcium-modulated guanylate cyclase transduction machinery in the photoreceptor–bipolar synaptic region. *Biochemistry* 42, 5640–5648. doi: 10.1021/bi034025x

Wen, X. H., Duda, T., Pertzev, A., Venkataraman, V., Makino, C. L., and Sharma, R. K. (2012). S100B serves as a Ca(2+) sensor for ROS-GC1 guanylate cyclase in cones but not in rods of the murine retina. *Cell. Physiol. Biochem.* 29, 417–430. doi: 10.1159/000338496

Weymouth, A. E., and Vingrys, A. J. (2008). Rodent electroretinography: methods for extraction and interpretation of rod and cone responses. *Prog. Retin. Eye Res.* 27, 1–44. doi: 10.1016/j.preteyeres.2007.09.003

Woodruff, M. L., Sampath, A. P., Matthews, H. R., Krasnoperova, N. V., Lem, J., and Fain, G. L. (2002). Measurement of cytoplasmic calcium concentration in the rods of wild-type and transducin knock-out mice. *J. Physiol.* 542(Pt 3), 843–854. doi: 10.1113/jphysiol.2001.013987

Yang, R. B., Robinson, S. W., Xiong, W. H., Yau, K. W., Birch, D. G., and Garbers, D. L. (1999). Disruption of a retinal guanylyl cyclase gene leads to cone-specific dystrophy and paradoxical rod behavior. *J. Neurosci.* 19, 5889–5897.

Zägel, P., and Koch, K.-W. (2014). Dysfunction of outer segment guanylate cyclase caused by retinal disease related mutations. *Front. Mol. Neurosci.* 7:4. doi: 10.3389/fnmol.2014.00004

Conflict of Interest Statement: The authors declare that the research was conducted in the absence of any commercial or financial relationships that could be construed as a potential conflict of interest.

Received: 20 December 2013; accepted: 05 March 2014; published online: 26 March 2014.

Citation: Sharma RK, Makino CL, Hicks D and Duda T (2014) ROS-GC interlocked Ca^{2+}-sensor S100B protein signaling in cone photoreceptors: review. Front. Mol. Neurosci. 7:21. doi: 10.3389/fnmol.2014.00021

This article was submitted to the journal Frontiers in Molecular Neuroscience.

frontiers in
MOLECULAR NEUROSCIENCE

ORIGINAL RESEARCH ARTICLE
published: 29 April 2014
doi: 10.3389/fnmol.2014.00034

Ca^{2+}-modulated ROS-GC1 transduction system in testes and its presence in the spermatogenic cells

Anna Jankowska[1]*, Rameshwar K. Sharma[2] and Teresa Duda[2]*

[1] The Unit of Molecular Biology, Department of Cell Biology, Poznan University of Medical Sciences, Poznan, Poland
[2] The Unit of Regulatory and Molecular Biology, Research Divisions of Biochemistry and Molecular Biology, Salus University, PA, USA

Edited by:
Clint Lawrence Makino, Massachusetts Eye and Ear Infirmary and Harvard Medical School, USA

Reviewed by:
Rosario Donato, University of Perugia, Italy
Andrzej Lukaszyk, Poznan University of Medical Sciences, Poland

****Correspondence:***
Anna Jankowska, The Unit of Molecular Biology, Department of Cell Biology, Poznan University of Medical Sciences, 5D Rokietnicka Street, 60-781 Poznan, Poland
e-mail: ajanko@ump.edu.pl;
Teresa Duda, The Unit of Regulatory and Molecular Biology, Research Divisions of Biochemistry and Molecular Biology, Salus University, 8360 Old York Road, Elkins Park, PA 19027, USA
e-mail: tduda@salus.edu

ROS-GC1 belongs to the Ca^{2+}-modulated sub-family of membrane guanylate cyclases. It primarily exists and is linked with signaling of the sensory neurons – sight, smell, taste, and pinealocytes. Exceptionally, it is also present and is Ca^{2+}-modulated in t he non-neuronal cells, the sperm cells in the testes, where S100B protein serves as its Ca^{2+} sensor. The present report demonstrates the identification of an additional Ca^{2+} sensor of ROS-GC1 in the testes, neurocalcin δ. Through mouse molecular genetic models, it compares and quantifies the relative input of the S100B and neurocalcin δ in regulating the Ca^{2+} signaling of ROS-GC1 transduction machinery, and via immunochemistry it demonstrates the co-presence of neurocalcin δ and ROS-GC1 in the spermatogenic cells of the testes. The suggestion is that in more ways than one the Ca^{2+}-modulated ROS-GC1 transduction system is linked with the testicular function. This non-neuronal transduction system may represent an illustration of the ROS-GC1 expanding role in the trans-signaling of the neural and non-neural systems.

Keywords: testes, neurocalcin δ, membrane guanylate cyclase, ROS-GC1, calcium ions

INTRODUCTION

Rod outer segment membrane guanylate cyclase, ROS-GC1 (known also as Ret-GC1 or GC-E), belongs to the family of membrane guanylate cyclases. Its discovery and molecular characterization was a land mark event in the field of phototransduction (reviewed in Pugh et al., 1997; Koch et al., 2010) as it identified the source of cyclic GMP that serves as a second messenger of the LIGHT signal. It also impacted the entire membrane guanylate cyclase field by dividing the guanylate cyclase family into two subfamilies, one comprising the hormone receptor cyclases, and the other, cyclases modulated by intracellular $[Ca^{2+}]_i$ signals (reviewed in: Sharma, 2010). ROS-GC1 belongs to the second subfamily together with another rod outer segment guanylate cyclase ROS-GC2 (Ret-GC2 or GC-F), and the olfactory neuroepithelial guanylate cyclase, ONE-GC (GC-D; reviewed in: Sharma, 2010).

The best-documented physiological function of ROS-GC1 and ROS-GC2 is in the recovery phase of phototransduction, to return the illuminated photoreceptors to the dark, resting state. Illumination of photoreceptors leads to activation of cyclic GMP phosphodiesterase, depletion of cyclic GMP, closure of the cyclic GMP gated (CNG) channels, lowering the free Ca^{2+} concentration, and hyperpolarization of the plasma membrane (reviewed in: Pugh et al., 1997; Koch et al., 2010). The ROS-GCs task is to restore the dark-level of cyclic GMP allowing opening of the CNG channels, increase of Ca^{2+} influx, and depolarization of plasma membrane. Ca^{2+} concentration, thus, determines the activities of ROS-GCs but in an indirect way. Guanylate cyclase activating proteins (GCAPs; GCAP1 and GCAP2) sense the post-illumination fall in Ca^{2+} and stimulate ROS-GCs to synthesize cyclic GMP at a faster rate and restore its dark level (reviewed in: Detwiler, 2000; Koch et al., 2010).

GCAPs, however, are not the only Ca^{2+} sensing modulators of ROS-GC activity. While increasing Ca^{2+} concentrations inhibit ROS-GCs activity through GCAPs, two other Ca^{2+} sensors, S100B and neurocalcin δ stimulate ROS-GC1 in a Ca^{2+}-dependent fashion (Pozdnyakov et al., 1995; Margulis et al., 1996; Duda et al., 1996a; Kumar et al., 1999). The Ca^{2+}-dependent S100B-mediated activation of ROS-GC1 operates in cones including their outer segments and pedicles (Duda et al., 2002; Wen et al., 2012). Its role in photo- and visual transductions remains to be established, but existing data indicate its involvement in transmission of the visual signal from cone ON-bipolar cells (Wen et al., 2012). Ca^{2+} signaling of ROS-GC1 activity mediated by neurocalcin δ is operative in retinal ganglion cells (Krishnan et al., 2004); and of ONE-GC in the olfactory neuroepithelium (Duda et al., 2001a, 2004).

Beyond the retina, ROS-GC1 is expressed in the pineal gland where in one subset of pinealocytes it co-localizes with GCAP1 and in another, with S100B (Venkataraman et al., 2000); in the mitral cells of the olfactory bulb where it co-localizes with GCAP1 (Duda et al., 2001b); and it co-immunoprecipitates with S100B in the gustatory epithelium (Duda and Sharma, 2004).

Neurocalcin δ (NCδ) belongs to a subfamily of neuronal calcium sensor (NCS) proteins called visinin like proteins (VSNLs).

Similar to other, but not all NCS proteins, it is acylated at the N-terminus by myristic acid and undergoes a classical calcium-myristoyl switch (Ladant, 1995) e.g., it buries the myristoyl group in a hydrophobic pocket in a Ca^{2+} free form and exposes it in Ca^{2+}-bound form, a phenomenon first observed for recoverin (Zozulya and Stryer, 1992). Myristoylation of neurocalcin δ allows its membrane association in response to changes in the intracellular Ca^{2+} concentration. However, once NCδ binds to the cellular membranes in a Ca^{2+}-dependent fashion, part of it remains membrane associated even after removing Ca^{2+} by the addition of ethylene glycol tetraacetic acid (EGTA; Krishnan et al., 2004). Although the highest level of NCδ has been detected in neuronal tissues, its expression in the periphery is also observed. Functionally, NCδ has been linked to a wide variety of processes such as receptor endocytosis through interaction with α- and β-clathrin and β-adaptin (Ivings et al., 2002), trafficking and membrane delivery of glutamate receptors of the kainate type (Coussen and Mulle, 2006), and with microtubule assembly (Iino et al., 1995). The presence of NCδ has been found in the inner plexiform layer of the retina, e.g., in the amacrine and ganglion cells (Krishnan et al., 2004), olfactory sensory neurons (Duda et al., 2001b, 2004) and in type II cells of mouse circumvallate taste papillae (Rebello et al., 2011).

In the inner retinal layer NCδ acts as Ca^{2+}-dependent modulator of membrane guanylate cyclase ROS-GC1 (Krishnan et al., 2004) and in the olfactory neuroepithelium, of ONE-GC (Duda et al., 2001a, 2004). The exact physiological significance of the ROS-GC1-NCδ signaling system in the retina is not known yet, it has, however, been proposed that the system may be involved in synaptic processes (Krishnan et al., 2004). In the olfactory neuroepithelium neurocalcin δ has been proposed as a Ca^{2+} sensor component of the two-step odorant uroguanylin signaling machinery (Duda and Sharma, 2009).

Outside the neuronal system, NCδ is expressed in the adrenal glomerulosa cells (Duda et al., 2012a,b). There it co-localizes with the member of receptor guanylate cyclase sub-family, atrial natriuretic factor receptor guanylate cyclase (ANF-RGC), and has been proposed to be involved in the inhibition of aldosterone synthesis (Duda et al., 2012a,b). Accordingly, a mouse model in which one copy of NCδ gene is deleted is inflicted with hyperaldosteronism and hypertension (Duda et al., 2012b).

Preliminary studies localize also ROS-GC1 outside the neuronal system, in male gonads, where it co-localizes with GCAP1 and S100B (Jankowska et al., 2007). It remains to be determined, whether, and how ROS-GC1 and its companion calcium binding proteins are involved in the physiology of the testis. Considering, however, that cyclic GMP and Ca^{2+} are genuine mediators of signal transduction in the testes in the physiology of fertilization (reviewed in: Garbers, 1989; Jankowska and Warchol, 2010) it is highly possible that ROS-GC1, stimulated or inhibited as needed, in a Ca^{2+}-dependent fashion by Ca^{2+}-binding proteins, is the provider of the physiologically necessary quantities of cyclic GMP. We now present new observations on co-presence of NCδ and ROS-GC1 in the spermatogenic cells and Ca^{2+}-dependent modes of NCδ and S100B in modulating ROS-GC1 signaling the mammalian testes.

MATERIALS AND METHODS

TISSUES

The study group consists of testes from human (obtained from consenting organ donors, $n = 5$), bovine (purchased from local slaughter house, $n = 3$), and Wistar rat (obtained form the Vivarium of Poznan University of Medical Sciences, Poznan, Poland, $n = 12$). The study was approved by the IACUC and Ethics Review Boards of all the involved Institutions.

GENETICALLY MODIFIED MICE

Care of the experimental animals conformed to the protocols approved by the IACUC at Salus University and was in strict compliance with the NIH guidelines. Construction of heterozygous NCδ-KO ($NC\delta^{+/-}$) mice is described in (Duda et al., 2012b). The S100B-KO mice are described in (Wen et al., 2012).

ANTIBODIES

Rabbit ROS-GC1 and NCδ antibodies were produced, characterized and affinity purified as in (Venkataraman et al., 2003; Krishnan et al., 2004). Secondary antibodies, AP-conjugated goat anti-rabbit IgG, preimmune rabbit serum, NBT/BCIP, and Cy3-conjugated sheep anti-rabbit IgG were purchased from Sigma-Aldrich.

REVERSE TRANSCRIPTION POLYMERASE CHAIN REACTION (RT-PCR)

Total RNA was isolated from seminiferous tubules and interstitial tissue using TriPure isolation reagent (Roche Diagnostics), according to the manufacturer's protocols. The cDNA library was constructed using Advantage RT for PCR kit (BD-Bioscience) and used for the amplification of ROS-GC1 and neurocalcin δ fragments. Sequences of primers used for the amplification are listed in **Table 1**. The amplified fragments were purified on agarose gel and sequenced to confirm their identities.

WESTERN BLOTTING

The procedure was carried out according to the previously published protocols (Venkataraman et al., 2000; Duda and Sharma, 2004; Jankowska et al., 2007). 150 mg of membrane fraction proteins were denatured in gel-loading buffer [62.5 mM Tris-HCl (pH 7.5), 2% SDS, 5% glycerol, 1 mM β-mercaptoethanol, and 0.005% bromophenol blue] in 95°C for 10 min. Samples were then subjected to SDS-PAGE in a buffer containing 0.025 mM Tris-HCl (pH 8.3), 0.192 M glycine, and 0.1% SDS. Afterwards the resolved proteins were transferred to nitrocellulose membranes. To avoid non-specific interactions membranes were incubated in Tris buffered saline containing 0.05% Tween 20 (TBS-T), 5% non-fat milk (blocking buffer) overnight at 4°C. ROS-GC1 and NCδ proteins were detected with specific rabbit polyclonal antibodies diluted 1:1500 and 1:1000, respectively. After 1 h incubation the blot was rinsed three times with TBS-T and incubated with anti-rabbit secondary antibodies conjugated with horseradish peroxidase (1:10 000).

To visualize the immunoreactive bands SuperSignal blaze chemiluminescent substrate (Pierce) was used according to the manufacturer's protocol. Signal was detected by exposing the blot

Table 1 | Primers used in PCR.

Species	Gene	PCR product	Primer sequence 5′	Primer sequence 3′	Amplified sequence
Human (*Homo sapiens)*	ROS-GC1Kin	553 bp	5′GGGAATAAGGTATCTGCACC3′	5′CCGGATCAGATCCTCCA3′	nt: 2028–2581 NM_000180
	NCALD	526 bp	5′ACAGCAAGCTGCGCCCGGAGGTC3′	5′ACAATGGACGGGTCGCTATTGGC3′	nt:407-933 NM_001040624
Rat (*Rattus Norvegicus)*	ROS-GC1Kin	566 bp	5′GAGATATCTCCACCATCGT3′	5′TAACTCCTCTGTGCGTTCT3′	nt: 2034-2600 L36029
	NCALD	526 bp	5′ACAGCAAGCTGCGCCCTGAAGTC 3′	5′ACAATGGAAGGGTCGCTTTTGGC3′	nt: 177-704 NM_001024371
Bovine (*Bos Taurus*)	ROS-GC1Kin	548 bp	5′ATAAGGTATCTGCACCATCGAG3′	5′CCGGATCAGGTCCTCCAGGTTC5′	nt: 2026-2574 NM_174548
	NCALD	527 bp	5′ACAGCAAGCTGCGCCCGGAGGTCA3′	5′ACAATGGACGGGTCGCTCTTGGC3′	nt:25-551 NM_174398

to Kodak X-ray film for 15 s. Then the X-ray film was scanned and processed using Photoshop 6.0 software.

IMMUNOHISTOCHEMISTRY

Paraffin sections of the testes fixed in 4% paraformaldehyde were used for immunohistochemical detecting of ROS-GC1 and NCδ. To block the non-specific binding the sections were first washed with TBS (100 mM Tris-HCl, 0.9% NaCl) and incubated in blocking solution consisting of TBS buffer containing 0.05% Tween 20 (TBS-T) and 1% BSA for 1 h at room temperature. After washing with TBS-T the sections were incubated with the respective primary antibodies for 60 min at 37°C and washed four times (15 min each) in TBS-T. Anti ROS-GC1 antibodies were diluted 1:200 and anti neurocalcin δ, 1:100. AP-conjugated anti-rabbit IgG, diluted 1:200 and NBT/BCIP as the substrate were used for detection. Controls included detection reactions carried out under identical conditions except that the primary antibodies were replaced by preimmune serum.

ISOLATION OF THE PARTICULATE FRACTION OF THE TESTES

Membrane fraction of the testes was isolated according to the protocol described previously (Marala and Sharma, 1988). The tissue was homogenized in a buffer containing 250 mM sucrose, 10 mM Tris-HCl (pH 7.4) and protease inhibitors. The homogenate was centrifuged at 400 *g* and then the supernatant at 10,000 *g* and finally, at 40,000 *g*. The resulting pellet represented the membrane fraction.

GUANYLATE CYCLASE ACTIVITY ASSAY

The particulate fraction was assayed for guanylate cyclase activity as described previously (Paul et al., 1987; Jankowska et al., 2007, 2008). Briefly, membranes were preincubated on an ice-bath with or without NCδ in an assay system containing 10 mM theophylline, 15 mM phosphocreatine, 20 μg creatine kinase, and 50 mM Tris-HCl (pH 7.5), adjusted to the appropriate free Ca^{2+} concentration with precalibrated Ca^{2}/EGTA solutions (Molecular Probes). The reaction was initiated by the addition of a substrate solution (4 mM $MgCl_2$ and 1 mM GTP, final concentration) and continued by incubation at 37°C for 10 min. The reaction was terminated by the addition of 50 mM sodium acetate (pH 6.2) followed by heating in a boiling water-bath for 3 min. The amount of cyclic GMP formed was determined by radioimmunoassay (Nambi et al., 1982; Jankowska et al., 2007, 2008).

STATISTICAL ANALYSES

The activity of guanylate cyclase was calculated as mean of at least six separate values ± SD.

RESULTS

General consensus has been that ROS-GC1 is expressed exclusively in the sensory as well as in the second order neurons of the retina and in the neurons of the pineal gland and the olfactory bulb (Hayashi and Yamazaki, 1991; Goraczniak et al., 1994; Liu et al., 1994; Yang et al., 1995; Venkataraman et al., 2000; Duda et al., 2001a). However, earlier results of these investigators provided the first indication that ROS-GC1 is also expressed outside the neuronal system, in bovine testes and sperm (Jankowska et al., 2007, 2008). In the sperm, it is co-expressed with calcium sensor S100B and neuronal calcium sensor proteins GCAP1 and NCδ (Jankowska et al., 2008). These results were striking enough to warrant more detailed studies. Present investigation represents a step in that direction.

MAMMALIAN TESTES EXPRESS ROS-GC1 AND NEUROCALCIN δ: ANALYSES AT THE mRNA LEVELS

The presence of ROS-GC1 and NCδ transcripts was analyzed in human, bovine, and rat testes. Using total RNA isolated from these tissues individual cDNA libraries were constructed and used for amplification of specific fragments of ROS-GC1 and NCδ cDNAs by polymerase chain reaction. For the amplification, distinct, species-specific primers for ROS-GC1 or NCδ were designed. These primers corresponded to the sequences located within so called "kinase-like domain" of ROS-GC1 cDNA and for NCδ they overlapped with the 5′- and 3′- ends of its coding sequence. The amplification yielded fragments of 553, 548, and 566 bp of the human, bovine, and rat ROS-GC1, respectively,

and 526 bp fragment of neurocalcin δ (**Table 1**). Sequencing of all amplified products confirmed their identities with ROS-GC1 or NCδ cDNAs. The ROS-GC1 fragments represented indeed sequence coding for the kinase-like domain, and the NCδ fragment had sequence identical with the predicted part of NCδ coding region. Amplification of uninterrupted coding sequences for ROS-GC1 and NCδ documented that the RNA used was not contaminated with genomic DNA. Thus both, ROS-GC1 and NCδ transcripts are present in human, bovine, and rat testes.

MAMMALIAN TESTES EXPRESS ROS-GC1 AND NEUROCALCIN δ: ANALYSES AT THE PROTEIN LEVELS

At the protein level, the expression of ROS-GC1 and NCδ in mammalian testes was tested in two ways. First, a rudimentary assessment of the expression of both types of proteins was obtained by Western blotting; this was followed by immunocytochemical localization of ROS-GC1 and NCδ in human and rat testes. In both types of analyses appropriate affinity purified antibodies, anti-ROS-GC1, or anti-NCδ were used. Immunostaining of bovine testis was performed in parallel as positive control.

After establishing that ROS-GC1 and NCδ transcripts are present in mammalian testes, their protein identity was scrutinized by Western blotting. The mobility of the ROS-GC1 or NCδ immunoreactive band, ∼116 kDa and ∼20 kDa, respectively, (**Figures 1A,B**) was identical to that observed previously for ROS-GC1 expressed in photoreceptor outer segments (Duda et al., 1996b) and NCδ expressed in the inner retina (Krishnan et al., 2004). These results clearly confirm that both proteins, ROS-GC1 and NCδ are expressed in human, rat, and bovine testes.

Detailed analyses of the localization of ROS-GC1 and NCδ in the mammalian testes were performed by immunocytochemistry. In human and rat testes ROS-GC1 immunostaining was randomly distributed in the seminiferous tubules (**Figures 2A,B**). The pattern of this staining was identical to that observed for bovine testes (**Figure 2C**). Visual analysis allowed localizing the staining to spermatogenic cells, especially to primary spermatocytes and spermatids. The majority of primary spermatocytes (**Figure 2**; indicated as Sc), spermatids (**Figure 2**; indicated as Sd) and single spermatogonias (**Figure 2**; indicated as Sg) were immunostained in all species tested, human, rat, and bovine. To verify specificity of the ROS-GC1 immunostaining a control reaction was performed in which ROS-GC1 antibody was omitted and substituted with the preimmune serum. Under these conditions no labeling was observed (**Figures 2A'–C'**).

In a similar manner the expression of NCδ in the human and rat testes was analyzed (**Figures 3A,B**) and compared with that in bovine testis (**Figure 3C**). NCδ immunoreactivity was observed in all types of germinal cells: spermatogonias (**Figure 3**: Sg), spermatocytes (**Figure 3**: Sc) and spermatids (**Figure 3**: Sd). Extremely strong staining was observed in spermatids localized close to seminiferous tubule lumen. No labeling was observed when the sections were incubated with preimmune rabbit serum instead of the NCδ antibody, attesting to the specificity of the staining (**Figures 3A'–C'**).

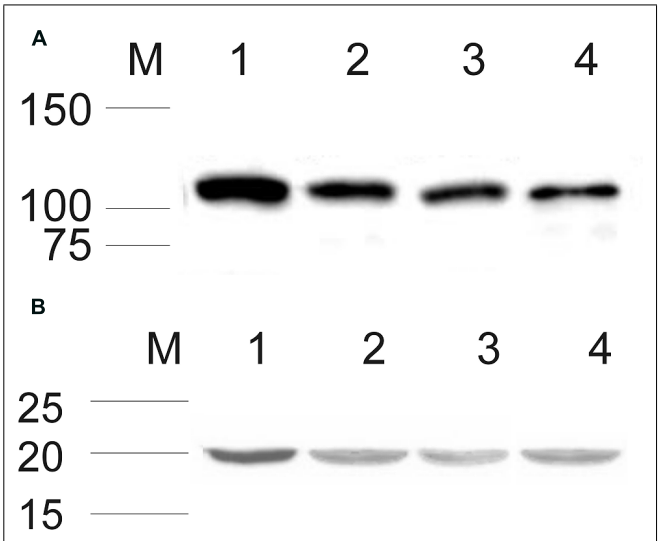

FIGURE 1 | Expression of ROS-GC1 and NCδ in the testes analyzed by Western blot. Membrane proteins from human, rat, and bovine testes were isolated and subjected to Western blot analyses with specific antibodies against ROS-GC1 **(A)**, and NCδ **(B)** as described in "Materials and Methods." Both types of analyzed proteins expressed in human, rat, and bovine testis are shown in lanes 2, 3, and 4, respectively. Western blotting of bovine retinal membranes was performed as a positive control and is shown in lane 1 in **(A)** and **(B)**. The positions of the molecular size markers are given alongside.

The results presented clearly demonstrate that both ROS-GC1 and NCδ are expressed in the mammalian testes and in the germinal cells. Importantly, the patterns of ROS-GC1 and NCδ immunoreactivities are identical in the species analyzed (compare **Figures 2** and **3**) strongly indicating that they co-localize with each other. Notably, the intensities of the immunostaining for ROS-GC1 or NCδ increase with the maturation of the spermatogenic cells.

Since the increase in the staining is observed across the cells in different stages of spermatogenesis process – the highest accumulation of analyzed proteins was observed in spermatocytes and spermatids – it indicates that ROS-GC1 and NCδ expression correlates with the stage of the seminiferous cycle.

NEUROCALCIN δ STIMULATES ROS-GC1 CATALYTIC ACTIVITY EXPRESSED IN THE TESTES: EVIDENCE FROM RECONSTITUTION EXPERIMENTS

To demonstrate that neurocalcin δ stimulates ROS-GC1 expressed in the testes, their membranes were analyzed for guanylate cyclase activity in the presence of NCδ. Membranes of human, bovine, and rat testes were isolated and incubated with increasing concentrations of NCδ and constant 100 μM Ca^{2+}. The amount of cyclic GMP formed was determined as a measure of guanylate cyclase activity. NCδ stimulated the cyclase activity in a dose-dependent fashion (**Figure 4**). Half-maximal stimulation (EC_{50}) was observed at ∼0.8 μM NCδ in all three species tested. The maximal stimulation of ∼2.2-fold above the basal value was at 2 μM NCδ. Importantly, the stimulatory profiles of guanylate cyclase in the analyzed membranes were very similar to those

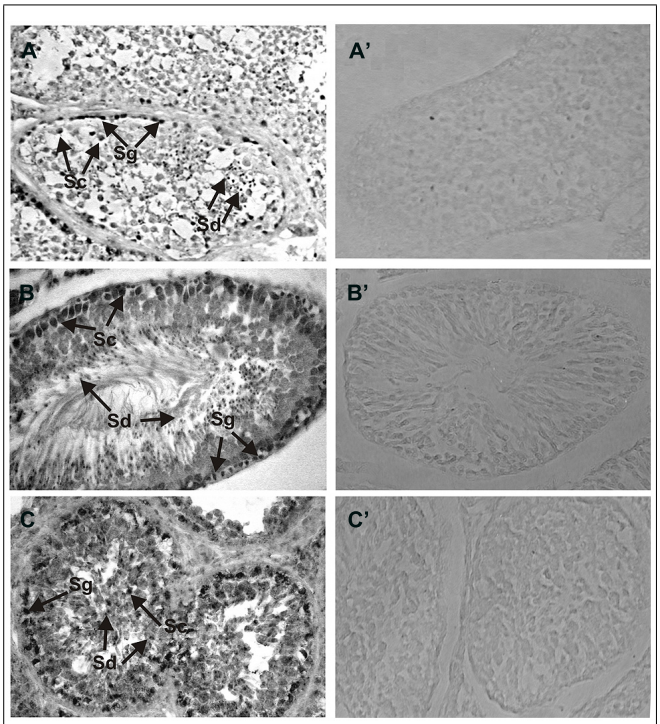

FIGURE 2 | Immunolocalization of ROS-GC1 in the testes. Immunohistochemistry was performed using specific antibodies against ROS-GC1 on paraffin sections of human **(A)**, rat **(B)**, and bovine **(C)** testes. The ROS-GC1 was localized in spermatogenic cells. In the testes positive staining was observed in spermatogonias (Sg), spermatocytes (Sc) and spermatids (Sd), as indicated by the arrows. Control staining was performed according to the procedure for ROS-GC1 detection, except that preimmune serum was used instead of the primary antibody **(A'–C')**. Original magnification 400X.

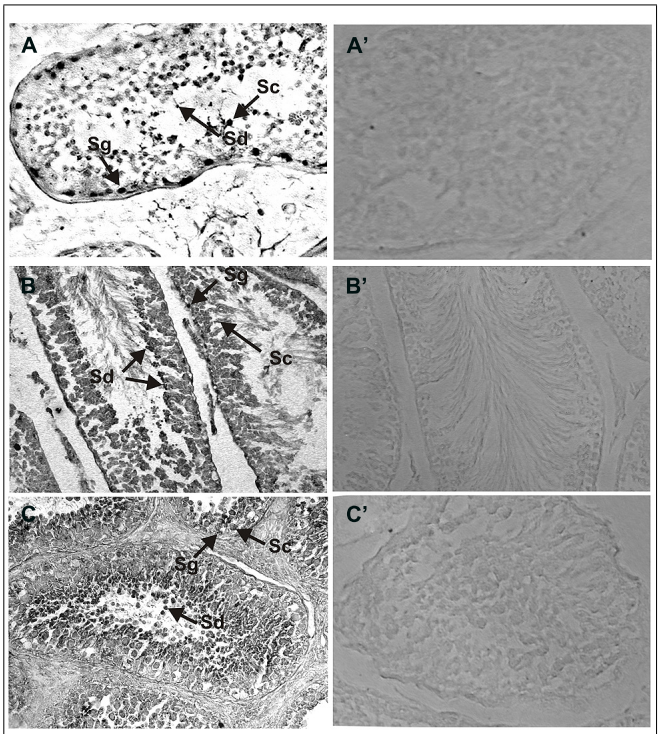

FIGURE 3 | Immunolocalization of NCδ in the testes. Paraffin sections of the testes were incubated with primary antibodies against NCδ. NCδ immunoreactivity was observed in all spermatogenic cells of human **(A)**, rat **(B)**, and bovine **(C)** testes. Particularly strong signal was detected in spermatocytes and spermatids localized close to lumen of the seminiferous tubule (indicated as Sc and Sd, respectively). Control staining was performed according to the procedure for NCδ detection, except that preimmune serum was used instead of the primary antibody **(A'–C')**. Original magnification 400X.

observed for the recombinant ROS-GC1 (Kumar et al., 1999) and ROS-GC1 native to the retinal photoreceptor outer segments and inner plexiform layer (Krishnan et al., 2004). These results show that NCδ indeed stimulates ROS-GC1 activity in the testes.

ROS-GC1 AND NCδ ARE FUNCTIONALLY LINKED: EVIDENCE FROM GENETICALLY MODIFIED MICE

Because the experiments described above were conducted on the native membranes of the testes but with exogenously supplied NCδ, they prove the ability of ROS-GC1 to respond to NCδ but they do not prove that these two together form a functional unit. To determine this, the mouse model with deletion of one copy of the NCδ gene, $NC\delta^{+/-}$, was used [mice with deletion of both copies of NCδ are not born (Duda et al., 2012b)]. It was reasoned that if NCδ is indeed the Ca^{2+}-sensor modulator of ROS-GC1 in the testes of these mice the NCδ-modulated Ca^{2+} signaling pathway should be half as active as in those of the wild type mice [wt ($NC\delta^{+/+}$)]. To test this prediction, the particulate fractions of the testes from wild type and $NC\delta^{+/-}$ mice were isolated in the presence of 100 μM Ca^{2+} and tested for guanylate cyclase activity in the presence and absence of Ca^{2+}. The reason for isolating the membranes in the presence of Ca^{2+} was that NCδ exhibits the property of "calcium-myristoyl switch" which means that in the presence of Ca^{2+} it is membrane bound and therefore would be present in the membrane fraction (Ladant, 1995; Krishnan et al., 2004). The guanylate cyclase activity assayed in the absence of Ca^{2+} (1 mM EGTA was present in the assay mixture) was 58 ± 7 pmol cyclic GMP min^{-1} (mg prot)$^{-1}$ for the wt and 63 ± 8 pmol cyclic GMP min^{-1} (mg prot)$^{-1}$ for the $NC\delta^{+/-}$ mice (**Figure 5**: panel "Ca^{2+}"). However, the cyclase activity determined in the presence of Ca^{2+} was strongly dependent on the mice genotype. With 1 μM Ca^{2+} present in the assay mixture the activity was 248 ± 17 pmol cyclic GMP min^{-1} (mg prot)$^{-1}$ for the wild type mice and 148 ± 16 pmol cyclic GMP min^{-1} (mg prot)$^{-1}$ for the $NC\delta^{+/-}$ mice (**Figure 5**: panel "+Ca^{2+} – basal"). These results, as predicted, demonstrate that the Ca^{2+}-dependent NCδ-modulated ROS-GC1 signaling pathway in the mice with one copy of NCδ gene deleted ($NC\delta^{+/-}$) is about half as active as in the wild type mice. To further validate that the lowering of the Ca^{2+}-dependent cyclase activity in the membranes of $NC\delta^{+/-}$ mice is the exclusive consequence of lower NCδ expression, 4 μM exogenous NCδ was added to the wild type and $NC\delta^{+/-}$ membranes and the cyclase activity was assessed in the presence of 1 μM Ca^{2+}. The cyclase activity in the wild type membranes increased only minimally, from 248 to 273 ± 25 pmol cyclic GMP

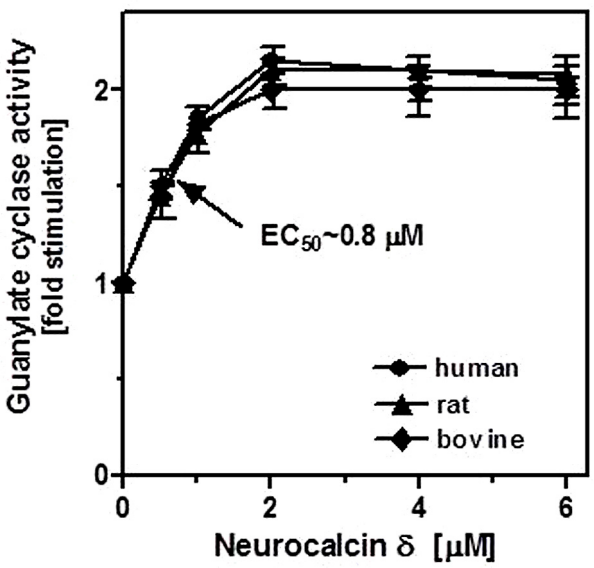

FIGURE 4 | Effect of NCδ on the guanylate cyclase activity in the membranes of testes. Membranes of human, rat, and bovine testes were isolated as described in "Materials and Methods". They were assayed for guanylate cyclase activity in the presence of indicated concentrations of NCδ and 100 μM Ca^{2+}. Each experiment was done in triplicate, and repeated two times. The results shown (mean ± SD) are from these experiments.

min^{-1} (mg prot)$^{-1}$but in the NCδ$^{+/-}$ membranes, from 148 to 258 ± 28 (**Figure 5**: panel "+Ca^{2+} + 4 μM NCδ"). Thus, the activity achieved was practically the same for both types of membranes. These results demonstrate that addition of exogenous NCδ to the NCδ$^{+/-}$ membranes restores the guanylate cyclase catalytic activity and brings it to the level of activity in the wild type membranes. The slight activity increase in the wild type membranes can be explained by a partial loss of the native NCδ during the membrane preparation procedure. Together these results demonstrate that functional ROS-GC1-NCδ-Ca^{2+} transduction system is operative and is the functional transduction element in the testes.

WHICH CA^{2+} SENSOR, NCδ OR S100B, IS THE MORE POTENT REGULATOR OF ROS-GC1 ACTIVITY?

Our previous investigation has shown that S100B is expressed in the testes (Jankowska et al., 2007) and the present results demonstrate that NCδ is also expressed there. Thus, two Ca^{2+}-dependent modulators of ROS-GC1 activity are present in the testes. Taking advantage of the availability of two types of genetically modified mice, NCδ$^{+/-}$ and S100B$^{-/-}$ we attempted comparing the relative inputs of NCδ and S100B into regulation of ROS-GC1 transduction machinery.

Testes were removed from the wild type, NCδ$^{+/-}$ and S100B$^{-/-}$ mice, their membrane fractions were isolated in the presence of 100 μM Ca^{2+} and assessed for guanylate cyclase activity. The results of this experiment are shown in **Figure 6**. In the absence of Ca^{2+} all three types of membranes exhibited comparable activity of ∼60 pmol cyclic GMP min^{-1} (mg prot)$^{-1}$ (**Figure 6A**: panel "basal") and, as expected, the activity was not affected by the addition of NCδ or S100B (**Figure 6A**: panels "+ncalc δ" and "+S100B"). However, when the cyclase activity was assayed in the presence of Ca^{2+} the values differed between the genotypes: 250 pmol cyclic GMP min^{-1} (mg prot)$^{-1}$ for the wild type, 150 pmol cyclic GMP min^{-1} (mg prot)$^{-1}$ for the NCδ$^{+/-}$ and 200 pmol cyclic GMP min^{-1} (mg prot)$^{-1}$ for the S100B$^{-/-}$ (**Figure 6B**: panel "basal"). These values describe the ROS-GC1 activity stimulated together by NCδ and S100B in the case of the wild type membranes; stimulated by half of wild type amount of NCδ and S100B in the case of NCδ$^{+/-}$ membranes; and stimulated by NCδ only in the case of S100B$^{-/-}$ membranes. Thus, the difference between ROS-GC1 activity in testes of the wild type mouse and the activity in the genetically modified mice (100 and 50 pmol pmol cyclic GMP min^{-1} (mg prot)$^{-1}$ for the NCδ$^{+/-}$ and S100B$^{-/-}$, respectively) describes the Ca^{2+}-dependent stimulatory effects lost due to the absence of half of the NCδ present in the wild type testes or to the total absence of S100B. Higher loss of activity resulting from deletion of one copy of NCδ gene than resulting from deletion of two copies of S100B gene indicates that NCδ is more potent than S100B in modulating the Ca^{2+}-dependent ROS-GC1 activity. One could argue, however, that this comparison might not be totally reflective of the *in vivo* contributions of NCδ and/or S100B, because there is a possibility that some of these proteins were lost during the membrane preparation process. To settle this possibility the ROS-GC1 activity was measured in the presence of individually added NCδ or S100B.

Addition of 4 μM NCδ (**Figure 6B**: panel "+ncalc δ") resulted in a small increase of the cyclase activity exhibited by the membranes isolated from the wild type testes (from ∼250 to ∼270 pmol cyclic GMP min^{-1} (mg prot)$^{-1}$ and isolated from the S100B$^{-/-}$

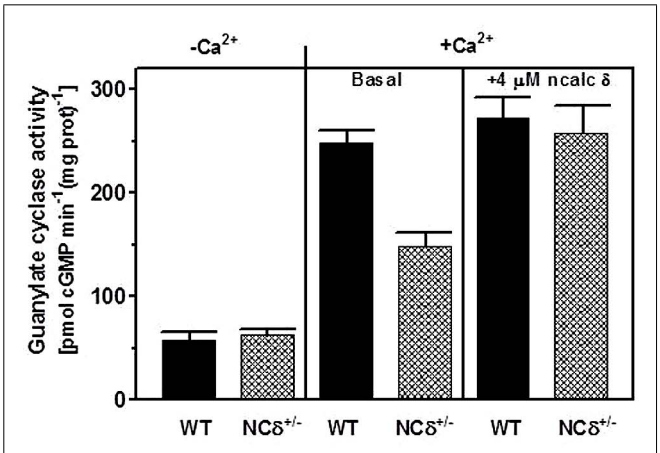

FIGURE 5 | NCδ modulates ROS-GC1 activity in mouse testes. Testes were removed from the wild type (WT) and NCδ$^{+/-}$ mice and their particulate fractions were isolated in the presence of 100 μM Ca^{2+}. These were assayed for guanylate cyclase activity in the presence of 1 mM EGTA or 10 μM Ca^{2+} (panel "−Ca^{2+}"- and "+Ca^{2+}"-basal). 4 μM myristoylated NCδ was added to the membranes and the guanylate cyclase activity was assessed in the presence of 10 μM Ca^{2+}. The experiment was done in triplicate and repeated with separate membrane preparations. The results are mean ± SD of these experiments.

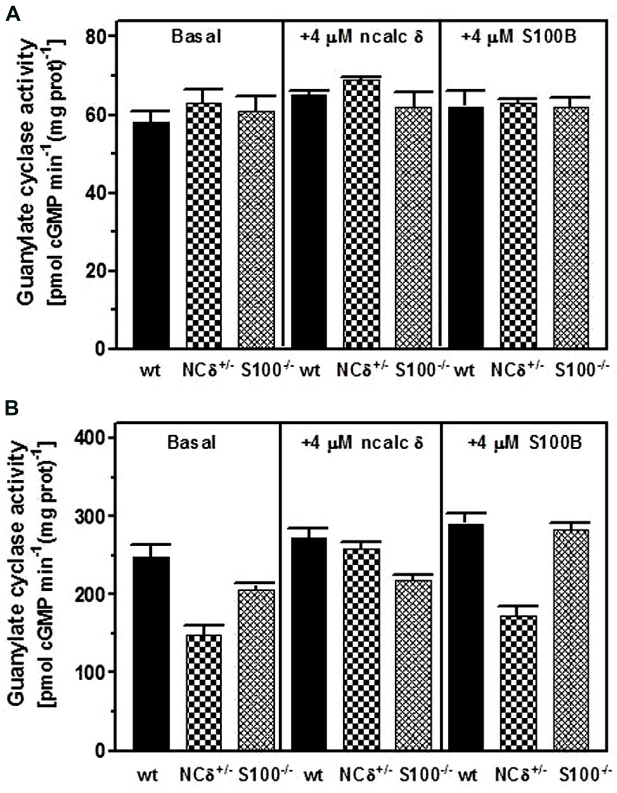

FIGURE 6 | Comparison of NCδ and S100B stimulatory effects on ROS-GC1 activity in mouse testes. Testes were removed from the wild type (WT), NCδ$^{+/-}$, and S100$^{-/-}$ mice and their particulate fractions were isolated in the presence of 100 μM Ca^{2+}. **(A)** The membranes were assayed for guanylate cyclase activity in the presence of 1 mM EGTA in the absence (panel "basal") or presence of 4 μM myristoylated NCδ (panel ("+ 4 μM ncalc δ") or 4 μM S100B (panel "+S100B"). **(B)** The membranes were assayed for guanylate cyclase activity in the presence of 10 μM Ca^{2+}("basal") or with the addition of 4 μM NCδ (panel "+ 4 μM ncalc δ") or 4 μM S100B (panel "+ 4 μM S100B"). The experiment was done in triplicate and repeated with separate membrane preparations. The results are mean ± SD of these experiments.

testes [from ∼200 to ∼220 pmol cyclic GMP min^{-1} (mg prot)$^{-1}$]. This non-significant to minimal increase of ROS-GC1 catalytic activity in these membranes indicates that if any NCδ was lost during the membrane preparation, it was only the insignificant amount. For the NCδ$^{+/-}$ membranes the increase was significant, from ∼150 to ∼260 pmol cyclic GMP min^{-1} (mg prot)$^{-1}$. Importantly, addition of 4 μM NCδ brought the ROS-GC1 activity in these membranes very close to the ROS-GC1 activity in the wild type membranes. Because only residual amount of NCδ was lost during membrane preparation, as concluded from the wild type and S100B$^{-/-}$ membranes, practically all the increase of activity in the NCδ$^{+/-}$ membranes accounts for the activity lost due to the expression of only half of the NCδ present in the membranes from wild type testes.

When the ROS-GC1 activity was assayed with 4 μM S100B added to the membranes (**Figure 6B**: panel "+S100B") it increased by ∼40 pmol cyclic GMP min^{-1} (mg prot)$^{-1}$ in the wild type and by 25 pmol cyclic GMP min^{-1} (mg prot)$^{-1}$in the NCδ$^{+/-}$ membranes indicating that some S100B was lost in membranes preparation. The increase was ∼80 pmol cyclic GMP min^{-1} (mg prot)$^{-1}$for the S100B$^{-/-}$ membranes [from 205 to 282 pmol cyclic GMP min^{-1} (mg prot)$^{-1}$] and this increase of activity in the S100B$^{-/-}$ membranes accounts for the activity lost due to the loss of S100B expression in the testes. Comparing the activity loss because of the absence of half of NCδ with the activity loss due to the total absence of S100B expression shows that neurocalcin δ is more significant contributor to ROS-GC1 Ca^{2+}-dependent activity than S100B. It could be estimated that NCδ contributes about 75% to ROS-GC1 Ca^{2+}-dependent activity and S100B, about 25%.

DISCUSSION

The core finding of this study is that it establishes the presence and molecular nature of a Ca^{2+}- modulated ROS-GC transduction system in all types of the germinal cells of the testes: spermatogonias, spermatocytes, and spermatids. Because abundance of this transduction system is present in the spermatids residing close to the seminiferous tubule lumen, it hints that the system is linked with the processes of spermatogenesis.

This Ca^{2+}-dependent cyclic GMP generating transduction system is composed of a transducer component ROS-GC1 and two Ca^{2+} sensor components, NCδ and S100B. NCδ is the major signal contributor responsible for about 75% of the guanylate cyclase stimulated catalytic activity, and S100B the relatively minor contributor, about 25% of signaling activity.

Cyclic GMP appears to be a critical second messenger in the physiology of the testes. In particular, it has been shown to influence motility in spermatozoa, development of testicular germ cells, relaxation of peritubular lamina propia cells, testosterone synthesis in Leydig cells, and dilatation of testicular blood vessels (Singh et al., 1988; Armstrong et al., 1994; Middendorff et al., 1997, 2000). Our immunostaining results demonstrate that both ROS-GC1 and NCδ immunoreactivity is present in all germ cells but its intensity is lowest in spermatogonias and highest in spermatids, hence, it increases with maturation, indicating that development of these cells may be directed by the activity of ROS-GC1.

The present study, of basic biochemical nature, brings to the fore several issues for future research. (1) What is the exact composition of the transduction system: does it represent a single pathway, composed of one ROS-GC1 and two Ca^{2+} sensors, NCδ, and S100B operating simultaneously? Or, two independent, but complementary pathways, each composed of one ROS-GC1 and one Ca^{2+} sensor, NCδ, or S100B? (2) What is the precise morphological residence of any of these transduction systems in the testicular cells? (3) What is the exact stoichiometry of these components in the given cell types? (4) What are the mechanistic details of the operational modes of this/these ROS-GC transduction pathways? (5) What is the physiological significance of these pathways to the testicular function, endocrine, fertility, including spermatogenesis; (6) what is the interplay between the Ca^{2+}-modulated ROS-GC1 signaling pathway and ANF-dependent ANF-RGC pathway, another cyclic GMP generating machinery functioning in the mammalian testes (Marala and Sharma, 1988; Pandey and Singh, 1990; Pandey et al., 1999; Mourdjeva et al., 2001) and finally,

(7) how this information can be translated to the clinical level to search for the pathway/s-linked diseases and finding their cures?

Handicapped with these informational gaps, it is difficult to construct a proper Ca^{2+}-modulated signal transduction model for any of the specific physiological function/s of the testes. However, a preliminary signal transduction scheme is conceptualized where $[Ca^{2+}]_i$ modulation of ROS-GC1 activity can occur through three modes. MODE 1 involves interaction of ROS-GC1 with its Ca^{2+} sensors, NCδ and S100B. The ROS-GC is stimulated in $[Ca^{2+}]_i$ – dependent manner and generates cyclic GMP. MODE 2 involves interaction of the ROS-GC1 with GCAP1 which is also present in the testes (Jankowska et al., 2007). It is recalled that GCAP1 signaling is opposite to that of NCδ or S100B; it stimulates ROS-GC1 catalytic activity in the absence of Ca^{2+} and progressively inhibits it with increasing Ca^{2+} concentration (Duda et al., 1996b). Thus, through GCAP1 $[Ca^{2+}]_i$ keeps the ROS-GC activity in the suppressed state. MODE 3, it is the most interesting scenario. ROS-GC1 is present together with the Ca^{2+}-dependent guanylate cyclase activators (CD-GCAPs)–NCδ, S100B – and with GCAP1. The ROS-GC activity oscillates between the GCAP1-dependent state and CD-GCAPs-dependent state. In these states the cyclase is a bimodal Ca^{2+} transduction switch. And it functions according to the principles established for the synapse region between the photoreceptor and ON-bipolar cells (Duda et al., 2002; Venkataraman et al., 2003). This mode of ROS-GC1 activity regulation is possible because each of the three modulators targets its individual domain in ROS-GC1. These domains have been mapped and are schematically shown in **Figure 7**. Neurocalcin δ targets the ROS-GC1 region V^{836}–D^{856} (Venkataraman et al., 2008); S100B, G^{962}–N^{981} and I^{1030}–Q^{1041} (Duda et al., 2002); GCAP1, M^{445}–L^{456} and L^{503}–1^{522} (Lange et al., 1999).

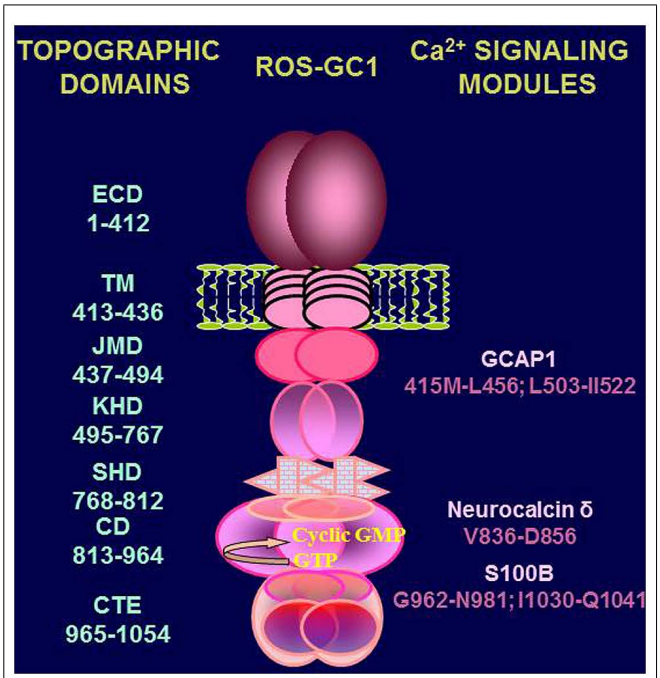

FIGURE 7 | Topography of ROS-GC1. A schematic diagram of ROS-GC1, with its multiple domains is provided. The extracellular (ECD), the transmembrane (TM), the juxtamembrane (JMD), the kinase homology (KHD), the signalling helix (SHD), the catalytic (CD), and the C-terminal extension (CTE) domains have been identified on the left-hand side; the GCAP1, NCδ, and S100B binding domains are indicated to the right.

MODE 3 – MODEL

Basal state – low Ca^{2+}: Ca^{2+}-free GCAP1 stimulates ROS-GC1 catalytic activity. Cyclic GMP formed in response to this stimulation opens some of the CNG channels present in the sperm membranes (Wiesner et al., 1998; Revelli et al., 2002). At least some of the Ca^{2+} ions entering the sperm through the open CNG channels are bound by neurocalcin δ and/or S100B. It is important to note that the half-maximal activation of ROS-GC1 by GCAP1 occurs at 707 nM Ca^{2+} (Hwang et al., 2003), the Ca^{2+} concentration at which neurocalcin δ and S100B are able to activate ROS-GC1 with approximately half-maximal effectiveness. With increasing Ca^{2+} concentrations GCAP1 inhibits ROS-GC1 activity while neurocalcin δ and S100B stimulate it. *Active state* – Ca^{2+}-bound NCδ and/or S100B further stimulate ROS-GC1 and cyclic GMP is formed in higher quantities leading to massive opening of CNG channels and influx of Ca^{2+} (Shapiro et al., 1990; Revelli et al., 2002). In this phase, the ROS-GC1 activity is resultant of two opposing effects, inhibitory through GCAP1 and stimulatory, through NCδ and S100B. *Signal termination*: when cyclic GMP and $[Ca^{2+}]_i$ reach the optimal level necessary for sperm membrane hyperpolarization and physiological function (e.g., capacitation and/or acrosome reaction; Galinado et al., 2000) combined effects of protein phosphorylation and phosphodiesterase activity (Su and Vacquier, 2006) lead to lowering of cyclic GMP levels, closure of the CNG channels and cessation of the Ca^{2+} influx.

CONCLUSION

Co-expression of NCδ, S100B, and GCAP1 with ROS-GC1 in mammalian spermatogenic cells confers bimodal Ca^{2+} sensitivity to cyclic GMP synthesis. The stimulatory arm of the switch operated by NCδ and S100B is essential for timely opening of the CNG channels by cyclic GMP produced and vast influx of Ca^{2+} necessary for the acrosome reaction. In this stimulatory arm NCδ appears to be a significantly more important player than S100B. The inhibitory arm operated by GCAP1 stops the cyclic GMP synthesis and therefore Ca^{2+} influx. Our findings demonstrate that ROS-GC1 transduction system and its bimodal Ca^{2+} modulation is not unique to neurosensory and neurosensory-linked systems and has a more widespread role in general Ca^{2+}-dependent signaling and may be a part of the fertilization machinery.

REFERENCES

Armstrong, V. L., Clulow, J., Murdoch, R. N., and Jones, R. C. (1994). Intracellular signal transduction mechanisms of rat epididymal spermatozoa and their relationship to motility and metabolism. *Mol. Reprod. Dev.* 38, 77–84. doi: 10.1002/mrd.1080380113

Coussen, F., and Mulle, C. (2006). Kainate receptor-interacting proteins and membrane trafficking. *Biochem. Soc. Trans.* 34, 927–930. doi: 10.1042/BST0340927

Detwiler, P. (2000). Open the loop: dissecting feedback regulation of a second messenger transduction cascade. *Neuron* 36, 3–4. doi: 10.1016/S0896-6273(02)00940-6

Duda, T., Fik-Rymarkiewicz, E., Venkataraman, V., Krishnan, A., and Sharma, R. K. (2004). Calcium-modulated ciliary membrane guanylate cyclase transduction machinery: constitution and operational principles. *Mol. Cell. Biochem.* 267, 107–122. doi: 10.1023/B:MCBI.0000049372.33965.4f

Duda, T., Goraczniak, R. M., and Sharma, R. K. (1996a). Molecular characterization of S100A1-S100B protein in retina and its activation mechanism of bovine photoreceptor guanylate cyclase. *Biochemistry* 35, 6263–6266. doi: 10.1021/bi960007m

Duda, T., Goraczniak, R., Surgucheva, I., Rudnicka-Nawrot, M., Gorczyca, W. A., Palczewski, K., et al. (1996b). Calcium modulation of bovine photoreceptor guanylate cyclase. *Biochemistry* 35, 8478–8482. doi: 10.1021/bi960752z

Duda, T., Jankowska, A., Venkataraman, V., Nagele, R. G., and Sharma, R. K. (2001a). A novel calcium-regulated membrane guanylate cyclase transduction system in the olfactory neuroepithelium. *Biochemistry* 40, 12067–12077. doi: 10.1021/bi0108406

Duda, T., Venkataraman, V., Krishnan, A., Nagele, R. G., and Sharma, R. K. (2001b). Negatively calcium-modulated membrane guanylate cyclase signaling system in the rat olfactory bulb. *Biochemistry* 40, 4654–4662. doi: 10.1021/bi0027985

Duda, T., Koch, K. W., Venkataraman, V., Lange, C., Beyermann, M., and Sharma, R. K. (2002). Ca^{2+} sensor S100beta-modulated sites of membrane guanylate cyclase in the photoreceptor-bipolar synapse. *EMBO J.* 21, 2547–2556. doi: 10.1093/emboj/21.11.2547

Duda, T., Pertzev, A., Koch, K. W., and Sharma, R. K. (2012a). Antithetical modes of and the Ca^{2+} sensors targeting in ANF-RGC and ROS-GC1 membrane guanylate cyclases. *Front. Mol. Neurosci.* 5:44. doi: 10.3389/fnmol.2012.00044

Duda, T., Pertzev, A., and Sharma, R. K. (2012b). Ca^{2+} modulation of ANF-RGC: new signaling paradigm interlocked with blood pressure regulation. *Biochemistry* 51, 9394–9405. doi: 10.1021/bi301176c

Duda, T., and Sharma, R. K. (2004). S100B-modulated Ca2+-dependentROS-GC1 transduction machinery in the gustatory epithelium: a new mechanism in gustatory transduction. *FEBS Lett.* 577, 393–398. doi: 10.1016/j.febslet.2004.09.089

Duda, T., and Sharma, R. K. (2009). Ca2+-modulated ONE-GC odorant signal transduction. *FEBS Lett.* 583, 1327–1330. doi: 10.1016/j.febslet.2009.03.036

Galinado, B. E., Beltrán, C., Cragoe, E. J. Jr., and Darszon, A. (2000). Participation of K+ channel modulated directly by cGMP in the speract-induced signaling cascade of *Strongylocentrotus purpuratus* sea urchin sperm. *Dev. Biol.* 221, 285–294. doi: 10.1006/dbio.2000.9678

Garbers, D. L. (1989). Molecular basis of signalling in the spermatozoon. *J. Androl.* 10, 99–107 doi: 10.1002/j.1939-4640.1989.tb00068.x

Goraczniak, R. M., Duda, T., Sitaramayya, A., and Sharma, R. K. (1994). Structural and functional characterization of the rod outer segment membrane guanylate cyclase. *Biochem. J.* 302, 455–461.

Hayashi, F., and Yamazaki, A. (1991). Polymorphism in purified guanylate cyclase from vertebrate rod photoreceptors. *Proc. Natl. Acad. Sci. U.S.A.* 88, 4746–4770. doi: 10.1073/pnas.88.11.4746

Hwang, J. Y., Lange, C., Helten, A., Höppner-Heitmann, D., Duda, T., Sharma, R. K., et al. (2003). Regulatory modes of rod outer segment membrane guanylate cyclase differ in catalytic efficiency and Ca2+-sensitivity. *Eur. J. Biochem.* 270, 3814–3821. doi: 10.1046/j.1432-1033.2003.03770.x

Iino, S., Kobayashi, S., Okazaki, K., and Hidaka, H. (1995). Immunohistochemical localization of neurocalcin in the rat inner ear. *Brain Res.* 680, 128–134. doi: 10.1016/0006-8993(95)00253-M

Ivings, L., Pennington, S. R., Jenkins, R., Weiss, J. L., and Burgoyne, R. D. (2002). Identification of Ca2+-dependent binding partners for the neuronal calcium sensor protein neurocalcin delta: interaction with actin, clathrin and tubulin. *Biochem. J.* 363, 599–608. doi: 10.1042/0264-6021:3630599

Jankowska, A., Burczynska, B., Duda, T., and Warchol, J. B. (2008). Rod outer segment membrane guanylate cyclase type 1, ROS-GC1, calcium-modulated transduction system in the sperm. *Fertil. Steril.* 93, 904–912. doi: 10.1016/j.fertnstert.2008.10.048

Jankowska, A., Burczynska, B., Duda, T., Warchol, J. B., and Sharma, R. K. (2007). Calcium-modulated rod outer segment membrane guanylate cyclase type 1 transduction machinery in the testes. *J. Androl.* 1, 50–58.

Jankowska, A., and Warchol, J. B. (2010). Ca^{2+}-modulated membrane guanylate cyclase in the testes. *Mol. Cell. Biochem.* 334, 169–179. doi: 10.1007/s11010-009-0329-5

Koch, K. W., Duda, T., and Sharma, R. K. (2010). Ca^{2+}-modulated vision-linked ROS-GC guanylate cyclase transduction machinery. *Mol. Cell. Biochem.* 334, 105–115. doi: 10.1007/s11010-009-0330-z

Krishnan, A., Venkataraman, V., Fik-Rymarkiewicz, E., Duda, T., and Sharma, R. K. (2004). Structural, biochemical and functional characterization of the calcium sensor neurocalcin δ in the inner retinal neurons and its linkage with the rod outer segment membrane guanylate cyclase transudation system. *Biochemistry* 43, 2708–2723. doi: 10.1021/bi035631v

Kumar, V. D., Vijay-Kumar, S., Krishnan, A., Duda, T., and Sharma, R. K. (1999). A second calcium regulator of rod outer segment membrane guanylate cyclase, ROS-GC1: neurocalcin. *Biochemistry* 38, 12614–12620. doi: 10.1021/bi990851n

Ladant, D. (1995). Calcium and membrane binding properties of bovine neurocalcin delta expressed in *Escherichia coli*. *J. Biol. Chem.* 270, 3179–3185.

Lange, C., Duda, T., Beyermann, M., Sharma, R. K., and Koch, K.-W. (1999). Regions in vertebrate photoreceptor guanylyl cyclase ROS-GC1 involved in Ca2+-dependent regulation by guanylyl cyclase-activating protein GCAP-1. *FEBS Lett.* 460, 27–31. doi: 10.1016/S0014-5793(99)01312-5

Liu, X., Seno, K., Nishizawa, Y., Hayashi, F., Yamazaki, A., Matsumoto, H., et al. (1994). Ultrastructural localization of retinal guanylate cyclase in human and monkey retinas. *Exp. Eye Res.* 59, 761–768. doi: 10.1006/exer.1994.1162

Marala, R. B., and Sharma, R. K. (1988). Characterization of atrial-natriuretic-factor-receptor-coupled membrane guanylate cyclase from rat and mouse testes. *Biochem. J.* 251, 301–304.

Margulis, A., Pozdnyakov, N., and Sitaramayya, A. (1996). Activation of bovine photoreceptor guanylate cyclase by S100 proteins. *Biochem. Biophys. Res. Commun.* 218, 243–247. doi: 10.1006/bbrc.1996.0043

Middendorff, R., Davidoff, M. S., Behrends, S., Mewe, M., Miethens, A., and Muller, D. (2000). Multiple roles of the messenger molecule cGMP in testicular function. *Andrologia* 32, 55–59.

Middendorff, R., Muller, D., Wichers, S., Holstein, A. F., and Davidoff, M. S. (1997). Evidence for production and functional activity of nitric oxide in seminiferous tubules and blood vessels of the human testes. *J. Clin. Endocrinol. Metab.* 82, 4154–4161.

Mourdjeva, M., Russinova, A., Kyurkchiev, S., and Kehayov, I. (2001). Spatial and temporal distribution of atrial natriuretic factor in the rat testis. *Biol. Cell* 93, 301–307. doi: 10.1016/S0248-4900(01)01119-4

Nambi, P., Aiyar, N. V., and Sharma, R. K. (1982). Adrenocorticotropin-dependent particulate guanylate cyclase in rat adrenal and adrenocortical carcinoma: comparison of its properties with soluble guanylate cyclase and its relationship with ACTH-induced steroidogenesis. *Arch. Biochem. Biophys.* 217, 638–646. doi: 10.1016/0003-9861(82)90545-8

Pandey, K. N., Oliver, P. M., Maeda, N., and Smithies, O. (1999). Hypertension associated with decreased testosterone levels in natriuretic peptide receptor-A gene-knockout and gene-duplicated mutant mouse models. *Endocrinology* 140, 5112–5119. doi: 10.1210/endo.140.11.7121

Pandey, K. N., and Singh, S. (1990). Molecular cloning and expression of murine guanylate cyclase/atrial natriuretic factor receptor cDNA. *J. Biol. Chem.* 265, 12342–12348.

Paul, A. K., Marala, R. B., Jaiswal, R. K., and Sharma, R. K. (1987). Coexistence of guanylate cyclase and atrial natriuretic factor receptor in a 180-kD protein. *Science* 235, 1224–1226. doi: 10.1126/science.2881352

Pozdnyakov, N., Yoshida, A., Cooper, N. G., Margulis, A., Duda, T., Sharma, R. K., et al. (1995). A novel calcium-dependent activator of retinal rod outer segment membrane guanylate cyclase. *Biochemistry* 34, 14279–14283. doi: 10.1021/bi00044a002

Pugh, E. N. Jr., Duda, T., Sitaramayya, A., and Sharma, R. K. (1997). Photoreceptor guanylate cyclases: a review. *Biosci. Rep.* 17, 429–473. doi: 10.1023/A:1027365520442

Rebello, M. R., Atkas, A., and Medle, K. F. (2011). Expression of calcium binding proteins in mouse type II taste cells. *J. Histochem. Cytochem.* 59, 530–539. doi: 10.1369/0022155411402352

Revelli, A., Ghigo, D., Moffa, F., Massobrio, M., and Tur-Kaspa, I. (2002). Guanylate cyclase activity and sperm function. *Endocr. Rev.* 23, 484–494. doi: 10.1210/er.2001-0020

Singh, S., Lowe, D. G., Thorpe, D. S., Rodriguez, H., Kuang, W. J., Dangott, L. J., et al. (1988). Membrane guanylate cyclase is a cell-surface receptor with homology to protein kinases. *Nature* 334, 708–712. doi: 10.1038/334708a0

Shapiro, B. M., Cook, S., Quest, A. F., Oberdorf, J., and Wothe, D. J. (1990). Molecular mechanisms of sea-urchin sperm activation before fertilization. *Reprod. Fertil.* 42, 3–8.

Sharma, R. K. (2010). Membrane guanylate cyclase is a beautiful signal transduction machine: overview. *Mol. Cell. Biochem.* 334, 3–6. doi: 10.1007/s11010-009-0336-6

Su, Y.-H., and Vacquier, V. D. (2006). Cyclic GMP-specific phosphodiesterase-5 regulates motility of sea urchin spermatozoa. *Mol. Biol. Cell.* 17, 114–121. doi: 10.1091/mbc.E05-08-0820

Venkataraman, V., Duda, T., Ravichandran, S., and Sharma, R. K. (2008). Neurocalcin delta modulation of ROS-GC1, a new model of Ca(2+) signaling. *Biochemistry* 47, 6590–6601. doi: 10.1021/bi800394s

Venkataraman, V., Duda, T., Vardi, N., Koch, K. W., and Sharma, R. K. (2003). Calcium-modulated guanylate cyclase transduction machinery in the photoreceptor – bipolar synaptic region. *Biochemistry* 40, 5640–5648. doi: 10.1021/bi034025x

Venkataraman, V., Nagele, R., Duda, T., and Sharma, R. K. (2000). Rod outer segment membrane guanylate cyclase type 1-linked stimulatory and inhibitory calcium signaling systems in the pineal gland: biochemical, molecular, and immunohistochemical evidence. *Biochemistry* 39, 6042–6052. doi: 10.1021/bi9929960

Wen, X. H., Duda, T., Pertzev, A., Venkataraman, V., Makino, C. L., and Sharma, R. K. (2012). S100B serves as a Ca(2+) sensor for ROS-GC1 guanylate cyclase in cones but not in rods of the murine retina. *Cell. Physiol. Biochem.* 29, 417–430. doi: 10.1159/000338496

Wiesner, B., Weiner, J., Middendorff, R., Hagen, V., Kaupp, U. B., and Weyand, I. (1998). Cyclic nucleotide-gated channels on the flagellum control Ca2+ entry into sperm. *J. Cell Biol.* 142, 473–484. doi: 10.1083/jcb.142.2.473

Yang, R. B., Foster, D. C., Garbers, D. L., and Fulle, H. J. (1995). Two membrane forms of guanylyl cyclase found in the eye. *Proc. Natl. Acad. Sci. U.S.A.* 92, 602–606. doi: 10.1073/pnas.92.2.602

Zozulya, S., and Stryer, L. (1992). Calcium-myristoyl protein switch. *Proc. Natl. Acad. Sci. U.S.A.* 89, 11569–11573. doi: 10.1073/pnas.89.23.11569

Conflict of Interest Statement: The authors declare that the research was conducted in the absence of any commercial or financial relationships that could be construed as a potential conflict of interest.

Received: 27 February 2014; accepted: 08 April 2014; published online: 29 April 2014.
*Citation: Jankowska A, Sharma RK and Duda T (2014) Ca^{2+}-modulated ROS-GC1 transduction system in testes and its presence in the spermatogenic cells. Front. Mol. Neurosci. **7**:34. doi: 10.3389/fnmol.2014.00034*
This article was submitted to the journal Frontiers in Molecular Neuroscience.

frontiers in
MOLECULAR NEUROSCIENCE

REVIEW ARTICLE
published: 17 March 2014
doi: 10.3389/fnmol.2014.00017

Atrial natriuretic factor receptor guanylate cyclase, ANF-RGC, transduces two independent signals, ANF and Ca^{2+}

Teresa Duda*, Alexandre Pertzev and Rameshwar K. Sharma

The Unit of Regulatory and Molecular Biology, Research Divisions of Biochemistry and Molecular Biology, Salus University, Elkins Park, PA, USA

Edited by:
Clint L. Makino, Massachusetts Eye and Ear Infirmary and Harvard Medical School, USA

Reviewed by:
Peter Jedlicka, Goethe University, Germany
Baojin Ding, University of Massachusetts Medical School, USA

****Correspondence:***
Teresa Duda, The Unit of Regulatory and Molecular Biology, Research Divisions of Biochemistry and Molecular Biology, Salus University, 8360 Old York Road, Elkins Park, PA 19027, USA
e-mail: tduda@salus.edu

Atrial natriuretic factor receptor guanylate cyclase (ANF-RGC), was the first discovered member of the mammalian membrane guanylate cyclase family. The hallmark feature of the family is that a single protein contains both the site for recognition of the regulatory signal and the ability to transduce it into the production of the second messenger, cyclic GMP. For over two decades, the family has been classified into two subfamilies, the hormone receptor subfamily with ANF-RGC being its paramount member, and the Ca^{2+} modulated subfamily, which includes the rod outer segment guanylate cyclases, ROS-GC1 and 2, and the olfactory neuroepithelial guanylate cyclase. ANF-RGC is the receptor and the signal transducer of the most hypotensive hormones, ANF– and B-type natriuretic peptide (BNP). After binding these hormones at the extracellular domain it, at its intracellular domain, signals activation of the C-terminal catalytic module and accelerates the production of cyclic GMP. Cyclic GMP then serves the second messenger role in biological responses of ANF and BNP such as natriuresis, diuresis, vasorelaxation, and anti-proliferation. Very recently another *modus operandus* for ANF-RGC was revealed. Its crux is that ANF-RGC activity is also regulated by Ca^{2+}. The Ca^{2+} sensor neurocalcin d mediates this signaling mechanism. Strikingly, the Ca^{2+} and ANF signaling mechanisms employ separate structural motifs of ANF-RGC in modulating its core catalytic domain in accelerating the production of cyclic GMP. In this review the biochemistry and physiology of these mechanisms with emphasis on cardiovascular regulation will be discussed.

Keywords: atrial natriuretic factor, atrial natriuretic factor receptor guanylate cyclase, calcium, cyclic GMP, neurocalcin δ, signal transduction

INTRODUCTION

In the 1980s, the field of cellular signal transduction underwent total metamorphosis. Until then only two major paradigms of signal transduction, that of cyclic AMP and that of IP_3 (inositol triphosphate) were known and were used to explain cellular signaling mechanisms and the second messenger concepts. Each of these two paradigms constituted an assemblage of three components – receptor, GTP binding protein, and the transducer catalyst – necessary for signal transduction. The astonishing discovery of a novel membrane protein that was simultaneously a receptor of a hormone and the transducer of its signal added a new dimension to our understanding of cellular signal transduction. The hormone was the newly described atrial natriuretic factor (ANF; de Bold, 1985) and the membrane protein was both its receptor and guanylate cyclase enzyme, termed therefore atrial natriuretic factor receptor guanylate cyclase (ANF-RGC; Kuno et al., 1986; Paul, 1986; Paul et al., 1987; Takayanagi et al., 1987; Meloche et al., 1988). Other terms to describe the protein are GC-A and NPR-A. ANF-RGC responded to ANF binding with accelerated synthesis of its second messenger cyclic GMP. The novelty of the system was 2-fold; first, a single protein, ANF-RGC, which contained both the ability to recognize the ANF hormonal signal and the activity to translate the hormonal information into the production of its second messenger, cyclic GMP was identified; and second, cyclic GMP was recognized as *bona fide* hormonal second messenger. Until then, the majority of laboratories forcefully denied the hormonal second messenger role of cyclic GMP (reviewed in Sharma, 2002, 2010).

The concept that ANF-RGC is indeed both hormone receptor and a catalyst was further supported by cloning studies (Chinkers et al., 1989; Lowe et al., 1989; Pandey and Singh, 1990; Duda et al., 1991; Marala et al., 1992). Homology cloning made possible finding other receptor membrane guanylate cyclases: C-type

Abbreviations: ANF, atrial natriuretic factor; ANF-RGC, atrial natriuretic factor receptor guanylate cyclase; ARM, ATP-regulatory module; ATP, adenosine triphosphate; BNP, B-type natriuretic peptide; CNP, C-type natriuretic peptide; CNP-RGC, C-type natriuretic peptide receptor guanylate cyclase; cyclic AMP, 3′,5′-cyclic adenosine monophosphate; cyclic GMP, 3′,5′-cyclic guanosine monophosphate; CNG channel, cyclic nucleotide gated channel; GCAP, guanylate cyclase activating protein; GC-A, guanylate cyclase-A; GC-B, guanylate cyclase-B; GC-C, guanylate cyclase-C; GC-D, guanylate cyclase-D; GC-E, guanylate cyclase-E; GC-F, guanylate cyclase-F; GC-G, guanylate cyclase-G; KHD, kinase homology domain; K-LD, kinase-like domain; NCδ, neurocalcin δ; NPR-A, natriuretic peptide receptor-A; ONE-GC, olfactory neuroepithelial guanylate cyclase; STa-RGC, heat-stable enterotoxin (also guanylin and uroguanylin) receptor guanylate cyclase; ROS-GC, rod outer segment guanylate cyclase.

natriuretic peptide receptor guanylate cyclase, CNP-RGC (also known as GC-B; Chang et al., 1989; Schulz et al., 1989; Duda et al., 1993b) and heat-stable enterotoxin (also guanylin and uroguanylin) receptor guanylate cyclase, STa-RGC (GC-C; Schulz et al., 1990; de Sauvage et al., 1991; Singh et al., 1991; Hamra et al., 1993; Khare et al., 1994). Identification of these three structurally and functionally related membrane guanylate cyclases that were receptors for hormonally active peptides resulted in a notion that all membrane guanylate cyclases, even those still to be discovered, were receptors for specific extracellular ligands.

The notion was short-lived, however. The next four, in chronological order, identified membrane guanylate cyclases: the rod outer segment guanylate cyclases, ROS-GC1 (also known as RetGC1 or GC-E; Koch, 1991; Shyjan et al., 1992; Goraczniak et al., 1994) and ROS-GC2 (RetGC2 or GC-F; Lowe et al., 1995; Yang et al., 1995; Goraczniak et al., 1998), the olfactory neuroepithelium guanylate cyclase, ONE-GC (also termed as GC-D) (Fulle et al., 1995; Duda et al., 2001a) and GC-G (Schulz et al., 1998), did not respond with increased activity to any extracellular ligand. They were therefore branded as "orphan receptors" (Fulle et al., 1995; Yang et al., 1995; Wedel and Garbers, 1997; Schulz et al., 1998).

ROS-GC1 and ROS-GC2 were not orphan RGC, however. Biochemical and physiological findings began to reveal that regulation of their catalytic activities is specific to their physiological function which is to return the illuminated photoreceptors to the dark, resting state. The illumination leads to activation of cyclic GMP phosphodiesterase, depletion of cyclic GMP, closure of the cyclic GMP gated (CNG) channels, and lowering the free Ca^{2+} concentration (reviewed in Pugh et al., 1997; Koch et al., 2010). The ROS-GCs' task is to restore the dark-level of cyclic GMP allowing opening of the CNG channels and increase of Ca^{2+} influx. Ca^{2+} concentration, thus, determines the activity of ROS-GCs but it occurs in an indirect way. Guanylate cyclase activating proteins (GCAPs) sense the post-illumination fall in Ca^{2+} and stimulate ROS-GCs to resynthesize cyclic GMP at a faster rate (reviewed in Detwiler, 2000; Koch et al., 2010). In this cyclic GMP-Ca^{2+} feedback mechanism, ROS-GCs do not respond to an extracellular ligand but to their intracellular Ca^{2+} sensing ligands, the GCAPs (Palczewski et al., 1994; Dizhoor et al., 1995; Duda et al., 1996b).

Soon thereafter the evidence began to emerge, primarily from our laboratory, that GCAPs are not the only Ca^{2+} sensing modulators of ROS-GC activity. While increasing Ca^{2+} concentrations inhibit ROS-GCs activity through GCAPs, two other Ca^{2+} sensors, S100B, and neurocalcin δ (NCδ) stimulate ROS-GC1 in a Ca^{2+}-dependent fashion (Pozdnyakov et al., 1995; Duda et al., 1996a; Margulis et al., 1996; Kumar et al., 1999). The Ca^{2+}-dependent S100B-mediated activation of ROS-GC operates in cones including their outer segments and pedicles (Wen et al., 2012). Its role in photo- and visual transductions remains to be established, but existing data indicate its involvement in transmission of the visual signal from cone ON-bipolar cells (Wen et al., 2012). Ca^{2+} signaling of ROS-GC activity mediated by NCδ is operative in retinal ganglion cells (Krishnan et al., 2004) but its linkage with the visual transduction is not clear yet.

Similar, but with additional twists, regulation of ONE-GC occurs in a subset of olfactory sensory neurons (Fulle et al., 1995; Duda et al., 2001a; Pertzev et al., 2010). The cyclase was initially classified as a member of the Ca^{2+} modulated subfamily (Duda et al., 2001a). Its activity is modulated in a Ca^{2+}-dependent fashion by NCδ (Duda et al., 2001a, 2004) and by GCAP1 (Duda et al., 2006, 2012a; Pertzev et al., 2010). Remarkably, the Ca^{2+}-GCAP1 pattern of ONE-GC modulation is opposite to that of ROS-GC modulation. Sensing increasing concentrations of Ca^{2+} GCAP1 stimulates ONE-GC while it inhibits ROS-GC (Duda et al., 2006, 2012a).

After the Ca^{2+}-dependent modulation of ONE-GC activity was demonstrated, an extracellular ligand of the cyclase was found. The ligand was the odorant uroguanylin (Leinders-Zufall et al., 2007; Duda and Sharma, 2008; reviewed in Sharma and Duda, 2010; Zufall and Munger, 2010). Hence, ONE-GC responds to both extracellular (uroguanylin) and intracellular Ca^{2+} signals. At this point a new, two-step "cross-talk" odorant transduction model was proposed (Duda and Sharma, 2009). In "step 1," the odorant uroguanylin interacts with the receptor domain of ONE-GC, causing its minimal activation. The cyclic GMP generated in response to uroguanylin signal opens a few of the CNG3 channels leading to some increase in $[Ca^{2+}]_i$ in the odorant receptor cell. In "step 2," the membrane bound NCδ and GCAP1 sense the increase in $[Ca^{2+}]_i$ and in their Ca^{2+}-bound states fully activate ONE-GC triggering maximal influx of $Ca^{2+}$and depolarization of the olfactory receptor cell membrane.

The odorant receptor ONE-GC linkage with the intracellular free Ca^{2+} signals brought forth a question whether this cyclase is a unique case of dually regulated membrane guanylate cyclase. Latest studies from our laboratory demonstrate that it is not. The nascent member of the hormone receptor subfamily, the ANF-RGC, is also responsive to Ca^{2+} (Duda et al., 2012a,b) and NCδ is the sensor protein which communicates the Ca^{2+} signal to ANF-RGC and in the Ca^{2+}-bound state, activates ANF-RGC activity. The two modes of ANF-RGC activation, hormonal and Ca^{2+}-dependent, engage their specific and independent pathways of transmitting the stimulatory signals to the catalytic domain. The end-product, however, is common, the second messenger cyclic GMP. Because of the individual signaling mechanisms involved in Ca^{2+} and hormonal signaling their net effects are multiplicative. Hence, in terms of the original sub-classification, the present day knowledge is that at least two cyclases, ANF-RGC and ONE-GC, are hybrids sensing both hormonal and Ca^{2+} signals.

The last cloned membrane guanylate cyclase was GC-G. Until today, the information of its function is very scarce. It was suggested that the mouse form of GC-G is selectively expressed in the sperm and may be involved in the process of capacitation (Kuhn et al., 2004). Other reports suggest that the cyclase is expressed in Grueneberg ganglion olfactory subsystem where it is responding to CO_2 (Chao et al., 2010) or to cool ambient temperature indicating its role in thermo-sensation (Mamasuew et al., 2008).

The following discussion is exclusively devoted to the ANF-RGC. It was the first template model, which established that cyclic GMP is a *bona fide* hormonal second messenger. The ongoing studies define the second ANF-RGC transduction model,

Ca^{2+}-modulated signaling. It makes ANF-RGC a bimodal switch, hormonal and Ca^{2+}. An additional significant part of the review is coverage of the manner in which these two models have now begun to explain the biochemical principles of cardiovascular, renal and endocrine homeostasis with special emphasis on blood pressure regulation.

HORMONAL SIGNALING OF ANF-RGC ACTIVATION

BINDING OF LIGAND-HORMONE ANF

Although intuitively expected, the first experimental evidence that the ANF binding site in ANF-RGC is located within the extracellular domain came first from the site-directed and deletion mutagenesis studies. A mutant ANF-RGC was cloned from rat adrenal cDNA library (Duda et al., 1991) and termed GCα. Its sequence differed from ANF-RGC by two amino acid substitutions $Q^{338} \rightarrow H$ and $L^{364} \rightarrow P$ which resulted from single nucleotide mutations, CAG → CAC and CTG → CCG, respectively. Expressed in heterologous system of COS cells, GCα was properly located in the plasma membrane and exhibited basal guanylate cyclase activity; it however, neither bound nor responded to ANF or other natriuretic peptides (Duda et al., 1991). These results demonstrated that the two amino acid substitutions exclusively abolished binding of ANF and therefore ANF signaling of the cyclase activity. Restoration by site-directed mutagenesis, glutamine at position 338 and leucine at position 364, reinstated ANF binding and ANF-dependent stimulation of the cyclase.

The site of ANF binding was further systematically analyzed (McNicoll et al., 1992, 1996; He et al., 1995; Misono, 2002). By cross-linking and proteinase digestion it was determined that the amino terminus of ANF is in contact with the region M^{173}-F^{188} of ANF-RGC, and the C-terminus, with D^{191}-R^{198} region. The fact that the identified contact sites were very close to each other was interpreted that the N- and C- termini of ANF interface distinct subunits of ANF-RGC homodimer. Importantly, it also implied that one ANF-RGC dimer binds one molecule of ANF.

Details of ANF binding to the ANF-RGC extracellular domain were unraveled by analyses of the extracellular domain of ANF-RGC co-crystallized with ANF (Ogawa et al., 2003, 2004). These analyses revealed that (1) the extracellular domain of ANF-RGC exists as a dimer in the head-to-head configuration; (2) one ANF-RGC dimer binds one molecule of ANF (2:1 complex); (3) the binding site in one monomer differs from that in the other - one monomer binds the N-terminal part of ANF and the other binds C-terminal part; (4) there is no preference in ANF binding to a specific monomer of the extracellular domain; bound ANF occurs in two alternate orientations of equal occurrence; (5) the membrane-distal portion of the extracellular domain contains chloride ion necessary for ANF binding.

TRANSMEMBRANE MIGRATION OF THE ANF BINDING SIGNAL

With the exception of enterotoxin RGC, all membrane guanylate cyclases contain a hinge region juxtaposed to the N-terminal side of the transmembrane domain. This region contains two conserved cysteine residues separated from each other by 6–8 residues. In ANF-RGC these residues are Cys^{423} and Cys^{432} and were indicated as a critical structural motif in ANF signaling (Huo et al., 1999; Labrecque et al., 1999; Miyagi and Misono, 2000). There was however no consensus on the mechanism of its operation. Based on results with intact cells transfected with ANF-RGC cDNA it was proposed that the cysteines are involved in dimerization through the formation of an inter-chain S-S bridge (Huo et al., 1999; Labrecque et al., 2001) or, that they form an intra-chain disulfide bridge (Huo et al., 1999; Miyagi and Misono, 2000). Analyses of guanylate cyclase activity in isolated membranes of COS cell expressing $C^{423}S$, $C^{432}S$, and $C^{423}S$, $C^{432}S$ mutants (Duda and Sharma, 2005) allowed to conclude that both C^{423} and C^{432} residues independently and equally control the catalytic activity of ANF-RGC and that activation of ANF-RGC does not involve interchain-disulfide bond formation. In the basal state, the disulfide motif keeps the ANF-RGC in its repressed catalytic state and ANF/ATP signaling brings it to the fully active state (Duda and Sharma, 2005).

A model of hormone-induced rotation has been proposed to explain how the extracellular signal is transmitted through the hinge region to the intracellular domain of ANF-RGC (Ogawa et al., 2004; Misono et al., 2005). Binding of ANF causes a twist motion of both ANF-RGC monomers centered on a support point close to the bound ANF. This twist motion translocates the juxtamembrane domains of both monomers with only minimal change in the distance between them. This movement constitutes a signal, which is transmitted through the transmembrane domain. Rotation of the transmembrane domain by 40 degrees occurs in response to ANF binding (Parat et al., 2010).

PASSAGE OF THE ANF SIGNAL THROUGH THE INTRACELLULAR DOMAIN

ANF signaling requires ATP

Early studies, before the biochemical characterization of ANF-RGC, demonstrated that activation by ANF is significantly amplified by ATP in the guanylate cyclase activation (Kurose et al., 1987; Cole et al., 1989; Chang et al., 1990; Larose et al., 1991; reviewed in Sharma, 2002; Duda et al., 2005). Subsequently, it was demonstrated that ATP is obligatory for ANF-dependent activation of ANF-RGC (Chinkers et al., 1991; Marala et al., 1991; Goraczniak et al., 1992; Wong et al., 1995; reviewed in Duda et al., 2005). Because the ATP effect was mimicked by its non-hydrolyzable analogs, ATPγS and AMP-PNP, it was suggested that ATP acts as an allosteric regulator (Chinkers et al., 1991; Marala et al., 1991; Goraczniak et al., 1992; Wong et al., 1995; reviewed in Duda et al., 2005). Shortly thereafter it was shown that ATP is also obligatory for the CNP-dependent stimulation of CNP-RGC (Duda et al., 1993a,b). Thus, it appears that the requirement of ATP is a common attribute of natriuretic peptide RGC signaling.

Studies with ANF-RGC deletion mutants revealed that the ATP regulated region resides in the intracellular portion of ANF-RGC between the transmembrane and the C-terminal catalytic domain (Chinkers and Garbers, 1989; Goraczniak et al., 1992). This region was named the kinase homology (or kinase-like domain; KHD or K-LD) because of its sequence similarity with the corresponding domains of tyrosine kinases (Chinkers et al., 1989; Chinkers and Garbers, 1989; Duda et al., 1991). A model for the ATP function was proposed that "binding of ANP to the extracellular domain of

its receptor initiates a conformational change in the protein K-LD, resulting in de-repression of guanylate cyclase activity" (Chinkers and Garbers, 1989). The central idea behind the model was that KHD in native ANF-RGC suppresses the catalytic module activity; ANF functions by relieving this suppression. Study from our group using two KHD deletion mutants, Δ506–677 and Δ555–762, negated this model and proposed an alternative one where ATP via ATP regulated module (ARM) potentiates the hormonal signal "(1) the signal is caused by the binding of the hormone to the receptor site; (2) there is a transmembrane migration of the signal; (3) the signal is potentiated by ATP at ARM; and (4) the amplified signal is finally transduced at the catalytic site" (Goraczniak et al., 1992).

ATP allosteric effect and the ARM domain

Within the KHD ANF-RGC contains a sequence, G^{503}-X-G^{505}-X-X-X-G^{509} (Goraczniak et al., 1992) which is a modified form of the protein kinases' nucleotide-binding consensus sequence G-X-G-X-X-G necessary for kinase activity (Wierenga and Hol, 1983; Hanks et al., 1988; Bratová et al., 2005). This motif was probed for its significance in ATP function in ANF signaling. Through analyses of a series of deletion and point mutants it was determined that the G^{503}-X-G^{505}-X-X-X-G^{509} motif is critical for the ATP function (Goraczniak et al., 1992; Duda et al., 1993a; Duda and Sharma, 1995; reviewed in Sharma, 2002; Duda et al., 2005). Although it is not involved in ATP binding it maintains the steric arrangements to fit the ATP molecule. For this reason, the motif has been named ARM (Goraczniak et al., 1992) and the KHD, where the ARM resides, was termed the ARM domain (Duda et al., 2001b; Sharma et al., 2001). To get an insight into the mechanism of ATP function, the structure of the ARM domain was simulated through computer-assisted homology based modeling (Duda et al., 2001b; Sharma et al., 2001; PDB ID 1T53). The basic structural features of the model have been experimentally validated through point mutation/expression studies (Duda et al., 2001b; Sharma et al., 2001; reviewed in Sharma, 2002; Duda et al., 2005).

Spatial determinants of the ARM domain. The domain comprises amino acid residues 496–771, which are arranged into two lobes: the smaller, N-terminal (91 aa residues: 496–586), and the larger, C-terminal (185 aa residues: 587–771; Duda et al., 2001b). Four antiparallel β strands and one α helix form the smaller lobe; the larger lobe is predominantly helical, composed of eight α-helices and two β strands (Duda et al., 2001b; Sharma et al., 2001). The ARM motif, G^{503}-X-G^{505}-X-X-X-G^{509}, is located within the smaller lobe.

The ATP-binding pocket. In order to identify the ARM domain residues potentially involved in ATP binding the model of this domain in its ATP-bound form was analyzed (Duda et al., 2005). A radius of 4 Å from the ATP molecule was chosen as the limiting distance for the electrostatic, hydrogen or van der Waals' interactions. Two sets of residues were identified (Figure 4 in reference Duda et al., 2005): (1) those forming the floor of the ATP binding pocket; (2) those surrounding ATP molecule. The residues in the first set are: G^{503}, R^{504}, G^{505}, S^{506}, N^{507}, Y^{508}, and G^{509}. These residues have no direct chemical interaction with ATP; they, however, provide necessary space to accommodate the ATP molecule. The residues in the second set surround the individual components of ATP, the adenine ring, the ribose ring and the triphosphate moiety. The adenine ring is surrounded by L^{511}, T^{513}, T^{514}, E^{515}, Q^{517}, A^{533}, T^{580}, E^{581}, C^{583}, V^{635}, and T^{645} and L^{511}, T^{513}, and C^{583} are within a distance shorter than 3 Å.

G^{503}, L^{511}, T^{513}, T^{514}, G^{580}, S^{587}, D^{590}surround the ribose ring with L^{511} and T^{514} located within 2.5 Å radius from the ribose. The phosphate groups are surrounded by R^{504}, G^{505}, L^{511}, K^{535}, N^{633}, D^{646}, and K^{535} is the nearest residue (2.6 Å) forming a hydrogen bond with the phosphate and has been shown to be critical for ATP regulation of ANF-dependent ANF-RGC activity; D^{646} interacts with the triphosphate group of ATP through the formation of a coordinate bond with the metal ion Mg^{2+}.

Interaction of ATP with the ARM domain. Kinetics of ATP binding to the ARM domain was determined through SPR spectroscopy (Burczynska et al., 2007). AMP-PNP, the non-hydrolyzable analog of ATP was used for the binding studies. Half-maximal binding (EC_{50}) occurred when the concentration of AMP-PNP was ∼0.2 mM and the calculated K_D value was 0.21 mM. Similar results (EC_{50} value of 0.15 mM and K_D of 0.13 mM) were obtained when 8-azido-ATP was used.

The model-predicted ATP binding pocket (*vide supra*) was authenticated experimentally by cross-linking of the purified isolated ARM domain protein with 8-azido-ATP, trypsin digestion of the cross-linked product and sequencing of the resulting peptides (Burczynska et al., 2007). Three peptides were found to be photoaffinity modified. The longest modified peptide was identified as G^{614}MLFLHNG-AICSHGNLKSSNCVVDGR^{639}and the shortest as S^{631}SNC^{634}V^{635}VDGR. In all three peptides $Cys^{634}$was modified indicating that this residue was the closest to the azido group. The G^{614}–R^{639} fragment contains six ATP-binding pocket-predicted residues (Duda et al., 2005): S^{625}, K^{630}, S^{631}, S^{632}, N^{633}, and V^{635}; and the shortest S^{631}–R^{639} fragment contains three residues: S^{631}, N^{633}, and V^{635}(Duda et al., 2005). The refined ARM model (Duda et al., 2005) predicts that V^{635} is within a 4 Å radius from the adenine ring; cross-linking of the neighboring residue to C^{634} validates that these residues are indeed the closest to the C-8 of the adenine ring.

ATP binding dependent changes in the ARM domain. If ATP binding to the ARM domain were to serve signaling purposes, it should induce structural changes that ultimately would signal activation of the catalytic domain. Comparative analyses of the ARM domain models in the apo and ATP-bound states identified such changes. They involve rotations of the β strands within the smaller lobe as well as movements of the β strands and α helices in the larger lobe (Duda et al., 2001b; Sharma et al., 2001; reviewed in Duda et al., 2005). Consequences of two such changes appear to be of particular importance: first, of the β1, β2 strands in the smaller lobe, and the second, of the EF and F helices in the larger lobe.

The β1 and β2 strands and the loop connecting them encompasses the G^{503}-X-G^{505}-X-X-X-G^{509} motif (Duda et al., 2001b; Sharma et al., 2001; reviewed in Duda et al., 2005), which is meshed

in and flanked by six phosphorylation sites, S^{497}, T^{500}, S^{502}, S^{506}, S^{510}, T^{513} (Potter and Hunter, 1998a, 1999a). The present consensus is that "phosphorylation of KHD is absolutely required for hormone-dependent activation of NPR-A" (Potter and Hunter, 1998a,b, 1999b). In this concept, hypothetical protein kinase and protein phosphatase co-exist with ANF-RGC (Foster and Garbers, 1998). Until now, however, neither the kinase nor the phosphatase has been identified.

Comparison of the ATP-free and ATP-bound ARM domain models allows explaining how ATP binding makes it possible for the serine and threonine residues to undergo phosphorylation. After ATP binds to the ARM domain, the β1, β2 strands, and the loop between them shift by ∼3–4 Å and rotate by ∼15° (Duda et al., 2001b; Sharma et al., 2001; reviewed in Duda et al., 2005). This movement triggers reorientation of the serine and threonine residues (**Figure 1**, red colored residues) causing the side chains and the OH groups of T^{500}, S^{502}, S^{506}, and T^{513} becoming directed toward the protein surface (**Figure 1**, compare the positions of the cyan- and red-colored OH groups). The change in the positions of the side chains is most drastic for the S^{502} and S^{506} residues. Although upon ATP binding there is no toward the surface reorientation of the S^{497} and S^{510} OH groups, the entire residues are shifted toward the surface (**Figure 1**). This structural rearrangement permits the hypothetical protein kinase to access the side chains of the residues and transfer the phosphate group (Duda et al., 2011).

Another important result of ATP binding on the dynamics within the ARM domain is the translocation within the larger lobe of two helices, EF and F. Their movement was characterized by analyzing the ATP-dependent changes in the fluorescence intensity and wavelength of two tryptophan residues W^{601} and W^{669} (Duda et al., 2009). Both residues reside in the larger lobe of the ARM domain, outside the ATP-binding pocket. The W^{601} residue is a part of the helix E structure (Duda et al., 2001b, 2005), its side-chain is oriented toward the protein surface, and it is flanked by several hydrophobic residues, F^{640}, L^{607}, S^{606}, and S^{596} (**Figure 2A**). These structural features define the fluorescence λ_{max} of W^{601} at 332 nm. W^{669} residue is located at the end of a loop connecting β8 strand and EF helix (Duda et al., 2009); it is a part of a conserved hydrophobic motif, ^{669}WTAPELL^{675}. The side chain of W^{669} is flanked by the polar residues: E^{699}, S^{631}, K^{667}, K^{630}, and L^{696} (**Figure 2B**). This environment causes red shifts in the fluorescence λ_{max} of W^{669} to 345 nm.

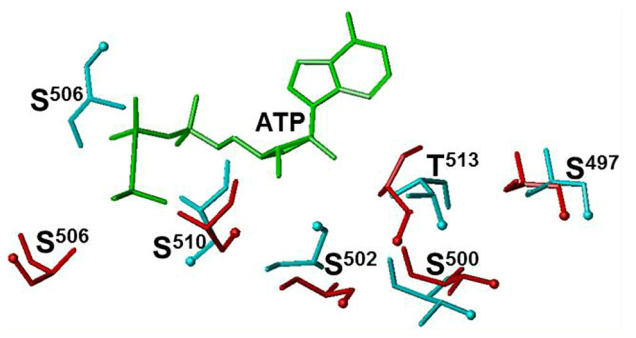

FIGURE 1 | ATP binding to the ARM domain affects the conformation of the six phosphorylable residues. The conformation of the six phosphorylated residues is shown before (cyan) and after (red) ATP binding. The ATP molecule is shown in green. The positions of the OH groups are indicated by cyan and red balls (reproduced with permission from ref. Duda et al., 2011).

Superimposition of the ATP-free and the ATP-bound forms indicates that ATP binding induces contraction of the entire ARM domain and affects the orientation and environment of W^{669}. The contraction results in shortening of the distance between W^{669} and the ATP binding pocket (**Figure 2C**). ATP binding also causes reorientation of the W^{669} side chain. It turns and becomes more shielded by the surrounding amino acids. Turning of the W^{669} side chain pushes the remainder of the motif, ^{670}TAPELL^{675}, to the surface resulting in its exposure. In general, the movement of a hydrophobic motif toward the surface of the protein indicates its readiness for interaction. For the ^{669}WTAPELL^{675} motif it was proposed that it interacts with subsequent transduction motif, possibly within the catalytic domain, propagates the ANF/ATP binding signal and activates the catalytic domain (Duda et al., 2009).

Based on the studies narrated above a model for ANF/ATP signaling of ANF-RGC activity was proposed: The ANF signal originates by the binding of one molecule of ANF to the extracellular dimer domain of ANF-RGC (Ogawa et al., 2004, 2009). The binding modifies the juxtamembrane region where the disulfide ^{423}Cys-Cys^{432} structural motif is a key element in this modification (Ogawa et al., 2004, 2009; Duda and Sharma, 2005). The signal twists the transmembrane domain (Parat et al., 2010), induces a structural change in the ARM domain, and prepares it for the ATP activation. ARM domain binds ATP to its pocket what leads to a cascade of temporal and spatial changes (Duda et al., 2001b; Sharma et al., 2001; reviewed in Duda et al., 2005). They result in (1) exposure of the hydrophobic ^{669}WTAPELL^{675} motif which directly (or indirectly) interacts with the catalytic domain causing its partial activation; and (2) exposure and phosphorylation of six serine, threonine residues and full activation of ANF-RGC. Concomitantly, phosphorylation converts ATP binding site from the high to low affinity, ATP dissociates and ANF-RGC returns to its ground state (Duda et al., 2011).

CATALYTIC DOMAIN

When more then 20 years ago an ANF RGC was purified to homogeneity and shown to contain the ANF binding and cyclic GMP forming activities on the same protein chain, the authors proposed a topological model for the transmembrane receptor enzyme in which the receptor part was extracellular and the cyclase catalytic domain was intracellular (Sharma et al., 1988a,b). The cloning studies confirmed this prediction. Alignment of the deduced amino acid sequences of the cloned guanylate cyclases indicated that the catalytic domain is located at the C-terminus of ANF-RGC and comprises 239 amino acid residues (Chinkers et al., 1989; Duda et al., 1991). This prediction was tested experimentally (Thorpe and Morkin, 1990; Thorpe et al., 1996). The carboxy terminal 293 amino acids fragment of ANF-RGC was expressed as a soluble protein and shown to exhibit guanylate cyclase activity. These results were in agreement with studies that determined through radiation inactivation experiments that the ANF-RGC

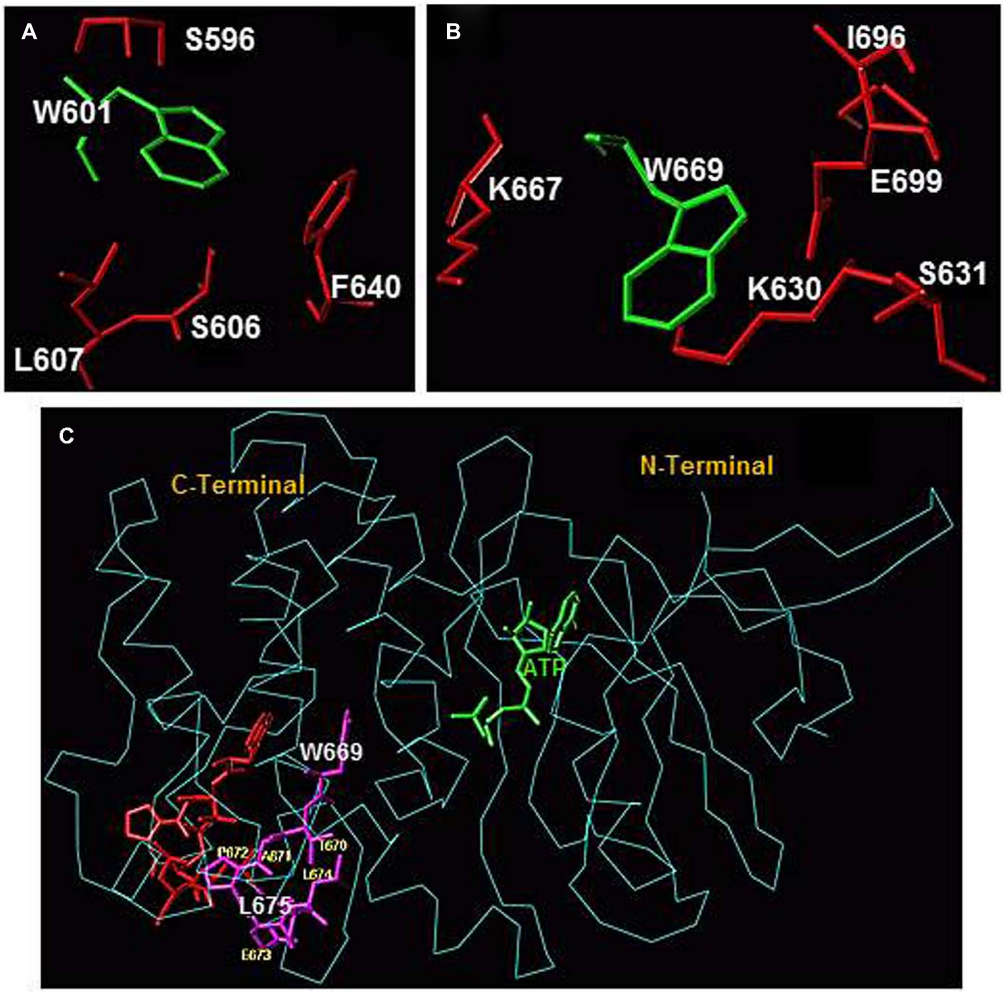

FIGURE 2 | (A) Amino acid residues surrounding W^{601} and **(B)** amino acid residues surrounding W^{669} within the ARM domain. Amino acid residues depicted in red are located within a 4 Å sphere from the respective tryptophan residue (green). **(C)** Conformational changes within the ^{669}WTAPELL^{675} motif induced by ATP binding to the ARM domain. The backbone structure of the ATP-bound ARM domain is shown in cyan and the ATP molecule is in green. The ^{669}WTAPELL^{675} motif is shown in magenta color. Apo structure of the ARM domain was superimposed on the ATP-bound form to assess the relative, ATP binding induced, conformational changes. For clarity, only the ^{669}WTAPELL^{675} motif (shown in red) of the apo-enzyme is visible. ATP binding results in a more compact structure of the ARM domain: the W^{669} side chain moves toward the ATP binding pocket while the side chains of T^{670}, E^{673}, L^{674}, and L^{675} move toward the protein surface [compare the orientation of side chain of these amino acid residues before (in red) and after (in magenta) ATP binding; fonts for W^{669} and L^{675} residues are increased for better visibility]. This movement changes the surface properties of the ARM domain. The movement toward the surface of the protein is poised to facilitate interaction of this amino acid stretch with subsequent transduction motif, possibly within the catalytic domain, propagation of the ANF/ATP binding signal and activation of the catalytic domain (reproduced with permission from ref. Duda et al., 2009).

fragment containing cyclase activity has a molecular weight of 32 ± 8 kDa (Tremblay et al., 1991). Further studies identified several residues within this region that appeared to be critical for the guanylate cyclase activity: L^{817} (Miao et al., 1995), D^{877}, K^{887}, D^{893}, G^{900}, H^{909}, R^{940}, and H^{944} (Thompson and Garbers, 1995). Their individual mutations to Ala resulted in ANF-RGC mutants without detectable guanylate cyclase activity. In contrast to these residues, mutation of E^{974} to Ala resulted in a hyperactive ANF-RGC mutant (Wedel et al., 1997). Based on these results it was concluded that the indicated residues are located within or close to the catalytic center or are critical for the proper folding of the catalytic center.

In the absence of a crystal structure of any membrane guanylate cyclase catalytic domain a model of the catalytic center of retGC-1, a mammalian membrane guanylate cyclase expressed in the retina, also known as ROS-GC1 was proposed (Liu et al., 1997). The model was built based on homology with the catalytic center of the adenylate cyclase. The modeling studies allowed identification of the critical residues constituting the catalytic core. Because the catalytic domains of all membrane guanylate cyclases are highly conserved (>95% of sequence identity), by homology substitution, the critical residues of the ANF-RGC catalytic center have been identified and they are described below.

The catalytic center is homodimeric. There are two GTP binding sites. Each GTP molecule interacts with both monomers. In the following description of the ANF-RGC catalytic center the monomers are labeled "A" and "B" and the location of each residue within a monomer A or B is indicated. Numbering of amino acids is according to the mature protein (Duda et al., 1991). R^{959}(B) and C^{961}(B) interact with guanine's O6; second NH_2 group of R^{959}(B) interacts with guanine's N1; the carboxy group of E^{889}(B) interacts with R^{959}(B) and through it with N1; G^{964}(B) interacts with N7; T^{854}(A), D^{893}(A) and N^{968}(B) form hydrogen bonds with ribose's OH (3′) group; R^{972}(B binds α phosphate group; R^{940}(A) binds β phosphate group; E^{974}(A) through Mg^{2+} interacts with β phosphate group; and S^{971}(A) binds γ phosphate group. Specificity toward GTP is determined by E^{889} and C^{961} of ANF-RGC. This conclusion is drawn based on studies showing that in ROS-GC1 mutation of the corresponding E to K and C to D converts guanylate cyclase activity into adenylate cyclase activity (Tucker et al., 1998).

Mechanism of ANF-RGC activation – the role of the ^{669}WTAPELL^{675} motif

An important feature of the model of ANF/ATP-dependent activation of ANF-RGC is the relay function of the ^{669}WTAPELL^{675} motif. It switches between the ATP-bound ARM domain and activates the catalytic domain. It was proposed that this motif interacts with and signals the antiparallel homo-dimer of the catalytic domain to undergo conformational changes and form a functional catalytic center (Duda et al., 2009). The exact site within the catalytic domain which is targeted by the ^{669}WTAPELL^{675} motif remains to be determined. Preliminary scanning experiments, however, suggest that the site may be located close to the E^{889}, a residue critical for cyclase specificity toward GTP (Tucker et al., 1998).

If the elements of the model are correct and the ^{669}WTAPELL^{675} motif is a switch, its deletion from the ANF-RGC should lead to a protein which binds ANF and ATP but is not able to respond to them with increased synthesis of cyclic GMP. This assumption was tested experimentally. An ANF-RGC mutant was created in which the ^{669}WTAPELL^{675} motif was deleted by mutagenesis. Wild type ANF-RGC and the mutant were expressed individually in COS cells and their membranes were analyzed (1) by Western blot to determine the proteins' levels of expression; (2) for basal guanylate cyclase activity; (3) for ANF binding; and (4) for K_M for the substrate GTP. The results demonstrated that (1) the wild type ANF-RGC and the ^{669}WTAPELL^{675} deletion mutant were expressed to the same level as determined by Western blot; (2) the basal cyclase activity of the mutant, 20 pmol cGMP min^{-1} (mg protein)$^{-1}$, was virtually identical to that of the wild type ANF-RGC, 21 pmol cGMP min^{-1} (mg protein) $^{-1}$; (3) their receptor activities were equal with the respective specific binding values of 9.7 ± 0.6 and 10.1 ± 0.9 pmol [^{125}I]ANF/mg protein and (4) the K_M values for the substrate GTP, 614 μM for the wild type and 608 μM for the mutant protein were identical. Thus, the basal integrity of the protein remained intact despite the deletion (Duda et al., 2009).

When the mutant was exposed to increasing concentrations of ANF and ATP its cyclase activity remained practically unchanged whereas under identical conditions wild type ANF-RGC was stimulated over 6-fold (Duda et al., 2009, 2013) demonstrating that in line with the original expectations the catalytic domain does not increase cyclic GMP synthesis in the presence of ANF/ATP. This type of outcome could only be observed if the mutant protein did not bind ANF and/or ATP or the catalytic domain lost its cyclase ability. Both of these possibilities were put to rest as the mutant and the wild type cyclase did not differ in ANF and ATP binding nor in enzymatic activity (*vide supra* and ref. Duda et al., 2009). Therefore the only explanation for the unchanged level of cyclic GMP synthesis is that the ^{669}WTAPELL^{675} deletion mutant is not able to respond to ANF and ATP. This leads to just one logical conclusion that in the absence of the ^{669}WTAPELL^{675} motif the ANF/ATP binding information is not transmitted to the catalytic domain. Thus, the ^{669}WTAPELL^{675} motif is the critical transmitter of the ATP-potentiated ANF signal to the catalytic domain where it is translated into generation of cyclic GMP.

Ca^{2+} SIGNALING OF ANF-RGC ACTIVITY

NEURONAL CALCIUM SENSOR NEUROCALCIN δ

Neurocalcin δ belongs to a distinct subfamily of neuronal calcium sensor proteins (NCS) together with visinin-like proteins (VILIPs) and hippocalcin. They all are acylated at the N-terminus by myristic acid and undergo a classical calcium-myristoyl switch (Ladant, 1995), e.g., they bury the myristoyl group in a hydrophobic pocket in Ca^{2+}−free form and expose it in Ca^{2+}-bound form, as first observed and described for recoverin (Zozulya and Stryer, 1992). Exposure of myristoyl group enables the protein association with the cell membrane. However, once it binds, in a Ca^{2+}-dependent fashion, to the membrane phospholipids, even after removing Ca^{2+} by the addition of EGTA part of it remains membrane bound (Krishnan et al., 2004). Although NCδ is primarily expressed in neuronal tissues, its expression in the periphery is also observed.

Functionally, NCδ has been linked to receptor endocytosis through interaction with α- and β-clathrin and β-adaptin (Ivings et al., 2002), trafficking and membrane delivery of glutamate receptors of the kainate type (Coussen and Mulle, 2006), and due to its Ca^{2+}-dependent affinity for S100B protein and tubulin β-chain (Okazaki et al., 1995), with microtubule assembly (Iino et al., 1995). In the sensory and sensory-linked neurons, the presence of NCδ has been found in the inner plexiform layer of the retina, e.g., in the amacrine and ganglion cells (Krishnan et al., 2004), olfactory sensory neurons (Duda et al., 2001a, 2004) and recently, it has been identified in type II cells of mouse circumvallate taste papillae, indicating its possible role in gustatory transduction (Rebello et al., 2011).

A relatively newly identified function of NCδ is its Ca^{2+}-dependent modulation of the activities of membrane guanylate cyclases ROS-GC1 in the retina and ONE-GC, in the olfactory neuroepithelium (Duda et al., 2001b, 2004; Krishnan et al., 2004). In these tissues NCδ co-localizes with its respective target cyclases. The exact physiological significance of the ROS-GC1- NCδ signaling system in the retinal neurons is not known yet. It can be, however, safely stated that the pathway is not present in the rod and cone outer segments, thus is not linked with the phototransduction machinery. The system has been localized to the lower strata

of the inner plexiform layer and to a subpopulation of ganglion cells (Krishnan et al., 2004).

In the olfactory neuroepithelium NCδ serves as a Ca^{2+} sensor component of the two-step odorant uroguanylin signaling machinery. This signaling mechanism was proposed to be initiated by uroguanylin interaction with the extracellular receptor domain of ONE-GC (Leinders-Zufall et al., 2007; Duda and Sharma, 2008; reviewed in Zufall and Munger, 2010; Sharma and Duda, 2010). This interaction leads to partial activation of ONE-GC, generation of small amount of cyclic GMP, partial opening of cyclic GMP-gated channel and influx of Ca^{2+} into the olfactory receptor neuron. In the next step, Ca^{2+} binds to NCδ which, then fully activates ONE-GC (Duda and Sharma, 2009).

FREE Ca^{2+} SIGNALS ANF-RGC ACTIVATION

In the course of mapping the NCδ targeted site on ROS-GC1 to which it binds and transmits the Ca^{2+} signal to the catalytic domain for signal translation into the generation of cyclic GMP, our group made a remarkable observation that NCδ binds directly to the catalytic domain and, thereby, activates ROS-GC1 (Venkataraman et al., 2008). Protein database comparison shows sequence conservation of the catalytic domain in the membrane guanylate cyclase family hinting at a possibility that other membrane guanylate cyclases might be activated by Ca^{2+} via NCδ as well. To test this possibility, ANF-RGC membrane guanylate cyclase, for which the only established signal transduction mechanism was through ANF/ATP (*vide supra*), was chosen. And indeed, in a recombinant system, myristoylated NCδ stimulated ANF-RGC activity in a dose- and Ca^{2+}-dependent manner; 0.5 μM Ca^{2+} and 0.5 μM NCδ triggered half-maximal activation of ANF-RGC (Duda et al., 2012a,b). These results for the first time demonstrated that ANF-RGC activity is dually regulated, by peptide hormones ANF and BNP, and by Ca^{2+}, thus, at least *in vitro* the cyclase was deemed a bimodal signal transducer.

Myristoylated dimeric form of neurocalcin δ is the transmitter of the Ca^{2+} signal

Since NCδ belongs to the family of NCS and myristoylation at N-terminus is a characteristic feature of a majority, but not all, of these proteins important for their cellular function, it was necessary to check whether myristoylation was required for NCδ to transmit the Ca^{2+} signal for ANF-RGC activation. Reconstitution experiments of ANF-RGC with both myristoylated and non-myristoylated NCδ showed that only the myristoylated NCδ stimulated the cyclase activity whereas the non-myristoylated form was ineffectual (Duda et al., 2012b). Importantly, both forms exhibited comparable affinity for ANF-RGC. In addition to activating ANF-RGC myristoylated NCδ also lowered the cyclase's K_M for substrate GTP and increased its catalytic efficiency, k_{cat}, from 6.5 ± 0.3 to 41.4 ± 0.5 pmol cyclic GMP/s.

The biochemical and homology based modeling studies indicate that the secondary structure of the functional form of all membrane guanylate cyclases is homodimeric (Rondeau et al., 1995; Liu et al., 1997; Venkataraman et al., 2008). The contact points for their homo-dimeric formation reside in their extracellular domain (Misono et al., 2011) and in the intracellular domain within the highly conserved dimerization domain (Wilson and Chinkers, 1995) and core catalytic core domain (Venkataraman et al., 2008). The X-ray crystallographic studies have demonstrated that NCδ also exists as a dimer (Vijay-Kumar and Kumar, 1999). Thus, it was reasonable to expect that the Ca^{2+}-modulated functional unit is NCδ dimer and ANF-RGC dimer.

This expectation was validated experimentally. When monomeric and dimeric forms of myristoylated NCδ were individually tested in reconstitution experiments for their abilities to stimulate ANF-RGC catalytic activity only the dimer was effective (Duda et al., 2012b). The stimulation by the monomeric form was only marginal, possibly resulting from spontaneous dimerization of the monomers when higher NCδ concentrations were used (Duda et al., 2012b). Thus indeed the functional Ca^{2+} signal transduction unit is composed of one NCδ dimer and one ANF-RGC dimer.

Neurocalcin δ targets directly the catalytic domain of ANF-RGC

The ANF-RGC fragment, aa 788–1029, encompassing the core catalytic domain, I^{820}–G^{1029}, was expressed as a soluble protein and tested for its basal and Ca^{2+}-dependent modulated *via* NCδ activities. The protein exhibited intrinsic guanylate cyclase activity (18 ± 4 pmol cyclic GMP min^{-1} mg $protein^{-1}$). This activity increased when Ca^{2+} and NCδ were added, and the increase was Ca^{2+} and NCδ-dose dependent (Duda et al., 2012b). Interestingly, the estimated EC_{50} for NCδ was comparable to that determined for full-length ANF-RGC strongly supporting the expectation that the NCδ signaling site resides within the catalytic domain.

The NCδ targeted site on ROS-GC1 was mapped to the aa segment V^{837}–L^{858}. The corresponding site on ANF-RGC, ^{849}DIVGFTALSAESTPMQVVTLLMQ^{871}, has 70% sequence conservation in comparison with ROS-GC1. When a synthetic peptide of this sequence was used in a functional interference experiment almost complete inhibition of the NCδ-stimulated ANF-RGC activity at 200 μM with an IC_{50} value of 80 μM was observed (Duda et al., 2012b). Because a scrambled peptide did not exhibit any inhibitory effect it was justified to conclude that the ANF-RGC region ^{849}DIVGFTALSAESTPMQVVTLLMQ^{871} mediates NCδ-dependent Ca^{2+} stimulation of ANF-RGC activity. This region is a part of the core catalytic domain and common to the corresponding sites in other membrane guanylate cyclases[28], it has a secondary structure of helix-loop-helix and is acidic in nature with a pI of 3.37 (Duda et al., 2012b).

The effects of ANF/ATP and Ca^{2+}-neurocalcin δ signaling of ANF-RGC activity are multiplicative

To determine the liaison between ANF/ATP and Ca^{2+}-NCδ signaling modes, ANF-RGC activity was analyzed first in the presence of 1 μM Ca^{2+} and 2 μM myristoylated NCδ and then with increasing concentrations, ranging from 10^{-11} M to 10^{-6} M, of ANF and constant 0.8 mM ATP. The presence of Ca^{2+} and NCδ resulted in stimulation of the cyclase activity approx. 3.5-fold above the basal activity. Addition of ANF and ATP resulted in additional 4.5-fold stimulation, demonstrating that the Ca^{2+}-NCδ and ANF/ATP effects are multiplicative (Duda et al., 2012b). It is noteworthy that in the absence of Ca^{2+} in the reaction mixture only the ANF/ATP-dependent stimulation of ANF-RGC activity was observed.

The preceding narration on the mechanisms involved in the hormone- or Ca^{2+}-NCδ-dependent stimulation of ANF-RGC activity explains the independence and multiplicativeness of the ANF and Ca^{2+}-NCδ signals in the activation of ANF-RGC. It is based on our evolving conceptual scheme whose central idea is that the functional specificity of a guanylate cyclase is determined by the structure of its modular blocks. The structural motif, ^{669}WTAPELL^{675} is involved in transmitting the ANF signal to the catalytic domain (Duda et al., 2009) but it is not involved in transmitting the Ca^{2+} signal to the catalytic domain; instead the ^{849}DIVGFTALSAESTPMQVVTLLMQ^{871} motif is involved (Duda et al., 2012b).

PHYSIOLOGICAL VALIDATION OF THE TWO SIGNALING MECHANISMS OF THE ANF-RGC ACTIVATION

The two described above signaling mechanisms of ANF-RGC activation are depicted in **Figure 3**. It is obvious from their description that they were developed based solely on biochemical observations. And although biochemically well-proven, they would have to be considered only hypothetical until their validity was confirmed *in vivo*. And this validation is narrated below.

SIGNALING THROUGH THE ^{669}WTAPELL^{675} MOTIF

In an *in vitro* reconstituted system the ^{669}WTAPELL^{675} motif is critical for the transmission of the ANF/ATP signal and activation of the ANF-RGC catalytic domain and its absence results in unresponsiveness of the mutated ANF-RGC to the signal so if the same happens *in vivo*, an animal model in which the sequence coding for the ^{669}WTAPELL^{675} motif is deleted from the ANF-RGC gene should be unresponsive to ANF and therefore exhibit all physiological consequences of this unresponsiveness. Following this logic, the ^{669}WTAPELL^{675} sequence was deleted in genetically altered mice (Duda et al., 2013). It is worth mentioning that up till now it is the only ANF-RGC domain-specific genetically modified animal model.

In agreement with the *in vitro* determinations, basal ANF-RGC activity in the membranes of the heart, adrenal gland and kidney, the primary tissues where ANF-RGC is expressed, was practically indistinguishable between the wild type control (ANF-RGC^{669}WTAPELL$^{675+/+}$), heterozygous (ANF-RGC^{669}WTAPELL$^{675+/-}$) and homozygous (ANF-RGC^{669}WTAPELL$^{675-/-}$) mice (Duda et al., 2013). However, the mutated cyclase expressed in these tissues did not respond to ANF/ATP stimulation. The cyclase activity in the membranes of the homozygous mice was the same when assayed in the presence of 10^{-7} M ANF and 0.8 mM ATP as when assayed in their absence. Interestingly, for the heterozygous mice, the cyclase remained responsive to ANF/ATP but the maximal achieved activity oscillated around 50% of the wild type values, clearly showing that in the heterozygous mice where the product of one ANF-RGC gene copy is of the wild type and the other, of the deletion-mutated cyclase, only the wild type ANF-RGC is responsive to ANF/ATP

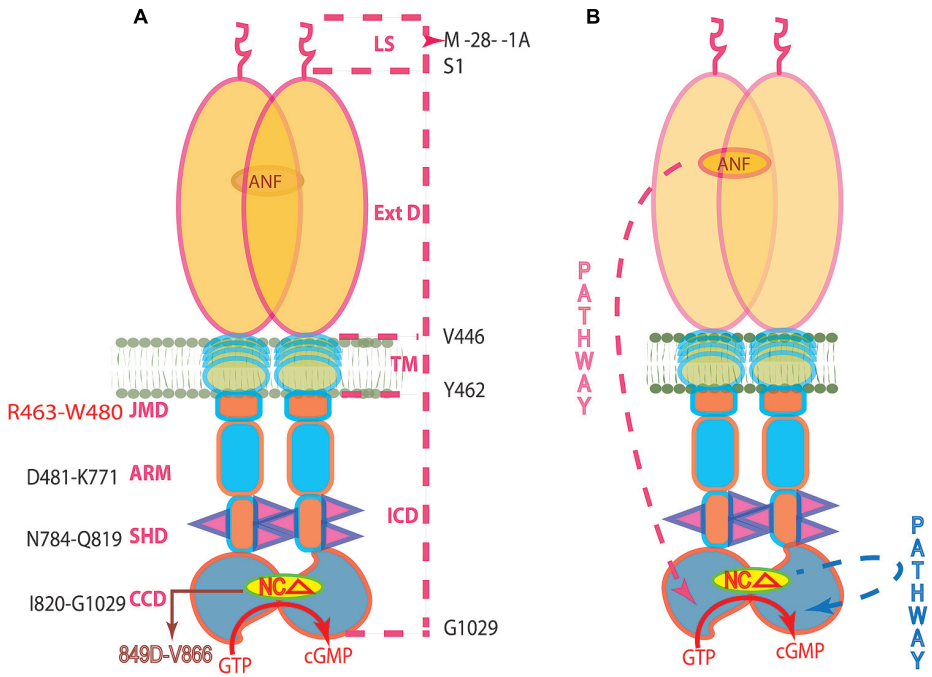

FIGURE 3 | (A) Topography of ANF-RGC. The dashed lines on the right show the boundaries of: LS, leader sequence; ExtD, extracellular domain; TM, transmembrane domain; ICD, intracellular domain. The functional domains in ICD, their names and the aa constituting their boundaries are indicated at the left: JMD, juxtamembrane domain; ARM, the ATP regulated module; SHD-signaling helix domain; CCD-core catalytic domain. The site targeted by NCδ (encircled) is within CCD. **(B)** The signaling pathways of ANF and of NCδ are independent. The trajectory of the ANF pathway is in red dashed arrow. From the ExtD, it passes through the TM, ARM and SHD in its course to CCD. The trajectory of the NCδ pathway (in blue dashed arrow) is within the CCD. The CCD exists as an antiparallel homodimer (reproduced with permission from ref. Duda et al., 2012b).

and the mutant is not (Duda et al., 2013). Thus, the *in vitro* activity characteristics were the mirror images of these *in vivo*.

Almost identical values of basal guanylate cyclase activity in various tissues of the ^{669}WTAPELL^{675} targeted mice and their isogenic controls implied that the expression of the mutant-cyclase must not differ from the expression of the wild type cyclase. This implication was confirmed by the results of immunocytochemical analyses. Side-by-side immunostaining with immunopurified anti ANF-RGC antibody resulted in identical images of the kidneys and adrenal glands of the wild type, heterozygous and homozygous ^{669}WTAPELL^{675} targeted mice. Also, visual examination of the stained sections as well as of the respective differential interference contrast images indicated that the targeting of the ^{669}WTAPELL^{675} motif does not change the integrity of these tissues (Duda et al., 2013).

The main function of ANF/ANF-RGC signaling system is to regulate natriuresis, diuresis, vasodilation, and prevent cardiac and renal hypertrophy. It regulates blood volume homeostasis and blood pressure by off-setting the renin-angiotensin-aldosterone system (RAAS): inhibiting renal renin secretion and aldosterone synthesis in the adrenocortical zona glomerulosa (Burnett et al., 1984; Brenner et al., 1990; Maack, 1996; Olson et al., 1998; Aoki et al., 2000; Shi et al., 2001). Therefore, elimination of ANF-RGC signaling through knocking-out either ANF-RGC or ANF gene leads to increased blood pressure, cardiac, and renal hypertrophy, fibrosis, to name some of the related pathological conditions (Dubois et al., 2000; Kishimoto et al., 2001; Ellmers et al., 2007; Das et al., 2010; Ellis et al., 2011; Pandey, 2011; Wadei and Textor, 2012). Since the ^{669}WTAPELL^{675} targeted mice have partially (heterozygous) and fully (homozygous) suppressed ANF-RGC response to ANF, but the basal cyclase activity is unaffected the critical question was: does this suppression lead to increased blood pressure and other physiological alterations in the genetically modified mice?

The answer obtained was clearly "yes." In comparison with the wild type the blood pressure of the heterozygous mice increased by ∼37% and of the homozygous mice by ∼56%. The increase was statistically highly significant with P value < 0.005 (Duda et al., 2013). It rose from 102 ± 9 mm Hg for the wild type mice to 134 ± 17 mm Hg for the heterozygous and 159 ± 11 mm Hg for the homozygous mice. These values showed that the progressive elevation of blood pressure directly correlates with the number of mutated ANF-RGC gene copies.

Because volume homeostasis and blood pressure are influenced by the mineralocorticoid hormone aldosterone secreted by the cells of the adrenocortical zona glomerulosa and the function of the ANF/ANF-RGC system is to inhibit this synthesis the obvious next question was whether the increased blood pressure in the ^{669}WTAPELL^{675} targeted mice is a consequence of the inability of the mutated ANF-RGC to transduce the ANF signal and to synthesize cyclic GMP sufficient quantities to inhibit aldosterone synthesis? A hint was provided by studies on ANF-RGC knockout mice showing that these mice had increased aldosterone level (Zhao et al., 2007).

The plasma aldosterone concentrations were measured in both types of genetically modified mice (hetero- and homozygous) and in their isogenic controls (wild type). The results demonstrated that, in comparison with the wild type mice, the plasma aldosterone concentration increased by approximately 40% (from 147 ± 12 to 204 ± 18 pg/ml) in the plasma of the heterozygous mice ($P < 0.005$) and by approximately 75% (up to 256 ± 22 pg/ml) in the plasma of the homozygous mice ($P < 0.005$) (Duda et al., 2013).

Chronic pressure overload is almost always accompanied by cardiac hypertrophy (reviewed in Katholi and Couri, 2011). The same is observed in the ^{669}WTAPELL^{675} targeted mice. The ratio of the heart weight (in mg) to whole body weight (in g) measured in 12 weeks old mice was 5.6 ± 0.3 and 6.1 ± 0.5 for the ^{669}WTAPELL$^{675(+/-)}$ and ^{669}WTAPELL$^{675(-/-)}$ mice, respectively, whereas it was 5 ± 0.3 for the wild type mice (Duda et al., 2013). However, hypertension is not the only cause of myocardial hypertrophy. Using animal models it has been shown that antihypertensive drugs do not always ameliorate cardiac hypertrophy (Knowles et al., 2001) and that even without systemic hypertension cardiac hypertrophy may occur (Oliver et al., 1997; Holtwick et al., 2003). Because deletion of the ^{669}WTAPELL^{675} motif from ANF-RGC results in decreased synthesis of cyclic GMP it was hypothesized that cardiomyocytes of the ^{669}WTAPELL^{675} targeted mice succumb to the insufficient quantities of cyclic GMP and normal inhibition of myocardial proliferative responses does not occur. Our ongoing studies indicate that indeed it is the case. The mice as young as 3 weeks of age (at weaning) exhibit significant cardiac hypertrophy. Which cyclic GMP-dependent signaling pathway involved in inhibition of myocardial proliferative responses is affected in these mice remains to be determined.

Taken together the biochemical and physiological evidence prove that the ^{669}WTAPELL^{675} motif is critical for the ANF-RGC function as the transducer of the ANF/ATP signal.

NEUROCALCIN δ Ca^{2+}-DEPENDENT SIGNALING OF ANF-RGC

To demonstrate that the ANF-RGC NCδ-Ca^{2+} signal transduction system is functional *in vivo* a mouse model with a disrupted NCδ gene was constructed and analyzed. Unfortunately, disruption of both copies of NCδ gene is lethal. Although it was unexpected at the time of developing the mouse line, it can be now understood in view of the results demonstrating that NCδ may be involved in spermatogenesis. Therefore, heterozygous, NCδ$^{+/-}$, line is viable.

Because earlier studies from our laboratory and others' had shown that NCδ is expressed in the adrenocortical zona glomerulosa (Nakano et al., 1993; Duda et al., 2012a) and that the adrenal gland also contains functional ANF-RGC transduction system (Takayanagi et al., 1987; Sharma et al., 1989; Duda et al., 1991; Rondeau et al., 1995) the adrenal gland appeared to be the tissue of choice for testing whether the ANF-RGC NCδ-Ca^{2+} signal transduction system is operational and of physiological significance there.

To show that NCδ is indeed the Ca^{2+}-sensor modulator of ANF-RGC in the adrenal gland the particulate fractions of the adrenal glands from wild type and NCδ$^{+/-}$ mice and their isogenic controls (NCδ$^{+/+}$) were tested for guanylate cyclase activity in the presence and absence of Ca^{2+}. The activity in membranes isolated in the absence of Ca^{2+} was about 66 pmol cyclic GMP

min^{-1} (mg protein) $^{-1}$ for the control and NCδ$^{+/-}$ mice and the activity was not affected by the presence or absence of Ca^{2+} in the assay mixture. However, the activity in membranes isolated in the presence of Ca^{2+} was strongly dependent on the mice genotype and Ca^{2+} in the assay mixture. When assessed in the absence of Ca^{2+}, the activity was ∼70 pmol cyclic GMP min^{-1} (mg protein) $^{-1}$ for the weight and NCδ$^{+/-}$ mice but when assessed in the presence of 1 μM Ca^{2+} the activity was 223 ± 20 pmol cyclic GMP min^{-1} (mg protein) $^{-1}$ for the wild type mice and 135 ± 10 pmol cyclic GMP min^{-1} (mg protein) $^{-1}$ for the NCδ$^{+/-}$ mice. Thus, the Ca^{2+}-dependent NCδ-modulated ANF-RGC signaling pathway in the mice with one copy of NCδ gene deleted (NCδ$^{+/-}$) is functionally half as active as in the wild type mice. To further authenticate that the lowering of the Ca^{2+}-dependent cyclase activity in the adrenal gland membranes of NCδ$^{+/-}$ mice is the exclusive consequence of lower NCδ expression, 2 μM exogenous NCδ was added to the NCδ$^{+/+}$ and NCδ$^{+/-}$ membranes (isolated in the presence of Ca^{2+}) and the cyclase activity was determined in the presence of 1 μM Ca^{2+}. The cyclase activity in the NCδ$^{+/+}$ adrenal membranes increased only minimally, from 220 to 279 ± 21 pmol cyclic GMP min^{-1} (mg protein) $^{-1}$ but in the NCδ$^{+/-}$ membranes, the increase was significantly larger, from 133 to 284 ± 24 (Duda et al., 2012b). Thus, the activity achieved was practically the same for both types of membranes. Hence, addition of exogenous NCδ to the NCδ$^{+/-}$ adrenal gland membranes restores the guanylate cyclase activity and brings it to the level of activity in the NCδ$^{+/+}$ membranes. We rationalized that the slight activity increase in the NCδ$^{+/+}$ membranes observed upon addition of exogenous NCδ is caused by a partial loss of the native NCδ during the membrane preparation.

What is the function of this pathway in the adrenal gland? In general, the primary role of ANF-RGC in the adrenal gland is to offset the renin-angiotensin system and inhibit aldosterone synthesis, and by doing this, to lower blood pressure (Burnett et al., 1984; Aoki et al., 2000; Shi et al., 2001). Therefore, is the Ca^{2+}-dependent ANF-RGC signal transduction machinery in the adrenal gland involved in aldosterone synthesis? Our ongoing studies indicate that indeed it is. The plasma aldosterone levels in the NCδ$^{+/-}$ mice are approximately 27% higher than in the plasma of the control (NCδ$^{+/+}$) mice. And the effect is exclusive for the aldosterone synthesizing glomerulosa cells, because corticosterone (synthesized in fasciculate cells) levels are unaffected by the absence of NCδ gene.

The increased plasma aldosterone level in the NCδ$^{+/-}$ mice correlates with the increase in blood pressure. Systolic blood pressure (measured by the non-invasive tail cuff method) was determined to be 92 ± 6 mm Hg for the wild type mice and 127 ± 9 mm Hg for the NCδ$^{+/-}$ mice. Therefore, the conclusion of these studies was that the ANF-RGC-Ca^{2+}-NCδ transduction system is not only physically present but is of physiological significance at least in the adrenal gland.

In summary, this review has high-lighted studies which define the molecular and physiological mechanisms of the hormonal signal transduction of ANF-RGC. In addition, a new signal transduction mechanism and its present state of validation has been narrated. In this model Ca^{2+} is the additional signal of ANF-RGC. By entirely different mechanism, it regulates ANF-RGC catalytic activity and controls its physiological functions.

FUTURE DIRECTIONS

There are three venues through which, in these authors' understanding, the future research will progress. The first venue is centered on the basic research to decipher (1) how the ^{669}WTAPELL^{675} motif "communicates" with the catalytic domain of ANF-RGC and signals its activation and (2) the mechanism of NCδ-Ca^{2+} signaling of ANF-RGC activity. The second venue relates to the physiology of both ANF-RGC signaling pathways (1) establishing whether the Ca^{2+} signaling mechanism is operative in other tissues in addition to the adrenal gland and (2) to determine the interrelationship of the hormonal and Ca^{2+} pathways. Finally, after deciphering the molecular and physiological details of the two signaling pathway the third venue will be translational, to design a molecule that can target directly the catalytic domain and bring ANF-RGC to its full activity and prevent the pandemic of hypertension, myocardial hypertrophy and obesity. The last objective is the most far-reaching, but hopefully can be achieved after the first two goals are accomplished.

ACKNOWLEDGMENTS

The numerous NIH and NSF support (Rameshwar K. Sharma) is acknowledged for the pioneering studies on ANF-RGC signal transduction field and the HL084584 and S82701 support (Teresa Duda) is acknowledged for the development of the ^{669}WTAPELL^{675} and Ca^{2+} signaling mechanisms.

REFERENCES

Aoki, H., Richmond, M., Izumo, S., and Sadoshima, J. (2000). Specific role of the extracellular signal-regulated kinase pathway in angiotensin II-induced cardiac hypertrophy in vitro. *Biochem. J.* 347, 275–284. doi: 10.1042/0264-6021:3470275

Bratová, I., Otyepka, M., Kříž, Z., and Koča, J. (2005). The mechanism of inhibition of the cyclin-dependent kinase-2 as revealed by the molecular dynamics study on the complex CDK2 with the peptide substrate HHASPRK. *Protein Sci.* 14, 445–451. doi: 10.1110/ps.04959705

Brenner, B. M., Ballermann, B. J., Gunning, M. E., and Zeidel, M. L. (1990). Diverse biological actions of atrial natriuretic peptide. *Physiol. Rev.* 7, 665–669.

Burczynska, B., Duda, T., and Sharma, R. K. (2007). ATP signaling site in the ARM domain of atrial natriuretic factor receptor guanylate cyclase. *Mol. Cell. Biochem.* 301, 193–207. doi: 10.1007/s11010-006-9400-7

Burnett, J. C. Jr., Granger, J. P., and Opgenorth, T. J. (1984). Effect of synthetic atrial natriuretic factor on renal function and rennin release. *Am. J. Physiol.* 247, F863–F866.

Chang, C. H., Kohse, K. P., Chang, B., Hirata, M., Jiang, B., Douglas, J. E., et al. (1990). Characterization of ATP-stimulated guanylate cyclase activation in rat lung membranes. *Biochim. Biophys. Acta* 1052, 159–165. doi: 10.1016/0167-4889(90)90071-K

Chang, M. S., Lowe, D. G., Lewis, M., Hellmiss, R., Chen, E., and Goeddel, D. V. (1989). Differential activation by atrial and brain natriuretic peptides of two different receptor guanylate cyclases. *Nature* 341, 68–72. doi: 10.1038/341068a0

Chao, Y.-C., Cheng, C.-J., Hsieh, H.-T., Lin, C.-C., Chen, C.-C., and Yang, R.-B. (2010). Guanylate cyclase-G, expressed in the Grueneberg ganglion olfactory subsystem, is activated by bicarbonate. *Biochem. J.* 432, 267–273. doi: 10.1042/BJ20100617

Chinkers, M., and Garbers, D. L. (1989). The protein kinase domain of the ANP receptor is required for signaling. *Science* 245, 1392–1394. doi: 10.1126/science.2571188

Chinkers, M., Garbers, D. L., Chang, M. S., Lowe, D. G., Chin, H. M., Goeddel, D. V., et al. (1989). A membrane form of guanylate cyclase is an atrial natriuretic peptide receptor. *Nature* 338, 78–83. doi: 10.1038/338078a0

Chinkers, M., Singh, S., and Garbers, D. L. (1991). Adenine nucleotides are required for activation of rat atrial natriuretic peptide receptor/guanylyl cyclase expressed in a baculovirus system. *J. Biol. Chem.* 266, 4088–4093.

Cole, F. E., Rondon, I., Iwata, T., Hardee, E., and Frohlich, E. D. (1989). Effect of ATP and amiloride on ANF binding and stimulation of cyclic GMP accumulation in rat glomerular membranes. *Life Sci.* 45, 477–484. doi: 10.1016/0024-3205(89)90097-0

Coussen, F., and Mulle, C. (2006). Kainate receptor-interacting proteins and membrane trafficking. *Biochem. Soc. Trans.* 34, 927–930. doi: 10.1042/BST0340927

Das, S., Au, E., Krazit, S. T., and Pandey, K. N. (2010). Targeted disruption of guanylyl cyclase-A/natriuretic peptide receptor-A gene provokes renal fibrosis and remodeling in null mutant mice: role of proinflammatory cytokines. *Endocrinology* 151, 5841–5850. doi: 10.1210/en.2010-0655

de Bold, A. J. (1985). Atrial natriuretic factor: a hormone produced by the heart. *Science* 230, 767–770. doi: 10.1126/science.2932797

de Sauvage, F. J., Camerato, T. R., and Goeddel, D. V. (1991). Primary structure and functional expression of the human receptor for *Escherichia coli* heat-stable enterotoxin. *J. Biol. Chem.* 266, 17912–17918.

Detwiler, P. (2000). Open the loop: dissecting feedback regulation of a second messenger transduction cascade. *Neuron* 36, 3–4. doi: 10.1016/S0896-6273(02)00940-6

Dizhoor, A. M., Olshevskaya, E. V., Henzel, W. J., Wong, S. C., Stults, J. T., Ankoudinova, I., et al. (1995). Cloning, sequencing, and expression of a 24-kDa Ca2+-binding protein activating photoreceptor guanylyl cyclase. *J. Biol. Chem.* 270, 25200–25206. doi: 10.1074/jbc.270.42.25200

Dubois, S. K., Kishimoto, I., Lillis, T. O., and Garbers, D. L. (2000). A genetic model defines the importance of the atrial natriuretic peptide receptor (guanylyl cyclase-A) in the regulation of kidney function. *Proc. Natl. Acad. Sci. U.S.A.* 97, 4369–4373. doi: 10.1073/pnas.97.8.4369

Duda, T., Bharill, S., Wojtas, I., Yadav, P., Gryczynski, I., Gryczynski, Z., et al. (2009). Atrial natriuretic factor receptor guanylate cyclase signaling: new ATP-regulated transduction motif. *Mol. Cell. Biochem.* 324, 39–53. doi: 10.1007/s11010-008-9983-2

Duda, T., Fik-Rymarkiewicz, E., Venkataraman, V., Krishnan, A., and Sharma, R. K. (2004). Calcium-modulated ciliary membrane guanylate cyclase transduction machinery: constitution and operational principles. *Mol. Cell. Biochem.* 267, 107–122. doi: 10.1023/B:MCBI.0000049372.33965.4f

Duda, T., Goraczniak, R. M., and Sharma, R. K. (1991). Site-directed mutational analysis of a membrane guanylate cyclase cDNA reveals the atrial natriuretic factor signaling site. *Proc. Natl. Acad. Sci. U.S.A.* 88, 7882–7886. doi: 10.1073/pnas.88.17.7882

Duda, T., Goraczniak, R. M., and Sharma, R. K. (1993a). The glycine residue of ATP regulatory module in receptor guanylate cyclases that is essential in natriuretic factor signaling. *FEBS Lett.* 335, 309–314. doi: 10.1016/0014-5793(93)80408-M

Duda, T., Goraczniak, R. M., Sitaramayya, A., and Sharma, R. K. (1993b). Cloning and expression of an ATP-regulated human retina C-type natriuretic factor receptor guanylate cyclase. *Biochemistry* 32, 1391–1395. doi: 10.1021/bi00057a001

Duda, T., Goraczniak, R. M., and Sharma, R. K. (1996a). Molecular characterization of S100A1-S100B protein in retina and its activation mechanism of bovine photoreceptor guanylate cyclase. *Biochemistry* 35, 6263–6266. doi: 10.1021/bi960007m

Duda, T., Goraczniak, R., Surgucheva, I., Rudnicka-Nawrot, M., Gorczyca, W. A., Palczewski, K., et al. (1996b). Calcium modulation of bovine photoreceptor guanylate cyclase. *Biochemistry* 35, 8478–8482. doi: 10.1021/bi960752z

Duda, T., Jankowska, A., Venkataraman, V., Nagele, R. G., and Sharma, R. K. (2001a). A novel calcium-regulated membrane guanylate cyclase transduction system in the olfactory neuroepithelium. *Biochemistry* 40, 12067–12077. doi: 10.1021/bi0108406

Duda, T., Yadav, P., Jankowska, A., Venkataraman, V., and Sharma, R. K. (2001b). Three dimensional atomic model and experimental validation for the ATP-Regulated Module (ARM) of the atrial natriuretic factor receptor guanylate cyclase. *Mol. Cell. Biochem.* 217, 165–172. doi: 10.1023/A:1007236917061

Duda, T., Krishnan, R., and Sharma, R. K. (2006). GCAP1: antithetical calcium sensor of ROS-GC transduction machinery. *Calcium Bind. Proteins* 1, 102–107.

Duda, T., Pertzev, A., Koch, K. W., and Sharma, R. K. (2012a). Antithetical modes of and the Ca2+ sensors targeting in ANF-RGC and ROS-GC1 membrane guanylate cyclases. *Front. Mol. Neurosci.* 5:44. doi: 10.3389/fnmol.2012.00044

Duda, T., Pertzev, A., and Sharma, R. K. (2012b). Ca(2+) modulation of ANF-RGC: new signaling paradigm interlocked with blood pressure regulation. *Biochemistry* 51, 9394–9405. doi: 10.1021/bi301176c

Duda, T., Pertzev, A., and Sharma, R. K. (2013). The ANF-RGC gene motif (669)WTAPELL(675) is vital for blood pressure regulation: Biochemical mechanism. *Biochemistry* 52, 2337–2334. doi: 10.1021/bi400175d

Duda, T., and Sharma, R. K. (1995). ATP bimodal switch that regulates the ligand binding and signal transduction activities of the atrial natriuretic factor receptor guanylate cyclase. *Biochem. Biophys. Res. Commun.* 209, 286–292. doi: 10.1006/bbrc.1995.1501

Duda, T., and Sharma, R. K. (2005). Two membrane juxtaposed signaling modules in ANF-RGC are interlocked. *Biochem. Biophys. Res. Commun.* 332, 149–156. doi: 10.1016/j.bbrc.2005.04.102

Duda, T., and Sharma, R. K. (2008). ONE-GC membrane guanylate cyclase, a trimodal odorant signal transducer. *Biochem. Biophys. Res. Commun.* 367, 440–444. doi: 10.1016/j.bbrc.2007.12.153

Duda., T., and Sharma, R. K. (2009). Ca2+-modulated ONE-GC odorant signal transduction. *FEBS Lett.* 583, 1327–1330. doi: 10.1016/j.febslet.2009.03.036

Duda, T., Venkataraman, V., Ravichandran, S., and Sharma, R. K. (2005). ATP-regulated module (ARM) of the atrial natriuretic factor receptor guanylate cyclase. *Peptides* 26, 969–984. doi: 10.1016/j.peptides.2004.08.032

Duda, T., Yadav, P., and Sharma, R. K. (2011). Allosteric modification, the primary ATP activation mechanism of atrial natriuretic factor receptor guanylate cyclase. *Biochemistry* 50, 1213–1212. doi: 10.1021/bi1018978

Ellis, K. L., Newton-Cheh, C., Wang, T. J., Frampton, C. M., Doughty, R. N., Whalley, G. A., et al. (2011). Association of genetic variation in the natriuretic peptide system with cardiovascular outcomes. *J. Mol. Cell. Cardiol.* 50, 695–701. doi: 10.1016/j.yjmcc.2011.01.010

Ellmers, L. J., Scott, N. J., Piuhola, J., Maeda, N., Smithies, O., Frampton, C. M., et al. (2007). Npr1-regulated gene pathways contributing to cardiac hypertrophy and fibrosis. *J. Mol. Endocrinol.* 38, 245–257. doi: 10.1677/jme.1.02138

Foster, D. C., and Garbers, D. L. (1998). Dual role for adenine nucleotides in the regulation of the atrial natriuretic peptide receptor, guanylyl cyclase-A. *J. Biol. Chem.* 273, 16311–16318. doi: 10.1074/jbc.273.26.16311

Fulle, H. J., Vassar, R., Foster, D. C., Yang, R. B., Axel, R., and Garbers, D. L. (1995). A receptor guanylyl cyclase expressed specifically in olfactory sensory neurons. *Proc. Natl. Acad. Sci. U.S.A.* 92, 3571–3575. doi: 10.1073/pnas.92.8.3571

Goraczniak, R. M., Duda, T., and Sharma, R. K. (1992). A structural motif that defines the ATP-regulatory module of guanylate cyclase in atrial natriuretic factor signalling. *Biochem. J.* 282, 533–537.

Goraczniak, R. M., Duda, T., and Sharma, R. K. (1998). Calcium modulated signaling site in type 2 rod outer segment membrane guanylate cyclase (ROS-GC2). *Biochem. Biophys. Res. Commun.* 245, 447–453. doi: 10.1006/bbrc.1998.8455

Goraczniak, R. M., Duda, T., Sitaramayya, A., and Sharma, R. K. (1994). Structural and functional characterization of the rod outer segment membrane guanylate cyclase. *Biochem. J.* 302, 455–461.

Hamra, F. K., Forte, L. R., Eber, S. L., Pidhorodeckyj, N. V., Krause, W. J., Freeman, R. H., et al. (1993). Uroguanylin: structure and activity of a second endogenous peptide that stimulates intestinal guanylate cyclase. *Proc. Natl. Acad. Sci. U.S.A.* 90, 10464–10468. doi: 10.1073/pnas.90.22.10464

Hanks, S. K., Quinn, A. M., and Hunter, T. (1988). The protein kinase family: conserved features and deduced phylogeny of the catalytic domains. *Science* 241, 42–52. doi: 10.1126/science.3291115

He, X., Nishio, K., and Misono, K. S. (1995). High-yield affinity alkylation of the atrial natriuretic factor receptor binding site. *Bioconjug. Chem.* 6, 541–548. doi: 10.1021/bc00035a007

Holtwick, R., van Eickels, M., Skryabin, B. V., Baba, H. A., Bubikat, A., Begrow, F., et al. (2003). Pressure independent cardiac hypertrophy in mice with cardiomyocyte-restricted inactivation of the atrial natriuretic peptide receptor guanyly cyclase-A. *J. Clin. Invest.* 111, 1399–1407. doi: 10.1172/JCI17061

Huo, X., Abe, T., and Misono, K. S. (1999). Ligand binding-dependent limited proteolysis of the atrial natriuretic peptide receptor: juxtamembrane hinge structure essential for transmembrane signal transduction. *Biochemistry* 38, 16941–16951. doi: 10.1021/bi9919448

Iino, S., Kobayashi, S., Okazaki, K., and Hidaka, H. (1995). Immunohistochemical localization of neurocalcin in the rat inner ear. *Brain Res.* 680, 128–134. doi: 10.1016/0006-8993(95)00253-M

Ivings, L., Pennington, S. R., Jenkins, R., Weiss, J. L., and Burgoyne, R. D. (2002). Identification of Ca2+-dependent binding partners for the neuronal calcium sensor protein neurocalcin delta: interaction with actin, clathrin and tubulin. *Biochem. J.* 363, 599–608. doi: 10.1042/0264-6021:3630599

Katholi, R. E., and Couri, D. M. (2011). Left ventricular hypertrophy: major risk factor in patients with hypertension: update and practical clinical applications. *Int. J. Hypertens.* 2011, 495349. doi: 10.4061/2011/495349

Khare, S., Wilson, D., Wali, R. K., Tien, X. Y., Bissonnette, M., Niedziela, S. M., et al. (1994). Guanylin activates rat colonic particulate guanylate cyclase. *Biochem. Biophys. Res. Commun.* 203, 1432–1437. doi: 10.1006/bbrc.1994.2345

Kishimoto, I., Rossi, K., and Garbers, D. L. (2001). A genetic model provides evidence that the receptor for atrial natriuretic peptide (guanylyl cyclase-A) inhibits cardiac ventricular myocyte hypertrophy. *Proc. Natl. Acad. Sci. U.S.A.* 98, 2703–2706. doi: 10.1073/pnas.051625598

Knowles, J. W., Esposito, G., Mao, L., Hagaman, J. R., Fox, J. E., Smithies, O., et al. (2001). Pressure independent enhancement of cardiac hypertrophy in natriuretic peptide receptor A-deficient mice. *J. Clin. Invest.* 107, 975–984. doi: 10.1172/JCI11273

Koch, K.-W. (1991). Purification and identification of photoreceptor guanylate cyclase. *J. Biol. Chem.* 266, 8634–8637.

Koch, K.-W., Duda, T., and Sharma, R. K. (2010). Ca2+-modulated vision-linked ROS-GC guanylate cyclase transduction machinery. *Mol. Cell. Biochem.* 334, 105–115. doi: 10.1007/s11010-009-0330-z

Kuhn, M., Ng, C. K., Su, Y. H., Kilić, A., Mitko, D., Bien-Ly, N., et al. (2004). Identification of an orphan guanylate cyclase receptor selectively expressed in mouse testis. *Biochem. J.* 379, 385–393. doi: 10.1042/BJ20031624

Kumar, V. D., Vijay-Kumar, S., Krishnan, A., Duda, T., and Sharma, R. K. (1999). A second calcium regulator of rod outer segment membrane guanylate cyclase, ROS-GC1: neurocalcin. *Biochemistry* 38, 12614–12620. doi: 10.1021/bi990851n

Krishnan, A., Venkataraman, V., Fik-Rymarkiewicz, E., Duda, T., and Sharma, R. K. (2004). Structural, biochemical, and functional characterization of the calcium sensor neurocalcin delta in the inner retinal neurons and its linkage with the rod outer segment membrane guanylate cyclase transduction system. *Biochemistry* 43, 2708–2723. doi: 10.1021/bi035631v

Kuno, T., Andresen, J. W., Kamisaki, Y., Waldman, S. A., Chang, L. Y., Saheki, S., et al. (1986). Co-purification of an atrial natriuretic factor receptor and particulate guanylate cyclase from rat lung. *J. Biol. Chem.* 261, 5817–5823.

Kurose, H., Inagami, T., and Ui, M. (1987). Participation of adenosine 5′-triphosphate in the activation of membrane-bound guanylate cyclase by the atrial natriuretic factor. *FEBS Lett.* 219, 375–379. doi: 10.1016/0014-5793(87)80256-9

Labrecque, J., Deschênes, J., McNicoll, N., and De Léan, A. (2001). Agonistic induction of a covalent dimer in a mutant of natriuretic peptide receptor-A documents a juxtamembrane interaction that accompanies receptor activation. *J. Biol. Chem.* 276, 8064–8072. doi: 10.1074/jbc.M005550200

Labrecque, J., Mc Nicoll, N., Marquis, M., and De Lean, A. (1999). A disulfide-bridged mutant of natriuretic peptide receptor-A displays constitutive activity. Role of receptor dimerization in signal transduction. *J. Biol. Chem.* 274, 9752–9759. doi: 10.1074/jbc.274.14.9752

Ladant, D. (1995). Calcium and membrane binding properties of bovine neurocalcin delta expressed in *Escherichia coli*. *J. Biol. Chem.* 270, 3179–3185.

Larose, L., McNicoll, N., Ong, H., and De Léan, A. (1991). Allosteric modulation by ATP of the bovine adrenal natriuretic factor R1 receptor functions. *Biochemistry* 30, 8990–8995. doi: 10.1021/bi00101a012

Leinders-Zufall, T., Cockerham, R. E., Michalakis, S., Biel, M., Garbers, D. L., Reed, R. R., et al. (2007). Contribution of the receptor guanylyl cyclase GC-D to chemosensory function in the olfactory epithelium. *Proc. Natl. Acad. Sci. U.S.A.* 104, 14507–14512. doi: 10.1073/pnas.0704965104

Liu, Y., Ruoho, A. E., Rao, V. D., and Hurley, J. H. (1997). Catalytic mechanism of the adenylyl and guanylyl cyclases: modeling and mutational analysis. *Proc. Natl. Acad. Sci. U.S.A.* 94, 13414–13419. doi: 10.1073/pnas.94.25.13414

Lowe, D. G., Chang, M. S., Hellmiss, R., Chen, E., Singh, S., Garbers, D. L., et al. (1989). Human atrial natriuretic peptide receptor defines a new paradigm for second messenger signal transduction. *EMBO J.* 8, 1377–13784.

Lowe, D. G., Dizhoor, A. M., Liu, K., Gu, Q., Spencer, M., Laura, R., et al. (1995). Cloning and expression of a second photoreceptor-specific membrane retina guanylyl cyclase (RetGC), RetGC-2. *Proc. Natl. Acad. Sci. U.S.A.* 92, 5535–5539. doi: 10.1073/pnas.92.12.5535

Maack, T. (1996). Role of atrial natriuretic factor in volume control. *Kidney Int.* 49, 1732–1737. doi: 10.1038/ki.1996.257

Mamasuew, K., Breer, H., and Fleischer, J. (2008). Gruenberg ganglion neurons respond to cool ambient temperatures. *Eur. J. Neurosci.* 28, 1775–1785. doi: 10.1111/j.1460-9568.2008.06465.x

Marala, R., Duda, T., Goraczniak, R. M., and Sharma, R. K. (1992). Genetically tailored atrial natriuretic factor-dependent guanylate cyclase. Immunological and functional identity with 180 kDa membrane guanylate cyclase and ATP signaling site. *FEBS Lett.* 296, 254–258. doi: 10.1016/0014-5793(92)80298-U

Marala, R. B., Sitaramayya, A., and Sharma, R. K. (1991). Dual regulation of atrial natriuretic factor-dependent guanylate cyclase activity by ATP. *FEBS Lett.* 281, 73–76. doi: 10.1016/0014-5793(91)80361-6

Margulis, A., Pozdnyakov, N., and Sitaramayya, A. (1996). Activation of bovine photoreceptor guanylate cyclase by S100 proteins. *Biochem. Biophys. Res. Commun.* 218, 243–247. doi: 10.1006/bbrc.1996.0043

McNicoll, N., Escher, E., Wilkes, B. C., Schiller, P. W., Ong, H., and De Léan, A. (1992). Highly efficient photoaffinity labeling of the hormone binding domain of atrial natriuretic factor receptor. *Biochemistry* 31, 4487–4493. doi: 10.1021/bi00133a015

McNicoll, N., Gagnon, J., Rondeau, J. J., Ong, H., and De Léan, A. (1996). Localization by photoaffinity labeling of natriuretic peptide receptor-A binding domain. *Biochemistry* 35, 12950–12956. doi: 10.1021/bi960818q

Meloche, S., McNicoll, N., Liu, B., Ong, H., and De Lean, A. (1988). Atrial natriuretic factor R1 receptor from bovine adrenal zona glomerulosa: purification, characterization, and modulation by amiloride. *Biochemistry* 27, 8151–8158. doi: 10.1021/bi00421a025

Miao, Z. H., Song, D. L., Douglas, J. G., and Chang, C. H. (1995). Mutational inactivation of the catalytic domain of guanylate cyclase-A receptor. *Hypertension* 25, 694–698. doi: 10.1161/01.HYP.25.4.694

Misono, K. S. (2002). Natriuretic peptide receptor: structure and signaling. *Mol. Cell. Biochem.* 230, 49–60. doi: 10.1023/A:1014257621362

Misono, K. S., Ogawa, H., Qiu, Y., and Ogata, C. M. (2005). Structural studies of the natriuretic peptide receptor: a novel hormone-induced rotation mechanism for transmembrane signal transduction. *Peptides* 26, 957–968. doi: 10.1016/j.peptides.2004.12.021

Misono, K. S., Philo, J. S., Arakawa, T., Ogata, C. M., Qiu, Y., Ogawa, H., et al. (2011). Structure, signaling mechanism and regulation of the natriuretic peptide receptor guanylate cyclase. *FEBS J.* 278, 1818–1829. doi: 10.1111/j.1742-4658.2011.08083.x

Miyagi, M., and Misono, K. S. (2000). Disulfide bond structure of the atrial natriuretic peptide receptor extracellular domain: conserved disulfide bonds among guanylate cyclase-coupled receptors. *Biochim. Biophys. Acta* 1478, 30–38. doi: 10.1016/S0167-4838(00)00002-9

Nakano, A., Terasawa, M., Watanabe, M., Okazaki, K., Inoue, S., Kato, M., et al. (1993). Distinct regional localization of neurocalcin, a Ca2+-binding protein, in the bovine adrenal gland. *J. Endocrinol.* 138, 283–290. doi: 10.1677/joe.0.1380283

Ogawa, H., Qiu, Y., Huang, L., Tam-Chang, S. W., Young, H. S., and Misono, K. S. (2009). Structure of the atrial natriuretic peptide receptor extracellular domain in the unbound and hormone-bound states by single-particle electron microscopy. *FEBS J.* 276, 1347–1355. doi: 10.1111/j.1742-4658.2009.06870.x

Ogawa, H., Qiu, Y., Ogata, C. M., and Misono, K. S. (2004). Crystal structure of hormone-bound atrial natriuretic peptide receptor extracellular domain: rotation mechanism for transmembrane signal transduction. *J. Biol. Chem.* 279, 28625–28631. doi: 10.1074/jbc.M313222200

Ogawa, H., Zhang, X., Qiu, Y., Ogata, C. M., and Misono, K. S. (2003). Crystallization and preliminary X-ray analysis of the atrial natriuretic peptide (ANP) receptor extracellular domain complex with ANP: use of ammonium sulfate as the cryosalt. *Acta Crystallogr. D Biol. Crystallogr.* 59, 1831–1833. doi: 10.1107/S0907444903016445

Okazaki, K., Obata, N. H., Inoue, S., and Hidaka, H. (1995). S100 beta is a target protein of neurocalcin delta, an abundant isoform in glial cells. *Biochem. J.* 306, 551–555.

Oliver, P. M., Fox, J. E., Kim, R., Rockman, H. A., Kim, H. S., Reddick, R. L., et al. (1997). Hypertension, cardiac hypertrophy, and sudden death in mice lacking natriuretic peptide receptor A. *Proc. Natl. Acad. Sci. U.S.A.* 94, 14730–14735. doi: 10.1073/pnas.94.26.14730

Olson, L. J., Ho, B., Cashdollar, L. W., and Drewett, J. G. (1998). Functionally active catalytic domain is essential of guanylyl cyclase-linked receptor mediated inhibition of human aldosterone synthesis. *Mol. Pharmacol.* 54, 761–769.

Palczewski, K., Subbaraya, I., Gorczyca, W. A., Helekar, B. S., Ruiz, C. C., Ohguro, H., et al. (1994). Molecular cloning and characterization of retinal photoreceptor guanylyl cyclase-activating protein. *Neuron* 13, 395–404. doi: 10.1016/0896-6273(94)90355-7

Pandey, K. N. (2011). Guanylyl cyclase/atrial natriuretic peptide receptor-A: role in the pathophysiology of cardiovascular regulation. *Can. J. Physiol. Pharmacol.* 89, 557–573. doi: 10.1139/y11-054

Pandey, K. N., and Singh, S. (1990). Molecular cloning and expression of murine guanylate cyclase/atrial natriuretic factor receptor cDNA. *J. Biol. Chem.* 265, 12342–12348.

Parat, M., Blanchet, J., and De Léan, A. (2010). Role of juxtamembrane and transmembrane domains in the mechanism of natriuretic peptide receptor A activation. *Biochemistry* 49, 4601–4610. doi: 10.1021/bi901711w

Paul, A. K. (1986). *Particulate Guanylate Cyclase from Adrenocortical Carcinoma 494. Purification, Biochemical and Immunological Characterization.* Ph.D. thesis, University of Tennessee.

Paul, A. K., Marala, R. B., Jaiswal, R. K., and Sharma, R. K. (1987). Coexistence of guanylate cyclase and atrial natriuretic factor receptor in a 180-kD protein. *Science* 235, 1224–1226. doi: 10.1126/science.2881352

Pertzev, A., Duda, T., and Sharma, R. K. (2010). Ca2+ sensor GCAP1: a constitutive element of the ONE-GC-modulated odorant signal transduction pathway. *Biochemistry* 49, 7303–7313. doi: 10.1021/bi101001v

Potter, L. R., and Hunter, T. (1998a). Phosphorylation of the kinase homology domain is essential for activation of the A-type natriuretic peptide receptor. *Mol. Cell. Biol.* 18, 2164–2172.

Potter, L. R., and Hunter, T. (1998b). Identification and characterization of the major phosphorylation sites of the B-type natriuretic peptide receptor. *J. Biol. Chem.* 273, 15533–15539. doi: 10.1074/jbc.273.25.15533

Potter, L. R., and Hunter, T. (1999a). Identification and characterization of the phosphorylation sites of the guanylyl cyclase-linked natriuretic peptide receptors A and B. *Methods* 19, 506–520. doi: 10.1006/meth.1999.0893

Potter, L. R., and Hunter, T. (1999b). A constitutively "phosphorylated" guanylyl cyclase-linked atrial natriuretic peptide receptor mutant is resistant to desensitization. *Mol. Biol. Cell* 10, 1811–1820. doi: 10.1091/mbc.10.6.1811

Pozdnyakov, N., Yoshida, A., Cooper, N. G., Margulis, A., Duda, T., Sharma, R. K., et al. (1995). A novel calcium-dependent activator of retinal rod outer segment membrane guanylate cyclase. *Biochemistry* 34, 14279–14283. doi: 10.1021/bi00044a002

Pugh, E. N. Jr., Duda, T., Sitaramayya, A., and Sharma, R. K. (1997). Photoreceptor guanylate cyclases: a review. *Biosci. Rep.* 17, 429–473. doi: 10.1023/A:1027365520442

Rebello, M. R., Aktas, A., and Medler, K. F. (2011). Expression of calcium binding proteins in mouse type II taste cells. *J. Histochem. Cytochem.* 59, 530–539. doi: 10.1369/0022155411402352

Rondeau, J. J., McNicoll, N., Gagnon, J., Bouchard, N., Ong, H., and De Léan, A. (1995). Stoichiometry of the atrial natriuretic factor-R1 receptor complex in the bovine zona glomerulosa. *Biochemistry* 34, 2130–2136. doi: 10.1021/bi00007a005

Schulz, S., Green, C. K., Yuen, P. S., and Garbers, D. L. (1990). Guanylyl cyclase is a heat-stable enterotoxin receptor. *Cell* 63, 941–948. doi: 10.1016/0092-8674(90)90497-3

Schulz, S., Singh, S., Bellet, R. A., Singh, G., Tubb, D. J., Chin, H., et al. (1989). The primary structure of a plasma membrane guanylate cyclase demonstrates diversity within this new receptor family. *Cell* 58, 1155–1162. doi: 10.1016/0092-8674(89)90513-8

Schulz, S., Wedel, B. J., Matthews, A., and Garbers, D. L. (1998). The cloning and expression of a new guanylyl cyclase orphan receptor. *J. Biol. Chem.* 273, 1032–1037. doi: 10.1074/jbc.273.2.1032

Sharma, R. K. (2002). Evolution of the membrane guanylate cyclase transduction system. *Mol. Cell. Biochem.* 230, 3–30. doi: 10.1023/A:1014280410459

Sharma, R. K. (2010). Membrane guanylate cyclase is a beautiful signal transduction machine: overview. *Mol. Cell. Biochem.* 334, 3–36. doi: 10.1007/s11010-009-0336-6

Sharma, R. K., and Duda, T. (2010). Odorant-linked ROS-GC subfamily membrane guanylate cyclase transduction system. *Mol. Cell. Biochem.* 334, 181–189. doi: 10.1007/s11010-009-0333-9

Sharma, R. K., Jaiswal, R. K., and Duda, T. (1988a). "Second messenger role of cyclic GMP in atrial natriuretic factor receptor mediated signal transduction: 180 kDa membrane guanylate cyclase, its coupling with atrial natriuretic factor receptor and its regulation by protein kinase C," in *Biological and Molecular Aspects of Atrial Factors*, ed. Needleman (New york: Alan R. Liss, Inc.), 77–96.

Sharma, R. K., Marala, R. B., and Paul, A. K. (1988b). "Mediatory role of cyclic GMP in receptor-mediated signal transduction: membrane guanylate cyclase and its coupling with atrial natriuretic factor receptor," in *American Society of Hypertension Symposium Series, Advances in Peptide Research*, Vol 2, eds B. M. Brenner and J. H. Laragh (New York: Raven Press), 61–77.

Sharma, R. K., Marala, R. B., and Duda, T. (1989). Purification and characterization of the 180-kDa membrane guanylate cyclase containing atrial natriuretic factor receptor from rat adrenal gland and its regulation by protein kinase C. *Steroids* 53, 437–460. doi: 10.1016/0039-128X(89)90024-X

Sharma, R. K., Yadav, P., and Duda, T. (2001). Allosteric regulatory step and configuration of the ATP-binding pocket in atrial natriuretic factor receptor guanylate cyclase transduction mechanism. *Can. J. Physiol. Pharmacol.* 79, 682–691. doi: 10.1139/y01-033

Shi, S.-J, Nguyen, H. T., Sharma, G. D., Navar, G., and Pandey, K. N. (2001). Genetic disruption of atrial natriuretic peptide receptor-A alters rennin and angiotensinII levels. *Am. J. Physiol. Renal Physiol.* 281, F665–F673.

Shyjan, A. W., de Sauvage, F. J., Gillett, N. A., Goeddel, D. V., and Lowe, D. G. (1992). Molecular cloning of a retina-specific membrane guanylyl cyclase. *Neuron* 9, 727–737. doi: 10.1016/0896-6273(92)90035-C

Singh, S., Singh, G., Heim, J. M., and Gerzer, R. (1991). Isolation and expression of a guanylate cyclase-coupled heat stable enterotoxin receptor cDNA from a human colonic cell line. *Biochem. Biophys. Res. Commun.* 179, 1455–1463. doi: 10.1016/0006-291X(91)91736-V

Takayanagi, R., Inagami, T., Snajdar, R. M., Imada, T., Tamura, M., and Misono, K. S. (1987). Two distinct forms of receptors for atrial natriuretic factor in bovine adrenocortical cells. Purification, ligand binding, and peptide mapping. *J. Biol. Chem.* 262, 12104–12113.

Thompson, D. K., and Garbers, D. L. (1995). Dominant negative mutations of the guanylyl cyclase-A receptor. Extracellular domain deletion and catalytic domain point mutations. *J. Biol. Chem.* 270, 425–430. doi: 10.1074/jbc.270.1.425

Thorpe, D. S., and Morkin, E. (1990). The carboxyl region contains the catalytic domain of the membrane form of guanylate cyclase. *J. Biol. Chem.* 265, 14717–14720.

Thorpe, D. S., Niu, S., and Morkin, E. (1996). The guanylyl cyclase core of an atrial natriuretic peptide receptor: enzymatic properties and basis for cooperativity. *Biochem. Biophys. Res. Commun.* 218, 670–673. doi: 10.1006/bbrc.1996.0120

Tremblay, J., Huot, C., Koch, C., and Potier, M. (1991). Characterization of the functional domains of the natriuretic peptide receptor/guanylate cyclase by radiation inactivation. *J. Biol. Chem.* 266, 8171–8175.

Tucker, C. L., Hurley, J. H., Miller, T. R., and Hurley, J. B. (1998). Two amino acid substitutions convert a guanylyl cyclase, RetGC-1, into an adenylyl cyclase. *Proc. Natl. Acad. Sci. U.S.A.* 95, 5993–5997. doi: 10.1073/pnas.95.11.5993

Venkataraman, V., Duda, T., Ravichandran, S., and Sharma, R. K. (2008). Neurocalcin delta modulation of ROS-GC1, a new model of Ca2+ signaling. *Biochemistry* 47, 6590–6601. doi: 10.1021/bi800394s

Vijay-Kumar, S., and Kumar, V. D. (1999). Crystal structure of recombinant bovine neurocalcin. *Nat. Struct. Biol.* 6, 80–88. doi: 10.1038/4956

Wadei, H. M., and Textor, S. C. (2012). The role of the kidney in regulating arterial blood pressure. *Nat. Rev. Nephrol.* 8, 602–609. doi: 10.1038/nrneph.2012.191

Wedel, B. J., Foster, D. C., Miller, D. E., and Garbers, D. L. (1997). A mutation of the atrial natriuretic peptide (guanylyl cyclase-A) receptor results in a constitutively hyperactive enzyme. *Proc. Natl. Acad. Sci. U.S.A.* 94, 459–462. doi: 10.1073/pnas.94.2.459

Wedel, B. J., and Garbers, D. L. (1997). New insights on the functions of the guanylyl cyclase receptors. *FEBS Lett.* 410, 29–33. doi: 10.1016/S0014-5793(97)00358-X

Wen, X. H., Duda, T., Pertzev, A., Venkataraman, V., Makino, C. L., and Sharma, R. K. (2012). S100B serves as a Ca2+ sensor for ROS-GC1 guanylate cyclase in cones but not in rods of the murine retina. *Cell. Physiol. Biochem.* 29, 417–430. doi: 10.1159/000338496

Wierenga, R. K., and Hol, W. G. (1983). Predicted nucleotide-binding properties of p21 protein and its cancer-associated variant. *Nature* 302, 842–844. doi: 10.1038/302842a0

Wilson, E. M., and Chinkers, M. (1995). Identification of sequences mediating guanylyl cyclase dimerization. *Biochemistry* 34, 4696–4701. doi: 10.1021/bi00014a025

Wong, S. K., Ma, C. P., Foster, D. C., Chen, A. Y., and Garbers, D. L. (1995). The guanylyl cyclase-A receptor transduces an atrial natriuretic peptide/ATP activation signal in the absence of other proteins. *J. Biol. Chem.* 270, 30818–30822. doi: 10.1074/jbc.270.51.30818

Yang, R. B., Foster, D. C., and Garbers, D. L., and Fulle, H. J. (1995). Two membrane forms of guanylyl cyclase found in the eye. *Proc. Natl. Acad. Sci. U.S.A.* 92, 602–606. doi: 10.1073/pnas.92.2.602

Zhao, D., Vellaichamy, E., Somanna, N. K., and Pandey, K. N. (2007). Guanylyl cyclase/natriuretic peptide receptor-A gene disruption causes increased adrenal angiotensin II and aldosterone levels. *Am. J. Physiol. Renal Physiol.* 293, F121–F127. doi: 10.1152/ajprenal.00478.2006

Zozulya, S., and Stryer, L. (1992). Calcium-myristoyl protein switch. *Proc. Natl. Acad. Sci. U.S.A.* 89, 11569–11573. doi: 10.1073/pnas.89.23.11569

Zufall, F., and Munger, S. D. (2010). Receptor guanylyl cyclases in mammalian olfactory function. *Mol. Cell. Biochem.* 334, 191–197. doi: 10.1007/s11010-009-0325-9

Conflict of Interest Statement: The authors declare that the research was conducted in the absence of any commercial or financial relationships that could be construed as a potential conflict of interest.

Received: 13 January 2014; accepted: 25 February 2014; published online: 17 March 2014.

*Citation: Duda T, Pertzev A and Sharma RK (2014) Atrial natriuretic factor receptor guanylate cyclase, ANF-RGC, transduces two independent signals, ANF and Ca^{2+}. Front. Mol. Neurosci. **7**:17. doi: 10.3389/fnmol.2014.00017*

This article was submitted to the journal Frontiers in Molecular Neuroscience.

frontiers in
MOLECULAR NEUROSCIENCE

REVIEW ARTICLE
published: 06 February 2014
doi: 10.3389/fnmol.2014.00003

Presynaptic [Ca^{2+}] and GCAPs: aspects on the structure and function of photoreceptor ribbon synapses

Frank Schmitz*

Department of Neuroanatomy, Institute for Anatomy and Cell Biology, Medical School Homburg/Saar, Saarland University, Saarland, Germany

Edited by:
Rameshwar K. Sharma, Salus University, USA

Reviewed by:
Matthias Kneussel, Zentrum für Molekulare Neurobiologie Hamburg, Germany
Noga Vardi, University of Pennsylvania, USA

***Correspondence:**
Frank Schmitz, Department of Neuroanatomy, Institute for Anatomy and Cell Biology, Medical School Homburg/Saar, Saarland University, Kirrbergerstrasse, University Campus, Building 61, Homburg/Saar 66421, Saarland, Germany
e-mail: frank.schmitz@uks.eu

Changes in intracellular calcium ions [Ca^{2+}] play important roles in photoreceptor signaling. Consequently, intracellular [Ca^{2+}] levels need to be tightly controlled. In the light-sensitive outer segments (OS) of photoreceptors, Ca^{2+} regulates the activity of retinal guanylate cyclases thus playing a central role in phototransduction and light-adaptation by restoring light-induced decreases in cGMP. In the synaptic terminals, changes of intracellular Ca^{2+} trigger various aspects of neurotransmission. Photoreceptors employ tonically active ribbon synapses that encode light-induced, graded changes of membrane potential into modulation of continuous synaptic vesicle exocytosis. The active zones of ribbon synapses contain large electron-dense structures, synaptic ribbons, that are associated with large numbers of synaptic vesicles. Synaptic coding at ribbon synapses differs from synaptic coding at conventional (phasic) synapses. Recent studies revealed new insights how synaptic ribbons are involved in this process. This review focuses on the regulation of [Ca^{2+}] in presynaptic photoreceptor terminals and on the function of a particular Ca^{2+}-regulated protein, the neuronal calcium sensor protein GCAP2 (guanylate cyclase-activating protein-2) in the photoreceptor ribbon synapse. GCAP2, an EF-hand-containing protein plays multiple roles in the OS and in the photoreceptor synapse. In the OS, GCAP2 works as a Ca^{2+}-sensor within a Ca^{2+}-regulated feedback loop that adjusts cGMP levels. In the photoreceptor synapse, GCAP2 binds to RIBEYE, a component of synaptic ribbons, and mediates Ca^{2+}-dependent plasticity at that site. Possible mechanisms are discussed.

Keywords: photoreceptor, ribbon synapse, synaptic ribbon, RIBEYE, Ca^{2+}, GCAP2

INTRODUCTION

PRESYNAPTIC [Ca^{2+}]: ASPECTS ON THE STRUCTURE AND FUNCTION OF PHOTORECEPTOR RIBBON SYNAPSES

Changes in presynaptic free cytosolic Ca^{2+} ions trigger important functions in the presynaptic terminals. These include synaptic vesicles exocytosis and the mediation of various forms of synaptic plasticity (Bliss and Collingridge, 1993; Malenka and Nicoll, 1999; Neher and Sakaba, 2008; Kawamoto et al., 2012; Rizo and Südhof, 2012; Catterall et al., 2013; Südhof, 2013). Ca^{2+} ions also have fundamental functions in photoreceptor synapses. Photoreceptors employ tonically active ribbon synapses that encode light-induced, graded changes of membrane potential into modulation of continuous synaptic vesicle exocytosis to transmit the light-induced signals to the inner retina. The active zones of ribbon synapses contain large electron-dense structures, synaptic ribbons, that are associated with large numbers of synaptic vesicles. Synaptic ribbons have a key importance for signaling at the ribbon synapse. This review focuses on the regulation of [Ca^{2+}] in presynaptic photoreceptor terminals and on the function of a particular Ca^{2+}-regulated protein, the neuronal calcium sensor (NCS) protein GCAP2 (guanylate cyclase-activating protein-2). GCAP2, an EF-hand-containing, Ca^{2+}-binding protein is strongly expressed in photoreceptors and plays multiple roles in the outer segments (OS) and in the photoreceptor synapse.

PHOTORECEPTORS

Photoreceptors are the principal light-sensitive neurons in the outer retina. They detect incoming light quanta (photons) and communicate the information to the inner retina for further processing. Rod photoreceptors operate at low light intensities and are capable of single-photon-detection. Cone photoreceptors operate at daylight conditions and mediate color vision (Abramov and Gordon, 1994). Both types of photoreceptors display a bipolar morphology with two processes emanating from opposite ends of the photoreceptor cell body (**Figure 1A**). (1) An outer process forms the outer segment (OS) that is responsible for phototransduction. During this process, light-sensitive photopigments in the OS transform light quanta into a change of the photoreceptor membrane potential. (2) An inner cell process emerges from the vitread portion of the photoreceptor soma. This inner process ends in a specialized presynaptic terminal that contains synaptic ribbons in their active zones (**Figures 1A** and **2**). At these

Abbreviations: CNG, cyclic nucleotide-gated channel; CRAC, Ca^{2+}-release-activated Ca^{2+}-channels; GCAP2, guanylate cyclase-activating protein 2; IS, inner segments; NAD(H), designates both the oxidized (NAD^+) as well as the reduced form (NADH) of nicotinamide adenine dinucleotide; OS, outer segments; PMCA, plasma membrane Ca^{2+}-ATPases; NCX, Na^+/Ca^{2+}-exchanger; RIM, rab3-interacting molecule; RIM-BP, RIM-binding protein; ret-GC, retinal guanylate cyclase; SERCA, sarco/endoplasmic reticulum Ca^{2+}-ATPase; SOCE, store-operated Ca^{2+}-entry; TIRF, total internal reflection fluorescence; VGCC, voltage-gated Ca^{2+}-channels; RE(A), RIBEYE(A)-domain; RE(B), RIBEYE(B)-domain.

ribbon-type active zones, signals generated by the absorption of light quanta in the OS are continuously transmitted to the inner retina (for review, see Wässle, 2004; Nassi and Callaway, 2009; Lee et al., 2010).

Ca^{2+}-DEPENDENT REGULATION OF PHOTOTRANSDUCTION IN PHOTORECEPTOR OUTER SEGMENTS

The OS contain dense and regular intracellular staples of membrane disks (for rods, **Figure 1**; for review, see Mustafi et al., 2009). These membrane-specializations are enriched with light-sensitive opsin-containing photopigments (Burns and Baylor, 2001; Chen, 2005). As light quanta are detected by the photopigments in the OS, a signal transduction cascade is initiated that finally leads via G-protein-mediated activation of a phosphodiesterase, phosphodiesterase 6 (PDE6), to the hydrolysis of cGMP (Burns and Baylor, 2001; Chen, 2005; Dell'Orco and Koch, 2010). The drop in cGMP leads to the closure of cyclic nucleotide-gated cation channels (CNG-channels) in the plasma membrane, a non-selective cation channel through which both Na^+- and Ca^{2+}-ions can pass from extra- to intracellular space along their electrochemical gradient. The light-induced closure of the CNG-channels generates a hyperpolarization response. The membrane potential ranges from ≈−40 mV in the dark to ≈−70 mV in bright light. The phototransduction system has a high dynamic range that is adjusted – not exclusively, but to a considerable extent – by Ca^{2+}-dependent processes (Arshavsky, 2002; Korenbrot and Rebrik, 2002; Sharma, 2002, 2010; Koch, 2006; Artemyev, 2008; Stephen et al., 2008; Dell'Orco and Koch, 2010; Sharma and Duda, 2012). The light-induced drop of Ca^{2+} is sensed by Ca^{2+}-binding, EF-hand-containing proteins, the guanylate cyclase-activating proteins (GCAPs; Korenbrot and Rebrik, 2002; Palczewski et al., 2004; Koch, 2006; Sakurai et al., 2011; Sharma and Duda, 2012). GCAPs are members of the family of NCS proteins (Sharma, 2002, 2010; Koch, 2006; Burgoyne, 2007; Baehr and Palczewski, 2009; Koch et al., 2010; Schmitz et al., 2012). GCAP2 (as well as its close relatives GCAP1 and GCAP3; for review, see Palczewski et al., 2004) contains four EF-hands. The first EF-hand is not able to bind Ca^{2+} due to exchange of critical amino acids (Palczewski et al., 2004; Koch, 2006; Burgoyne, 2007; Schmitz et al., 2012). Thus, under light stimulation, when Ca^{2+} is low, GCAPs activate the photoreceptor retinal guanylate cyclase (ret-GC) thus restoring cGMP baseline levels (Burns and Baylor, 2001; Sharma, 2002, 2010; Chen, 2005; Sharma and Duda, 2012). In the dark, at elevated Ca^{2+}, GCAPs inhibit ret-GCs activity and prevent overproduction of cGMP. These Ca^{2+}-/GCAP-dependent processes set the dynamic range of phototransduction and keep the OS and phototransduction operational at different levels of photon fluxes (Koch, 2006; Stephen et al., 2008; Sharma and Duda, 2012). GCAPs are myristoylated at their N-terminus. Remarkably, in contrast to other members of the NCS family, GCAPs do not perform a Ca^{2+}-dependent myristoyl switch at the N-terminus (Stephen et al., 2007). Instead, the N-terminal myristoyl-group remains buried in the inside of the molecule both in the Ca^{2+}-bound and Ca^{2+}-free state where it is essential to stabilize the protein (Stephen et al., 2007). Unusually, the C-terminus of GCAP2 performs a Ca^{2+}-dependent conformational change (Peshenko et al., 2004).

THE PHOTORECEPTOR RIBBON SYNAPSE OF THE MATURE RETINA: ULTRASTRUCTURE AND MOLECULAR ANATOMY OF THE SYNAPTIC RIBBON COMPLEX

Photoreceptors are non-spiking neurons and communicate light-induced, graded changes of membrane potential into modulations of tonic neurotransmitter release rates at the presynaptic terminals (Heidelberger et al., 2005; Matthews and Fuchs, 2010; Mercer and Thoreson, 2011). For this purpose, photoreceptor terminals are equipped with large active zones to which conspicuous presynaptic specializations, the synaptic ribbons, are attached (for review, see tom Dieck and Brandstätter, 2006; Schmitz, 2009; Matthews and Fuchs, 2010; Mercer and Thoreson, 2011; Schmitz et al., 2012).

The synaptic ribbon is a large, electron-dense structure that is associated with large numbers of synaptic vesicles along its entire surface (**Figure 2**; see also Schmitz, 2009). In photoreceptor ribbon synapses, the synaptic ribbon usually appears as a bar-shaped structure of several 100 nm in length in the transmission electron microscope (Schmitz, 2009; Mercer and Thoreson, 2011; Schmitz et al., 2012). Three-dimensional reconstructions of the synaptic ribbon revealed that this bar-shaped profile is a cross-section of a plate-shaped structure of the synaptic ribbon (**Figures 2** and **3E**; Rao-Mirotznik et al., 1995; for review, see also Schmitz, 2009; Mercer and Thoreson, 2011; Schmitz et al., 2012). Furthermore, the synaptic ribbon is bended in a horseshoe-shaped manner along the invaginated presynaptic plasma membrane of the photoreceptor terminal. The horseshoe-shaped synaptic ribbon can have a depth of about 1 μm (Schmitz, 2009; Schmitz et al., 2012). Rod photoreceptor presynaptic terminals usually possess a single active zone and a single synaptic ribbon; cone presynaptic terminals possess multiple active zones and multiple, though typically smaller synaptic ribbons (**Figure 2**; Wässle, 2004; Schmitz, 2009; Mercer and Thoreson, 2011; Regus-Leidig and Brandstätter, 2012; Schmitz et al., 2012). In photoreceptor ribbon synapses, synaptic ribbons are anchored to the arciform density. The arciform density corresponds to the presynaptic projections of conventional synapses (tom Dieck and Brandstätter, 2006; Schmitz, 2009; Mercer and Thoreson, 2011; **Figure 2**). At the plasma membrane of the active zone, L-type voltage-gated Ca^{2+}-channels (VGCC) are clustered. Ca^{2+}-influx through these channels triggers release at the photoreceptor synapse (see below). The active zone with the attached synaptic ribbon is opposed by the tips of multiple postsynaptic dendritic endings from horizontal and bipolar cells. These dendritic tips are located in a cavity formed by an invagination of the presynaptic photoreceptor terminal. The dendritic tips contain metabotropic glutamate receptors (in case of invaginating ON bipolar cells) or ionotropic glutamate receptors (in case of horizontal cells and OFF bipolar cells; Nomura et al., 1994; De Vries and Schwartz, 1999; De Vries, 2000; Wässle, 2004; De Vries et al., 2006; for review, see Dhingra and Vardi, 2012). Retinal bipolar cells, photoreceptor-like neurons in the pineal gland, inner ear hair cells, and vestibular hair cells also build ribbon synapses in mammals (Moser et al., 2006; Schmitz, 2009; Matthews and Fuchs, 2010; Mercer and Thoreson, 2011; Safieddine et al., 2012; Schmitz et al., 2012).

RIBEYE is a unique and major component of synaptic ribbons (Schmitz et al., 2000, 2012; Wan et al., 2005; Schmitz, 2009; Mercer

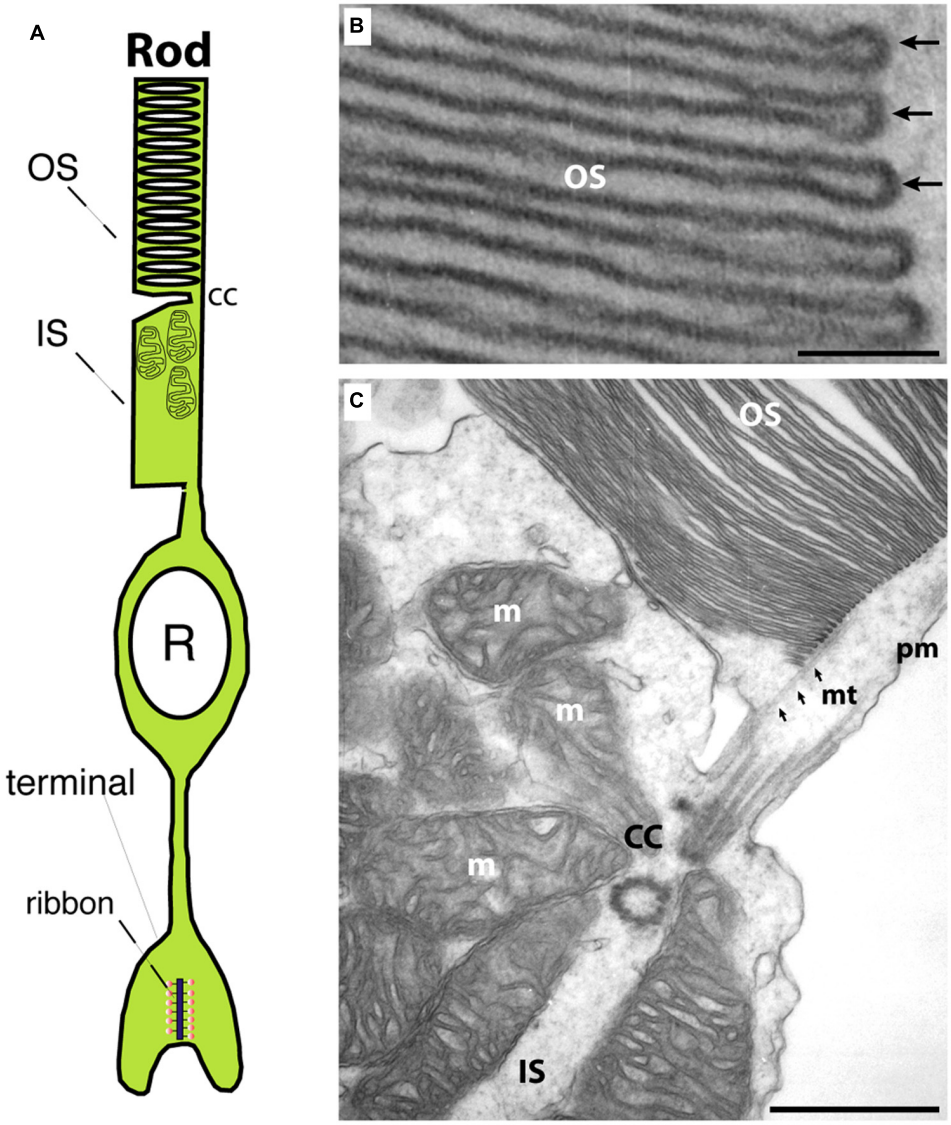

FIGURE 1 | (A) Photoreceptors show a bipolar morphology. A distal process forms the outer segment (OS) and the inner segment (IS). The OS is the place where phototransduction takes place. The IS represents the metabolic center of the photoreceptor. An inner, vitread process ends in the presynaptic terminal that contains a synaptic ribbon at the active zone. **(B)** Transmission electron micrograph of an outer segment (OS). Densely packed arrays of membrane disks can be observed. The arrows in **(B)** point to individual disks. In the OS, phototransduction occurs and GCAP proteins perform a Ca^{2+}-dependent feedback on guanylate cyclases. **(C)** Transmission electron micrograph at the junctional zone between OS and IS. OS and IS are connected by the connecting cilum (cc) that organizes mt-dependent vesicle transport into the outer segment (Sung and Chuang, 2010). OS, outer segment; IS, inner segment; m, mitochondrion; cc, connecting cilium linking OS and IS; mt, microtubule; pm, plasma membrane. Scale bars: 50 nm **(B)**, 250 nm **(C)**.

and Thoreson, 2011). RIBEYE is the only known protein specific to synaptic ribbons (Schmitz et al., 2000; Magupalli et al., 2008; for review, see Schmitz, 2009; Mercer and Thoreson, 2011; Schmitz et al., 2012). RIBEYE consists of a unique A-domain that is specific to synaptic ribbons and a B-domain that is largely identical to CtBP2. Using different promoters, RIBEYE and CtBP2 are transcribed from the same gene (Schmitz, 2009). While CtBP2 is expressed in most if not all cells; the expression of RIBEYE expression is limited to cells that form ribbon synapses. Particularly the A-domain contains many interaction sites, at which RIBEYE can bind to neighboring RIBEYE molecules. These multiple RIBEYE–RIBEYE interactions could allow the assembly of multiple RIBEYE molecules into ribbon-like structures (Magupalli et al., 2008; for review, see Schmitz, 2009; Mercer and Thoreson, 2011; Schmitz et al., 2012). These primitive, spherical ribbon precursors could then assemble into mature, bar-/plate-shaped synaptic ribbons in mature photoreceptors (see below). RIBEYE appears to be the main building block of synaptic ribbons. Additional proteins are needed to generate mature, functional synaptic ribbons (see below).

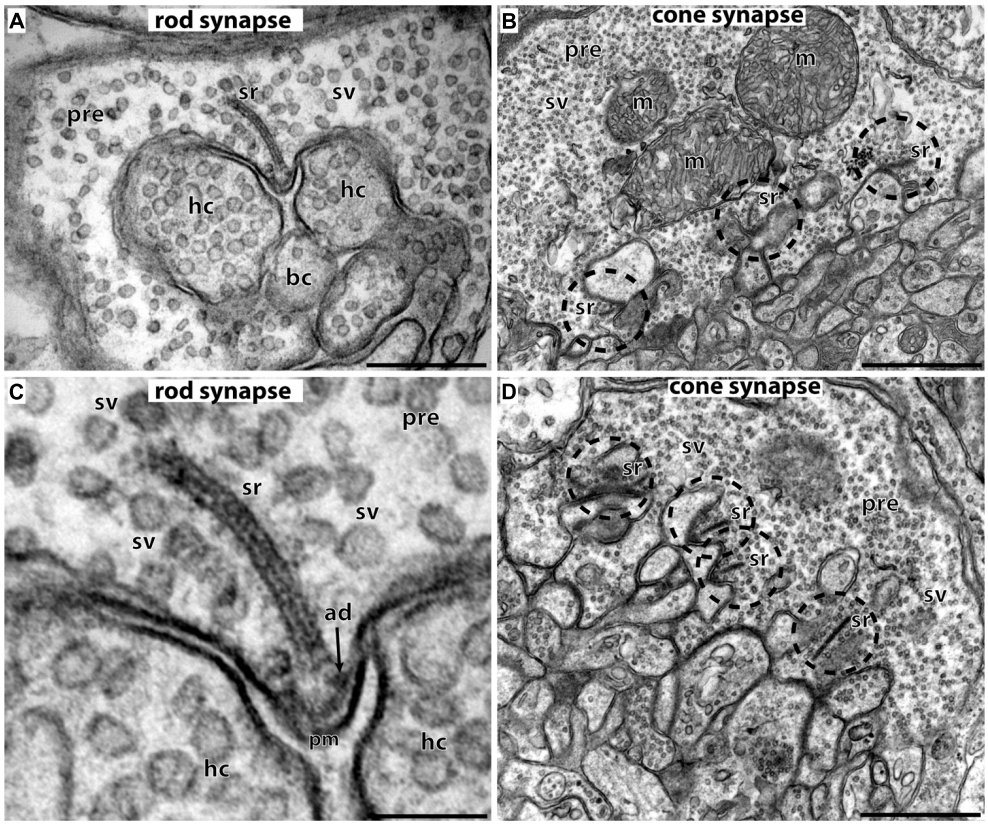

FIGURE 2 | Photoreceptor ribbon synapses. In **(A,C)** rod photoreceptor ribbon synapses are shown by transmission electron microscopy; in **(B,D)** cone photoreceptor ribbon synapses. **(A,B)** The large presynaptic terminals are filled with numerous synaptic vesicles (sv). The active zone is characterized by specialized presynaptic densities, the arciform densities (ad). The synaptic ribbon (sr) is anchored to the arciform density. The synaptic ribbon is associated with large numbers of synaptic vesicles. Opposite to the active zones are the dendritic tips of horizontal cells (hc) and bipolar cells (bc) that contain ionotropic and metabotropic glutamate receptors for signaling. The dendritic tips are located within an invagination of the presynaptic terminal. Cone synapses **(B,D)** are larger in diameter than rod synapses and contain multiple active zones (dashed circles) and multiple synaptic ribbons (sr). sr, synaptic ribbon; sv, synaptic vesicles; ad, arciform density; pre, presynaptic terminal; m, mitochondrium; hc, dendritic tips of horizontal cells; bc, dendritic tips of bipolar cells; pm, presynaptic plasma membrane. Scale bars: 400 nm **(A)**, 1 μm **(B)**, 150 nm **(C)**, 800 nm **(D)**.

Both RIBEYE(B)-domain and CtBP1/CtBP2 bind NAD(H) (Schmitz et al., 2000). In case of CtBP1/CtBP2, binding of NADH regulates interaction with nuclear proteins (Fjeld et al., 2003). This NAD(H)-regulated interaction can switch on or off distinct target genes relevant, e.g., for cellular migration, adhesion, and apoptosis (Paliwal et al., 2006, 2007, 2012; Chinnadurai, 2009). In the synapse, NAD(H) promotes interaction of RIBEYE with other synaptic proteins, e.g., the NCS protein GCAP2 (Venkatesan et al., 2010; López-del Hoyo et al., 2012). RIBEYE–GCAP2 interaction appears to be relevant for mediating Ca^{2+}-dependent effects on synaptic ribbon dynamics (see below). Other protein–protein interactions of RIBEYE do not depend on NADH, e.g., RIBEYE–Munc119 interaction (Alpadi et al., 2008) or have not been analyzed for their NADH-dependence, e.g., in case of RIBEYE-Bassoon (tom Dieck et al., 2005). While RIBEYE appears to be the only unique and major protein of the synaptic ribbon, there are other ribbon proteins which are also present in the active zone of non-ribbon containing synapses (for review, see tom Dieck and Brandstätter, 2006; Schmitz, 2009; Mercer and Thoreson, 2011; Schmitz et al., 2012). Bassoon is localized in the active zone of photoreceptors, bipolar cells, and hair cells (in addition to the active zone localization of conventional synapses) and is considered as an important anchor for the synaptic ribbon in ribbon synapses. Bassoon knockout mice display non-plasma membrane-anchored "floating" ribbons in photoreceptor and hair cells (Khimich et al., 2005; tom Dieck et al., 2005), though not in retinal bipolar cells. Bassoon is also present in retinal bipolar cells (Deguchi-Tawarada et al., 2006). Therefore, additional anchoring mechanisms for the synaptic ribbon might exist. Bassoon was also been reported to be linked to presynaptic Cav-channels recently (Nishimune et al., 2004, 2012; see also below). Piccolo, like bassoon a very large multidomain-protein, is present both in conventional and ribbon-type synapses. Recently, a splice variant of piccolo was described, named piccolino, that is preferentially expressed at ribbon synapses (Regus-Leidig et al., 2013). Proteins known to be essential for synapse function in conventional synapses are the multi-domain rab3-interacting molecule (RIM) protein family (Wang et al., 1997; Kaeser et al., 2011, 2012; for review, see Südhof, 2013). These proteins have been localized to the synaptic ribbon. The long isoforms of RIM contain a N-terminal Zn-finger, central

PDZ-domain and two C2-domains (Südhof, 2012a,b, 2013) that enable them to perform key synaptic functions. RIM proteins control synaptic vesicle docking and vesicle priming as well as Ca^{2+}-channel localization (for review, see Südhof, 2012b, 2013). Their function in the ribbon synapse is less clear. RIM2 appears to be localized at the base of the synaptic ribbon and RIM1 at the body of the synaptic ribbon (tom Dieck et al., 2005). RIM proteins interact with Munc13 proteins in conventional synapses to mediate vesicle priming (Deng et al., 2011). While in conventional synapses, RIMs interact with Munc13-1; Munc13-1 is missing in photoreceptor synapses (Schmitz et al., 2001; Cooper et al., 2012). Instead of Munc13-1, ubMunc13-2 is expressed in photoreceptor synapses (Cooper et al., 2012). Other active zone proteins [e.g., CAST/ELKS; RIM-binding proteins (RIM-BPs)] are also present at photoreceptor ribbon synapses partly differentially distributed in distinct sub-compartments of the synapse (for review, see tom Dieck and Brandstätter, 2006; Mercer and Thoreson, 2011; Schmitz et al., 2012).

SYNAPTIC RIBBONS: FUNCTIONAL CONSIDERATIONS

The synaptic ribbon is the most prominent structural feature of photoreceptor ribbon synapses. The function of the synaptic ribbon is still unclear. The synaptic vesicles attached to the synaptic ribbon have been functionally correlated to different synaptic vesicle pools (for review, see Heidelberger et al., 2005; Matthews and Fuchs, 2010; Mercer and Thoreson, 2011). Total internal reflection fluorescence (TIRF) microscopy studies of individual synaptic vesicles demonstrated that the base of the ribbon is a hotspot of synaptic vesicle exocytosis (Zenisek et al., 2000; Chen et al., 2013). The basal row of synaptic vesicles attached to the synaptic ribbon represents the vesicle pool that can be immediately released (the "RRP," readily releasable pool). Therefore, one role of the ribbon might be to position this basal row of synaptic vesicles in a "strike-distance" for SNARE proteins to rapidly execute Ca^{2+}-triggered exocytosis (Zenisek et al., 2000). The synaptic ribbon seems to be needed for both fast, synchronous release as well as for slow, asynchronous release components (Khimich et al., 2005; Zenisek, 2008; Frank et al., 2010 Snellman et al., 2011).

Exocytosis was frequently observed at ribbon-containing sites if exocytosis was induced by mild stimuli, e.g., weak depolarizations (Chen et al., 2013). If longer depolarizations were applied, exocytosis also occurred at non-ribbon-containing sites, i.e., in some distance from the presynaptic Ca^{2+}-channels (Midorikawa et al., 2007; Zenisek, 2008; Chen et al., 2013). Exocytosis of synaptic vesicles at these non-ribbon-containing sites could contribute to the asynchronous release component (Midorikawa et al., 2007; Zenisek, 2008).

The large dimensions of the synaptic ribbon allow many vesicles to be docked at the base of the synaptic ribbon (Matthews and Fuchs, 2010; Mercer and Thoreson, 2011; Schmitz et al., 2012). This is quite likely necessary to support coordinated multivesicular vesicle fusion at the synaptic ribbon (Glowatzki and Fuchs, 2002; Singer et al., 2004; Khimich et al., 2005; Graydon et al., 2011). The synaptic vesicles attached to the synaptic ribbon in a more distant position (also denoted as "tethered vesicles"; Heidelberger et al., 2005; Matthews and Fuchs, 2010; Mercer and Thoreson, 2011) could contribute to the synaptic vesicle pool that is released with a slower kinetics, the slowly releasable pool ("SRP"). The tethered synaptic vesicles could possibly move down toward the base of the synaptic ribbon before they finally fuse at the active zone ("conveyor belt" hypothesis of the synaptic ribbon; Lenzi and von Gersdorff, 2001; Parsons and Sterling, 2003).

Recently, it was shown that the synaptic ribbon has also an important role in the replenishment of synaptic vesicles (Jackman et al., 2009; Snellman et al., 2011; Chen et al., 2013; see also below). Regulation of synaptic vesicle replenishment could be a major function of synaptic ribbons (Jackman et al., 2009; Chen et al., 2013). It was shown that tonic release at the photoreceptor ribbon synapse leads to vesicle depletion at the base of the ribbon. Based on that suggestion, the ribbon would work as a capacitor for synaptic vesicles that reloads the empty release sites at the base of the synaptic ribbon (Jackman et al., 2009; Snellman et al., 2011; Chen et al., 2013). The ribbon capacitor will be re-charged with synaptic vesicles in the light phase when vesicle exocytosis is low. This recharged ribbon capacitor will provide release-ready vesicles in the dark when the photoreceptor depolarizes (Jackman et al., 2009; Chen et al., 2013). According to this hypothesis, the rate of release is determined by the rate of vesicle replenishment at the synaptic ribbon. In agreement with this assumption, it was recently shown that major endocytic proteins were strongly enriched in the periactive zone around the synaptic ribbon (Wahl et al., 2013).

SYNAPTIC CODING AT RIBBON SYNAPSES IN COMPARISON TO CODING IN CONVENTIONAL SYNAPSES

Synaptic coding in ribbon synapses differs from coding in conventional synapses. Conventional synapses are typically phasic synapses that initiate synaptic vesicle exocytosis only when a stimulus, usually an action potential, reaches the presynaptic terminal. The depolarization of the presynaptic terminal opens VGCC, typically P-/Q-/N-type calcium channels in phasic synapses (for review, see Catterall et al., 2005; Striessnig et al., 2010; Catterall, 2011; Südhof, 2012a,b, 2013). The subsequent Ca^{2+}-influx initiates synaptic vesicle fusion at the active zone (for review, see Südhof, 2012a,b, 2013). In contrast, ribbon synapses are tonically active synapses that continuously fuse synaptic vesicles with the presynaptic plasma membrane. The basal rate of synaptic vesicle exocytosis is modulated in response to graded changes of the membrane potential. In photoreceptors, exocytosis is high in the dark when the photoreceptor is depolarized. The rate of exocytosis is diminished in the light when the photoreceptor hyperpolarizes (Jackman et al., 2009). Synaptic vesicle exocytosis at ribbon synapses is also initiated by influx of Ca^{2+} through VGCC. But ribbon synapses typically use other Ca^{2+}-channels than phasic synapses (see below). As mentioned above, exocytosis of synaptic vesicles preferentially occurs at the base of the synaptic ribbon (Zenisek et al., 2000; Chen et al., 2013). Ribbon synapses can fuse several hundreds of synaptic vesicles per second and ribbon (Heidelberger et al., 2005; Schmitz, 2009). Rod photoreceptors maintain continuous exocytosis at physiological membrane potentials indicating a high vesicle release probability in ribbon synapses (Jackman et al., 2009; Chen et al., 2013). How this is achieved is not clear but could be based on a high Ca^{2+}-sensitivity of the release machinery and/or an

efficient coupling of the release machinery to the presynaptic L-type Ca^{2+}-channels (see below). In contrast, release probability in conventional, phasic synapses is typically much lower than in ribbon synapses (for review, see Nicoll and Schmitz, 2005; Rusakov, 2006; Fioravante and Regehr, 2011; Regehr, 2012).

At the single vesicle level, using TIRF microscopy it was shown that synaptic vesicles did not fuse immediately after they appeared at the plasma membrane but paused at the base of the ribbon for about 60 ms before fusion finally occurred (Zenisek et al., 2000; Chen et al., 2013). Sixty-millisecond is a relatively long time delay and indicates that the speed of single vesicle exocytosis cannot be the main determinant for synaptic coding and its temporal fidelity at ribbon synapses.

The retrieval of synaptic vesicles has been recently appreciated as an important aspect of signaling at ribbon synapses (see also above). Continuous exocytosis in photoreceptor ribbon synapses caused depletion of synaptic vesicles at the base of the synaptic ribbon at physiological membrane potentials (Jackman et al., 2009; Chen et al., 2013). This depletion of presynaptic release sites during tonic exocytosis at physiological membrane potentials suggested that synaptic vesicle replenishment is rate-limiting for exocytosis and an important aspect for signaling at ribbon synapses (Jackman et al., 2009; Chen et al., 2013). The rate of vesicle replenishment would thus determine how smooth exocytosis could proceed. Gaps in continuous synaptic vesicle exocytosis at the ribbon synapse, e.g., as a result of insufficient vesicle replenishment, could contribute important signaling informations.

Despite the large physiological differences between ribbon synapses and conventional synapses, these synapses do not differ strongly in the composition of the exocytotic machinery (for review, see Schmitz, 2009; Matthews and Fuchs, 2010; Mercer and Thoreson, 2011; Schmitz et al., 2012). In photoreceptor ribbon synapses, syntaxin 1 is replaced by syntaxin 3b (Curtis et al., 2008, 2010); complexin 1/2 by complexin 3/4 (Reim et al., 2005, 2009); Munc13-1 by ubMunc13-2 (Schmitz et al., 2001; Cooper et al., 2012); piccolo by piccolino (Regus-Leidig et al., 2013). But the key players of exocytosis are remarkably conserved.

It should be mentioned that ribbon synapses are not a uniform population of synapses but display both structural and functional differences (Heidelberger et al., 2005; Moser et al., 2006; Matthews and Fuchs, 2010; Mercer and Thoreson, 2011). Exocytosis in ribbon synapses of hair cells in the inner ear operates in a fundamentally different manner and appears to function without neuronal SNARE proteins (Nouvian et al., 2011).

DEVELOPMENT OF THE SYNAPTIC RIBBON COMPLEX

Photoreceptor ribbon synapses of the mouse retina develop postnatally (Olney, 1968; Blanks et al., 1974). The assembly of the synaptic ribbon complex in photoreceptors occurs via distinct steps. Starting around postnatal day 4 (P4) small, spherical ribbon precursors are anchored at the arciform density of the photoreceptor active zone as judged by electron microscopy and immunofluorescence microscopy with antibodies against RIBEYE (Olney, 1968; Hermes et al., 1992; Regus-Leidig et al., 2010a,b; Liu et al., 2013; Zabouri and Haverkamp, 2013). Starting around P10 and proceeding with the time of eye opening, the immature, short spherical ribbons develop into the mature form of the synaptic ribbon which is bar-shaped in cross sections and plate-shaped in three-dimensional representations (**Figures 3C,F**; Hermes et al., 1992; Vollrath and Spiwoks-Becker, 1996; Adly et al., 1999; Schmitz et al., 2006; Regus-Leidig et al., 2010a,b; Liu et al., 2013).

Recent studies demonstrated that VGCC have a key role for the developmental organization of the presynaptic cytoskeleton including the synaptic ribbons.

SYNAPTIC RIBBONS AND VOLTAGE-GATED Ca^{2+} CHANNELS

L-type VGCC are clustered at the basal end of the synaptic ribbon (Heidelberger et al., 2005; Doering et al., 2007; Striessnig et al., 2010; Mercer and Thoreson, 2011; Mercer et al., 2011a; Schmitz et al., 2012). The site is a hotspot of exocytosis (Zenisek et al., 2000). Entry of Ca^{2+} through L-type VGCC is essential for triggering exocytosis at the photoreceptor synapse (Dacheux and Miller, 1976; Schmitz and Witkovsky, 1997; Witkovsky et al., 1997; Heidelberger et al., 2005). The VGCC at the active zone of photoreceptors consists of a pore-forming transmembrane α1 subunit (Cav1.4, in photoreceptors; Cav1.3 in inner hair cells), an auxiliary β2-subunit and the α2δ4-subunit (Ball et al., 2002, 2011; Catterall et al., 2005; Morgans et al., 2005; Wycisk et al., 2006; Buraei and Yang, 2010; Striessnig et al., 2010; Catterall, 2011; Mercer et al., 2011a; Schmitz et al., 2012; Liu et al., 2013). Few Cav-channels at the base of the synaptic ribbons are sufficient to drive exocytosis (Brandt et al., 2005; Bartoletti et al., 2011). L-type VGCC in photoreceptors are well suited to support tonical exocytosis at ribbon synapses because these channels do not show Ca^{2+}-dependent inactivation (CDI) and little voltage-dependent inactivation (VDI; Singh et al., 2006; Striessnig et al., 2010; Catterall, 2011; Shaltiel et al., 2012). Furthermore, the Ca^{2+}-sensitivity of release is high and exocytosis is triggered by low, submicromolar Ca^{2+}-concentrations (Rieke and Schwartz, 1996; Thoreson et al., 2004; Heidelberger et al., 2005; Sheng et al., 2007; Choi et al., 2008; Jarsky et al., 2010). In addition to L-type channels, retinal bipolar cells also express transient, T-type VGCC (Pan et al., 2001; Ma and Pan, 2003; Hu et al., 2009).

In the development of the outer retina, Cav-channels associate early with synaptic ribbon precursors and synaptic ribbons (Liu et al., 2013; Zabouri and Haverkamp, 2013). Synaptic ribbons do not form properly, if the L-type calcium channels are missing, e.g., in Cav1.4 mouse knockout models (Mansergh et al., 2005; Chang et al., 2006; Raven et al., 2007; Lodha et al., 2010). In the different available Cav1.4 mouse knockout models, the Cav1.4-channel was shown to exert a strong, severe influence on synaptic ribbon localization and assembly. Some quantitative differences were observed in the different available Cav1.4 mouse knockout models (Mansergh et al., 2005; Chang et al., 2006; Raven et al., 2007; Lodha et al., 2010).

Two recent studies (Liu et al., 2013; Zabouri and Haverkamp, 2013) analyzed in detail the relevance of the Cav-channels for distinct steps of synaptic ribbon assembly at the active zone and for the subsequent maturation of the synaptic ribbon complex (Liu et al., 2013; Zabouri and Haverkamp, 2013). Initially, at early stages of development, immature ribbon precursors are clustered in the

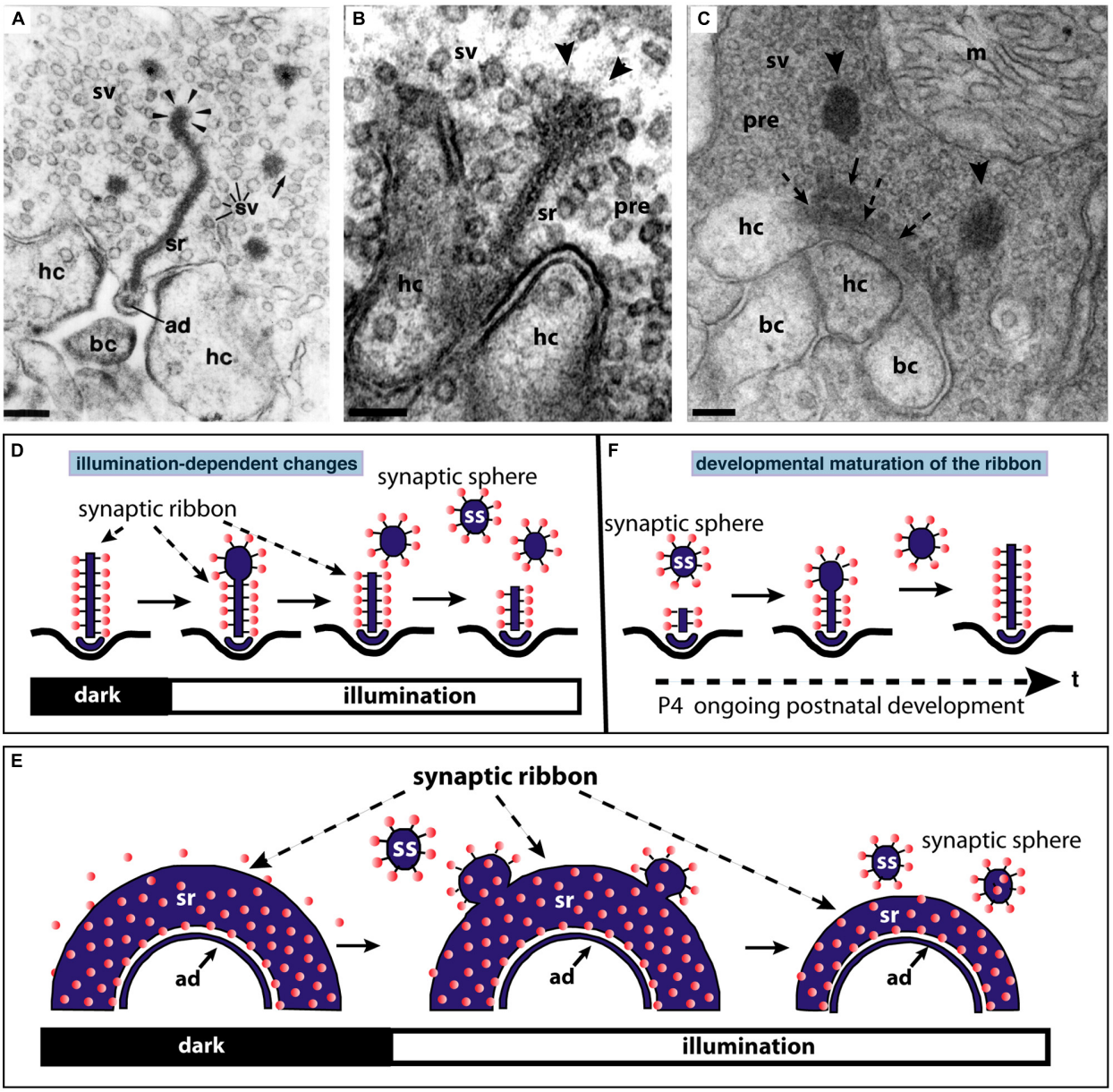

FIGURE 3 | The synaptic ribbon is a dynamic structure, both in the mature retina (A,B,D,E) as well as in the immature retina during early postnatal retinal development (C,F). Panels **(A,B)** show disassemblying synaptic ribbons in the mature retina. The mature, bar-shaped synaptic ribbon disassembles via spherical structures, the synaptic spheres (arrowheads in **A,B**). Disassembly into synaptic spheres occurs at the cytosolic, non-plasma membrane-anchored end of the synaptic ribbon (arrowheads in **A,B**). At this end, the synaptic ribbon appears enlarged before the spherical synaptic spheres detach from it **(A,B)**. The spherical synaptic ribbons are still associated with synaptic vesicles via thin connections. But they are no longer anchored to the presynaptic plasma membrane. Panel **(A)** is modified from Schmitz and Drenckhahn (1993) with permission from Springer-Verlag, Berlin, Heidelberg, Germany. **(C)** Assembly of the mature, bar-shaped synaptic ribbon during postnatal development. The arciform density (ad) is clearly visible at the active zone (dashed arrowheads in **C**). In the synapse shown in **(C)**, the assembly of the synaptic ribbon just started. A small piece of the ribbon is already assembled (small black arrow in **C**) and anchored at the arciform density. Most of the ribbon is still present as immature synaptic spheres (arrowheads) located in vicinity to the small anchored ribbon primer (arrow in **C**). Later in development, the spherical synaptic ribbons (arrowheads) coalesce with the anchored ribbon primer (small black arrow in **C**) to form the mature, bar-shaped synaptic ribbon. RIBEYE–RIBEYE interactions might mediate this process. Panel **(C)** is taken from Schmitz et al. (2006) with permission from PNAS (copyright (2006) National Academy of Sciences, USA). Panels **(D,E)** schematically depict the illumination-induced disassembly of the synaptic ribbon (see also **A,B**). Panel **(F)** summarizes the possible sequence of synaptic ribbon assembly that occurs during postnatal development. sr, synaptic ribbon; ss, synaptic sphere; pre, presynaptic, sv, synaptic vesicle; bc, bipolar cell dendritic tip; hc, horizontal cell dendritic tip; m, mitochondrium; P4, postnatal day 4. Arrowheads in **(A,B)** point to synaptic spheres forming at the distal, non-membrane-anchored end of the synaptic ribbon. Dashed arrows in **(C)** point to the arciform density, which is the presynaptic density in ribbon synapses. The spheres colored in red in **(D–F)** represent synaptic vesicles. Panels **(D–F)** were re-drawn based on figures by Adly et al. (1999) and Spiwoks-Becker et al. (2004). Scale bars: 100 nm **(A–C)**.

terminal and probably anchored to the active zone (Zabouri and Haverkamp, 2013) even if the Cav-channels are missing. But – in contrast to the wildtype – these immature ribbon precursors are not aligned and thus functionally linked with postsynaptic glutamate receptors in the Cav1.4 knockout (Liu et al., 2013). Furthermore, without proper channel activity, these immature ribbon precursors do not mature into the bar-shaped synaptic ribbons but remain immature (Liu et al., 2013; Zabouri and Haverkamp, 2013). Interestingly, normal physiological activity of the Cav-channel is needed to transform immature ribbons into mature ribbons. Both loss-of-function mutants as well as gain-of-function mutants (Knoflach et al., 2013; Liu et al., 2013) of the Cav-channels prevented proper maturation of the synaptic ribbon complex (Liu et al., 2013).

Similarly, also knockout models of various proteins linked to the Cav1.4-channel (i.e., β2-subunit of Cav1.4 channels, CaBP4, bassoon, and laminin β2 (for review, see Nishimune, 2012) displayed absent, smaller or non-attached "floating" synaptic ribbons (Libby et al., 1999; Ball et al., 2002; Dick et al., 2003; Haeseleer et al., 2004; Nishimune et al., 2004; Nishimune, 2012). In agreement with these findings, voltage-gated Cav-channels in the inner ear were shown to regulate synaptic ribbon size (Frank et al., 2009, 2010; Sheets et al., 2011, 2012).

Zabouri and Haverkamp (2013) demonstrated that Cav-channels are not only important for the proper development of the synaptic ribbon complex but also for the development of the presynaptic cytoskeleton in photoreceptors. Deletion of Cav1.4 lead to misassembly of many components of the presynaptic photoreceptor cytoskeleton including PSD95, the plasma membrane Ca^{2+}-ATPase (PMCA), Veli3, β-dystroglycan, bassoon, and RIM2. As consequence, the architecture of the synaptic terminal was profoundly altered.

These data argue that the Cav1.4 channel in photoreceptors is a central organizer of the photoreceptor ribbon synapse active zone in general and for the synaptic ribbon complex in particular. Several molecules are candidates that could provide a link between synaptic ribbons and voltage-gated Cav1.4 calcium channels. The RIM multi-domain family of proteins are essential components of the active zones in conventional and ribbon synapses (Wang et al., 1997; Südhof, 2013). In conventional active zones, they are found at presynaptic densities; in ribbon synapses both at the active zone (arciform densities; RIM2; tom Dieck et al., 2005) and also at the proper synaptic ribbon (RIM1, tom Dieck et al., 2005). RIMs are important for various central aspects of synapse function (Deng et al., 2011; Han et al., 2011; Kaeser et al., 2011; for review, see Südhof, 2013). RIM proteins are crucial for anchoring P/Q/N-type VGCC at the active zone in conventional synapses via a direct PDZ-domain interaction (Deng et al., 2011; Han et al., 2011; Kaeser et al., 2011; for review, see Südhof, 2013). RIMs indirectly interact with L-type Ca^{2+}-channels via RIM-BPs (Hibino et al., 2002). Besides immobilizing VGCC, RIMs are essential for vesicle priming via interaction with Munc13 and for synaptic vesicle docking via interaction with rab3/rab27 (Deng et al., 2011; Han et al., 2011; Kaeser et al., 2011; for review, see Südhof, 2013).

RIM1 has also been reported to be associated with the β-subunits (β4, β2a) of VGCC (Kiyonaka et al., 2007; Miki et al., 2007). This interaction was suggested to suppress inactivation of VGCC (Kiyonaka et al., 2007; Miki et al., 2007). Interestingly, a point mutation in the C2A-domain of RIM1 is responsible for a cone rod-dystrophy (CORD7; Johnson et al., 2003). CAST/ELKS proteins that are also present at the synaptic ribbon complex have been recently reported to be also associated with β-subunits of VGCC (Chen et al., 2011; Kiyonaka et al., 2012). Similarly, bassoon has been described to be associated with β-subunits of VGCC (Chen et al., 2011; Nishimune et al., 2012). The binding of bassoon to β-subunits of VGCC is compatible with the finding that the organization of VGCC was disturbed in inner ear ribbon synapses of bassoon-deficient mice (Frank et al., 2010). Thus, the active zone with the synaptic ribbons appears to be intimately associated with VGCC and organized by these channels by a multitude of different protein–protein interactions.

PRESYNAPTIC Ca^{2+}, GCAP2, AND SYNAPTIC RIBBON DYNAMICS

In the mature adult mouse retina, synaptic ribbons also underlie changes in size. These changes are illumination-dependent and appear to be regulated by Ca^{2+} (Vollrath and Spiwoks-Becker, 1996; Adly et al., 1999; Spiwoks-Becker et al., 2004; Schmitz, 2009; Regus-Leidig et al., 2010a). Several studies observed a light-induced reduction in the size of synaptic ribbons in the mouse retina (Adly et al., 1999; Spiwoks-Becker et al., 2004; Regus-Leidig et al., 2010a; Fuchs et al., 2013). The bar-shaped ribbons appear to disassemble (and re-assemble) from the free cytosolic, non-membrane-anchored end (**Figure 3**). From this end of the bar-shaped ribbon, spherical ribbons, the synaptic spheres, detach (**Figure 3**). Thus, this illumination-dependent growth and disassembly of the synaptic ribbon appears to employ similar intermediate structures as in development (**Figure 3C**). These spherical intermediates are similar in appearance as the spherical synaptic ribbons of hair cells in the inner ear (for review, see Moser et al., 2006). The synaptic spheres are still associated with numerous synaptic vesicles (**Figures 3A–C**). Spherical ribbons were added to remaining ribbons during darkness (Spiwoks-Becker et al., 2004; Regus-Leidig et al., 2010a).

The light-induced reduction of synaptic ribbon size could be mimicked by lowering intracellular Ca^{2+} (Adly et al., 1999; Spiwoks-Becker et al., 2004) suggesting that Ca^{2+} is an important factor that regulates ribbon size. In fact, while lowering intracellular Ca^{2+} lead to a reduction of synaptic ribbon size, increases of intracellular Ca^{2+} resulted in increased ribbon sizes (Spiwoks-Becker et al., 2004; Regus-Leidig et al., 2010a). The genetic background of animals also influences synaptic ribbon dynamics. Synaptic ribbon size plasticity has been reported to be stronger in albinotic mice than in pigmented mice (Fuchs et al., 2013).

Mechanisms of assembly and disassembly of synaptic ribbons in the mature retina are still largely unknown. The NCS protein GCAP2 is involved in the Ca^{2+}-dependent disassembly of synaptic ribbons (Venkatesan et al., 2010; López-del Hoyo et al., 2012). RIBEYE, the main component of synaptic ribbons, binds the NCS protein GCAP2 (Venkatesan et al., 2010). GCAP2 is the only known Ca^{2+}-binding protein of synaptic ribbons. Interaction between RIBEYE and GCAP2 occurs via the B-domain of RIBEYE and the C-terminal region (CTR) of GCAP2

(Venkatesan et al., 2010; for review, see Schmitz et al., 2012). The CTR of GCAP2 is divergent in sequence between GCAP1 and GCAP2. In agreement, GCAP1 does not bind to RIBEYE while GCAP2 does (Venkatesan et al., 2010). Recent ultrastructural analyses, using postembedding immunogold electron microscopy demonstrated that GCAP2 is a component of synaptic ribbons that is directly localized at the synaptic ribbon body (López-del Hoyo et al., 2012). Viral overexpression of GCAP2 in organotypical retina cultures leads to a disassembly of synaptic ribbons (Venkatesan et al., 2010). Similarly, in GCAP2 – overexpressing transgenic mice, synaptic ribbons also tend to disassemble more easily than in the wildtype retinas (López-del Hoyo et al., 2012) although the synaptic ribbon complex as such is normally formed in GCAP2 knockout mice.

Low intracellular Ca^{2+}-concentrations lead to dimerization and also to conformational changes in the CTR of GCAP2 (Olshevskaya et al., 1999; Peshenko et al., 2004). In particular, low intracellular Ca^{2+} leads to exposure of the CTR of GCAP2 (Peshenko et al., 2004). In the Ca^{2+}-free form of GCAP2, the CTR is exposed while in the Ca^{2+}-bound state it is not (or much less; Peshenko et al., 2004). Therefore, RIBEYE–GCAP2 interaction is most likely favored by conditions of low intracellular Ca^{2+}, e.g., at illumination. Furthermore, while RIBEYE–GCAP2 interaction is promoted by NAD(H) (Venkatesan et al., 2010), NADH destabilizes the RIBEYE–RIBEYE interaction network (i.e., RE(A)-RE(B) interaction ; Magupalli et al., 2008) which would lead to an overall tendency of reduced RIBEYE–RIBEYE interaction. By this mechanism, depletion of Ca^{2+} from GCAP2 could contribute to the disassembly of synaptic ribbons in photoreceptor synapses. By this way of thinking, GCAP2 binding to the synaptic ribbon could thus be involved in the regulation of the Ca^{2+}-dependent dynamics of synaptic ribbons.

The conformational change of GCAP2 induced by low Ca^{2+} could thus lead to a severing and subsequent disassembly of the ribbon body into spherical structures, the synaptic spheres (**Figure 4**). The immunogold electron microscopic studies by López-del Hoyo et al. (2012) showed that GCAP2 is not homogeneously distributed along the entire ribbon body (as is RIBEYE; Schmitz et al., 2000), but is clustered at hotspots at the synaptic ribbon surface. These hot spots of GCAP2 immunoreactivity on the synaptic ribbon could represent sites of ribbon disassembly (**Figure 4**).

INTRACELLULAR MODULATION OF Ca^{2+}-SIGNALS IN PHOTORECEPTOR TERMINALS

Ca^{2+} signals generated by influx through VGCC are modulated by various intracellular mechanisms that can subsequently increase or decrease cytosolic Ca^{2+}-concentration. The final Ca^{2+}-signal in the presynaptic terminal is shaped by the temporal and spatial interactions of these mechanisms (Krizaj and Copenhagen, 2002; Szikra and Krizaj, 2006).

The smooth endoplasmic reticulum (ER) is a main intracellular Ca^{2+}-source (Parekh, 2011) and located close to the synaptic ribbon in photoreceptor ribbon synapses as judged by immunolabeling with antibodies against ER components, e.g., the sarco(endo)plasmic reticulum Ca^{2+}-ATPase (SERCA)-2 protein (Johnson et al., 2007; Babai et al., 2010). Ca^{2+}-induced Ca^{2+}-release (CICR) from the ER can amplify Ca^{2+}-signals and enhance signal transmission (Krizaj et al., 1999; Krizaj, 2003; Cadetti et al., 2006; Suryanarayanan and Slaughter, 2006; Szikra and Krizaj, 2007; Szikra et al., 2008, 2009; Babai et al., 2010). Several studies showed that CICR contributes to tonic release at the photoreceptor synapse (Krizaj et al., 1999; Cadetti et al., 2006; Suryanarayanan and Slaughter, 2006; Babai et al., 2010). Both classes of ER-localized receptors responsible for mobilization of Ca^{2+} from the ER, i.e., ryanodine receptors (RyR) and IP3 receptors (IP3R) have been localized to photoreceptor terminals (Peng et al., 1991; Krizaj et al., 1999; Krizaj, 2003). CICR can also activate Ca^{2+}-activated Cl^--channels at the presynaptic plasma membrane. TMEM16B-type of Ca^{2+}-activated Cl^--channels have been localized to the photoreceptor terminal (Lalonde et al., 2009; Stöhr et al., 2009; Mercer et al., 2011b). Activation of Ca^{2+}-activated Cl^--channels in photoreceptor terminals should lead to depolarization because the membrane potential of about ≈–40 mV at darkness is more negative than the Cl^--equilibrium potential of −20 mV in rod photoreceptor synapses (Thoreson et al., 2002; Babai et al., 2010).

If intracellular Ca^{2+}-stores are exhausted, store-operated calcium entry (SOCE) mechanisms can replenish them (for review, see Parekh and Putney, 2005; Lewis, 2011; Soboloff et al., 2012; Gudlur et al., 2013). The ER-localized EF-hand-containing Ca^{2+}-sensor protein STIM activates Ca^{2+}-selective, plasma membrane located Ca^{2+}-release-activated Ca^{2+} (CRAC)-channels in case of store-depletion. CRAC channels contain Orai-proteins as major components that allow Ca^{2+} influx through the plasma membrane and subsequent Ca^{2+} replenishment of the emptied ER store (Lewis, 2011; Soboloff et al., 2012; Gudlur et al., 2013). TRPC1 proteins also contribute to CRAC channel activity (Szikra et al., 2009; Molnar et al., 2012). Silencing of TRPC1 by RNA interference abolished SOCE in rods but not in cones indicating that TRPC1 could be an important component of SOCE in rods (Szikra et al., 2008). STIM1 proteins have been recently localized to the photoreceptor terminal (Szikra et al., 2009). The SERCA2 ATPase (see below) has been suggested to be the "third element" of SOCE that mediates influx of Ca^{2+} into the ER after it has entered the cytosol via the CRAC channels (Manjarrés et al., 2010, 2011; Alonso et al., 2012). Store-operated Ca^{2+}-channels could contribute to sustained Ca^{2+} signals and extend the dynamic range of signaling in the tonically active photoreceptor ribbon synapse.

The PMCAs represent a family of transmembrane proteins (Carafoli, 1999; Tempel and Shilling, 2007) that extrudes Ca^{2+} from the cytosol into the extracellular space in an ATP-dependent manner (Carafoli, 1999; Tempel and Shilling, 2007). The PMCA is immobilized in the plasma membrane of the presynaptic terminal that is scaffolded by PSD95, MPP4, and VELI3 (Aartsen et al., 2006, 2009; Yang et al., 2007; Förster et al., 2009). Proper localization of PMCA in the presynaptic plasma membrane also depends on VGCC (Xing et al., 2012). The PMCA has a strong influence on presynaptic Ca^{2+}-signaling (Duncan et al., 2006; Szikra and Krizaj, 2006) and also on synaptic ribbon length dynamics (Yang et al., 2007; Aartsen et al., 2009). Deletion of the MPP4 gene leads to a loss of PMCA from the plasma membrane of the presynaptic photoreceptor terminals (Yang et al., 2007;

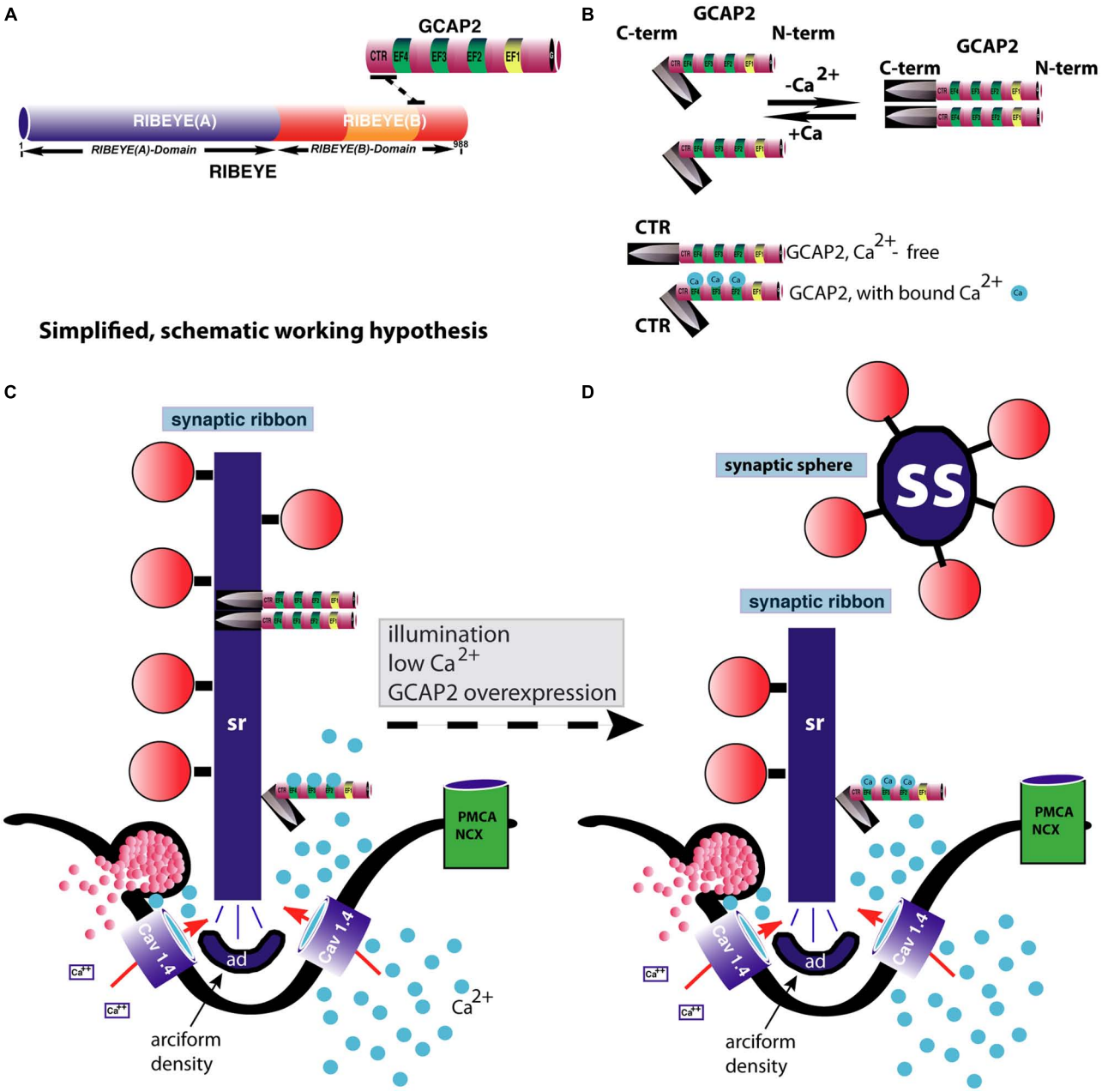

FIGURE 4 | GCAP2-mediated disassembly of the synaptic ribbon. (A) Previous studies have shown that GCAP2 interacts with RIBEYE, the main component of synaptic ribbons (Venkatesan et al., 2010). The drawing in **(A)** schematically summarizes the interaction between GCAP2 and RIBEYE. The C-terminal region (CTR) of GCAP2 interacts with the hinge region of RIBEYE(B)-domain that connects the NAD(H)-binding sub-domain with the substrate-binding sub-domain of RIBEYE (Venkatesan et al., 2010; Schmitz et al., 2012). This interaction is promoted by NAD(H). **(B)** GCAP2 performs a Ca^{2+}-dependent conformational change of its C-terminal region (CTR). In the Ca^{2+}-free form, the CTR is exposed, whereas in its Ca^{2+}-bound form it is less exposed (Peshenko et al., 2004). In addition, GCAP2 dimerizes at low Ca^{2+} (Olshevskaya et al., 1999). The CTR is responsible for the binding to RIBEYE (Venkatesan et al., 2010). **(C,D)** Binding of GCAP2 to RIBEYE of synaptic ribbons might lead to severing of the synaptic ribbon via exposure of the CTR. Exposure of the CTR occurs if Ca^{2+} is low, e.g., at illumination or if intracellular Ca^{2+} is buffered away by chelators. As a consequence, ribbons are getting shorter. Spherical ribbons, synaptic spheres, dissociate from the free cytosolic end of the synaptic ribbon. While NAD(H) favors binding of GCAP2 to RIBEYE, it weakens RIBEYE–RIBEYE interactions which might ease disassembly of the synaptic ribbon (Magupalli et al., 2008). For sake of clarity, intracellular membrane system, e.g., ER, and mitochondria which could influence intracellular Ca^{2+}-levels were omitted in the schematic drawing. These compartments can be expected to further shape the Ca^{2+}-signal in the presynaptic terminal. PMCA and NCX-proteins are schematically depicted. The C-terminus (CTR) of GCAP2 that interacts with RIBEYE and which is exposed particularly in the Ca^{2+}-free form of GCAP2 is schematically depicted as a knife-like structure because it is proposed to severe the synaptic ribbon structure. The spheres colored in blue in **(B–D)** represent Ca^{2+}-ions. sr, synaptic ribbon; ss, synaptic sphere; CTR, C-terminal region of GCAP2; PMCA, plasma membrane Ca^{2+}-ATPases; NCX, Na^{+}/Ca^{2+}-exchanger; ad, arciform density (i.e., the presynaptic density of photoreceptor ribbon synapses); EF, EF-hand.

Aartsen et al., 2009). The subsequent loss of extrusion activity leads to increased intracellular Ca^{2+} and enlarged synaptic ribbons (Yang et al., 2007; Aartsen et al., 2009). Na^{+}/Ca^{2+} exchangers (NCXs) extrude Ca^{2+} from the cytosol into the extracellular space under physiological conditions (Lytton, 2007). NCX proteins are closely localized to the synaptic ribbon and thus can be expected to strongly influence synaptic transmission and ribbon dynamics (Duncan et al., 2006; Johnson et al., 2007). PMCA appears to be predominantly expressed in rod spherules; NCX is predominantly expressed in cone pedicles (Johnson et al., 2007). The SERCA can lower intracellular Ca^{2+} by pumping Ca^{2+} from the cytosol into the ER (Bublitz et al., 2013). In photoreceptor synapses, the SERCA pump has been localized in close proximity to the synaptic ribbon (Yang et al., 2007; Babai et al., 2010). The described Ca^{2+}-extruding systems are important to restore resting levels of Ca^{2+} after depolarization-induced increases (Duncan et al., 2006; Szikra and Krizaj, 2006; Johnson et al., 2007; Mercer and Thoreson, 2011; Wan et al., 2012; Bublitz et al., 2013). Photoreceptor terminals often contain also mitochondria in proximity to the synaptic ribbon (Johnson et al., 2007). Mitochondria have been suggested to be able to take up large amounts of Ca^{2+} (Rizzuto et al., 2004; Parekh and Putney, 2005; Rizzuto and Pozzan, 2006). In ribbon terminals, Ca^{2+}-uptake by mitochondria was found to be only functionally relevant if the Ca^{2+}-load was particularly high (Zenisek and Matthews, 2000).

THE SYNAPTIC RIBBON SIZE IN PHOTORECEPTOR SYNAPSES: A PROXY FOR PRESYNAPTIC Ca^{2+}-CONCENTRATION?

As summarized above, there are multiple links between Cav-channels, presynaptic Ca^{2+}-levels, synaptic signaling and the synaptic ribbons. Ca^{2+}-flux through VGCC as well as the subsequent cross-talk to other Ca^{2+}-regulating systems in the presynaptic terminal affect structural plasticity and developmental maturation of the synaptic ribbon in photoreceptor synapses. In the light, when Ca^{2+} is low in presynaptic photoreceptor terminals (Thoreson et al., 2004; Choi et al., 2005, 2008; Sheng et al., 2007; Jackman et al., 2009), synaptic ribbons appear to be smaller than in the dark (Adly et al., 1999; Balkema et al., 2001; Spiwoks-Becker et al., 2004; Hull et al., 2006; Regus-Leidig et al., 2010a). Similarly, in knockout mouse models in which extrusion of Ca^{2+} is disturbed and presynaptic Ca^{2+} increased, synaptic ribbons were longer than in control animals (Yang et al., 2007; Aartsen et al., 2009). On the other hand, in mouse knockout models where Cav-channels were deleted, synaptic ribbons were smaller and did not develop into mature, large synaptic ribbons. Therefore, the size of the synaptic ribbon could appear as a readout of presynaptic Ca^{2+}. A recent publication (Liu et al., 2013) indicated, that the Ca^{2+}-mediated dynamics of synaptic ribbons – at least in development – is more complex. Also gain-of-function mutations of the Cav1.4 channel, which lead to an activation of the Cav1.4 channel already at more negative membrane potentials, displayed shorter than normal synaptic ribbons (Liu et al., 2013). Future investigation need to provide a more detailed picture about the assembly and disassembly of the synaptic ribbon, its regulation and its consequences for signaling at the photoreceptor synapse.

SUMMARY AND OUTLOOK

Biochemical and molecular analyses identified the protein composition of synaptic ribbons to a large extent. Surprisingly, most of the ribbon proteins are not only present in ribbon synapses but also in conventional synapses. RIBEYE is the only major building block unique to synaptic ribbons. Still, many questions concerning the structure, assembly, and function of synaptic ribbons remain to be elucidated. How is the assembly of synaptic ribbons regulated? How do immature ribbons develop into mature ribbons? How does Ca^{2+} exerts its influence on synaptic ribbons? Does Ca^{2+}-dependent phosphorylation of ribbon proteins play a role? Why are there so many links between presynaptic Ca^{2+}-channels and synaptic ribbons? How can very few ribbon synapse-specific components build such a fundamentally different synapse? How are the synaptic ribbon components mechanistically linked to the proposed functions of synaptic ribbons? The application of innovative physiological tools and the analysis of mouse knockout models are needed to answer these questions.

ACKNOWLEDGMENTS

Work of the author was supported by research grants from the German Research Community (DFG) SFB894, GRK1326 and by the Human Frontiers Science Organization HFSP. Thanks to Dr. Jutta Schmitz-Kraemer and Prof. Dr. Doris M. Kraemer (University of Oldenburg) for critically reading the manuscript. The author apologizes that not all relevant original papers could be cited due to limitations in space.

REFERENCES

Aartsen, W. M., Arsanto, J. P., Chauvin, J. P., Vos, R. M., Versteeg, I., Cardozo, B. N., et al. (2009). PSD95b regulates plasma membrane Ca(2+) pump localization at the photoreceptor synapse. *Mol. Cell. Neurosci.* 41, 156–165. doi: 10.1016/j.mcn.2009.02.003

Aartsen, W. M., Kantardzhieva, A., Klooster, J., van Rossum, A. G., van de Pavert, S. A., Versteeg, I., et al. (2006). MPP4 recruits PSD95 and veli3 towards the photoreceptor synapse. *Hum. Mol. Genet.* 15, 1291–1302. doi: 10.1093/hmg/ddl047

Abramov, I., and Gordon, J. (1994). Color appearance: on seeing red- or yellow, or green, or blue. *Annu. Rev. Psychol.* 45, 451–485. doi: 10.1146/annurev.ps.45.020194.002315

Adly, M., Spiwoks-Becker, I., and Vollrath, L. (1999). Ultrastructural changes of photoreceptor synaptic ribbons in relation to time of day and illumination. *Invest. Ophthalmol. Vis. Sci.* 40, 2165–2172.

Alonso, M. T., Manjarrés, I. M., and García-Sancho, J. (2012). Privileged coupling between Ca^{2+} entry through plasma membrane store-operated Ca^{2+} channels and the endoplasmic reticulum Ca^{2+}-pump. *Mol. Cell. Endocrinol.* 353, 37–44. doi: 10.1016/j.mce.2011.08.021

Alpadi, K., Magupalli, V. G., Käppel, S., Köblitz, L., Schwarz, K., Seigel, G. M., et al. (2008). RIBEYE recruits Munc119, the mammalian ortholog of the *Caenorhabditis elegans* protein unc119 to synaptic ribbons of photoreceptor synapses. *J. Biol. Chem.* 283, 26461–26467. doi: 10.1074/jbc.M801625200

Arshavsky, V. Y. (2002). Rhodopsin phosphorylation: from terminating single photon responses to photoreceptor adaptation. *Trends Neurosci.* 25, 124–126. doi: 10.1016/S0166-2236(00)02094-4

Artemyev, N. O. (2008). Light-dependent compartmentalization of transducin in rod photoreceptors. *Mol. Neurobiol.* 37, 44–51. doi: 10.1007/s12035-008-8015-2

Babai, N., Morgans, C. W., and Thoreson, W. B. (2010). Calcium-induced calcium release contributes to synaptic release from mouse rod photoreceptors. *Neuroscience* 165, 1447–1456. doi: 10.1016/j.neuroscience.2009.11.032

Baehr, W., and Palczewski, K. (2009). Focus on molecules: guanylate cyclase-activating proteins (GCAPs). *Exp. Eye Res.* 89, 2–3. doi: 10.1016/j.exer.2008.12.016

Balkema, G. W., Cusick, K., and Nguyen, T. H. (2001). Diurnal variation in synaptic ribbon length and visual threshold. *Vis. Neurosci.* 18, 789–792. doi: 10.1017/S0952523801185123

Ball, S. L., McEnery, M. W., Yunker, A. M., Shin, H. S., and Gregg, R. G. (2011). Distribution of voltage gated calcium channel β-subunits in the mouse retina. *Brain Res.* 1412, 1–8. doi: 10.1016/j.brainres.2011.07.033

Ball, S. L., Powers, P. A., Shin, H. S., Morgans, C. W., Peachey, N. S., and Gregg, R. G. (2002). Role of the β2 subunit of voltage-dependent calcium channels in the retinal outer plexiform layer. *Invest. Ophthalmol. Vis. Sci.* 43, 1595–1603.

Bartoletti, T. M., Jackman, S. L., Babai, N., Mercer, A. J., Kramer, R. H., and Thoreson, W. B. (2011). Release from the cone ribbon synapse under bright light conditions can be controlled by the opening of few $Ca(^{2+})$ channels. *J. Neurophysiol.* 106, 2922–2935. doi: 10.1152/jn.00634.2011

Blanks, J. C., Adinolfi, A. M., and Lolley, R. N. (1974). Synaptogenesis in the photoreceptor terminal of the mouse retina. *J. Comp. Neurol.* 156, 81–93. doi: 10.1002/cne.901560107

Bliss, T. V., and Collingridge, G. (1993). A synaptic model of memory: long-term potentiation in the hippocampus. *Nature* 361, 31–39. doi: 10.1038/361031a0

Brandt, A., Khimich, D., and Moser, T. (2005). Few Cav1.3 channels regulate the exocytosis of a synaptic vesicle at the hair cell ribbon synapse. *J. Neurosci.* 25, 11577–11585. doi: 10.1523/JNEUROSCI.3411-05.2005

Bublitz, M., Musgaard, M., Poulsen, H., Thogersen, L., Olesen, C., Schiott, B., et al. (2013). Ion pathways in the sarcoplasmic reticulum Ca^{2+} ATPase. *J. Biol. Chem.* 288, 10759–10765. doi: 10.1074/jbc.R112.436550

Buraei, Z., and Yang, Y. (2010). The β-subunit of Ca^{2+}-channels. *Physiol. Rev.* 90, 1461–1506. doi: 10.1152/physrev.00057.2009

Burgoyne, R. D. (2007). Neuronal calcium sensor proteins: generating diversity in neuronal Ca^{2+}-signalling. *Nat. Rev. Neurosci.* 8, 182–193. doi: 10.1038/nrn2093

Burns, M. E., and Baylor, D. E. (2001). Activation, deactivation, and adaptation in vertebrate photoreceptor cells. *Annu. Rev. Neurosci.* 24, 779–805. doi: 10.1146/annurev.neuro.24.1.779

Cadetti, L., Bryson, E. J., Ciccone, C. A., Rabl, K., and Thoreson, W. B. (2006). Calcium-induced calcium release in rod photoreceptors boosts synaptic transmission during maintained depolarization. *Eur. J. Neurosci.* 23, 2983–2990. doi: 10.1111/j.1460-9568.2006.04845.x

Carafoli, E. (1999). The plasma membrane calcium pump: structure, function and regulation. *Biochem. Soc. Trans.* 17, 808–810.

Catterall, W. A. (2011). Voltage-gated calcium channels. *Cold Spring Harb. Perspect. Biol.* 3, a003947. doi: 10.1101/cshperspect.a003947

Catterall, W. A., Leal, K., and Nanou, E. (2013). Calcium channels and short-term synaptic plasticity. *J. Biol. Chem.* 288, 10742–10749. doi: 10.1074/jbc.R112.411645

Catterall, W. A., Perez-Reyes, E., Snutch, T. P., and Striessnig, J. (2005). International union of pharmacology. XLVIII. Nomenclature and structure-function relationships of voltage-gated calcium channels. *Pharmacol. Rev.* 57, 411–425. doi: 10.1124/pr.57.4.5

Chang, B., Heckenlively, J. R., Bayley, P. R., Brecha, N. C., Davisson, M. C., Hawes, N. L., et al. (2006). The nob2 mouse, a null mutation in cacna1f: anatomical and functional abnormalities in the outer retina and their consequences on ganglion cells visual responses. *Vis. Neurosci.* 23, 11–24. doi: 10.1017/S095252380623102X

Chen, J., Billings, S. E., and Nishimune, H. (2011). Calcium channels link the muscle-derived synapse organizer laminin b2 to bassoon and CAST/ERC2 to organize presynaptic active zones. *J. Neurosci.* 31, 512–525. doi: 10.1523/JNEUROSCI.3771-10.2011

Chen, K. (2005). The vertebrate phototransduction cascade: amplification and termination mechanisms. *Rev. Physiol. Biochem. Pharmacol.* 154, 101–121.

Chen, M., van Hook, M., Zenisek, D., and Thoreson, W. B. (2013). Properties of ribbon and non-ribbon release from rod photoreceptors by visualizing individual synaptic vesicles. *J. Neurosci.* 33, 2071–2086. doi: 10.1523/JNEUROSCI.3426-12.2013

Chinnadurai, G. (2009). The transcriptional corepressor CtBP: a foe of multiple tumor suppressors. *Cancer Res.* 69, 731–734. doi: 10.1158/0008-5472.CAN-08-3349

Choi, S. Y., Borghuis, B. G., Rea, R., Levitan, E. S., Sterling, P., and Kramer, R. H. (2005). Encoding light intensity by the cone photoreceptor synapse. *Neuron* 48, 555–562. doi: 10.1016/j.neuron.2005.09.011

Choi, S. Y., Jackman, S., Thoreson, W. B., and Kramer, R. H. (2008). Light regulation of Ca^{2+} in the cone photoreceptor synaptic terminal. *Vis. Neurosci.* 25, 693–700. doi: 10.1017/S0952523808080814

Cooper, B., Hemmerlein, M., Ammermüller, J., Imig, C., Reim, K., Lipstein, N., et al. (2012). Munc13-independent vesicle priming at mouse photoreceptor ribbon synapses. *J. Neurosci.* 32, 8040–8052. doi: 10.1523/JNEUROSCI.4240-11.2012

Curtis, L., Datta, P., Liu, X., Bogdanova, N., Heidelberger, R., and Janz, R. (2010). Syntaxin3b is essential for the exocytosis of synaptic vesicles in ribbon synapses of the retina. *Neurosci.* 166, 832–841. doi: 10.1016/j.neuroscience.2009.12.075

Curtis, L. B., Doneske, B., Liu, X., Thaller, C., McNew, J. A., and Janz, R. (2008). Syntaxin3b is a t-SNARE specific for ribbon synapses of the retina. *J. Comp. Neurol.* 510, 550–559. doi: 10.1002/cne.21806

Dacheux, R. F., and Miller, R. F. (1976). Photoreceptor-bipolar cell transmission in the perfused retina eyecup of the mudpuppy. *Science* 191, 963–964. doi: 10.1126/science.175443

Deguchi-Tawarada, M., Inoue, E., Takao-Rikitsu, E., Inoue, M., Kitajima, I., Ohtsuka, T., et al. (2006). Active zone protein CAST is a component of conventional and ribbon synapses in the mouse retina. *J. Comp. Neurol.* 495, 480–496. doi: 10.1002/cne.20893

Dell'Orco, D., and Koch, K. W. (2010). Systems biochemistry approaches to vertebrate phototransduction: towards a molecular understanding of disease. *Biochem. Soc. Trans.* 38, 1275–1280. doi: 10.1042/BST0381275

Deng, L., Kaeser, P. S., Xu, W., and Südhof, T. C. (2011). RIM proteins activate vesicle priming by reversing autoinhibitory homodimerization of Munc13. *Neuron* 69, 317–331. doi: 10.1016/j.neuron.2011.01.005

De Vries, S. H. (2000). Bipolar cells use kainite and AMPA receptors to filter visual informations into separate channels. *Neuron* 28, 847–856. doi: 10.1016/S0896-6273(00)00158-6

De Vries, S. H., Li, W., and Saszik, S. (2006). Parallel processing in two transmitter microenvironments at the cone photoreceptor synapse. *Neuron* 50, 735–748. doi: 10.1016/j.neuron.2006.04.034

De Vries, S. H., and Schwartz, E. A. (1999). Kainate receptors mediate synaptic transmission between cones and "OFF" bipolar cells in a mammalian retina. *Nature* 397, 157–160. doi: 10.1038/16462

Dhingra, A., and Vardi, N. (2012). "mGlu receptors in the retina" – WIREs membrane transport and signaling. *Wiley Interdiscip. Rev. Membr. Transp. Signal.* 1, 641–653. doi: 10.1002/wmts.43

Dick, O., tom Dieck, S., Altrock, W. D., Ammermüller, J., Weiler, R., Garner, C. C., et al. (2003). The presynaptic active zone protein bassoon is essential for photoreceptor ribbon synapse formation in the retina. *Neuron* 37, 775–786. doi: 10.1016/S0896-6273(03)00086-2

Doering, C. J., Peloquin, J. B., and McRory, J. E. (2007). The CaV1.4 channel. *Channels* 1, 3–10. doi: 10.4161/chan.3938

Duncan, J. L., Yang, H., Doan, T., Silverstein, R. S., Murphy, G. J., Nune, G., et al. (2006). Scotopic visual signalling in the mouse retina is modulated by high-affinity plasma membrane calcium extrusion. *J. Neurosci.* 26, 7201–7211. doi: 10.1523/JNEUROSCI.5230-05.2006

Fioravante, D., and Regehr, W. G. (2011). Short-term forms of presynaptic plasticity. *Curr. Opin. Neurobiol.* 21, 269–274. doi: 10.1016/j.conb.2011.02.003

Fjeld, C. C., Birdsong, W. T., and Goodman, R. H. (2003). Differential binding of NAD^+ and NADH allows the transcriptional corepressor carboxy-terminal binding protein to serve as a metabolic sensor. *Proc. Natl. Acad. Sci. U.S.A.* 100, 9202–9207. doi: 10.1073/pnas.1633591100

Förster, J. R., Lochnit, G., and Stöhr, H. (2009). Proteomic analysis of the membrane palmitoylated protein-4 (MPP4)-associated protein complex in the retina. *Exp. Eye Res.* 88, 39–48. doi: 10.1016/j.exer.2008.09.016

Frank, T., Khimich, D., Neef, A., and Moser, T. (2009). Mechanisms contributing to synaptic Ca^{2+} signals and their heterogeneity in hair cells. *Proc. Natl. Acad. Sci. U.S.A.* 106, 4483–4488. doi: 10.1073/pnas.0813213106

Frank, T., Rutherford, M. A., Strenzke, N., Neef, A., Pangrsic, T., Khimich, D., et al. (2010). Bassoon and the synaptic ribbon organize Ca(2+)-channels and vesicles to add release sites and promote refilling. *Neuron* 68, 724–738. doi: 10.1016/j.neuron.2010.10.027

Fuchs, M., Sendelbeck, A., Atorf, J., Kremers, J., and Brandstätter, J. H. (2013). Strain differences in illumination-dependent structural changes at mouse photoreceptor ribbon synapses. *J. Comp. Neurol.* 521, 68–78. doi: 10.1002/cne.23161

Glowatzki, E., and Fuchs, P. (2002). Transmitter release at the hair cell ribbon synapse. *Nat. Neurosci.* 5, 147–154. doi: 10.1038/nn796

Graydon, C. W., Cho, S., Li, G. L., Kachar, B., and von Gersdorff, H. (2011). Sharp Ca^{2+} nanodomains beneath the ribbon promote highly synchronous multivesicular release at hair cell synapses. *J. Neurosci.* 31, 16637–16650. doi: 10.1523/JNEUROSCI.1866-11.2011

Gudlur, A., Zhou, Y., and Hogan, P. G. (2013). STIM–ORAI interactions that control the CRAC channel. *Curr. Top. Membr.* 71, 33–58. doi: 10.1016/B978-0-12-407870-3.00002-0

Haeseleer, F., Imanishi, Y., Maeda, T., Possin, D. E., Maeda, A., Lee, A., et al. (2004). Essential role of Ca^{2+}-binding protein 4, a Cav1.4 channel regulator, in photoreceptor synaptic function. *Nat. Neurosci.* 7, 1079–1087. doi: 10.1038/nn1320

Han, Y., Kaeser, P. S., Südhof, T. C., and Schneggenburger, R. (2011). RIM determines Ca(2+)-channel density and vesicle docking at the presynaptic active zone. *Neuron* 69, 304–316. doi: 10.1016/j.neuron.2010.12.014

Heidelberger, R., Thoreson, W. B., and Witkovsky, P. (2005). Synaptic transmission retinal ribbon synapses. *Prog. Retin. Eye Res.* 24, 682–720. doi: 10.1016/j.preteyeres.2005.04.002

Hermes, B., Reuss, S., and Vollrath, L. (1992). Synaptic ribbons, spheres and intermediate structures in the developing rat retina. *Int. J. Dev. Neurosci.* 10, 215–223. doi: 10.1016/0736-5748(92)90061-4

Hibino, H., Pironkova, R., Onwumere, O., Vologodkaia, M., Hudspeth, A. J., and Lesage, F. (2002). RIM binding proteins (RBPs) couple Rab3-interacting molecules (RIMs) to voltage-gated Ca^{2+}-channels. *Neuron* 34, 411–423. doi: 10.1016/S0896-6273(02)00667-0

Hu, C., Bi, A., and Pan, Z. H. (2009). Differential expression of three T-type calcium channels in retinal bipolar cells in rats. *Vis. Neurosci.* 26, 177–187. doi: 10.1017/S0952523809090026

Hull, C., Studholme, K., Yazulla, S., and von Gersdorff, H. (2006). Diurnal changes in exocytosis and the number of synaptic ribbons at active zones of an ON-type bipolar cell terminal. *J. Neurophysiol.* 96, 2025–2033. doi: 10.1152/jn.00364.2006

Jackman, S. L., Choi, S. Y., Thoreson, W. B., Rabl, K., Bartoletti, T. M., and Kramer, R. H. (2009). Role of the synaptic ribbon in transmitting the cone light response. *Nat. Neurosci.* 12, 303–310. doi: 10.1038/nn.2267

Jarsky, T., Tian, M., and Singer, J. H. (2010). Nanodomain control of exocytosis is responsible for the signaling capability of a retinal ribbon synapse. *J. Neurosci.* 30, 11885–11895. doi: 10.1523/JNEUROSCI.1415-10.2010

Johnson, J. E. Jr., Perkins, G. A., Anand Giddabasappa, C. S., Chaney, S., Xiao, W., White, A. D., et al. (2007). Spatiotemporal regulation of ATP and Ca^{2+} dynamics in vertebrate rod and cone ribbon synapses. *Mol. Vis.* 13, 887–919.

Johnson, S., Halford, S., Morris, A. G., Patel, R. J., Wilkie, S. E., Hardcastle, A. J., et al. (2003). Genomic organization and alternative splicing of human RIM1, a gene implicated in autosomal dominant cone-rod dystrophy (CORD7). *Genomics* 81, 304–314. doi: 10.1016/S0888-7543(03)00010-7

Kaeser, P. S., Deng, L., Fan, M., and Südhof, T. C. (2012). RIM genes differentially contribute to organizing presynaptic release sites. *Proc. Natl. Acad. Sci. U.S.A.* 109, 11830–11835. doi: 10.1073/pnas.1209318109

Kaeser, P. S., Deng, L., Wang, Y., Dulubova, I., Liu, X., Rizo, J., et al. (2011). RIM tethers Ca^{2+}-channels to presynaptic active zones via a direct PDZ-domain interaction. *Cell* 144, 282–295. doi: 10.1016/j.cell.2010.12.029

Kawamoto, E. M., Vivar, C., and Camandola, S. (2012). Physiology and pathology of calcium signaling in the brain. *Front. Pharmacol.* 3:61. doi: 10.3389/fphar.2012.00061

Khimich, D., Nouvian, R., Pujol, R., tom Dieck, S., Egner, A., Gundelfinger, E. D., et al. (2005). Hair cell synaptic ribbons are essential for synchronous auditory signalling. *Nature* 434, 889–894. doi: 10.1038/nature03418

Kiyonaka, S., Nakajima, H., Takada, Y., Hida, Y., Yoshioka, T., Hagiwara, A., et al. (2012). Physical and functional interaction of the active zone protein CAST/ERC2 and the β-subunit of the voltage-dependent Ca^{2+}-channel. *J. Biochem.* 152, 149–159. doi: 10.1093/jb/mvs054

Kiyonaka, S., Wakamori, M., Miki, T., Uriu, Y., Nonaka, M., Bito, H., et al. (2007). RIM1 confers sustained activity and neurotransmitter vesicle anchoring to presynaptic Ca^{2+}-channels. *Nat. Neurosci.* 10, 691–701. doi: 10.1038/nn1904

Knoflach, D., Kerov, V., Sartori, S. B., Obermair, G. J., Schmuckermair, C., Liu, X., et al. (2013). Cav1.4 IT mouse as a model for vision impairment in human congenital stationary night blindness type 2. *Channels* 7, 6. doi: 10.4161/chan.26368

Koch, K. W. (2006). GCAPs, the classical neuronal calcium sensors in the retina. A Ca^{2+}-relay model of guanylate cyclase activation. *Calcium Binding Proteins* 1, 3–6.

Koch, K. W., Duda, T., and Sharma, R. K. (2010). Ca^{2+}-modulated vision-linked ROS-GC guanylate cyclase transduction machinery. *Mol Cell. Biochem.* 334, 105–115. doi: 10.1007/s11010-009-0330-z

Korenbrot, J. I., and Rebrik, T. I. (2002). Tuning outer segment homeostasis to phototransduction in rods and cones. *Adv. Exp. Med. Biol.* 514, 179–203. doi: 10.1007/978-1-4615-0121-3_11

Krizaj, D., Bao, I. X., Schmitz, Y., Witkovsky, P., and Copenhagen, D. R. (1999). Caffeine-sensitive stores regulate synaptic transmission from retinal rod photoreceptors. *J. Neurosci.* 19, 7249–7261.

Krizaj, D. (2003). Properties of exocytic response in vertebrate photoreceptors. *J. Neurophysiol.* 90, 218–225. doi: 10.1152/jn.01025.2002

Krizaj, D., and Copenhagen, D. R. (2002). Calcium regulation in photoreceptors. *Front. Biosci.* 7:d2023–d2044. doi: 10.2741/krizaj

Krizaj, D., Lai, F. A., and Copenhagen, D. R. (2003). Ryanodine stores and calcium regulation in the inner segments of salamander rods and cones. *J. Physiol. (Lond.)* 547, 761–774. doi: 10.1113/jphysiol.2002.035683

Lalonde, M. R., Kelly, M. E., and Barnes, S. (2009). Calcium-activated chloride channels in the retina. *Channels (Austin)* 24, 252–260. doi: 10.4161/chan.2.4.6704

Lee, B. B., Martin, P. R., and Grünert, U. (2010). Retinal connectivity and primate vision. *Prog. Retin. Eye Res.* 29, 622–639. doi: 10.1016/j.preteyeres.2010.08.004

Lenzi, D., and von Gersdorff, H. (2001). Structure suggests function: the case for synaptic ribbons as exocytotic nanomachines. *Bioessays* 23, 831–840. doi: 10.1002/bies.1118

Lewis, R. S. (2011). Store-operated calcium channels: new perspectives on mechanism and function. *Cold Spring Harb. Perspect. Biol.* 3, a003970. doi: 10.1101/cshperspect.a003970

Libby, R. T., Lavallee, C. R., Balkema, G. W., Brunken, W. J., and Hunter, D. D. (1999). Disruption of laminin beta2 chain production causes alterations in morphology and function in the CNS. *J. Neurosci.* 19, 9399–9411.

Liu, X., Kerov, V., Haeseleer, F., Majumder, A., Artemyev, N., Baker, S. A., et al. (2013). Dysregulation of Cav1.4 channels disrupts the maturation of photoreceptor synaptic ribbons in congenital stationary night blindness type 2. *Channels* 24, 7.

Lodha, N., Bonfield, S., Orton, N. C., Doering, C. J., McRory, J. E., Mema, S.C., et al. (2010). Congenital stationary night blindness in mice – a tale of two caca1f mutants. *Adv. Exp. Med. Biol.* 664, 549–558. doi: 10.1007/978-1-4419-1399-9_63

López-del Hoyo, N., Fazioli, L., López-Begines, S., Fernández-Sanchez, L., Cuenca, N., Llorens, J., et al. (2012). Overexpression of guanylate cyclase activating protein 2 in rod photoreceptors in vivo leads to morphological changes at the synaptic Ribbon. *PLoS ONE* 7:e42994. doi: 10.1371/journal.pone.0042994

Lytton, J. (2007). Na^+/Ca^{2+}-exchangers: three mammalian genes families control Ca^{2+} transport. *Biochem. J.* 406, 365–382. doi: 10.1042/BJ20070619

Ma, Y. P., and Pan, Z. H. (2003). Spontaneous regenerative activity in mammalian retinal bipolar cells: roles of multiple subtypes of voltage-dependent Ca(2+) channels. *Vis. Neurosci.* 20, 131–139. doi: 10.1017/S0952523803202042

Magupalli, V. G., Schwarz, K., Alpadi, K., Natarajan, S., Seigel, G. M., and Schmitz, F. (2008). Multiple RIBEYE–RIBEYE interactions create a dynamic scaffold for the formation of synaptic ribbons. *J. Neurosci.* 28, 7954–7967. doi: 10.1523/JNEUROSCI.1964-08.2008

Malenka, R. C., and Nicoll, R. A. (1999). Long-term potentiation – a decade of progress? *Science* 285, 1870–1874. doi: 10.1126/science.285.5435.1870

Manjarrés, I. M., Alonso, M. T., and García-Sancho, J. (2011). Calcium entry-calcium refilling (CECR) coupling between store-operated Ca^{2+} entry and sarco/endoplasmic reticulum ATPase. *Cell Calcium* 49, 153–161. doi: 10.1016/j.ceca.2011.01.007

Manjarrés, I. M., Rodriguez-Garcia, A., Alonso, M. T., and García-Sancho, J. (2010). The sarco/endoplasmic reticulum Ca(2+)-ATPase (SERCA) is the third element in capacitive calcium entry. *Cell Calcium* 47, 412–418. doi: 10.1016/j.ceca.2010.03.001

Mansergh, F., Orton, N. C., Vessey, J. P., Lalonde, M. R., Stell, W. K., Tremblay, F., et al. (2005). Mutation of the calcium channel gene Cacna1f disrupts calcium signaling, synaptic transmission and cellular organization in mouse retina. *Hum. Mol. Genet.* 14, 3035–3046. doi: 10.1093/hmg/ddi336

Matthews, G., and Fuchs, P. (2010). The diverse roles of ribbon synapses in sensory neurotransmission. *Nat. Rev. Neurosci.* 11, 812–822. doi: 10.1038/nrn2924

Mercer, A. J., Chen, M., and Thoreson, W. B. (2011a). Lateral mobility of presynaptic L-type calcium channels at photoreceptor ribbon synapses. *J. Neurosci.* 31, 4397–4406. doi: 10.1523/JNEUROSCI.5921-10.2011

Mercer, A. J., Rabl, K., Riccardi, G. E., Brecha, N. C., Stella, S. L. Jr., and Thoreson, W. B. (2011b). Location of release sites and calcium-activated chloride channels relative to calcium channels at the photoreceptor ribbon synapse. *J. Neurophysiol.* 105, 321–335. doi: 10.1152/jn.00332.2010

Mercer, A. J., and Thoreson, W. B. (2011). The dynamic architecture of photoreceptor ribbon synapses: cytoskeletal, extracellular matrix, and intramembrane proteins. *Vis. Neurosci.* 28, 453–471. doi: 10.1017/S0952523811000356

Midorikawa, M., Tsukamoto, Y., Berglund, K., Ishii, M., and Tachibana, M. (2007). Different roles of ribbon-associated and ribbon-free active zones in retinal bipolar cells. *Nat. Neurosci.* 10, 1268–1276. doi: 10.1038/nn1963

Miki, T., Kiyonaka, S., Uriu, Y., deWaard, M., Wakamori, M., Beedle, A. M., et al. (2007). Mutation associated with an autosomal dominant cone-rod dystrophy CORD7 modifies RIM1-mediated modulation of voltage-gated Ca^{2+}-channels. *Channels* 1, 144–147.

Molnar, T., Barabas, P., Birnbaumer, L., Punzo, C., Kefalov, V., and Krizaj, D. (2012). Store-operated channels regulate intracellular calcium in mammalian rods. *J. Physiol.* 590, 3465–3481. doi: 10.1113/jphysiol.2012.234641

Morgans, C. W., Bayley, P. R., Oesch, N., Ren, G., Akileswaran, L., and Taylor, W. R. (2005). Photoreceptor calcium channels: insight from night blindness. *Vis. Neurosci.* 22, 561–568. doi: 10.1017/S0952523805225038

Moser, T., Brandt, A., and Lysakowski, A. (2006). Hair cell ribbon synapses. *Cell Tissue Res.* 326, 347–359. doi: 10.1007/s00441-006-0276-3

Mustafi, D., Engel, A. H., and Palczewski, K. (2009). Structure of cone photoreceptors. *Prog. Retin. Eye Res.* 28, 289–302. doi: 10.1016/j.preteyeres.2009.05.003

Nassi, J. J., and Callaway, E. M. (2009). Parallel processing strategies of the primate visual system. *Nat. Rev. Neurosci.* 10, 360–372. doi: 10.1038/nrn2619

Neher, E., and Sakaba, T. (2008). Multiple roles of calcium ions in the regulation of neurotransmitter release. *Neuron* 59, 861–872. doi: 10.1016/j.neuron.2008.08.019

Nicoll, R. A., and Schmitz, D. (2005). Synaptic plasticity at hippocampal mossy fibre synapses. *Nat. Rev. Neurosci.* 6, 863–876. doi: 10.1038/nrn1786

Nishimune, H. (2012). Active zones of mammalian neuromuscular junctions: formation, density, and aging. *Ann. N. Y. Acad. Sci.* 1274, 24–32. doi: 10.1111/j.1749-6632.2012.06836.x

Nishimune, H., Numata, T., Chen, J., Aoki, Y., Wang, Y., Starr, M. P., et al. (2012). Active zone protein bassoon co-localizes with presynaptic calcium channels, modifies channel function, and recovers from aging related loss by exercise. *PLoS ONE* 7:e38029. doi: 10.1371/journal.pone.0038029

Nishimune, H., Sanes, J. R., and Carlson, S. S. (2004). A synaptic laminin–calcium channel interaction organizes active zones in motor nerve terminals. *Nature* 432, 580–587. doi: 10.1038/nature03112

Nomura, A., Shigemoto, R., Nakanishi, Y., Okamoto, N., Mizuno, N., and Nakanishi, S. (1994). Developmentally regulated postsynaptic localization of a metabotropic glutamate receptor in rat rod bipolar cells. *Cell* 77, 361–369. doi: 10.1016/0092-8674(94)90151-1

Nouvian, R., Neef, J., Bulankina, A., Reisinger, E., Pangrsic, T., Frank, T., et al. (2011). Exocytosis at the hair cell ribbon synapse operates without neuronal SNARE proteins. *Nat. Neurosci.* 14, 411–413. doi: 10.1038/nn.2774

Olney, J. W. (1968). An electron microscopic study of synapse formation, receptor outer segment development, and other aspects of developing mouse retinas. *Invest. Ophthalmol.* 7, 250–268.

Olshevskaya, E. V., Ermilov, A. N., and Dizhoor, A. M. (1999). Dimerization of guanylyl cyclase-activating protein and a mechanism of photoreceptor guanylyl cyclase activation. *J. Biol. Chem.* 274, 25583–25587. doi: 10.1074/jbc.274.36.25583

Palczewski, K., Sokal, I., and Baehr, W. (2004). Guanylate cyclase-activating proteins: structure, function and diversity. *Biochem. Biophys. Res. Commun.* 322, 1123–1130. doi: 10.1016/j.bbrc.2004.07.122

Paliwal, S., Ho, N., Parker, D., and Grossman, S. R. (2012). CtBP2 promotes human cancer cell migration by transcriptional activation of Tiam1. *Genes Cancer* 3, 481–490. doi: 10.1177/1947601912463695.

Paliwal, S., Kovi, R., Nath, B., Chen, Y., Lewis, B., and Grossman, S. R. (2007). ARF antagonizes cancer cell migration via interaction with CtBP corepressor. *Cancer Res.* 67, 9322–9329. doi: 10.1158/0008-5472.CAN-07-1743

Paliwal, S., Pande, S., Kovi, R., Shapless, N., Bardeesy, N., and Grossman, S. R. (2006). Targeting of C-terminal binding protein by ARF results in p53-independent apoptosis. *Mol. Cell. Biol.* 26, 2360–2372. doi: 10.1128/MCB.26.6.2360-2372.2006

Pan, Z. H., Hu, H. J., Perring, P., and Andrade, R. (2001). T-type Ca^{2+}-channels mediate neurotransmitter release in retinal bipolar cells. *Neuron* 32, 89–98. doi: 10.1016/S0896-6273(01)00454-8

Parekh, A. B. (2011). Decoding cytoplasmic Ca^{2+} oscillations. *Trends Biochem. Sci.* 36, 78–87. doi: 10.1016/j.tibs.2010.07.013

Parekh, A. B., and Putney, J. W. Jr. (2005). Store-operated calcium channels. *Physiol. Rev.* 85, 757–810. doi: 10.1152/physrev.00057.2003

Parsons, T. D., and Sterling, P. (2003). Synaptic ribbon. Conveyor belt or safety belt? *Neuron* 37, 379–382. doi: 10.1016/S0896-6273(03)00062-X

Peng, Y. W., Sharp, A. H., Snyder, S. H., and Yau, K. W. (1991). Localization of the inositol 1,4,5-trisphosphate receptor in synaptic terminals in the vertebrate retina. *Neuron* 6, 525–531. doi: 10.1016/0896-6273(91)90055-5

Peshenko, I. V., Olshevskaya, E. V., and Dizhoor, A. M. (2004). Ca^{2+}-dependent conformational changes in guanylyl cyclase-activating protein 2 (GCAP2) revealed by site-specific phosphorylation and partial proteolysis. *J. Biol. Chem.* 279, 50342–50349. doi: 10.1074/jbc.M408683200

Rao-Mirotznik, R., Harkins, A. B., Buchsbaum, G., and Sterling, P. (1995). Mammalian rod terminal: architecture of a binary synapse. *Neuron* 14, 561–569. doi: 10.1016/0896-6273(95)90312-7

Raven, M. A., Orton, N. C., Nassar, H., William, G. A., Stell, W. K., Jacobs, G. H., et al. (2007). Early afferent signaling in the outer plexiform layer regulates the development of horizontal cell morphology. *J. Comp. Neurol.* 506, 745–758. doi: 10.1002/cne.21526

Regehr, W. G. (2012). Short-term plasticity. *Cold Spring Harb. Perspect. Biol.* 4, a005702. doi: 10.1101/cshperspect.a005702

Regus-Leidig, H., and Brandstätter, J. H. (2012). Structure and function of a complex sensory synapse. *Acta Physiol. (Oxf.)* 204, 479–486. doi: 10.1111/j.1748-1716.2011.02355.x

Regus-Leidig, H., Ott, C., Löhner, M., Atorf, J., Fuchs, M., Sedmak, T., et al. (2013). Identification and immunocytochemical characterization of piccolino, a novel splice variant selectively expressed at sensory ribbon synapses of the eye and ear. *PLoS ONE* 8:e70373. doi: 10.1371/journal.pone.0070373

Regus-Leidig, H., Specht, D., tom Dieck, S., and Brandstätter, J. H. (2010a). Stability of active zone components at the photoreceptor ribbon complex. *Mol. Vis.* 16, 2690–2770.

Regus-Leidig, H., tom Dieck, S., and Brandstätter, J. H. (2010b). Absence of functional active zone protein bassoon affects assembly and transport of ribbon precursors during early steps of photoreceptor synaptogenesis. *Mol. Vis.* 16, 2699–2700.

Reim, K., Regus-Leidig, H., Ammermüller, J., El-Kordi, A., Radyushkin, K., Ehrenreich, H., et al. (2009). Aberrant function and structure of retinal ribbon synapses in the absence of complexin 3 and complexin 4. *J. Cell Sci.* 122, 1352–1361. doi: 10.1242/jcs.045401

Reim, K., Wegmeyer, H., Brandstätter, J. H., Xue, M., Rosenmund, C., Dresbach, T., et al. (2005). Structurally and functionally unique complexins at retinal ribbon synapses. *J. Cell Biol.* 169, 669–680. doi: 10.1083/jcb.200502115

Rieke, F., and Schwartz, E. A. (1996). Asynchronous transmitter release: control of exocytosis and endocytosis at the salamander rod synapse. *J. Physiol.* 493, 1–8.

Rizo, J., and Südhof, T. C. (2012). The membrane fusion enigma: SNAREs, sec1/Munc18 proteins, and their complices-guilty as charged? *Annu. Rev. Cell Dev. Biol.* 28, 279–308. doi: 10.1146/annurev-cellbio-101011-155818

Rizzuto, R., Duchen, M. R., and Pozzan, T. (2004). Flirting in little space: the ER/mitochondria liaison. *Sci STKE* 215, re1. doi: 10.1126/stke.2152004re1

Rizzuto, R., and Pozzan, T. (2006). Microdomains of intracellular Ca^{2+}: molecular determinants and functional consequences. *Physiol. Rev.* 86, 369–408. doi: 10.1152/physrev.00004.2005

Rusakov, D. A. (2006). Ca^{2+}-dependent mechanisms of presynaptic control at central synapses. *Neuroscientist* 12, 317–326. doi: 10.1177/1073858405284672

Safieddine, S., El-Amraoui, A., and Petit, C. (2012). The auditory hair cell ribbon synapse: from assembly to function. *Annu. Rev. Neurosci.* 35, 509–528. doi: 10.1146/annurev-neuro-061010-113705

Sakurai, K., Chen, J., and Kefalov, V. J. (2011). Role of guanylyl cyclase modulation in mouse cone phototransduction. *J. Neurosci.* 31, 7991–8000. doi: 10.1523/JNEUROSCI.6650-10.2011

Schmitz, F. (2009). The making of synaptic ribbons: how they are built and what they do. *Neuroscientist* 15, 611–624. doi: 10.1177/1073858409340253

Schmitz, F., Augustin, I., and Brose, N. (2001). Absence of the synaptic vesicle priming protein Munc13-1 from tonically active ribbon synapses of the rat retina. *Brain Res.* 895, 258–263. doi: 10.1016/S0006-8993(01)02078-9

Schmitz, F., and Drenckhahn, D. (1993). Intermediate stages in the disassembly of synaptic ribbons in cone photoreceptors of the crucian carp, *Carassius carassius*. *Cell Tissue Res.* 272, 487–490. doi: 10.1007/BF00318554

Schmitz, F., Königstorfer, A., and Südhof, T. C. (2000). RIBEYE, a component of synaptic ribbons: a protein's journey through evolution provides insights into synaptic ribbon function. *Neuron* 28, 857–872. doi: 10.1016/S0896-6273(00)00159-8

Schmitz, F., Natarajan, N., Venkatesan, J. K., Wahl, S., Schwarz, K., and Grabner, C. P. (2012). EF hand-mediated Ca^{2+}- and cGMP-signaling in photoreceptor synaptic terminals. *Front. Mol. Neurosci.* 5:26. doi: 10.3389/fnmol.2012.00026

Schmitz, F., Tabares, L., Khimich, D., Strenzke, N., de la Villa-Polo, P., Castellano-Munoz, M., et al. (2006). CSPalpha-deficiency causes massive and rapid photoreceptor degeneration. *Proc. Natl. Acad. Sci. U.S.A.* 103, 2926–2931. doi: 10.1073/pnas.0510060103

Schmitz, Y., and Witkovsky, P. (1997). Dependence of photoreceptor glutamate release on a dihydropyridine-sensitive calcium channel. *Neuroscience* 78, 1209–1216. doi: 10.1016/S0306-4522(96)00678-1

Shaltiel, L., Paparizos, C., Fenske, S., Hassan, S., Gruner, C., Rötzer, K., et al. (2012). Complex regulation of voltage-dependent activation and inactivation properties of retinal voltage-gated Cav1.4 L-type Ca^{2+} channels by Ca^{2+}-binding protein 4 (CaBP4). *J. Biol. Chem.* 287, 36312–36321. doi: 10.1074/jbc.M112.392811

Sharma, R. K. (2002). Evolution of the membrane guanylate cyclase transduction system. *Mol. Cell. Biochem.* 230, 3–30. doi: 10.1023/A:1014280410459

Sharma, R. K. (2010). Membrane guanylate cyclase is a beautiful signal transduction machinery. *Mol. Cell. Biochem.* 334, 3–36. doi: 10.1007/s11010-009-0336-6

Sharma, R. K., and Duda, T. (2012). Ca^{2+}-sensors and ROS-GC: interlocked sensory transduction elements: a review. *Front. Mol. Neurosci.* 5:42. doi: 10.3389/fnmol.2012.00042

Sheets, L., Kindt, K. S., and Nicolson, T. (2012). Presynaptic CaV1.3 channels regulate synaptic ribbon size and are required for synaptic maintenance in sensory hair cells. *J. Neurosci.* 28, 17273–17286. doi: 10.1523/JNEUROSCI.3005-12.2012

Sheets, L., Trapani, J. G., Mo, W., Obholzer, N., and Nicolson, T. (2011). RIBEYE is required for presynaptic Ca(V)1.3 channel localization and afferent innervation of sensory hair cells. *Development* 138, 1309–1319. doi: 10.1242/dev.059451

Sheng, Z., Choi, S. Y., Dharia, A., Li, J., Sterling, P., and Kramer, R. H. (2007). Synaptic Ca^{2+} in darkness is lower in rods than in cones, causing slower tonic release of vesicles. *J. Neurosci.* 27, 5033–5042. doi: 10.1523/JNEUROSCI.5386-06.2007

Singer, J. H., Lassová, L., Vardi, N., and Singer, J. S. (2004). Coordinated multivesicular release at a mammalian ribbon synapse. *Nat. Neurosci.* 7, 826–833. doi: 10.1038/nn1280

Singh, A., Hamedinger, D., Hoda, J. C., Gebhart, M., Koschak, A., Romanin, C., et al. (2006). C-terminal modulator controls Ca^{2+}-dependent gating of Ca(v)1.4 L-type Ca^{2+} channels. *Nat. Neurosci.* 9, 1108–1116. doi: 10.1038/nn1751

Snellman, J., Mehta, B., Babai, N., Bartoletti, T. M., Akmentin, W., Francis, A., et al. (2011). Acute destruction of the synaptic ribbon reveals a role for the ribbon in vesicle priming. *Nat. Neurosci.* 14, 1135–1141. doi: 10.1038/nn.2870

Soboloff, J., Rothberg, B. S., Madesh, M., and Gill, D. L. (2012). STIM proteins: dynamic calcium signal transducers. *Nat. Rev. Mol. Cell Biol.* 13, 549–565. doi: 10.1038/nrm3414

Spiwoks-Becker, I., Glas, M., Lasarzik, I., and Vollrath, L. (2004). Synaptic ribbons lose and regain material in response to illumination changes. *Eur. J. Neurosci.* 19, 1559–1571. doi: 10.1111/j.1460-9568.2004.03198.x

Stephen, R., Bereta, G., Golczak, M., Palczewski, K., and Souza, M. C. (2007). Stabilizing function for myristoyl group revealed by the crystal structure of a neuronal calcium sensor, the guanylate cyclase-activating protein1. *Structure* 15, 1392–1402. doi: 10.1016/j.str.2007.09.013

Stephen, R., Filipek, S., Palczewski, K., and Souza, M. C. (2008). Ca^{2+}-dependent regulation of phototransduction. *Photochem. Photobiol.* 84, 903–910. doi: 10.1111/j.1751-1097.2008.00323.x

Stöhr, H., Heisig, J. B., Benz, P. M., Schöberl, S., Milenkovic, V. M., Strauss, O., et al. (2009). TMEM16B, a novel protein with calcium-dependent chloride channel activity, associates with a presynaptic protein complex in photoreceptor terminals. *J. Neurosci.* 29, 6809–6818. doi: 10.1523/JNEUROSCI.5546-08.2009

Striessnig, J., Bolz, H. J., and Koschak, A. (2010). Channelopathies in CaV1.1, CaV1.3, and CaV1.4 voltage-gated L-type Ca^{2+}-channels. *Pflügers Arch.* 460, 361–374. doi: 10.1007/s00424-010-0800-x

Südhof, T. C. (2012a). Calcium control of neurotransmitter release. *Cold Spring Harb. Perspect. Biol.* 4, a011353. doi: 10.1101/cshperspect.a011353

Südhof, T. C. (2012b). The presynaptic active zone. *Neuron* 75, 11–25. doi: 10.1016/j.neuron.2012.06.012

Südhof, T. C. (2013). A molecular machine for neurotransmitter release: synaptotagmin and beyond. *Nat. Med.* 19, 1227–1231. doi: 10.1038/nm.3338

Sung, C.-H., and Chuang, J. Z. (2010). The cell biology of vision. *J. Cell Biol.* 190, 953–963. doi: 10.1083/jcb.201006020

Suryanarayanan, A., and Slaughter, M. M. (2006). Synaptic transmission mediated by internal calcium stores in rod photoreceptors. *J. Neurosci.* 26, 1759–1766. doi: 10.1523/JNEUROSCI.3895-05.2006

Szikra, T., and Krizaj, D. (2006). The dynamic range and domain-specific signals of intracellular calcium in photoreceptors. *Neuroscience* 141, 143–155. doi: 10.1016/j.neuroscience.2006.03.054

Szikra, T., and Krizaj, D. (2007). Intracellular organelles and calcium homeostasis in rods and cones. *Vis. Neurosci.* 24, 733–743. doi: 10.1017/S0952523807070587

Szikra, T., Barabas, P., Bartoletti, T. M., Huang, W., Akopian, A., Thoreson, W. B., et al. (2009). Calcium homeostasis and cone signalling are regulated by interactions between calcium stores and plasma membrane ion channels *PLoS ONE* 4:e6723. doi: 10.1371/journal.pone.0006723

Szikra, T., Cusato, K., Thoreson, W. B., Barabas, P., Bartoletti, T. M., and Krizaj, D. (2008). Depletion of calcium stores regulates calcium influx and signal transmission in rod photoreceptors. *J. Physiol.* 586, 4859–4875. doi: 10.1113/jphysiol.2008.160051

Tempel, B. L., and Shilling, D. J. (2007). The plasma membrane calcium ATPase and disease. *Subcell. Biochem.* 45, 365–383. doi: 10.1007/978-1-4020-6191-2_13

Thoreson, W. B., Rabl, K., Townes-Anderson, E., and Heidelberger, R. (2004). A highly Ca^{2+}-sensitive pool of synaptic vesicles contributes to linearity at the rod photoreceptor ribbon synapse. *Neuron* 42, 595–605. doi: 10.1016/S0896-6273(04)00254-5

Thoreson, W. B., Stella, S. L. Jr., Bryson, E. L., Clements, J., and Witkovsky, P. (2002). D2-like dopamine receptors promote interactions between calcium and chloride channels that diminish rod synaptic transfer in the salamander retina. *Vis. Neurosci.* 19, 235–247. doi: 10.1017/S0952523802192017

tom Dieck, S., Altrock, W. D., Kessels, M. M., Qualmann, B., Regus, H., Brauner, D., et al. (2005). Molecular dissection of the photoreceptor ribbon synapse: physical interaction of bassoon and RIBEYE is essential for the development of the ribbon complex. *J. Cell Biol.* 168, 825–836. doi: 10.1083/jcb.200408157

tom Dieck, S., and Brandstätter, J. H. (2006). Ribbon synapses of the retina. *Cell Tissue Res.* 326, 339–346. doi: 10.1007/s00441-006-0234-0

Venkatesan, J. K., Natarajan, S., Schwarz, K., Mayer, S. I., Alpadi, K., Magupalli, V. G., et al. (2010). Nicotinamide adenine dinucleotide-dependent binding of the neuronal Ca^{2+} sensor protein GCAP2 to photoreceptor synaptic ribbons. *J. Neurosci.* 30, 6559–6567. doi: 10.1523/JNEUROSCI.3701-09.2010

Vollrath, L., and Spiwoks-Becker, I. (1996). Plasticity of retinal ribbon synapses. *Microsc. Res. Tech.* 35, 472–487. doi: 10.1002/(SICI)1097-0029(19961215)35:6<472::AID-JEMT6>3.0.CO;2-K

Wahl, S., Katiyar, R., and Schmitz, F. (2013). A local, periactive zone endocytic machinery at photoreceptor synapses in close vicinity to synaptic ribbons. *J. Neurosci.* 33, 10278–10300. doi: 10.1523/JNEUROSCI.5048-12.2013

Wan, L., Almers, W., and Chen, W. (2005). Two ribeye genes in teleosts: the role of RIBEYE in ribbon formation and bipolar cell development. *J. Neurosci.* 25, 941–949. doi: 10.1523/JNEUROSCI.4657-04.2005

Wan, Q. F., Nixon, E., and Heidelberger, R. (2012). Regulation of presynaptic calcium in a mammalian synaptic terminal. *J. Neurophysiol.* 108, 3059–3067. doi: 10.1152/jn.00213.2012

Wang, Y., Okamoto, M., Schmitz, F., Hofmann, K., and Südhof, T. C. (1997). RIM is a putative effector in regulating synaptic-vesicle fusion. *Nature* 388, 593–598. doi: 10.1038/41580

Wässle, H. (2004). Parallel processing in the mammalian retina. *Nat. Rev. Neurosci.* 5, 1–12. doi: 10.1038/nrn1497

Witkovsky, P., Schmitz, Y., Akopian, A., Krizaj, D., and Tranchina, D. (1997). Gain of rod to horizontal cell synaptic transfer: relation to glutamate release

and a dihydropyridine-sensitive calcium current. *J. Neurosci.* 17, 7297–7306.

Wycisk, K. A., Budde, B., Feil, S., Skosyrski, S., Buzzi, F., Neidhardt, J., et al. (2006). Structural and functional abnormalities of retinal ribbon synapses due to cacna2d4 mutations. *Invest. Ophthalmol. Vis. Sci.* 47, 3523–3530. doi: 10.1167/iovs.06-0271

Xing, W., Akopian, A., and Krizaj, D. (2012). Trafficking of the presynaptic PMCA signaling complexes in mouse photoreceptors requires Cav1.4 β1-subunits. *Adv. Exp. Med. Biol.* 723, 739–744. doi: 10.1007/978-1-4614-0631-0_94

Yang, J., Pawlyk, B., Wen, X. H., Adamian, M., Soloview, M., Michaud, N., et al. (2007). MPP4 is required for the proper localization of plasma membrane calcium ATPases and maintain calcium homeostasis at the rod photoreceptor synaptic terminal. *Hum. Mol. Genet.* 16, 1017–1029. doi: 10.1093/hmg/ddm047

Zabouri, N., and Haverkamp, S. (2013). Calcium channel-dependent molecular maturation of photoreceptor synapses. *PLoS ONE* 8:e63853. doi: 10.1371/journal.pone.0063853

Zenisek, D. (2008). Vesicle association and exocytosis at ribbon and extraribbon sites in retinal bipolar cell presynaptic terminals. *Proc. Natl. Acad. Sci. U.S.A.* 105, 4922–4927. doi: 10.1073/pnas.0709067105

Zenisek, D., and Matthews, G. (2000). The role of mitochondria in presynaptic calcium handling at a ribbon synapse. *Neuron* 25, 229–237. doi: 10.1016/S0896-6273(00)80885-5

Zenisek, D., Steyer, J. A., and Almers, W. (2000). Transport, capture and exocytosis of synaptic vesicles at active zones. *Nature* 406, 849–854. doi: 10.1038/35022500

Conflict of Interest Statement: The author declares that the research was conducted in the absence of any commercial or financial relationships that could be construed as a potential conflict of interest.

Received: 30 October 2013; accepted: 15 January 2014; published online: 06 February 2014.

*Citation: Schmitz F (2014) Presynaptic [Ca^{2+}] and GCAPs: aspects on the structure and function of photoreceptor ribbon synapses. Front. Mol. Neurosci. **7**:3. doi: 10.3389/fnmol.2014.00003*

This article was submitted to the journal Frontiers in Molecular Neuroscience.

frontiers in
MOLECULAR NEUROSCIENCE

MINI REVIEW ARTICLE
published: 26 May 2014
doi: 10.3389/fnmol.2014.00044

Insights into the role of RD3 in guanylate cyclase trafficking, photoreceptor degeneration, and Leber congenital amaurosis

Laurie L. Molday, Thomas Jefferies and Robert S. Molday*

Department of Biochemistry and Molecular Biology, Center for Macular Research, University of British Columbia, Vancouver, BC, USA

Edited by:
Wolfgang Baehr, University of Utah, USA

Reviewed by:
John Oberdick, The Ohio State University, USA
Johann H. Brandstätter, Friedrich-Alexander-Universität Erlangen-Nuremberg, Germany

***Correspondence:**
Robert S. Molday, Department of Biochemistry and Molecular Biology, Center for Macular Research, University of British Columbia, 2350 Health Sciences Mall, Vancouver, BC V6T 1Z3, Canada
e-mail: molday@mail.ubc.ca

Retinal degeneration 3 (RD3) is an evolutionarily conserved 23 kDa protein expressed in rod and cone photoreceptor cells. Mutations in the gene encoding RD3 resulting in unstable non-functional C-terminal truncated proteins are responsible for early onset photoreceptor degeneration in Leber Congenital Amaurosis 12 patients, the *rd3* mice, and the *rcd2* collies. Recent studies have shown that RD3 interacts with guanylate cyclases GC1 and GC2 in retinal cell extracts and HEK293 cells co-expressing GC and RD3. This interaction inhibits GC catalytic activity and promotes the exit of GC1 and GC2 from the endoplasmic reticulum and their trafficking to photoreceptor outer segments. Adeno-associated viral vector delivery of the normal *RD3* gene to photoreceptors of the *rd3* mouse restores GC1 and GC2 expression and outer segment localization and leads to the long-term recovery of visual function and photoreceptor cell survival. This review focuses on the genetic and biochemical studies that have provided insight into the role of RD3 in photoreceptor function and survival.

Keywords: retinal degeneration 3, guanylate cyclase, photoreceptor cells, protein trafficking, photoreceptor degeneration, Leber congenital amaurosis, gene therapy

INTRODUCTION

Guanylate cyclase (GC) plays a key role in phototransduction by catalyzing the synthesis of cGMP. In the dark the basal catalytic activity of GC in photoreceptor outer segments (OS) is balanced by the basal activity of phosphodiesterase (PDE) to maintain cGMP at a level sufficient for maintaining a significant fraction of cGMP-gated channels in their open state. This allows the influx of Ca^{2+} and Na^{+} into the OS with the intracellular Ca^{2+} level reaching 250–500 nM (Gray-Keller and Detwiler, 1994; Woodruff et al., 2002). At this concentration, guanylate cyclase activating proteins (GCAPs) with bound Ca^{2+} maintain GC at its basal level (Gorczyca et al., 1994; Dizhoor et al., 1995; Polans et al., 1996). Following photoexcitation the Ca^{2+} level decreases to less than 25 nM through the combined closure of the cGMP-gated channels and continued efflux of Ca^{2+} by the Na/Ca-K exchanger (Woodruff et al., 2002). The reduced Ca^{2+} concentration triggers the exchange of Ca^{2+} for Mg^{2+} on GCAPs resulting in the activation GC (Peshenko and Dizhoor, 2006; Dizhoor et al., 2010). The increase in cGMP reopens the cGMP-gated channels and restores Ca^{2+} and cGMP to their dark state levels.

Vertebrate photoreceptors contain two membrane-bound GCs, generally called GC1 and GC2, that share a high degree of sequence identity (∼49%) and structural organization (Shyjan et al., 1992; Lowe et al., 1995; Baehr et al., 2007; Karan et al., 2011). They consist of an N-terminal signal sequence followed by an extracellular domain, a transmembrane segment, a kinase homology domain, a dimerization domain, a cyclase catalytic domain, and a carboxyl-terminal extension. GC1 and GC2 exist as homodimers which localize to disk membranes of photoreceptor OS (Yang and Garbers, 1997; Ramamurthy et al., 2001). GC1 is present at relatively high concentrations in rod and cone OS, whereas GC2 is restricted to rod OS in mice and humans (Baehr et al., 2007; Azadi et al., 2010). The relative amounts of GC1 and GC2 vary with species with a GC1 to GC2 ratio of 4:1 in mouse (Peshenko et al., 2011b) and 30:1 in bovine photoreceptors (Helten et al., 2007; Kwok et al., 2008). The importance of GC1 and GC2 in the visual response and photoreceptor survival has been determined in knockout mice. In GC1 knockout mice, the cone photoresponse is absent and these cells undergo rapid degeneration (Baehr et al., 2007; Karan et al., 2010). Rod photoreceptors remain viable and functional due to the presence of GC2. In the GC1/GC2 double knockout mice, the rod and cone photoresponse is undetectable and both cell types undergo degeneration. The importance of GC1 in rod and cone function and survival is further highlighted by the finding that mutations in the *GUCY2D* gene encoding human GC1 cause Leber Congenital Amaurosis (LCA) Type 1 (LCA1), a severe early onset retinal dystrophy, and cone-rod dystrophy (Perrault et al., 1996; Kelsell et al., 1998; Karan et al., 2010).

Photoreceptor cells are highly polarized neurons with the OS segregated from the rest of the cell by a thin cilium. OS proteins must be efficiently transported from the endoplasmic reticulum (ER) in the inner segment through the cilium since OS turnover every 10 days through the phagocytosis of aged OS membranes by retinal pigment epithelial cells and the addition of new membrane at the base of the OS (Sung and Chuang, 2010). The molecular machinery which orchestrates the transport of proteins to the OS is highly complex involving vesicle

budding, fusion, and motorized transport along microtubules and other cytoskeletal elements in the inner segment and cilium. Molecular-based studies indicate that the C-terminal targeting segment of several OS membrane proteins including rhodopsin and perpherin-2 play an essential role in vesicle trafficking through protein–protein interactions (Tam et al., 2000, 2004; Deretic et al., 2005; Chuang et al., 2007; Mazelova et al., 2009). The vesicle transport pathways, however, appear to be distinct for various OS membrane proteins (Fariss et al., 1997). Efforts to define a sequence required to transport GC to outer segments have been inconclusive (Karan et al., 2011). Recently, retinal degeneration 3 (RD3), a photoreceptor protein encoded by the gene associated with retinal degeneration in the *rd3* mouse, *rcd2* collie, and LCA12 patients has been shown to play a crucial role in the trafficking of GC1 and GC2 in photoreceptors (Azadi et al., 2010). In this review, we focus on the molecular properties of RD3 and its role in GC trafficking, catalytic activity, and photoreceptor degeneration.

GENETIC AND PROTEIN ANALYSIS OF THE RD3

The gene responsible for retinal degeneration in the *rd3* mouse was first identified as an uncharacterized transcript in an *in silico* search of retina-specific transcripts and called *C1orf36* for Chromosome 1 open reading frame 36 (Lavorgna et al., 2003). The gene now known as *RD3* consists of 3 exons spanning the 5′ and 3′ untranslated region with the open reading frame comprised of part of exon 2 (amino acids 1–99) and exon 3 (100–195). RT-PCR and *in situ* hybridization confirmed the presence of *RD3* in the retina with high expression in the photoreceptors.

The RD3 protein encoded by the *RD3* gene is highly conserved across vertebrates with the human protein consisting of 195 amino acids and sharing 95% sequence identity with other primates, 86% with mouse and rat, 83% with bovine, 67% with chicken, and 50–60% with lower vertebrates including *Danio rerio* (Zebrafish) and *Xenopus tropicalis* (Western clawed frog). Computer algorithms indicate that RD3 lacks any known homology domains or transmembrane segments. RD3 is predicted to have a high α-helix content (∼43%), no β-sheets and considerable disordered regions (**Figure 1**). There are four conserved stretches of predicted α-helices (H1–H4) with the first helix consisting of 34 amino acids and the last helix having 39 amino acids. Additional conserved features include a putative coil–coil region between amino acids 22–54 and several predicted phosphorylation sites.

RD3 has been isolated from retinal homogenates and HEK293 cells and bacteria expressing the recombinant protein (Azadi et al., 2010; Peshenko et al., 2011a). On SDS gels RD3 migrates as a 23 kDa protein consistent with its amino acid sequence. Dynamic light scattering and gel filtration chromatography, however, indicate that purified RD3 in solution exists as a polydispersed oligomeric protein.

TRUNCATION MUTATIONS IN RD3 CAUSE PHOTORECEPTOR DEGENERATION

The *rd3* mouse was one of the first naturally occurring murine strains found to display early onset rod and cone degeneration (Chang et al., 1993). The rate of degeneration varies with the background strain (Linberg et al., 2005; Friedman et al., 2006; Danciger et al., 2008; Molday et al., 2013). The albino RBF/DnJ strain shows the fastest rate of degeneration with only a monolayer of photoreceptor nuclei present 8 weeks after birth. The pigmented In(5) 30RK/J strain displays the slowest rate with some photoreceptors still present after 30 weeks. The Rb(11.13)4Bnr/J strain is intermediate in its rate of degeneration. Rod-derived scotopic electroretinograms (ERG) are measurable in all strains at an early age prior to significant photoreceptor degeneration (∼24–35 days postnatal), but a cone response has only been reported in the In(5) 30RK/J strain (Friedman et al., 2006; Molday et al., 2013). The mutation which causes photoreceptor degeneration in all strains was first reported by Friedman et al. (2006). They identified a homozygous C→T substitution (c.319C→T) in the *Rd3* gene which causes a premature stop codon resulting in a protein lacking the last 99 amino acids.

An extensive human *RD3* mutational screen was carried out on individuals with autosomal dominant and recessive retinal degenerative diseases. A homozygous G → A transition in the donor splice site at the end of exon 2 was found in two siblings from a family with LCA (Friedman et al., 2006). This mutation causes a premature stop codon following codon 99 of the *RD3* gene. The *RD3* gene was the twelfth gene associated with LCA and accordingly this subclass is called LCA12. Subsequent genetic screens revealed homozygous mutations in *RD3* with severely truncated proteins in other LCA families (Preising et al., 2012; Perrault et al., 2013). World-wide genetic screens indicate that mutations in the *RD3* gene causing LCA are rare. In addition to truncation mutations, missense mutations in *RD3* have been observed in individuals with other retinopathies (Friedman et al., 2006). However, additional studies are needed to determine if these mutations are directly responsible for the disease.

A mutation in the canine *Rd3* gene causes rod-cone dysplasia 2 (*rcd2*) in a strain of collies (Kukekova et al., 2009). An insertion in the gene leads to an alteration in the last 61 codons and a further extension of the open reading frame.

Biochemical studies indicate that the truncated RD3 proteins associated with photoreceptor degeneration in the *rd3* mouse and LCA12 patients are highly unstable and non-functional (Friedman et al., 2006; Peshenko et al., 2011a). These studies support a crucial role of the C-terminal segment in the stability and function of RD3.

INTERACTION OF RD3 WITH GC1 AND GC2

RD3 was first detected in a mass-spectrometry-based proteomic analysis of bovine photoreceptor OS (Kwok et al., 2008). Monoclonal and polyclonal antibodies against RD3 confirmed the presence of the 23 kDa RD3 protein in mouse retinal extracts by western blotting (Azadi et al., 2010). These antibodies, however, proved to be problematic for immunolocalizing RD3 in photoreceptors as they failed to consistently label retinal cryosections above background levels due to either the inaccessibility of the epitopes or the low level of RD3 expression. One polyclonal antibody showed some immunoreactivity in outer and inner segment layers above control retinas, but in subsequent studies this observation could not be reproduced (Azadi et al., 2010). Additional studies

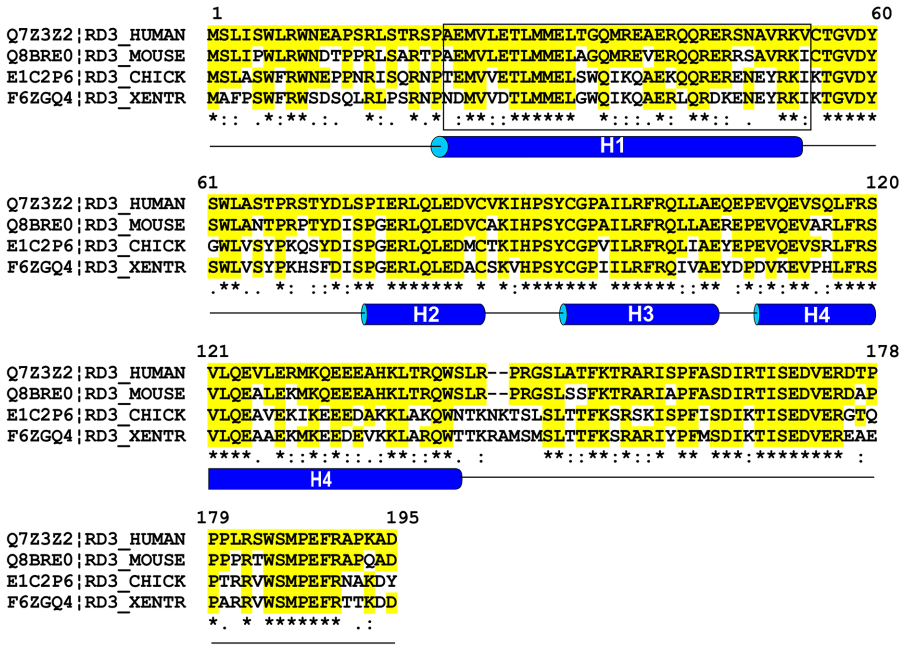

FIGURE 1 | Sequence alignment of RD3 proteins from various vertebrates. Sequences of human, mouse, chick, and *Xenopus tropocalis* RD3 were aligned using Clustal W multiple alignment program. Sequence identities relative to human RD3 are shown in yellow and * and similarities are indicated by (:). Helical predictions were based on the PSIPRED protein structure prediction program and coil–coil domain (enclosed in a rectangle) was predicted using Coils program found in the web-based ExPASy Bioinformatics Resource portal.

are needed to definitively determine the subcellular localization of RD3 in photoreceptor cells.

The first insight into the possible role of RD3 in photoreceptors was obtained from co-immunoprecipitation experiments. A monoclonal antibody to murine RD3 coupled to Sepharose immunoprecipitated GC1 and GC2 together with RD3 from mouse retinal extracts (Azadi et al., 2010). The interaction of RD3 and GC1 was confirmed in co-expression and co-immunoprecipitation studies. When RD3 and GC1 were co-expressed in HEK293 cells, an anti-RD3 antibody co-precipitated GC1 with RD3 and in a reverse experiment an anti-GC1 antibody co-immunoprecipitated RD3 with GC1 confirming the direct interaction between these proteins (Azadi et al., 2010). Analysis of GC1 deletion mutants further indicated that the C-terminus of GC1 is required for binding of RD3.

RD3 IS IMPORTANT FOR THE EXPRESSION AND LOCALIZATION OF GUANYLATE CYCLASES

To determine the significance of the RD3-GC interaction, the expression and localization of GC1 and GC2 in the *rd3* mouse was compared with age-matched wild-type (WT) mice by western blotting and confocal microscopy (Azadi et al., 2010). GC1 and GC2 from WT mouse retina migrated as 120 and 125 kDa proteins on SDS gels, but were absent or present in reduced amounts in extracts from *rd3* mice depending on the strain used for the analysis (Azadi et al., 2010; Molday et al., 2013). At a subcellular level, GC1 and GC2 was localized to the photoreceptor OS of WT mice with GC1 present in rod and cones and GC2 restricted to rod cells as reported previously (Karan et al., 2010). In contrast, GC1 and GC2 immunolabeling was absent in 21-day old Rb(11.13)4Bnr/J *rd3* mice and mislocalized to the inner segment of the In(5)30RK/J strain (Azadi et al., 2010; Cheng and Molday, 2013; Molday et al., 2013). GCAP1 and GCAP2 were detected at a reduced level in *rd3* mice and primarily confined to the inner segments as observed in GC1/GC2 knockout mice (Azadi et al., 2010; Karan et al., 2010). Other photoreceptor OS proteins including the cyclic GMP-gated channel, PDE6, peripherin-2, rhodopsin, and cone arrestin targeted normally to the OS of the *rd3* mice. Gene expression observed by microarray analysis indicated that the expression levels of genes encoding RD3, GC1 and GC2 in 21 day old (Rb(11.13)4Bnr *rd3* mice were similar to age-matched WT mice. Up-regulation of endothelin 2 (*EDn2*), glial fibrillary acid protein (*Gfap*), and complement component factor 1 (*Cf1*) and down-regulation of phosducin (*Pdc*), gap junction protein α5 (*Gja5*) and retinal G protein – coupled receptor (*Rgr*) genes, however, were observed for the *rd3* retina (Cheng and Molday, 2013).

The expression and distribution of GC1 was also examined in the In(5)30RK/J strain of *rd3* mice by immunofluorescence microscopy (Molday et al., 2013). GC1 was detected at reduced levels in this strain and confined primarily to the inner segments where it co-localized with the anti-KDEL ER marker. A small amount of GC1 was detected in the OS layer which may account for the attenuated scotopic and photopic ERGs observed in this strain. Similar mislocalization of GC in the *rcd2* collie has been observed. When the normal murine *Rd3* gene was delivered to photoreceptor cells of either strain of *rd3* mice using adeno-associated virus

(AAV), GC1 and GC2 expressed at levels comparable to that of WT mice and localized normally to the photoreceptor OS layer (Molday et al., 2013). Collectively, these studies indicate that RD3 is required for efficient expression and localization of GCs to the photoreceptor OS.

The effect of RD3 expression on the localization of GC was also examined in transfected culture cells (Azadi et al., 2010). GC1 primarily localized to the ER of transfected cells in the absence of RD3, whereas RD3 co-localized with Rab11 in endosomes. Co-expression of GC1 and RD3 resulted in the exit of GC1 from the ER and colocalization with RD3 in Rab11 containing vesicles. These studies are consistent with the observed effect of RD3 in promoting the exit of GC from the ER in photoreceptor cells.

RD3 INHIBITS GUANYLATE CYCLASE ACTIVITY

In addition to altering the expression level and trafficking of GC, RD3 inhibits its catalytic activity (Peshenko et al., 2011a). In the absence of GCAPs, RD3 expressed in either bacteria or HEK293 cells inhibited the basal and GCAP-activated GC catalytic activity at submicromolar concentrations, but did not alter the Ca^{2+} sensitivity of GCAPs. It remains to be determined if RD3 plays a significant role in modulating the activity of GCs during phototransduction. It is possible that RD3 only plays an important role in inhibiting cyclase activity during the trafficking of GCs within the inner segments. At present the quantity of RD3 in photoreceptors remains to be determined, but in *in vitro* measurements, RD3 at nanomolar concentrations competitively inhibited the activation of GC by GCAP (Peshenko et al., 2011a).

The effect of the RD3 mutation (F100ter) associated with LCA12 and other possible disease-linked missense mutations on the interaction of RD3 with GC was studied (Peshenko et al., 2011a). The F100ter and the G57V mutants were undetectable when expressed in HEK293 cells, but were expressed at significant levels in *E. Coli*. Other missense mutants (K130M, G35R, R68W, W6R/E23D) expressed at levels comparable to WT RD3 and bound GC1. The F100ter mutant had no effect of the cyclase activity, whereas the missense mutations inhibited GC activity to varying degrees. The W6R/E23D and G35R mutations inhibited the cyclase activity at a similar concentration as WT RD3, whereas the R68W, K130M and G57V were less effective. It remains to be determined if these missense mutations in RD3 alter the ability of RD3 to function in GC trafficking in photoreceptors.

MODELS FOR THE ROLE OF RD3 IN PHOTORECEPTORS

Studies carried out to date suggest that RD3 serves two roles in photoreceptor cells. A primary function of RD3 is to facilitate the exit of GC from the ER and its trafficking to the photoreceptor cilium (**Figure 2**). RD3 may also be involved in the trafficking of GC within the cilium although this remains to be determined.

A second function of RD3 is to inhibit GC catalytic activity (Peshenko et al., 2011a). The inhibition of GC activity by RD3 may be crucial for insuring that cGMP is not produced in the inner segment of photoreceptors cells during the trafficking of GC to the outer segment. In the absence of RD3 inhibition, GC could either use up the supply of GTP required for the function of other proteins including small G-proteins such as Rabs required for protein vesicle trafficking or overproduction of cGMP in the inner segment could be toxic to photoreceptors. In this regard it is interesting to note that an early study reported that retinal extracts from the *rcd2* collie showed a 10 times higher level of cGMP than control retinas during a 2–8 week period with only 25% reduction in PDE activity (Woodford et al., 1982).

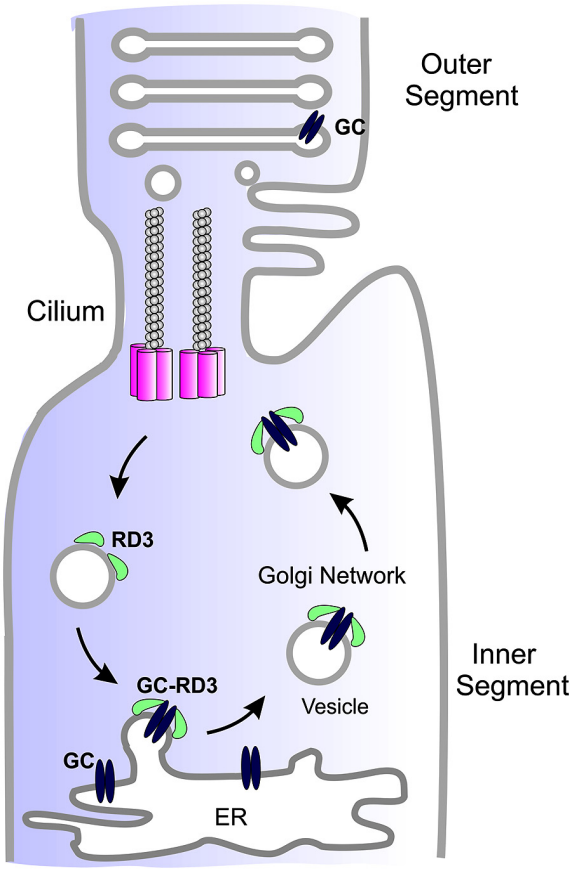

FIGURE 2 | Simplified diagram showing the role of RD3 in GC trafficking. GC synthesized in the endoplasmic reticulum (ER) of photoreceptor inner segments binds to RD3 on the cytoplasmic side of the ER membrane. This interaction may induce membrane curvature required for the budding of GC-RD3 from the ER in the form of small vesicles. RD3 also inhibits the cyclase activity of GC. The RD3-GC complex together with other adaptor proteins is translocated through the Golgi to the base of the connecting cilium where GC perhaps in the absence of RD3 is transported through the cilium to the base of the outer segments where it is incorporated into disk membranes. At some point RD3 dissociates from GC possibly through phosphorylation or other post-translational modifications or protein–protein interaction. RD3 associated with endosomes is returned to the ER to initiate another cycle of RD3-mediated GC transport.

ROLE OF RD3 IN PHOTORECEPTOR CELL SURVIVAL

The mechanism by which loss in RD3 causes photoreceptor degeneration remains to be determined. Here we discuss two possible mechanisms. The first mechanism is centered on the role of GC and cGMP in maintaining calcium homeostasis in photoreceptors. It is generally known that too high or too low Ca^{2+} levels

can be toxic to cells (Fain, 2006). Calcium homeostasis in OS is maintained by the influx of Ca^{2+} through the cGMP-gated channels and the efflux through the Na/Ca-K exchanger. In the absence of GC in the OS, cGMP will not be produced resulting in permanent closure of cGMP-gated channels and a reduction in intracellular Ca^{2+} below a threshold required for photoreceptor survival. In this case the mechanism of photoreceptor degeneration in the *rd3* mouse and LCA12 patients would be similar to photoreceptor degeneration in the GC1/GC2 knockout mouse and LCA1 patients. Direct comparison of the rate of photoreceptor degeneration in the *rd3* mouse and GC1/GC2 knockout mouse is complicated by the large variation in the rate of degeneration observed for different strains of *rd3* mice, although in general degeneration in the *rd3* mouse appears to be more rapid. Comparison of LCA12 with LCA1 patients is complicated by the presence of functional GC2 in rod photoreceptors of LCA1 patients. However, limited clinical assessment of these patients suggests that LCA12 is more severe (Preising et al., 2012; Perrault et al., 2013).

A second mechanism involves the role of RD3 in the inhibition of GC activity (Peshenko et al., 2011a). In the absence of RD3, GC in photoreceptor inner segments is likely to be active in catalyzing the production of cGMP (Woodford et al., 1982). Elevated cGMP levels can be toxic through the unregulated activation of cGMP-dependent enzymes. High cGMP levels have been implicated in photoreceptor cell death in the *rd1* and *rd10* mice linked to mutations in the β-subunit of PDE (Bowes et al., 1990; Chang et al., 2007), mice deficient in the A3 subunit of the cone cGMP-gated channel (Xu et al., 2013), and transgenic mice harboring an Y99C mutation in GCAP1 (Olshevskaya et al., 2004). Both the loss in RD3 chaperone activity and inhibition of GC activity may contribute to photoreceptor degeneration.

ACKNOWLEDGMENTS

This work was supported by grants from the National Institutes of Health (EY02422-33) and the Macular Vision Research Foundation.

REFERENCES

Azadi, S., Molday, L. L., and Molday, R. S. (2010). RD3, the protein associated with Leber congenital amaurosis type 12, is required for guanylate cyclase trafficking in photoreceptor cells. *Proc. Natl. Acad. Sci. U.S.A.* 107, 21158–21163. doi: 10.1073/pnas.1010460107

Baehr, W., Karan, S., Maeda, T., Luo, D. G., Li, S., Bronson, J. D., et al. (2007). The function of guanylate cyclase 1 and guanylate cyclase 2 in rod and cone photoreceptors. *J. Biol. Chem.* 282, 8837–8847. doi: 10.1074/jbc.M610369200

Bowes, C., Li, T., Danciger, M., Baxter, L. C., Applebury, M. L., and Farber, D. B. (1990). Retinal degeneration in the rd mouse is caused by a defect in the beta subunit of rod cGMP-phosphodiesterase. *Nature* 347, 677–680. doi: 10.1038/347677a0

Chang, B., Hawes, N. L., Pardue, M. T., German, A. M., Hurd, R. E., Davisson, M. T., et al. (2007). Two mouse retinal degenerations caused by missense mutations in the beta-subunit of rod cGMP phosphodiesterase gene. *Vision Res.* 47, 624–633. doi: 10.1016/j.visres.2006.11.020

Chang, B., Heckenlively, J. R., Hawes, N. L., and Roderick, T. H. (1993). New mouse primary retinal degeneration (rd-3). *Genomics* 16, 45–49. doi: 10.1006/geno.1993.1138

Cheng, C. L., and Molday, R. S. (2013). Changes in gene expression associated with retinal degeneration in the rd3 mouse. *Mol. Vis.* 19, 955–969.

Chuang, J. Z., Zhao, Y., and Sung, C. H. (2007). SARA-regulated vesicular targeting underlies formation of the light-sensing organelle in mammalian rods. *Cell* 130, 535–547. doi: 10.1016/j.cell.2007.06.030

Danciger, M., Ogando, D., Yang, H., Matthes, M. T., Yu, N., Ahern, K., et al. (2008). Genetic modifiers of retinal degeneration in the rd3 mouse. *Invest. Ophthalmol. Vis. Sci.* 49, 2863–2869. doi: 10.1167/iovs.08-1715

Deretic, D., Williams, A. H., Ransom, N., Morel, V., Hargrave, P. A., and Arendt, A. (2005). Rhodopsin C terminus, the site of mutations causing retinal disease, regulates trafficking by binding to ADP-ribosylation factor 4 (ARF4). *Proc. Natl. Acad. Sci. U.S.A.* 102, 3301–3306. doi: 10.1073/pnas.0500095102

Dizhoor, A. M., Olshevskaya, E. V., Henzel, W. J., Wong, S. C., Stults, J. T., Ankoudinova, I., et al. (1995). Cloning, sequencing, and expression of a 24-kDa Ca(2+)-binding protein activating photoreceptor guanylyl cyclase. *J. Biol. Chem.* 270, 25200–25206. doi: 10.1074/jbc.270.42.25200

Dizhoor, A. M., Olshevskaya, E. V., and Peshenko, I. V. (2010). Mg^{2+}/Ca^{2+} cation binding cycle of guanylyl cyclase activating proteins (GCAPs): role in regulation of photoreceptor guanylyl cyclase. *Mol. Cell. Biochem.* 334, 117–124. doi: 10.1007/s11010-009-0328-6

Fain, G. L. (2006). Why photoreceptors die (and why they don't). *Bioessays* 28, 344–354. doi: 10.1002/bies.20382

Fariss, R. N., Molday, R. S., Fisher, S. K., and Matsumoto, B. (1997). Evidence from normal and degenerating photoreceptors that two outer segment integral membrane proteins have separate transport pathways. *J. Comp. Neurol.* 387, 148–156. doi: 10.1002/(SICI)1096-9861(19971013)387:1<148::AID-CNE12>3.0.CO;2-Q

Friedman, J. S., Chang, B., Kannabiran, C., Chakarova, C., Singh, H. P., Jalali, S., et al. (2006). Premature truncation of a novel protein, RD3, exhibiting subnuclear localization is associated with retinal degeneration. *Am. J. Hum. Genet.* 79, 1059–1070. doi: 10.1086/510021

Gorczyca, W. A., Gray-Keller, M. P., Detwiler, P. B., and Palczewski, K. (1994). Purification and physiological evaluation of a guanylate cyclase activating protein from retinal rods. *Proc. Natl. Acad. Sci. U.S.A.* 91, 4014–4018. doi: 10.1073/pnas.91.9.4014

Gray-Keller, M. P., and Detwiler, P. B. (1994). The calcium feedback signal in the phototransduction cascade of vertebrate rods. *Neuron* 13, 849–861. doi: 10.1016/0896-6273(94)90251-8

Helten, A., Saftel, W., and Koch, K. W. (2007). Expression level and activity profile of membrane bound guanylate cyclase type 2 in rod outer segments. *J. Neurochem.* 103, 1439–1446. doi: 10.1111/j.1471-4159.2007.04923.x

Karan, S., Frederick, J. M., and Baehr, W. (2010). Novel functions of photoreceptor guanylate cyclases revealed by targeted deletion. *Mol. Cell. Biochem.* 334, 141–155. doi: 10.1007/s11010-009-0322-z

Karan, S., Tam, B. M., Moritz, O. L., and Baehr, W. (2011). Targeting of mouse guanylate cyclase 1 (Gucy2e) to *Xenopus laevis* rod outer segments. *Vision Res.* 51, 2304–2311. doi: 10.1016/j.visres.2011.09.001

Kelsell, R. E., Gregory-Evans, K., Payne, A. M., Perrault, I., Kaplan, J., Yang, R. B., et al. (1998). Mutations in the retinal guanylate cyclase (RETGC-1) gene in dominant cone-rod dystrophy. *Hum. Mol. Genet.* 7, 1179–1184. doi: 10.1093/hmg/7.7.1179

Kukekova, A. V., Goldstein, O., Johnson, J. L., Richardson, M. A., Pearce-Kelling, S. E., Swaroop, A., et al. (2009). Canine RD3 mutation establishes rod-cone dysplasia type 2 (rcd2) as ortholog of human and murine rd3. *Mamm. Genome* 20, 109–123. doi: 10.1007/s00335-008-9163-4

Kwok, M. C., Holopainen, J. M., Molday, L. L., Foster, L. J., and Molday, R. S. (2008). Proteomics of photoreceptor outer segments identifies a subset of SNARE and Rab proteins implicated in membrane vesicle trafficking and fusion. *Mol. Cell. Proteomics* 7, 1053–1066. doi: 10.1074/mcp.M700571-MCP200

Lavorgna, G., Lestingi, M., Ziviello, C., Testa, F., Simonelli, F., Manitto, M. P., et al. (2003). Identification and characterization of C1orf36, a transcript highly expressed in photoreceptor cells, and mutation analysis in retinitis pigmentosa. *Biochem. Biophys. Res. Commun.* 308, 414–421. doi: 10.1016/S0006-291X(03)01410-4

Linberg, K. A., Fariss, R. N., Heckenlively, J. R., Farber, D. B., and Fisher, S. K. (2005). Morphological characterization of the retinal degeneration in three strains of mice carrying the rd-3 mutation. *Vis. Neurosci.* 22, 721–734. doi: 10.1017/S0952523805226044

Lowe, D. G., Dizhoor, A. M., Liu, K., Gu, Q., Spencer, M., Laura, R., et al. (1995). Cloning and expression of a second photoreceptor-specific membrane retina guanylyl cyclase (RetGC), RetGC-2. *Proc. Natl. Acad. Sci. U.S.A.* 92, 5535–5539. doi: 10.1073/pnas.92.12.5535

Mazelova, J., Astuto-Gribble, L., Inoue, H., Tam, B. M., Schonteich, E., Prekeris, R., et al. (2009). Ciliary targeting motif VxPx directs assembly of a trafficking module through Arf4. *EMBO J.* 28, 183–192. doi: 10.1038/emboj.2008.267

Molday, L. L., Djajadi, H., Yan, P., Szczygiel, L., Boye, S. L., Chiodo, V. A., et al. (2013). RD3 gene delivery restores guanylate cyclase localization and rescues photoreceptors in the Rd3 mouse model of Leber congenital amaurosis 12. *Hum. Mol. Genet.* 22, 3894–3905. doi: 10.1093/hmg/ddt244

Olshevskaya, E. V., Calvert, P. D., Woodruff, M. L., Peshenko, I. V., Savchenko, A. B., Makino, C. L., et al. (2004). The Y99C mutation in guanylyl cyclase-activating protein 1 increases intracellular Ca^{2+} and causes photoreceptor degeneration in transgenic mice. *J. Neurosci.* 24, 6078–6085. doi: 10.1523/JNEUROSCI.0963-04.2004

Perrault, I., Estrada-Cuzcano, A., Lopez, I., Kohl, S., Li, S., Testa, F., et al. (2013). Union makes strength: a worldwide collaborative genetic and clinical study to provide a comprehensive survey of RD3 mutations and delineate the associated phenotype. *PLoS ONE* 8:e51622. doi: 10.1371/journal.pone.0051622

Perrault, I., Rozet, J. M., Calvas, P., Gerber, S., Camuzat, A., Dollfus, H., et al. (1996). Retinal-specific guanylate cyclase gene mutations in Leber's congenital amaurosis. *Nat. Genet.* 14, 461–464. doi: 10.1038/ng1296-461

Peshenko, I. V., and Dizhoor, A. M. (2006). Ca^{2+} and Mg^{2+} binding properties of GCAP-1. Evidence that Mg^{2+}-bound form is the physiological activator of photoreceptor guanylyl cyclase. *J. Biol. Chem.* 281, 23830–23841. doi: 10.1074/jbc.M600257200

Peshenko, I. V., Olshevskaya, E. V., Azadi, S., Molday, L. L., Molday, R. S., and Dizhoor, A. M. (2011a). Retinal degeneration 3 (RD3) protein inhibits catalytic activity of retinal membrane guanylyl cyclase (RetGC) and its stimulation by activating proteins. *Biochemistry* 50, 9511–9519. doi: 10.1021/bi201342b

Peshenko, I. V., Olshevskaya, E. V., Savchenko, A. B., Karan, S., Palczewski, K., Baehr, W., et al. (2011b). Enzymatic properties and regulation of the native isozymes of retinal membrane guanylyl cyclase (RetGC) from mouse photoreceptors. *Biochemistry* 50, 5590–5600. doi: 10.1021/bi200491b

Polans, A., Baehr, W., and Palczewski, K. (1996). Turned on by Ca^{2+}! The physiology and pathology of Ca(2+)-binding proteins in the retina. *Trends Neurosci.* 19, 547–554. doi: 10.1016/S0166-2236(96)10059-X

Preising, M. N., Hausotter-Will, N., Solbach, M. C., Friedburg, C., Ruschendorf, F., and Lorenz, B. (2012). Mutations in RD3 are associated with an extremely rare and severe form of early onset retinal dystrophy. *Invest. Ophthalmol. Vis. Sci.* 53, 3463–3472. doi: 10.1167/iovs.12-9519

Ramamurthy, V., Tucker, C., Wilkie, S. E., Daggett, V., Hunt, D. M., and Hurley, J. B. (2001). Interactions within the coiled-coil domain of RetGC-1 guanylyl cyclase are optimized for regulation rather than for high affinity. *J. Biol. Chem.* 276, 26218–26229. doi: 10.1074/jbc.M010495200

Shyjan, A. W., De Sauvage, F. J., Gillett, N. A., Goeddel, D. V., and Lowe, D. G. (1992). Molecular cloning of a retina-specific membrane guanylyl cyclase. *Neuron* 9, 727–737. doi: 10.1016/0896-6273(92)90035-C

Sung, C. H., and Chuang, J. Z. (2010). The cell biology of vision. *J. Cell Biol.* 190, 953–963. doi: 10.1083/jcb.201006020

Tam, B. M., Moritz, O. L., Hurd, L. B., and Papermaster, D. S. (2000). Identification of an outer segment targeting signal in the COOH terminus of rhodopsin using transgenic *Xenopus laevis*. *J. Cell Biol.* 151, 1369–1380. doi: 10.1083/jcb.151.7.1369

Tam, B. M., Moritz, O. L., and Papermaster, D. S. (2004). The C terminus of peripherin/rds participates in rod outer segment targeting and alignment of disk incisures. *Mol. Biol. Cell* 15, 2027–2037. doi: 10.1091/mbc.E03-09-0650

Woodford, B. J., Liu, Y., Fletcher, R. T., Chader, G. J., Farber, D. B., Santos-Anderson, R., et al. (1982). Cyclic nucleotide metabolism in inherited retinopathy in collies: a biochemical and histochemical study. *Exp. Eye Res.* 34, 703–714. doi: 10.1016/S0014-4835(82)80031-6

Woodruff, M. L., Sampath, A. P., Matthews, H. R., Krasnoperova, N. V., Lem, J., and Fain, G. L. (2002). Measurement of cytoplasmic calcium concentration in the rods of wild-type and transducin knock-out mice. *J. Physiol.* 542, 843–854. doi: 10.1113/jphysiol.2001.013987

Xu, J., Morris, L., Thapa, A., Ma, H., Michalakis, S., Biel, M., et al. (2013). cGMP accumulation causes photoreceptor degeneration in CNG channel deficiency: evidence of cGMP cytotoxicity independently of enhanced CNG channel function. *J. Neurosci.* 33, 14939–14948. doi: 10.1523/JNEUROSCI.0909-13.2013

Yang, R. B., and Garbers, D. L. (1997). Two eye guanylyl cyclases are expressed in the same photoreceptor cells and form homomers in preference to heteromers. *J. Biol. Chem.* 272, 13738–13742. doi: 10.1074/jbc.272.21.13738

Conflict of Interest Statement: The authors declare that the research was conducted in the absence of any commercial or financial relationships that could be construed as a potential conflict of interest.

Received: 28 February 2014; accepted: 29 April 2014; published online: 26 May 2014.
*Citation: Molday LL, Jefferies T and Molday RS (2014) Insights into the role of RD3 in guanylate cyclase trafficking, photoreceptor degeneration, and Leber congenital amaurosis. Front. Mol. Neurosci. **7**:44. doi: 10.3389/fnmol.2014.00044*
This article was submitted to the journal Frontiers in Molecular Neuroscience.

frontiers in
MOLECULAR NEUROSCIENCE

REVIEW ARTICLE
published: 02 June 2014
doi: 10.3389/fnmol.2014.00045

Membrane guanylyl cyclase complexes shape the photoresponses of retinal rods and cones

***Xiao-Hong Wen*[1] *, *Alexander M Dizhoor*[2] *and Clint L Makino*[1]**

[1] *Department of Ophthalmology, Massachusetts Eye and Ear Infirmary and Harvard Medical School, Boston, MA, USA*
[2] *Department of Basic Sciences Research and Pennsylvania College of Optometry, Salus University, Elkins Park, PA, USA*

Edited by:
Wolfgang Baehr, University of Utah, USA

Reviewed by:
Daniele Bottai, University of Milan, Italy
Trevor Lamb, Australian National University, Australia

****Correspondence:***
Xiao-Hong Wen, Department of Ophthalmology, Massachusetts Eye and Ear Infirmary and Harvard Medical School, Boston, MA 02114, USA
e-mail: wenx@meei.harvard.edu

In vertebrate rods and cones, photon capture by rhodopsin leads to the destruction of cyclic GMP (cGMP) and the subsequent closure of cyclic nucleotide gated ion channels in the outer segment plasma membrane. Replenishment of cGMP and reopening of the channels limit the growth of the photon response and are requisite for its recovery. In different vertebrate retinas, there may be as many as four types of membrane guanylyl cyclases (GCs) for cGMP synthesis. Ten neuronal Ca^{2+} sensor proteins could potentially modulate their activities. The mouse is proving to be an effective model for characterizing the roles of individual components because its relative simplicity can be reduced further by genetic engineering. There are two types of GC activating proteins (GCAPs) and two types of GCs in mouse rods, whereas cones express one type of GCAP and one type of GC. Mutant mouse rods and cones bereft of both GCAPs have large, long lasting photon responses. Thus, GCAPs normally mediate negative feedback tied to the light-induced decline in intracellular Ca^{2+} that accelerates GC activity to curtail the growth and duration of the photon response. Rods from other mutant mice that express a single GCAP type reveal how the two GCAPs normally work together as a team. Because of its lower Ca^{2+} affinity, GCAP1 is the first responder that senses the initial decrease in Ca^{2+} following photon absorption and acts to limit response amplitude. GCAP2, with a higher Ca^{2+} affinity, is recruited later during the course of the photon response as Ca^{2+} levels continue to decline further. The main role of GCAP2 is to provide for a timely response recovery and it is particularly important after exposure to very bright light. The multiplicity of GC isozymes and GCAP homologs in the retinas of other vertebrates confers greater flexibility in shaping the photon responses in order to tune visual sensitivity, dynamic range and frequency response.

Keywords: guanylate cyclase, guanylyl cyclase activating protein, Ca^{2+} feedback, Ca^{2+}-binding protein, phototransduction, rod and cone photoreceptors, knockout mouse, neuronal calcium sensors

INTRODUCTION

Unlike most neurons, retinal rods and cones are partially depolarized while at rest (in darkness). Cation channels in the open state permit an influx of Na^{+} and also some Ca^{2+} that is termed the "dark" current. When rods and cones receive light, photon capture by visual pigment within the outer segment is amplified by the subsequent activation of many transducin (G-protein) molecules, each of which stimulate phosphodiesterase (PDE) enzymatic activity. Cyclic GMP (cGMP) hydrolysis leads to closure of cyclic nucleotide-gated (CNG) channels thereby blocking the dark current. The ensuing hyperpolarization of membrane potential spreads through the photoreceptor to reduce neurotransmitter release at the synaptic terminal. To recover quickly from stimulation by light, cGMP, the second messenger that links photon capture to CNG channel opening, must be restored (for reviews on phototransduction, see Luo et al., 2008; Wensel, 2008; Gross and Wensel, 2011; Korenbrot, 2012).

Membrane guanylyl cyclases (GCs) catalyze the synthesis of cGMP. As opposed to other membrane GCs, those of photoreceptors do not respond to extracellular ligands, but instead are subject to regulation by Ca^{2+}-binding, EF-hand bearing, GC activating protein (GCAP) subunits (reviewed in Sharma and Duda, 2012; Koch and Dell'Orco, 2013; Lim et al., 2014). GCAP suppresses synthesis of cGMP by GC in darkness, when intracellular Ca^{2+} is relatively high. After light closes the CNG channels and blocks Ca^{2+} influx, continued extrusion by Na^{+}/K^{+}, Ca^{2+} exchangers lowers intracellular Ca^{2+}. Ca^{2+} dissociates from GCAP allowing it to bind Mg^{2+} instead, whereupon it stimulates GC activity.

Negative feedback onto cGMP synthesis provided by a Ca^{2+} sensing GCAP is likely to have already been in place in very ancient ciliary photoreceptors (reviewed in Lamb, 2013). Two rounds of whole-genome duplications predating the origin of vertebrates could have generated multiple isoforms. A third genome duplication in fish could explain why they have at least four GCs and eight GCAPs (Imanishi et al., 2004), although it is not clear whether all are expressed in photoreceptors (**Figure 1**). The existence of multiple isoforms of GC and GCAP provided a substrate for natural selection to optimize the photon response for particular visual ecologies. Where an overly complex system

of GCs and GCAPs was not needed, components were eventually lost. For example in mouse, three frame deletions degraded the GUCA1C gene for GCAP3 into a pseudogene (Imanishi et al., 2002). But multiple GCs and GCAPs were retained in some species and were possibly even supplemented with GC inhibitory protein (GCIP; **Figure 1**), that inhibits GC at high Ca^{2+} but does not stimulate it at low Ca^{2+} (Li et al., 1998), and unrelated S100 proteins that stimulate GC1 at high Ca^{2+} (reviewed by Sharma et al., 2014), to tune GC synthesis in order to meet more challenging demands on vision. Over 400 million years of evolution, GCAP1 and GCAP2 genes are ubiquitously preserved in mammals in a tail-to-tail array (Surguchov et al., 1997). In human, there are two isoforms of GCs, RetGC1, and RetGC2 (Lowe et al., 1995), and two isoforms of GCAPs (GCAP1 and GCAP2) in rods (Dizhoor et al., 1994; Palczewski et al., 1994), while at least some cones express an additional GCAP3 (Haeseleer et al., 1999) and possibly only one type of GC (Karan et al., 2010). Three types of GCs and six types of GCAPs are expressed in zebrafish UV cones (Imanishi et al., 2002, 2004; Rätscho et al., 2009), although it remains to be seen whether all are present in the outer segment (**Table 1**). GCs and GCAPs have responsibilities in the inner segment (reviewed in Karan et al., 2010) and synapse of photoreceptors (reviewed by Schmitz, 2014), both of which constitute separate Ca^{2+} compartments. Here, we review the progress that has been made in understanding why so many types of GCs

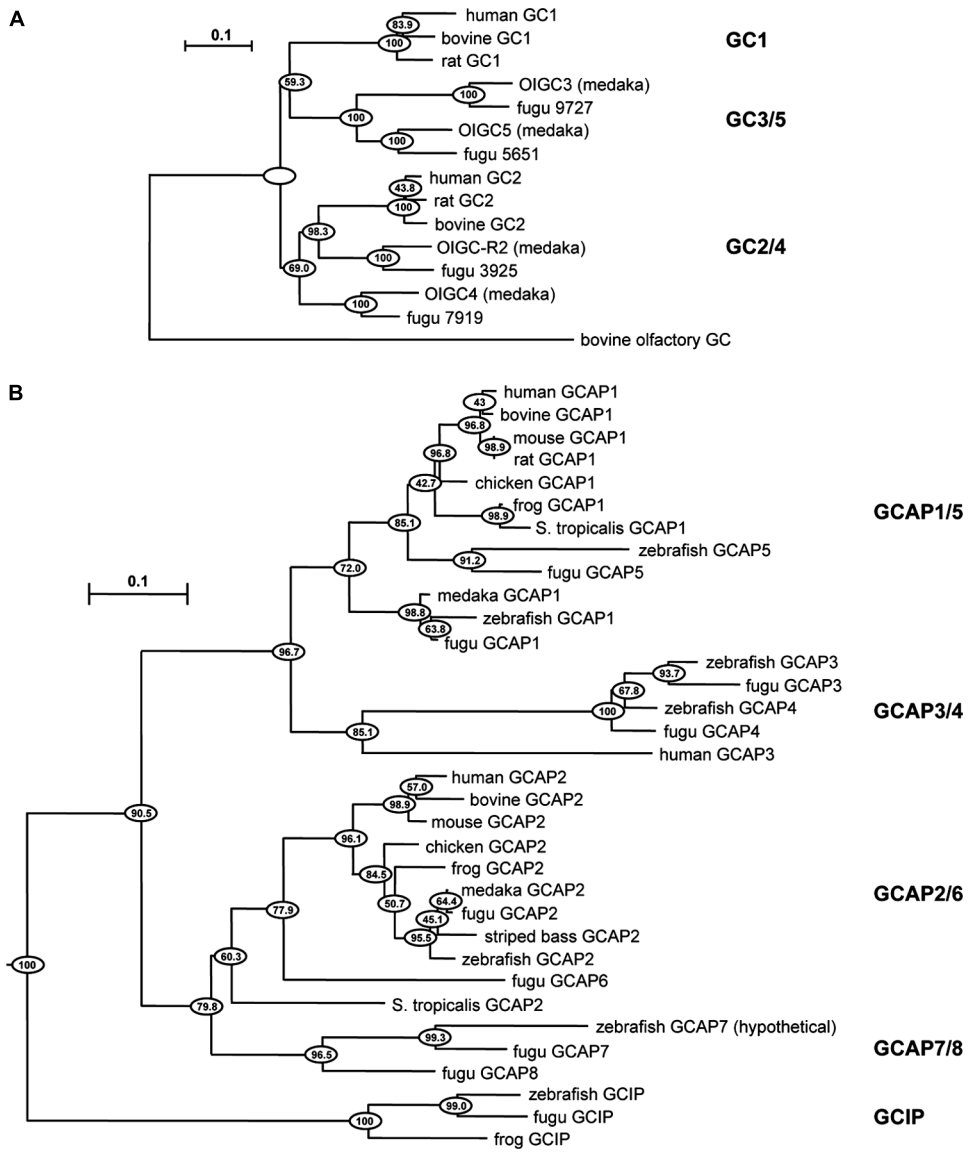

FIGURE 1 | Evolutionary relationships of GC and GCAP isoforms in vertebrates. Horizontal branch lengths for GC **(A)** and GCAP **(B)** isoforms are proportional to genetic distances. The scale bar indicates 0.1 amino acid substitutions per site. Clustering percentages at the nodes derived from 1000 bootstrap resamplings. Modified from Imanishi et al. (2004) with permission from Springer.

Table 1 | Distribution of GCs and GCAPs in photoreceptors of mouse, carp, and zebrafish.

	Mouse		Carp		Zebrafish			
	Rod, μM	Cone	Rod, μM	Cone, μM	Rod	UV cone	B cone	R/G Double cone
GC1	3.2–5.8	+	3.9	–	+	+	–	–
GC2	0.8–1.4	–	0.3	–	+	+	–	–
GC3	–	–	–	–	–	+	+	+
GC5	–	–	–	72	?	?	?	?
GCAP1	+*	+	0.84	–	+	+	–	–
GCAP2	+*	–	1.8	–	+	+	–	–
GCAP3	–	–	–	33	–	+	+	+
GCAP4	–	–	–	–	–	+	+	+
GCAP5	–	–	–	–	–	+	+	+
GCAP7	–	–	–	–	–	+	+	+

*Results on mouse and carp refer to photoreceptor outer segments, while results on zebrafish were obtained from an analysis of mRNA so the proteins may not necessarily localize to the outer segments. No distinctions are made for cones of different spectral type in mouse or carp. Where the concentrations have not been determined, positive expression is marked with (+), lack of expression is marked with (–), unknown status is marked with (?). Expression of GC2 and GCAP2 is negligible in mouse cones [neither GC2 nor GCAP2 is expressed in the all-cone retina of Nrl$^{-/-}$ mouse Xu et al., 2013]. Expression of GCAPs 4 and 7 is presumed to be absent in carp retina based on exceedingly low mRNA levels. Expression of GCAP4 is moderate in zebrafish UV cones. GCAP7 is present in zebrafish cones but at very low levels. *Total concentration of GCAPs 1 and 2 in mouse rods is likely between 3 and 9 μM. From Howes et al., 1998; Imanishi et al., 2002, 2004; Baehr et al., 2007; Rätscho et al., 2009; Takemoto et al., 2009; Peshenko et al., 2011; Scholten and Koch, 2011.*

and GCAPs are involved in phototransduction. First, we will consider a relatively simple system that utilizes predominantly two components, GC1 and GCAP1. The impact of genetically deleting the GCAP revealed its role in shaping the response to light. Next, we will describe how this approach was extended to a more complex system that utilizes two additional components. Finally, an extrapolation will be made to other systems in which genetic studies have not yet been carried out or are still in early stages.

A SIMPLE SYSTEM IN MOUSE CONES

Mouse cones use a simple system for cGMP synthesis with a single type of GC, GC1, coupled almost exclusively to GCAP1 (**Table 1**). To understand how the Ca^{2+} feedback onto cGMP synthesis influences the cone photoresponse, it is useful to simplify the system further by genetic engineering. The tacit assumption is that the genetic manipulation "cleanly" removes a targeted protein(s) in an otherwise undisturbed system. Caution is necessary because full verification is impossible and there may be unpredictable consequences. As an illustration, knockout of GC1 in mice interferes with the expression of many cone phototransduction proteins, including transducin, PDE, GCAP1, and arrestin, and the cones eventually degenerate. Surprisingly, small cone ERG responses to light were detected at 1 month of age (Yang et al., 1999), but they soon vanished over the next few weeks as the cones degenerated (Yang et al., 1999; Baehr et al., 2007).

Genetic deletion of GCAPs (GCAPs$^{-/-}$) may be a more specific experimental perturbation and cones retain good health. **Figure 2A** shows that the single photon response of a GCAPs$^{-/-}$ cone rises normally, but continues to do so for twice as long to finally reach a peak after 220 ms that is 2.7-fold higher than normal (Sakurai et al., 2011). Integration time, calculated as the integral of the response divided by response amplitude, increases by 2.3-fold. Loading a WT cone with a Ca^{2+} buffer to delay the onset of Ca^{2+}-dependent feedback also prolongs its photon response but such treatment does not affect the flash response of a GCAPs$^{-/-}$ cone because GCAP1, the main mediator of the Ca^{2+}-dependent negative feedback onto the phototransduction cascade that dynamically shapes the photon response in mouse cones, is not present.

Since responses to dim steady light summate the responses to individual photons, the large, slow photon responses in GCAPs$^{-/-}$ cones should shift the response-intensity relation for steps of light to light intensities $(2.7 \times 2.3) = 6.2$ times lower. There is such a shift for very weak responses, however, GCAPs$^{-/-}$ cones are about 20-fold more sensitive than wild type (WT) cones at the half maximal response level (**Figure 2B**; Sakurai et al., 2011). The extra shift suggests that the feedback regulation provided by GCAP1 becomes more vigorous when extended exposures to brighter light cause Ca^{2+} to drop lower than the minimum reached during a single photon response. The steeper GCAPs$^{-/-}$ response-intensity relation for steps of light shows that GCAP1 normally enables cones to operate over a wider range of intensities.

Thus GCAP1 restricts the growth and quickens the recovery of the single photon response in mouse cones, making them less sensitive but improving their temporal resolution. GCAP1 also extends the operating range of cones by preventing saturation when cones are exposed to bright, steady illumination.

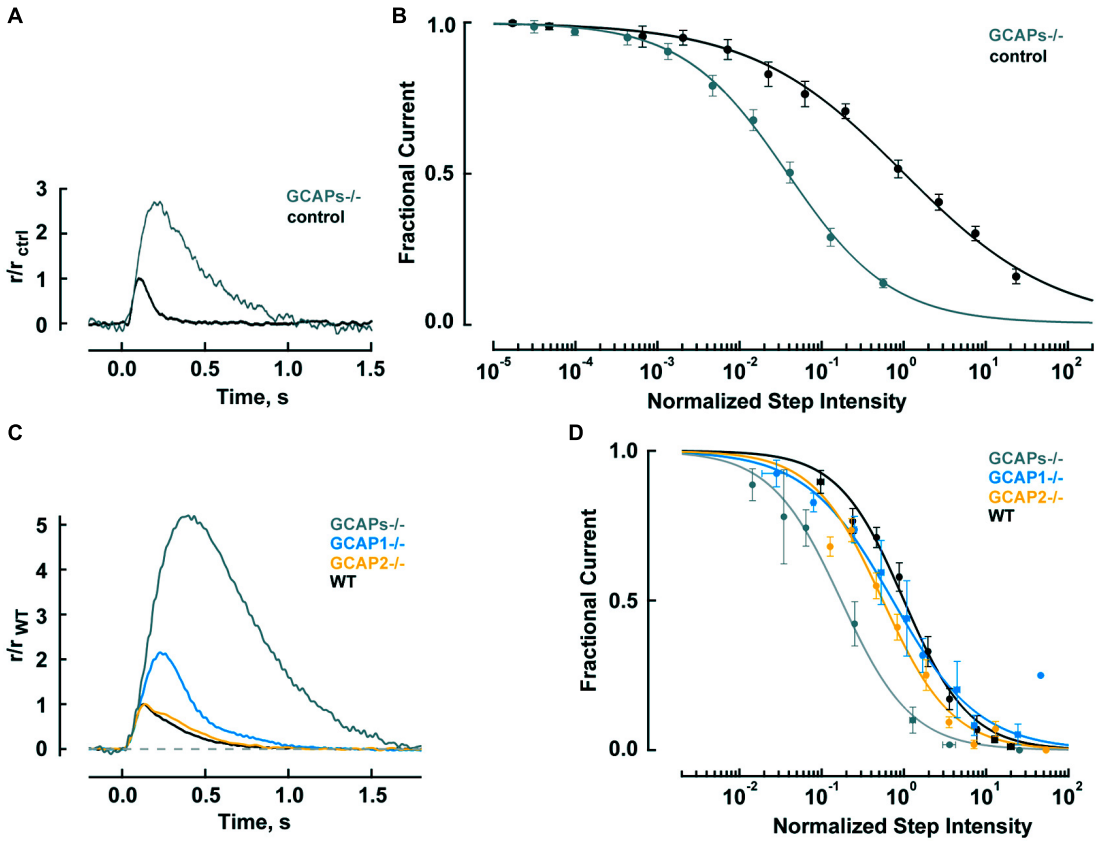

FIGURE 2 | GCAPs shape the photon responses and set the operating ranges of cones and rods. (A) Enlarged, slowed photon response of cones from mice lacking the α-subunit of rod transducin, to render rods unresponsive to light, and both GCAPs (Gnat1$^{-/-}$, GCAPs$^{-/-}$). Control response is from Gnat1$^{-/-}$ cones. Mean responses to flashes given at time zero are normalized by the peak amplitude of the control cone response, 0.01 pA. For reasons that are not known, cone response kinetics of this study were slower than those reported by Cao et al. (2014) in **Table 2**. **(B)** Shift in the operating range of GCAPs$^{-/-}$ cones to lower intensities. Fractional current is that present 2 s after light onset. Step intensities are normalized to the mean intensity suppressing half of the dark current for controls, $I_{1/2}$ = 94,300 hυ μm^{-2} s^{-1}. Continuous lines are fits with the Hill equation for GCAPs$^{-/-}$ and control cones with Hill coefficients of 0.78 and 0.49, respectively. **(A,B)** were adapted from Sakurai et al. (2011) with permission from Society for Neuroscience. **(C)** Mean single photon responses of WT, GCAP1$^{-/-}$, GCAP2$^{-/-}$, and GCAPs$^{-/-}$ rods with amplitudes of 0.47, 1.02, 0.43, and 2.34 pA, respectively, before normalization, includes results from Makino et al. (2008, 2012b). **(D)** Progressive shift in the rod operating range to lower intensities as one or both GCAPs are knocked out. Fractional current is that remaining after 10 s of illumination. The mean $I_{1/2}$ for WT rods was 480 hυ μm^{-2} s^{-1}. Traces show fits with Hill equation with Hill coefficients of: 1.1, 0.8, 1.0, and 1.0 for WT, GCAP1$^{-/-}$, GCAP2$^{-/-}$ and GCAPs$^{-/-}$. **(B,D)** Error bars show SEM.

GREATER COMPLEXITY IN MOUSE RODS

In mouse rod outer segments, two GCs coupled to two GCAPs are responsible for cGMP synthesis (**Table 1**). As with mouse cones, a genetic approach is useful for trying to understand how the system works, but with rods, it is necessary to knock out components individually and in combinations to isolate the physiological function of each component (Yang et al., 1999; Baehr et al., 2007; Makino et al., 2008, 2012b). Mutant mice induced to express transgenes for either GCAP1 or GCAP2 on the GCAPs$^{-/-}$ background are also informative (Mendez et al., 2001; Howes et al., 2002; Pennesi et al., 2003).

Rods are tasked with counting single photons and are therefore designed to be far more sensitive than cones. Major modifications in rods include slowing of the shutoff and recovery phases of the cascade to grant the photon response time to rise to a large size (reviewed in Luo et al., 2008; Gross and Wensel, 2011; Korenbrot, 2012). In mouse, the rod photon response peaks after 140 ms at an amplitude of 0.6 pA, compared to 80 ms and 0.012 pA in cones (**Table 2**). Negative feedback provided by GCAPs is a key factor. The feedback during the single photon response is somewhat more powerful in mouse rods than in mouse cones (**Figure 2**). In the absence of both GCAPs the rod response rises for three times longer than normal to reach an amplitude that is four times larger (Mendez et al., 2001; Burns et al., 2002). The shift in sensitivity for the GCAPs$^{-/-}$ rod is to flashes 6–8 times dimmer compared to WT rods, greater than the shift of 2–3 times for cones after knockout of both GCAPs (**Figure 2A**). When GCAP2 alone is missing (GCAP2$^{-/-}$), the size of the single photon response in rods is normal and the only change is a slightly slower recovery (Makino et al., 2008). Knockout of GCAP1 alone in rods (GCAP1$^{-/-}$) produces a single photon response roughly twice the normal size (Makino et al., 2012b). So between the two GCAPs, GCAP1 must be the

Table 2 | Flash response kinetics and relative sensitivity.

	Rod/cone	a, pA	t_p, ms	t_i, ms	$i_{1/2}$, hυ μm^{-2}
Monkey	Rod	0.7	190	275	16
Mouse	Rod	0.6	142	269	56
Chipmunk	Rod	0.5	116	183	153
Monkey	Cone	0.035	48	49	1744
Mouse	Cone	0.012	82	87	5330
Squirrel	Cone	0.005	29	37	16115
Salamander	S cone	0.3	459	1209	235
	L cone	0.03	155	325	1409

T = 35–38° C for mammalian cells, T = 20–22° C for salamander cells. Amplitude (a), time to peak (t_p) and integration time (t_i) are for the single photon response, typically obtained by analysis of dim flash responses in the linear range. Values for $i_{1/2}$ give the flash strengths at λ_{max} that elicit a half maximal response and are thus inversely proportional to relative sensitivity. Flash responses of different spectral types of mammalian cones do not vary so they were averaged: L, M, S cones for primates; M, S for mouse and squirrel. From Baylor et al., 1984; Schnapf et al., 1990; Perry and McNaughton, 1991; Zhang et al., 2003; Isayama et al., 2006, 2014; Cao et al., 2014. The single photon response amplitude from chipmunk rods studied in Zhang et al. (2003) was provided by T. Kraft, personal communication. Results from mouse were selected from the most recent reports where all parameters were available and in which recording methods were similar: Yang et al., 1999; Mendez et al., 2001; Makino et al., 2004, 2012a,b; Luo and Yau, 2005; Tsang et al., 2006; Krispel et al., 2007; Woodruff et al., 2007; Herrmann et al., 2010.

primary determinant for setting single photon response amplitude. GCAP2 assumes greater importance with stronger flashes (Mendez et al., 2001; Makino et al., 2008). Bright flashes saturate the rod response; the brighter the flash, the longer it takes for the response to emerge from saturation. GCAP2 acts to reduce the saturation time to an extent roughly equivalent to lowering flash strength 3.8-fold (Makino et al., 2008). Loading WT rods with a Ca^{2+} buffer increases the size of the photon response and alters its kinetics but has no effect on GCAPs$^{-/-}$ rods, indicating that as with cones, no other major Ca^{2+} feedback besides GC/GCAP comes into play during the flash response (Burns et al., 2002).

It might seem that enlarged single photon responses should improve the ability of GCAPs$^{-/-}$ and GCAP1$^{-/-}$ rods to count photons. But when GCAPs are not present, there is a 40-fold greater variance of the dark noise (Burns et al., 2002), which would instead diminish the accuracy of detecting photons. Phototransduction noise stems from two sources: discrete noise due to the thermal activations of rhodopsin (Baylor et al., 1980) and continuous noise due to spontaneous PDE activation (Rieke and Baylor, 1996). GCAPs counteract the cGMP depletion caused by both components (Burns et al., 2002). GCAP1$^{-/-}$ rods are also noisy, albeit somewhat less so, whereas GCAP2$^{-/-}$ rods appear to be normal, indicating that GCAP1 is more important for dampening the noise although GCAP2 likely comes into play when GCAP1 is not present (**Figure 3A**).

In steady light, given that stimulation of GC activity by GCAPs increases with light intensity as Ca^{2+} is driven down to lower and lower levels, one might expect GCAPs to extend the operating range of rods by keeping them out of saturation, just as GCAP1 does in cones (**Figure 2B**). But that does not happen; the relation between fractional current and light intensity does not fall more gradually in WT rods compared to GCAPs$^{-/-}$ rods (**Figure 2D**). One explanation might be that something happens at higher light intensities, such as the summation of long lasting, aberrant photon responses (see below), which undermines the efforts of GCAPs in their attempt to help rods evade saturation. Interestingly, knockout of GCAP1$^{-/-}$ does extend the operating range of rods, perhaps compensatory overexpression of GCAP2 boosts the maximal GC activity and the stimulation of GC activity is concentrated at higher intensities (Makino et al., 2012b).

Mammalian rods possess an odd characteristic: about once per several hundred events, rods generate an aberrant single photon response that climbs to an amplitude nearly twofold larger than normal and then remains at that amplitude for an average of 3–6 s, before recovering. In individual trials, the duration is unpredictable and some aberrant responses last for tens of seconds (Baylor et al., 1984; Chen et al., 1995; Kraft and Schnapf, 1998). Apparently, rhodopsin excitations are not always shut off properly by phosphorylation and arrestin binding (Chen et al., 1995, 1999). The aberrant response is enhanced in the absence of GCAP1, to a greater extent than the normal single photon response (Makino et al., 2012b). Even though aberrant responses are relatively rare, they have a significant physiological impact, because they produce a "tail" that delays the recovery after bright flashes. Tails are especially prominent when GCAP1 is missing (**Figure 3B**).

The basis for the different roles of GCAP1 and GCAP2 lies in their Ca^{2+} sensitivities. GCAP1 has a lower affinity for Ca^{2+} than GCAP2 (**Figure 4A**). The $K_{1/2}$ for Ca^{2+} of GCAP1 in the mouse rod is 130–140 nM, while that of GCAP2 is 50–60 nM (Makino et al., 2008; Peshenko et al., 2011). Levels of free Ca^{2+} inside a mouse rod range from 250 nM in darkness to 23 nM in saturating light (**Table 3**). So during the initial fall in Ca^{2+} incurred during the photon response, many more GCAP1 molecules release their Ca^{2+} than GCAP2. The majority of GCAP2 molecules only release their bound Ca^{2+} when intracellular Ca^{2+} plummets, during the saturating response to very bright light. A model illustrating the actions of GCAP1 and GCAP2 is shown in **Figure 4B**. A similar "relay" model was proposed earlier (Koch and Dell'Orco, 2013) but we here prefer the term "recruitment" model to avoid

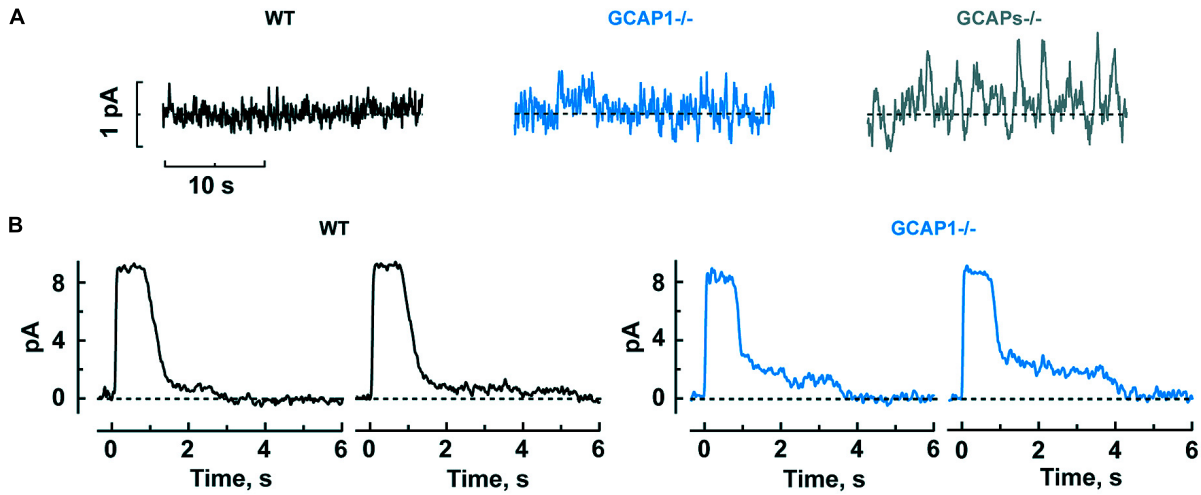

FIGURE 3 | GCAP1 reduces the cGMP fluctuations underlying the dark noise and response tails after exposure to bright light in rods. **(A)** Progressive increase in dark noise after GCAP1 and GCAPs knockout, respectively. **(B)** More prominent photocurrent tails that prolong the recovery after bright light in GCAP1$^{-/-}$ rods. The staircased recovery reflects the stochastic shutoff of aberrant single photon responses generated during the light exposure. Traces are from single trials, where a bright flash was turned on at time zero. Reproduced from Makino et al. (2012b).

conveying inadvertently the impression that GCAP2 stimulation substitutes for GCAP1 stimulation at low Ca^{2+}. "Recruitment" emphasizes that GCAP2 adds to stimulation of GC by GCAP1.

The timing of Ca^{2+} feedback onto GC activity during the photon response is shown in **Figure 5A**. GC activity ascends at the same rate as the electrical response with a ~40 ms delay, then declines sharply and falls briefly to a level less than the dark value. GCAP1's lower affinity to Ca^{2+} makes it the logical "first responder" to the initial decrease in Ca^{2+} (**Figure 4**). Although it could have been the case that GCAP2 responds later because it has a slower release of Ca^{2+} than GCAP1 after a sudden drop in intracellular Ca^{2+}, it will be argued below that both GCAPs are rapid Ca^{2+} sensors. **Figure 5B** shows the rising phases of the photon responses of mouse rods lacking GCAP1, GCAP2, or both. The GCAPs$^{-/-}$ response is the first to diverge at ~80 ms after the flash, while the GCAP2$^{-/-}$ response is the last to diverge. Based on this pattern, it may be inferred that GCAP1 senses the fall in Ca^{2+} and begins to stimulate GC by 80 ms post-flash. GCAP1$^{-/-}$ rods are highly variable in their response waveforms apparently because they upregulate GCAP2 expression and the degree of compensation differs from rod to rod. Rods with the least compensation show response divergence from the WT response nearly as early as the GCAPs$^{-/-}$ response. Accordingly, GCAP2 must respond rapidly to the initial fall in Ca^{2+}. At normal expression levels, the paltry number of GCAP2 molecules responding to the initial fall in Ca^{2+} is unable to make its presence felt. But the mutant rods show that given enough GCAP2, its feedback onto GC does restrain the early rising phase of the response.

As one might expect, knockout of both GCs in rods eliminates the dark current, sabotaging their capacity for phototransduction (Baehr et al., 2007). Deleting GC2 alone seems to have little effect on the dark current or on flash response kinetics and sensitivity in recordings from individual mouse rods (Baehr et al., 2007). In contrast, GC1 deletion compromises the expression of both GCAPs revealing differences between the duties of the two GCs not directly related to phototransduction in the outer segment. There is an increase in flash sensitivity and a delayed time to peak of the photon response (Yang et al., 1999; Baehr et al., 2007), as predicted from the reduced levels of GCAPs (Mendez et al., 2001). Paradoxically, elimination of GC1 also accelerated the rod response recovery (Yang et al., 1999).

In summary, the functional significance to phototransduction of expressing two types of GCs in rods is not yet clear. For GCAPs, there is a division of labor. GCAP1 helps to achieve the proper balance of keeping noise to a minimum while restricting photon response size to optimize the range of flash strengths and light intensities over which the rod operates. Contrary to the situation in cones, the shutoffs of photoexcited visual pigment and activated transducin are slow in rods to allow the photon response to grow. The slow shutoffs pose a problem with bright flashes because the time that the rod stays in saturation gets prolonged. GCAP2 addresses that problem by boosting GC activity to bring the rod out of saturation sooner.

TUNING Ca^{2+} FEEDBACK WITH ADDITIONAL GCs AND GCAPs BETWEEN DIFFERENT ANIMAL SPECIES

While it is generally true that the photon response of rods is larger and slower than that of cones, the response can vary across rods and across cones of different species. The preceding sections described how Ca^{2+} feedback onto cGMP synthesis reduces the size of the single photon response and quickens its kinetics in mouse rods and cones. The extent to which that occurs is dependent upon the selective expressions of GC(s) and GCAP(s). Therefore, variation that exists in the sensitivity and flash response kinetics of rods and cones from

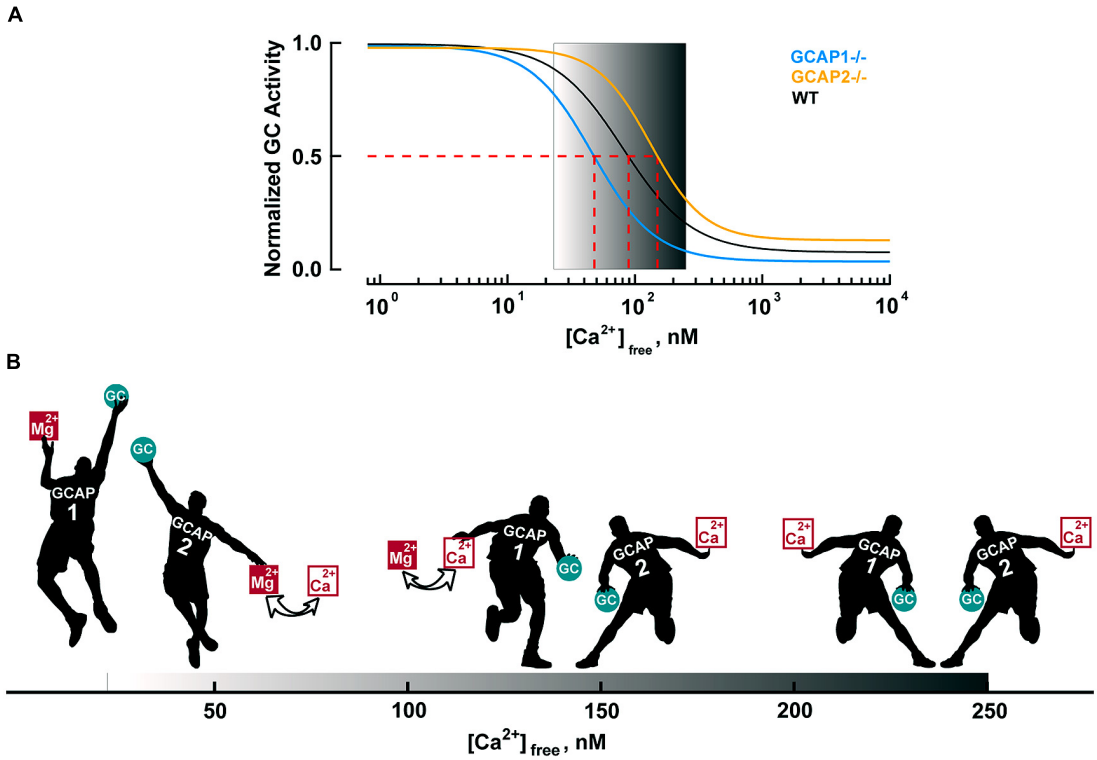

FIGURE 4 | Ca^{2+}-dependent regulation of GC activity in mouse rods. **(A)** Ca^{2+} dependence of GC activity for each GCAP isoform and for the mixture in mouse rods. GC activities are normalized to their respective maxima and follow the Hill equation: $A = (A_{max}–A_{min})/(1 + ([Ca^{2+}]/K_{1/2})^{nH}) + A_{min}$ with nH values of 1.8, 1.6, and 2.1 for WT, GCAP1$^{-/-}$ and GCAP2$^{-/-}$, respectively. The physiological range of internal free Ca^{2+} is 23 nM in the light to 250 nM in the dark, as demarcated by the gradient background. Modified from Makino et al. (2008, 2012b). **(B)** Recruitment model. The physiological free Ca^{2+} concentration range shown by the black progression at the bottom of the figure. In darkness (right), nearly all of the GCAP1 and 2 "players" bind Ca^{2+} and suppress GC activity (only a single representative player of each type is shown). Soon after illumination, both GCAPs respond to the light-induced Ca^{2+} concentration decrease. The disparity in Ca^{2+} affinity causes many more GCAP1 players to release their bound Ca^{2+} than GCAP2 players. In that sense, GCAP1 is the "first responder". Mg^{2+} replaces the released Ca^{2+} on GCAP, prompting it to raise GC activity (Peshenko and Dizhoor, 2004). As intracellular Ca^{2+} falls further, the rest of the GCAP2 players exchange Mg^{2+} for bound Ca^{2+} and they join the GCAP1 players in lifting GC activity. Very few GCAP2s exchange Ca^{2+} for Mg^{2+} during the single photon response, but with bright light, all GCAP1 and GCAP2 players get involved (far left). During the recovery of the response to light, cyclic nucleotide gated (CNG) channels reopen to allow Ca^{2+} back in. GCAP2 players regain their Ca^{2+} first and begin to restrain GC. Gradually, as intracellular Ca^{2+} levels return to baseline, GCAP1 players also regain Ca^{2+} and turn down GC activity.

Table 3 | Dynamics of intracellular free Ca^{2+} in the outer segments of rods and cones.

Type	Time constants, ms	$[Ca^{2+}]_{dark}$, nM	$[Ca^{2+}]_{light}$, nM	$[Ca^{2+}]_{dark}/[Ca^{2+}]_{light}$
Mouse rod	154, 540	250	23	11
Lizard rod	580, 5450	554	50	11
Salamander rod	260, 2200	410–670	30	14–22
Salamander cone	43, 640	410	5	82

Intracellular free Ca^{2+} declines after sudden closure of CNG channels by bright light as the sum of two exponential functions. The two time constants listed are from measurements of fluorescent Ca^{2+} indicators. Electrophysiological measurements of Ca^{2+} exchange are not included because they often do not resolve the second, slower component. T = 37° C for mouse rod, and T = 16–23° C for lizard and salamander cells. From Woodruff et al., 2002; Gray-Keller and Detwiler, 1994; Lagnado et al., 1992, Sampath et al., 1998, 1999.

other vertebrates is likely to arise at least in part from differences in their cGMP synthetic machinery. This section will present a few examples of the variation between species and lay out three mechanisms by which cGMP production could be altered to tune the photon response: by augmenting the amounts of GC and GCAP expressed, by a change in intracellular Ca^{2+} dynamics or by a switch in the types of GCs or GCAPs expressed.

In comparison to mouse rods, primate rods have a single photon response that peaks later whereas the response of chipmunk

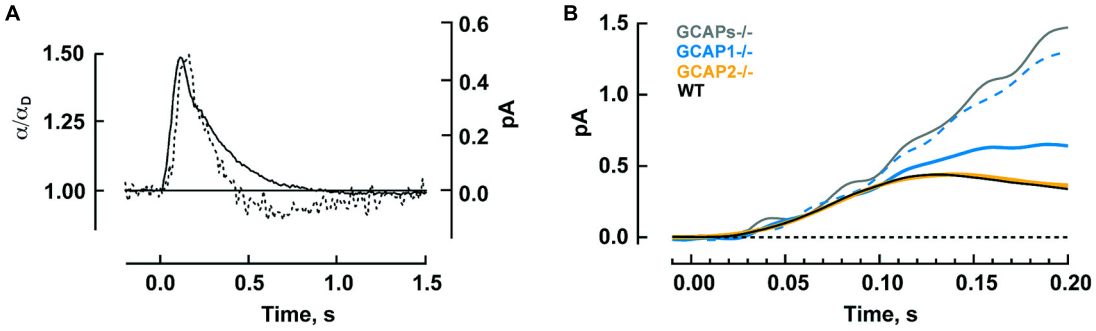

FIGURE 5 | Timeline for GCAP regulated GC activity during the photon response in mouse rods. (A) The calculated time course of GC activity α normalized to the basal value in darkness (broken trace) overlaid on the single photon response (solid trace). The two curves rise with similar slopes to reach their peaks 40 ms apart. Thereafter, GC activity declines sharply. Reproduced from Burns et al. (2002) with permission from Elsevier. **(B)** Divergent rising phases of the photon responses of WT rods and rods lacking either or both GCAPs. The GCAPs$^{-/-}$ response separates from the WT response at 70–80 ms after the flash. Separation of the larger response of those GCAP1$^{-/-}$ rods presumed to have little GCAP2 overexpression (dashed blue trace) is next, at 90–100 ms, followed by the smaller response of those GCAP1$^{-/-}$ rods presumed to have the most GCAP2 overexpression (solid blue trace) at 100–110 ms. The response of GCAP2$^{-/-}$ rods overlays the WT until well after the peak. Includes results from Makino et al. (2008, 2012b).

rods peaks and recovers earlier (**Table 2**). In general, the single photon response of cones is far smaller and peaks much sooner than the response of rods in the same animal. Across species, ground squirrel cones generate smaller, faster photon responses than mouse cones (**Figure 6**; **Table 2**). At present, primate cones are something of an enigma. Their single photon response kinetics are faster than those of mouse yet the single photon response is larger and relative sensitivity is greater. In initial studies on isolated primate retina, cone flash responses exhibited a prominent and reproducible undershoot to the recovery (Baylor et al., 1987; Schnapf et al., 1987; Schnapf et al., 1990). Under the same conditions, cones of other mammals did not generally have undershoots, with the possible exception of chipmunk cones (Zhang et al., 2003). However, in a later study on primate cones, undershoots were absent or only seen occasionally (**Figure 6**) and kinetics inferred for cones in the intact human eye lack the undershoot (van Hateren and Lamb, 2006). Although flash response kinetics are invariant across cone spectral type in mammal (e.g., Baylor et al., 1987 and Cao et al., 2014), there are distinct differences across cone type in fish and amphibians where faster time to peak corresponds with reduced sensitivity (Perry and McNaughton, 1991; Miller and Korenbrot, 1993; Isayama et al., 2006, 2014). After a partial bleach of the visual pigment content, flash responses of salamander L cones develop an undershoot but flash responses of S cones do not (cf. Figures 4–6 of Isayama et al., 2006).

It has been proposed that an enhanced expression of GC in cones accounts, in part, for their faster flash response kinetics and their ability to signal over an enormous range of light intensities (Takemoto et al., 2009). Expression of GC is 17 times higher in carp cones than in rods (**Table 1**) and the basal rate of cGMP synthesis in cones is an order of magnitude higher. The differential appears to be lower in salamander to account for a basal rate that is only ~3-fold higher in their cones compared to their rods (Cornwall and Fain, 1994; Cornwall et al., 1995). But despite the higher basal activity in cones, the fold change in stimulation of GC activity in the light is greater in rods than in cones for both carp and salamander. GC will function in the absence of GCAP, so a lower fold change in GC synthesis at low Ca^{2+} could be achieved by reducing the ratio of GCAP to GC. That turns out not to be the case in carp, indicating that there are quantitative differences in the way that the cGMP synthetic machineries of rods and cones respond to low Ca^{2+} and/or differences in their Ca^{2+} dynamics (Takemoto et al., 2009).

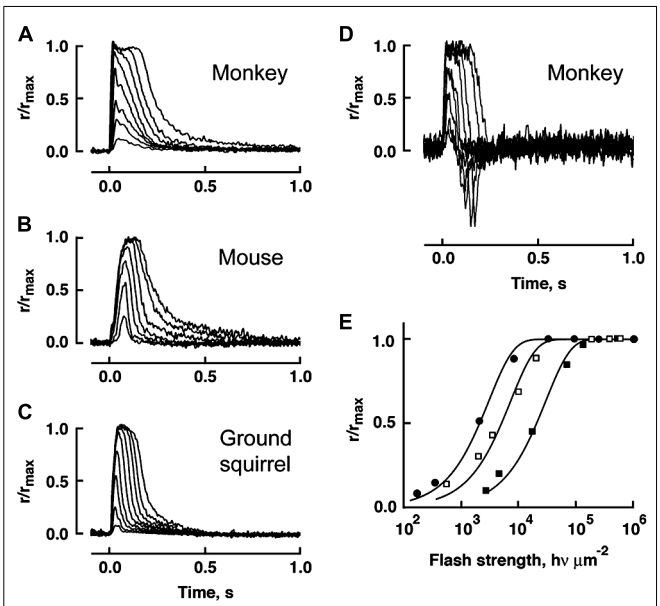

FIGURE 6 | Variation in flash response kinetics and sensitivity across mammalian cones for monkey (A), mouse (B) and squirrel (C). A monkey cone with an undershoot is shown in **D**. **(E)** The stimulus-response relations for the cones in **A–C** showing the order of relative flash sensitivity. The monkey cone (circles) is more sensitive than the mouse cone (open squares), which is more sensitive than the squirrel cone (filled squares). Modified with permission from Cao et al. (2014).

Dissimilarities in the operation of the same cGMP synthetic machinery may exist across photoreceptors because of how they

handle Ca^{2+}. Ca^{2+} dynamics in the outer segment depend upon the rates of Ca^{2+} entry through the CNG channel and removal by a Na^+/K^+, Ca^{2+} exchanger, as well as Ca^{2+} buffering and outer segment surface to volume ratio. In cones, the fraction of circulating current into the outer segment carried by Ca^{2+} is roughly twice that in rods, due to a greater permeability of the cone CNG channel for Ca^{2+} (Nakatani and Yau, 1988; Perry and McNaughton, 1991; Ohyama et al., 2000). It is not clear whether the cone exchanger operates at a faster rate than the rod exchanger, but surface to volume is greater in cone outer segments and their time constant for Ca^{2+} extrusion is faster (Sampath et al., 1999; Paillart et al., 2007). As a result, $[Ca^{2+}]$ changes more rapidly and the fold change in Ca^{2+} levels is bigger in cones than in rods (**Table 3**). In salamander, a faster rate of Ca^{2+} extrusion in L cones than in S cones may contribute to faster response kinetics of L cones (Perry and McNaughton, 1991). In both salamander rods and cones, the dark level of Ca^{2+} is higher than in mouse rods, and in salamander cone, the light induced fall in Ca^{2+} is to 5 nM, a lower level than that in mouse rod, 23 nM (Sampath et al., 1999; Woodruff et al., 2002). For feedback on cGMP synthesis to operate over the full range of Ca^{2+} concentrations, the choice of GCAP(s) expressed will need to be based in part on Ca^{2+} affinity.

The occurrence of isoforms of GC and GCAP allows for adjustments to be made in their biochemical properties: $K_{1/2}$ for Ca^{2+}, cooperativity for Ca^{2+} binding, maximal and basal rates of cGMP synthetic activity. Further flexibility stems from having maximal stimulation of GC depend on the pairing of a GC with specific GCAP isoforms. The unstimulated rate of cGMP synthesis by mouse GC1 is nearly 10-fold less than that of GC2. But stimulation of GC1 activity by GCAP1 and GCAP2 is 28-fold and 13-fold, respectively, whereas for GC2 activity, it is only sixfold and fivefold, respectively (Peshenko et al., 2011). In some cases, the effects of GCAPs on GC are species dependent. Zebrafish GCAP5 will stimulate carp rod GCs severalfold at low Ca^{2+} concentration but has little effect on carp cone GC (Takemoto et al., 2009). The 6 zebrafish GCAPs differ in the degree to which they will stimulate bovine rod GC activity, ranging from 1.5- to 13-fold (**Figure 7**), but stimulation of zebrafish GC3 by GCAPs 3–5 and 7 is more uniform at ∼2-fold (Fries et al., 2013). Carp GCAP1 stimulates carp GC preparations consisting mostly of GC1 to a greater extent than GCAP2 (Takemoto et al., 2009), which is just the opposite of the effect of these zebrafish GCAPs on bovine GC (Scholten and Koch, 2011). These comparisons do not carry physiological significance, nonetheless, it is clear that switching GC and GCAP types is important for setting the basal rate of cGMP synthesis at high Ca^{2+}, the maximal rate at low Ca^{2+}, and the fold activation. In contrast to mouse cones that express GC1 alone, mouse rods add a second GC with a ratio of GC1/GC2 of (4:1) (Peshenko et al., 2011), similar to the (3:1) ratio in bovine rods (Skiba et al., 2013). It should be noted that these recent determinations indicate that the fraction of RetGC2 in mammalian rods is much higher than previously thought (Hwang et al., 2003; Helten et al., 2007).

GCAPs also vary in their $K_{1/2}$ for Ca^{2+} (Hwang et al., 2003; Peshenko et al., 2011), a property that would appear to be important for optimizing feedback onto cGMP synthesis to the light induced fall in Ca^{2+}. For example, with $K_{1/2}$ values of 130–140 nM and 50–60 nM (Makino et al., 2008; Peshenko et al., 2011), mouse GCAPs 1 and 2 provide little or no incremental activation of GC below ∼10 nM (**Figure 4A**), but intracellular $[Ca^{2+}]$ in salamander cones falls to 5 nM upon exposure to bright light. So another GCAP with lower $K_{1/2}$ for Ca^{2+} is needed if cGMP synthetic rate is to increase over the entire Ca^{2+} range. $K_{1/2}$ values for zebrafish GCAPs 1–3 cluster at about 30 nM (**Figure 7**). It remains to be seen whether lower values are possible. Certainly GCAPs, e.g., zGCAPs 4,5, can have $K_{1/2}$ values higher than those of mouse GCAPs (**Figure 7**), but while such GCAPs may be useful for photoreceptors of lizards and salamanders (**Table 3**), they cause degenerative retinal disease in mammals (reviewed in Behnen et al., 2010). Ca^{2+}-dependent activation of GC by GCAPs is cooperative (reviewed in Luo et al., 2008; Gross and Wensel, 2011; Korenbrot, 2012) but so far, there is no evidence for differences in their cooperativity (e.g., Peshenko and Dizhoor, 2004) or in the rapidity of their response to low Ca^{2+} (see above). Given the differences in the composition of their cGMP machineries (**Table 1**), it may be predicted that the physiological properties of zebrafish cones will vary with spectral type.

The selectivity rules for forming GC complexes are not completely understood. The apparent affinity of mouse GC2 is slightly higher for GCAP2 than for GCAP1 *in vitro* (Peshenko et al., 2011), yet in living mouse rods, regulation of RetGC2 is heavily dominated by GCAP2 with very little, if any, contribution from GCAP1 (Olshevskaya et al., 2012). Apparently, the selectivity mechanism taking place *in vivo* is not governed strictly by binding affinity observed *in vitro*. Thus while the Ca^{2+} sensitivity of the regulation is determined by the type of GCAP rather than isozyme of the cyclase (Peshenko et al., 2011), the type of GC expressed could shift the GCAP dominance and the Ca^{2+} sensitivity.

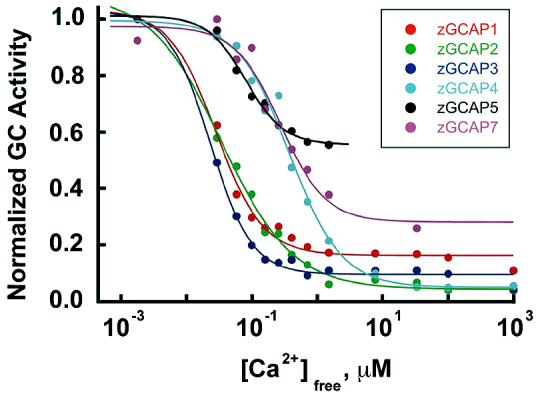

FIGURE 7 | Ca^{2+} dependence and extent of GC activation by zebrafish GCAPs. Reconstituted zebrafish GCAPs were assayed *in vitro* against bovine rod outer segment membranes that were stripped of native GCAPs but contained a mixture of GC1 and GC2, with GC1 predominating. Activity is plotted relative to the maximum rate for each isoform. $K_{1/2}$ values are 30, 35, 25, 520, 440 and 180 nM, and the fold activation values are 3, 10, 6, 13, 1.5, and 2 for zGCAP1-5 and 7, respectively. From Scholten and Koch (2011).

It may be argued that Nature could have given mouse rods a single GCAP having a $K_{1/2}$ for Ca^{2+} that matches the value obtained by their mixture of GCAPs 1 and 2. This path was not chosen, perhaps because the flexibility of a mixture of components allowed for adjustments to be made on a shorter evolutionary time scale to accommodate other changes in the phototransduction cascade, as rods evolved as photoreceptors (Lamb, 2013).

On a much shorter time scale, relevant to the lifetime of an individual, the complexity of a mixture of components leaves open many options for plasticity. The absence of GCAP5 transcripts in zebrafish until 15 dpf (Rätscho et al., 2009), even though at least some cones are present by 3 dpf suggests a changeover in the type of GCAP expressed with age. Since each GC has a rank order of preference for GCAPs with which it will form a complex (Takemoto et al., 2009; Peshenko et al., 2011; Scholten and Koch, 2011; Olshevskaya et al., 2012), relative expression levels of each GCAP may be a factor in determining which GC/GCAP complexes predominate. In zebrafish cones, GCAP3 expression exceeds GC3 expression by an order of magnitude, yet there is no change in optomotor behavior upon knockdown of GCAP3 (Fries et al., 2013). Presumably, GCAP3 is replaced with a GCAP having similar properties. However, it is possible that reduced expression of a different GCAP would result in greater incorporation of GCAP3 with a change in visual function. In mice, knockout of GCAP2 has no effect on GCAP1 expression, but knockout of GCAP1 drives an increase in GCAP2 expression with a greater fractional incorporation of GCAP2 into GC complexes that yields a higher maximal GC activity at low Ca^{2+} (Makino et al., 2012b). It is tempting to speculate that GCAP1 expression may fall under transcriptional control by some conditions. Exposure to bright light reduced PDEα mRNA levels in mice by twofold (Krishnan et al., 2008) and PDEα and PDEβ protein levels in rat by threefold (Hajkova et al., 2010). In rat, there were no changes in GC1 (GC-E) expression; other cGMP synthetic machinery components were not reported. Then unless another GC activity went down, cGMP levels would have risen. GCAPs are sensitive to the $[Mg^{2+}]$, which allows them to maintain their cyclase activating conformation in the light and affects the $[Ca^{2+}]$ at which they de-activate GC (Peshenko and Dizhoor, 2004). However, evidence so far indicates that internal $[Mg^{2+}]$ does not change in rods or in cones upon exposure to light and remains in the vicinity of 1 mM (Chen et al., 2003). So while the potential exists for changes in the choice of GC or GCAP expressed and in their relative levels of expression during development or in response to environmental conditions, the issue of plasticity is at present, unresolved.

Evolution has favored the occurrence of multiple isoforms of GCAPs that vary in their Ca^{2+} affinity and GCs with different activities and preferences for the type of GCAP bound. By expressing selected components and regulating their levels of expression, vertebrates "design" the cGMP synthetic machinery in their photoreceptors in order to adjust their physiological responses to light stimuli. The possibility exists for plasticity during development or on a shorter time scale to meet changing visual demands.

ACKNOWLEDGMENTS

This work was supported by the Howe Laboratory Endowment of the Massachusetts Eye and Ear Infirmary, Research to Prevent Blindness, National Eye Institute EY014104, EY011522. Alexander M. Dizhoor is the Martin and Florence Hafter Chair Professor of Pharmacology. The authors bear sole responsibility for the contents herein. The views expressed do not necessarily convey those of the National Eye Institute.

REFERENCES

Baehr, W., Karan, S., Maeda, T., Luo, D.-G., Li, S., Bronson, J. D., et al. (2007). The function of guanylate cyclase 1 and guanylate cyclase 2 in rod and cone photoreceptors. *J. Biol. Chem.* 282, 8837–8847. doi: 10.1074/jbc.M610369200

Baylor, D. A., Matthews, G., and Yau, K.-W. (1980). Two components of electrical dark noise in toad retinal rod outer segments. *J. Physiol.* 309, 591–621.

Baylor, D. A., Nunn, B. J., and Schnapf, J. L. (1984). The photocurrent, noise and spectral sensitivity of rods of the monkey *Macaca fascicularis*. *J. Physiol.* 357, 575–607.

Baylor, D. A., Nunn, B. J., and Schnapf, J. L. (1987). Spectral sensitivity of cones of the monkey *Macaca fascicularis*. *J. Physiol.* 390, 145–160.

Behnen, P., Dell'Orco, D., and Koch, K.-W. (2010). Involvement of the calcium sensor GCAP1 in hereditary cone dystrophies. *Biol. Chem.* 391, 631–637. doi: 10.1515/BC.2010.063

Burns, M. E., Mendez, A., Chen, J., and Baylor, D. A. (2002). Dynamics of cyclic GMP synthesis in retinal rods. *Neuron* 36, 81–91. doi: 10.1016/S0896-6273(02)00911-X

Cao, L.-H., Luo, D.-G., and Yau, K.-W. (2014). Light responses of primate and other mammalian cones. *Proc. Natl. Acad. Sci. U.S.A.* 111, 2752–2757. doi: 10.1073/pnas.1400268111

Chen, C., Nakatani, K., and Koutalos, Y. (2003). Free magnesium concentration in salamander photoreceptor outer segments. *J. Physiol.* 553, 125–135. doi: 10.1113/jphysiol.2003.053280

Chen, C. K., Burns, M. E., Spencer, M., Niemi, G. A., Chen, J., Hurley, J. B., et al. (1999). Abnormal photoresponses and light-induced apoptosis in rods lacking rhodopsin kinase. *Proc. Natl. Acad. Sci. U.S.A.* 96, 3718–3722. doi: 10.1073/pnas.96.7.3718

Chen, J., Makino, C. L., Peachey, N. S., Baylor, D. A., and Simon, M. I. (1995). Mechanisms of rhodopsin inactivation in vivo as revealed by a COOH-terminal truncation mutant. *Science* 267, 374–377. doi: 10.1126/science.7824934

Cornwall, M. C., and Fain, G. L. (1994). Bleached pigment activates transduction in isolated rods of the salamander retina. *J. Physiol.* 480, 261–279.

Cornwall, M. C., Matthews, H. R., Crouch, R. K., and Fain, G. L. (1995). Bleached pigment activates transduction in salamander cones. *J. Gen. Physiol.* 106, 543–557. doi: 10.1085/jgp.106.3.543

Dizhoor, A. M., Lowe, D. G., Olshevskaya, E. V., Laura, R. P., and Hurley, J. B. (1994). The human photoreceptor membrane guanylyl cyclase, RetGC, is present in outer segments and is regulated by calcium and a soluble activator. *Neuron* 12, 1345–1352. doi: 10.1016/0896-6273(94)90449-9

Fries, R., Scholten, A., Säftel, W., and Koch, K.-W. (2013). Zebrafish guanylate cyclase type 3 signaling in cone photoreceptors. *PLoS ONE* 8:e69656. doi: 10.1371/journal.pone.0069656

Gray-Keller, M. P., and Detwiler, P. B. (1994). The calcium feedback signal in the phototransduction cascade of vertebrate rods. *Neuron* 13, 849–861. doi: 10.1016/0896-6273(94)90251-8

Gross, A. K., and Wensel, T. G. (2011). "Biochemical cascade of phototransduction," in *Adler's Physiology of the Eye*, 11th Edn, eds L. A. Levin, S. F. E. Nilsson, J. Ver Hoeve, S. M. Wu, P. L. Kaufman, and A. Alm (Philadelphia: Saunders/Elsevier B.V.), 394–410.

Haeseleer, F., Sokal, I., Li, N., Pettenati, M., Rao, N., Bronson, D., et al. (1999). Molecular characterization of a third member of the guanylyl cyclase-activating protein subfamily. *J. Biol. Chem.* 274, 6526–6535. doi: 10.1074/jbc.274.10.6526

Hajkova, D., Imanishi, Y., Palamalai, V., Rao, K. C. S., Yuan, C., Sheng, Q., et al. (2010). Proteomic changes in the photoreceptor outer segment upon intense light exposure. *J. Proteome Res.* 9, 1173–1181. doi: 10.1021/pr900819k

Helten, A., Säftel, W., and Koch, K.-W. (2007). Expression level and activity profile of membrane bound guanylate cyclase type 2 in rod outer segments. *J. Neurochem.* 103, 1439–1446. doi: 10.1111/j.1471-4159.2007.04923.x

Herrmann, R., Lobanova, E. S., Hammond, T., Kessler, C., Burns, M. E., Frishman, L. J., et al. (2010). Phosducin regulates transmission at the photoreceptor-to-ON-bipolar cell synapse. *J. Neurosci.* 30, 3239–3253. doi: 10.1523/JNEUROSCI.4775-09.2010

Howes, K., Bronson, J. D., Dang, Y. L., Li, N., Zhang, K., Ruiz, C., et al. (1998). Gene array and expression of mouse retina guanylate cyclase activating proteins 1 and 2. *Invest. Ophthalmol. Vis. Sci.* 39, 867–875.

Howes, K. A., Pennesi, M. E., Sokal, I., Church-Kopish, J., Schmidt, B., Margolis, D., et al. (2002). GCAP1 rescues rod photoreceptor response in GCAP1/GCAP2 knockout mice. *EMBO J.* 21, 1545–1554. doi: 10.1093/emboj/21.7.1545

Hwang, J.-Y., Lange, C., Helten, A., Höppner-Heitmann, D., Duda, T., Sharma, R. K., et al. (2003). Regulatory modes of rod outer segment membrane guanylate cyclase differ in catalytic efficiency and Ca^{2+}-sensitivity. *Eur. J. Biochem.* 270, 3814–3821. doi: 10.1046/j.1432-1033.2003.03770.x

Imanishi, Y., Li, N., Sokal, I., Sowa, M. E., Lichtarge, O., Wensel, T. G., et al. (2002). Characterization of retinal guanylate cyclase-activating protein 3 (GCAP3) from zebrafish to man. *Eur. J. Neurosci.* 15, 63–78. doi: 10.1046/j.0953-816x.2001.01835.x

Imanishi, Y., Yang, L., Sokal, I., Filipek, S., Palczewski, K., and Baehr, W. (2004). Diversity of guanylate cyclase-activating proteins (GCAPs) in teleost fish: characterization of three novel GCAPs (GCAP4, GCAP5, GCAP7) from zebrafish (*Danio rerio*) and prediction of eight GCAPs (GCAP1-8) in pufferfish (*Fugu rubripes*). *J. Mol. Evol.* 59, 204–217. doi: 10.1007/s00239-004-2614-y

Isayama, T., Chen, Y., Kono, M., DeGrip, W. J., Ma, J.-X., Crouch, R. K., et al. (2006). Differences in the pharmacological activation of visual opsins. *Vis. Neurosci.* 23, 899–908. doi: 10.1017/S0952523806230256

Isayama, T., Chen, Y., Kono, M., Fabre, E., Slavsky, M., DeGrip, W. J., et al. (2014). Coexpression of three opsins in cone photoreceptors of the salamander, *Ambystoma tigrinum*. *J. Comp. Neurol.* 522, 2249–2265. doi: 10.1002/cne.23531

Karan, S., Frederick, J. M., and Baehr, W. (2010). Novel functions of photoreceptor guanylate cyclases revealed by targeted deletion. *Mol. Cell. Biochem.* 334, 141–155. doi: 10.1007/s11010-009-0322-z

Koch, K.-W., and Dell'Orco, D. (2013). A calcium-relay mechanism in vertebrate phototransduction. *ACS Chem. Neurosci.* 4, 909–917. doi: 10.1021/cn400027z

Korenbrot, J. I. (2012). Speed, sensitivity, and stability of the light response in rod and cone photoreceptors: facts and models. *Prog. Retin. Eye Res.* 31, 442–466. doi: 10.1016/j.preteyeres.2012.05.002

Kraft, T. W., and Schnapf, J. L. (1998). Aberrant photon responses in rods of the macaque monkey. *Vis. Neurosci.* 15, 153–159. doi: 10.1017/S0952523898151131

Krishnan, J., Chen, J., Shin, K.-J., Hwang, J.-I., Han, S.-U., Lee, G., et al. (2008). Gene expression profiling of light-induced retinal degeneration in phototransduction gene knockout mice. *Exp. Mol. Med.* 40, 495–504. doi: 10.3858/emm.2008.40.5.495

Krispel, C. M., Sokolov, M., Chen, Y.-M., Song, H., Herrmann, R., Arshavsky, V. Y., et al. (2007). Phosducin regulates the expression of transducin $\beta\gamma$ subunits in rod photoreceptors and does not contribute to phototransduction adaptation. *J. Gen. Physiol.* 130, 303–312. doi: 10.1085/jgp.200709812

Lagnado, L., Cervetto, L., and McNaughton, P. A. (1992). Calcium homeostasis in the outer segments of retinal rods from the tiger salamander. *J. Physiol.* 455, 111–142.

Lamb, T. D. (2013). Evolution of phototransduction, vertebrate photoreceptors and retina. *Prog. Retin. Eye Res.* 36, 52–119. doi: 10.1016/j.preteyeres.2013.06.001

Li, N., Fariss, R. N., Zhang, K., Otto-Bruc, A., Haeseleer, F., Bronson, D., et al. (1998). Guanylate-cyclase-inhibitory protein is a frog retinal Ca^{2+}-binding protein related to mammalian guanylate-cyclase-activating proteins. *Eur. J. Biochem.* 252, 591–599. doi: 10.1046/j.1432-1327.1998.2520591.x

Lim, S., Dizhoor, A. M., and Ames, J. B. (2014). Structural diversity of neuronal calcium sensor proteins and insights for activation of retinal guanylyl cyclase by GCAP1. *Front. Mol. Neurosci.* 7:19. doi: 10.3389/fnmol.2014.00019

Lowe, D. G., Dizhoor, A. M., Liu, K., Gu, Q., Spencer, M., Laura, R., et al. (1995). Cloning and expression of a second photoreceptor-specific membrane retina guanylyl cyclase (RetGC), RetGC-2. *Proc. Natl. Acad. Sci. U.S.A.* 92, 5535–5539. doi: 10.1073/pnas.92.12.5535

Luo, D.-G., Xue, T., and Yau, K.-W. (2008). How vision begins: an odyssey. *Proc. Natl. Acad. Sci. U.S.A.* 105, 9855–9862. doi: 10.1073/pnas.0708405105

Luo, D.-G., and Yau, K.-W. (2005). Rod sensitivity of neonatal mouse and rat. *J. Gen. Physiol.* 126, 263–269. doi: 10.1085/jgp.200509342

Makino, C. L., Dodd, R. L., Chen, J., Burns, M. E., Roca, A., Simon, M. I., et al. (2004). Recoverin regulates light-dependent phosphodiesterase activity in retinal rods. *J. Gen. Physiol.* 123, 729–741. doi: 10.1085/jgp.200308994

Makino, C. L., Peshenko, I. V., Wen, X.-H., Olshevskaya, E. V., Barrett, R., and Dizhoor, A. M. (2008). A role for GCAP2 in regulating the photoresponse. Guanylyl cyclase activation and rod electrophysiology in GUCA1B knock-out mice. *J. Biol. Chem.* 283, 29135–29143. doi: 10.1074/jbc.M804445200

Makino, C. L., Wen, X.-H., Michaud, N. A., Covington, H. I., DiBenedetto, E., Hamm, H. E., et al. (2012a). Rhodopsin expression level affects rod outer segment morphology and photoresponse kinetics. *PLoS ONE* 7:e37832. doi: 10.1371/journal.pone.0037832

Makino, C. L., Wen, X.-H., Olshevskaya, E. V., Peshenko, I. V., Savchenko, A. B., and Dizhoor, A. M. (2012b). Enzymatic relay mechanism stimulates cyclic GMP synthesis in rod photoresponse: biochemical and physiological study in guanylyl cyclase activating protein 1 knockout mice. *PLoS ONE* 7:e47637. doi: 10.1371/journal.pone.0047637

Mendez, A., Burns, M. E., Sokal, I., Dizhoor, A. M., Baehr, W., Palczewski, K., et al. (2001). Role of guanylate cyclase-activating proteins (GCAPs) in setting the flash sensitivity of rod photoreceptors. *Proc. Natl. Acad. Sci. U.S.A.* 98, 9948–9953. doi: 10.1073/pnas.171308998

Miller, J. L., and Korenbrot, J. I. (1993). Phototransduction and adaptation in rods, single cones, and twin cones of the striped bass retina: a comparative study. *Vis. Neurosci.* 10, 653–667. doi: 10.1017/S0952523800005356

Nakatani, K., and Yau, K.-W. (1988). Calcium and magnesium fluxes across the plasma membrane of the toad rod outer segment. *J. Physiol.* 395, 695–729.

Ohyama, T., Hackos, D. H., Frings, S., Hagen, V., Kaupp, U. B., and Korenbrot, J. I. (2000). Fraction of the dark current carried by Ca^{2+} through cGMP-gated ion channels of intact rod and cone photoreceptors. *J. Gen. Physiol.* 116, 735–754. doi: 10.1085/jgp.116.6.735

Olshevskaya, E. V., Peshenko, I. V., Savchenko, A. B., and Dizhoor, A. M. (2012). Retinal guanylyl cyclase isozyme 1 is the preferential in vivo target for constitutively active GCAP1 mutants causing congenital degeneration of photoreceptors. *J. Neurosci.* 32, 7208–7217. doi: 10.1523/JNEUROSCI.0976-12.2012

Paillart, C., Winkfein, R. J., Schnetkamp, P. P. M., and Korenbrot, J. I. (2007). Functional characterization and molecular cloning of the K^+-dependent Na^+/Ca^{2+} exchanger in intact retinal cone photoreceptors. *J. Gen. Physiol.* 129, 1–16. doi: 10.1085/jgp.200609652

Palczewski, K., Subbaraya, I., Gorczyca, W. A., Helekar, B. S., Ruiz, C. C., Ohguro, H., et al. (1994). Molecular cloning and characterization of retinal photoreceptor guanylyl cyclase-activating protein. *Neuron* 13, 395–404. doi: 10.1016/0896-6273(94)90355-7

Pennesi, M. E., Howes, K. A., Baehr, W., and Wu, S. M. (2003). Guanylate cyclase-activating protein (GCAP) 1 rescues cone recovery kinetics in GCAP1/GCAP2 knockout mice. *Proc. Natl. Acad. Sci. U.S.A.* 100, 6783–6788. doi: 10.1073/pnas.1130102100

Perry, R. J., and McNaughton, P. A. (1991). Response properties of cones from the retina of the tiger salamander. *J. Physiol.* 433, 561–587.

Peshenko, I. V., and Dizhoor, A. M. (2004). Guanylyl cyclase-activating proteins (GCAPs) are Ca^{2+}/Mg^{2+} sensors: implications for photoreceptor guanylyl cyclase (RetGC) regulation in mammalian photoreceptors. *J. Biol. Chem.* 279, 16903–16906. doi: 10.1074/jbc.C400065200

Peshenko, I. V., Olshevskaya, E. V., Savchenko, A. B., Karan, S., Palczewski, K., Baehr, W., et al. (2011). Enzymatic properties and regulation of the native isozymes of retinal membrane guanylyl cyclase (RetGC) from mouse photoreceptors. *Biochemistry* 50, 5590–5600. doi: 10.1021/bi200491b

Rätscho, N., Scholten, A., and Koch, K.-W. (2009). Expression profiles of three novel sensory guanylate cyclases and guanylate cyclase-activating proteins in the zebrafish retina. *Biochim. Biophys. Acta* 1793, 1110–1114. doi: 10.1016/j.bbamcr.2008.12.021

Rieke, F., and Baylor, D. A. (1996). Molecular origin of continuous dark noise in rod photoreceptors. *Biophys. J.* 71, 2553–2572. doi: 10.1016/S0006-3495(96)79448-1

Sakurai, K., Chen, J., and Kefalov, V. J. (2011). Role of guanylyl cyclase modulation in mouse cone phototransduction. *J. Neurosci.* 31, 7991–8000. doi: 10.1523/JNEUROSCI.6650-10.2011

Sampath, A. P., Matthews, H. R., Cornwall, M. C., Bandarchi, J., and Fain, G. L. (1999). Light-dependent changes in outer segment free-Ca^{2+} concentration in salamander cone photoreceptors. *J. Gen. Physiol.* 113, 267–277. doi: 10.1085/jgp.113.2.267

Sampath, A. P., Matthews, H. R., Cornwall, M. C., and Fain, G. L. (1998). Bleached pigment produces a maintained decrease in outer segment Ca^{2+} in salamander rods. *J. Gen. Physiol.* 111, 53–64. doi: 10.1085/jgp.111.1.53

Schmitz, F. (2014). Presynaptic [Ca^{2+}] and GCAPs: aspects on the structure and function of photoreceptor ribbon synapses. *Front. Mol. Neurosci.* 7:3. doi: 10.3389/fnmol.2014.00003

Schnapf, J. L., Kraft, T. W., and Baylor, D. A. (1987). Spectral sensitivity of human cone photoreceptors. *Nature* 325, 439–441. doi: 10.1038/325439a0

Schnapf, J. L., Nunn, B. J., Meister, M., and Baylor, D. A. (1990). Visual transduction in cones of the monkey *Macaca fascicularis*. *J. Physiol.* 427, 681–713.

Scholten, A., and Koch, K.-W. (2011). Differential calcium signaling by cone specific guanylate cyclase-activating proteins from the zebrafish retina. *PLoS ONE* 6:e23117. doi: 10.1371/journal.pone.0023117

Sharma, R. K., and Duda, T. (2012). Ca^{2+}-sensors and ROS-GC: interlocked sensory transduction elements: a review. *Front. Mol. Neurosci.* 5:42. doi: 10.3389/fnmol.2012.00042

Sharma, R. K., Makino, C. L., Hicks, D., and Duda, T. (2014). ROS-GC interlocked Ca^{2+}-sensor S100B protein signaling in cone photoreceptors: a review. *Front. Mol. Neurosci.* 7:21. doi: 10.3389/fnmol.2014.00021

Skiba, N. P., Spencer, W. J., Salinas, R. Y., Lieu, E. C., Thompson, J. W., and Arshavsky, V. Y. (2013). Proteomic identification of unique photoreceptor disc components reveals the presence of PRCD, a protein linked to retinal degeneration. *J. Proteome Res.* 12, 3010–3018. doi: 10.1021/pr4003678

Surguchov, A., Bronson, J. D., Banerjee, P., Knowles, J. A., Ruiz, C., Subbaraya, I., et al. (1997). The human GCAP1 and GCAP2 genes are arranged in a tail-to-tail array on the short arm of chromosome 6 (p21.1). *Genomics* 39, 312–322. doi: 10.1006/geno.1996.4513

Takemoto, N., Tachibanaki, S., and Kawamura, S. (2009). High cGMP synthetic activity in carp cones. *Proc. Natl. Acad. Sci. U.S.A.* 106, 11788–11793. doi: 10.1073/pnas.0812781106

Tsang, S. H., Woodruff, M. L., Chen, C.-K., Yamashita, C. Y., Cilluffo, M. C., Rao, A. L., et al. (2006). GAP-independent termination of photoreceptor light response by excess γ subunit of the cGMP-phosphodiesterase. *J. Neurosci.* 26, 4472–4480. doi: 10.1523/JNEUROSCI.4775-05.2006

van Hateren, J. H., and Lamb, T. D. (2006). The photocurrent response of human cones is fast and monophasic. *BMC Neurosci.* 7:34. doi: 10.1186/1471-2202-7–34

Wensel, T. G. (2008). Signal transducing membrane complexes of photoreceptor outer segments. *Vision Res.* 48, 2052–2061. doi: 10.1016/j.visres.2008.03.010

Woodruff, M. L., Olshevskaya, E. V., Savchenko, A. B., Peshenko, I. V., Barrett, R., Bush, R. A., et al. (2007). Constitutive excitation by Gly90Asp rhodopsin rescues rods from degeneration caused by elevated production of cGMP in the dark. *J. Neurosci.* 27, 8805–8815. doi: 10.1523/JNEUROSCI.2751-07.2007

Woodruff, M. L., Sampath, A. P., Matthews, H. R., Krasnoperova, N. V., Lem, J., and Fain, G. L. (2002). Measurement of cytoplasmic calcium concentration in the rods of wild-type and transducin knock-out mice. *J. Physiol.* 542, 843–854. doi: 10.1113/jphysiol.2001.013987

Xu, J., Morris, L., Thapa, A., Ma, H., Michalakis, S., Biel, M., et al. (2013). cGMP accumulation causes photoreceptor degeneration in CNG channel deficiency: evidence of cGMP cytotoxicity independently of enhanced CNG channel function. *J. Neurosci.* 33, 14939–14948. doi: 10.1523/JNEUROSCI.0909-13.2013

Yang, R.-B., Robinson, S. W., Xiong, W.-H., Yau, K.-W., Birch, D. G., and Garbers, D. L. (1999). Disruption of a retinal guanylyl cyclase gene leads to cone-specific dystrophy and paradoxical rod behavior. *J. Neurosci.* 19, 5889–5897.

Zhang, X., Wensel, T. G., and Kraft, T. W. (2003). GTPase regulators and photoresponses in cones of the eastern chipmunk. *J. Neurosci.* 23, 1287–1297.

Conflict of Interest Statement: The authors declare that the research was conducted in the absence of any commercial or financial relationships that could be construed as a potential conflict of interest.

Received: 05 February 2014; accepted: 01 May 2014; published online: 02 June 2014.
Citation: Wen X-H, Dizhoor AM and Makino CL (2014) Membrane guanylyl cyclase complexes shape the photoresponses of retinal rods and cones. Front. Mol. Neurosci. 7:45. doi: 10.3389/fnmol.2014.00045
This article was submitted to the journal Frontiers in Molecular Neuroscience.

frontiers in
MOLECULAR NEUROSCIENCE

ORIGINAL RESEARCH ARTICLE
published: 27 June 2014
doi: 10.3389/fnmol.2014.00060

PDE9A is expressed in the inner retina and contributes to the normal shape of the photopic ERG waveform

Anuradha Dhingra[1†], Shanti R. Tummala[1†], Arkady Lyubarsky[2] and Noga Vardi[1]*

[1] *Retina Lab, Department of Neuroscience, University of Pennsylvania, Philadelphia, PA, USA*
[2] *Department of Ophthalmology, University of Pennsylvania, Philadelphia, PA, USA*

Edited by:
Rameshwar K. Sharma, Salus University, USA

Reviewed by:
Laura J. Frishman, University of Houston, USA
Edward N. Pugh, University of California, Davis, USA

***Correspondence:**
Noga Vardi, Retina Lab, Department of Neuroscience, University of Pennsylvania, 123 Anat-Chem Bldg., Philadelphia, PA 19104, USA
e-mail: noga@mail.med.upenn.edu

† These authors have contributed equally to this work.

The ubiquitous second messenger cGMP is synthesized by guanylyl cyclase and hydrolyzed by phosphodiesterase (PDE). cGMP mediates numerous signaling pathways in multiple tissues. In the retina, cGMP regulates signaling in nearly every cell class including photoreceptors, bipolar cells, amacrine cells, and ganglion cells. In order to understand the specific role of cGMP and its regulating enzymes in different cell types, it is first necessary to localize these components and dissect their influence on the circuits. Here we tested the contribution of PDE9A to retinal processing by recording the electroretinograms (ERG) of *PDE9A*$^{-/-}$ (KO) mice and by localizing the enzyme. We found that while the scotopic ERG of KO was the same as that of wild type (WT) in both amplitude and kinetics, the photopic ERG was greatly affected. The greatest effect was on the recovery of the b-wave; the falling phase and the b-wave duration were significantly longer in the KO mice for all photopic stimuli (UV, green, or saturating white flashes). The rising phase was slower in KO than in WT for UV and green stimuli. For certain stimuli, amplitudes of both the a- and b-waves were smaller than in WT. Using *Lac-Z* expression in KO retinas as a reporter for PDE9A expression pattern, we found that PDE9A is localized to GABA-positive and GABA-negative amacrine cells, and likely also to certain types of ganglion cells. Our results indicate that PDE9A, by controlling the level of cGMP, modulates inhibitory processes within the cone pathway. We speculate that these circuits involve NO/cGMP signaling pathways.

Keywords: ERG, serial inhibition, amacrine cells, cyclic GMP, cone pathways, ciliary body

INTRODUCTION

The ubiquitous second messenger cGMP, which is synthesized by guanylyl cyclases (GC) and hydrolyzed by phospodiesterases (PDE), controls a variety of processes from smooth muscle cell contraction in the vasculature to signaling in the central nervous system (Beavo, 1995; Polson and Strada, 1996; Juilfs et al., 1999). cGMP typically accomplishes these functions either by gating cyclic nucleotide-gated (CNG) channels or by activating cGMP-dependent kinases and phosphatases. In the retina, cGMP regulates nearly every step of signal processing. At the first step of retinal processing, rod and cone photoreceptors use cGMP to gate CNG channels. In these cells, light activates PDE6, which hydrolyzes cGMP; this closes the CNG channels and the cells hyperpolarize (Lamb and Pugh, 1992; Hsu and Molday, 1993; Yau, 1994). At the next step of retinal processing, ON bipolar cells (rod bipolar that mediate night vision and ON cone bipolar cells that signal light increments in daylight vision) appear to use cGMP, but its function is still unclear. cGMP was initially thought to gate a CNG channel similar to photoreceptors (Nawy and Jahr, 1990; Shiells and Falk, 1990, 1992; de la Villa et al., 1995). It is now known that ON bipolar cells use the non-selective cation channel TRPM1, which is not gated by cGMP (Morgans et al., 2009; Koike et al., 2010). Instead, some evidence suggests that cGMP potentiates the light response at low light intensities (Nawy, 1999; Shiells and Falk, 2002; Snellman and Nawy, 2004). At the next stage of visual processing, some third order neurons (including certain types of amacrine and ganglion cells) modulate cGMP, often in response to NO (Ahmad et al., 1994; Gotzes et al., 1998; Chun et al., 1999; Blute et al., 2003). The NO/cGMP pathway is also critical for modulating coupling conductance between the AII amacrine cells and ON cone bipolar cells (Mills and Massey, 1995). The exact role and mechanism of cGMP regulation in second and third order neurons is not clear. In order to better understand the role of cGMP in different steps of processing, and especially in ON bipolar cells, it is important to localize PDE enzymes in retina. To this end, using our ON bipolar cell cDNA library, we identified a PDE isoform *PDE9A* and determined that these cells express the transcript for this isoform (Dhingra et al., 2008). Moreover analysis of the retinal transcriptome database (Siegert et al., 2009) showed that several amacrine and ganglion cell types also express *PDE9A* transcripts. Because PDE9A is expressed predominately in neurons (van Staveren and Markerink-van Ittersum, 2005), and hydrolyses cGMP with a very low Km (Fisher et al., 1998), it likely contributes to retinal function. Here, using *PDE9A*$^{-/-}$ (KO) mouse, we report that PDE9A contributes to the normal kinetics of the photopic electroretinogram (ERG). PDE9A is localized to amacrine cells, ganglion cells, and to the ciliary body, but not ON bipolar cells. We therefore

conclude that inner retinal expression of PDE9A in amacrine cells contributes to response kinetics of the ERG b-wave.

MATERIALS AND METHODS

GENERATION OF *PDE9A* KNOCKOUT MICE

PDE9A$^{-/-}$ (KO) mice were obtained from Pfizer (Menniti et al., 2008) and were initially generated by Deltagen (San Mateo, CA). Briefly, a targeting construct with neomycin resistance (neo) and bacterial *LacZ* (coding for β-galactosidase or β-gal) genes was designed to disrupt the *PDE9A* gene (Accession # AF031147) in ES cells by homologous recombination. The resultant allele had a replacement of part of exon 11/12 of *PDE9A* with neo-*LacZ* cassette that shifted the downstream sequence out of the open reading frame. The ES cells were injected into blastocysts and the resulting chimeras were tested for germ line transmission. The following primers were used for genotyping:

GS (E) (CACAGATGATGTACAGTATGGTCTGG);
GS (T,E) (TGCAGTCATCAGGACCAAGATGTCC); and
Neo (T) (GACGAGTTCTTCTGAGGGGATCGATC).

Genotyping was performed on tail DNA using a multiplex PCR reaction: GS (T, E) + Neo (T) for targeted allele (expected size 599 bp); GS (E) + GS (T, E) for endogenous allele (expected size 256 bp). KO mice were bred to homogenicity by multiple back-crossings (>6) with C57BL6/J mates. Mouse colonies were maintained by breeding KO mice; no specific behavioral phenotypes were observed in these mice. Age matched C57BL6/J (WT) were purchased from Jackson Labs (Bar Harbor, Maine). All experiments were done in compliance with federal regulations and the protocol was reviewed and approved by the Institutional Animal Care and Use Committee of the University of Pennsylvania. Both male and female mice were used for all experiments.

ELECTRORETINOGRAM

The ERG recording setup and methods have been described elaborately (Lyubarsky et al., 1999, 2000; Ng et al., 2010). In short, mice were dark-adapted, deeply anesthetized intraperitoneally under dim light with ketamine/xylazine/urethane (20, 8, and 800 μg/gm bodyweight, respectively) and were placed on a platform maintained at 37–38°C. Pupils were dilated with 1% tropicamide saline solution (Mydriacyl, Alconox). A platinum electrode was inserted into the mouth to serve as a reference and ground electrode, and another platinum electrode was placed on the cornea. Mice were placed inside a light-proof Ganzfield Faraday cage. ERG recordings from KO and age matched WT mice were performed on the same day under identical settings and conditions. Light stimuli were either 4 ms flashes produced by a light-emitting diode (LED) stimulator or <1 ms flashes produced by a Xenon tube delivered in the Ganzfeld (Espion Electrophysiology System; Diagnosys). For scotopic ERG, intensities of light flashes were converted to the estimated number of photoisomerizations (R^*) per rod as described previously (Lyubarsky et al., 2004). For photopic ERG, light intensity was converted to number of photons per μm^2 at the cornea as described previously (Lyubarsky et al., 1999, 2000). For photopic stimuli, a rod-suppressing step of light (30 scot cd m^{-2}) was given every 5.5 s and a light flash was superimposed on it 2 s after the onset of the step. ERGs were recorded from both eyes using differential amplifiers with a bandwidth of 0.1 Hz–1 kHz, and a sampling interval of 1 ms. Depending on the signal-to-noise ratio, each record was an average of 3–25 individual trials.

The various parameters characterizing the ERG waveform were determined using a user-defined MATLAB® (Mathworks, MA) program. The amplitude of the b-wave was quantified by subtracting the peak of the a-wave from the peak of the b-wave. The functional characteristics of phototransduction in photoreceptors in WT and KO animals were determined from the ERG a-wave by fitting the rising phase of the a-wave with the transduction cascade activation model (Breton et al., 1994; Lyubarsky and Pugh, 1996) as follows:

$$F(t) = \exp[-0.5\Phi A\left(t - t_{eff}\right)^2], \quad (1)$$

where $F(t)$ is the a-wave amplitude at time t after a brief flash normalized to the saturated amplitude; Φ is the number of photoisomerizations per rod; t_{eff} a brief delay; A is the amplification constant whose value is estimated by the best fit. ERG data presented in this paper were performed on 12 WT and 14 KO mice, but occasional records were too noisy and were not considered. Values of the measured response parameters for the left and right eyes were averaged and treated as a single data point. The number of animals or data points acquired for each stimulus condition is specified in the Results section. All data values in the figures are presented as mean ± s.e.m. Unless stated otherwise, statistical comparison of a parameter between groups of WT and KO was performed using two-tailed Student's t-test. A p-value of less than 0.05 ($p < 0.05$) was considered significant and $p < 0.01$ was considered highly significant.

β-GALACTOSIDASE ASSAY

Mice were deeply anesthetized with an intraperitoneal injection of ketamine and xylazine (100 and 10 μg/gm bodyweight). Eyes were enucleated and incised just below the limbus. Eyeballs were fixed in 4% paraformaldehyde for 10 min, and rinsed in 0.1 M phosphate buffer. For cryosections, eyeballs were cryoprotected by soaking overnight at 4°C in 0.1 M phosphate buffer containing 30% sucrose and embedded in a mixture of two parts 20% sucrose in phosphate buffer and one part optimal cutting temperature compound (Tissue Tek, Electron Microscopy Sciences, Hatfield, PA, USA). Radial sections (15–20 μm) were cut on a cryostat (Leica) at −20°C and collected on superfrost plus slides (Fisher Scientific, Pittsburgh, PA, USA). β-galactosidase expression was detected enzymatically using X-gal (5-bromo-3-indoyl-b-D-galactopyranoside stock solution) as substrate. Briefly, whole mount or retinal sections were pre-incubated in a detergent buffer (0.02% Nonidet P-40, 0.01% Sodium Deoxycholate, and 2 mM $MgCl_2$ in 0.1 M phosphate buffer, pH 7.3) for about 10 mins at room temperature (RT), incubated for 2–4 days in staining buffer (0.02% Nonidet P-40, 0.01% Sodium Deoxycholate, 5 mM Potassium Ferricyanide, 5 mM Potassium Ferrocyanide, and 2 mM $MgCl_2$ in 0.1 M phosphate buffer, pH 7.3 containing 1–1.5 mg/ml X-gal) and finally rinsed twice in detergent buffer (5 min each).

IMMUNOFLUORESCENCE

Sections were permeabilized and blocked with 10% normal goat serum, 5% sucrose and 0.5% Triton X-100 in phosphate buffer for 1 h at RT. Sections were incubated in primary antibodies (diluted in blocking solution) at 4°C overnight or occasionally for 3 days. Primary antibodies were washed 3 times in 5% sucrose in phosphate buffer at RT. Sections were then incubated in secondary antibodies at RT for 3 h, washed, mounted with Vectashield mounting medium (Vector Laboratories, Burlingame, CA, USA) and coverslipped. To identify X-gal-stained cells in the inner retina, some retinal sections were first stained for GABA and then processed for X-gal staining, and others were first processed for X-gal staining, and then immunostained for GABA. For double staining on the whole mount, we first stained for GABA overnight and then with x-gal for at least 3 days; after imaging, the retinas were also stained with DAPI. To avoid collapse of retinal layers, retinas were mounted between number 0 cover slips, which served to support the coverslip. The blue staining corresponding to the sites of β-galactosidase activity and the fluorescent stainings were examined with a conventional microscope (Nikon Eclipse TE-300 microscope; Nikon Inc., Melville, NY, USA).

Antibodies

Rabbit anti-PDE9A (1:100–500, GTX14625 from Genetex, Irvine, CA); rabbit anti-PDE9A (1:100, PD9A-101AP from FabGennix, Frisco, TX); guinea-pig anti-GABA (1:1000, AB175, Chemicon International, Temecula, CA); mouse anti-β-gal antibodies (a monoclonal; 1:200, Promega, Madison, WI); and chicken anti-β-gal (1:500, Aves labs Inc., Tigard, Oregon).

RESULTS

ABSENCE OF PDE9A DOES NOT AFFECT THE SCOTOPIC ERG, BUT DECREASES THE AMPLITUDE OF THE ROD/CONE-GENERATED ERG a-WAVE

To determine if PDE9A contributes to visual processing, we recorded ERGs from WT and *PDE9A* KO mice. We first presented a series of scotopic flash intensities under dark-adapted conditions and measured the amplitude of the b-wave. There was no significant difference in the ERG b-wave amplitude between KO and WT (**Figures 1A–C**). To assess the response kinetics, we measured the time it took the b-wave to rise to 66% of its peak amplitude, the time it took to fall to 66% of its peak amplitude, and the 66% maximum width (as in **Figure 1D**). We also analyzed the half width; however, because responses of dark-adapted mice at high intensities often do not return to baseline in the sampled duration of 500 ms, this measure is less reliable and is not reported here. Under scotopic conditions, the kinetic parameters of KO and WT ERGs were similar (**Figure 1E**).

Next, to determine the possible contribution of PDE9A to the a-wave, we presented strong saturating flashes that stimulate both rods and cones (**Figure 2A**). In response to the strongest flash ($I = 9.3 \times 10^5$ R^*/rod), both the a- and b-wave amplitudes were significantly lower in KO than in WT. The a-wave saturating amplitude in KO (227 μV) was 36% lower than in WT (357 μV; $p = 0.002$), and the b-wave saturating amplitude of KO was 30% lower (411 μV in KO vs. 601 in WT; $p = 0.009$; **Figure 2B**). The ratios of b-wave to a-wave amplitude for the three intensities were similar in KO and WT (ranged from 1.7 in WT and 1.8 in KO for the lower intensity to 3.6 and 3.7 for the higher intensity).

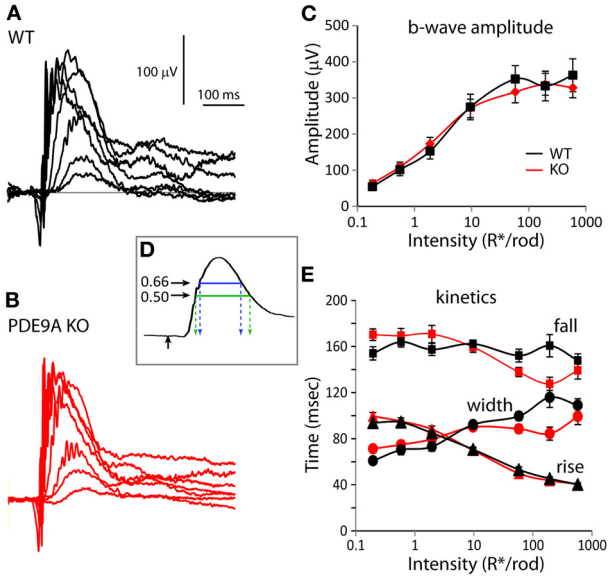

FIGURE 1 | PDE9A does not contribute to the ERG under scotopic conditions. For all figures, WT is drawn in black and KO in red. Also for all figures, data are plotted as average ±s.e.m. When the s.e.m. cannot be seen, it is smaller than the symbol. **(A,B)** Representative responses to increasing light intensities (0.2– 600 R^*/rod) from age matched WT **(A)** and *PDE9A* KO **(B)** retinas. **(C)** Average b-wave amplitudes vs. flash intensity for WT (black squares; 16–22 records) and KO (red diamonds; 18–28 records) mice. **(D)** Illustration of the parameters used to characterize the kinetics of the b-wave. Stimulus onset is designated by an upward black arrow, 66% of the peak amplitude is indicated by the blue line and 50% by the green line. Time taken by the b-wave to rise from the stimulus onset to 66% of its peak amplitude (left dashed blue arrow) or to 50% of its amplitude (left dashed green arrow) were used for comparison of its kinetics. Time taken by the b-wave to fall to 66 or 50% of its peak amplitude is indicated by the right blue and green arrows. **(E)** Times taken by the b-wave to rise (triangles) and fall (squares) to 66% of its amplitude, and the duration between them (width, circles) at the measured intensities.

To determine if the reduced a-wave was due to compromised photoreceptor function, we computed the Lamb and Pugh amplification constant "*A*." This constant provides a measure of the gain of the photoreceptor transduction cascade that is independent of light intensity for low-to-moderate intensities (Lyubarsky and Pugh, 1996). The amplification constant *A* was computed by fitting the a-wave component of two flash intensities (460 and 1860 R^*/rod) to Equation 1 (**Figure 2C**; the fit is shown with dashed lines). The amplification constant *A* in WT (3.5) was not statistically different from that in KO mice (4.3; **Figure 2D**; $p = 0.11$), indicating that deletion of *PDE9A* does not affect phototransduction. Next, we looked at the shape of the rod/cone mixed response and computed the 66% maximum width. As expected, in both WT and KO, the rise time of the b-wave decreased slightly and the fall time increased substantially with increasing intensity. The curves of the rise time as a function of intensity for KO and WT were very similar. The curves of the fall time and 66%

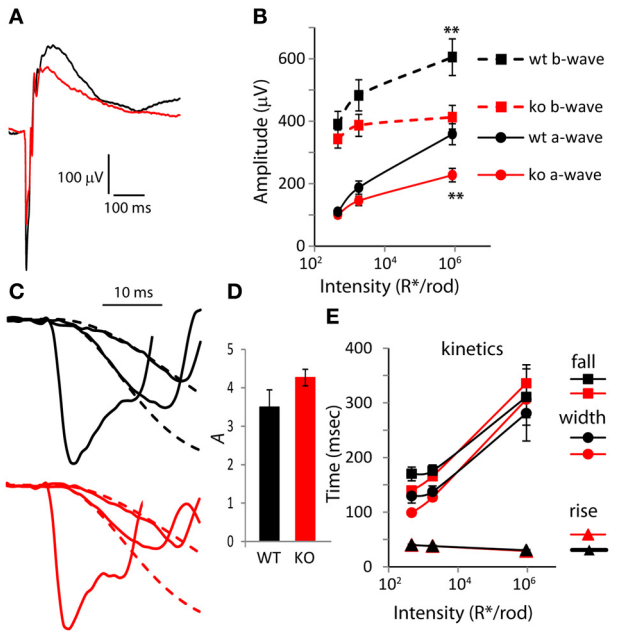

FIGURE 2 | The amplitude of the a-wave is smaller in *PDE9A* KO but its kinetics is largely unaffected. (A) Average response from WT and KO retinas to a rod saturating flash (~10^6 *R**/rod). **(B)** Average a-wave and b-wave amplitudes (dark-adapted, rod and cone generated responses). Both a-wave and b-wave amplitudes in KO ($n = 14$ mice for all intensities) are significantly different from WT ($n = 12$) at the two highest intensities. Unless otherwise stated, for all figures, "$*$" designates $p < 0.05$ and $^{**}p < 0.01$. **(C)** Expanded ERG responses from a KO and WT animal at the flash intensities in **(B)** showing the a-waves and their Lamb and Pugh curve fits (red and black dashed lines for KO and WT, respectively). The Lamb and Pugh equation was fit to the average a-wave from both eyes of the animal to estimate the amplification constant. **(D)** The Lamb and Pugh amplification constants as estimated by regression in WT and KO animals are similar. **(E)** The time taken by the b-wave to rise and fall to 66% of its amplitude and the duration (width). For the highest intensity, the b-wave fell to 66% of its amplitude only in 50% of WT and in 82% of KO.

maximum duration for KO crossed those of WT: at lower intensities KOs were slightly faster, and at the highest intensity tested, the KOs took longer to recover (**Figure 2E**). However, neither of these differences was significantly different between WT and KO.

ABSENCE OF PDE9A SLOWS DOWN THE PHOTOPIC RESPONSE

To test the effect of deleting PDE9A on the photopic ERG wave, we suppressed rod responses using a light step of 30 scotopic cd m^{-2} and superimposed (in sequence, with 5.5 s delay between trials) a saturating white flash of 1000 scot cd s m^{-2}, UV flashes ($\lambda = 365$ nm; 4×10^3, 8×10^3, and 1.65×10^4 photon/μm^2), green flashes ($\lambda = 513$ nm; 8×10^3, 1.6×10^4, and 3.2×10^4 photon/μm^2) and another saturating white flash of 1000 scot cd s m^{-2}. In light-adapted rodents, the ERG a-wave is small and it reflects the activity of cones and the OFF pathway; the b-wave predominantly reflects the activity of ON cone bipolar cells and to a smaller extent that of the inner retina (Xu et al., 2003; Sharma et al., 2005; Shirato et al., 2008). For the saturated flashes, the average WT a-wave (combining the amplitude of both the first and the last flash) was 37.3 μV and in KO mice, it was 23.5 μV; significantly smaller than in WT ($p = 0.004$). The WT b-wave (170 μV) was larger than that of KO (137 μV) by 20% (albeit not significantly, $p = 0.09$; **Figures 3A,B**). Thus, absence of PDE9A greatly reduced the photopic a-wave amplitude, and only mildly effected the b-wave. Examination of the wave shape (**Figure 3C**) showed that while the times for the b-wave to rise to 66% of the peak in KO (40 ms) were similar to those in WT (41 ms) ($p = 0.56$), the time it took the b-wave to fall to 66% of its peak amplitude was highly significantly longer in KO (227 in KO vs. 156 ms in WT; $p = 0.0001$). Consequently, the 66% maximum width was also highly significantly longer in KO (201 in KO vs. 116 ms in WT; $p = 0.0001$).

Because photopic ERG responses were slower in KO than in WT, we wondered if light adaptation contributed to this difference. We therefore compared the first saturating response to the last saturating response in each experiment. Recall that the last saturating flash was presented after the UV and green flashes, so the eyes were exposed to the adapting light step for 12 min longer (**Figures 3D–F**). In WT, the kinetics of the b-wave in the first and last saturating flashes were similar, while in KO, the second presentation of the saturating flash resulted in a slower decay. The difference in the 66% maximum width was not significant (paired t-test; $p = 0.1$), but the 50% maximum width in KO was significantly longer in the second saturating flash ($p = 0.007$; **Figure 3F**). This suggests that PDE9A contributes to the kinetics of the cone-generated response, and that this contribution may be affected by the state of light adaptation.

To see if the effect of PDE9A's absence is specific to high intensities, or perhaps to different cone pathways, we examined the responses to low intensities of UV and green flashes. In response to UV flashes, both a- and b-waves amplitudes were similar in KO and WT (**Figures 4A,B**). However, in response to green flashes, both a- and b-wave amplitudes were significantly smaller in KO (**Figures 4D,E**). Like the saturating response, the time for the b-wave to decay to 66% and the 66% maximum duration were significantly longer for both wavelengths at all intensities ($p < 0.01$; **Figures 4C,F**). In addition, at these wavelengths, the time to rise to 66% of the peak amplitude was also significantly longer ($p < 0.001$). Consequently, the time to peak in KO for all intensities at both wavelengths was also significantly longer. Taken together, our ERG results suggest that the main effect of deleting PDE9A is on the photopic ERG which reflects activity in the cone pathways.

PDE9A IS LOCALIZED TO CELLS IN THE GANGLION AND AMACRINE CELL LAYERS

To understand the mechanism by which PDE9A affects retinal processing, it is essential to determine its cellular localization. We initially attempted to localize PDE9A using two commercial antibodies; both gave intense staining in several layers of the retina. However, when the antibodies were applied to KO retinas, the staining patterns were similar to those of WT, suggesting that the antibodies cross-react with other proteins (not shown). We similarly obtained non-specific bands using Western blots with these antibodies. To get a reliable localization pattern, we stained retinas for the reporter *Lac-Z* that replaced

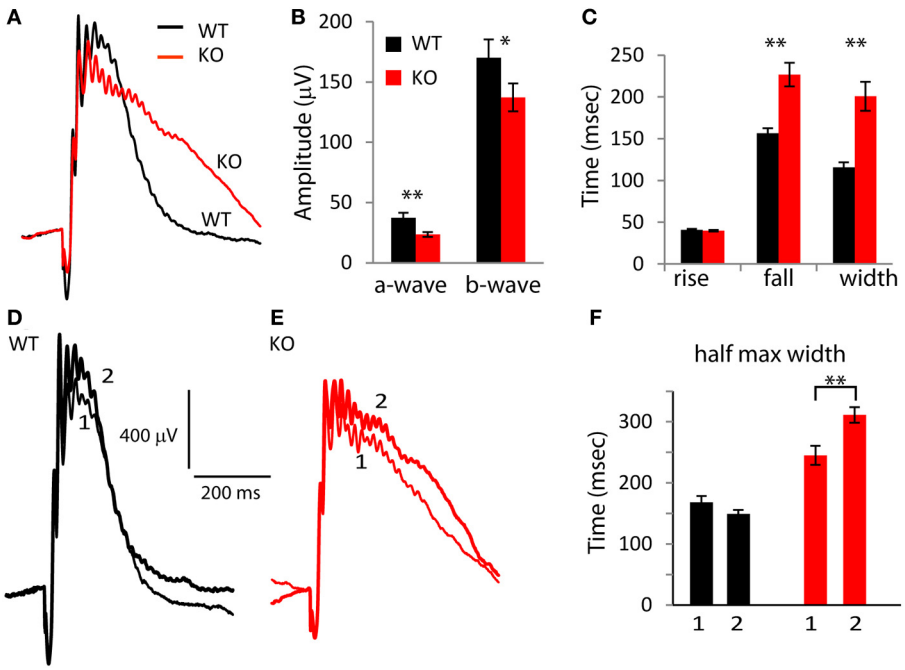

FIGURE 3 | Absence of PDE9A slows the falling phase of the b-wave of a saturating flash under photopic conditions. (A) Average responses of WT and KO retinas to a saturating flash (1000 scot cd s m^{-2}) after 2 s light adaptation. The responses to both the first and second saturating flashes (presented before and after stimulation with UV and green light, respectively) in each retina were averaged. **(B)** Response amplitudes of the a- and b-waves at the saturating flash are reduced in KO (13 WT and 14 KO mice). **(C)** The times taken by the b-wave to rise and fall to 66% of its amplitude and the duration between them. **(D,E)** Average response of WT and KO retinas to the first (1) and second (2) saturating flash. **(F)** The width of the b-wave at 50% of its amplitude for the first (1) and second (2) saturating flashes increased in KO.

PDE9A in KO. We first attempted to immunostain for β-gal, but there was no specific staining; instead we used the X-gal assay. In whole mount KO retinas, staining was present throughout the ganglion cell layer (GCL) (**Figures 5A,B**). No staining was found in WT, suggesting that this staining is specific and is present only in cells that normally express PDE9A. We determined the percentage of PDE9A-expressing cells within the GCL by co-staining the retina with DAPI. In a total GCL area of 150,000 μm^2 (3 retinas combined) we found 1844 somas of which 28% were stained for X-gal. We also performed X-gal staining on vertical cryosections of the retina. Most staining was observed in cells of the GCL, but some staining was also observed in the somas of amacrine cells in the inner nuclear layer (**Figure 5C**).

Based on transcript presence and pharmacological blocking of certain PDE isoforms, it was suggested that retinal pigment epithelium (RPE) expresses PDE9A (Diederen et al., 2007). If so, absence of PDE9A from these cells may be able to explain the slow b-wave. We have therefore examined retinal cryosections that had RPE and choroid layers intact. There was no X-gal staining in the RPE; however we observed staining in the non-pigmented epithelium of the ciliary body (**Figure 5D**), in certain unidentified cells in the sclera, and in the lens (not shown). We further examined whole mounts of the pigment epithelium layer, but did not observe any staining.

To determine whether the cells in the GCL were amacrine or ganglion cells, we immunostained the X-gal stained retina for the amacrine cell markers GABA and glycine (**Figure 6**). Our antibody against glycine gave a high general background without specific staining, so the analysis relied on staining for GABA. We found that most X-gal-stained cells in the GCL were negative for GABA (e.g., cells 2, 6, 8 in **Figures 6A–C**), but many were positive (e.g., cells 1, 7). Similarly, in the inner nuclear layer, most X-gal-stained cells were negative for GABA but some were positive. To determine the percent of X-gal-stained cells that use GABA and the percent of GABA-immunoreactive cells that express β-gal, we co-stained whole mount retinas with X-gal and for GABA (**Figure 6D**). We found that in the GCL, 20% of X-gal-stained cells also stained for GABA, and 20% of GABAergic cells also stained with X-gal (3 retinas, **Table 1**). In the INL, 27% of X-gal-stained cells stained for GABA, but only 7% of the GABAergic cells stained with X-gal. This experiment suggests that PDE9A is present in one or more types of GABAergic amacrine cells, but mostly in GABA-negative cells.

DISCUSSION

We report here on two main findings. First, within the retina, PDE9A is restricted to the inner layers: it is widely distributed within the GCL and less widely within the amacrine tier of the inner nuclear layer. Second, PDE9A contributes to the amplitude and kinetics of the photopic ERG.

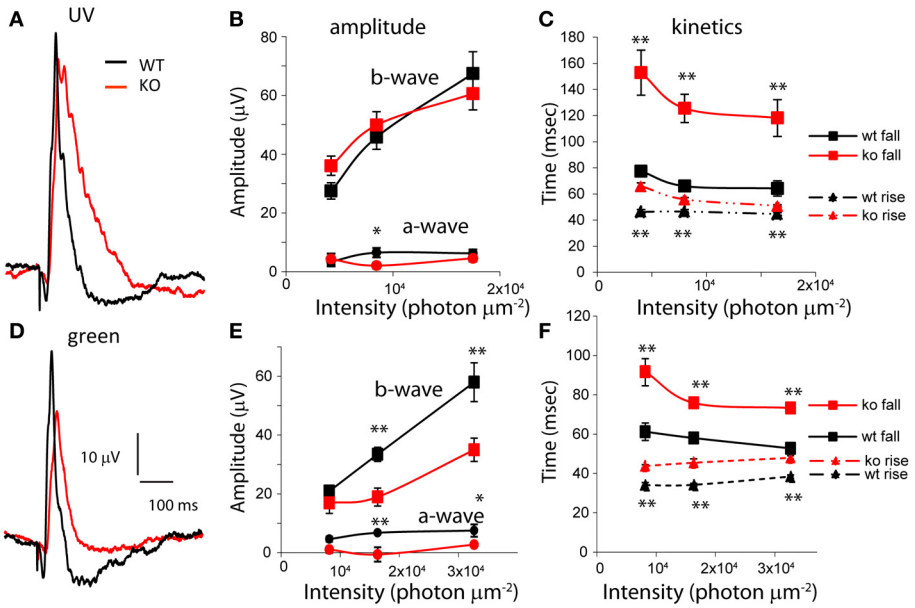

FIGURE 4 | PDE9A accelerates the kinetics of the photopic b-wave. **(A)** Average responses from WT and KO retinas to ultra-violet (UV) light of intensity 1.65×10^4 photons μm^{-2} (17 records were averaged for WT and 24 for KO). **(B)** Amplitudes of the a- and b-waves from WT ($n = 9$–12 mice) and KO ($n = 12$–13) retinas at increasing intensities of UV light. **(C)** The time taken by the b-wave to rise and fall to 66% of its amplitude at different intensities of stimulation. The time taken by the b-wave to rise and decay to 66% of its amplitude was significantly longer in KO at all intensities. **(D)** Average response of WT and KO retinas to green light of intensity 3.2×10^4 photons μm^{-2} ($n = 16$ for WT and 19 for KO). **(E)** Amplitudes of the a- and b-waves from WT ($n = 7$–11) and KO ($n = 2$–11). Mice at increasing intensities of green light. **(F)** The times taken by the b-wave to rise and fall to 66% of its amplitude: both parameters are significantly longer in KO.

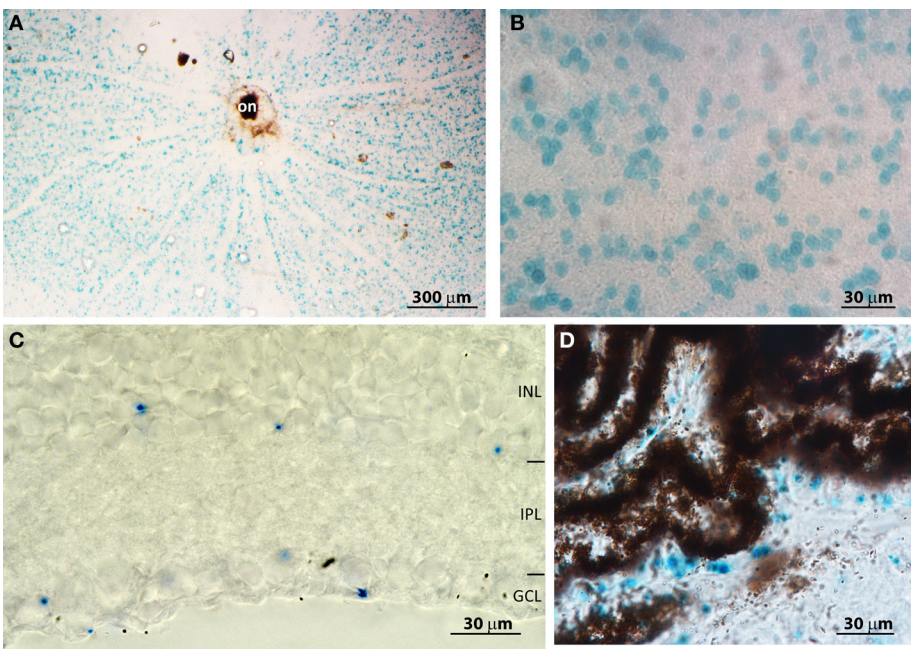

FIGURE 5 | PDE9A is localized in the inner retina. (A) Low magnification (4×) image of a whole mount *PDE9A* KO retina stained for X-gal (blue); on, optic nerve head. **(B)** Higher magnification (40×) image of the ganglion cell layer (GCL) in the same retina as in **(A)**: the stained cells occupy less than 50% of the area. **(C)** A cryosection of a KO retina stained for X-gal. X-gal staining is present in both the inner nuclear layer (INL) and GCL. IPL: inner plexiform layer. **(D)** Cryosection of KO retina showing X-gal staining in the ciliary body.

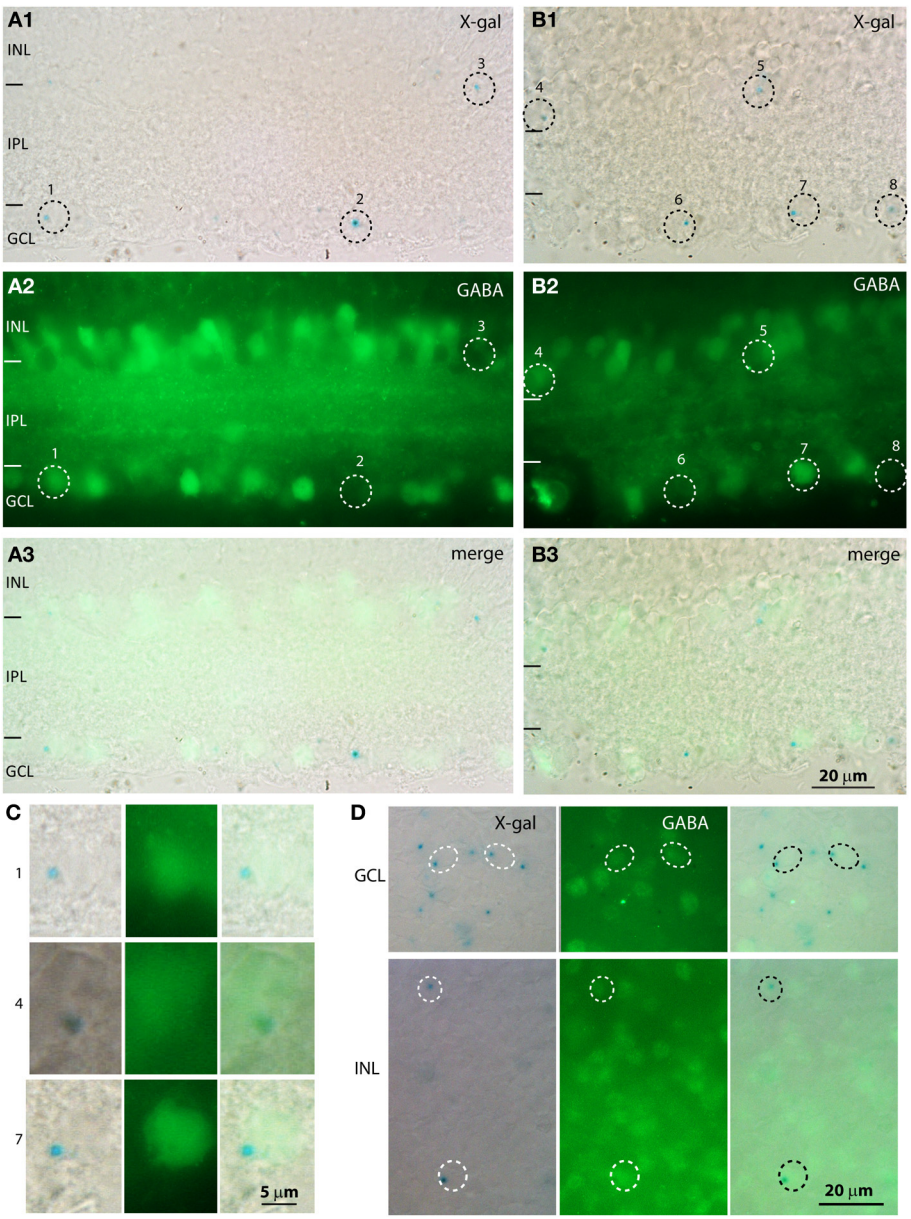

FIGURE 6 | A population of X-gal positive cells is positive for GABA. **(A,B)** Cryosections from KO retinas double stained with X-gal (**A_1,B_1;** blue, visualized with DIC microscopy) and for GABA (**A_2,B_2**, visualized with fluorescence microscopy). Dotted circles indicate the location of the somas of the cells that are positive for X-gal. The merged images **(A_3,B_3)** show that some cells positive for X-gal are also positive for GABA and others are negative for GABA. **(C)** Magnified images of the X-gal positive cells (numbers on the side correspond to numbers on the low magnification images) that are also positive for GABA. Cells 1, 7 are located in the GCL and cell 4 is located in the INL. **(D)** Whole mount preparations stained with X-gal reagent and for GABA show that some cells in both GCL and INL stained for both (circles), while several X-gal stained cells were negative for GABA and numerous GABA-immunoreactive cells were not stained with X-gal.

PDE9A IS LOCALIZED TO SEVERAL RETINAL CELL TYPES

Our experiments identify at least three retinal cell types that express PDE9A: GABAergic amacrine cells, non-GABAergic amacrine cells (hence, glycinergic), and ganglion cells. The GABAergic amacrine cell type was identified by GABA-positive staining in a subset of X-gal-stained cells. We know that our immunostaining for GABA is genuine because we have previously shown that all cells that immunostain for GABA also express GAD_{65} or GAD_{67} (Vardi and Auerbach, 1995). In the inner retina, cGMP is predominantly synthesized by the soluble isoform of guanylate cyclase (sGC), which is activated by nitric oxide (NO). Immunostaining for the β1 subunit of sGC (the obligatory subunit of the heterodimer in neurons) in rat retina shows that sGC is expressed in a subset of amacrine cells, some of which are GABAergic (Ding and Weinberg, 2007). Given that the retinas of rats and mice are sufficiently similar, it is likely that these cells may

Table 1 | Percentage of PDE9A-expressing cells in retina (averages of 3 retinas).

	GCL	INL
No. of X-gal-stained cells/206,000 μm^2	495	219
No. of GABA-stained cells	325	509
% of X-gal cells that use GABA	20%	27%
% of GABA cells that expresses X-gal	20%	7%

be the GABAergic PDE9A-expressing amacrine cells. It remains to be determined whether the GABA-stained amacrine cells in the GCL are of the same type as those in the INL (but displaced), or if they represent a different amacrine cell type. The glycinergic type is inferred because nearly all amacrine cells in the INL stain either for GABA or for glycine (Marc et al., 1995; Vardi and Auerbach, 1995; Kalloniatis et al., 1996), thus it is highly likely that the GABA-negative X-gal stained amacrine cells are glycinergic. This inference agrees with a previous report that NO-stimulated cGMP production is localized to glycinergic amacrine cells (Yu and Eldred, 2005). We think that one or more ganglion cell types express PDE9A because of the following facts: (1) about 40% of the GCL cells are ganglion cells (Jeon et al., 1998); (2) only few glycinergic amacrine cells are present in the GCL (Pourcho and Goebel, 1985, 1987; Marc et al., 1995); and (3) the PDE9A-expressing cells in the GCL are more numerous than those in the INL, in fact about 30% of cells in GCL express PDE9A (this study). This agrees with presence of *PDE9A* transcript in ganglion cells (Siegert et al., 2009) and with reports that NO stimulates production of cGMP in certain ganglion cells (Ahmad et al., 1994; Blute et al., 2003).

PDE9A ACCELERATES THE PHOTOPIC ERG b-WAVE BY ENHANCING SERIAL INHIBITORY RESPONSES

The most striking phenotype of deleting PDE9A is the change in the kinetics of the photopic b-wave. Under light-adapted conditions, at the tested UV, green, and saturating white light intensities, the falling phase of the b-wave in KO was slower, and the wave was wider than in WT. For UV and green flashes, the rising phase of the b-wave was also slower. Slower ERG b-wave in light-adapted conditions had been reported following intravitreal injection of TTX in mouse (Miura et al., 2009) and rat (Bui and Fortune, 2004; Mojumder et al., 2008). Similar effects of TTX on ERG kinetics were also reported in rabbit after 5 min of dark adaptation (Dong and Hare, 2000). Even a greater effect on the photpic ERG kinetics was found following injection of PDA (cis-2, 3-piperidinedicarboxylic acid which blocks transmission to hyperpolarizing 2nd order and all 3rd order neurons), or CNQX (Sharma et al., 2005; Miura et al., 2009). Another common qualitative outcome to the *PDE9A* KO and to applications of TTX, PDA, or CNQX is the reduced b-wave amplitude. While some of the effect of TTX in the light adapted retina is due to sodium channels in certain ON cone bipolar cells (Mojumder et al., 2008), an additional effect must be due to contribution from the inner retina, suggesting that spiking amacrine cells enhance and speed up the ON cone bipolar cells' responses. The precise mechanisms by which amacrine cells affect the b-wave are not known. However, it is known that cone bipolar cells receive different types of inhibitory input from amacrine cells and that these amacrine cells themselves receive inhibitory input (serial inhibition). Furthermore, it has been shown by whole cell recordings and ERG recordings that these inhibitory circuits accelerate and often enhance bipolar cells' responses (e.g., Dong and Hare, 2000, 2002; Molnar and Werblin, 2007; Eggers and Lukasiewicz, 2011; Eggers et al., 2013).

How can deletion of PDE9A mimic this effect? It is well known that many amacrine cells use cGMP to modulate their activity. For example, light stimulation increases NO levels in the IPL (Eldred and Blute, 2005) and this increases the levels of cGMP. NOS1 (the enzyme that produces NO in neurons) is expressed in certain types of GABAergic amacrine cells, and NO stimulates the production of cGMP in neighboring sGC expressing cells (Ding and Weinberg, 2007). It is possible that these sGC expressing amacrine cells are those that express PDE9A, and that these two enzymes regulate cGMP in a light-dependent manner. Since cGMP activates cGMP-dependent kinases (such as PKG), and since phosphorylation crucially controls exocytosis and endocytosis (Liu, 1997), absence of PDE9A can alter neurotransmiter release. Thus, if PDE9A-expressing cells inhibit bipolar cells in a time-dependent manner to regulate their response size and kinetics; absence of PDE9A, which likely causes an accumulation of cGMP, would render bipolar cells' responses slower. Based on the characteristics of the b-wave seen in the absence of PDE9A and their resemblance to the pharmacological results described above, we predict that these cells spike at photopic intensities. Finally, although PDE9A is likely present also in ganglion cells, we do not think that they contribute to reducing the ERG b-wave and slowing down its kinetics because in WT, ganglion cells do not contribute to the ERG a- and b- waves (Bui and Fortune, 2004; Li et al., 2005; Mojumder et al., 2008). Ganglion cells, however, do contribute to the photopic negative response (PhNR) (Li et al., 2005), and although not quantified here, this wave might have been affected.

PDE9A LIKELY REDUCES THE CONE-GENERATED a-WAVE DUE TO AN EFFECT ON THE OFF PATHWAY

We found that in the absence of PDE9A, the photopic a-wave elicited by both green and saturating flashes was smaller. In rodents, the photopic a-wave is generated by the activity of cones and post-receptoral neurons, which includes a small contribution from OFF bipolar cells and horizontal, and perhaps a larger contribution from amacrine cells (Xu et al., 2003; Sharma et al., 2005; Mojumder et al., 2008; Shirato et al., 2008). We think that the reduced a-wave in KO represents reduced current contribution from the inner retinal cells and not reduced cone activity because cones do not express PDE9A. Thus, the same disrupted signal processing that explains the reduced ON bipolar cells' activity, as reflected by the ERG b-wave in KO, could explain the reduced inner retina component of the photopic a-wave (either an indirect influence on OFF bipolar cells' activity or reduced current from amacrine cells). This interpretation also explains why the a-wave of the mix rod-cone ERG was smaller in KO than in WT retina. With such bright flashes, both cones and inner retinal cells likely contribute to the negative a-wave. In contrast, rod function

has not been altered, as can be inferred from both the similar Lamb and Pugh amplification constants and the similar scotopic responses in KO and WT.

CONCLUSION

The results of our study indicate that PDE9A, by hydrolyzing cGMP, controls its levels and thereby modulates inhibitory processes in the retina. We speculate that light increases nitric oxide levels in the cone pathway of the inner retina; this stimulates sGCs, increases cGMP levels, and modulates inhibition. By hydrolyzing cGMP, PDE9A restricts the duration of the inhibitory processes, thus sharpening and accelerating retinal signaling.

ACKNOWLEDGMENTS

This work was supported by National Institutes of Health Grants EY11105 (Noga Vardi), EY013333 (Michael A. Freed), and NEI P30 EY01583 (Vision Research Core of the University of Pennsylvania). We thank Pfizer and especially Dr. Rita Balice Gordon and Dr. Frank S. Menniti for providing the PDE9A KO mice. We also thank Drs. Sergei Nikonov, Michael A. Freed, and Robert Smith for multiple useful discussions, Dr. Narender Dhingra for reading the manuscript, and Dr. Sergei Nikonov and Richard Zorger for writing the MATLAB program to analyze ERG.

REFERENCES

Ahmad, I., Leinders-Zufall, T., Kocsis, J. D., Shepherd, G. M., Zufall, F., and Barnstable, C. J. (1994). Retinal ganglion cells express a cGMP-gated cation conductance activatable by nitric oxide donors. *Neuron* 12, 155–165. doi: 10.1016/0896-6273(94)90160-0

Beavo, J. A. (1995). Cyclic nucleotide phosphodiesterases: functional implications of multiple isoforms. *Physiol. Rev.* 75, 725–748.

Blute, T. A., Strang, C., Keyser, K. T., and Eldred, W. D. (2003). Activation of the cGMP/nitric oxide signal transduction system by nicotine in the retina. *Vis. Neurosci.* 20, 165–176. doi: 10.1017/S0952523803202078

Breton, M. E., Schueller, A. W., Lamb, T. D., and Pugh, E. N. Jr. (1994). Analysis of ERG a-wave amplification and kinetics in terms of the G-protein cascade of phototransduction. *Invest. Ophthalmol. Vis. Sci.* 35, 295–309.

Bui, B. V., and Fortune, B. (2004). Ganglion cell contributions to the rat full-field electroretinogram. *J. Physiol.* 555, 153–173. doi: 10.1113/jphysiol.2003.052738

Chun, M. H., Oh, S. J., Kim, I. B., and Kim, K. Y. (1999). Light and electron microscopical analysis of nitric oxide synthase-like immunoreactive neurons in the rat retina. *Vis. Neurosci.* 16, 379–389. doi: 10.1017/S0952523899162175

de la Villa, P., Kurahashi, T., and Kaneko, A. (1995). L-glutamate-induced responses and cGMP-activated channels in three subtypes of retinal bipolar cells dissociated from the cat. *J. Neurosci.* 15, 3571–3582.

Dhingra, A., Sulaiman, P., Xu, Y., Fina, M. E., Veh, R. W., and Vardi, N. (2008). Probing neurochemical structure and function of retinal ON bipolar cells with a transgenic mouse. *J. Comp. Neurol.* 510, 484–496. doi: 10.1002/cne.21807

Diederen, R. M., La Heij, E. C., Markerink-van Ittersum, M., Kijlstra, A., Hendrikse, F., and de Vente, J. (2007). Selective blockade of phosphodiesterase types 2, 5 and 9 results in cyclic 3′5′ guanosine monophosphate accumulation in retinal pigment epithelium cells. *Br. J. Ophthalmol.* 91, 379–384. doi: 10.1136/bjo.2006.100628

Ding, J. D., and Weinberg, R. J. (2007). Distribution of soluble guanylyl cyclase in rat retina. *J. Comp. Neurol.* 502, 734–745. doi: 10.1002/cne.21206

Dong, C. J., and Hare, W. A. (2000). Contribution to the kinetics and amplitude of the electroretinogram b-wave by third-order retinal neurons in the rabbit retina. *Vision Res.* 40, 579–589. doi: 10.1016/S0042-6989(99)00203-5

Dong, C. J., and Hare, W. A. (2002). GABAc feedback pathway modulates the amplitude and kinetics of ERG b-wave in a mammalian retina *in vivo*. *Vision Res.* 42, 1081–1087. doi: 10.1016/S0042-6989(02)00032-9

Eggers, E. D., and Lukasiewicz, P. D. (2011). Multiple pathways of inhibition shape bipolar cell responses in the retina. *Vis. Neurosci.* 28, 95–108. doi: 10.1017/S0952523810000209

Eggers, E. D., Mazade, R. E., and Klein, J. S. (2013). Inhibition to retinal rod bipolar cells is regulated by light levels. *J. Neurophysiol.* 110, 153–161. doi: 10.1152/jn.00872.2012

Eldred, W. D., and Blute, T. A. (2005). Imaging of nitric oxide in the retina. *Vision Res.* 45, 3469–3486. doi: 10.1016/j.visres.2005.07.033

Fisher, D. A., Smith, J. F., Pillar, J. S., St. Denis, S. H., and Cheng, J. B. (1998). Isolation and characterization of PDE9A, a novel human cGMP-specific phosphodiesterase. *J. Biol. Chem.* 273, 15559–15564. doi: 10.1074/jbc.273.25.15559

Gotzes, S., de Vente, J., and Muller, F. (1998). Nitric oxide modulates cGMP levels in neurons of the inner and outer retina in opposite ways. *Vis. Neurosci.* 15, 945–955. doi: 10.1017/S0952523898155141

Hsu, Y. T., and Molday, R. S. (1993). Modulation of the cGMP-gated channel of rod photoreceptor cells by calmodulin. *Nature* 361, 76–79. doi: 10.1038/361076a0

Jeon, C. J., Strettoi, E., and Masland, R. H. (1998). The major cell populations of the mouse retina. *J. Neurosci.* 18, 8936–8946.

Juilfs, D. M., Soderling, T. R., Burns, F., and Beavo, J. A. (1999). Cyclic GMP as substrate and regulator of cyclic nucleotide phosphodiesterases (PDEs). *Rev. Physiol. Biochem. Pharmacol.* 135, 67–103. doi: 10.1007/BFb0033670

Kalloniatis, M., Marc, R. E., and Murry, R. F. (1996). Amino acid signatures in the primate retina. *J. Neurosci.* 16, 6807–6829.

Koike, C., Obara, T., Uriu, Y., Numata, T., Sanuki, R., Miyata, K., et al. (2010). TRPM1 is a component of the retinal ON bipolar cell transduction channel in the mGluR6 cascade. *Proc. Natl. Acad. Sci. U.S.A.* 107, 332–337. doi: 10.1073/pnas.0912730107

Lamb, T. D., and Pugh, E. N. Jr. (1992). G-protein cascades: gain and kinetics. *Trends Neurosci.* 15, 291–298. doi: 10.1016/0166-2236(92)90079-N

Li, B., Barnes, G. E., and Holt, W. F. (2005). The decline of the photopic negative response (PhNR) in the rat after optic nerve transection. *Doc. Ophthalmol.* 111, 23–31. doi: 10.1007/s10633-005-2629-8

Liu, J. P. (1997). Protein phosphorylation events in exocytosis and endocytosis. *Clin. Exp. Pharmacol. Physiol.* 24, 611–618. doi: 10.1111/j.1440-1681.1997.tb02101.x

Lyubarsky, A. L., Daniele, L. L., and Pugh, E. N. Jr. (2004). From candelas to photoisomerizations in the mouse eye by rhodopsin bleaching *in situ* and the light-rearing dependence of the major components of the mouse ERG. *Vision Res.* 44, 3235–3251. doi: 10.1016/j.visres.2004.09.019

Lyubarsky, A. L., Chen, C., Simon, M. I., and Pugh, E. N. Jr. (2000). Mice lacking G-protein receptor kinase 1 have profoundly slowed recovery of cone-driven retinal responses. *J. Neurosci.* 20, 2209–2217.

Lyubarsky, A. L., Falsini, B., Pennesi, M. E., Valentini, P., and Pugh, E. N. Jr. (1999). UV- and midwave-sensitive cone-driven retinal responses of the mouse: a possible phenotype for coexpression of cone photopigments. *J. Neurosci.* 19, 442–455.

Lyubarsky, A. L., and Pugh, E. N. Jr. (1996). Recovery phase of the murine rod photoresponse reconstructed from electroretinographic recordings. *J. Neurosci.* 16, 563–571.

Marc, R. E., Murry, R. F., and Basinger, S. F. (1995). Pattern recognition of amino acid signatures in retinal neurons. *J. Neurosci.* 15, 5106–5129.

Menniti, F., Kleiman, R., and Schmidt, C. (2008). PDE9A-mediated regulation of cGMP: impact on synaptic plasticity. *Schizophr. Res.* 102(Suppl. 2), 38. doi: 10.1016/S0920-9964(08)70122-1

Mills, S. L., and Massey, S. C. (1995). Differential properties of two gap junctional pathways made by AII amacrine cells. *Nature* 377, 734–737. doi: 10.1038/377734a0

Miura, G., Wang, M. H., Ivers, K. M., and Frishman, L. J. (2009). Retinal pathway origins of the pattern ERG of the mouse. *Exp. Eye Res.* 89, 49–62. doi: 10.1016/j.exer.2009.02.009

Mojumder, D. K., Sherry, D. M., and Frishman, L. J. (2008). Contribution of voltage-gated sodium channels to the b-wave of the mammalian flash electroretinogram. *J. Physiol.* 586, 2551–2580. doi: 10.1113/jphysiol.2008.150755

Molnar, A., and Werblin, F. (2007). Inhibitory feedback shapes bipolar cell responses in the rabbit retina. *J. Neurophysiol.* 98, 3423–3435. doi: 10.1152/jn.00838.2007

Morgans, C. W., Zhang, J., Jeffrey, B. G., Nelson, S. M., Burke, N. S., Duvoisin, R. M., et al. (2009). TRPM1 is required for the depolarizing light response in retinal ON-bipolar cells. *Proc. Natl. Acad. Sci. U.S.A.* 106, 19174–19178. doi: 10.1073/pnas.0908711106

Nawy, S. (1999). The metabotropic receptor mGluR6 may signal through G(o), but not phosphodiesterase, in retinal bipolar cells. *J. Neurosci.* 19, 2938–2944.

Nawy, S., and Jahr, C. E. (1990). Suppression by glutamate of cGMP-activated conductance in retinal bipolar cells. *Nature* 346, 269–271. doi: 10.1038/346269a0

Ng, L., Lyubarsky, A., Nikonov, S. S., Ma, M., Srinivas, M., Kefas, B., et al. (2010). Type 3 deiodinase, a thyroid-hormone-inactivating enzyme, controls survival and maturation of cone photoreceptors. *J. Neurosci.* 30, 3347–3357. doi: 10.1523/JNEUROSCI.5267-09.2010

Polson, J. B., and Strada, S. J. (1996). Cyclic nucleotide phosphordiesterases and vascular smooth muscle. *Ann Rev Pharmacol Toxicol* 36, 403–427. doi: 10.1146/annurev.pa.36.040196.002155

Pourcho, R. G., and Goebel, D. J. (1985). A combined Golgi and autoradiographic study of (3 H)glycine-accumulating amacrine cells in the cat retina. *J. Comp. Neurol.* 233, 473–480. doi: 10.1002/cne.902330406

Pourcho, R. G., and Goebel, D. J. (1987). Visualization of endogenous glycine in cat retina: an immunocytochemical study with Fab fragments. *J. Neurosci.* 7, 1189–1197.

Sharma, S., Ball, S. L., and Peachey, N. S. (2005). Pharmacological studies of the mouse cone electroretinogram. *Vis. Neurosci.* 22, 631–636. doi: 10.1017/S0952523805225129

Shiells, R. A., and Falk, G. (1990). Glutamate receptors of rod bipolar cells are linked to a cyclic GMP cascade via a G-protein. *Proc. Biol. Sci.* 242, 91–94. doi: 10.1098/rspb.1990.0109

Shiells, R. A., and Falk, G. (1992). Properties of the cGMP-activated channel of retinal on-bipolar cells. *Proc. Biol. Sci.* 247, 21–25. doi: 10.1098/rspb.1992.0004

Shiells, R. A., and Falk, G. (2002). Potentiation of 'on' bipolar cell flash responses by dim background light and cGMP in dogfish retinal slices. *J. Physiol.* 542, 211–220. doi: 10.1113/jphysiol.2002.019752

Shirato, S., Maeda, H., Miura, G., and Frishman, L. J. (2008). Postreceptoral contributions to the light-adapted ERG of mice lacking b-waves. *Exp. Eye Res.* 86, 914–928. doi: 10.1016/j.exer.2008.03.008

Siegert, S., Scherf, B. G., Del Punta, K., Didkovsky, N., Heintz, N., and Roska, B. (2009). Genetic address book for retinal cell types. *Nat. Neurosci.* 12, 1197–1204. doi: 10.1038/nn.2370

Snellman, J., and Nawy, S. (2004). cGMP-dependent kinase regulates response sensitivity of the mouse on bipolar cell. *J. Neurosci.* 24, 6621–6628. doi: 10.1523/JNEUROSCI.1474-04.2004

van Staveren, W. C., and Markerink-van Ittersum, M. (2005). Localization of cyclic guanosine 3′,5′-monophosphate-hydrolyzing phosphodiesterase type 9 in rat brain by nonradioactive *in situ* hydridization. *Methods Mol. Biol.* 307, 75–84. doi: 10.1385/1-59259-839-0:075

Vardi, N., and Auerbach, P. (1995). Specific cell types in cat retina express different forms of glutamic acid decarboxylase. *J. Comp. Neurol.* 351, 374–384. doi: 10.1002/cne.903510305

Xu, L., Ball, S. L., Alexander, K. R., and Peachey, N. S. (2003). Pharmacological analysis of the rat cone electroretinogram. *Vis. Neurosci.* 20, 297–306. doi: 10.1017/S0952523803203084

Yau, K. W. (1994). Phototransduction mechanism in retinal rods and cones. *Invest. Ophthalmol. Vis. Sci.* 35, 9–32.

Yu, D., and Eldred, W. D. (2005). Gycine and GABA interact to regulate the nitric oxide/cGMP signaling pathway in the turtle retina. *Vis. Neurosci.* 22, 825–838. doi: 10.1017/S0952523805226123

Conflict of Interest Statement: The authors declare that the research was conducted in the absence of any commercial or financial relationships that could be construed as a potential conflict of interest.

Received: 26 March 2014; accepted: 09 June 2014; published online: 27 June 2014.
Citation: Dhingra A, Tummala SR, Lyubarsky A and Vardi N (2014) PDE9A is expressed in the inner retina and contributes to the normal shape of the photopic ERG waveform. Front. Mol. Neurosci. 7:60. doi: 10.3389/fnmol.2014.00060
This article was submitted to the journal Frontiers in Molecular Neuroscience.

frontiers in
MOLECULAR NEUROSCIENCE

REVIEW ARTICLE
published: 22 August 2014
doi: 10.3389/fnmol.2014.00075

Guanylyl cyclase/natriuretic peptide receptor-A signaling antagonizes phosphoinositide hydrolysis, Ca^{2+} release, and activation of protein kinase C

Kailash N. Pandey*

Department of Physiology, School of Medicine, Tulane University Health Sciences Center, New Orleans, LA, USA

Edited by:
Teresa Duda, Salus University, USA

Reviewed by:
Sandhya Srikant Visweswariah, Indian Institute of Science, India
Teresa Duda, Salus University, USA

****Correspondence:***
Kailash N. Pandey, Department of Physiology, School of Medicine, Tulane University Health Sciences Center, 1430 Tulane Avenue, New Orleans, LA 70112, USA
e-mail: kpandey@tulane.edu

Thus far, three related natriuretic peptides (NPs) and three distinct sub-types of cognate NP receptors have been identified and characterized based on the specific ligand binding affinities, guanylyl cyclase activity, and generation of intracellular cGMP. Atrial and brain natriuretic peptides (ANP and BNP) specifically bind and activate guanylyl cyclase/natriuretic peptide receptor-A (GC-A/NPRA), and C-type natriuretic peptide (CNP) shows specificity to activate guanylyl cyclase/natriuretic peptide receptor-B (GC-B/NPRB). All three NPs bind to natriuretic peptide receptor-C (NPRC), which is also known as clearance or silent receptor. The NPRA is considered the principal biologically active receptor of NP family; however, the molecular signaling mechanisms of NP receptors are not well understood. The activation of NPRA and NPRB produces the intracellular second messenger cGMP, which serves as the major signaling molecule of all three NPs. The activation of NPRB in response to CNP also produces the intracellular cGMP; however, at lower magnitude than that of NPRA, which is activated by ANP and BNP. In addition to enhanced accumulation of intracellular cGMP in response to all three NPs, the levels of cAMP, Ca^{2+} and inositol triphosphate (IP_3) have also been reported to be altered in different cells and tissue types. Interestingly, ANP has been found to lower the concentrations of cAMP, Ca^{2+}, and IP_3; however, NPRC has been proposed to increase the levels of these metabolic signaling molecules. The mechanistic studies of decreased and/or increased levels of cAMP, Ca^{2+}, and IP_3 in response to NPs and their receptors have not yet been clearly established. This review focuses on the signaling mechanisms of ANP/NPRA and their biological effects involving an increased level of intracellular accumulation of cGMP and a decreased level of cAMP, Ca^{2+}, and IP_3 in different cells and tissue systems.

Keywords: natriuretic peptides, natriuretic peptide receptors, membrane guanylyl cyclases, cGMP, cAMP, Ca^{2+}, inositol triphosphate

INTRODUCTION

Atrial natriuretic factor/peptide (ANF/ANP) is produced and secreted in the specific granules of cardiac atrial myocytes, which participates in the control of extracellular fluid volume, electrolyte balance, and mean arterial pressure, thus, it plays a central role in the maintenance and regulation of cardiovascular homeostasis (de Bold et al., 1981; de Bold, 1985; Brenner et al., 1990; Anand-Srivastava and Trachte, 1993; Pandey, 2005, 2011). In addition to its natriuretic, diuretic, vasorelaxant, antimitogenic, antihypertrophic, and anti-inflammatory activities, ANP inhibits the release of renin from the kidneys, aldosterone from the adrenal glands, vasopressin from posterior pituitary, and progesterone from Leydig tumor (MA-10) cells, while stimulating the synthesis and release of testosterone from normal Leydig cells in the testes, progesterone from granulosa-leuteal cells, and luteinizing hormone from anterior pituitary gland (Inagami, 1989; Brenner et al., 1990; Levin et al., 1998; Pandey, 2005). A number of studies have documented that ANP has always been found to increase the intracellular accumulation of cGMP, however, to decrease the levels of cAMP; Ca^{2+}, and inositol triphosphate (IP_3) in agonist hormone-treated cells and tissues (Waldman et al., 1984; Pandey et al., 1985, 1988; Khurana and Pandey, 1993, 1996; Pandey, 2005; Turovsky et al., 2013). It has also been suggested that ANP decreases the cAMP levels by stimulating the cGMP-specific phosphodiesterases; however, in certain cells and tissue types, ANP did not decrease or change the cAMP concentrations. Several studies have indicated that ANP diminishes the Ca^{2+} signals probably by activating the Ca^{2+} extrusion processes by protein kinase-G (PKG) specifically in endothelial and vascular smooth muscle cells (VSMCs; Rashatwar et al., 1987; Zolle et al., 2000; Pandey, 2005).

Among the natriuretic peptides (NPs) hormone family, ANP is the first described member, later, two other members of NP family; brain natriuretic peptide (BNP) and C-type natriuretic peptide (CNP) were identified and characterized, which also exhibited biochemical and structural properties similar to ANP; however, each prepro NP hormone is encoded from a separate gene (Rosenzweig and Seidman, 1991; Levin et al., 1998). Although, all three NPs (ANP, BNP, and CNP) have highly homologous structure, they bind to specific NP receptors and elicit discrete biological

and physiological functions (Brenner et al., 1990). There have been three subtypes of NP receptors, namely; NP receptor-A, NP receptor-B, and NP peptide receptor-C (NPRA, NPRB, and NPRC, respectively), which were identified and characterized by molecular cloning (Pandey and Singh, 1990; Garbers, 1992). Interestingly, both ANP and BNP bind to NPRA, which produces the intracellular second messenger cGMP; however, CNP binds NPRB, which also generates cGMP, but all three NPs indiscriminately bind and activate NPRC, which lacks GC catalytic domain (Fuller et al., 1988; Drewett and Garbers, 1994; Lucas et al., 2000; Sharma, 2002; Pandey, 2005). The cellular, biochemical, and pharmacological aspects of NPs and their cognate receptors have revealed classic hallmark of physiological and pathophysiological functional significance, including; renal, cardiac, vascular, neuronal, and immunological aspects in health and disease (Pandey, 2005, 2011; Kishimoto et al., 2011). It has been suggested that ANP suppresses Na^+-reabsorption at the collecting duct of the kidneys, inhibits renin synthesis and release, and stimulates natriuresis and diuresis, thereby, lowers blood pressure and blood volume and maintains cardiovascular homeostasis (de Bold, 1985; Brenner et al., 1990; Levin et al., 1998; Pandey, 2005). In the vasculature, ANP relaxes VSMCs thus causing the immediate vasorelaxant effect in the vascular bed (Levin et al., 1998; Pandey, 2005).

The expression and activity of NPRA is regulated by various hormonal agents, including its ligand ANP (Pandey, 1993, 2005; Cao et al., 1995; Pandey et al., 2002). The studies detailing the *Npr1* (coding for NPRA) gene-disruption in mice have revealed the functional significance of NPRA in the control of blood pressure and cardiovascular disease states (Oliver et al., 1997; Shi et al., 2001; Holtwick et al., 2002; Vellaichamy et al., 2005; Kishimoto et al., 2011; Pandey, 2011; Yoshihara et al., 2014). Mice lacking NPRA develop high blood pressure and severe cardiac hypertrophy, fibrosis, and disorders that are reminiscent of heart disease as seen in untreated human hypertensive patients (Vellaichamy et al., 2007, 2014; Zhao et al., 2013). The regulated expression of CNP is derived from endothelial cells, which targets NPRB on the adjacent smooth muscle cells (Suga et al., 1992). Thus, the principal role of CNP is considered as a direct vasodilator involved in the regulation of vascular tone through activation of GC-B/NPRB on smooth muscle cells in the vascular beds (Hama et al., 1994). The objective of this current review is to summarize and document the findings and discoveries with particular emphasis of cellular signaling and physiological and pathological significance of ANP/NPRA in relation to the increased production of intracellular second messenger cGMP and inhibition of the phosphoinositide (IP_3) hydrolysis, Ca^{2+} release, and protein kinase C (PKC) activity in target cells.

HISTORICAL BACKGROUND

Thirty-three years ago, the pioneer discovery by de Bold and his coworkers established that atrial extracts contained natriuretic and diuretic activity which led to the isolation and nomenclature of ANF, usually referred to as ANP (de Bold et al., 1981; de Bold, 1985). Now, it is considered that ANP is primarily synthesized and secreted in the granules of heart atrium and BNP is largely synthesized in the heart ventricle and displays most variability in the primary structure. Although, the atrium is the primary site of synthesis for ANP, however, ventricle also produces ANP but at the levels of 100-fold to 1000-fold lower than that of the atrium, respectively (Kojima et al., 1989). CNP was isolated from the porcine brain, however, is mostly present in the endothelial cells of the vasculature and is highly conserved among the mammalian species (Rosenzweig and Seidman, 1991). The primary structure deduced from the cDNA synthesis, suggested that ANP is synthesized first as the 152-amino acid prepro-ANP molecule that contains sequences of active peptide in its carboxyl-terminal region (Maki et al., 1984). The biologically active ANP is released by proteolytic cleavage of pro-ANP molecule into predominantly 28-amino acid active (residues 99–126) and the 98 amino acid inactive (residues 1–98) molecules. The active form of ANP has a disulfide-bonded loop between cysteine 105 and 121, which seems to be essential for the biological activity (Brenner et al., 1990). Initially, different lengths of sequences of ANP were identified and synthesized for the studies of structure-activity relationship, and it was suggested that the ring structure of ANP with a disulfide-bonded loop is essential for its biological activities (Rosenzweig and Seidman, 1991). All three NPs contain highly conserved amino acid sequences with a 17-residues disulfide-bonded ring but deviate from each other in the N-terminal and C-terminal flanking amino acid sequences. Furthermore, the C-terminal sequence extending from the ring structure to Asn-Phe-Arg-Tyr is essential for the biological activity of ANP. The amino acid sequence of ANP is almost identical across the mammalian species, except at the position 10, which is substituted with isoleucine in rat, mouse, and rabbit, however, in human, dog, and bovine, ANPs have methionine in this position (Misono et al., 1984). Subsequently, BNP and CNP were both isolated and characterized from the porcine brain extracts (Sudoh et al., 1988, 1990). BNP is predominantly synthesized and secreted from the heart ventricle (Phillips et al., 1991). Similarly, CNP is predominantly localized in the central nervous system and endothelial cells and is considered as a non-circulatory peptide hormone (Suga et al., 1992).

NATRIURETIC PEPTIDES SYNTHESIS AND SECRETION

It has been suggested that the processing of preprohormone to prohormone molecule and the cleavage and secretion of biologically active mature 28-residue ANP molecule occurs predominantly in response to atrial distension (de Bold, 1985; Brenner et al., 1990). Usually, ANP concentration ranges from 50 to 100-fold higher than BNP; however, the expression of both ANP and BNP increases dramatically in the atrium and ventricle in the condition of cardiac disorders and heart failure (Mukoyama et al., 1991). During the disease states, the ventricle becomes the primary site of synthesis and release for BNP. In congestive heart failure (CHF) patients, the concentrations of both ANP and BNP increase greater than the control values, however, the BNP concentration increases 10-fold to 50-fold higher than a comparative increases in the ANP levels (Mukoyama et al., 1991). Those previous findings indicated that ANP and BNP elicit distinct physiological and pathophysiological effects, nevertheless, both hormones show similar hemodynamic responses, but BNP exerts a longer duration of action and causes enhanced natriuretic responses as compared

with ANP (Yoshimura et al., 1991; Omland et al., 1996). It has been suggested that the cardiac atrium expresses almost 50-fold to 100-fold or even higher levels of ANP mRNA as compared with extra -cardiac tissues (Gardner et al., 1986). Interestingly, higher ventricular ANP levels have been found in the developing embryos and fetuses; however, both mRNA and peptide levels of ANP decline rapidly during the prenatal period (Cameron et al., 1996). On the other hand, CNP does not seem to behave as a cardiac hormone and its concentration is extremely low in the circulation (Igaki et al., 1996). It is believed that CNP is largely localized in the central nervous system and in the vascular endothelial cells (Ogawa et al., 1992; Suga et al., 1992, 1993; Tamura et al., 1996; Chen and Burnett, 1998). Another class of NPs is the D-type natriuretic peptide (DNP) that represents an additional member in the NP hormone family and is largely present in the venom of the green mamba (*Dendroaspis angusticeps*) as a 38-amino acid peptide molecule (Schweitz et al., 1992; Lisy et al., 1999). In addition, a 32-amino acid peptide termed as urodilatin (URO) is identical to C-terminal sequence of pro-ANP, which is largely present only in the urine (Schulz-Knappe et al., 1988). Initially, URO was purified from the human urine and is considered to be synthesized only in the kidneys (Saxenhofer et al., 1990). The immunohistochemical staining indicated that URO is largely present in the cortical tubules around the collecting ducts of the kidneys (Meyer et al., 1996; Doust et al., 2005).

In the circulation, the half-life of BNP is greater than ANP, thus the evaluation of the diagnostic importance of the NPs have mostly favored BNP. The inactive N-terminal fragment of BNP (NT-proBNP) has even a greater half-life than the BNP. The plasma levels of both BNP and NT-proBNP are markedly elevated under the pathophysiological conditions of cardiac dysfunction, including diastolic dysfunction, CHF, and pulmonary embolism (Felker et al., 2006; Jaffe et al., 2006). The basal plasma levels of BNP vary from 5 to 50 pg/ml and NT-proBNP levels range from 10 to 150 pg/ml. An abnormal range is considered as 100 pg/ml for BNP and 125 pg/ml for NT-proBNP (Felker et al., 2006). Nevertheless, the secretion of both ANP and BNP from the ventricular myocytes increases proportionally in relation to the magnitude of cardiac dysfunction or heart failure condition (Yoshimura et al., 1993). It has been suggested that BNP acts as an important prognostic indicator in the CHF patients, however, NT-proBNP is considered to be a stronger risk bio-indicator for cardiovascular events (Doust et al., 2005). Both BNP and NT-proBNP seem to provide an ideal tool to be utilized as blood tests to diagnose cardiac disorders in patients with high risk of heart failure, diabetes, chronic kidney disease, and coronary artery disease (Khan et al., 2006; Freestone et al., 2008; Czucz et al., 2011; Ganem et al., 2011). The BNP level is increased to almost 200 pg/ml and NT-proBNP levels reaches to approximately 1200 pg/ml in patients with reduced creatinin clearance (McCullough et al., 2003; Anwaruddin et al., 2006).

IDENTIFICATION AND CHARACTERIZATION OF RECEPTOR MEMBRANE GUANYLYL CYCLASE

The previous studies using cross-linking and photoaffinity labeling procedures, have shown the existence of NP receptors with a wide range of molecular weight (M_r) of the 60–180 kDa (Misono et al., 1985; Schenk et al., 1985; Vandlen et al., 1985; Meloche et al., 1986; Pandey et al., 1986). Initially, NP receptors were identified with varying receptor density in different cells and tissue types (**Table 1**). Subsequently, high affinity ANP binding sites were with GC activity were co-purified (Kuno et al., 1986; Paul et al., 1987; Takayanagi et al., 1987; Meloche et al., 1988) On the basis of biological activity of different ANP analogs, NP receptors were classified and characterized as biologically active and clearance or silent receptors (Maack et al., 1987). Subsequently, three distinct subtypes of NP receptors were identified, which appeared to be specific to different cells and tissues (Pandey et al., 1988). Based on the cellular, biochemical, and molecular biological studies, the NPs and their receptors are quite widespread in cell and tissue distributions (Leitman et al., 1988; Pandey et al., 1988; Brenner et al., 1990; Marala et al., 1992; Levin et al., 1998; Pandey, 2005). Molecular cloning and expression of cDNA from mouse, rate, and human, led to identify and characterize the primary structure of three distinct subtypes of NP receptors, which are currently designated as GC-A/NPRA, GC-B/NPRB, and NPRC (Fuller et al.,

Table 1 | ANP-dependent binding parameters of GC-A/NPRA and intracellular accumulation of cGMP in different cell types.

Cell type	ANP-dependent Intracellular cGMP (fold stimulation)	Ligand binding parameters of NPRA	
		kd value (Molar)	B_{max} (receptor site/cell)
Endothelial cells	15	10–100 pM	0.5×10^5
Granulosa cells	30	10–100 pM	0.5×10^5
Glomerulosa cells	50	100–1 pM	2×10^5
MA-10 cells	1,500	100–1 nM	1×10^6
MDCK cells	50	10–100 pM	0.5×10^5
N4TG1 cells	30	1–100 pM	0.5×10^5
Primary Ledig cells	60	10–100 pM	0.5×10^5
RTASM cells	10	1–100 pM	0.2×10^5

HEK-293 cells, human embryonic Kidney-293 cells; kd, dissociation constant; B_{max}, receptor density; MA-10 cells, Leydig tumor cells; MDCK cells, Maiden-Darby kidney epithelial cells; N4TG1 cells, neuroblastoma cells; RTASM, rat thoracic aortic smooth muscle cells.

1988; Chinkers et al., 1989; Schulz et al., 1989; Pandey and Singh, 1990; Duda et al., 1991). The general topological structures of GC-A/NPRA and GC-B/NPRB are consistent with at least four distinct domains, including extracellular ligand-binding domain, a single transmembrane spanning region, and intracellular protein kinase-like homology domain (protein-KHD), and GC catalytic domain. The transmembrane GC receptors contain a single cyclase catalytic site per protein molecule, however, based on the structural modeling data two polypeptide chains seem to be required to activate GC-A/NPRA (Wilson and Chinkers, 1995; Labrecque et al., 1999; van den Akker et al., 2000). It has been indicated that the dimerization region of the receptor is located between the KHD and GC catalytic domain that has been predicted to form an amphipathic alpha helix structure. The GC-B/NPRB has the overall domain structure similar to that of GC-A/NPRA with binding affinity to CNP also produces the intracellular second messenger cGMP (Schulz et al., 1989; Koller et al., 1991; Lucas et al., 2000). NPRA is considered as the dominant subtype of the NP receptors found in peripheral organs and mediates most of the known functions of ANP and BNP hormones. Nevertheless, NPRB is localized mainly in the central nervous system and vascular tissues, which is thought to mediate the actions of CNP in the brain and also in the vascular bed. There are increasing numbers of other GC receptors; however, the specific ligands for these receptors are still being identified (**Table 2**). The third member of the NP receptor family, NPRC, constitutes a large extracellular domain of 496-amino acids, a single transmembrane domain, and a very short 37-amino acid cytoplasmic tail that contains no sequence homology with any other known membrane receptor proteins and has been given the name by default as clearance receptor (Fuller et al., 1988). The extracellular region of NPRC is approximately 30% identical to both GC-A/NPRA and GC-B/NPRB. Studies using the ligand receptor binding as a criterion, have shown that NPRC has much less stringent specificity and affinity for structural variants of ANP than does NPRA (Bovy, 1990). The extracellular domain of NPRC possesses two pairs of cysteine residues along with one isolated cysteine near the transmembrane domain of the receptor. However, three potential signals for N-glycosylation and several serine and threonine for O-linked glycosylation sites are known to be present in the extracellular domain of NPRC (Fuller et al., 1988). Previously, it has been suggested that NPRC may function as a clearance receptor to remove and clear NPs from the circulation, however, a number of studies have provided the evidence that NPRC plays roles in the biological actions of NPs (Anand-Srivastava and Trachte, 1993; Matsukawa et al., 1999; Zhou and Murthy, 2003). Thus, it is evident that the clearance name carries only by a default nomenclature to NPRC.

INTERNALIZATION AND DOWN-REGULATION OF GC-A/NPRA

The ligand-dependent internalization plays important role in the receptor down-regulation and signaling process. Down-regulation of GC-A/NPRA has been reported in a number of cells, including PC-12 cells containing endogenous receptors and transfected

Table 2 | The distribution of natriuretic peptide receptors (NPRA, NPRB, and NPRC) and their gene-knockout phenotype.

Receptor	Ligand	Tissue-specific distribution	Cell-specific distribution	Gene-knockout phenotype
NPRA *(Npr1)*	ANP/BNP	Kidney, adrenal glands, brain, heart, liver, lung, olfactory, ovary, pituitary gland, placenta, testis, thymus, vascular beds, liver, ileum	Renal epithelial and mesangial cells, vascular smooth muscle cells, endothelial cells, Leydig cells, granulosa cells, fibroblasts, Neuroblastoma, LLCPk-1, MDCK cells	High blood pressure, hypertension, cardiac hypertrophy and fibrosis, inflammation, volume overload, reduced testosterone
NPRB *(Npr2)*	CNP	Adrenal glands, brain, cartilage, fibroblast, heart, lung, ovary, pituitary gland, placenta, testis, thymus, vascular beds	Vascular smooth muscle cells, fibroblasts, chondrocytes	Dwarfism, decreased adiposity, female sterility, seizures, vascular complication
NPRC *(Npr3)*	ANP, BNP, CNP	Kidney, heart, brain liver, vascular bed, intestine	Vascular smooth muscle cells, endothelial cells, mesangial cells, fibroblasts	Bone deformation, skeletal over-growth, long bone overgrowth
GC-D	Guanylyn/uroguanylyn	Olfactory neuroepithelium		
GC-E/(ROS-GC-1)	Ca^{2+}-binding proteins	Retina, pineal gland		
GC-F/(ROS-GC-2)	Ca^{2+}-binding proteins	Retina, rod outer segment		
GC-G	Orphan	Skeletal muscle, lung, intestine, and kidney		
GC-Y-X1	Orphan	Sensory neurons of *C. elegans*		

NPRA, natriuretic peptide receptor-A; Npr1, coding for guanylyl cyclase/natriuretic peptide receptor-A; NPRB, natriuretic peptide receptor-B; Npr2, coding for guanylyl cyclase/natriuretic peptide receptor-B; NPRC, natriuretic peptide receptor-C; Npr3, coding for natriuretic peptide clearance receptor.

COS-7 and HEK-293 cells harboring recombinant receptors (Rathinavelu and Isom, 1991; Pandey, 1993; Pandey et al., 2000a, 2002). The carboxyl-terminal deletion mutation has shown that the specific sites in the GC catalytic domain and KHD of NPRA, play critical roles in the endocytosis and sequestration of the receptor (Pandey et al., 2000a). Previous studies have also indicated that after prolonged treatment of cultured cells with ANP, both the receptor density and GC activity were decreased with simultaneous reduction in mRNA of levels NPRA (Fujio et al., 1994; Cao et al., 1995, 1998; Hum et al., 2004). In addition, transforming growth factor-β1 (TGF-β1), angiotensin II (ANG II), and endothelin (ET-1) have also been shown to reduce mRNA levels of NPRA in various types of cultured cells (Fujio et al., 1994; Chen and Gardner, 2003; Garg and Pandey, 2003; Arise and Pandey, 2006). Those previous studies demonstrated that a decrease in mRNA levels of GC-A/NPRA correlated with the repressed transcriptional activity of the receptor. On the other hand, mRNA levels of NPRA are greatly increased by retinoic acid and histonedeacetylase inhibitor treatments (Kumar et al., 2010, 2014a,b). It has been suggested that NPRA exists in the phosphorylated state and the addition of ANP causes a decrease in the phosphate contents as well as reduction or desensitization of the ANP-dependent GC catalytic activity of NPRA Potter and Garbers, 1992). The apparent mechanism of desensitization of NPRA is in contrast to many other cell-surface hormone receptors, which appear to be desensitized by phosphorylation (Sibley et al., 1987; Hugnir and Greengard, 1990; Lefkowitz et al., 1998; Sorkin and von Zastrow, 2002). The initial findings have also indicated that ANP stimulates phosphorylation of NPRA (Ballerman et al., 1988; Pandey, 1989; Duda and Sharma, 1990; Larose et al., 1992). Later, it was suggested that cGMP-dependent PKG, a serine/threonine kinase is also phosphorylates NPRA (Airhart et al., 2003).

The down-regulation of NPRC also seems to be associated with increased internalization of the ligand-receptor complexes involving receptor-mediated endocytosis and trafficking mechanisms of this receptor protein (Pandey, 1992). The phenomenon of down-regulation of NPRC has been largely documented in cultured VSMCs, which predominantly contain a high density of NPRC (Neuser and Bellermann, 1986; Hirata et al., 1987; Hughes et al., 1987; Pandey, 1992; Anand-Srivastava, 2000). The metabolic processing of ANP involving NPRC has been reported by several investigators utilizing VSMCs (Hirata et al., 1985; Napier et al., 1986; Murthy et al., 1989; Nussenzveig et al., 1990; Pandey, 1992, 2005; Cohen et al., 1996; Anand-Srivastava, 2000). It has been suggested that a population of the internalized NPRC also recycles back to the plasma membrane (Pandey, 1992).

ACTIVATION OF GC-A/NPRA GENERATES INTRACELLULAR SECOND MESSENGER cGMP

It is believed that cGMP is generated as a result of ANP binding to the extracellular domain of GC-A/NPRA, which probably allosterically regulates an increased activity of the receptor protein (Pandey, 1993, 2005, 2011; Drewett and Garbers, 1994; Pandey et al., 2002; Sharma, 2002; Sharma and Duda, 2010). The initial findings showed that ANP markedly increases cGMP in target tissues in a dose-related manner (Hamet et al., 1984; Waldman et al., 1984; Pandey et al., 1985). Previous studies have also indicated that the binding of ANP to GC-A/NPRA by itself is probably not sufficient to stimulate GC catalytic activity and the production of cGMP, however, it requires ATP (Kurose et al., 1987; Chinkers et al., 1991; Goraczniak et al., 1992). Because the non-hydrolyzable analogs of ATP mimicked ANP effect, it was suggested that ATP acts directly by allosteric regulation of GC catalytic activity of NPRA. Both the ligand binding and the interaction of ATP with the KHD of the receptor increase the cGMP production without affecting the affinity for the substrate (Kurose et al., 1987; Chang et al., 1990; Duda et al., 1991). Molecular cloning and overexpression of NPRA demonstrated that GC catalytic domain cannot be activated by ANP alone without ATP-binding to KHD region of the receptor (Chinkers et al., 1991; Larose et al., 1991; Wong et al., 1995). Further studies provided the evidence that ATP binding to KHD of NPRA is important for the effectors coupling of GC family of receptors (Goraczniak et al., 1992; Sharma, 2002).

Deletion of the KHD of GC-A/NPRA and GC-B/NPRB has been suggested that KHD represses the GC catalytic activity of these receptors (Chinkers et al., 1989). At the same time, another model was proposed indicating that KHD was not a repressor; however, ATP was required to activate the catalytic domain of NPRA (Goraczniak et al., 1992; Sharma, 2002). Both NPRA and NPRB contain a glycine-rich ATP binding motif within the KHD, which is known as glycine-rich consensus sequence (Duda et al., 1991, 1993; Goraczniak et al., 1992). The juxtamembrane hinge structure of NPRA undergoes a significant conformational change in response to ligand binding, and it may play an important role in transmembrane signaling process (Huo et al., 1999). The amino acid sequence near the transmembrane region is well conserved in GC-A/NPRA that contains several closely located proline residues and a pair of cysteine residues. The mutation of one of the proline in this region renders the receptor to bind the ligand but blocks GC catalytic activity (Huo et al., 1999). Similarly, in the juxtamembrane hinge region, the elimination of disulfide bond of cysteine residues resulted in constitutive activation of NPRA. Those previous findings suggested that juxtamembrane hinge region of NPRA may play a critical role in receptor activation and signal transduction mechanisms of GC-coupled receptors.

The glycosylation of the receptor seems to be essential for ligand binding activity of GC-A/NPRA (Lowe and Fendly, 1992; Fenrick et al., 1997). However, it has also been suggested that glycosylation may not be required for ligand binding of NPRA (Miyagi et al., 2000). The mutational analyses of N-linked glycosylation consensus sites in guanylyl cyclase-C (GC-C) have indicated that certain amino acid residues might be important for receptor stability (Hesegawa et al., 1999). The glycosylation sites onto the GC-A/NPRA binding domain have been found to be scattered on the surface of the receptor with the exception of the hormone binding site and dimer interface (van den Akker, 2001). The glycosylation sites have been implicated to function in proper folding and stability of NPRA (Lowe and Fendly, 1992; Koller et al., 1993; Heim et al., 1996). Nevertheless, the glycosylation of the extracellular domain of NPRA can be considered of significant importance for receptor orientation and packaging on the cell surface similar to that of other plasma membrane receptor proteins (Wormald

and Dwek, 1999). Nevertheless, it should be noted that there is no appreciable conservation of the precise position of the glycosylation sites within the members of GC-receptor family. Clearly, more studies are needed to confirm the functional roles of glycosylation in the transmembrane signaling processes of both GC-A/NPRA and GC-B/NPRB protein molecules.

ANP/NPRA SIGNALING INHIBITS PHOSPHOINOSITIDE HYDROLYSIS, Ca^{2+} RELEASE, AND PKC ACTIVITY

Previous studies have demonstrated that ANP significantly decreased the hydrolysis of phosphoinositide in murine Leydig tumor (MA-10) cells in a dose-dependent manner and the H-8, a specific inhibitor of PKG, reversed the inhibitory effect of ANP on the generation of inositol phosphates, supporting the involvement of PKG in this process (Khurana and Pandey, 1995). ANP has also been shown to inhibit both autophosphorylation and enzymatic activity of PKC in different cell systems (Pandey, 1989, 1994a,b; Kumar et al., 1997). It is not yet clear if the ANP-dependent inhibitory effects on the phosphoinositide metabolism and PKC autophosphorylation and/or enzyme activity are exerted in a composite manner to negatively regulate the phosphoinositide, Ca^{2+}, and PKC involving ANP/NPRA/cGMP/PKG cascade. It is also possible that the effect of ANP is transmitted to block the IP_3 and Ca^{2+} signaling pathways independently in response to particular agonist stimulation. It has been suggested that potassium channels can be stimulated by ANP through the activation of PKGs, which require ATP and G-proteins (White et al., 1993). However, the possible involvements of potassium channels in the ANP-dependent inhibitory responses on the generation of inositol phosphates are not yet clearly understood. ANP has also been shown to stimulate the formation of inositol phosphates in cultured VSMCs, however, in the inner medullary collecting duct cells and smooth muscle tissues, ANP stimulated the production of inositol phosphates at lower dosages, and inhibited the formation of these metabolites at higher dosages, which increase intracellular generation of cGMP (Resink et al., 1988; Hirata et al., 1989; Teitelbaum et al., 1990; Berl et al., 1991). Thus the heterogeneity of NP receptors and their diverse cellular distribution suggest that different mechanisms might be involved in the cellular action of ANP/NPRA/cGMP (Anand-Srivastava and Trachte, 1993; Pandey, 2001, 2002, 2011). It has also been shown that ANP inhibits the thrombin-induced synthesis and release of endothelin in cultured rat aortic endothelial cells by blocking the phosphoinositide breakdown (Emori et al., 1993).

In addition to the stimulatory effect of ANP on GC activity, it has also been shown to reduce adenylyl cyclase and phospholipase C activities, sodium influx, and Ca^{2+} concentrations (Brenner et al., 1990; Anand-Srivastava and Trachte, 1993; Pandey, 2005). The increased production of cGMP in response to ANP correlates with the effects of dibutyryl-cGMP. The most compelling evidence supporting a role for cGMP effects was obtained with selective NPRA antagonists, A71915 and HS-121-1 in the kidneys (von Geldern et al., 1990; Sano et al., 1992). Those previous studies established that ANP effect is largely mediated by cGMP through the activation of GC-A/NPRA. In general, evidence suggests that biological activity of ANP/NPRA enhances the generation of the intracellular second messenger cGMP and decreases the levels of cAMP, Ca^{2+}, and IP_3 along with the antagonistic effects on PKC and mitogen-activated protein kinases (MAPKs) in target cells (**Figure 1**). ANP has been reported to induce cGMP-dependent acrosomal reaction in both capacitated and non-capacitated spermatozoa (Anderson et al., 1994). Furthermore, the acrosome reaction was essentially equal in magnitude when induced with ANP or Ca^{2+} ionophore A23187. However, higher concentrations of ANP were required to induce acrosomal reaction in capacitated as compared with non-capacitated spermatozoa. Those previous findings indicated that ANP-induced human acrosomal reaction does not require physiological concentrations of extracellular Ca^{2+}. Acrosomal reaction is known to involve various extracellular signals, including cAMP (Anderson et al., 1992), cGMP (Komatsu et al., 1990), prostaglandins, Ca^{2+} and IP_3 (Thomas and Meizel, 1989), and diacylglycerol (Breitbart et al., 1992).

The established biochemical and cellular effects of ANP in the adrenal glomerulosa cells showed the activation of GC activity and K^+ channel conductance; whereas T-type Ca^{2+} channels conductance and adenylyl cyclase activity are suppressed (Anand-Srivastava and Trachte, 1993). The correlative evidence between ANP-induced cGMP accumulation and vasodilation has suggested the role of cGMP as the intracellular second messenger of dilator responses to ANP (Brenner et al., 1990; Anand-Srivastava and Trachte, 1993; Cao et al., 1995; Pandey, 2005). ANP as well as cGMP analogs have been found to reduce the agonist-induced increases in cytosolic Ca^{2+} concentrations (Hassid, 1986; Lincoln et al., 1994; Pandey, 2005). It has been suggested that cGMP activates sarcolemmal Ca^{2+}-ATPase, and this mechanism seems to be important in the ANP-induced decreases in cytosolic Ca^{2+} in VSMCs (Rashatwar et al., 1987; Cornwell and Lincoln, 1989; Levin et al., 1998; Pandey, 2005). Nevertheless, it is anticipated that the ultimate effect of ANP in VSMCs could be due to production of cGMP and the activation of PKG (Lincoln et al., 1994; Kumar et al., 1997). However, more studies are needed to define the biochemical and molecular basis of NP actions in vasculature, including VSMCs and endothelial cells.

Initial studies from our laboratory and data published from others have also shown that both ANP and cGMP inhibited the autophosphorylation and enzymatic activity of PKC in the plasma membrane preparations of various target cells (Rogers et al., 1988; Sauro and Fitzpatrick, 1990; Pandey, 1994a,b; Kumar et al., 1997). The activation of PKC triggers the agonist-dependent phosphorylation and activity of numerous cellular proteins causing alteration in many physiological and pathophysiological conditions, including hypertension, cardiac hypertrophy, ischemia, atherosclerosis, stroke, and neurological disorders (Louis et al., 1988; Turla et al., 1990; Komuro et al., 1991; Kumar et al., 1997). PKC is believed to be a multigene family, consisting of at least 12 isoenzymes that can be classified into classical, novel, and atypical forms (Hug and Sarre, 1993; Dekker and Parker, 1994). These PKC isoenzymes are multifunctional serine/threonine kinases that are largely activated by Ca^{2+}/phospholipids and phorbol esters. However, some of these isoforms (e, δ, ή, and φ) do not require Ca^{2+}, while other isoforms (ζ and ε) do not require Ca^{2+} or phospholipid for PKC enzymatic activity. Previous studies have indicated that vasoconstrictive agents, including ANG II and

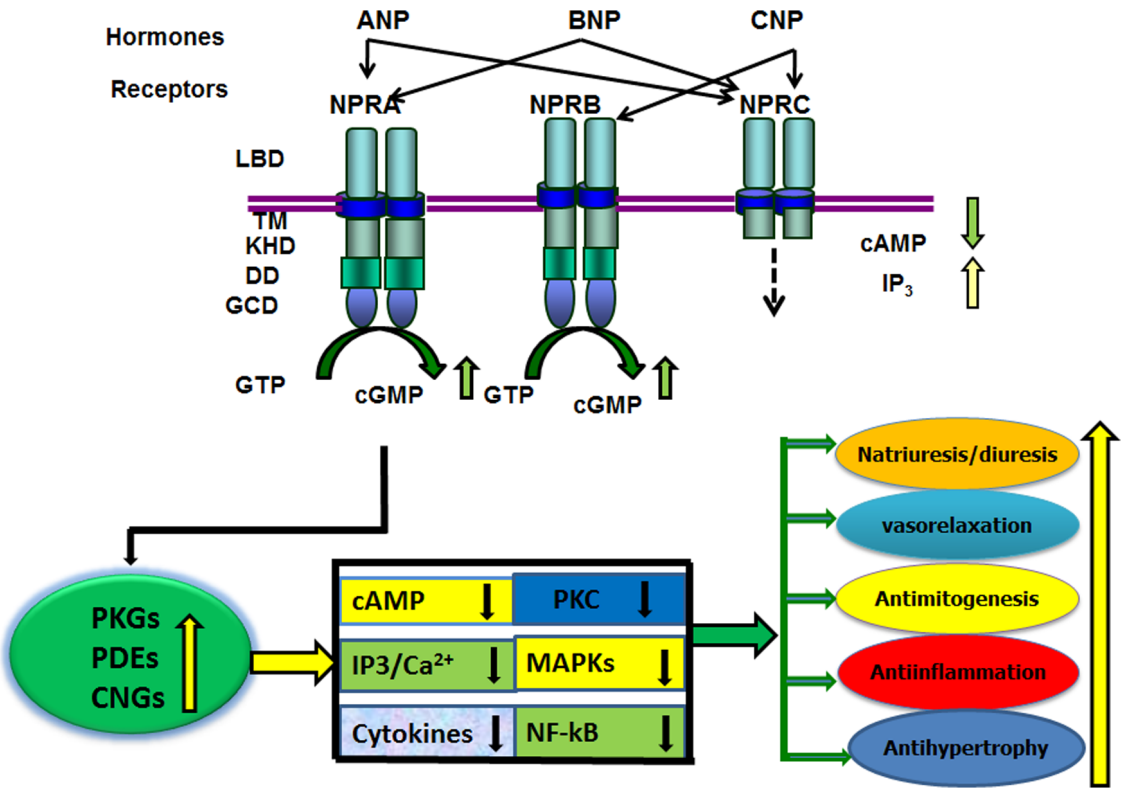

FIGURE 1 | Diagram represents the ligand specificity and physiological function(s) of GC-A/NPRA. The ligand-binding to NPRA generates second messenger cGMP from the hydrolysis of GTP. An increased level of intracellular cGMP is produced, which activates three known cGMP effecter molecules namely; cGMP-dependent protein kinases (PKGs), cGMP-dependent phosphodiesterases (PDEs), and cGMP-dependent ion-gated channels (CNGs). The ANP/NPRA/cGMP signaling may antagonize a number of pathways including; intracellular formation of cAMP, Ca^{2+}, IP_3; cytokine expression; and the activation of protein kinase C (PKC) and mitogen-activated protein kinases (MAPKs). The resulting signaling cascade can mimic the physiological responses of ANP/NPRA. LBD, ligand binding domain; TM transmembrane region; protein-KHD, protein kinase-like homology domain; and GCD, guanylyl cyclase catalytic domain; DD, dimerization domain of NPRA and NPRB. The ligand binding region, transmembrane domain, and small intracellular tail region of NPRC are indicated.

ET-1, were able to activate several-fold PKC activity in cultured VSMCs, however, ANP potently antagonized the ANG II- and ET-1-stimulated PKC activity in the ANP/NPRA-dependent manner (Kumar et al., 1997; Pandey, 2005). The inhibitory effect of ANP was greatly amplified if cell were transfected with both PKC-α and NPRA cDNAs. The pretreatment of cells with NPRA antagonist A-71915, significantly blocked the production of cGMP as well as the inhibitory effect of ANP on PKC activity (Kumar et al., 1997). The results of those previous studies provided strong evidence that ANP antagonizes the PKC activation involving ANP/NPRA/cGMP signaling cascade. Agonists that activate PKC also produce two distinct second messengers, IP3, which activates cytosolic free Ca^{2+} and diacylglycesol, which stimulates PKC activity (Berridge and Irvine, 1989; Exton, 1990; Rasmussen et al., 1995; Kumar et al., 1997). Our previous studies have suggested that ANP inhibits the formation of IP3 in a cGMP-dependent manner in the intact cells, suggesting that the inhibitory effect of ANP on PKC activity might be linked with its antagonistic action on IP_3 formation, however, more studies are needed to support these observations in various ANP-responsive cell and tissues systems.

EFFECT OF NPRA ON THE INHIBITION OF MAPKs ACTIVITY AND CELL PROLIFERATION

It has been shown that cGMP analogs mimicked the antiproliferative action of ANP, indicating that it exerts the antimitogenic effects largely through the intracellular second messenger cGMP (Lincoln et al., 1994; Hutchinson et al., 1997; Pandey et al., 2000b; Sharma et al., 2002). ANP has been shown to inhibit collagen synthesis in cardiac fibroblasts and also it inhibits hypertrophy of cardiac myocytes (Calderone et al., 1998; Masciotra et al., 1999; Silberbach et al., 1999; Horio et al., 2000; Gopi et al., 2013). Similarly, PKG has been shown to suppress extracellular matrix production in VSMCs (Dey et al., 1998). Both NPRA and NPRC, have been suggested to play a role in ANP-dependent antimitogenic responses (Prins et al., 1996; Hutchinson et al., 1997; Pandey et al., 2000b; Sharma et al., 2002; Tripathi and Pandey, 2012). ANP has been shown to act as a growth suppressor in a variety of cell types including; kidney, heart, neurons, thymus, vasculature, and fibroblasts (Levin et al., 1998; Pandey, 2005). Previous studies have demonstrated that ANP inhibits ANGII- and platelet-derived growth factor (PDGF) -dependent MAPK activity in different tissues and cell types (Sugimoto et al., 1993; Prins

et al., 1996; Pandey et al., 2000b; Sharma et al., 2002; Tripathi and Pandey, 2012). However, in astroglial cells, ANP was shown to inhibit extracellular-regulated MAPK (Erk1/2) activity through NPRC (Prins et al., 1996). In contrast, recent findings have indicated that des- (Cys^{105}–Cys^{121}) -ANP, a ligand selective to NPRC, did not inhibit basal or serum-stimulated MAPK, however, CNP, which acts through NPRB, potently inhibited MAPK activity in fibroblasts in a cGMP-dependent manner (Chrisman and Garbers, 1999).

It has been postulated that cGMP-dependent signaling mechanisms of GC-A/NPRA are initiated probably at the level of gene transcription; however, the exact mechanism of this activation remains to be elucidated. A previous report also indicated that cGMP/PKG signaling was able to increase the MAPK activity in contractile rat VSMCs (Komalavilas et al., 1999). However, the process by which cGMP/PKG leads to the activation of MAPKs is unclear. Similarly, cAMP- and PKG have also been shown to inhibit as well as to activate MAPKs pathways, depending on the cell types and culture conditions (Bornfildt and Krebs, 1999). However, the involvement of specific ANP receptor subtypes in the inhibitory effects of ANP on the agonist-stimulated MAPKs activity is controversial. Indeed, more studies are needed to establish the underlying mechanisms of the antiproliferative effect of ANP in target cells. ANP has also been shown to induce apoptosis in cultured VSMCs and in neonatal rat cardiac myocytes (Trindade et al., 1995; Wu et al., 1997). The apoptotic effect of ANP was mimicked by 8-bromo-cGMP, a membrane-permeable analog of cGMP, and also by nitroprusside, an activator of soluble guanylyl cyclase. Furthermore, the effect of ANP was greatly potentiated by a cGMP-specific phosphodiesterase inhibitor zaprinast. It has been indicated that norepinephrine, a myocyte growth and proliferative effector molecule, inhibited ANP-induced apoptosis via activation of β-adrenergic receptor and elevation of cAMP (Wu et al., 1997). The existence of a complementary ANP-mediated mechanism to inhibit cell growth and proliferation is not anticipated. Nevertheless, the inhibition of cell proliferation is often accompanied by an increased probability of apoptosis, whereas, growth-promoting agents and agonist hormones tend to promote cell growth and proliferation. For instance, ANG II inhibits apoptosis, in contrast, ANP and nitric oxide, both potently inhibit cell growth and proliferation and induce apoptosis (Pollman et al., 1996; Wu et al., 1997). It has been suggested that the anti-apoptotic molecule Bcl-2 homolog Mcl-1 might serve as an important target in ANP-induced apoptosis. Intriguing was the finding that the Bcl-2 homolog Mcl-1 was initially identified as a protein marker, which was up-regulated during the differentiation of the monocytoid cell line ML-1 cells (Kozopas et al., 1993; Kiefer et al., 1995; Wu et al., 1997).

GENE-TARGETING OF *Nppa* AND *Npr1*

Genetic-targeting strategies in mice have provided novel approaches to study the physiological responses corresponding to gene-dosage *in vivo* (Takahashi and Smithies, 1999; Kim et al., 2002). Genetically modified mice carrying *Npr1* gene-disruption or gene-duplication have provided strong support for the physiological roles of NPs and their receptors in the intact animals (John et al., 1995; Lopez et al., 1995; Kishimoto et al., 1996; Oliver et al., 1997, 1998; Matsukawa et al., 1999; Pandey et al., 1999; Shi et al., 2001, 2003; Holtwick et al., 2002; Vellaichamy et al., 2005; Das et al., 2012; Zhao et al., 2013). Numerous studies have examined the quantitative contributions and possible mechanisms mediating the responses of *Npr1* gene copies by determining the renal plasma flow (RPF), glomerular filtration rate (GFR), urine flow, and sodium excretion following blood volume expansion in *Npr1* homozygous null mutant ($Npr1^{-/-}$; 0-copy), wild-type ($Npr1^{+/+}$; 2-copy), and gene-duplicated ($Npr1^{++/++}$; 4-copy) mice in a *Npr1* gene-dose-dependent manner (Shi et al., 2003). Although, the blood volume expansion stimulated the release of ANP in all three *Npr1* genotypes of mice, significant functional responses (RPF, GFR, and sodium excretion) occurred only in $Npr1^{-/-}$ and $Npr1^{++/++}$ mice but not in $Npr1^{-/-}$ mice. These findings demonstrated that the ANP/NPRA axis is primarily responsible for mediating the renal hemodynamic and sodium excretory responses to intravascular blood volume expansion. ANP responses to volume expansion led to the significantly lesser excretion of Na^+ and water in 0-copy null mutant mice and significantly greater excretory responses along with reduced tubular reabsorption in 4-copy mice as compared with 2-copy wild-type mice. Similarly, during the volume expansion, urinary cGMP concentration was significantly lower in null mutant mice and greater in gene-duplicated mice. Our previous findings have established that NPRA is a hallmark receptor, which plays a critical role in mediating the natriuresis, diuresis, and renal hemodynamic responses to acute blood volume expansion (Shi et al., 2003).

Genetic mouse models with disruption of both *Nppa* and *Npr1* genes have provided strong support for the role of this hormone-receptor system in the regulation of blood pressure, cardiac hypertrophy, and other physiological functions (John et al., 1995; Lopez et al., 1995; Oliver et al., 1997, 1998; Melo et al., 1999; Pandey et al., 1999; Shi et al., 2001, 2003; Holtwick et al., 2002; Vellaichamy et al., 2005; Kishimoto et al., 2011; Pandey, 2011). Therefore, the genetic defects that reduce the activity of ANP and its receptor system can be considered as candidate contributors to essential hypertension and CHF (John et al., 1995; Pandey et al., 1999; Zhao et al., 1999; Knowles et al., 2001; Holtwick et al., 2002; Shi et al., 2003; Vellaichamy et al., 2005). Interestingly, complete absence of NPRA causes hypertension in mice and leads to altered renin and ANG II levels, cardiac hypertrophy, and lethal vascular events similar to those seen in untreated human hypertensive patients (Oliver et al., 1997; Shi et al., 2001, 2003; Zhao et al., 2007). In contrast, increased expression of *Npr1* reduces the blood pressures and inflammatory responses, protects heart, and increases the intracellular second messenger cGMP concentrations corresponding to the increasing number of *Npr1* gene copies (Oliver et al., 1998; Pandey et al., 1999; Shi et al., 2003; Vellaichamy et al., 2007, 2014; Zhao et al., 2013). Recent evidence also indicates that CNP and its receptor NPRB can play important role in regulating the cardiac hypertrophy and remodeling as a potential drug target for the treatment of cardiovascular diseases (Del Ry, 2013).

CONCLUSION

The field of NPs has been advanced to examine the function and signaling mechanisms of their receptors and the role of

second messenger cGMP in physiology and pathophysiology of hypertension, renal hemodynamics, cardiovascular functions, and neural plasticity. The development of gene-knockout and gene-duplication mouse models along with transgenic mice have provided a framework for understanding both the physiological and pathophysiological functions of NPs and their receptors in the intact animals *in vivo*. Although, a considerable progress has been made, the transmembrane signal transduction mechanisms of NPs and their receptors remain unresolved. Future investigations should include; the identification and characterization of cellular targets of intracellular second messenger cGMP produced by NPs, including cytosolic and nuclear proteins, role in gene transcription, cell growth and proliferation, apoptosis, and differentiation. A more vigorous studies of the crosstalk with other signaling mechanisms namely, PKC, MAPKs, cAMP, Ca^{2+}, and IP_3 needs to be pursued systematically. NPs are considered as circulating markers of CHF, however, their therapeutic potential for the treatment of cardiovascular diseases such as hypertension, renal insufficiency, cardiac hypertrophy, CHF, and stroke is still lacking. The ultimate goal of the investigations is this field is to fully appreciate the mechanisms of cGMP generation after ligand binding to GC-coupled receptors and the pathways leading to elicit cellular and physiological functions in relation to other signaling molecules with special emphasis to Ca^{2+}, IP_3, and cAMP levels. Identification of the discrete switch points in signal transmission of NPs and their cognate receptors that specify unique directional responses need to be vigorously pursued.

ACKNOWLEDGMENTS

I thank my wife Kamala Pandey for her generous help in the preparation of this manuscript. The research in the author's laboratory is supported by the grants from the National Institutes of Health (HL 57531 and HL 62147).

REFERENCES

Airhart, N., Yang, Y. F., Roberts, C. T. Jr., and Silberbach, M. (2003). Atrial natriuretic peptide induces natriuretic peptide receptor-cGMP-dependent protein kinase interaction. *J. Biol. Chem.* 278, 38693–38698. doi: 10.1074/jbc.M304098200

Anand-Srivastava, M. B. (2000). Down-regulation of atrial natriuretic peptide ANP-C receptor is associated with alteration in G-protein expression in A10 smooth muscle cells. *Biochemistry* 39, 6503–6513. doi: 10.1021/bi992660q

Anand-Srivastava, M. B., and Trachte, G. J. (1993). Atrial natriuretic factor receptors and signal transduction mechanisms. *Pharmacol. Rev.* 45, 455–497. doi: 10.1007/s11010-009-0335-7

Anderson, R. A., Feathergill, K. A., De Jonge, C., Mack, S. R., and Zaneveld, L. J. D. (1992). Facilitative effect of pulsed addition of dibutyryl-cAMP on the acrosome reaction of noncapacitated human spermotazoa. *J. Androl.* 13, 398–408.

Anderson, R. A., Feathergill, K. A., Drisdel, R. C., Rawlins, R. G., Mack, S. R., and Zaneveld, L. J. D. (1994). Atrial natriuretic peptide (ANP) as a stimulus of the human acrosome reaction and a component of ovarian follicular fluid: correlation of follicular ANP content with in vitro fertilization outcome. *J. Androl.* 15, 61–70. doi: 10.1002/j.1939-4640.1994.tb01685.x

Anwaruddin, S., Lloyd-Jones, D. M., Baggish, A., Chen, A., Krauser, D., Tung, R., et al. (2006). Renal function, congestive heart failure, and amino-terminal pro-brain natriuretic petpide measurement: results from the proBNP investigation of dyspnea in the emergency Department (PRIDE) study. *J. Am. Coll. Cardiol.* 47, 91–97. doi: 10.1016/j.jacc.2005.08.051

Arise, K. K., and Pandey, K. N. (2006). Inhibition and down-regulation of gene transcription and guanylyl cyclase activity of NPRA by angiotensin II involving protein kinase C. *Biochem. Biophys. Res. Commun.* 349, 131–135. doi: 10.1016/j.bbrc.2006.08.003

Ballerman, B. J., Marala, R. B., and Sharma, R. K. (1988). Characterization and regulation by protein kinase C of renal glomerular atrial natriuretic peptide receptor-coupled guanylate cyclase. *Biochem. Biophys. Res. Commun.* 157, 755–761. doi: 10.1016/S0006-291X(88)80314-0

Berl, T., Mansour, J., and Teitelbaum, I. (1991). ANP stimulates phospholipase C in cultured RIMCT cells: roles of protein kinases and G proteins. *Am. J. Physiol.* 260, F590–F595.

Berridge, M. J., and Irvine, R. F. (1989). Inositol phosphates adn cel signaling. *Nature* 341, 197–205. doi: 10.1038/341197a0

Bornfildt, K. E., and Krebs, E. G. (1999). Crosstalk between protein kinase A and growth factor receptor signaling pathways in arterial smooth muscle. *Cell. Signal.* 11, 465–477. doi: 10.1016/S0898-6568(99)00020-0

Bovy, P. R. (1990). Structure activity in the atrial natriuretic peptide (ANP) family. *Med. Res. Rev.* 10, 115–142. doi: 10.1002/med.2610100105

Breitbart, H., Lax, J., Rotem, R., and Naor, J. (1992). Role of protein kinase C in the acrosome reaction of mammalian spermatozoa. *Biochem. J.* 281, 473–476.

Brenner, B. M., Ballermann, B. J., Gunning, M. E., and Zeidel, M. L. (1990). Diverse biological actions of atrial natriuretic peptide. *Physiol. Rev.* 70, 665–699.

Calderone, A., Thaik, C. M., Takahashi, N., Chang, D. L. F., and Colucci, W. S. (1998). Nitric oxide, atrial natriuretic peptide, and cyclic GMP inhibit the growth-promoting effects of norepinephrine in cardiac myocytes and fibroblasts. *J. Clin. Invest.* 101, 812–818. doi: 10.1172/JCI119883

Cameron, V. A., Aitken, G. D., Ellmers, L. J., Kennedy, M. A., and Espiner, E. A. (1996). The sites of gene expression of atrial, brain, and C-type natriuretic peptides in mouse fetal development: temporal changes in embryos and placenta. *Endocrinology* 137, 817–824.

Cao, L., Chen, S. C., Humphreys, M. H., and Gardner, D. G. (1998). Ligand-dependent regulation of NPR-A gene expression in inner medullary collecting duct cells. *Am. J. Physiol.* 275, F119–F125.

Cao, L., Wu, J., and Gardner, D. G. (1995). Atrial natriuretic peptide suppresses the transcription of its guanylyl cyclase-linked receptor. *J. Biol. Chem.* 270, 24891–24897. doi: 10.1074/jbc.270.42.24891

Chang, C.-H., Kohse, K. P., Chang, B., Hirata, M., Jiang, B., Douglas, J. E., et al. (1990). Characterization of ATP-stimulated guanylyl cyclase activation in rat lung membranes. *Biochim. Biophys. Acta* 1052, 159–165. doi: 10.1016/0167-4889(90)90071-K

Chen, H. H., and Burnett, J. C. Jr. (1998). C-type natriuretic peptide: the endothelial component of the natriuretic peptide system. *J. Cardiovasc. Pharmacol.* 32(Suppl. 3), S22–S28. doi: 10.1038/jcbfm.2013.234

Chen, Y. O., and Gardner, D. G. (2003). Endothelin inhibits NPR-A and stimulates eNOS gene expression in rat IMCD cells. *Hypertension* 41 675–681. doi: 10.1161/01.HYP.0000047204.72286.34

Chinkers, M., Garbers, D. L., Chang, M. S., Lowe, D. G., Chin, H. M., Goeddel, D. V., et al. (1989). A membrane form of guanylate cyclase is an atrial natriuretic peptide receptor. *Nature* 338, 78–83. doi: 10.1038/338078a0

Chinkers, M., Singh, S., and Garbers, D. L. (1991). Adenine nucleotides are required for activation of rat atrial natriuretic peptide receptor/guanylyl cyclase expressed in a baculovirus system. *J. Biol. Chem.* 266, 4088–4093.

Chrisman, T. D., and Garbers, D. L. (1999). Reciprocal antagonism coordinates C-type natriuretic peptide and mitogen-signaling pathways in fibroblasts. *J. Biol. Chem.* 274, 4293–4299. doi: 10.1074/jbc.274.7.4293

Cohen, D., Koh, G. Y., Nikonova, L. N., Porter, J. G., and Maack, T. (1996). Molecular determinants of the clearance function of type-C receptor of natriuretic peptides. *J. Biol. Chem.* 271, 9863–9869. doi: 10.1074/jbc.271.16.9863

Cornwell, T. L., and Lincoln, T. M. (1989). Regulation of intracellular Ca2+ levels in cultured vascular smooth muscle cells. Reduction of Ca^{2+} by atriopeptin and 8-bromo-cyclic GMP is mediated by cyclic GMP-dependent protein kinase. *J. Biol. Chem.* 264, 1146–1155.

Czucz, J., Cervenak, L., Forhecz, Z., Gombos, T., Pozsonyi, Z., Kunde, J., et al. (2011). Serum soluble E-selectin and NT-proBNP levels additively predict mortality in diabetic patients with chronic heart failure. *Clin. Res. Cardiol.* 100, 587–594. doi: 10.1007/s00392-011-0283-6

Das, S., Periyasamy, R., and Pandey, K. N. (2012). Activation of IKK/NF-kappaB provokes renal inflammatory responses in guanylyl cyclase/natriuretic peptide receptor-A gene-knockout mice. *Physiol. Genomics* 44, 430–442. doi: 10.1152/physiolgenomics.00147.2011

de Bold, A. J. (1985). Atrial natriuretic factor: a hormone produced by the heart. *Science* 230, 767–770. doi: 10.1126/science.2932797

de Bold, A. J., Borenstein, H. B., Veress, A. T., and Sonnenberg, H. (1981). A rapid and potent natriuretic response to intravenous injection of atrial myocardial extract in rats. *Life Sci.* 28, 89–94. doi: 10.1016/0024-3205(81)90370-2

Dekker, L. V., and Parker, P. J. (1994). Protein kinase C: a question of specficicit. *Trends Biochem. Sci.* 19, 73–77. doi: 10.1016/0968-0004(94)90038-8

Del Ry, S. (2013). C-type natriuretic peptide: a new cardiac mediator. *Peptides* 40, 93–98. doi: 10.1016/j.peptides.2012.12.010

Dey, N. B., Boerth, N. J., Murphy-Ullrich, J. E., Chang, P. L., Prince, C. W., and Lincoln, T. M. (1998). Cyclic GMP-dependent protein kinase inhibits osteopontin and thrombospondin production in rat aortic smooth muscle cells. *Circ. Res.* 82 139–146. doi: 10.1161/01.RES.82.2.139

Doust, J. A., Pietrzak, E., Dobson, A., and Glasziou, P. (2005). How well does B-type natriuretic peptide predict death and cardiac events in patients with heart failure: systematic review. *BMJ* 330, 625. doi: 10.1136/bmj.330.7492.625

Drewett, J. G., and Garbers, D. L. (1994). The family of guanylyl cyclase receptors and their ligands. *Endocr. Rev.* 15, 135–162. doi: 10.1210/edrv-15-2-135

Duda, T., Goraczniak, R. M., and Sharma, R. K. (1991). Site-directed mutational analysis of a membrane guanylate cyclase cDNA reveals the atrial natriuretic factor signaling site. *Proc. Natl. Acad. Sci. U.S.A.* 88, 7882–7886. doi: 10.1073/pnas.88.17.7882

Duda, T., Goraczniak, R. M., and Sharma, R. K. (1993). Core sequence of ATP regulatory module in receptor guanylate cyclases. *FEBS Lett.* 315, 143–148. doi: 10.1016/0014-5793(93)81151-O

Duda, T., and Sharma, R. K. (1990). Regulation of guanylate cyclase activity by atrial natriuretic factor and protein kinase C. *Mol. Cell. Biochem.* 93, 179–184. doi: 10.1007/BF00226190

Emori, T., Hirata, Y., Imai, T., Eguchi, S., Kanno, K., and Marumos, F. (1993). Cellular mechanism of natriuretic peptides-induced inhibition of endothelin-1 biosynthesis in rat endothelial cells. *Endocrinology* 133, 2474–2480.

Exton, J. H. (1990). Signaling through phosphatidylcholine breakdow. *J. Biol. Chem.* 265, 1–4.

Felker, G. M., Petersen, J. W., and Mark, D. W. (2006). Natriuretic peptides in the diagnosis and management of heart failure. *CMAJ* 175, 611–617. doi: 10.1503/cmaj.060236

Fenrick, R., Bouchard, N., Mcnicoll, N., and De Lean, A. (1997). Glycosylation of asparagines 24 of the natriuretic peptide receptor-B is crucial for the formation of a competent ligand binding domain. *Mol. Cell. Biochem.* 173, 25–32. doi: 10.1023/A:1006855522272

Freestone, B., Gustafsson, F., Chong, A. Y., Corell, P., Kistorp, C., Hildebrandt, P., et al. (2008). Influence of atrial fibrillation on plasma von willebrand factor, soluble E-selectin, and N-terminal pro B-type natriuretic peptide levels in systolic heart failure. *Chest* 133, 1203–1208. doi: 10.1378/chest.07-2557

Fujio, N., Gossard, F., Bayard, F., and Tremblay, J. (1994). Regulation of natriuretic peptide receptor A and B expression by transforming growth factor-beta 1 in cultured aortic smooth muscle cells. *Hypertension* 23, 908–913. doi: 10.1161/01.HYP.23.6.908

Fuller, F., Porter, J. G., Arfsten, A. E., Miller, J., Schilling, J. W., Scarborough, R. M., et al. (1988). Atrial natriuretic peptide clearance receptor. Complete sequence and functional expression of cDNA clones. *J. Biol. Chem.* 263, 9395–9401.

Ganem, F., Serrano, C. V. Jr., Fernandes, J. L., Blotta, M. H., Souza, J. A., and Nicolau, J. C. (2011). Preoperative B-type natriuretic peptide, and not the inflammation status, predicts an adverse outcome for patients undergoing heart surgery. *Interact. Cardiovasc. Thorac. Surg.* 12, 778–783. doi: 10.1510/icvts.2010.255257

Garbers, D. L. (1992). Guanylyl cyclase receptors and their endocrine, paracrine, and autocrine ligands. *Cell* 71, 1–4. doi: 10.1016/0092-8674(92)90258-E

Gardner, D. G., Deschepper, C. F., Ganong, W. F., Hane, S., Fiddes, J., Baxter, J. D., et al. (1986). Extra-atrial expression of the gene for atrial natriuretic factor. *Proc. Natl. Acad. Sci. U.S.A.* 83, 6697–6701. doi: 10.1073/pnas.83.18.6697

Garg, R., and Pandey, K. N. (2003). Angiotensin II-mediated negative regulation of Npr1 promoter activity and gene transcription. *Hypertension* 41, 730–736. doi: 10.1161/01.HYP.0000051890.68573.94

Gopi, V., Parthasarathy, A., Umadevi, S., and Vellaichamy, E. (2013). Angiotensin-II down-regulates cardiac natriuretic peptide receptor-A mediated anti-hypertrophic signaling in experimental rat hearts. *Indian J. Exp. Biol.* 51, 48–55.

Goraczniak, R. M., Duda, T., and Sharma, R. K. (1992). A structural motif that defines the ATP-regulatory module of guanylate cyclase in atrial natriuretic factor signalling. *Biochem. J.* 282(Pt 2), 533–537.

Hama, N., Itoh, H., Shirakami, G., Suga, S., Komatsu, Y., Yoshimasa, T., et al. (1994). Detection of C-type natriuretic peptide in human circulation and marked increase of plasma CNP level in septic shock patients. *Biochem. Biophys. Res. Commun.* 198, 1177–1182. doi: 10.1006/bbrc.1994.1166

Hamet, P., Tremblay, J., Pang, S. C., Garcia, R., Thibault, G., Gutkowska, J., et al. (1984). Effect of native and synthetic atrial natriuretic factor on cyclic GMP. *Biochem. Biophys. Res. Commun.* 123, 515–527. doi: 10.1016/0006-291X(84)90260-2

Hassid, A. (1986). Atriopeptin II decreases cytosolic free Ca^{2+} in cultured vascular smooth muscle cells. *Am. J. Physiol.* 251, C681–C686.

Heim, J. M., Singh, S., and Gerzer, R. (1996). Effect of glycosylation on cloned ANF-sensitive guanylyl cyclase. *Life Sci.* 59, L61–L68. doi: 10.1016/0024-3205(96)00306-2

Hesegawa, M., Hidaka, Y., Wada, A., Hirayama, T., and Shimonishi, Y. (1999). The relevance of N-linked glycosylation to the binding of a ligand to guanylate cyclase C. *Eur. J. Biochem.* 263, 338–346. doi: 10.1046/j.1432-1327.1999.00488.x

Hirata, M., Chang, C. M., and Murad, F. (1989). Stimulatory effect of atrial natriuretic factor on phosphoinositide hydrolysis in cultured bovine aortic smooth muscle cells. *Biochim. Biophys. Acta* 1010, 346–351. doi: 10.1016/0167-4889(89)90060-8

Hirata, Y., Hirose, S., Takada, S., Takagi, Y., and Matsubara, H. (1987). Down-regulation of atrial natriuretic peptide receptor and cyclic GMP response in cultured rat vascular smooth muscle cells. *Eur. J. Pharmacol.* 135, 439–442. doi: 10.1016/0014-2999(87)90697-2

Hirata, Y., Takata, S., Tomita, M., and Takaichi, S. (1985). Binding, internalization, and degradation of atrial natriuretic peptide in cultured vascular smooth muscle cells of rat. *Biochem. Biophys. Res. Commun.* 132, 976–984. doi: 10.1016/0006-291X(85)91903-5

Holtwick, R., Baba, H. A., Ehler, E., Risse-Vob, M. D., Gehrmann, J., Pierkes, M., et al. (2002). Left but not right cardiac hypertrophy in atrial natriuretic peptide receptor-deficient mice is prevented by angiotensin type 1 receptor antagonist losartan. *J. Cardiovasc. Pharmacol.* 40, 725–734. doi: 10.1097/00005344-200211000-00010

Horio, T., Nishikimi, T., Yoshihara, F., Matsuo, H., Takishita, S., and Kangawa, K. (2000). Inhibitory regulation of hypertrophy by endogenous atrial natriuretic peptide in cultured cardiac myocytes. *Hypertension* 35, 19–24. doi: 10.1161/01.HYP.35.1.19

Hug, H., and Sarre, T. F. (1993). Protein kinase C isoenzymes: divergence in signal transduction. *Biochem. J.* 291, 329–343.

Hughes, R. J., Struthers, R. S., Fong, A. M., and Insel, P. A. (1987). Regulation of the atrial natriuretic peptide receptor on a smooth muscle cell. *Am. J. Physiol.* 253, C809–C816.

Hugnir, R. I., and Greengard, P. (1990). Regulation of neurotransmitter receptor desensitization by protein phosphorylation. *Neuron* 5, 555–567. doi: 10.1016/0896-6273(90)90211-W

Hum, D., Besnard, S., Sanchez, R., Devost, D., Gossard, F., Hamet, P., et al. (2004). Characterization of a cGMP-response element in the guanylyl cyclase/natriuretic peptide receptor A gene promoter. *Hypertension* 43, 1270–1278. doi: 10.1161/01.HYP.0000126920.93207.53

Huo, X., Abe, T., and Misono, K. S. (1999). Ligand binding-dependent limited proteolysis of the atrial natriuretic peptide juxtamembrane hinge structure essential for transmembrane signal transduction. *Biochemistry* 38, 16941–16951. doi: 10.1021/bi9919448

Hutchinson, H. G., Trinadade, P. T., Cunanan, D. B., Wu, C. F., and Pratt, R. E. (1997). Mechanisms of natriuretic-peptide-induced growth inhibition of vascular smooth muscle cells. *Cardiovasc. Res.* 35 158–167. doi: 10.1016/S0008-6363(97)00086-2

Igaki, T., Itoh, H., Suga, S., Hama, N., Ogawa, Y., Komatsu, Y., et al. (1996). C-type natriuretic peptide in chronic renal failure and its action in humans. *Kidney Int. Suppl.* 55, S144–S147.

Inagami, T. (1989). Atrial natriuretic factor. *J. Biol. Chem.* 264, 3043–3046.

Jaffe, A. S., Babuin, L., and Apple, F. S. (2006). Biomarkers in acute cardiac disease: the present and the future. *J. Am. Coll. Cardiol.* 48, 1–11. doi: 10.1016/j.jacc.2006.02.056

John, S. W., Krege, J. H., Oliver, P. M., Hagaman, J. R., Hodgin, J. B., Pang, S. C., et al. (1995). Genetic decreases in atrial natriuretic peptide and salt-sensitive hypertension. *Science* 267, 679–681. doi: 10.1126/science.7839143

Khan, I. A., Fink, J., Nass, C., Chen, H., Christenson, R., and Defilippi, C. R. (2006). N-terminal pro-B-type natriuretic peptide and B-type natriuretic peptide for identifying coronary artery disease and left ventricular hypertrophy in ambulatory chronic kidney disease patients. *Am. J. Cardiol.* 97, 1530–1534. doi: 10.1016/j.amjcard.2005.11.090

Khurana, M. L., and Pandey, K. N. (1993). Receptor-mediated stimulatory effect of atrial natriuretic factor, brain natriuretic peptide, and C-type natriuretic peptide on testosterone production in purified mouse Leydig cells: activation of cholesterol side-chain cleavage enzyme. *Endocrinology* 133, 2141–2149.

Khurana, M. L., and Pandey, K. N. (1995). Catalytic activation of guanylate cyclase/atrial natriuretic factor receptor by combined effects of ANF and GTP gamma S in plasma membranes of Leydig tumor cells: involvement of G-proteins. *Arch. Biochem. Biophys.* 316, 392–398. doi: 10.1006/abbi.1995.1052

Khurana, M. L., and Pandey, K. N. (1996). Atrial natriuretic peptide inhibits the phosphoinositide hydrolysis in murine Leydig tumor cells. *Mol. Cell. Biochem.* 158, 97–105. doi: 10.1007/BF00225834

Kiefer, M. C., Brauer, M. J., Powers, V. C., Wu, J. J., Umansky, S. R., Tomel, L. D., et al. (1995). Modulation of apoptosis by the widely distributed Bcl-2 homologue Bak. *Nature* 374, 736–739. doi: 10.1038/374736a0

Kim, H. S., Lu, G., John, S. W. M., Maeda, N., and Smithies, O. (2002). Molecular phenotyping for analyzing subtle genetic effects in mice application to an angiotensinogen gene titration. *Proc. Natl. Acad. Sci. U.S.A.* 99, 4602–4607. doi: 10.1073/pnas.072083799

Kishimoto, I., Dubois, S. K., and Garbers, D. L. (1996). The heart communicates with the kidney exclusively through the guanylyl cyclase-A receptor: acute handling of sodium and water in response to volume expansion. *Proc. Natl. Acad. Sci. U.S.A.* 93, 6215–6219. doi: 10.1073/pnas.93.12.6215

Kishimoto, I., Tokudome, T., Nakao, K., and Kangawa, K. (2011). Natriuretic peptide system: an overview of studies using genetically engineered animal models. *FEBS J.* 278, 1830–1841. doi: 10.1111/j.1742-4658.2011.08116.x

Knowles, J. W., Esposito, G., Mao, L., Hagaman, J. R., Fox, J. E., Smithies, O., et al. (2001). Pressure-independent enhancement of cardiac hypertrophy in natriuretic peptide receptor A-deficient mice. *J. Clin. Invest.* 107, 975–984. doi: 10.1172/JCI11273

Kojima, M., Minamino, N., Kangawa, K., and Matsuo, H. (1989). Cloning and sequence analysis of cDNA encoding a precursor for rat brain natriuretic peptide. *Biochem. Biophys. Res. Commun.* 159, 1420–1426. doi: 10.1016/0006-291X(89)92268-7

Koller, K. J., Lipari, M. T., and Goeddel, D. V. (1993). Proper glycosylation and phosphorylation of the type A natriuretic peptide receptor are required for hormone-stimulated guanylyl cyclase activity. *J. Biol. Chem.* 268, 5997–6003.

Koller, K. J., Lowe, D. G., Bennett, G. L., Minamino, N., Kangawa, K., Matsuo, H., et al. (1991). Selective activation of the B natriuretic peptide receptor by C-type natriuretic peptide (CNP). *Science* 252, 120–123. doi: 10.1126/science.1672777

Komalavilas, P., Shah, P. K., Jo, H., and Lincoln, T. M. (1999). Activation of mitogen-activated protein kinase pathways by cyclic GMP and cyclic GMP-dependent protein kinase in contractile vascular smooth muscle cells. *J. Biol. Chem.* 274, 34301–34309. doi: 10.1074/jbc.274.48.34301

Komatsu, Y., Endo, Y., and Suzaki, S. (1990). Changes in protein phoshorylation during acrosome reaction of mouse sperm. *Yakugaku Zasshi* 110, 325–331.

Komuro, I., Katoh, Y., Kaida, T., Shibazaki, Y., Kurabayashi, M., Hoh, E., et al. (1991). Mechanical loading stimulates cell hypertrophy and specific gene expression in cultured rat cardiac myocytes. Possible role of protein kinase C activation. *J. Biol. Chem.* 266, 1265–1268.

Kozopas, K. M., Yang, T., Buchan, H. L., Zhou, P., and Craig, R. W. (1993). MCLI, a gene expressed in programmed myeloid cell differentiation, has sequence similarity to BCL2. *Proc. Natl. Acad. Sci. U.S.A.* 90, 3516–3520. doi: 10.1073/pnas.90.8.3516

Kumar, P., Garg, R., Bolden, G., and Pandey, K. N. (2010). Interactive roles of Ets-1, Sp1, and acetylated histones in the retinoic acid-dependent activation of guanylyl cyclase/atrial natriuretic peptide receptor-A gene transcription. *J. Biol. Chem.* 285, 37521–37530. doi: 10.1074/jbc.M110.132795

Kumar, P., Periyasamy, R., Das, S., Neerukonda, S., Mani, I., and Pandey, K. N. (2014a). All-trans retinoic acid and sodium butyrate enhance natriuretic peptide receptor a gene transcription: role of histone modification. *Mol. Pharmacol.* 85, 946–957. doi: 10.1124/mol.114.092221

Kumar, P., Tripathi, S., and Pandey, K. N. (2014b). Histone deacetylase inhibitors modulate the transcriptional regulation of guanylyl cyclase/natriuretic peptide receptor-A gene: interactive roles of modified histones, HATS, p300, and Sp1. *J. Biol. Chem.* 289, 6991–7002. doi: 10.1074/jbc.M113.511444

Kumar, R., Cartledge, W. A., Lincoln, T. M., and Pandey, K. N. (1997). Expression of guanylyl cyclase-A/atrial natriuretic peptide receptor blocks the activation of protein kinase C in vascular smooth muscle cells. Role of cGMP and cGMP-dependent protein kinase. *Hypertension* 29, 414–421. doi: 10.1161/01.HYP.29.1.414

Kuno, T., Andresen, J. W., Kamisaki, Y., Waldman, S. A., Chang, L. Y., Saheki, S., et al. (1986). Co-purification of an atrial natriuretic factor receptor and particulate guanylate cyclase from rat lung. *J. Biol. Chem.* 261, 5817–5823.

Kurose, H., Inagami, T., and Ui, M. (1987). Participation of adenosine 5'-triphosphate in the activation of membrane-bound guanylate cyclase by the atrial natriuretic factor. *FEBS Lett.* 219, 375–379. doi: 10.1016/0014-5793(87)80256-9

Labrecque, J., Mcnicoll, N., Marquis, M., and De Lean, A. (1999). A disulfide-bridged mutant of natriuretic peptide receptor-A displays constitutive activity. Role of receptor dimerization in signal transduction. *J. Biol. Chem.* 274, 9752–9759. doi: 10.1074/jbc.274.14.9752

Larose, L., Mcnicoll, N., Ong, H., and De Lean, A. (1991). Allosteric modulation by ATP of the bovine adrenal natriuretic factor R1 receptor functions. *Biochemistry* 30, 8990–8995. doi: 10.1021/bi00101a012

Larose, L., Rondeau, J. J., Ong, H., and De Lean, A. (1992). Phosphorylation of atrial natriuretic factor R1 receptor by serine/threonine protein kinases: evidences for receptor regulation. *Mol. Cell. Biochem.* 115, 203–211. doi: 10.1007/BF00230332

Lefkowitz, R. J., Pitcher, J., Krueger, K., and Daaka, Y. (1998). Mechanisms of β-adrenergic receptor desensitization and resensitization. *Adv. Pharmacol.* 42, 416–420. doi: 10.1016/S1054-3589(08)60777-2

Leitman, D. C., Andresen, J. W., Catalano, R. M., Waldman, S. A., Tuan, J. J., and Murad, F. (1988). Atrial natriuretic peptide binding, cross-linking, and stimulation of cyclic GMP accumulation and particulate guanylate cyclase activity in cultured cells. *J. Biol. Chem.* 263, 3720–3728.

Levin, E. R., Gardner, D. G., and Samson, W. K. (1998). Natriuretic peptides. *N. Engl. J. Med.* 339, 321–328. doi: 10.1056/NEJM199807303390507

Lincoln, T. M., Komalavilas, P., and Cornwell, T. L. (1994). Pleiotropic regulation of vascular smooth muscle tone by cyclic GMP-dependent protein kinase. *Hypertension* 243, 383–385.

Lisy, O., Jougasaki, M., Heublein, D. M., Schirger, J. A., Chen, H. H., Wennberg, P. W., et al. (1999). Renal actions of synthetic *Dendroaspis* natriuretic peptide. *Kidney Int.* 56, 502–508. doi: 10.1046/j.1523-1755.1999.00573.x

Lopez, M. J., Wong, S. K.-F., Kishimoto, I., Dubois, S., Mach, V., Friesen, J., et al. (1995). Salt-resistant hypertension in mice lacking the guanylyl cyclase-A receptor for atrial natriuretic peptide. *Nature* 378, 65–68. doi: 10.1038/378065a0

Louis, J. C., Magal, E., and Yavin, E. (1988). Protein kinase C alterations in the fetal rat brain after global ischemia. *J. Biol. Chem.* 263, 19282–19285.

Lowe, D. G., and Fendly, B. M. (1992). Human natriuretic peptide receptor-A guanylyl cyclase. Hormone cross-linking and antibody reactivity distinguish receptor glycoforms. *J. Biol. Chem.* 267, 21691–21697.

Lucas, K. A., Pitari, G. M., Kazerounian, S., Ruiz-Stewart, I., Park, J., Schulz, S., et al. (2000). Guanylyl cyclases and signaling by cyclic GMP. *Pharmacol. Rev.* 52, 375–414.

Maack, T., Suzuki, M., Almeida, F. A., Nussenzveig, D., Scarborough, R. M., Mcenroe, G. A., et al. (1987). Physiological role of silent receptors of atrial natriuretic factor. *Science* 238, 675–678. doi: 10.1126/science.2823385

Maki, M., Takayanagi, R., Misono, K. S., Pandey, K. N., Tibbetts, C., and Inagami, T. (1984). Structure of rat atrial natriuretic factor precursor deduced from cDNA sequence. *Nature* 309, 722–724. doi: 10.1038/309722a0

Marala, R., Duda, T., Goraczniak, R. M., and Sharma, R. K. (1992). Genetically tailored atrial natriuretic factor-dependent guanylate cyclase. Immunological and functional identity with 180 kDa membrane guanylate cyclase and ATP signaling site. *FEBS Lett.* 296, 254–258. doi: 10.1016/0014-5793(92)80298-U

Masciotra, S., Picard, S., and Deschepper, C. F. (1999). Cosegregation analysis in genetic crosses suggests a protective role for atrial natriuretic factor against ventricular hypertrophy. *Circ. Res.* 84, 1453–1458. doi: 10.1161/01.RES.84.12.1453

Matsukawa, N., Grzesik, W. J., Takahashi, N., Pandey, K. N., Pang, S., Yamauchi, M., et al. (1999). The natriuretic peptide clearance receptor locally modulates the physiological effects of the natriuretic peptide system. *Proc. Natl. Acad. Sci. U.S.A.* 96, 7403–7408. doi: 10.1073/pnas.96.13.7403

McCullough, P. A., Duc, P., Omland, T., Mccord, J., Nowak, R. M., Hollander, J. E., et al. (2003). B-type natriuretic peptide and renal function in the diagnosis

of heart failure: an analysis from the breathing not properly multinational study. *Am. J. Kidney Dis.* 41, 571–579. doi: 10.1053/ajkd.2003.50118

Melo, L. G., Veress, A. T., Ackermann, U., Steinhelper, M. E., Pang, S. C., Tse, Y., et al. (1999). Chronic regulation of arterial blood pressure in ANP transgenic and knockout mice: role of cardiovascular sympathetic tone. *Cardiovasc. Res.* 43, 437–444. doi: 10.1016/S0008-6363(99)00104-2

Meloche, S., Mcnicoll, N., Liu, B., Ong, H., and De Lean, A. (1988). Atrial natriuretic factor R1 receptor from bovine adrenal zona glomerulosa: purification, characterization, and modulation by amiloride. *Biochemistry* 27, 8151–8158. doi: 10.1021/bi00421a025

Meloche, S., Ong, H., Cantin, M., and De Lean, A. (1986). Affinity cross-linking of atrial natriuretic factor to its receptor in bovine adrenal zona glomerulosa. *J. Biol. Chem.* 261, 1525–1528.

Meyer, M., Richter, R., Brunkhorst, R., Wrenger, E., Schulz-Knappe, P., Kist, A., et al. (1996). Urodilatin is involved in sodium homeostasis and exerts sodium-state-dependent natriuretic and diuretic effects. *Am. J. Physiol.* 271, F489–F497.

Misono, K. S., Fukumi, H., Grammer, R. T., and Inagami, T. (1984). Rat atrial natriuretic factor: complete amino acid sequence and disulfide linkage essential for biological activity. *Biochem. Biophys. Res. Commun.* 119, 524–529. doi: 10.1016/S0006-291X(84)80279-X

Misono, K. S., Grammer, R. T., Rigby, J. W., and Inagami, T. (1985). Photoaffinity labeling of atrial natriuretic factor receptor in bovine and rat adrenal cortical membranes. *Biochem. Biophys. Res. Commun.* 130, 994–1001. doi: 10.1016/0006-291X(85)91713-9

Miyagi, M., Zhang, X., and Misono, K. S. (2000). Glycosylation sites in the atrial natriuretic peptide receptor oligosaccharide structures are not required for hormone binding. *Eur. J. Biochem.* 267, 5758–5768. doi: 10.1046/j.1432-1327.2000.01647.x

Mukoyama, M., Nakao, K., Hosoda, K., Suga, S., Saito, Y., Ogawa, Y., et al. (1991). Brain natriuretic peptide as a novel cardiac hormone in humans. Evidence for an exquisite dual natriuretic peptide system, atrial natriuretic peptide and brain natriuretic peptide. *J. Clin. Invest.* 87, 1402–1412. doi: 10.1172/JCI115146

Murthy, K. K., Thibault, G., and Cantin, M. (1989). Binding and intracellular degradation of atrial natriuretic factor by cultured vascular smooth muscle cells. *Mol. Cell. Endocrinol.* 67, 195–206. doi: 10.1016/0303-7207(89)90210-4

Napier, M., Arcuri, K., and Vandlen, R. (1986). Binding and internalization of atrial natriuretic factor by high-affinity receptors in A10 smooth muscle cells. *Arch. Biochem. Biophys.* 248, 516–522. doi: 10.1016/0003-9861(86)90504-7

Neuser, D., and Bellermann, P. (1986). Receptor binding, cGMP stimulation and receptor desensitization by atrial natriuretic peptides in cultured A10 vascular smooth muscle cells. *FEBS Lett.* 209, 347–351. doi: 10.1016/0014-5793(86)81140-1

Nussenzveig, D. R., Lewicki, J. A., and Maack, T. (1990). Cellular mechanisms of the clearance function of type-C receptors of atrial natriuretic factor. *J. Biol. Chem.* 265, 20952–20958.

Ogawa, Y., Nakao, K., Nakagawa, O., Komatsu, Y., Hosoda, K., Suga, S., et al. (1992). Human C-type natriuretic peptide. Characterization of the gene and peptide. *Hypertension* 19, 809–813. doi: 10.1161/01.HYP.19.6.809

Oliver, P. M., Fox, J. E., Kim, R., Rockman, H. A., Kim, H. S., Reddick, R. L., et al. (1997). Hypertension, cardiac hypertrophy, and sudden death in mice lacking natriuretic peptide receptor A. *Proc. Natl. Acad. Sci. U.S.A.* 94, 14730–14735. doi: 10.1073/pnas.94.26.14730

Oliver, P. M., John, S. W., Purdy, K. E., Kim, R., Maeda, N., Goy, M. F., et al. (1998). Natriuretic peptide receptor 1 expression influences blood pressures of mice in a dose-dependent manner. *Proc. Natl. Acad. Sci. U.S.A.* 95 2547–2551. doi: 10.1073/pnas.95.5.2547

Omland, T., Aakvaag, A., Bonarjee, V. V., Caidahl, K., Lie, R. T., Nilsen, D. W., et al. (1996). Plasma brain natriuretic peptide as an indicator of left ventricular systolic function and long-term survival after acute myocardial infarction. Comparison with plasma atrial natriuretic peptide and N-terminal proatrial natriuretic peptide. *Circulation* 93, 1963–1969. doi: 10.1161/01.CIR.93.11.1963

Pandey, K., Kumar, R., Li, M., and Nguyen, H. T. (2000a). Functional domains and expression of truncated atrial natriuretic peptide receptor-A: the carboxyl-terminal regions direct the receptor internalization and sequestration in COS-7 cells. *Mol. Pharmacol.* 57, 259–267.

Pandey, K. N., Nguyen, H. T., Li, M., and Boyle, J. W. (2000b). Natriuretic peptide receptor-A negatively regulates mitogen-activated protein kinase and proliferation of mesangial cells: role of cGMP-dependent protein kinase. *Biochem. Biophys. Res. Commun.* 271, 374–379. doi: 10.1006/bbrc.2000.2627

Pandey, K. N. (1989). Stimulation of protein phosphorylation by atrial natriuretic factor in plasma membranes of bovine adrenal cortical cells. *Biochem. Biophys. Res. Commun.* 163, 988–994. doi: 10.1016/0006-291X(89)92319-X

Pandey, K. N. (1992). Kinetic analysis of internalization, recycling and redistribution of atrial natriuretic factor-receptor complex in cultured vascular smooth-muscle cells. Ligand-dependent receptor down-regulation. *Biochem. J.* 288, 55–61.

Pandey, K. N. (1993). Stoichiometric analysis of internalization, recycling, and redistribution of photoaffinity-labeled guanylate cyclase/atrial natriuretic factor receptors in cultured murine Leydig tumor cells. *J. Biol. Chem.* 268, 4382–4390.

Pandey, K. N. (1994a). Atrial natriuretic factor inhibits autophosphorylation of protein kinase C and A 240-kDa protein in plasma membranes of bovine adrenal glomerulosa cells: involvement of cGMP-dependent and independent signal transduction mechanisms. *Mol. Cell. Biochem.* 141, 103–111. doi: 10.1007/BF00926173

Pandey, K. N. (1994b). Atrial natriuretic factor inhibits the phosphorylation of protein kinase C in plasma membrane preparations of cultured Leydig tumor cells. *J. Androl.* 15, 100–109. doi: 10.1007/BF00926173

Pandey, K. N. (2001). Dynamics of internalization and sequestration of guanylyl cyclase/atrial natriuretic peptide receptor-A. *Can. J. Physiol. Pharmacol.* 79, 631–639. doi: 10.1139/y01-035

Pandey, K. N. (2002). Intracellular trafficking and metabolic turnover of ligand-bound guanylyl cyclase/atrial natriuretic peptide receptor-A into subcellular compartments. *Mol. Cell. Biochem.* 230, 61–72. doi: 10.1023/A:1014240006767

Pandey, K. N. (2005). Biology of natriuretic peptides and their receptors. *Peptides* 26, 901–932. doi: 10.1016/j.peptides.2004.09.024

Pandey, K. N. (2011). The functional genomics of guanylyl cyclase/natriuretic peptide receptor-A: perspectives and paradigms. *FEBS J.* 278, 1792–1807. doi: 10.1111/j.1742-4658.2011.08081.x

Pandey, K. N., Inagami, T., and Misono, K. S. (1986). Atrial natriuretic factor receptor on cultured Leydig tumor cells: ligand binding and photoaffinity labeling. *Biochemistry* 25, 8467–8472. doi: 10.1021/bi00374a022

Pandey, K. N., Kovacs, W. J., and Inagami, T. (1985). The inhibition of progesterone secretion and the regulation of cyclic nucleotides by atrial natriuretic factor in gonadotropin responsive murine Leydig tumor cells. *Biochem. Biophys. Res. Commun.* 133, 800–806. doi: 10.1016/0006-291X(85)90975-1

Pandey, K. N., Nguyen, H. T., Sharma, G. D., Shi, S. J., and Kriegel, A. M. (2002). Ligand-regulated internalization, trafficking, and down-regulation of guanylyl cyclase/atrial natriuretic peptide receptor-A in human embryonic kidney 293 cells. *J. Biol. Chem.* 277, 4618–4627. doi: 10.1074/jbc.M106436200

Pandey, K. N., Oliver, P. M., Maeda, N., and Smithies, O. (1999). Hypertension associated with decreased testosterone levels in natriuretic peptide receptor-A gene-knockout and gene-duplicated mutant mouse models. *Endocrinology* 140, 5112–5119.

Pandey, K. N., Pavlou, S. N., and Inagami, T. (1988). Identification and characterization of three distinct atrial natriuretic factor receptors. Evidence for tissue-specific heterogeneity of receptor subtypes in vascular smooth muscle, kidney tubular epithelium, and Leydig tumor cells by ligand binding, photoaffinity labeling, and tryptic proteolysis. *J. Biol. Chem.* 263, 13406–13413.

Pandey, K. N., and Singh, S. (1990). Molecular cloning and expression of murine guanylate cyclase/atrial natriuretic factor receptor cDNA. *J. Biol. Chem.* 265, 12342–12348.

Paul, A. K., Marala, R. B., Jaiswal, R. K., and Sharma, R. K. (1987). Coexistence of guanylate cyclase and atrial natriuretic factor receptor in a 180-kD protein. *Science* 235, 1224–1226. doi: 10.1126/science.2881352

Phillips, R. A., Ardeljan, M., Shimabukuro, S., Goldman, M. E., Garbowit, D. L., Eison, H. B., et al. (1991). Normalization of left ventricular mass and associated changes in neurohormones and atrial natriuretic peptide after 1 year of sustained nifedipine therapy for severe hypertension. *J. Am. Coll. Cardiol.* 17, 1595–1602. doi: 10.1016/0735-1097(91)90654-R

Pollman, M. J., Yamada, T., Horiuchi, M., and Gibbons, G. H. (1996). Vasoactive substances regulate vascular smooth muscle cell apoptosis. *Circ. Res.* 79 748–756. doi: 10.1161/01.RES.79.4.748

Potter, L. R., and Garbers, D. L. (1992). Dephosphorylation of the guanylyl cyclase-A receptor causes desensitization. *J. Biol. Chem.* 267, 14531–14534.

Prins, B. A., Weber, M. J., Hu, R. -M., Pedram, A., Daniels, M., and Levin, E. R. (1996). Atrial natriuretic peptide inhibits mitogen-activated protein kinase through the

clearance receptor Potential role in the inhibition of astrocyte proliferation. *J. Biol. Chem.* 271, 14156–14162. doi: 10.1074/jbc.271.24.14156

Rashatwar, S. S., Cornwell, T. L., and Lincoln, T. M. (1987). Effect of 8-bromo cGMP on Ca2+-ATPase by cGMP dependent protein kinase. *Proc. Natl. Acad. Sci. U.S.A* 84, 5685–5689. doi: 10.1073/pnas.84.16.5685

Rasmussen, H., Isales, C. M., Calle, R. A., Throckmorton, D., Anderson, M., Gasalla-Harraiz, J., et al. (1995). Diacylglycerol production, Ca^{2+} influx and protein kinase c activation in sustained cellular responses. *Endocr. Rev.* 16, 649–681.

Rathinavelu, A., and Isom, G. E. (1991). Differential internalization and precessing of atrial natriuretic factor B and C receptors in PC-12 cells. *Biochem. J.* 276, 493–497.

Resink, T. J., Scott-Burden, T., Baur, U., Jones, C. R., and Buhler, F. R. (1988). Atrial natriuretic peptide induces breakdown of phosphatidylinositol phosphates in cultured vascular smooth muscle cells. *Eur. J. Biochem.* 172, 499–505. doi: 10.1111/j.1432-1033.1988.tb13915.x

Rogers, J., Hughes, R. J., and Mathes, E. K. (1988). cGMP inhibits protein kinase C-mediated secretion in rat pancreatic acini. *J. Biol. Chem.* 263, 3713–3719.

Rosenzweig, A., and Seidman, C. E. (1991). Atrial natriuretic factor and related peptide hormones. *Annu. Rev. Biochem.* 60, 229–255. doi: 10.1146/annurev.bi.60.070191.001305

Sano, T., Morishita, Y., Matsuda, Y., and Yamada, K. (1992). Pharmacological profile of HS-142-1, a novel nonpeptide atrial natriuretic peptide antagonist of microbial origin I. Selective inhibition of the actions of natriuretic peptides in anesthetized rats. *J. Pharmacol. Exp. Ther.* 260, 825–831.

Sauro, M. D., and Fitzpatrick, D. F. (1990). Atrial natriuretic peptides inhibit protien kinase C activation in rat aortic smooth muscle. *Pept. Res.* 3, 138–141.

Saxenhofer, H., Raselli, A., Weidmann, P., Forssmann, W. G., Bub, A., Ferrari, P., et al. (1990). Urodilatin, a natriuretic factor from kidneys, can modify renal and cardiovascular function in men. *Am. J. Physiol.* 259, F832–F838.

Schenk, D. B., Phelps, M. N., Porter, J. G., Scarborough, R. M., Mcenroe, G. A., and Lewicki, J. A. (1985). Identification of the receptor for atrial natriuretic factor on cultured vascular cells. *J. Biol. Chem.* 260, 14887–14890.

Schulz-Knappe, P., Forssmann, K., Herbst, F., Hock, D., Pipkorn, R., and Forssmann, W. G. (1988). Isolation and structural analysis of "urodilatin", a new peptide of the cardiodilatin-(ANP)-family, extracted from human urine. *Klin. Wochenschr.* 66, 752–759. doi: 10.1007/BF01726570

Schulz, S., Singh, S., Bellet, R. A., Singh, G., Tubb, D. J., Chin, H., et al. (1989). The primary structure of a plasma membrane guanylate cyclase demonstrates diversity within this new receptor family. *Cell* 58, 1155–1162. doi: 10.1016/0092-8674(89)90513-8

Schweitz, H., Vigne, P., Moinier, D., Frelin, C., and Lazdunski, M. (1992). A new member of the natriuretic peptide family is present in the venom of the green mamba (*Dendroaspis angusticeps*). *J. Biol. Chem.* 267, 13928–13932.

Sharma, G. D., Nguyen, H. T., Antonov, A. S., Gerrity, R. G., Von Geldern, T., and Pandey, K. N. (2002). Expression of atrial natriuretic peptide receptor-A antagonizes the mitogen-activated protein kinases (Erk2 and P38MAPK) in cultured human vascular smooth muscle cells. *Mol. Cell. Biochem.* 233, 165–173. doi: 10.1023/A:1015882302796

Sharma, R. K. (2002). Evolution of the membrane guanylate cyclase transduction system. *Mol. Cell. Biochem.* 230, 3–30. doi: 10.1023/A:1014280410459

Sharma, R. K., and Duda, T. (2010). ROS-GC subfamily membrane guanylate cyclase-linked transduction systems: taste, pineal gland and hippocampus. *Mol. Cell. Biochem.* 334, 199–206. doi: 10.1007/s11010-009-0334-8

Shi, S. J., Nguyen, H. T., Sharma, G. D., Navar, L. G., and Pandey, K. N. (2001). Genetic disruption of atrial natriuretic peptide receptor-A alters renin and angiotensin II levels. *Am. J. Physiol.* 281, F665–F673.

Shi, S. J., Vellaichamy, E., Chin, S. Y., Smithies, O., Navar, L. G., and Pandey, K. N. (2003). Natriuretic peptide receptor A mediates renal sodium excretory responses to blood volume expansion. *Am. J. Physiol.* 285, F694–F702.

Sibley, D. R., Benovic, J. L., Caron, M. G., and Lefkowitz, R. J. (1987). Regulation of transmembrane signaling by receptor phosphorylation. *Cell* 48, 913–933. doi: 10.1016/0092-8674(87)90700-8

Silberbach, M., Gorenc, T., Hershberger, R. E., Stork, P. J. S., Steyger, P. S., and Roberts, C. T. J. (1999). Extracellular signal-regulated protein kinase activation is required for the anti-hypertrophic effect of atrial natriuretic factor in neonatal rat ventricular myocytes. *J. Biol. Chem.* 274, 24858–24864. doi: 10.1074/jbc.274.35.24858

Sorkin, A., and von Zastrow, M. (2002). Signal transduction and endocytosis close encounters of many kinds. *Nat. Rev. Mol. Cell Biol.* 3, 600–614. doi: 10.1038/nrm883

Sudoh, T., Minamino, N., Kangawa, K., and Matsuo, H. (1988). Brain natriuretic peptide-32: N-terminal six amino acid extended form of brain natriuretic peptide identified in porcine brain. *Biochem. Biophys. Res. Commun.* 155, 726–732. doi: 10.1016/S0006-291X(88)80555-2

Sudoh, T., Minamino, N., Kangawa, K., and Matsuo, H. (1990). C-type natriuretic peptide (CNP): a new member of natriuretic peptide family identified in porcine brain. *Biochem. Biophys. Res. Commun.* 168, 863–870. doi: 10.1016/0006-291X(90)92401-K

Suga, S., Itoh, H., Komatsu, Y., Ogawa, Y., Hama, N., Yoshimasa, T., et al. (1993). Cytokine-induced C-type natriuretic peptide (CNP) secretion from vascular endothelial cells–evidence for CNP as a novel autocrine/paracrine regulator from endothelial cells. *Endocrinology* 133, 3038–3041.

Suga, S., Nakao, K., Itoh, H., Komatsu, Y., Ogawa, Y., Hama, N., et al. (1992). Endothelial production of C-type natriuretic peptide and its marked augmentation by transforming growth factor-beta. Possible existence of "vascular natriuretic peptide system." *J. Clin. Invest.* 90, 1145–1149. doi: 10.1172/JCI115933

Sugimoto, T., Kikkawa, R., Haneda, M., and Shigeta, Y. (1993). Atrial natriuretic peptide inhibits endothelin-1 induced activation of mitogen-activated protein kinase in cultured rat mesangial cells. *Biochem. Biophys. Res. Commun.* 195, 72–78. doi: 10.1006/bbrc.1993.2011

Takahashi, N., and Smithies, O. (1999). Gene targeting approaches to analyzing hypertension. *J. Am. Soc. Nephrol.* 10, 1598–1605.

Takayanagi, R., Snajdar, R. M., Imada, T., Tamura, M., Pandey, K. N., Misono, K. S., et al. (1987). Purification and characterization of two types of atrial natriuretic factor receptors from bovine adrenal cortex: guanylate cyclase-linked and cyclase-free receptors. *Biochem. Biophys. Res. Commun.* 144, 244–250. doi: 10.1016/S0006-291X(87)80502-8

Tamura, N., Ogawa, Y., Yasoda, A., Itoh, H., Saito, Y., and Nakao, K. (1996). Two cardiac natriuretic peptide genes (atrial natriuretic peptide and brain natriuretic peptide) are organized in tandem in the mouse and human genomes. *J. Mol. Cell Cardiol.* 28, 1811–1815. doi: 10.1006/jmcc.1996.0170

Teitelbaum, I., Strasheim, A., and Berl, T. (1990). Epidermal growth factor-stimulated phosphonositide hydrolysis in cultured rat inner medullary collecting tubule cells. Regulation by G protein, calcium, and protein kinase C. *J. Clin. Invest.* 85, 1044–1050. doi: 10.1172/JCI114534

Thomas, P., and Meizel, S. (1989). Phosphatidylinositol 4,5-bisphosphate hydrolysis in human sperm stimulated with follicular fluid or progesterone is dependent upon Ca^{2+} influx. *Biochem. J.* 264, 539–546.

Trindade, P., Hutchinson, H. G., Pollman, M. J., Gibbons, G. H., and Pratt, R. E. (1995). Atrial natriuretic peptide (ANP) and C-type natriuretic peptide (CNP) induce apoptosis in vascular smooth muscle cells (VMSC). *Circulation* 92, 1–696.

Tripathi, S., and Pandey, K. N. (2012). Guanylyl cyclase/natriuretic peptide receptor-A signaling antagonizes the vascular endothelial growth factor-stimulated MAPKs and downstream effectors AP-1 and CREB in mouse mesangial cells. *Mol. Cell. Biochem.* 368, 47–59. doi: 10.1007/s11010-012-1341-8

Turla, M. B., Park, S. M., and Webb, R. C. (1990). Vascular responsiveness to phorbol esters in coarctation-hypertensive rats. *J. Hypertens.* 8, 191–196. doi: 10.1097/00004872-199002000-00015

Turovsky, E. A., Turovskaya, M. V., Dolgacheva, L. P., Zinchenko, V. P., and Dynnik, V. V. (2013). Acetylcholine promotes Ca^{2+} and NO-oscillations in adipocytes implicating Ca2+– > NO– > cGMP– > cADP-ribose– > Ca2+ positive feedback loop – modulatory effects of norepinephrine and atrial natriuretic peptide. *PLoS ONE* 8:e63483. doi: 10.1371/journal.pone.0063483

van den Akker, F. (2001). Structural insights into the ligand binding domains of membrane bound guanylyl cyclases and natriuretic peptide receptors. *J. Mol. Biol.* 311, 923–937. doi: 10.1006/jmbi.2001.4922

van den Akker, F., Zhang, X., Miyagi, M., Huo, X., Misono, K. S., and Yee, V. C. (2000). Structure of the dimerized hormone-binding domain of a guanylyl-cyclase-coupled receptor. *Nature* 406, 101–104. doi: 10.1038/35017602

Vandlen, R. L., Arcuri, K. E., and Napier, M. A. (1985). Identification of a receptor for atrial natriuretic factor in rabbit aorta membranes by affinity cross-linking. *J. Biol. Chem.* 260, 10889–10892.

Vellaichamy, E., Das, S., Subramanian, U., Maeda, N., and Pandey, K. N. (2014). Genetically altered mutant mouse models of guanylyl cyclase/natriuretic

peptide receptor-A exhibit the cardiac expression of proinflammatory mediators in a gene-dose-dependent manner. *Endocrinology* 155, 1045–1056. doi: 10.1210/en.2013-1416

Vellaichamy, E., Khurana, M. L., Fink, J., and Pandey, K. N. (2005). Involvement of the NF-kappa B/matrix metalloproteinase pathway in cardiac fibrosis of mice lacking guanylyl cyclase/natriuretic peptide receptor A. *J. Biol. Chem.* 280, 19230–19242. doi: 10.1074/jbc.M411373200

Vellaichamy, E., Zhao, D., Somanna, N., and Pandey, K. N. (2007). Genetic disruption of guanylyl cyclase/natriuretic peptide receptor-A upregulates ACE and AT1 receptor gene expression and signaling: role in cardiac hypertrophy. *Physiol. Genomics* 31, 193–202. doi: 10.1152/physiolgenomics.00079.2007

von Geldern, T. W., Budzik, G. P., Dillon, T. P., Holleman, W. H., Holst, M. A., Ksio, Y., et al. (1990). Atrial natriuretic peptide antagonists biological evaluation and structural correlations. *Mol. Pharmacol.* 38, 771–778.

Waldman, S. A., Rapoport, R. M., and Murad, F. (1984). Atrial natriuretic factor selectively activates particulate guanylate cyclase and elevates cyclic GMP in rat tissues. *J. Biol. Chem.* 259, 14332–14334.

White, R. E., Lee, A. B., Shcherbatko, A. D., Lincoln, T. M., Schonbrunn, A., and Armstrong, D. L. (1993). Potassium channel stimulation by natriuretic peptides through cGMP-dependent dephosphorylation. *Nature* 361, 263–266. doi: 10.1038/361263a0

Wilson, E. M., and Chinkers, M. (1995). Identification of sequences mediating guanylyl cyclase dimerization. *Biochemistry* 34, 4696–4701. doi: 10.1021/bi00014a025

Wong, S. K., Ma, C. P., Foster, D. C., Chen, A. Y., and Garbers, D. L. (1995). The guanylyl cyclase-A receptor transduces an atrial natriuretic peptide/ATP activation signal in the absence of other proteins. *J. Biol. Chem.* 270, 30818–30822. doi: 10.1074/jbc.270.51.30818

Wormald, M. R., and Dwek, R. A. (1999). Glycoproteins glycan presentation and protein-fold stability. *Structure* 7, R155–R160. doi: 10.1016/S0969-2126(99)80095-1

Wu, C. F., Bishopric, N. H., and Pratt, R. E. (1997). Atrial natriuretic peptide induces apoptosis in neonatal rat cardiac myocytes. *J. Biol. Chem.* 272, 14860–14866. doi: 10.1074/jbc.272.23.14860

Yoshihara, F., Tokudome, T., Kishimoto, I., Otani, K., Kuwabara, A., Horio, T., et al. (2014). Aggravated renal tubular damage and interstitial fibrosis in mice lacking guanylyl cyclase-A (GC-A), a receptor for atrial and B-type natriuretic peptides. *Clin. Exp. Nephrol.* doi: 10.1007/s10157-014-0982-1 [Epub ahead of print].

Yoshimura, M., Yasue, H., Morita, E., Sakaino, N., Jougasaki, M., Kurose, M., et al. (1991). Hemodynamic, renal, and hormonal responses to brain natriuretic peptide infusion in patients with congestive heart failure. *Circulation* 84, 1581–1588. doi: 10.1161/01.CIR.84.4.1581

Yoshimura, M., Yasue, H., Okumura, K., Ogawa, H., Jougasaki, M., Mukoyama, M., et al. (1993). Different secretion patterns of atrial natriuretic peptide and brain natriuretic peptide in patients with congestive heart failure. *Circulation* 87, 464–469. doi: 10.1161/01.CIR.87.2.464

Zhao, D., Das, S., and Pandey, K. N. (2013). Interactive roles of NPR1 gene-dosage and salt diets on cardiac angiotensin II, aldosterone and proinflammatory cytokines levels in mutant mice. *J. Hypertens.* 31, 134–144. doi: 10.1097/HJH.0b013e32835ac15f

Zhao, D., Vellaichamy, E., Somanna, N. K., and Pandey, K. N. (2007). Guanylyl cyclase/natriuretic peptide receptor-A gene disruption causes increased adrenal angiotensin II and aldosterone levels. *Am. J. Physiol.* 293, F121–F127. doi: 10.1152/ajprenal.00478.2006

Zhao, L., Long, L., and Morrell, N. W. (1999). NPRA-deficient mice show increased susceptibility to hypoxia-induced pulmonary hypertension. *Circulation* 99, 605–607. doi: 10.1161/01.CIR.99.5.605

Zhou, H., and Murthy, K. S. (2003). Identification of the G-protein activation sequence of the single-transmembrane natriuretic peptide receptor C (NPR-C). *Am. J. Cell. Physiol.* 284, C1255–C1261. doi: 10.1152/ajpcell.00520.2002

Zolle, O., Lawrie, A. M., and Simpson, A. W. (2000). Activation of the particulate and not the soluble guanylate cyclase leads to the inhibition of Ca^{2+} extrusion through localized elevation of cGMP. *J. Biol. Chem.* 275, 25892–25899. doi: 10.1074/jbc.M000786200

Conflict of Interest Statement: The author declares that the research was conducted in the absence of any commercial or financial relationships that could be construed as a potential conflict of interest.

Received: 10 April 2014; accepted: 05 August 2014; published online: 22 August 2014.
*Citation: Pandey KN (2014) Guanylyl cyclase/natriuretic peptide receptor-A signaling antagonizes phosphoinositide hydrolysis, Ca^{2+} release, and activation of protein kinase C. Front. Mol. Neurosci. **7**:75. doi: 10.3389/fnmol.2014.00075*
This article was submitted to the journal Frontiers in Molecular Neuroscience.

frontiers in
MOLECULAR NEUROSCIENCE

ORIGINAL RESEARCH ARTICLE
published: 01 December 2014
doi: 10.3389/fnmol.2014.00095

Regulation of hippocampal synaptic plasticity thresholds and changes in exploratory and learning behavior in dominant negative NPR-B mutant rats

Gleb Barmashenko[1,2], Jens Buttgereit[3,4], Neil Herring[4,5], Michael Bader[4], Cemil Özcelik[3,4†], Denise Manahan-Vaughan[2] and Karl H. Braunewell[1]*

[1] Guest Group, In vitro-Electrophysiology Laboratory, Department of Neurophysiology, Medical Faculty, Ruhr University Bochum, Bochum, Germany
[2] Department of Neurophysiology, Medical Faculty, Ruhr University Bochum, Bochum, Germany
[3] Experimental and Clinical Research Center, Max Delbrück Center for Molecular Medicine, Charité Medical Faculty, Berlin, Germany
[4] Max Delbrück Center for Molecular Medicine, Berlin, Germany
[5] Department of Physiology, Anatomy and Genetics, Burdon Sanderson Cardiac Science Centre – BHF Centre of Research Excellence, University of Oxford, Oxford, UK

Edited by:
Clint Lawrence Makino, Massachusetts Eye and Ear Infirmary and Harvard Medical School, USA

Reviewed by:
Yi-Ping Hsueh, Institute of Molecular Biology – Academia Sinica, Taiwan
Teresa Duda, Salus University, USA

***Correspondence:**
Karl H. Braunewell, Guest Group, In vitro-Electrophysiology Laboratory, Department of Neurophysiology, Medical Faculty, Ruhr University Bochum, Universitätsstraße 150, Building MA 4/150, 44780 Bochum, Germany
e-mail: kbraunewell@gmail.com

†**Present address:**
Cemil Özcelik, KLINIKUM VEST GmbH, Dorstener Straße 151, 45657 Recklinghausen, Germany

The second messenger cyclic GMP affects synaptic transmission and modulates synaptic plasticity and certain types of learning and memory processes. The impact of the natriuretic peptide receptor B (NPR-B) and its ligand C-type natriuretic peptide (CNP), one of several cGMP producing signaling systems, on hippocampal synaptic plasticity and learning is, however, less well understood. We have previously shown that the NPR-B ligand CNP increases the magnitude of long-term depression (LTD) in hippocampal area CA1, while reducing the induction of long-term potentiation (LTP). We have extended this line of research to show that bidirectional plasticity is affected in the opposite way in rats expressing a dominant-negative mutant of NPR-B (NSE-NPR-BΔKC) lacking the intracellular guanylyl cyclase domain under control of a promoter for neuron-specific enolase. The brain cells of these transgenic rats express functional dimers of the NPR-B receptor containing the dominant-negative NPR-BΔKC mutant, and therefore show decreased CNP-stimulated cGMP-production in brain membranes. The NPR-B transgenic rats display enhanced LTP but reduced LTD in hippocampal slices. When the frequency-dependence of synaptic modification to afferent stimulation in the range of 1–100 Hz was assessed in transgenic rats, the threshold for both, LTP and LTD induction, was shifted to lower frequencies. In parallel, NPR-BΔKC rats exhibited an enhancement in exploratory and learning behavior. These results indicate that bidirectional plasticity and learning and memory mechanism are affected in transgenic rats expressing a dominant-negative mutant of NPR-B. Our data substantiate the hypothesis that NPR-B-dependent cGMP signaling has a modulatory role for synaptic information storage and learning.

Keywords: cGMP, exploratory, hippocampus, LTP, LTD, metaplasticity, NPR-B, memory

INTRODUCTION

The natriuretic peptides, ANP, BNP, and CNP (A-, B-, and C- type natriuretic peptide) and their receptors, the natriuretic peptide receptors (NPRs) are widely distributed in the central nervous system (CNS). They constitute a peptide hormone-receptor signaling system with a variety of potential roles in modulating physiological brain functions (Potter et al., 2009; Potter, 2011). Whereas ANP and BNP activate the type I transmembrane guanylyl cyclase receptor, natriuretic peptide receptor-A (NPR-A), CNP activates a related cyclase, the natriuretic peptide receptor-B (NPR-B), leading to the production of the second messenger cGMP (Potter et al., 2009). NPR-A and -B display several functional domains, including an extracellular ligand-binding domain, a transmembrane domain, and an intracellular domain, which consists of a kinase homology domain (KHD), a hinge region, and a guanylyl cyclase domain catalyzing the conversion of Mg-GTP into cGMP. A ligand-dependent receptor homodimerization is essential for the enzymatic activity of the guanylyl cyclase domain (Potter, 2011).

Natriuretic peptide receptor-B leads to various physiological effects ranging from bone growth (Bartels et al., 2004; Potter et al., 2009; Potter, 2011) to CNS effects, such as axonal sprouting in dorsal root ganglion neurons (Schmidt et al., 2007; Potter et al., 2009), effects on synaptic plasticity (Decker et al., 2008, 2009, 2010), and anxiogenic effects in rats and humans (Jahn et al., 2001; Kellner et al., 2003). CNP and its receptor NPR-B are widely expressed in the rat brain including expression in the limbic system, particularly in the hippocampal regions CA1-3 (Langub et al., 1995; Herman et al., 1996). In the hippocampus NPR-B is expressed in pyramidal cells and GAD (65/67)-immunopositive interneurons. Sub-cellular expression of NPR-B can be demonstrated in neuronal process in primary hippocampal cell cultures (Brackmann et al., 2005). The second messenger cGMP and cGMP signaling-cascades are implicated

in the modulation of long term potentiation (LTP), long-term depression (LTD) as well as other forms of synaptic plasticity, such as short-term plasticity (Schuman and Madison, 1991; Arancio et al., 1996; Son et al., 1998). The effect of cGMP on synaptic plasticity has been attributed to the activity of soluble guanylyl cyclases (sGCs; Arancio et al., 1996). Moreover, downstream cGMP targets such as cyclic nucleotide-gated channels and cGMP-dependent kinases (cGK or protein kinase G, PKG) contribute to different forms of synaptic plasticity (Klyachko et al., 2001; Kleppisch et al., 2003; Liu et al., 2003). More recently, we investigated whether activation of another cGMP-signaling system, the membrane guanylyl cyclase NPR-B, via activation of by its ligand CNP has an effect on hippocampal synaptic plasticity (Decker et al., 2008, 2009, 2010). When LTD and LTP stimulation was applied in area CA1 at 1 and 5 Hz and 30–100 Hz, respectively, CNP increased the magnitude of LTD while LTP induction was reduced. Thus, in the presence of CNP the threshold for LTP induction was shifted to higher stimulus frequencies (Decker et al., 2010). C-type natriuretic peptide (CNP) also decreased hippocampal network oscillations in adult rats *in vitro*, which are believed to be involved in storage of information and memory consolidation *in vivo* (Decker et al., 2009). In line with these results earlier work showed that direct application of CNP into the lateral brain ventricles affects the performance of rats in a passive avoidance learning paradigm (Telegdy et al., 1999, 2000).

Knock out of the gene for NPR-B in mice causes severe dwarfism, and the NPR-B knock out mice display seizures, female sterility, and priapism and are therefore not suitable for detailed cardiovascular or neurophysiological phenotyping (Tamura et al., 2004). To overcome this limitation, transgenic rats with ubiquitous overexpression of a dominant-negative NPR-B mutant, lacking the cytoplasmic domain (CMV-NPR-BΔKC) were generated (Langenickel et al., 2006). Receptor homodimerization of NPR-B, leading to a tight contact between the guanylyl cyclase domains, is essential for enzymatic activity. Interestingly, Tamura and Garbers (2003) have described that different NPR-B isoforms resulting from alternative splicing of the primary transcript are present in mouse tissues. In addition to full-length GC-B1, GC-B2 contains a 25 aa deletion in the KHD, and GC-B3 only retains a part of the extracellular ligand-binding domain. When GC-B2 or GC-B3 is expressed coincident with GC-B1, they act as dominant negative isoforms by virtue of blocking formation of active GC-B1 homodimers (Tamura and Garbers, 2003). It appears that these splice variants serve as dominant negative regulators of full-length GC-B. Similarly, overexpression of NPR-BΔKC leads to functional down-regulation of NPR-B signaling as indicated by blunted CNP-induced cGMP production (Langenickel et al., 2006).

In order to test whether cGMP signaling via neuronal NPR-B affects bidirectional synaptic plasticity in the rat hippocampus, and simultaneously learning and memory, we have generated dominant-negative NPR-B mutant under the control of a neuron-specific promoter (NSE-NPR-BΔKC) to specifically inhibit NPR-B signaling in the brain. After confirming the expression of the NPR-BΔKC mutant and reduction of CNP-dependent cGMP generation in brain membranes we have analyzed bidirectional plasticity *in vitro* over the range of 1–100 Hz stimulation in the hippocampal CA1 region. To further evaluate these animals in behavioral experiments we have performed open field, novel object recognition and spatial object recognition (SOR) tests. Our results support the hypothesis that the cGMP-signaling cascade linked to NPR-B and its ligand CNP play an important role in the brain, and in the hippocampus in particular, to modulate bidirectional synaptic plasticity and learning behavior.

MATERIALS AND METHODS

GENERATION OF TRANSGENIC RATS WITH SPECIFIC INHIBITION OF NPR-B SIGNALING IN NEURONS

Transgenic rats overexpressing a dominant-negative NPR-B mutant under the control of a neuron-specific promoter (NSE-NPR-BΔKC; **Figure 1A**) were generated and identified by Southern blotting (**Figure 1B**) essentially as previously described (Langenickel et al., 2006). After breeding rats to homozygosity, tissue-specific expression of NSE-NPR-BΔKC in the brain was verified by reverse transcription (RT)-PCR and Western blotting. RT-PCR, Western blotting and measuring of cGMP levels in brain membrane preparation was performed as previously described (Langenickel et al., 2006; Buttgereit et al., 2010). Primary anti-flag antibodies (Life Technologies, Carlsbad, CA, USA) in combination with secondary anti-rabbit-HRP antibodies were used for detection of NSE-NPR-BΔKC-flag in Western blots. For RT-PCR the following primer pairs were used: NSE-NPR-BΔKC forward: GACAGAGAGACTGATTTCGTCC, reverse: TCACTTGTCGTCATCGTCTTTG: GAPDH: forward: CCATGGAGAAGGCTGGGG, reverse: CAAAGTTGTCATGGATGACC. Transgenic rats and control Sprague Dawley rats, aged 6–8 weeks were kept under standard conditions with 12-h light–dark cycle and free access to water and food. The present study was carried out in accordance with the European Communities Council Directive of 24 November 1986 (86/609/EEC) for care of laboratory animals and after approval of the local government ethics committee. All efforts were made to minimize the number of animals used.

SLICE PREPARATION

Animals were decapitated under deep ether anesthesia. The brain was rapidly taken out of the skull and immersed in ice-cold (1–4°C) sucrose-based solution (87 mM NaCl, 25 mM $NaHCO_3$, 10 mM D-glucose, 75 mM sucrose, 2.5 mM KCl, 1.25 mM NaH_2PO_4, 0.5 mM $CaCl_2$, 7 mM $MgCl_2$, bubbled with 95% O_2 and 5% CO_2, pH 7.4). Horizontal hippocampal slices (400 μm) were cut on a vibratome (Leica VT 1200S). Slices were kept at room temperature. For recordings, the slices were transferred to a submerged recording chamber. During the experiments, the chamber was perfused at a flow rate of 3 ml/min with oxygenated artificial cerebrospinal fluid (ACSF; 125 mM NaCl, 2.5 mM KCl, 1.25 mM NaH_2PO_4, 25 mM $NaHCO_3$, 25 mM D-glucose, 2 mM $CaCl_2$, 1 mM $MgCl_2$, pH 7.4). All recordings were performed at 32°C.

RECORDING OF EXTRACELLULAR FIELD POTENTIALS

Recording electrodes were pulled from borosilicate glass and filled with standard Artificial Cerebrospinal Fluid (ACSF, resistance 1–3 MΩ). Extracellular field potentials (FPs) were recorded from

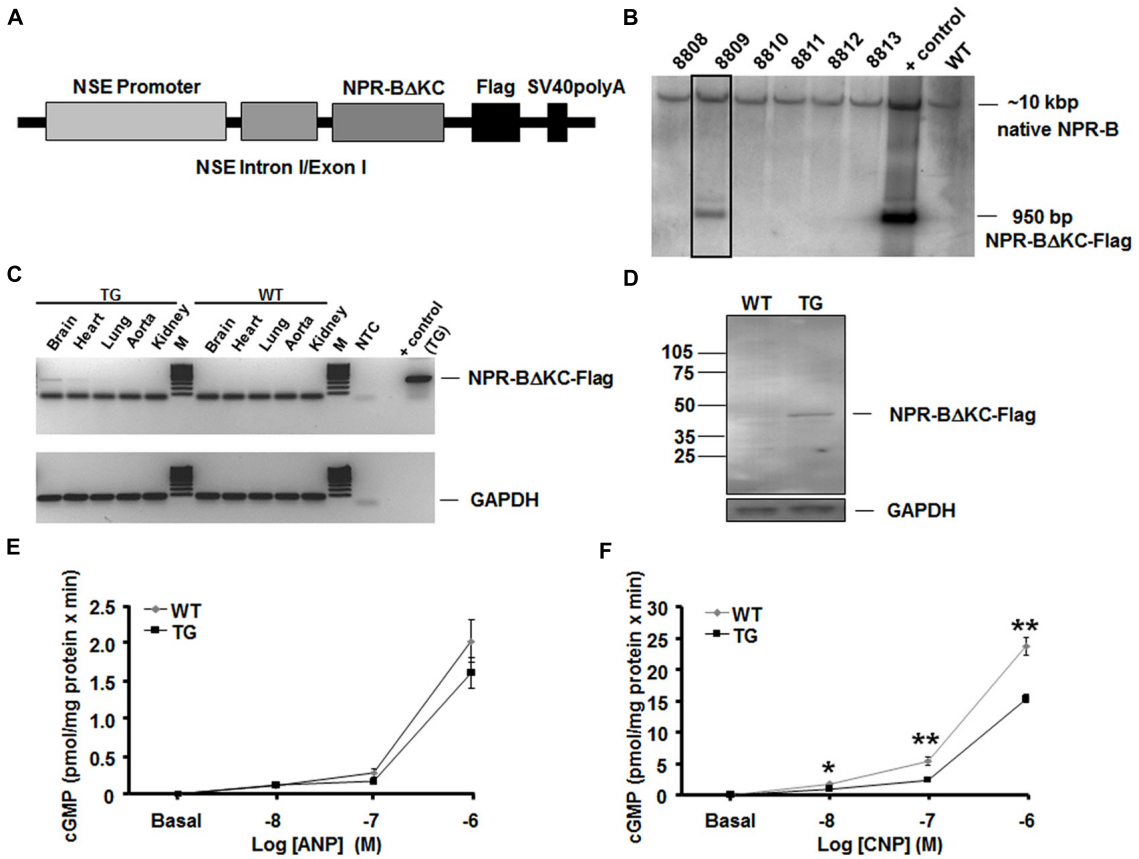

FIGURE 1 | Generation of transgenic rats. (A) Structure of NSE-NPR-BΔKC transgenic construct using the neuron-specific enolase promoter (NSE) for neuron-specific expression. The flag/tag was used for immunodetection of the expressed protein. **(B)** Detection of a founder animal (8809, boxed lane) by Southern blotting. Native NPR-B is present in wild type animals (WT), and native NPR-B and transgene are present in the positive control and founder animal 8809. The transgene construct has a size of 950 bp, and native NPR-B of approximately 10 kbp. **(C)** Specific expression of NPR-BΔKC-Flag was demonstrated by RT-PCR. Negative control (NTC) and positive control (control + transgene) are shown for the RT-PCR showing NPR-BΔKC-Flag expression. PCR for GAPDH expression was used as loading control. M indicates a 100 bp DNA fragment ladder. **(D)** Specific expression of NPR-BΔKC-Flag as shown by Western blotting using an anti-flag antibody using extracts from brain, heart, lung, aorta, and kidney. GAPDH expression is shown as a loading control. **(E,F)** NPR-BΔKC overexpression significantly reduced CNP-dependent, but not ANP-dependent cGMP production in brain membrane preparations in transgene animals (TG) compared to wild-type animals (WT). $*p < 0.05$, $**p < 0.01$ vs. wild-type ($n = 6$ per group).

stratum radiatum (SR) of area CA1 every 60 s for at least 10 min (baseline recording) and then for at least 60 min following high- or low frequency stimulation (HFS or LFS). A concentric bipolar stimulation electrode was placed in SR of area CA1 to stimulate Schaffer collaterals and commissural fibers. FPs were recorded using a MultiClamp 700B amplifier, filtered at 3 kHz and sampled to a computer disk at 10 kHz using the Clampex 10.2 software (Molecular Devices, Sunnyvale, CA, USA). The stimulus intensity was set to evoke 30% of the maximum FP response in LTP, and 50% in LTD experiments (50–200 μA with stimulus duration of 100 μs). The HFS paradigm applied to SR consisted of a 1 s long stimulus train applied at frequencies of 100, 50, 30, or 10 Hz (pulse duration: 100 μs, each). For LFS trains 900 pulses were applied at 1 or 5 Hz (pulse duration: 100 μs, each; 4–6). FP recordings obtained from SR were analyzed by determining the slope of the ?eld excitatory postsynaptic potential (EPSP) between 10 and 90% of the peak amplitude. Summary graphs were prepared by normalizing all responses to the baseline obtained during 10 min prior to HFS or LFS and then averaged across experiments. Only slices with a stable baseline FP response were used for further analysis. All changes in long-term synaptic plasticity were evaluated by averaging responses at 50–60 min post-HFS or LFS and averaging across experiments. For metaplasticity experiments, the frequencies used were HFS 100 Hz for 1 s and LFS 1 Hz for 900 times for 15 min. After the first HFS or LFS for 15 min, LTP was measured for 60 min, then a second HFS or LFS for 15 min was applied, and LTP was measured for another 60 min. CNP (Calbiochem, Merck KGaA, Darmstadt, Germany) was prepared as stock solution, frozen, finally thawed on the day of the experiment and added to ACSF to reach the desired final concentration (100 nM).

BEHAVIORAL TESTS

The temporal order to test the 11 wild type and the 12 transgenic rats were chosen randomly and changed for each experiment. All trials were recorded by a video camera and exploration time was

measured by video analysis. The rats' behavior was determined as exploration time when the animal approached closer than 2 cm to an object with its snout or forepaws (or both). After each trial, the arena and objects were cleaned carefully to avoid the presence of olfactory cues for the next rat. The available objects differed slightly in their shape, size and color. Before the first test – the novel object recognition task – rats were allowed to explore the arena during a habituation trial for 5 min, so that they could adapt to the new environment.

The object recognition task (ORT) was conducted in a square-shaped arena (100 cm × 100 cm), and used a similar approach as described in a previous report Goh and Manahan-Vaughan (2013). In the training trial (1st trial), two novel objects (i.e., A and B) were presented. Fifty minutes later (second trial) one familiar and one novel object (i.e., A and C) were presented. A further 24 h later (third trial) object A was presented with a new object (D). The objects were presented in the same location as the objects in the first trial. The objects and the recording chambers were cleaned thoroughly between task trials to ensure the absence of olfactory cues. The objects were distinctly different from one another and heavy so that they could not be moved by the rats.

In the SOR task the objects always remained the same (A and B), and the task was performed as previously described Goh and Manahan-Vaughan (2013). The position of object A remained constant, but in the second and third trial object B was placed in a distinctly new position in the chamber. As in the ORT experiments, the animals were allowed to explore the objects for 5 min. The second and third trials began 50 min and 24 h after the first trials, respectively.

In the open field locomotion test we examined motor function by means of measuring spontaneous activity in an open field (100 cm × 100 cm). Here, we differentiated between the entire running time of the animals and the time spent in the center of the area (without touching the walls).

DATA ANALYSIS

Data were expressed as mean ± SEM. Statistical analysis was done with the aid of SigmaStat software (SPSS Inc., Chicago, IL, USA) performing Student's *t*-test (unpaired), Mann–Whitney *U*-test or one-way analysis of variance (ANOVA) with repeated measures. The sample sizes (*n* values) for electrophysiological experiments indicate the number of slices from at least three different animals. Differences were considered significant with $^{*}p < 0.05$ or $^{**}p < 0.01$.

RESULTS

NPR-B-DEPENDENT cGMP SIGNALING IN NSE-NPR-BΔKC RATS

Transgenic rats overexpressing a dominant-negative NPR-B mutant under the control of a neuron-specific promoter (NSE-NPR-BΔKC; **Figure 1A**) were generated and identified by Southern blotting (**Figure 1B**). After breeding rats to homozygosity, tissue-specific expression of NSE-NPR-BΔKC in the brain was verified by RT-PCR. Other tissues, such as heart, lung, aorta and kidney do not express the transgene (**Figure 1C**). Western blot analysis showed that the NPR-B deletion construct was properly translated into a protein with the expected Mw of about 45 kDa in the transgenic animals but not in wild type rats (**Figure 1D**). To test whether expression of the dominant negative NSE-NPR-BΔKC mutant leads to the functional down-regulation of the NPR-B signaling, guanylyl cyclase assays in brain membrane preparations were performed (**Figures 1E,F**). The cGMP production of brain membranes derived from NSE-NPR-BΔKC rats stimulated with 10, 100, and 1000 nM ANP was comparable with those derived from wild-type rats, indicating that signaling via NPR-A was not affected in the transgene line (**Figure 1E**). In contrast, after stimulation with the same doses of CNP cGMP production significantly dampened in brain membrane preparations from NSE-NPR-BΔKC rats compared to wild-type rats. This result confirms the receptor-specific dominant-negative effect of the transgene expression on NPR-B signaling in the brain (**Figure 1F**).

EFFECT OF NPR-B-DEPENDENT cGMP SIGNALING ON SYNAPTIC PLASTICITY IN HIPPOCAMPAL SLICES *IN VITRO*

Here, we investigated the role of NPR-B and cGMP signaling in hippocampal synaptic plasticity. Field extracellular postsynaptic potentials (EPSP) were recorded from the SR of the CA1 by stimulating the Schaffer collaterals using high-frequency stimulation (HFS) at 100 Hz, which typically produces potentiation of the EPSP in the form of LTP. HFS resulted in LTP of 157 ± 12% 1 h after HFS was applied ($n = 13$) compared to baseline in wild-type (wt) rats (**Figure 2A**). In NPR-BΔKC rats, showing reduced CNP-dependent cGMP levels in brain membranes, HFS resulted in LTP that in its induction phase was similar to that seen in wt slices but after 60 min reached 285 ± 17% of baseline levels ($n = 16$, $p < 0.01$). On the opposite, application of 100 nM CNP to activate hippocampal NPR-B significantly inhibited LTP in wt rats (115 ± 10%, $n = 7$). Since the EPSP recordings in NPR-BΔKC rats did not reach saturation levels 60 min after HFS (**Figure 2A**), a longer time period of 200 min was recorded (**Figure 2B**). EPSP recordings showed a steep rise over the first 30 min, followed by a slower rise over the next 100 min and finally reached saturation levels at ∼250% of baseline values. This potentiation subsequently decreased somewhat to ∼200% of baseline values 180 min after HFS (**Figure 2B**).

THE FREQUENCY-DEPENDENCE OF LTP AND LTD IS MODULATED BY NPR-B ACTIVATION THROUGH CNP AND FUNCTIONAL DOWN-REGULATION OF NPR-B SIGNALING

Next, we compared the frequency-dependence of synaptic plasticity in wt, homo- and heterozygous NPR-BΔKC animals. The extent of change of synaptic strength was assessed 60 min after application of afferent stimulation of Schaffer collateral-CA1 synapses (**Figure 3**). In wt animals LTD was elicited at frequencies of 1, 5, and 10 Hz stimulation. Stimulation at 30, 50, and 100 Hz led to potentiation of EPSP over baseline. In hetero- and homozygous NPR-BΔKC animals the frequency-dependence of synaptic plasticity was distinctly different to wt controls at frequencies of 5, 10, 30, 50, and 100 Hz ($p < 0.01$, $p = 0.36$ for 1 Hz stimulation, **Figure 3**). Thus, depending on gene dose the NPR-BΔKC mutation shifts LTP induction to lower stimulation frequencies compared to wt rats.

We then tested the effect of CNP application (100 nM) on synaptic plasticity in wt slices (**Figure 3**). Here, we observed

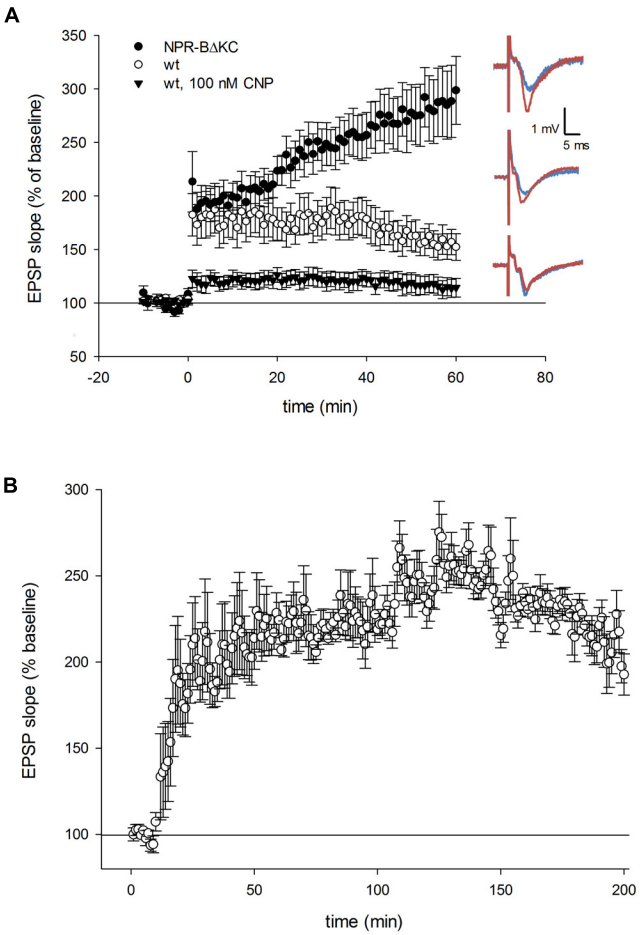

FIGURE 2 | (A) Time course of the relative changes in the excitatory postsynaptic potential (EPSP) slope expressed in % of baseline stimulation induced by 100 Hz HFS for 1 s in hippocampal slices from NPR-BΔKC, from wild type rats (wt) and from wild type slices incubated with the NPR-B agonist CNP (100 nM). Sample traces of the electrically evoked EPSPs for the NPR-BΔKC, wild type slices, and wild type slices incubated with 100 nM CNP are shown on the right, and were recorded 10 min before and 60 min following high frequency stimulation (HFS, 100 Hz for 1 s). Note that LTP was more strongly expressed in slices from NPR-BΔKC rats (black circles) compared to wt (white circles). Bath application of 100 nM CNP (black triangles) caused attenuation of LTP. **(B)** The increase of the EPSP slope in NPR-BΔKC rats reaches saturation levels at 285% of baseline stimulation after 120 min. EPSPs decrease slowly to ~200% of baseline stimulation after 180 min.

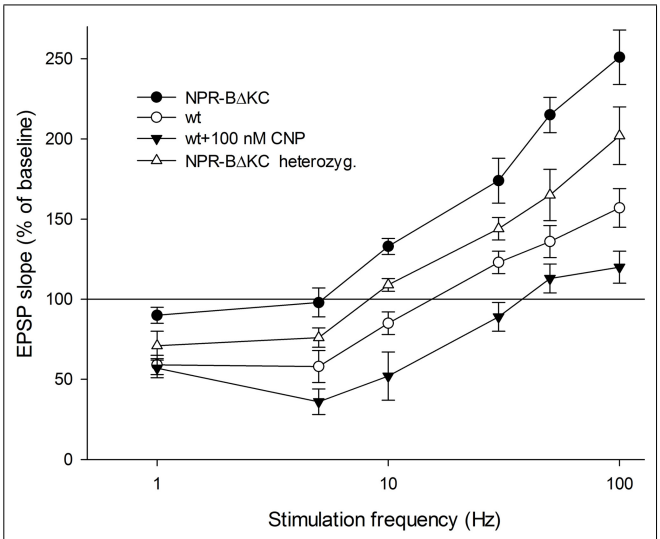

FIGURE 3 | Relative changes in the EPSP slope expressed in % of baseline stimulation after HF stimulation at 100 Hz for 1 s as recorded 50–60 min after stimulation in hippocampal slices from homozygous NPR-BΔKC rats, heterozygous NPR-BΔKC rats, slices from wild type rats (wt) and slices from wild type rats incubated with the NPR-B agonist CNP (100 nM). Stimulation frequencies used were 1, 5, 10, 30, 50, and 100 Hz.

that although LTD which was elicited using 1 Hz stimulation was equivalent to that seen in untreated wt controls, LTD induced by 5 Hz stimulation was significantly enhanced, and potent LTD was elicited by 10 Hz stimulation. In contrast, CNP-treatment resulted in a failure to induce LTP using 30 Hz stimulation. Stimulation at 50 and 100 Hz resulted in only a very small potentiation that was significantly less than that seen in untreated wt controls ($p < 0.01$). Taken together, these data suggest that under conditions of low cGMP levels the threshold for induction of LTP is lowered, whereas when cGMP is strongly elevated via the CNP/NPR-B/cGMP pathway the threshold for LTP induction is raised and LTD induction is facilitated.

POSSIBLE MECHANISMS OF THE EFFECT OF FUNCTIONAL DOWN-REGULATION OF NPR-B SIGNALING ON LTP AND LTD IN HIPPOCAMPAL SLICES *IN VITRO*

In search of possible molecular and cellular mechanisms responsible for the observed steady increase in EPSPs over a 60 min period following HFS, we repeated the experiments in the presence of anisomycin (20 μM), an inhibitor of protein synthesis (**Figure 4**). Anisomycin did not influence the induction of LTP but slightly reduced the potentiation of the EPSP signals in slices from wt rats, and reduced potentiation back to control levels in slices of NPR-BΔKC rats. These results indicate that protein synthesis is involved in the continuous increase of EPSP over a 60 min period in slices of NPR-BΔKC rats. However, the induction of LTP was unaffected by anisomycin in control and NPR-BΔKC rats.

We then tested whether NPR-BΔKC affects the intrinsic excitability in hippocampal neurons. Here we measured the EPSP in relation to the stimulation current (**Figure 5A**). We observed significantly higher responses in slices of NPR-BΔKC rats compared to wt using stimulation currents of 0.5–2 mA ($p < 0.05$). This increase in the input–output relationship indicates positive plastic changes in intrinsic excitability caused by reduced cGMP signaling that may underlie the observed lowering of LTP induction thresholds in NPR-BΔKC rats compared to wt rats.

Moreover, to test whether hippocampal inhibitory activity is affected in NPR-BΔKC rats we measured paired-pulse facilitation. Using different interpulse intervals (**Figure 5B**) we show larger facilitation in slices of NPR-BΔKC rats, particularly at the interpulse interval of 20 and 25 ms ($p < 0.01$), which is typically indicative of a loss of inhibitory GABAergic activity.

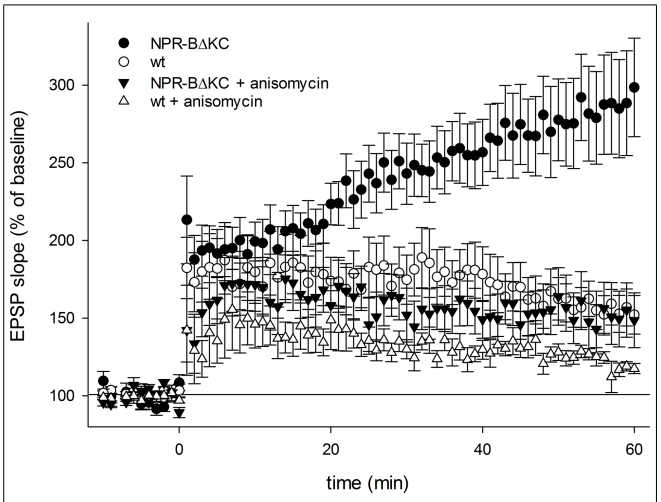

FIGURE 4 | Time course of the relative changes in the EPSP slope expressed in % of baseline stimulation induced by 100 Hz HFS for 1 s in hippocampal slices from NPR-BΔKC rats, wild type rats (wt), NPR-BΔKC rats incubated with anisomycin (20 μM) and wild type slices incubated with anisomycin (20 μM).

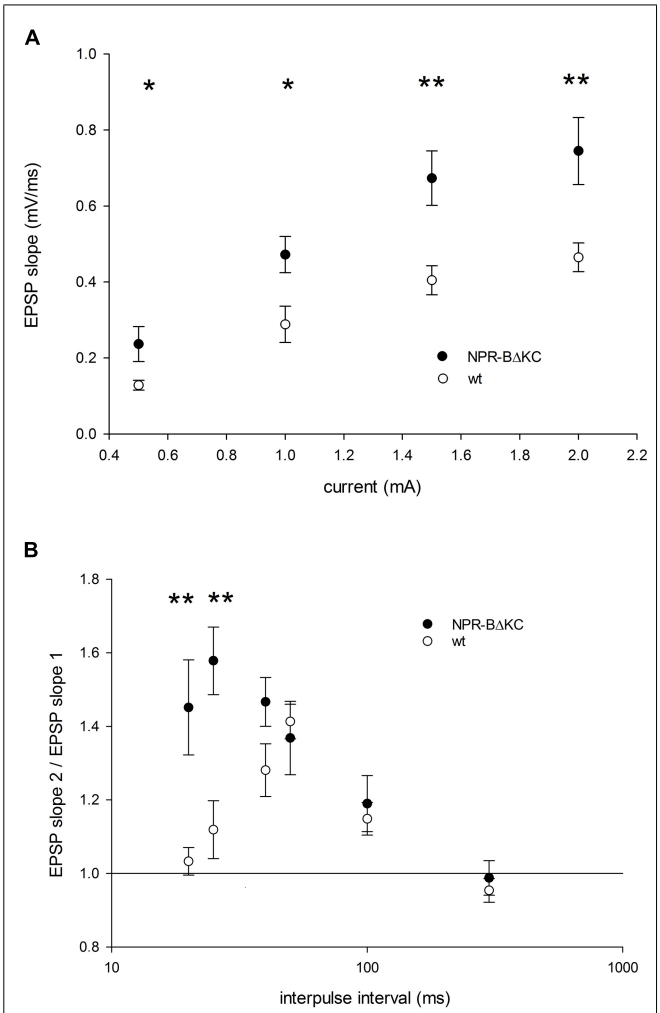

FIGURE 5 | (A) EPSP slope as a function of stimulus current in slices of NPR-BΔKC (functional down-regulation of NPR-B signaling) and wild type (wt) rats. EPSP slopes recorded as mV/ms were determined between 0.5 and 2 mV. Note the greater excitability in hippocampal slices of NPR-BΔKC rats with significant differences at 0.5–2 mV stimulus current. **(B)** Paired-pulse facilitation as a function of interpulse interval current in slices of NPR-BΔKC (NPR-B) and wild type (wt) rats. Paired pulses as determined by the ratio of EPSP slope 2/EPSP slope 1 were recorded at 20, 25, 40, 50, 100, and 300 ms time intervals. Note the larger facilitation in slices of NPR-BΔKC rats at interpulse intervals of 20 and 25 ms. Asterisks indicate significant changes (*$p < 0.05$ and **$p < 0.01$).

THE EFFECT OF FUNCTIONAL DOWN-REGULATION OF NPR-B SIGNALING ON METAPLASTICITY IN HIPPOCAMPAL SLICES *IN VITRO*

Long-term potentiation and LTD depend on the current state of synapses as modulated by intrinsic but also extrinsic influences (Goh and Manahan-Vaughan, 2013). In other words, synaptic plasticity can be modified by activity including previous synaptic inhibition, the activity of modulatory afferents, and hormonal activity, for instance, of natriuretic peptide hormones. This plasticity of synaptic plasticity, also called metaplasticity, may play a role in some mechanisms of memory and learning (Dudek and Bear, 1993). Thus, we assessed effects of NPR-BΔKC on metaplasticity using repetitive HFS (100 Hz) or LFS (1 Hz) 60 min after an initial HFS (100 Hz) or LFS (1 Hz; **Figure 6**). Pretreatment with HFS did not increase LTP further following the second HFS in wild type rats, but increased LTP in NPR-BΔKC rats. Pretreatment with HFS abolished LTD in response to LFS in wt rats, but further increased LTP in NPR-BΔKC rats. Similarly, LFS pretreatment further increased LTP following the second HFS in NPR-BΔKC rats, but had no effect in the LFS/LFS combination. Thus, in all combinations of LFS and HFS a significant bigger potentiation was observed after the second stimulation (% of potentiation 60 min after first stimulation) in NPR-BΔKC rats compared to wt rats ($p < 0.05$). These results indicate that the effect of the NPR-B/cGMP signaling system on LTP and LTD also affects metaplasticity.

MEASURING ANXIETY/CURIOSITY AND LEARNING AND MEMORY IN TRANSGENIC RATS EXPRESSING DOMINANT-NEGATIVE NPR-BΔKC

To evaluate changes in learning behavior of NPR-BΔKC animals in behavioral experiments, and relate these results with effects of NPR-BΔKC on synaptic plasticity, we performed open field, novel object recognition and SOR tests. In the open field test, anxiety and curiosity were compared between NPR-BΔKC and control rats. We observed significant differences in locomotion of NPR-BΔKC rats in the first trial in the arena (habituation; **Figure 7A**, $p < 0.01$). The greater willingness of NPR-BΔKC rats to run can be understood as a sign of greater curiosity and reduced anxiety. However, in the second and third trial after 5 min and 1 h, respectively, the rats from both groups did not show significant differences in the total distance moved. On the other hand, the NPR-BΔKC rats moved significantly longer distances in the central area of the arena compared to the total distance traveled (**Figure 7B**, $p < 0.05$). NPR-BΔKC rats also made significantly more visits to the central area (**Figure 7B**, $p < 0.01$). These results indicate that NPR-BΔKC rats

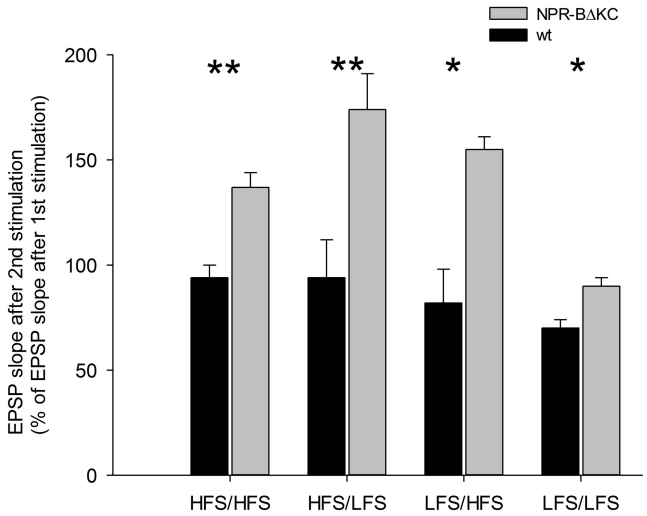

FIGURE 6 | Metaplasticity of EPSP when slices were stimulated a second time with HFS or LFS after an initial HFS, or with HFS or LFS after an initial LFS. LFS,1Hz; HFS, 100 Hz. Bars represent mean values ± SEM of the relative changes in EPSP slope 50–60 min after the second stimulation in % of EPSP slope 50–60 min after the first stimulation. Note that LTP is significantly stronger expressed in slices from NPR-BΔKC rats in all cases. Asterisks indicate significant changes (*$p < 0.05$ and **$p < 0.01$).

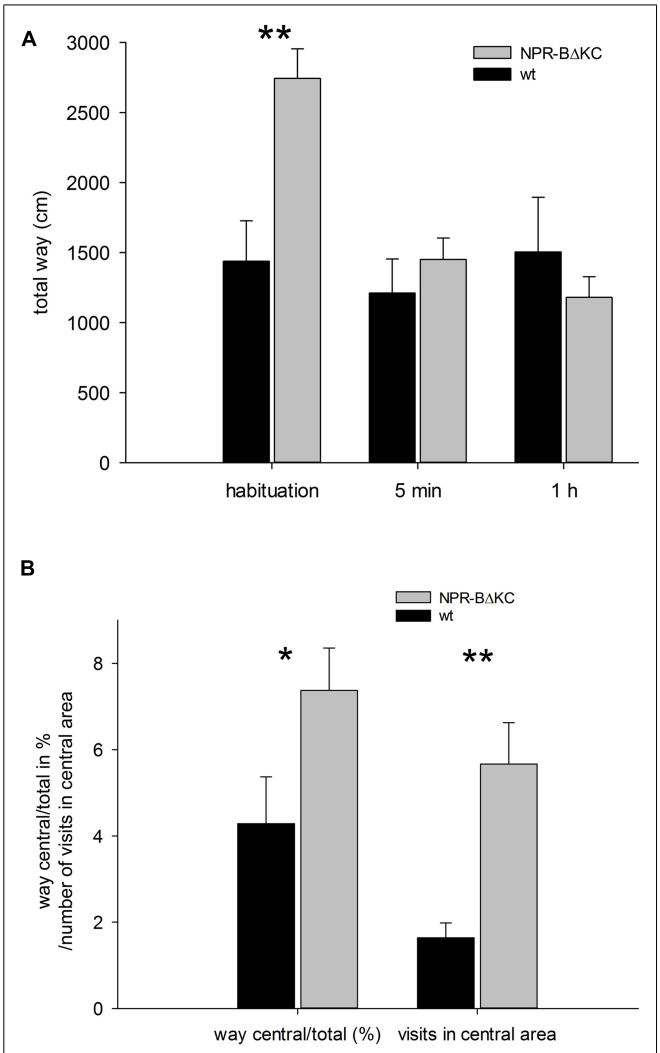

FIGURE 7 | In the open field test NPR-BΔKC and wild type rats (wt) were placed in an open field arena and movement of animals was observed to examine exploratory behavior and anxiety. (A) NPR-BΔKC rats moved more (total way in cm) during initial habituation. In the second trial after 5 min and the third trial after 1 h the rats from both groups did not show significant differences in the total distance moved. **(B)** NPR-BΔKC rats showed a higher ratio of movement in the central area versus total movement (way central/total in %). Transgenic animals also demonstrated an increase in the number of visits in the central area as compared to wt animals. Asterisks indicate significant changes (*$p < 0.05$ and **$p < 0.01$).

show reduced levels of anxiety leading to enhanced exploratory behavior.

In the novel object recognition test (ORT), upon exposure to the familiar object (A) and the unfamiliar object (C at 50 min, D at 24 h), one would expect that the animals show a markedly greater interest in the unfamiliar objects compared to object A (22). This was the case both for wt and transgenic animals (**Figure 8A**). The analysis also revealed a significantly higher exploratory activity for NPR-BΔKC rats in the initial 5 min when objects (A and B) were introduced into the arena (**Figure 8A**, $p = 0.065$). Object discrimination ratios were calculated to verify that the animals showed a preference of the novel vs. the familiar object (**Figure 8B**). No significantly different discrimination ratios were recorded in the first trial suggesting that the animals found both novel objects equally interesting. Upon exposure to object A and novel object C in the second trial, a significant preference for object C over object A was seen in both animal groups. A preference for the novel object was still evident 24 h after first object exposure, whereby the transgenic animals showed a significantly greater preference for object D compared to wt controls ($p < 0.05$). This indicates that long term memory is facilitated in NPR-BΔKC rats. In the SOR test, the two groups exhibited the expected learning performance, but no significant differences between the two groups were observed (**Figure 9A**). In the first trial AB1, the second trial after 50 min. and the third trial after 24 h NPR-BΔKC rats did not exhibited a significantly changed discrimination ratio (**Figure 9B**). Although NPR-BΔKC rats showed a tendency for an increased discrimination ratio AB3 in the third trial (**Figure 9B**), SOR was not significantly different between NPR-BΔKC rats and wt animals.

DISCUSSION

The second messenger cGMP modulates synaptic transmission and learning processes. This has been attributed mainly to calcium- and nitric oxide (NO)-dependent activation of sGCs (Schuman and Madison, 1991; Arancio et al., 1996; Son et al., 1998). However, other cGMP-producing enzymes including the transmembrane guanylyl cyclase NPR-B are expressed in the brain, including the hippocampal formation. NPR-B is activated by the CNP and produces cGMP in hippocampal neurons (Brackmann et al., 2005). CNP and its receptor NPR-B are strongly expressed in hippocampal regions CA1-3 (Langub et al., 1995; Herman et al., 1996), which are well-described model systems for studying

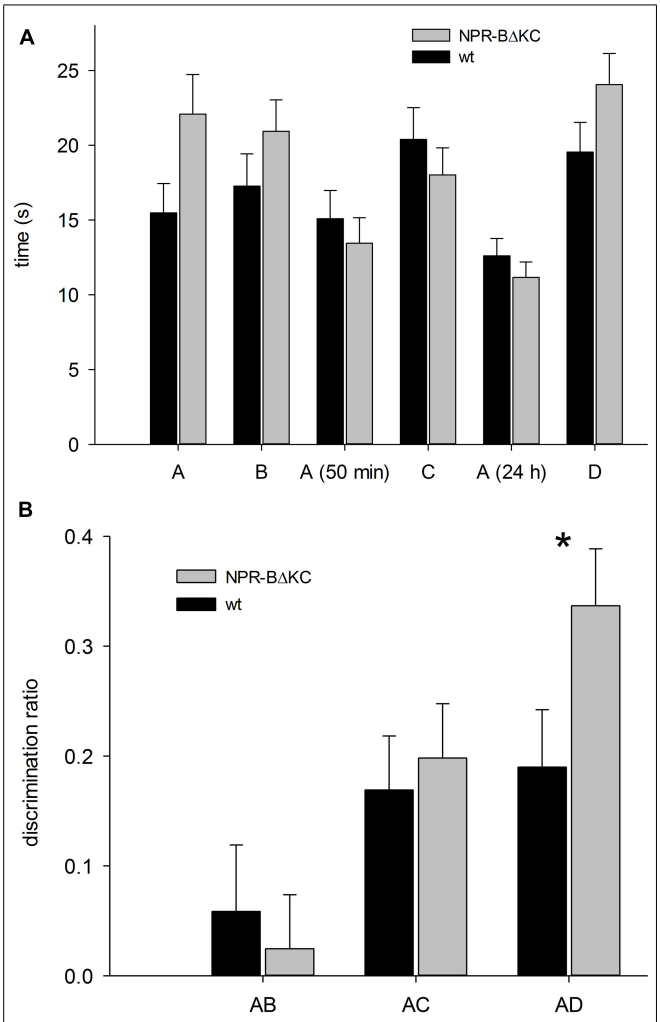

FIGURE 8 | In the novel ORT NPR-BΔKC rats and wild type rats (wt) were placed in an open field arena with novel and familiar objects. **(A)** NPR-BΔKC rats revealed higher exploratory activity when different objects (A and B) were presented as measured by the time spent in the vicinity to the objects (time in s). Exposure to the familiar (A) or a novel object after 50 min (C) or 24 h (D) demonstrated that NPR-BΔKC rats had an increased preference for novel object D after 24 h compared to wt animals. **(B)** Transgenic animals showed a significantly greater preference for the novel object compared to wt controls as analyzed by the discrimination ratio of exploration between new and old object after 24 h (AD) compared to wt control animals. Asterisks indicate significant changes ($*p < 0.05$).

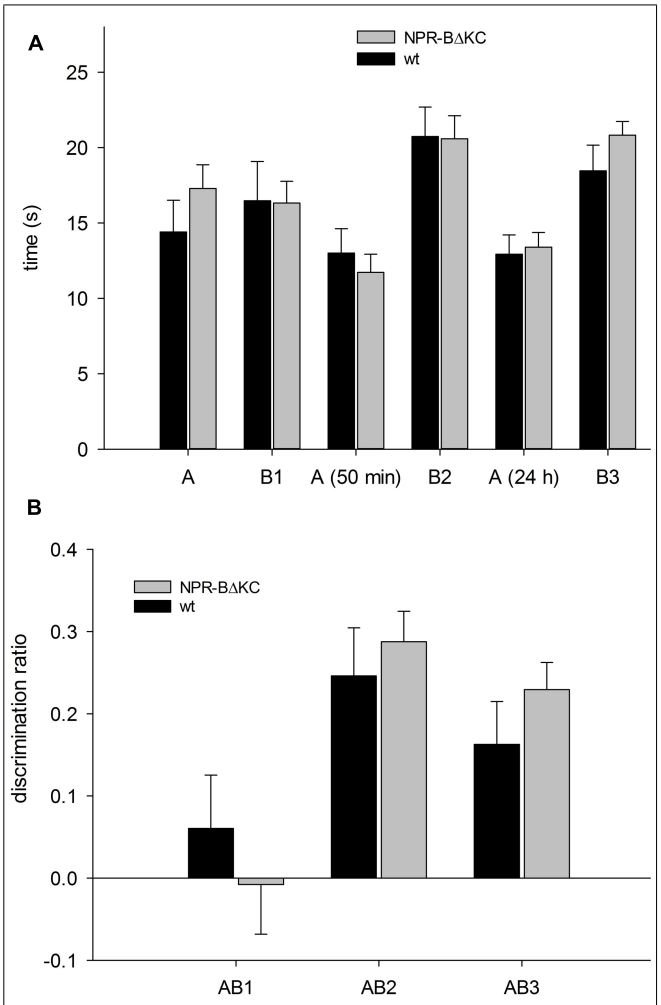

FIGURE 9 | In the spatial object recognition test NPR-BΔKC and wild type rats (wt) were placed in an open field arena with two objects (A and B1, B2, or B3), and with objects B2 and B3 moved to a different place after 50 min and 24 h, respectively. **(A)** Both, NPR-BΔKC and wild type rats (wt) showed enhanced interest for the object in a novel place after 50 min (B2) and 24 h (B3). **(B)** The calculation of the discrimination ratio calculation reveals no significant differences in the interest for the object in a novel place after 50 min (B2) and 24 h (B3) between NPR-BΔKC and wild type rats (wt).

synaptic plasticity and metaplasticity and their relation to learning and memory (Dudek and Bear, 1993; Manahan-Vaughan and Braunewell, 1999; Braunewell and Manahan-Vaughan, 2001). Evidence that the CNP/NPR-B system is able to modulate synaptic transmission came from our recent study showing that application of CNP, the ligand for NPR-B, negatively affects LTP, but positively affects LTD in hippocampal slices (Decker et al., 2008, 2009, 2010). Our present results indicate that transgenic rats expressing a dominant-negative mutant (NPR-BΔKC) of NPR-B in the brain, display changes of bidirectional plasticity in the opposite way. Rats expressing the NPR-BΔKC mutant, which specifically inhibits cGMP production of NPR-B without affecting NPR-A, showed enhanced LTP and reduced LTD induction. When frequency-dependence of synaptic modification in the range of 1–100 Hz was assessed transgenic rats expressed LTP at lower stimulation frequencies than wild-type controls and at the same time exhibited enhancements in exploratory and learning behavior. These results indicate that modulation of bidirectional plasticity via NPR-B-dependent cGMP signaling is related to learning and memory behavior in rats, and are in line with the notion that NPR-B and the associated cGMP signaling pathway constitutes a negative feed forward or feedback loop regulating synaptic plasticity.

It is worth mentioning that exploratory activity and spatial learning are associated with LTP and LTD. In rats, exploratory behavior of a new environment containing unfamiliar objects

and/or familiar objects in new locations facilitated LTD and impaired LTP, whereas exploration of the new environment itself, in the absence of objects, impaired LTD and facilitated LTP (Manahan-Vaughan and Braunewell, 1999; Braunewell and Manahan-Vaughan, 2001; Kemp and Manahan-Vaughan, 2004, 2007, 2008). More recently, it was shown in mice that object recognition facilitates hippocampal LTD and impairs LTP, indicating that both forms of plasticity work in concert in the creation of spatial memory. However, LTP and LTD might contribute to different components of a spatial representation and learning (Goh and Manahan-Vaughan, 2013). In NPR-BΔKC mutant rats, showing enhanced LTP and reduced LTD, we found improved object recognition. Although our experiments did not investigate the exact contributions of LTP and LTD to SOR, these results further substantiate the link between LTP and LTD as cellular mechanism required for spatial memory tasks (Goh and Manahan-Vaughan, 2013), and link cGMP signaling via NPR-B with synaptic plasticity and learning.

In regard to the possible molecular and cellular mechanisms of how NPR-B affects synaptic plasticity in the hippocampal network, our results indicate that protein synthesis is involved in the observed effect on EPSPs. The late onset but continuous increase of EPSPs over a prolonged time period in NPR-BΔKC mutant rats was sensitive to the protein synthesis inhibitor anisomycin, indicating that the link between reduced cGMP production and enhanced LTP involves protein synthesis. Moreover, the increase in the input-output relationship of LTP indicates positive alterations in the intrinsic excitability of neurons probably leading to the shift in LTP induction frequencies. This is most likely a sign of loss of inhibitory GABAergic activity in the slices of NPR-BΔKC mutant rats. This assumption is in agreement with our previous results showing that CNP activation of NPR-B in hippocampal slices leads to inhibition of LTP by modulating GABA(A)-mediated inhibition of the hippocampal network (Decker et al., 2008, 2009, 2010). Similarly, the effect of the inhibition of NPR-B-dependent cyclase activity on metaplasticity also indicates that there is a loss of negative feedback in the hippocampus of transgenic rats. In our experiments all combinations of LFS and HFS, with the exception of the LFS/LFS combination, led to a significant increase in LTP after the second stimulation in NPR-BΔKC rats. These differences in metaplasticity are most likely explained by the fact that 1 Hz LFS did not induce LTD in the transgenic rats, and that LTP may not have been saturated at 1 h and typically reached much higher levels than in wt animals. These differences likely contribute to the observed changes in metaplasticity in transgenic animals. Thus, the NPR-B/cGMP signaling system may play a role in metaplasticity, for instance as one of the regulatory feedback mechanism, to link previous experience or the hormonal state of the organism to synaptic plasticity.

In our previous studies we have postulated that the physiological significance of the CNP/NPR-B signaling system in the hippocampus may be to restrict synaptic plasticity and possibly learning and memory behaviors in stress-linked situations and thus link anxiogenic and limbic functions. This assumption was based on preclinical studies in rats and human studies which have shown that natriuretic peptides differentially modulate endocrine and behavioral stress responses (Kellner et al., 2003). CNP enhances the release of ACTH and cortisol (Kellner et al., 2003) and had anxiogenic effects in rats and in humans (Jahn et al., 2001). We have previously shown that exposure of rat strains to stress, in form of a novel open platform environment, induced a significant elevation in serum corticosterone levels but did not facilitate LTD expression (Manahan-Vaughan and Braunewell, 1999). However, different or longer lasting forms of stress activating the NPR-B system are likely to modulate bidirectional plasticity and thus lead to reduced learning and memory-related behavior. Interestingly, in the transgenic rats showing reduction of the NPR-B and cGMP signaling system we observe reduced anxiety levels which are observed as an enhanced exploratory behavior in the open field test as well as in object recognition tests. Enhanced exploratory and novelty seeking behavior is likely linked to learning and memory behavior (Manahan-Vaughan and Braunewell, 1999; Braunewell and Manahan-Vaughan, 2001). Although we have seen significant differences in learning behavior only in novel object recognition and not in the SOR test, enhanced exploratory behavior was noticed in open field and object recognition tests alike. More detailed behavioral analysis will be necessary to further characterize the role of NPR-B for distinct learning and memory paradigms.

Interestingly, GC-C another member of the family of transmembrane guanylyl cyclases (Potter et al., 2009; Potter, 2011), previously thought to be expressed mainly in neurons of the intestine, was identified in midbrain dopaminergic neurons, particularly in midbrain ventral tegmental area and substantia nigra compacta (VTA/SNc) neurons that regulate many important behavioral processes (Gong et al., 2011). Dysfunction of these neurons is associated with attention deficit hyperactivity disorder (ADHD) and schizophrenia. Mice in which GC-C has been knocked out exhibit hyperactivity and attention deficits which resemble behavioral symptoms of ADHD (Gong et al., 2011). Similarly, the functional down regulation of NPR-B in NPR-BΔKC rats showed increased activity and exploratory behavior. Thus, dysfunction of receptor guanylyl cyclases and the cGMP-pathway may be involved in a variety of additional CNS disorders, for instance deficits in cGMP signaling pathways and neuroplasticity are hypothesized to underlie the pathophysiology of major depressive disorder (MDD; Reierson et al., 2011). This is in line with the hypothesis that increased cGMP signaling in the brain restricts excitability of neurons, and thereby controls a range of behaviors including hyperactivity, anxiety, attention, learning and memory.

ACKNOWLEDGMENTS

This work was conducted within the framework of the national priority program (Schwerpunktprogram) SPP1226 Nicotine: molecular and physiological mechanisms in the central nervous system (www.nicotine-research.com) funded by the German Research Foundation (Deutsche Forschungsgemeinschaft, grant DFG 1579/8-1 and 2 to Karl H. Braunewell, MA1843/6 to Denise Manahan-Vaughan). Generation of transgenic rats was supported by DFG grants to Michael Bader and Jens Buttgereit (BA1374/14-1).

REFERENCES

Arancio, O., Kiebler, M., Lee, C. J., Lev-Ram, V., Tsien, R. Y., Kandel, E. R., et al. (1996). Nitric oxide acts directly in the presynaptic neuron to produce long-term potentiation in cultured hippocampal neurons. *Cell* 87, 1025–1035. doi: 10.1016/S0092-8674(00)81797-3

Bartels, C. F., Bukulmez, H., Padayatti, P. R., Ravenswaaijart, C., and Pauli, R. M. (2004). Mutations in the transmembrane natriuretic peptide receptor NPR-B impair skeletal growth and cause acromesomelic dysplisia, type maroteaux. *Am. J. Hum. Genet.* 75, 27–34. doi: 10.1086/422013

Brackmann, M., Schuchmann, S., Anand, R., and Braunewell, K. H. (2005). Neuronal Ca2+ sensor protein VILIP-1 affects cGMP signalling of guanylyl cyclase B by regulating clathrin dependent receptor recycling in hippocampal neurons. *J. Cell Sci.* 118, 2495–2505. doi: 10.1242/jcs.02376

Braunewell, K. H., and Manahan-Vaughan, D. (2001). Long-term depression: a cellular basis for learning? *Rev. Neurosci.* 12, 121–140. doi: 10.1515/REVNEURO.2001.12.2.121

Buttgereit, J., Qadri, F., Monti, J., Langenickel, T. H., Dietz, R., Braunewell, K. H., et al. (2010). Visinin-like protein 1 regulates natriuretic peptide receptor B in the heart. *Regul. Pept.* 161, 51–57. doi: 10.1016/j.regpep.2009.12.019

Decker, J. M., Wójtowicz, A. M., Bartsch, J. C., Liotta, A., Braunewell, K. H., Heinemann, U., et al. (2010). C-type natriuretic peptide modulates bidirectional plasticity in hippocampal area CA1 in vitro. *Neuroscience* 169, 8–22. doi: 10.1016/j.neuroscience.2010.04.064

Decker, J. M., Wojtowicz, A., Heinemann, U., and Braunewell, K. H. (2008). C-Type natriuretic peptide modulates pre- and postsynaptic properties in hippocampal area CA1 in vitro. *Biochem. Biophys. Res. Commun.* 377, 820–825. doi: 10.1016/j.bbrc.2008.10.070

Decker, J. M., Wójtowicz, A. M., Ul Haq, R., Braunewell, K. H., Heinemann, U., and Behrens, C. J. (2009). C-type natriuretic peptide decreases hippocampal network oscillations in adult rats in vitro. *Neuroscience* 164, 1764–1775. doi: 10.1016/j.neuroscience.2009.09.036

Dudek, S. M., and Bear, M. F. (1993). Bidirectional long-term modification of synaptic effectiveness in the adult and immature hippocampus. *J. Neurosci.* 13, 2910–2918.

Goh, J. J., and Manahan-Vaughan, D. (2013). Spatial object recognition enables endogenous LTD that curtails LTP in the mouse hippocampus. *Cereb. Cortex* 23, 1118–1125. doi: 10.1093/cercor/bhs089

Gong, R., Ding, C., Hu, J., Lu, Y., Liu, F., Mann, E., et al. (2011). Role for the membrane receptor guanylyl cyclase-C in attention deficiency and hyperactive behavior. *Science* 333, 1642–1646. doi: 10.1126/science.1207675

Herman, J. P., Drucker, D., and Langub, M. C. Jr. (1996). Localization of natriuretic peptide-activated guanylate cyclase mRNAs in the rat brain. *J. Comp. Neurol.* 369, 165–187. doi: 10.1002/(SICI)1096-9861(19960527)369:2<165::AID-CNE1>3.0.CO;2-1

Jahn, H. A., Knaudt, K., Ströhle, A., Kiefer, F., Schick, M., and Wiedemann, K. (2001). Alpha-helical-corticotrophin-releasing hormone reverses anxiogenic effects of C-type natriuretic peptide in rats. *Brain Res.* 893, 21–28. doi: 10.1016/S0006-8993(00)03275-3

Kellner, M., Jahn, H., and Wiedemann, K. (2003). Natriuretic peptides and panic disorder: therapeutic prospects. *Expert Rev. Neurother.* 3, 381–386. doi: 10.1586/14737175.3.3.381

Kemp, A., and Manahan-Vaughan, D. (2004). Hippocampal long-term depression and long-term potentiation encode different aspects of novelty acquisition. *Proc. Natl. Acad. Sci. U.S.A.* 101, 8192–8197. doi: 10.1073/pnas.0402650101

Kemp, A., and Manahan-Vaughan, D. (2007). Hippocampal long-term depression: master or minion in declarative memory processes? *Trends Neurosci.* 30, 111–118. doi: 10.1016/j.tins.2007.01.002

Kemp, A., and Manahan-Vaughan, D. (2008). The hippocampal CA1 region and dentate gyrus differentiate between environmental and spatial feature encoding through long-term depression. *Cereb. Cortex* 18, 968–977. doi: 10.1093/cercor/bhm136

Kleppisch, T., Wolfsgruber, W., Feil, S., Allmann, R., Wotjak, C. T., Goebbels, S., et al. (2003). Hippocampal cGMP-dependent protein kinase I supports an age- and protein synthesis-dependent component of long-term potentiation but is not essential for spatial reference and contextual memory. *J. Neurosci.* 23, 6005–6012.

Klyachko, V. A., Ahern, G. P., and Jackson, M. B. (2001). cGMP-mediated facilitation in nerve terminals by enhancement of the spike afterhyperpolarization. *Neuron* 31, 1015–1025. doi: 10.1016/S0896-6273(01)00449-4

Langenickel, T. H., Buttgereit, J., Pagel-Langenickel, I., Lindner, M., Monti, J., Beuerlein, K., et al. (2006). Cardiac hypertrophy in transgenic rats expressing a dominant-negative mutant of the natriuretic peptide receptor B. *Proc. Natl. Acad. Sci. U.S.A.* 103, 4735–4740. doi: 10.1073/pnas.0510019103

Langub, M. C. Jr., Watson, R. E. Jr., and Herman, J. P. (1995). Distribution of natriuretic peptide precursor mRNAs in the rat brain. *J. Comp. Neurol.* 356, 183–199. doi: 10.1002/cne.903560205

Liu, S., Rao, Y., and Daw, N. (2003). Roles of protein kinase A and protein kinase G in synaptic plasticity in the visual cortex. *Cereb. Cortex* 13, 864–869. doi: 10.1093/cercor/13.8.864

Manahan-Vaughan, D., and Braunewell, K. H. (1999). Novelty acquisition is associated with induction of hippocampal long-term depression. *Proc. Natl. Acad. Sci. U.S.A.* 96, 8739–8744. doi: 10.1073/pnas.96.15.8739

Potter, L. R. (2011). Guanylyl cyclase structure, function and regulation. *Cell. Signal.* 23, 1921–1926. doi: 10.1016/j.cellsig.2011.09.001

Potter, L. R., Yoder, A. R., Flora, D. R., Antos, L. K., and Dickey, D. M. (2009). Natriuretic peptides: their structures, receptors, physiologic functions and therapeutic applications. *Handb. Exp. Pharmacol.* 191, 341–366. doi: 10.1007/978-3-540-68964-5_15

Reierson, G. W., Guo, S., Mastronardi, C., Licinio, J., and Wong, M. L. (2011). cGMP signaling, phosphodiesterases and major depressive disorder. *Curr. Neuropharmacol.* 9, 715–727. doi: 10.2174/157015911798376271

Schmidt, H., Stonkute, A., Jüttner, R., Schäffer, S., Buttgereit, J., Feil, R., et al. (2007). The receptor guanylyl cyclase Npr2 is essential for sensory axon bifurcation within the spinal cord. *J. Cell Biol.* 179, 331–340. doi: 10.1083/jcb.200707176

Schuman, E. M., and Madison, D. V. (1991). A requirement for the intercellular messenger nitric oxide in long-term potentiation. *Science* 254, 1503–1506. doi: 10.1126/science.1720572

Son, H., Yun, F. L., Min, Z., Arancio, O., Kandel, E. R., and Hawkins, R. D. (1998). The specific role of cGMP in hippocampal LTP. *Learn. Mem.* 5, 231–245.

Tamura, N., Doolittle, L. K., Hammer, R. E., Shelton, J. M., Richardson, J. A., and Garbers, D. L. (2004). Critical roles of the guanylyl cyclase B receptor in endochondral ossification and development of female reproductive organs. *Proc. Natl. Acad. Sci. U.S.A.* 101, 17300–17305. doi: 10.1073/pnas.0407894101

Tamura, N., and Garbers, D. L. (2003). Regulation of the guanylyl cyclase-B receptor by alternative splicing. *J. Biol. Chem.* 278, 48880–48889. doi: 10.1074/jbc.M308680200

Telegdy, G., Adamik, A., and Glover, V. (2000). The action of isatin (2,3-dioxoindole) an endogenous indole on brain natriuretic and C-type natriuretic peptide-induced facilitation of memory consolidation in passive-avoidance learning in rats. *Brain Res. Bull.* 53, 367–370. doi: 10.1016/S0361-9230(00)00359-2

Telegdy, G., Kokavszky, K., and Nyerges, A. (1999). Action of C-type natriuretic peptide (CNP) on passive avoidance learning in rats: involvement of transmitters. *Eur. J. Neurosci.* 11, 3302–3306. doi: 10.1046/j.1460-9568.1999.00750.x

Conflict of Interest Statement: The authors declare that the research was conducted in the absence of any commercial or financial relationships that could be construed as a potential conflict of interest.

Received: 16 September 2014; accepted: 12 November 2014; published online: 01 December 2014.

Citation: Barmashenko G, Buttgereit J, Herring N, Bader M, Özcelik C, Manahan-Vaughan D and Braunewell KH (2014) Regulation of hippocampal synaptic plasticity thresholds and changes in exploratory and learning behavior in dominant negative NPR-B mutant rats. Front. Mol. Neurosci. 7:95. doi: 10.3389/fnmol.2014.00095

This article was submitted to the journal Frontiers in Molecular Neuroscience.

frontiers in
MOLECULAR NEUROSCIENCE

ORIGINAL RESEARCH ARTICLE
published: 26 February 2014
doi: 10.3389/fnmol.2014.00004

Dysfunction of outer segment guanylate cyclase caused by retinal disease related mutations

***Patrick Zägel*[1] *and Karl-Wilhelm Koch*[1,2] ***

[1] *Biochemistry Group, Department of Neurosciences, Carl von Ossietzky University Oldenburg, Oldenburg, Germany*
[2] *Research Center Neurosensory Science, Carl von Ossietzky University Oldenburg, Oldenburg, Germany*

Edited by:
Rameshwar K. Sharma, Salus University, USA

Reviewed by:
Rameshwar K. Sharma, Salus University, USA
Teresa Duda, Salus University, USA

****Correspondence:***
Karl-Wilhelm Koch, Biochemistry Group, Department of Neurosciences, Carl von Ossietzky University Oldenburg, Oldenburg D-26111, Germany
e-mail: karl.w.koch@uni-oldenburg.de

Membrane bound guanylate cyclases are expressed in rod and cone cells of the vertebrate retina and mutations in several domains of rod outer segment guanylate cyclase 1 (ROS-GC1 encoded by the gene *GUCY2D*) correlate with different forms of retinal degenerations. In the present work we investigated the biochemical consequences of three point mutations, one is located in position P575L in the juxtamembrane domain close to the kinase homology domain and two are located in the cyclase catalytic domain at H1019P and P1069R. These mutations correlate with various retinal diseases like autosomal dominant progressive cone degeneration, e.g., Leber Congenital Amaurosis and a juvenile form of retinitis pigmentosa. Wildtype and mutant forms of ROS-GC1 were heterologously expressed in HEK cells, their cellular distribution was investigated and activity profiles in the presence and absence of guanylate cyclase-activating proteins were measured. The mutant P575L was active under all tested conditions, but it displayed a twofold shift in the Ca^{2+}-sensitivity, whereas the mutant P1069R remained inactive despite normal expression levels. The mutation H1019P caused the cyclase to become more labile. The different biochemical consequences of these mutations seem to reflect the different clinical symptoms. The mutation P575L induces a dysregulation of the Ca^{2+}-sensitive cyclase activation profile causing a slow progression of the disease by the distortion of the Ca^{2+}-cGMP homeostasis. In contrast, a strong reduction in cGMP synthesis due to an inactive or structurally unstable ROS-GC1 would trigger more severe forms of retinal diseases.

Keywords: photoreceptor guanylate cyclase, GCAP, retinal dystrophy, neuronal calcium sensor, phototransduction

INTRODUCTION

Inherited retinal diseases are caused by a heterogeneous group of mutations in retinal genes (Perrault et al., 2000; den Hollander et al., 2008; Athanasiou et al., 2013). Among them are a large number of genes coding for proteins involved in phototransduction processes in the outer segments of rods and cones. Genetic heterogeneity is paralleled by diverse phenotypical and clinical characteristics of retinal degenerations, which are classified in disorders like cone-rod dystrophies, retinitis pigmentosa, and leber congenital amaurosis (LCA). These disease forms lead to a loss of visual function, but they differ in the progression of specific visual impairments.

Phototransduction in rods and cones is centered on the light-triggered hydrolysis of the second messenger cyclic GMP, its powerful re-synthesis after illumination and its role as a ligand targeting a cyclic nucleotide-gated channel in the plasma membrane (Pugh and Lamb, 2000; Kaupp and Seifert, 2002; Luo et al., 2008). Phototransduction is further under control of several negative feedback loops that are important for recovery of the photoresponse from illumination and for adjusting the cell performance to ambient background light (Fain et al., 2001). One crucial molecular factor involved in the regulation of phototransduction is Ca^{2+}, which binds to and dissociates from Ca^{2+}-sensor proteins under oscillating changes in cytoplasmic Ca^{2+}-concentration $[Ca^{2+}]$. A multi-protein complex operating at the interface between changing concentrations of cGMP and $[Ca^{2+}]$ consists of a sensory type membrane-bound guanylate cyclase that is regulated by guanylate cyclase-activating proteins (GCAPs; Stephen et al., 2008; Dizhoor et al., 2010; Koch et al., 2010; Koch and Dell'Orco, 2013). So far, mutations in patients suffering from retinal diseases are found in the gene *GUCA1A* encoding the Ca^{2+}-sensor GCAP1 and *GUCY2D* coding for the outer segment guanylate cyclase type 1 (ROS-GC1) (Kitiratschky et al., 2008; Behnen et al., 2010; Hunt et al., 2010). Previous research was focused on elucidating the molecular causes and cellular consequences of point mutations in ROS-GC1 and GCAP1 and in a further step to test therapeutic strategies involving RNA interference techniques and transgenic mouse lines (Buch et al., 2011; Jiang et al., 2011; Boye et al., 2013).

However, disease causing mutations can also point to critical amino acid positions that determine structure-function relationships in natively folded protein structures and therefore might help to gain mechanistic insights of protein function and regulation (Duda et al., 1999a, 2000; Ramamurthy et al., 2001). For example, a biochemical study on mutations in the so-called dimerization domain of ROS-GC1 correlating with cone-rod dystrophy recently revealed that this dimerization or linker domain operates as a Ca^{2+}-sensitive control switch module (Zägel et al., 2013).

In the present work we tested the biochemical consequences of three point mutations (**Figure 1**). The mutation P575L was found in a family, where clinically affected members suffer from progressive cone degeneration (Small et al., 2008). The amino acid substitution is located in the juxtamembrane domain (JMD), which is a specific region of sensory GCs upstream of the kinase homology domain (KHD). H1019P is located in the cyclase catalytic domain (CCD) and patients with this missense mutation show the typical clinical symptoms of LCA type 1 suffering from severe visual impairment at birth (Perrault et al., 2000). Finally, P1069R is also within the CCD and a patient carrying this mutation was diagnosed with juvenile retinitis pigmentosa (Booji et al., 2005).

So far, none of these mutations have been investigated on a molecular level. Two of the main questions are for example what the consequences on guanylate cyclase activity are and which Ca^{2+}-dependent activation profiles can be observed in the presence of GCAPs. These topics are addressed in the present contribution.

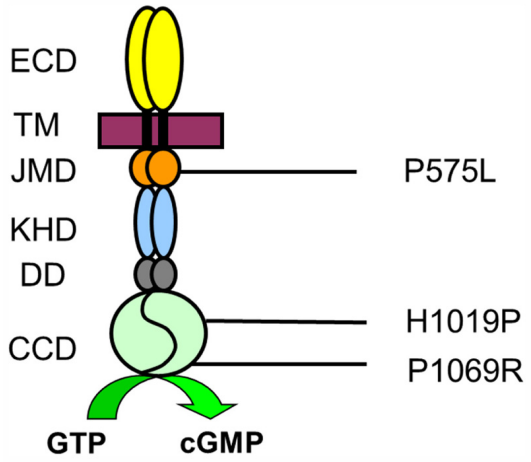

FIGURE 1 | Amino acid positions of mutations in ROS-GC1. Topology of ROS-GC1 domains is indicated as extracellular domain (ECD) corresponding to the intradiscal region when cyclases are expressed in rod outer segments, transmembrane domain (TM), JMD, KHD, dimerization domain, and cyclase catalytic domain (CCD). Numbers correspond to the unprocessed human sequence.

MATERIALS AND METHODS

CLONING AND SITE-DIRECTED MUTAGENESIS OF HUMAN ROS-GC1 CONSTRUCTS

The cDNA of human ROS-GC1 was cloned into the vector pIRES2-eGFP (Clonetech) exactly as described previously (Zägel et al., 2013). DNA was prepared by using the DNA purification kit of Promega according to manufacturer's instruction. The mutant P575L was produced by using the following primers for PCR amplification: 5′-GCTATCCGCCTAGCAACCAAGACG-3′ (forward) and 5′-CGTCTTGGTTGCTAGGCGGATAGC-3′ (reverse). Site-directed mutagenesis yielding the mutants H1019P and P1069R was achieved by performing two PCRs each using the ROS-GC1-WT gene in the pIRES2-eGFP vector as template. Primers for the PCR were for creating H1019P: 5′-CCTTACCGCATCCCCGTGAACTTGAG-3′ and 5′-TCAAGAGAACTGGCCCGGCCGC-3′ (forward and reverse primer, first PCR) and 5′-AAAGCTAGCCACCATGACCGCC-TGCGCCCGCC-3′ and 5′-CTCAAGTTCACGGGGATGCGG-TAAGG-3′ (forward and reverse primer, second PCR). P1069R was obtained with 5′-CCCATCCCCAAACGGCCTGACCTG-3′ and 5′-TCAAGAGAACTGGCCCGGCCGC-3′ (forward and reverse primer in the first PCR) and 5′-AAAGCTAGCCACCATGACCGC CTGCGCCCGCC-3′ and 5′-CAGGTCAGGCCGTTTGGG-GATGGG-3′ (forward and reverse primer in the second PCR). The resulting two fragments were used in a further PCR to obtain a complete mutated ROS-GC1-DNA construct (3320 bp) by employing the primers 5′-AAAGCTAGCCACCATGACCGCCTG-CGCCCGCC-3′ and 5′-TCAAGAGAACTGGCCCGGCCGC-3′. The final construct was cut with Nhe I, phosphorylated with T4 polynucleotide kinase and ligated in the pIRES2-EGFP vector that was cut by Nhe I/Sma I. Clone products were verified by sequencing.

HETEROLOGOUS EXPRESSION OF ROS-GC1 AND GCAPs

WT and mutant forms of ROS-GC1 were expressed in HEK flip 293 cells. For this purpose cells were cultivated in minimal essential medium under standard conditions as described (Koch and Helten, 2008). After culturing 3–5 × 10^6 cells were harvested in 100 μL of a buffer containing 5 mM KCl, 20 mM $MgCl_2$, and 150 mM phosphate buffer pH 7.2. For transfection, 5 μg of DNA was added and cells were electroporated with the CLB system (Lonza). Further treatment of cells and harvesting for subsequent guanylate cyclase assays was done exactly as described (Zägel et al., 2013). GCAP1 and GCAP2 were expressed in *E. coli* and purified to homogeneity by anion exchange and size exclusion chromatography as previously reported (Hwang et al., 2003; Koch and Helten, 2008). Myristoylation of GCAPs during bacterial expression was accomplished by co-transforming *E. coli* cells with *N*-myristoyl-transferase from yeast and supplementation with myristic acid. To ensure a high degree of myristoylation of GCAP1, which lacks the consensus site for yeast *N*-myristoyl-transferase, we used the D^6S-mutant of GCAP1 (Krylov et al., 1999; Hwang et al., 2003). The degree of myristoylation of both GCAPs was typically higher than 90% as checked by using an analytical HPLC run on a reverse-phase column.

GUANYLATE CYCLASE ASSAY

Recombinant human ROS-GC1 in HEK cell membranes was measured as described before (Koch and Helten, 2008; Zägel et al., 2013). In addition to measuring the basal guanylate cyclase activity we mainly tested two effects of GCAPs on the activation profile of the cyclase. In a first set we added purified bovine GCAP1 or GCAP2 at saturating 10 μM to washed HEK cell membranes and incubated samples at different free [Ca^{2+}] using a Ca^{2+}-EGTA buffer system. Details of the procedure have been described in several previous publications (Hwang et al., 2003; Koch and Helten, 2008; Zägel et al., 2013). Data were evaluated to obtain the [Ca^{2+}], at which the activation is half-maximal (IC_{50}). In a second set of guanylate cyclase

assays we incubated recombinant ROS-GC1 with increasing concentrations of GCAP1 and GCAP2 (0–20 μM) for 30 min under Ca^{2+}-free conditions. GCAPs were liganded with Mg^{2+} (Peshenko and Dizhoor, 2004) using the same buffer composition as described (Koch and Helten, 2008). The latter activity measurements yielded apparent affinities (EC_{50}-values) of GCAPs for WT and mutant ROS-GC1. Activity values were obtained from at least 3–4 different data sets and were used to calculate the mean ± standard deviation (SD). A student's *t*-test was performed to check for significant differences between two sets of data.

IMMUNOHISTOCHEMISTRY

Localization of ROS-GC1 WT and mutants in HEK cells by immunofluorescence microscopy was done as described before using an Olympus fluorescence microscope (Zägel et al., 2013). The following primary antibodies were used for detection: anti-ROS-GC1 (1:100; ROS-GC1 (H-225), sc50512, rabbit polyclonal IgG; Santa Cruz Biotechnology), anti-Na^+/K^+-ATPase (1:200; Na^+/K^+-ATPase, a (H-3), sc-48345, mouse monoclonal IgG_{2b}; Santa Cruz Biotechnology), and anti-calnexin [1:200; calnexin (E-10), sc-46669, mouse monoclonal IgG_{2a}; Santa Cruz Biotechnology]. Secondary antibodies were donkey anti-rabbit conjugated to Fura350 (dilution 1:200) from Invitrogen and goat anti-mouse conjugated with Dylight594 from Thermo Scientific, USA used in a dilution of 1:500. Incubation and washing buffers were exactly as described (Zägel et al., 2013).

RESULTS AND DISCUSSION

LOCALIZATION OF ROS-GC1 CONSTRUCTS

Previous work has shown that ROS-GC1 can be expressed heterologously in HEK293 cells in sufficient quantity to allow subsequent biochemical studies (Hwang et al., 2003; Koch and Helten, 2008; Zägel et al., 2013). In HEK293 cells the enzyme was found to be present in cell membranes and mainly co-localized with the endoplasmic reticulum. Probing the cells with an anti-ROS-GC1 antibody (**Figure 2A**, middle panel) and using specific markers for the plasma membrane (anti-Na^+/K^+-ATPase antibody, top left panel in **Figure 2A**) and for the endoplasmic reticulum (anti-calnexin, top right panel) we obtained a staining pattern in the overlay image (**Figure 2A**, bottom panels) in agreement with published results (Peshenko et al., 2008; Zägel et al., 2013). The localization of all investigated mutants was very similar to the cellular localization of the WT. Using western blotting we further estimated that the amount of ROS-GC1 WT and mutants was nearly the same in a suspension of cells having a similar cell density (**Figure 2B**, also Zägel et al., 2013).

BASAL GUANYLATE CYCLASE ACTIVITIES

The mutant P575L exhibited similar basal GC activities as WT (**Figure 3**). Activities in the presence of GCAP1 and 2 at saturating [Ca^{2+}] revealed almost no difference between P575L and WT. However, a difference was observed, when GCAP1 and 2 were incubated with ROS-GC1 at low [Ca^{2+}] (EGTA columns in **Figure 3**) resulting in a 25–30% decrease of maximal activity.

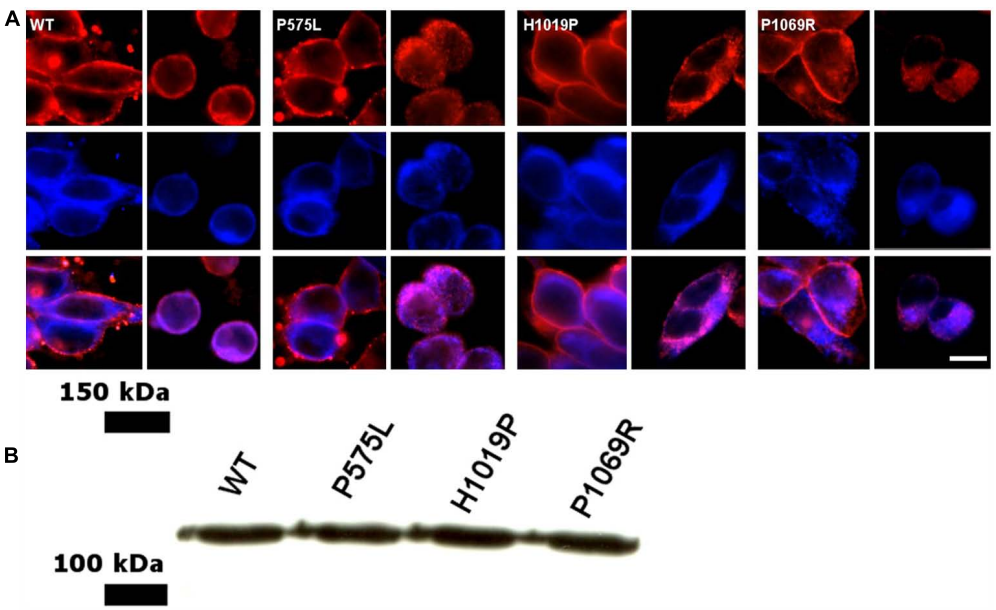

FIGURE 2 | Cellular localization ofWT and ROS-GC1 mutants in HEK293 cells. (A) Cells were stably transfected with human ROS-GC1 constructs and were probed with different antibodies; the corresponding ROS-GC1 construct used for transfection is indicated in the corner of the upper left panel. Anti-Na^+/K^+-ATPase was used as plasma membrane marker (upper left panel, red staining); anti-calnexin antibodies as marker for the endoplasmic reticulum (top right panel, red staining); anti-ROS-GC1 antibody (middle panels, blue staining); overlay of ROS-GC1 staining and membrane specific localization (lower panels). Secondary antibodies were indicated in the Methods section. Visualization was done in an Olympus fluorescence microscope. Cells were fixed either with paraformaldehyde (localization of plasma membrane) or with paraformaldehyde-methanol (endoplasmic reticulum). Scale bar = 10 μm. **(B)** Western blot of HEK293 cells expressing human ROS-GC1, WT and the mutants P575L, H1019P, and P1069R. Blots were probed with a primary antibody against ROS-GC1 (GC1#3, dilution 1:2000) and a secondary anti-rabbit antibody from Dianova (dilution 1:4000) as described (Zägel et al., 2013).

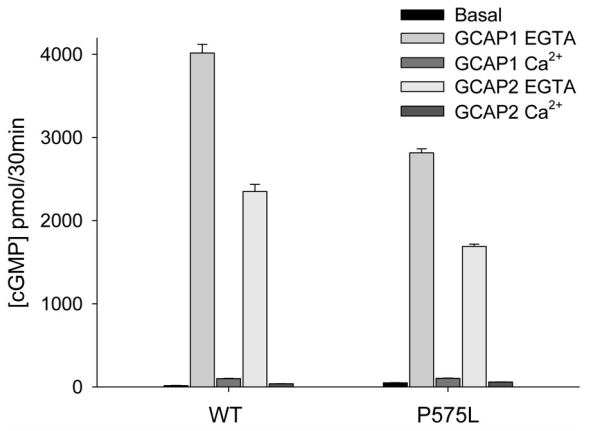

FIGURE 3 | Guanylate cyclase activities of WT and the P575L mutant. Ca^{2+}-bound and Ca^{2+}-free (EGTA) GCAP1 or GCAP2 were added to HEK293 cell membranes expressing human ROS-GC1 (inset) yielding a final concentration of 10 μM. Ca^{2+} was either at 33 μM or <10 nM (EGTA). Assay incubations were performed with equal amounts of WT and mutant guanylate cyclase in membranes, which was verified by western blotting (see **Figure 2B**). Some error bars are not visible due to the scaling of the figure. Differences between data sets were highly significant yielding $***P \leq 0.001$, except for P575L; when its basal activity was compared with the activity in the presence of Ca^{2+}-bound GCAP2, it resulted in $**P \leq 0.01$.

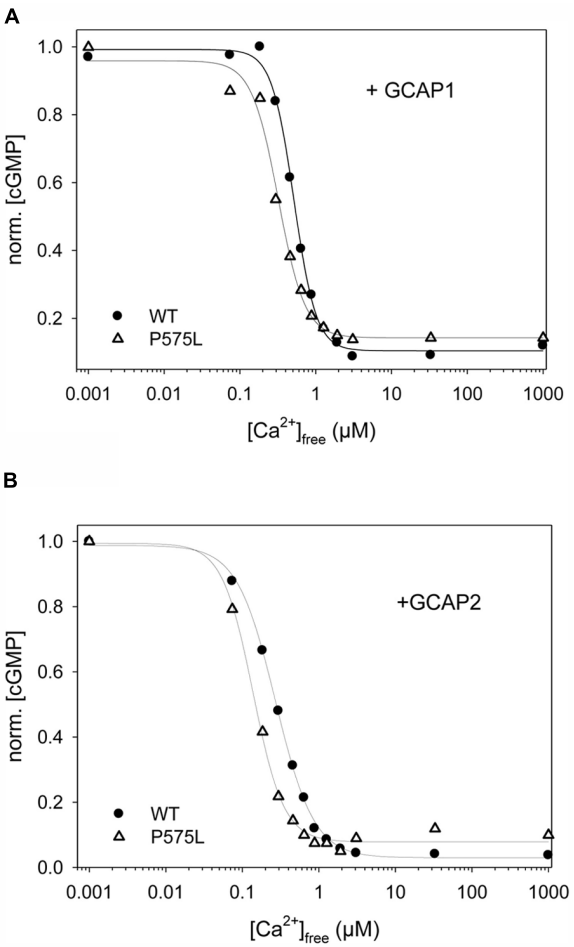

FIGURE 4 | Ca^{2+}-sensitive activity profiles of WT and ROS-GC1 mutant P575L. Guanylate cyclase activities were measured as a function of free [Ca^{2+}] for samples as indicated **(A)** WT or P575L, in the presence of 10 μM GCAP1. **(B)** WT or P575L, in the presence of 10 μM GCAP2. Incubation time was 30 min. Activities are normalized to allow comparison of IC_{50} values ($[Ca^{2+}]_{free}$ at which activity is halfmaximal). Data are representative of three to four sets of incubations.

In sharp contrast to P575L, the mutant P1069R did not exhibit any activity, neither in the presence nor in the absence of Ca^{2+}, EGTA, or GCAPs (data not shown). We also tested activities of cells transiently expressing the mutant or a stably transfected cell line. Since the cellular localization of this mutant appeared normal and was very similar to the active WT and P575L forms (**Figure 2A**), we conclude that the lack of GC activity was a consequence of an impaired catalytic domain.

A special case was observed with the mutant H1019P: we were unable to obtain consistent activity profiles as we did with WT and the P575L mutant. In some cell batches we observed activation by GCAP1, but not by GCAP2, whereas in other batches both GCAPs were able to activate the cyclase or the enzyme was inactive under all conditions. The large scattering of the results seems to indicate a general instability of the mutant.

GCAP-MEDIATED ACTIVATION

The key feature among ROS-GC1 properties is the Ca^{2+}-dependent activation under control of GCAPs. We tested this activation of P575L by GCAPs and compared it with the WT activity profile. Representative data sets are shown in **Figure 4A** (+GCAP1) and **Figure 4B** (+GCAP2), a summary of the IC_{50} values (mean ± SD) is displayed in **Table 1**. For both Ca^{2+}-sensor proteins we observed a similar two-fold shift of the IC_{50} values to lower [Ca^{2+}], in the presence of GCAP1 from 0.529 (WT) to 0.270 μM (P575L) and in the presence of GCAP2 from 0.269 μ(WT) to 0.128 μM (P575L).

A shift in the IC_{50} values had previously been reported for some autosomal cone dystrophy related mutations that are located in a so-called "mutation hotspot" region within or near the residue R838 in the dimerization domain (Duda et al. 1999a, 2000; Wilkie et al., 2000; Kitiratschky et al., 2008; Zägel et al., 2013). One reasonable model explaining this observed effect states that the shift in Ca^{2+}-sensitivity originates from different apparent affinities of WT and mutant ROS-GC1 for the Ca^{2+}-free form of GCAPs

Table 1 | Summary of IC_{50} and EC_{50} values for WT and P575L mutant.

ROS-GC1	IC_{50} (μM)	EC_{50} (μM)
WT + GCAP1	0.529 ± 0.006	2.93 ± 0.37
WT + GCAP2	0.269 ± 0.009	8.34^{+} ± 0.36
P575L + GCAP1	0.270* ± 0.018	3.32^{+} ± 0.39
P575L + GCAP2	0.128 ± 0.014	7.44 ± 1.26

**Six data sets; $^{+}$two data sets.*
Values are the mean ± SD of mainly three to four independent measurements, if not indicated otherwise.

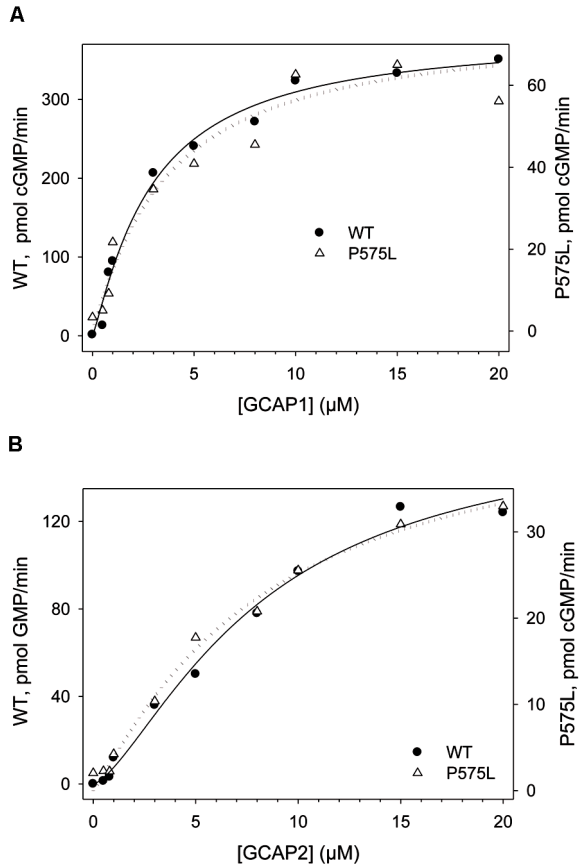

FIGURE 5 | GCAP-dependency of WT and P575L to determine apparent affinities (EC_{50}). WT and mutant P575L (see inset) were incubated with Ca^{2+}-free (Mg^{2+}-bound) GCAP1 **(A)** and GCAP2 **(B)**. The amount of cGMP produced by ROS-GC1 is shown as a function of the GCAP concentration. Incubation time was 30 min.

(Peshenko et al., 2004). We tested this hypothesis for the P575L mutant by measuring the GC activities at increasing GCAP concentrations (**Figure 5**). GCAP1 and 2 were Ca^{2+}-free, but they had Mg^{2+}-bound (Peshenko and Dizhoor, 2004) under the assay conditions. Apparent affinities expressed as EC_{50}-values differed only minimally between WT and the P575L mutant and overlapped within the measured standard deviations (**Table 1**). Thus, we conclude that differences in apparent affinities for GCAPs cannot account for the observed shifts in Ca^{2+}-sensitivity of the P575L mutant.

STRUCTURE-FUNCTION RELATIONSHIPS

The single point mutation P575L is located in direct C-terminal neighborhood of a small stretch of 20 amino acids, which was previously identified as an essential regulatory and/ or interaction site in bovine ROS-GC1 for GCAP1 (L559–I578 corresponding to peptide #34a in Lange et al., 1999). The region is highly conserved among different species and encompasses also the point mutation F565S (human sequence) that is linked to LCA type 1 (Perrault et al., 1996). However, the biochemical consequences of these two mutations differ significantly, since F565S leads to a more than 10-fold lower basal cyclase synthesis rate, but also to a complete loss of the GCAP1-stimulated GC activity (Duda et al., 1999b). These biochemical consequences are in contrast to the less severe effects caused by the P575L mutation.

The position H1019P is located in the short β6-sheet of the CCD in close vicinity of the β5-sheet that harbors amino acids R995, C997, L998, and F999, which are critical for binding the purine ring of the GTP substrate (Tucker et al., 1998). Replacement of H by P might cause a "kink" of the β6-sheet and therefore disrupts or destabilize the catalytic center. A mutation of A to P in α-synuclein for example was reported to have long-range and short-range effects on the three-dimensional structure including a decrease of β-sheet content (Wise-Scira et al., 2013). Furthermore, the position H1019P is also located in the GCAP2 binding site that was previously narrowed down to the amino acid stretch Y1012-N1037 in the bovine sequence (Duda et al., 2005; Pettelkau et al., 2012). In summary, these results might explain the large scattering of GC activities observed in the *in vitro* assays.

In our test system the mutation P1069R had the most dramatic consequences leading to a completely inactive enzyme. This position is sandwiched between the binding sites of GCAP2 and S100β (Duda et al., 2002) and we can only speculate that it might have the function to integrate diverse signals. Furthermore, it seems to be indispensable for the basal catalysis of ROS-GC1.

CONCLUSION

Inherited retinal disorders can affect visual function in different manners. In the present study we investigated the biochemical consequences of three point mutations in the GUCY2D gene, which cause different forms of visual impairment. The mutation P575L causes a progressive form of cone degeneration in affected patients, which very often correlates with symptoms of photophobia, decrease of central vision and impairment of color vision. Since the mutation did not lead to a complete loss of guanylate cyclase function, cone cells expressing the mutated ROS-GC1 protein very likely maintain key features of photoreceptor physiology. But since the mutation induces a dysregulation of the Ca^{2+}-sensitive cyclase activation profile, it seems to have long-term effects in the distortion of the Ca^{2+}-cGMP homeostasis triggering apoptotic pathways. Similar consequences have been discussed for GCAP1 mutations correlating with certain forms of cone-rod dystrophies (Behnen et al., 2010; Hunt et al., 2010). The other two point mutations that were investigated in the present study correlate with LCA and a juvenile form of retinitis pigmentosa. Both mutations have more severe pathological consequences. Typical clinical features are for example an early onset of the disease in childhood and a strongly reduced or even non-recordable electroretinogram (Perrault et al., 2000; Booji et al., 2005). Clinical manifestations of the point mutations appear to be mirrored in the biochemical properties of the expressed ROS-GC1 protein as there are: synthesis of cGMP by ROS-GC1 is either severely disrupted due to protein instability (H1019P) or completely abolished (P1069R). Thus, light-triggered hydrolysis of cGMP cannot adequately be balanced by the second photoreceptor specific guanylate cyclase (ROS-GC2, GC-F), which has a much lower expression level, at least in cone cells (Olshevskaya

et al., 2002; Baehr et al., 2007). The cGMP level in photoreceptor cells would be lower than in non-affected cell. This in turn would keep a lower number of cyclic nucleotide-gated channels open in the dark state. Since the cytoplasmic cGMP pool that is hydrolyzed after illumination is already reduced in the dark, amplitude and kinetics of the photoresponse are expected to be smaller and faster.

ACKNOWLEDGMENT

We thank Jutta Appelt for technical assistance in the cell culture laboratory and Dr. Alexander Scholten for fruitful discussions. This study was supported by a grant from the Deutsche Forschungsgemeinschaft (DFG) to Karl-Wilhelm Koch (KO948/10-1).

REFERENCES

Athanasiou, D., Aguila, M., Bevilacqua, D., Novoselov, S. S., Parfitt, D. A., and Cheetham, M. E. (2013). The cell stress machinery and retinal degeneration. *FEBS Lett.* 587, 2008–2017. doi: 10.1016/j.febslet.2013.05.020

Baehr, W., Karan, S., Maeda, T., Luo, D.-G., Li, S., Bronson, J. D., et al. (2007). The function of guanylate cyclase 1 (GC1) and guanylate cyclase 2 (GC2) in rod and cone photoreceptors. *J. Biol. Chem.* 282, 8837–8847. doi: 10.1074/jbc.M610369200

Behnen, P., Dell'Orco, D., and Koch, K.-W. (2010). Involvement of the calcium sensor GCAP1 in hereditary cone dystrophies. *Biol. Chem.* 391, 631–637. doi: 10.1515/bc.2010.063

Booji, J. C., Florijn, R. J., ten Brink, J. B., Loves, W., Meire, F., von Schooneveld, M. J., et al. (2005). Identification of mutations in the AIPL1, CRB1, GUCY2D, RPE65, and RPGRIP1 genes in patients with juvenile retinitis pigmentosa. *J. Med. Genet.* 42, e67. doi: 10.1136/jmg.2005.035121

Boye, S. L., Peshenko, I. V., Huang, W. C., Min, S. H., McDoom, I., Kay, C. N., et al. (2013). AAV-mediated gene therapy in the guanylate cyclase (RetGC1/RetGC2) double knockout mouse model of Leber congenital amaurosis. *Hum. Gene. Ther.* 24, 189–202. doi: 10.1089/hum.2012.193

Buch, P. K., Mihelec, M., Cottrill, P., Wilkie, S. E., Pearson, R. A., Duran, Y., et al. (2011). Dominant cone-rod dystrophy: a mouse model generated by gene targeting of the GCAP1/Guca1a gene. *PLoS ONE* 6:e18089. doi: 10.1371/journal.pone.0018089

den Hollander, A. I., Roepman, R., Koenekoop, R. K., and Cremers, F. P. M. (2008). Leber congenital amaurosis: genes, proteins and disease mechanisms. *Prog. Retin. Eye Res.* 27, 391–419. doi: 10.1016/j.preteyeres.2008.05.003

Dizhoor, A. M., Olshevskaya, E. V., and Peshenko, I. V. (2010). Mg^{2+}/Ca^{2+} cation binding cycle of guanylyl cyclase activating proteins (GCAPs): role in regulation of photoreceptor guanylyl cyclase. *Mol. Cell. Biochem.* 334, 117–124. doi: 10.1007/s11010-009-0328-6

Duda, T., Fik-Rymarkiewicz, E., Venkataraman, V., Krishnan, R., Koch, K.-W., and Sharma, R. K. (2005). The calcium-sensor guanylate cyclase activating protein type 2-specific site in rod outer segment membrane guanylate cyclase type 1. *Biochemistry* 44, 7336–7345. doi: 10.1021/bi050068x

Duda, T., Koch, K.-W., Venkataraman, V., Lange, C., Beyermann, M., and Sharma, R. K. (2002). Ca^{2+}-sensor S100 modulated sites of membrane guanylate cyclase in the photoreceptor-bipolar synapse. *EMBO J.* 21, 2547–2556. doi: 10.1093/emboj/21.11.2547

Duda, T., Krishnan, A., Venkataraman, V., Lange, C., Koch, K.-W., and Sharma, R. K. (1999a). Mutations in the rod outer segment membrane guanylate cyclase (ROS-GC1) in a cone-rod dystrophy cause defects in calcium signaling. *Biochemistry* 38, 13912–13919. doi: 10.1021/bi9915972

Duda, T., Venkataraman, V., Goraczniak, R., Lange, C., Koch, K.-W., and Sharma, R. K. (1999b). Functional consequences of a rod outer segment membrane guanylate cyclase (ROS-GC1) gene mutation linked with Leber's congenital amaurosis. *Biochemistry* 38, 509–515. doi: 10.1021/bi9824137

Duda, T., Venkataraman, V., Jankowska, A., Lange, C., Koch, K.-W., and Sharma, R. K. (2000). Impairment of the rod outer segment membrane guanylate cyclase dimerization in a cone-rod dystrophy results in defective calcium signaling. *Biochemistry* 39, 12522–12533. doi: 10.1021/bi001514d

Fain, G. L., Matthews, H. R., Cornwall, M. C., and Koutalos, Y. (2001). Adaptation in vertebrate photoreceptors. *Physiol. Rev.* 81, 117–151.

Hunt, D. M., Buch, P., and Michaelides, M. (2010). Guanylate cyclases and associated activator proteins in retinal disease. *Mol. Cell. Biochem.* 334, 157–168. doi: 10.1007/s11010-009-0331-y

Hwang, J.-Y., Lange, C., Helten, A., Höppner-Heitmann, D., Duda, T., Sharma, R. K., et al. (2003). Regulatory modes of rod outer segment membrane guanylate cyclase differ in catalytic efficiency and Ca^{2+}-sensitivity. *Eur. J. Biochem.* 270, 3814–3821. doi: 10.1046/j.1432-1033.2003.03770.x

Jiang, L., Zhang, H., Dizhoor, A. M., Boye, S. E., Hauswirth, W. W., Frederick, J. M., et al. (2011). Long-term RNA interference gene therapy in a dominant retinitis pigmentosa mouse model. *Proc. Natl. Acad. Sci. U.S.A.* 108, 18476–18481. doi: 10.1073/pnas.1112758108

Kaupp, U. B., and Seifert, R. (2002). Cyclic nucleotide-gated ion channels. *Physiol. Rev.* 82, 769–824.

Kitiratschky, V. B., Wilke, R., Renner, A. B., Kellner, U., Vadalà, M., Birch, D. G., et al. (2008). Mutation analysis identifies GUCY2D as the major gene responsible for autosomal dominant progressive cone degeneration. *Invest. Ophthalmol. Vis. Sci.* 49, 5015–5023. doi: 10.1167/iovs.08-1901

Koch, K.-W., and Dell'Orco, D. (2013). A calcium–relay mechanism in vertebrate phototransduction. *ACS Chem. Neurosci.* 4, 909–917. doi: 10.1021/cn400027z

Koch, K.-W., Duda, T., and Sharma, R. K. (2010). Ca^{2+}-modulated vision-linked ROS-GC guanylate cyclase transduction machinery. *Mol. Cell. Biochem.* 334, 105–115. doi: 10.1007/s11010-009-0330-z

Koch, K.-W., and Helten, A. (2008). "Guanylate cyclase-based signaling in photoreceptors and retina," in *Signal Transduction in the Retina*, Chap. 6 eds S. J. Fliesler and O. G. Kisselev (North Tonawanda, NY: Taylor and Francis CRC Press), 121–143.

Krylov, D. M., Niemi, G. A., Dizhoor, A. M., and Hurley, J. B. (1999). Mapping sites in guanylyl cyclase activating protein-1 required for regulation of photoreceptor membrane guanylyl cyclases. *J. Biol. Chem.* 274, 10833–10839. doi: 10.1074/jbc.274.16.10833

Lange, C., Duda, T., Beyermann, M., Sharma, R. K., and Koch, K.-W. (1999). Regions in vertebrate photoreceptor guanylyl cyclase ROS-GC1 involved in Ca^{2+}-dependent regulation by guanyly cyclase-activating protein GCAP-1. *FEBS Lett.* 460, 27–31. doi: 10.1016/S0014-5793(99)01312-5

Luo, D. G., Xue, T., and Yau, K.-W. (2008). How vision begins: an odyssey. *Proc. Natl. Acad. Sci. U.S.A.* 105, 9855–9862. doi: 10.1073/pnas.0708405105

Olshevskaya, E. V., Ermilov, A. N., and Dizhoor, A. M. (2002). Factors that affect regulation of cGMP synthesis in vertebrate photoreceptors and their genetic link to human retinal degeneration. *Mol. Cell. Biochem.* 230, 139–147. doi: 10.1023/A:1014248208584

Perrault, I., Rozet, J. M., Calvas, P., Gerber, S., Camuzat, A., Dollfus, H., et al. (1996). Retinal-specific guanylate cyclase gene mutations in leber's congenital amaurosis. *Nat. Genet.* 14, 461–464. doi: 10.1038/ng1296-461

Perrault, I., Rozet, J. M., Gerber, S., Ghazi, I., Ducroq, D., Souied, E., et al. (2000). Spectrum of retGC1 mutations in Leber's congenital amaurosis. *Eur. J. Hum. Genet.* 8, 578–582. doi: 10.1038/sj.ejhg.5200503

Peshenko, I. V., and Dizhoor, A. M. (2004). Guanylyl cyclase-activating proteins (GCAPs) are Ca^{2+}/Mg^{2+} sensors: implications for photoreceptor guanylyl cyclase (RetGC) regulation in mammalian photoreceptors. *J. Biol. Chem.* 279, 16903–16906. doi: 10.1074/jbc.C400065200

Peshenko, I. V., Moiseyev, G. P., Olshevskaya, E. V., and Dizhoor, A. M. (2004). Factors that determine Ca^{2+} sensitivity of photoreceptor guanylyl cyclase. Kinetic analysis of the interaction between the Ca^{2+}-bound and the Ca^{2+}-free guanylyl cyclase activating proteins (GCAPs) and recombinant photoreceptor guanylyl cyclase 1 (RetGC-1). *Biochemistry* 43, 13796–13804. doi: 10.1021/bi048943m

Peshenko, I. V., Olshevskaya, E., and Dizhoor, A. M. (2008). Binding of guanylyl cyclase activating protein 1 (GCAP1) to retinal guanylyl cyclase (RetGC1). *J. Biol. Chem.* 283, 21747–21757. doi: 10.1074/jbc.M801899200

Pettelkau, J., Schröder, T., Ihling, C. H., Olausson, B. E., Kölbel, K., Lange, C., et al. (2012). Structural insights into retinal guanylylcyclase-GCAP-2 interaction determined by cross-linking and mass spectrometry. *Biochemistry* 51, 4932–4949. doi: 10.1021/bi300064v

Pugh, E. N. Jr., and Lamb, T. D. (2000). "Phototransduction in vertebrate rods and cones: molecular mechanisms of amplification, recovery and light adaptation," in *Handbook of Biological Physics*, eds D. G. Stavenga, W. J. DeGrip, and E. N. Pugh Jr. (Leiden: Elsevier Science), 183–255.

Ramamurthy, V., Tucker, C., Wilkie, S. E., Daggett, V., Hunt, D. M., and Hurley, J. B. (2001). Interactions within the coiled-coil domain of RetGC-1 guanylyl cyclase are optimized for regulation rather than for high affinity. *J. Biol. Chem.* 276, 26218–26229. doi: 10.1074/jbc.M010495200

Small, K. W., Silva-Garcia, R., Udar, N., Nguyen, E. V., and Heckenlively, J. R. (2008). New mutation, P575L, in the GUCY2D gene in a family with autosomal dominant progressive cone degeneration. *Arch. Ophthalmol.* 126, 397–403. doi: 10.1001/archopht.126.3.397

Stephen, R., Filipek, S., Palczewski, K., and Sousa, M. C. (2008). Ca^{2+}-dependent regulation of phototransduction. *Photochem. Photobiol.* 84, 903–910. doi: 10.1111/j.1751-1097.2008.00323.x

Tucker, C. L., Hurley, J. H., Miller, T. R., and Hurley, J. B. (1998). Two amino acid substitutions convert a guanylyl cyclase, RetGC-1, into an adenylyl cyclase. *Proc. Natl. Acad. Sci. U.S.A.* 95, 5993–5997. doi: 10.1073/pnas.95.11.5993

Wilkie, S. E., Newbold, R. J., Deery, E., Walker, C. E., Stinton, I., Ramamurthy, V., et al. (2000). Functional characterization of missense mutations at codon 838 in retinal guanylate cyclase correlates with disease severity in patients with autosomal dominant cone-roddystrophy. *Hum. Mol. Genet.* 9, 3065–3073. doi: 10.1093/hmg/9.20.3065

Wise-Scira, O., Aloglu, A. K., Dunn, A., Sakallioglu, I. T., and Coskuner, O. (2013). Structures and free energy landscapes of the wild-type and A30P mutant-type α-synuclein proteins with dynamics. *ACS Chem. Neurosci.* 4, 486–497. doi: 10.1021/cn300198q

Zägel, P., Dell'Orco, D., and Koch, K.-W. (2013). The dimerization domain in outer segment guanylate cyclase is a Ca^{2+} -sensitive control switch module. *Biochemistry* 52, 5065–5074. doi: 10.1021/bi400288p

Conflict of Interest Statement: The authors declare that the research was conducted in the absence of any commercial or financial relationships that could be construed as a potential conflict of interest.

Received: 25 November 2013; accepted: 10 February 2014; published online: 26 February 2014.

*Citation: Zägel P and Koch K-W (2014) Dysfunction of outer segment guanylate cyclase caused by retinal disease related mutations. Front. Mol. Neurosci. **7**:4. doi: 10.3389/fnmol.2014.00004*

This article was submitted to the journal Frontiers in Molecular Neuroscience.

frontiers in
MOLECULAR NEUROSCIENCE

REVIEW ARTICLE
published: 14 May 2014
doi: 10.3389/fnmol.2014.00043

Insights gained from gene therapy in animal models of retGC1 deficiency

Shannon E. Boye*

Department of Ophthalmology, University of Florida, Gainesville, FL, USA

Edited by:
Wolfgang Baehr, University of Utah, USA

Reviewed by:
Wolfgang Baehr, University of Utah, USA
Izhak Michaelevski, Tel Aviv University, Israel

****Correspondence:***
Shannon E. Boye, Department of Ophthalmology, University of Florida, P.O. Box 100284, Gainesville, FL 32610, USA
e-mail: shannon.boye@eye.ufl.edu

Vertebrate species possess two retinal guanylate cyclases (retGC1 and retGC2) and at least two guanylate cyclase activating proteins (GCAPs), GCAP1 and GCAP2. GCAPs function as Ca^{2+} sensors that regulate the activity of guanylate cyclases. Together, these proteins regulate cGMP and Ca^{2+} levels within the outer segments of rod and cone photoreceptors. Mutations in *GUCY2D*, the gene that encodes retGC1, are a leading cause of the most severe form of early onset retinal dystrophy, Leber congenital amaurosis (LCA1). These mutations, which reduce or abolish the ability of retGC1 to replenish cGMP in photoreceptors, are thought to lead to the biochemical equivalent of chronic light exposure in these cells. In spite of this, the majority of LCA1 patients retain normal photoreceptor laminar architecture aside from foveal cone outer segment abnormalities, suggesting they may be good candidates for gene replacement therapy. Work began in the 1980s to characterize multiple animal models of retGC1 deficiency. 34 years later, all models have been used in proof of concept gene replacement studies toward the goal of developing a therapy to treat *GUCY2D*-LCA1. Here we use the results of these studies as well as those of recent clinical studies to address specific questions relating to clinical application of a gene therapy for treatment of LCA1.

Keywords: LCA1, Leber congenital amaurosis, *GUCY2D*, retGC1, GC1, guanylate cyclase, retinal gene therapy, AAV

INTRODUCTION

The ability to process light into an electrochemical signal depends on the precise regulation of levels of cGMP and Ca^{2+} within the outer segments of rod and cone photoreceptor cells. In the absence of light stimulation, intracellular cGMP and Ca^{2+} levels are high and a continuous flow of Na^{+} and Ca^{2+} ions through cGMP-gated channels and Na^{+}/Ca^{2+} exchangers keeps the cell in a depolarized state. Activation of rhodopsin or cone opsins in rod and cone outer segments, respectively, leads to activation of transducin that in turn activates cGMP phosphodiesterase (PDE) leading to a reduction in the concentration of cGMP in the outer segment. Reduction of cGMP leads to closure of cGMP-gated channels, reduced Na^{+}/Ca^{2+} influx and hyperpolarization of the cell (Pugh et al., 1997). Recovery of light stimulated photoreceptors to the dark state is hastened by the decrease in intracellular Ca^{2+} that results from continued expulsion of Ca^{2+} by Na^{+}/Ca^{2+}-K^{+} exchangers. Calcium has several roles in photoreceptor cells, one of which is to regulate the activity of retinal guanylate cyclases, retGC1 and retGC2 (Koch and Stryer, 1988). It does so by binding to guanylate cyclase activating proteins (GCAPs), a family of calcium-binding proteins that regulate the activity of retGCs (Polans et al., 1996). Two variants of guanylate cyclases (retGC1 and retGC2) and at least two variants of GCAPs (GCAP1 and GCAP2) are present in the outer segments of vertebrate photoreceptors (Shyjan et al., 1992; Margulis et al., 1993; Dizhoor et al., 1994; Goraczniak et al., 1994, 1997; Palczewski et al., 1994; Lowe et al., 1995; Yang et al., 1995; Imanishi et al., 2004). In the dark, high levels of intracellular Ca^{2+} promote its binding to GCAP and inhibit the ability of this protein to activate retGCs. Reduction of free, intracellular Ca^{2+} following light stimulation leads to a decrease in the amount of Ca^{2+} bound to GCAP in exchange for Mg^{2+}, which allows this protein to activate retGCs (Peshenko and Dizhoor, 2006; **Figure 1**). *In vivo*, retGC1 is the preferred target of GCAP1 (Olshevskaya et al., 2012). *In vitro*, some studies show that GCAP1 and GCAP2 can activate both retGCs, albeit with slightly different affinities and sensitivity to Ca^{2+} (Hwang et al., 2003; Peshenko and Dizhoor, 2004; Peshenko et al., 2011) while another shows that GCAP1 cannot activate retGC2 (Haeseleer et al., 1999).

Mutations in *GUCY2D*, the gene that encodes retGC1, are associated with the severe, early onset, autosomal recessive disorder Leber congenital amaurosis-1 (LCA1; Perrault et al., 1996, 2000). LCA1 causing mutations are found throughout *GUCY2D*, can alter the enzyme's structure or stability, affect transport of other peripheral membrane associated protein, and are frequently null (Karan et al., 2010; Jacobson et al., 2013). Without fully functional retGC1 to replenish intracellular cGMP, as is the case in LCA1, cGMP-gated cation channels will remain closed as they are in the light stimulated state. Hence, mutations in *GUCY2D* are thought to induce the biochemical equivalent of chronic light exposure in photoreceptors. LCA1 patients routinely present with severely reduced visual acuities, attenuated or extinguished electroretinogram (ERG), nystagmus, digito-ocular signs, and apparently normal fundus appearance (Perrault et al., 1999a, 2000; Hanein et al., 2004; Yzer et al., 2006; den Hollander et al., 2008). While early reports indicated retinal degeneration was associated with this form of LCA (Milam et al., 2003; Porto et al., 2003),

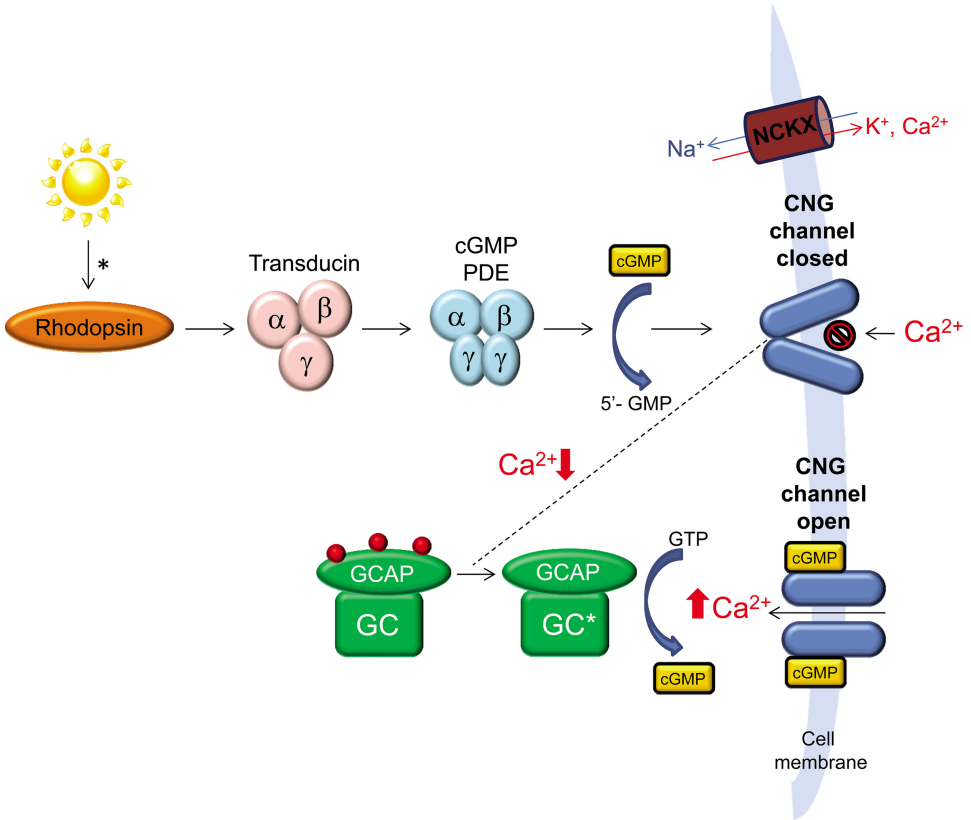

FIGURE 1 | The role of retinal guanylate cyclase (retGC) in phototransduction. A photon of light activates rhodopsin initiating a cascade of events, the end result of which is reduction of cGMP, closure of cGMP-gated channels and reduction of intracellular Ca^{2+} in photoreceptor outer segments. Continued expulsion of Ca^{2+} by Na^{+}/Ca^{2+}-K^{+} exchangers (NCKX) results in activation of retGC by GCAP. retGC replenishes intracellular cGMP which reopens cGMP-gated channels allowing for Ca^{2+} influx and a return of the photoreceptor to its dark-adapted state.

later studies revealed preservation of retinal laminar architecture in LCA1 patients (Simonelli et al., 2007; Pasadhika et al., 2010; Jacobson et al., 2013).

Preservation of retinal structure despite profound visual disturbance suggests that LCA1 patients would be good candidates for gene replacement therapy. Before initiating such clinical trials there are major questions that need to be answered. Here we stepwise address these questions by reviewing findings of proof of concept studies utilizing different animal models of retGC1 deficiency (results summarized in **Table 1**). Additionally, we provide an update on efforts to clinically apply a gene therapy for LCA1.

WILL *GUCY2D* GENE REPLACEMENT RESTORE RETINAL FUNCTION *IN VIVO*?

The first animal model used to investigate gene replacement for retGC1 was the *retinal degeneration* (*rd*) chicken, also referred to as the GUCY1*B chicken. This cone- dominant, avian model carries a null, naturally occurring deletion/insertion mutation in the gene encoding retGC1 (Semple-Rowland et al., 1998). As a consequence of retGC1 deficiency, photoreceptors of post-hatch day 1 (P1) GUCY1*B chickens have only 10–20% cGMP relative to that found in age-matched, wild type controls and affected chickens are blind at hatch. They have unrecordable ERGs and lack optokinetic and volitional visual behavior (Ulshafer et al., 1984; Williams et al., 2006). These biochemical and visual disturbances occur prior to photoreceptor loss which doesnot begin until 1 week post-hatch (Cheng et al., 1980; Ulshafer et al., 1984) and proceeds in a central to peripheral fashion with cones completely lost by 3.5 months and rods lost by 8 months (Ulshafer and Allen, 1985a,b).

Due to the technical difficulty associated with performing subretinal injections in chicken, an *in ovo* treatment paradigm was developed. For its ability to stably transduce retinal progenitor cells (Miyoshi et al., 1997), HIV-1-based lentivirus (LV) was used to deliver a cDNA encoding bovine retGC1 under the control of an elongation factor 1 alpha (EF1α) promoter to the neural tube of developing GUCY1*B embryos (Williams et al., 2006). Bovine retGC1 (bGC1) was chosen for its verified activity in the presence of chicken GCAPs *in vitro* (Williams et al., 2006). At 1 month post-hatch, ERG testing under both dark and light-adapted conditions revealed that LV-EF1α-bGC1 treatment produced modest increases in photoreceptor-mediated a-wave amplitudes in treated chickens (~6% of wild type). These results were the first demonstration that retGC1 gene replacement could restore retinal function. ERG improvements were associated with a restoration of visually guided behavior, as assessed by

Table 1 | Summary of proof of concept experiments.

Animal model	Vector	Treatment age	ERG results	Behavior outcomes	Structural results	Length of study
GUCY1*B chicken	LV-EF1α-*bGC1*	E2	Cones/rods: up to 6% of WT	Cone-mediated OKN reflex/volitional behavior	Degeneration slowed	5 weeks
GC1KO mouse	AAV5-smCBA-*Gucy2e*	P14–P25	Cones: up to ∼45% of WT	Cone-mediated OKN reflex	Cone preservation	3 months, 1 year
	AAV5-hGRK1-*Gucy2e*	P14–P25	Cones: up to ∼45% of WT	Cone-mediated OKN reflex	Cone preservation	3 months, 1 year
	AAV8-hGRK1-*GUCY2D*	P10	Cones: up to ∼65% of WT Rods: up to 100% of WT	Cone-mediated OKN reflex	Cone preservation	6 months
	AAV8(Y733F)-hGRK1-*Gucy2e*	P14–P25	Cones: up to ∼45% of WT	Cone-mediated OKN reflex	Cone preservation	1 year
GC1/GC2DKO mouse	AAV8(Y733F)-hGRK1-*Gucy2e*	P21–P108	Cones: up to ∼42% of WT Rods: up to ∼44% of WT	Cone-mediated OKN reflex Cone and rod-mediated visual acuity	Cone/rod preservation	1 year

optokinetic reflex testing (Wallman and Velez, 1985) and volitional visually guided behavior tests (Williams et al., 2006). In addition, a slowing of retinal degeneration was observed (Williams et al., 2006). Taken together, these results were exciting proof of concept that gene replacement therapy could be effective for treatment of LCA1. However, there were multiple limitations associated with this study that needed to be overcome. First, the therapeutic effect was transient, with ERG and behavioral responses disappearing after the latest time points analyzed (5 weeks post-hatch) and retinal degeneration continuing unabated (Williams et al., 2006; Verrier et al., 2011). Second, multiple facets of the therapeutic strategy lacked clinical translatability- (1) Therapeutic retGC1 was delivered embryonically, a currently untenable task in patients and also requiring in-utero genotyping. (2) An integrating, lentiviral vector was used. While proven effective for transducing retinal precursors, LV has demonstrated little to no ability to transduce post-mitotic photoreceptors (Miyoshi et al., 1997; Bainbridge et al., 2001; Pang et al., 2006; Lipinski et al., 2014). (3) Data was obtained in a non-mammalian model of retGC1 deficiency. Together, this highlighted the need to test therapy using more clinically relevant animal models and vector platform.

WILL POST-NATALLY DELIVERED retGC1 RESTORE RETINAL FUNCTION IN A MAMMALIAN MODEL OF retGC1 DEFICIENCY?

The first mammalian model retGC1 deficiency to be described was the guanylate cyclase-1 knockout (GC1KO) mouse (Yang et al., 1999). Insertion of a neomycin resistance cassette in exon 5 of *Gucy2e* (the murine homolog of *GUCY2D*) resulted in truncation of retGC1, rendering it null (Yang et al., 1999). Cone-mediated ERGs are unrecordable by 5 weeks but cones are not completely degenerated in this mouse until ∼6 months of age (Yang et al., 1999; Coleman et al., 2004). Rods, on the other hand, do not degenerate and maintain variable levels of function (∼30–50% of WT; Yang et al., 1999) which is owed to the presence of retGC2 in those cells (Baehr et al., 2007). GCAP1 and GCAP2 transcripts and GCAP1 expression are down-regulated (Coleman et al., 2004) and light-induced translocation of cone arrestin is disrupted as a result of retGC1 deficiency in this model (Coleman and Semple-Rowland, 2005). The temporal dissociation between loss of cone function and structure in GC1KO mice, provides a window of therapy for gene replacement.

For its safety profile and proven ability to transduce post-mitotic photoreceptors following subretinal injection of murine retina (Yang et al., 2002), a serotype 5 adeno associated virus (AAV) was chosen to deliver bovine retGC1 (the same cDNA delivered to the GUCY1*B chicken) under the control of either the ubiquitous, small CBA (smCBA) or photoreceptor-specific, murine opsin (MOPS) promoter to the GC1KO mouse (Haire et al., 2006). Post-natal day 21 (P21) treatment with AAV5-bGC1 failed to improve retinal function (ERG) in treated mice. However, AAV-mediated retGC1 expression was restricted to photoreceptor outer segments and restoration of light-induced cone arrestin translocation, a biochemical correlate of functionality in these cells, was observed at 4 weeks post-treatment (Haire et al., 2006), suggesting that the light signaling cascade in GC1KO cones had been at least partially reset following treatment.

Investigators speculated that the species non-specific nature of the delivered transgene may have dampened the therapeutic outcome. Indeed, subretinal delivery of murine *Gucy2e* via an AAV5 vector containing either the ubiquitous smCBA or photoreceptor-specific human rhodopsin kinase (hGRK1) promoter led to robust improvements (∼45% of WT) in cone-mediated ERGs (Boye et al., 2010). These improvements were stable over the course of this initial study (at least 3 months post-treatment) and provided the first evidence that an AAV-based vector could restore retinal function to a mammalian model of retGC1 deficiency (Boye et al.,

2010). Later studies would go on to show that stable restoration of cone function (ERG) is achievable over the long term (Boye et al., 2011; Mihelec et al., 2011). Subretinally delivered AAV8 containing the hGRK1 promoter and human *GUCY2D* cDNA stably restored cone function (∼65% of WT) for at least 6 months (Mihelec et al., 2011). In the longest follow up reported to date, subretinally delivered AAV5 or capsid mutant AAV8(Y733F) containing either the smCBA or hGRK1 promoter and murine *Gucy2e* cDNA stably restored cone function (∼45% of WT) for at least 1 year post-treatment (Boye et al., 2011). A notable difference between these two studies was the level of cone function achieved (65 vs. 45% of WT). Mihelec et al. (2011) subretinally delivered AAV-*GUCY2D* to GC1KO mice at P10 (an age prior to natural eye opening) whereas Boye et al. (2011) delivered AAV-*Gucy2e* between P14–P25. Earlier intervention was likely more effective at combating the chronic effects of hyperpolarization that GC1KO cones endure upon light stimulation. Regardless of these differences, the robust and stable functional improvements in cone function following AAV-retGC1 treatment (including with a clinically relevant human cDNA) in GC1KO mice laid the groundwork for development of an AAV-based treatment for LCA1.

As a follow up to these studies, cone-mediated function was also evaluated in the retGC1/retGC2 double knockout (GCDKO mouse following subretinal delivery of AAV8(Y733F)-hGRK1-*Gucy2e* (Boye et al., 2013). Treatment of this model, in which cones and rods are functionally silent and progressively degenerate, also resulted in stable and robust improvements in cone function for at least 1 year post-treatment (Boye et al., 2013). As in all GC1KO studies, AAV-mediated retGC1 expression was restricted to the outer segments of rods and cones in treated GCDKO mice. The GCDKO mouse and gene replacement experiments in this model will be discussed in more detail below.

DOES RESTORATION OF CONE FUNCTION TRANSLATE INTO USEFUL VISION?

Adeno associated virus-mediated expression of retGC1 in photoreceptors of GC1KO mice effectively reset the phototransduction cascade in cones, allowing them to send electrochemical signals to downstream neurons which were detected via full field ERG electrodes (Boye et al., 2010, 2011; Mihelec et al., 2011). However, the existence of functional neural circuits within the retina does not ensure that electrochemical signals are properly relayed to higher order processing centers in the brain and experienced as "vision." Even if the biochemical defect within photoreceptors is corrected via restoration of retGC1, it is unclear what role amblyopia (the inability of the retina to send visual information to the brain) will play on the treatment outcome. To gain insight into this question, multiple visually guided behavior tests were used to further characterize therapy in AAV-treated GC1KO mice.

Two tests, each of which evaluates the integrity of different visual processing centers of the brain, were used to determine whether useful cone vision could be restored to treated mice. A virtual optokinetic system was used to evaluate the integrity of subcortical retinal efferents (Douglas et al., 2005). While untreated GC1KO mice lack cone-mediated behavior, significant improvements in cone-mediated spatial frequency thresholds and contrast sensitivities were seen in GC1KO mice treated with AAV5-hGRK1-*Gucy2e*, AAV5-smCBA-*Gucy2e*, AAV8(Y733F)-hGRK1-*Gucy2e* or AAV8-hGRK1-*GUCY2D* (Boye et al., 2010, 2011; Mihelec et al., 2011) with behavior resembling that of normal, sighted congenic mice. Improvements in cone-mediated behavior were observed out to 4 months post-treatment (Mihelec et al., 2011), the latest time point evaluated in this mouse model. Analysis of cone-mediated behavior was also evaluated in GCDKO mice via Morris Water Maze (under photopic conditions), a test used to analyze cortically driven visual behavior (Boye et al., 2013). AAV8(Y733F)-hGRK1-*Gucy2e* treated mice exhibited significantly reduced escape latencies (the amount of time required to escape water bath via a platform demarcated with a flag) relative to untreated controls. Importantly, behavior of treated mice was not significantly different from age-matched WT controls. Notably, these results were obtained in 1 year old GCDKO mice treated 11 months prior, highlighting that retGC1 supplementation confers useful cone-mediated vision to mammalian models of LCA1 over the long term. This is significant as humans rely heavily on their cone-mediated vision for activities of daily living. It is also interesting to note that while cone-mediated ERG improvements in both GC1KO and GCDKO controls ranged between 45 and 65% that of WT controls, cone-mediated behavior was restored to "normal" in AAV-treated mice supporting previous work showing that behavior is a more sensitive indicator of therapy (Williams and Jacobs, 2007). This was also shown to be the case in LV-retGC1 treated GUCY1*B chickens whose modest ERG responses corresponded, albeit transiently, to robust visually guided behavior (Williams et al., 2006).

HOW DO ROD PHOTORECEPTORS RESPOND TO TREATMENT?

Prior to the most comprehensive clinical characterization of LCA1 patients published to date (Jacobson et al., 2013), multiple reports had described that both rod/cone function and rod/cone structure were compromised (Perrault et al., 1999a,b; Milam et al., 2003; Porto et al., 2003; den Hollander et al., 2008; Chung and Traboulsi, 2009; Jacobson et al., 2013). It was clear that, despite the presence of retGC2 in these cells (Lowe et al., 1995), rod photoreceptors of LCA1 patients are negatively impacted by retGC1 deficiency. Thus, the specific effects of post-natal gene replacement therapy on this photoreceptor subclass needed to be analyzed. Prior studies were conducted in a model that lacks rod degeneration and retains variable levels of rod function throughout its life, the GC1KO mouse. For these reasons, it was not possible to address whether gene replacement would prevent degeneration of rods or definitively restore their function, respectively. Significant improvements in rod-mediated ERGs were only obtained when vector was delivered prior to natural eye opening (P10; Mihelec et al., 2011), but it is difficult to ascertain whether these gains are meaningful because GC1KO mice exhibit normal rod-mediated visual behavior. It was not until generation of the GCDKO mouse that it became possible to ask these questions (Baehr et al., 2007).

Deletion of both retGC1 and retGC2 in the GCDKO mouse (Baehr et al., 2007) renders both cones and rods functionally silent

(ERGs are unrecordable) and degenerative (Baehr et al., 2007). Several cone proteins (GCAP1, GCAP2, cone opsins, cone transducin, cone PDE, GRK1) are downregulated/mislocalized) and PDE6 is absent from rods (Baehr et al., 2007) in this model. By 2 months of age, overall outer segment length is reduced to 30–50% of normal (Baehr et al., 2007). Appreciable thinning of the outer nuclear layer (ONL) is apparent by ∼3.5 months of age and by 6 months, only 3–4 photoreceptor nuclei remain (Boye et al., 2013).

For its success in the studies described above, AAV8(Y733)-hGRK1 was chosen to subretinally deliver *Gucy2e* to cohorts of GCDKO mice of various age groups (P18, P21–P25, P37–P49, and P108). ERG revealed that, like the cone results described above, rod function was also stably restored to ∼40% of normal (at least 1 year post-treatment; Boye et al., 2013). Morris Water Maze testing revealed that these functional gains translated to useful rod-mediated vision, with AAV-retGC1- treated GCDKO mice performing the task at speeds that did not differ significantly from age-matched WT controls (Boye et al., 2013). As in the treated GC1KO mice, WT-like behavior was achievable in GCDKO mice that exhibited only partial ERG recovery. Optical coherence tomography (OCT) was used to monitor the rate of photoreceptor degeneration (predominantly rods) in treated vs. untreated mice. By 7–12 months post-treatment, there was significant structural preservation in all treated GCDKOs, barring those treated at the latest time point (P108), although retinas in these mice still exhibited greater preservation than controls (Boye et al., 2013). Importantly, the rate of photoreceptor cell loss in GCDKO mice treated as late as P49 was no different from that of age-matched WT controls. GCAP1 and GCAP2 were expressed at WT-like levels at 1 year post-injection and cone opsins were present only in treated cones (Boye et al., 2013). Taken together, this study showed for the first time that, along with the rescue effects seen on cones, AAV-mediated retGC1 expression can restore rod photoreceptor function and rod-mediated visual behavior and preserve rod structure over the long term in an animal model of LCA1.

WHAT IS THE FUNCTIONAL EFFICIENCY OF AAV- DELIVERED retGC1 ENZYME?

In considering clinical application of a gene therapy, an important question becomes "how efficient is the vector-derived, recombinant gene product relative to the native protein?" The ability to assess this *in vivo* provides a powerful bioassay which can be used to establish dose-response relationships and equivalencies for batches of clinical vectors. Guanylate cyclase activity assays are performed on dark-adapted retinas to determine how much cGMP is produced by retGCs in the presence of a [α-^{32}P]GTP substrate (Olshevskaya et al., 2004; Peshenko et al., 2011). This assay doesnot discriminate between the activity of retGC1 and retGC2. Therefore, isolating the functional efficiency of exogenous retGC1 requires delivery to photoreceptors that lack both endogenous retGC1 and retGC2, such as those in the GCDKO mouse. Boye et al. (2013) compared retGC activity in retinas of GCDKO mice that were treated subretinally between P30–P60 with AAV8(Y733F)-hGRK1-*Gucy2e*, relative to untreated GCDKO or WT controls and those that received a serotype-matched control vector expressing GFP. Maximal retGC activity in AAV-*Gucy2e* treated retinas was ∼63% of normal. The known contribution to total cyclase activity by retGC2 in this assay is between 20 and 28% (Peshenko et al., 2011). In addition, the area of retGC1 expression in treated retinas is known to be restricted to the subretinal injection bleb (Timmers et al., 2001; Cideciyan et al., 2008). "Good" subretinal injections typically result in ∼80–90% detachment meaning not all photoreceptors expressed the enzyme. Taking these two factors into account, the level of retGC1 activity suggested its near-complete restoration in the area exposed to vector. When the maximal activity of AAV-retGC1 was normalized to that seen in WT retinas, it was determined that the calcium sensitivity of the exogenous and endogenous enzymes were identical (Boye et al., 2013). Moving forward, this assay may be used to evaluate the relative potency of clinical vectors.

WHAT ARE THE CONSEQUENCES OF retGC1 DEFICIENCY ON HUMAN ROD AND CONE PHOTORECEPTOR STRUCTURE AND FUNCTION?

While there is general consensus that LCA1 is associated with severely attenuated or ablated ERG (Perrault et al., 1999b, 2000; Hanein et al., 2004; Yzer et al., 2006; den Hollander et al., 2008), reports on the extent of photoreceptor degeneration associated with this form of LCA have been conflicting (Milam et al., 2003; Porto et al., 2003; Simonelli et al., 2007; Pasadhika et al., 2010). The most thorough clinical characterization of LCA1 performed to date focused on a cohort of patients ranging in age from 6 months to 37 years with different mutations in *GUCY2D* and has provided new insight on the effects of retGC1 deficiency on retinal structure and function (Jacobson et al., 2013).

Similar to previous reports Simonelli et al. (2007), Pasadhika et al. (2010), Jacobson et al. (2013) found that LCA1 patients retained normal retinal laminar architecture aside from foveal cone outer segment abnormalities and, in some cases, foveal cone loss. Within rod-dominant retina, ONL thickness and outer segment lengths were normal in all patients (Jacobson et al., 2013). Unlike previous reports, Jacobson et al. (2013) found that LCA1 patients can retain substantial rod function. Full field sensitivity testing (FST) revealed all patients effectively used their rods to detect blue stimuli, albeit at reduced sensitivities. These psychophysical findings were supported by ERG, pupillometry and mobility testing, all of which revealed variable levels of retained rod function that did not correlate with the patient's age (Jacobson et al., 2013). In contrast, the majority of patients lacked cone sensitivity (FST) which correlated to severely reduced visual acuity and a lack of color perception. FST, microperimetry and mobility tests revealed a small subset had detectable, but reduced cone function with central fixation and some color perception. None of the patients had recordable cone-mediated ERGs (Jacobson et al., 2013).

To better understand these differential cone phenotypes, Jacobson et al. (2013) investigated the activity of patient-specific retGC1 mutants *in vitro*. Their activity was assayed by transfecting cDNA for each form, along with GCAPs in HEK293 cells under appropriate ionic conditions and quantifying the amount of cGMP produced relative to that achieved with wild type retGC1. Of the

patient-specific mutants tested, some exhibited reduced catalytic activity (4–5 fold lower than WT) while others demonstrated no loss of function (Jacobson et al., 2013). Not surprisingly, those mutants that retained biochemical activity were expressed by LCA1 patients with measurable cone function. It is expected that those with normal activity *in vitro* may exhibit defective folding, expression or impaired trafficking to photoreceptor outer segments *in situ*. Investigations are currently underway to understand the fate of these mutants *in vivo* via AAV-mediated expression in GCDKO mice. retGC1 mutants that exhibited no activity *in vitro* corresponded to patients with profound loss of cone function (Jacobson et al., 2013).

WHAT FORM MIGHT A CLINICAL TRIAL FOR *GUCY2D*-LCA1 TAKE?

A few important choices must be made prior to clinical application of a gene replacement therapy for LCA1. These include the injection route and location, AAV serotype and promoter, and therapeutic endpoints. Route and location of injection should be dictated by the calculated risk(s)/benefit. The structural integrity of the patient's retina and locus of existing vision must be considered. Evidence suggests *GUCY2D*-LCA1 is unlike any form of LCA studied in detail to date (Jacobson et al., 1998, 2003, 2005, 2007a,b, 2009b, 2011; Cideciyan et al., 2007). Their hallmark retinal preservation suggests that LCA1 patients may be good candidates for subretinal injection of AAV-*GUCY2D* (Simonelli et al., 2007; Pasadhika et al., 2010; Jacobson et al., 2013). Because retGC1 deficiency leads to profound visual impairment, stemming primarily from cones, the central retina should be the treatment target. In the small subset of patients that exhibit foveal cone losses, para- or peri-foveal areas may be targeted in the hopes that, like some *RPE65*-LCA2 patients, they will develop an eccentric locus of fixation (Cideciyan et al., 2009).

AAV5 and AAV8-based vectors were used in the aforementioned studies for developing a treatment for LCA1. These vectors have proven utility for photoreceptor-targeted therapy following subretinal injection in multiple mouse and dog models of inherited retinal disease (Min et al., 2005; Alexander et al., 2007; Boye et al., 2010, 2013; Gorbatyuk et al., 2010; Komaromy et al., 2010; Mao et al., 2011; Pang et al., 2011, 2012; Yao et al., 2011; Beltran et al., 2012; Petit et al., 2012; Lheriteau et al., 2014). Because AAV transduction profiles and the activity of promoters can vary across species, the final decision should be dictated by the serotype and promoter combination's behavior in a species most closely related to man, non-human primate (NHP). In LCA1, photoreceptors of the central retina are the treatment target. Therefore, serotype and promoter combinations that effectively transduce cone photoreceptors in NHP are required. Transduction of both AAV5 and AAV8 vectors have recently been described in subretinally injected NHP (Boye et al., 2012; Vandenberghe et al., 2013). Only partial cone transduction was achieved following subretinal delivery of elevated doses of AAV8 containing the ubiquitous CMV promoter driving GFP (10^{11} vg delivered; Vandenberghe et al., 2011, 2013). At a lower dose (10^{10} vg delivered), AAV8-CMV-GFP failed to transduce foveal, parafoveal or perifoveal cones (Vandenberghe et al., 2011). In contrast, foveal, parafoveal, perifoveal and peripheral cones of NHP (as well as rods) were all effectively transduced following subretinal delivery of an AAV5 vector containing the photoreceptor-specific hGRK1 promoter (10^{10} vg delivered; Boye et al., 2012). This mirrors earlier findings in rodent that hGRK1 has exclusive activity in cones and rods (Khani et al., 2007; Tan et al., 2009; Boye et al., 2010, 2011; Pawlyk et al., 2010; Sun et al., 2010). Taken together, these results support the use of subretinally delivered AAV5-hGRK1-*GUCY2D* in a clinical setting.

Because LCA1 patients exhibit profound cone-mediated visual impairment and variable levels of rod-mediated vision, typical measures of vision must be supplemented with assays that are more suited to this severe disease. Most patients have nystagmus, making full field ERG recordings difficult. Additionally, because many LCA1 patients have unrecordable ERGs to begin with, it would be impossible to measure any negative treatment-associated changes with this assay. Tests which control for nystagmus such as microperimetry can be used to assess cone-mediated central vision (Cideciyan et al., 2012). Tests such as chromatic FST which was used in the most recent clinical characterization (Jacobson et al., 2013) and in the clinical trial for RPE65-LCA2 (Jacobson et al., 2012) could be used to measure localized improvements in rod function. The limits of variability for this assay have already been defined in patients with various retinal degenerations, including LCA (Roman et al., 2005; Roman et al., 2007; Jacobson et al., 2009a). OCT should be performed to monitor the safety of injections performed under the fovea or para/peri- fovea, with emphasis placed on the former given the slow return of cone outer segment structure observed in LCA2 patients treated subfoveally (Jacobson et al., 2012). The potential effects of amblyopia must also be considered. It is possible that AAV-mediated expression of wild type retGC1 in cones of LCA1 patients will reset their signaling cascade allowing for electrochemical signals to propagate through the retina, but that these signals will not be effectively relayed to the brain. Magnetic resonance imaging studies could be used to confirm the integrity of higher order visual processing pathways prior to treatment. Fully understanding how the brain of an LCA1 patient will accommodate *GUCY2D* gene replacement and whether this will differ depending the patient's mutation and/or level of cone preservation will only be accomplished through a clinical trial.

CONCLUSION

Information gleaned from proof of concept experiments in multiple animal models of retGC1 deficiency have laid the groundwork for development of an AAV-based treatment for *GUCY2D*-LCA1 (Haire et al., 2006; Williams et al., 2006; Boye et al., 2010, 2011; Mihelec et al., 2011). Thorough clinical characterization of patients has provided new insights into the pathophysiology of this severe early onset inherited retinal disease, pointing to the central retina as the target for treatment and highlighting the importance of selecting appropriate outcome measures by which to score therapeutic efficacy in a clinical trial (Jacobson et al., 2013). Studies in NHP have revealed an optimal AAV serotype (AAV5) and promoter (hGRK1) combination for delivery of therapeutic transgene to all cone subclasses and rods (Boye et al., 2012). The majority of genes (13/19) known to account for some form of

LCA, including *GUCY2D*, encode photoreceptor specific proteins (den Hollander et al., 2008; Wang et al., 2009; Estrada-Cuzcano et al., 2011; Sergouniotis et al., 2011; Abu-Safieh et al., 2013). In fact, inherited retinal diseases as a whole are caused primarily by defects in proteins expressed by photoreceptors (Wright et al., 2010), a cell type yet to be targeted by AAV in a clinical setting. Thus, developing a treatment for *GUCY2D*-LCA1 will serve as a framework for other photoreceptor-targeted gene replacement strategies.

ACKNOWLEDGMENT

I would like to thank Sanford L. Boye for his thoughtful critique of this review.

REFERENCES

Abu-Safieh, L., Alrashed, M., Anazi, S., Alkuraya, H., Khan, A. O., Al-Owain, M., et al. (2013). Autozygome-guided exome sequencing in retinal dystrophy patients reveals pathogenetic mutations and novel candidate disease genes. *Genome Res.* 23, 236–247. doi: 10.1101/gr.144105.112

Alexander, J. J., Umino, Y., Everhart, D., Chang, B., Min, S. H., Li, Q., et al. (2007). Restoration of cone vision in a mouse model of achromatopsia. *Nat. Med.* 13, 685–687. doi: 10.1038/nm1596

Baehr, W., Karan, S., Maeda, T., Luo, D. G., Li, S., Bronson, J. D., et al. (2007). The function of guanylate cyclase 1 (GC1) and guanylate cyclase 2 (GC2) in rod and cone photoreceptors. *J. Biol. Chem.* 282, 8837–8847. doi: 10.1074/jbc.M610369200

Bainbridge, J. W., Stephens, C., Parsley, K., Demaison, C., Halfyard, A., Thrasher, A. J., et al. (2001). In vivo gene transfer to the mouse eye using an HIV-based lentiviral vector; efficient long-term transduction of corneal endothelium and retinal pigment epithelium. *Gene Ther.* 8, 1665–1668. doi: 10.1038/sj.gt.3301574

Beltran, W. A., Cideciyan, A. V., Lewin, A. S., Iwabe, S., Khanna, H., Sumaroka, A., et al. (2012). Gene therapy rescues photoreceptor blindness in dogs and paves the way for treating human X-linked retinitis pigmentosa. *Proc. Natl. Acad. Sci. U.S.A.* 109, 2132–2137. doi: 10.1073/pnas.1118847109

Boye, S. E., Alexander, J. J., Boye, S. L., Witherspoon, C. D., Sandefer, K. J., Conlon, T. J., et al. (2012). The human rhodopsin kinase promoter in an AAV5 vector confers rod- and cone-specific expression in the primate retina. *Hum. Gene Ther.* 23, 1101–1115. doi: 10.1089/hum.2012.125

Boye, S. E., Boye, S. L., Pang, J., Ryals, R., Everhart, D., Umino, Y., et al. (2010). Functional and behavioral restoration of vision by gene therapy in the guanylate cyclase-1 (GC1) knockout mouse. *PLoS ONE* 5:e11306. doi: 10.1371/journal.pone.0011306

Boye, S. L., Conlon, T., Erger, K., Ryals, R., Neeley, A., Cossette, T., et al. (2011). Long-term preservation of cone photoreceptors and restoration of cone function by gene therapy in the guanylate cyclase-1 knockout (GC1KO) mouse. *Invest. Ophthalmol. Vis. Sci.* 52, 7098–7108. doi: 10.1167/iovs.11-7867

Boye, S. L., Peshenko, I. V., Huang, W. C., Min, S. H., McDoom, I., Kay, C. N., et al. (2013). AAV-mediated gene therapy in the guanylate cyclase (RetGC1/RetGC2) double knockout mouse model of Leber congenital amaurosis. *Hum. Gene Ther.* 24, 189–202. doi: 10.1089/hum.2012.193

Cheng, K. M., Shoffner, R. N., Gelatt, K. N., Gum, G. G., Otis, J. S., and Bitgood, J. J. (1980). An autosomal recessive blind mutant in the chicken. *Poult. Sci.* 59, 2179–2181. doi: 10.3382/ps.0592179

Chung, D. C., and Traboulsi, E. I. (2009). Leber congenital amaurosis: clinical correlations with genotypes, gene therapy trials update, and future directions. *J. AAPOS* 13, 587–592. doi: 10.1016/j.jaapos.2009.10.004

Cideciyan, A. V., Aleman, T. S., Boye, S. L., Schwartz, S. B., Kaushal, S., Roman, A. J., et al. (2008). Human gene therapy for RPE65 isomerase deficiency activates the retinoid cycle of vision but with slow rod kinetics. *Proc. Natl. Acad. Sci. U.S.A.* 105, 15112–15117. doi: 10.1073/pnas.0807027105

Cideciyan, A. V., Aleman, T. S., Jacobson, S. G., Khanna, H., Sumaroka, A., Aguirre, G. K., et al. (2007). Centrosomal-ciliary gene CEP290/NPHP6 mutations result in blindness with unexpected sparing of photoreceptors and visual brain: implications for therapy of Leber congenital amaurosis. *Hum. Mutat.* 28, 1074–1083. doi: 10.1002/humu.20565

Cideciyan, A. V., Hauswirth, W. W., Aleman, T. S., Kaushal, S., Schwartz, S. B., Boye, S. L., et al. (2009). Human RPE65 gene therapy for Leber congenital amaurosis: persistence of early visual improvements and safety at 1 year. *Hum. Gene Ther.* 20, 999–1004. doi: 10.1089/hum.2009.086

Cideciyan, A. V., Swider, M., Aleman, T. S., Feuer, W. J., Schwartz, S. B., Russell, R. C., et al. (2012). Macular function in macular degenerations: repeatability of microperimetry as a potential outcome measure for ABCA4-associated retinopathy trials. *Invest. Ophthalmol. Vis. Sci.* 53, 841–852. doi: 10.1167/iovs.11-8415

Coleman, J. E., and Semple-Rowland, S. L. (2005). GC1 deletion prevents light-dependent arrestin translocation in mouse cone photoreceptor cells. *Invest. Ophthalmol. Vis. Sci.* 46, 12–16. doi: 10.1167/iovs.04-0691

Coleman, J. E., Zhang, Y., Brown, G. A., and Semple-Rowland, S. L. (2004). Cone cell survival and downregulation of GCAP1 protein in the retinas of GC1 knockout mice. *Invest. Ophthalmol. Vis. Sci.* 45, 3397–3403. doi: 10.1167/iovs.04-0392

den Hollander, A. I., Roepman, R., Koenekoop, R. K., and Cremers, F. P. (2008). Leber congenital amaurosis: genes, proteins and disease mechanisms. *Prog. Retin. Eye Res.* 27, 391–419. doi: 10.1016/j.preteyeres.2008.05.003

Dizhoor, A. M., Lowe, D. G., Olshevskaya, E. V., Laura, R. P., and Hurley, J. B. (1994). The human photoreceptor membrane guanylyl cyclase, RetGC, is present in outer segments and is regulated by calcium and a soluble activator. *Neuron* 12, 1345–1352. doi: 10.1016/0896-6273(94)90449-9

Douglas, R. M., Alam, N. M., Silver, B. D., McGill, T. J., Tschetter, W. W., and Prusky, G. T. (2005). Independent visual threshold measurements in the two eyes of freely moving rats and mice using a virtual-reality optokinetic system. *Vis. Neurosci.* 22, 677–684. doi: 10.1017/S0952523805225166

Estrada-Cuzcano, A., Koenekoop, R. K., Coppieters, F., Kohl, S., Lopez, I., Collin, R. W., et al. (2011). IQCB1 mutations in patients with leber congenital amaurosis. *Invest. Ophthalmol. Vis. Sci.* 52, 834–839. doi: 10.1167/iovs.10-5221

Goraczniak, R., Duda, T., and Sharma, R. K. (1997). Structural and functional characterization of a second subfamily member of the calcium-modulated bovine rod outer segment membrane guanylate cyclase, ROS-GC2. *Biochem. Biophys. Res. Commun.* 234, 666–670. doi: 10.1006/bbrc.1997.6579

Goraczniak, R. M., Duda, T., Sitaramayya, A., and Sharma, R. K. (1994). Structural and functional characterization of the rod outer segment membrane guanylate cyclase. *Biochem. J.* 302(Pt 2), 455–461.

Gorbatyuk, M. S., Knox, T., LaVail, M. M., Gorbatyuk, O. S., Noorwez, S. M., Hauswirth, W. W., et al. (2010). Restoration of visual function in P23H rhodopsin transgenic rats by gene delivery of BiP/Grp78. *Proc. Natl. Acad. Sci. U.S.A.* 107, 5961–5966. doi: 10.1073/pnas.0911991107

Haeseleer, F., Sokal, I., Li, N., Pettenati, M., Rao, N., Bronson, D., et al. (1999). Molecular characterization of a third member of the guanylyl cyclase-activating protein subfamily. *J. Biol. Chem.* 274, 6526–6535. doi: 10.1074/jbc.274.10.6526

Haire, S. E., Pang, J., Boye, S. L., Sokal, I., Craft, C. M., Palczewski, K., et al. (2006). Light-driven cone arrestin translocation in cones of postnatal guanylate cyclase-1 knockout mouse retina treated with AAV-GC1. *Invest. Ophthalmol. Vis. Sci.* 47, 3745–3753. doi: 10.1167/iovs.06-0086

Hanein, S., Perrault, I., Gerber, S., Tanguy, G., Barbet, F., Ducroq, D., et al. (2004). Leber congenital amaurosis: comprehensive survey of the genetic heterogeneity, refinement of the clinical definition, and genotype-phenotype correlations as a strategy for molecular diagnosis. *Hum. Mutat.* 23, 306–317. doi: 10.1002/humu.20010

Hwang, J. Y., Lange, C., Helten, A., Hoppner-Heitmann, D., Duda, T., Sharma, R. K., et al. (2003). Regulatory modes of rod outer segment membrane guanylate cyclase differ in catalytic efficiency and Ca(2+)-sensitivity. *Eur. J. Biochem.* 270, 3814–3821. doi: 10.1046/j.1432-1033.2003.03770.x

Imanishi, Y., Yang, L., Sokal, I., Filipek, S., Palczewski, K., and Baehr, W. (2004). Diversity of guanylate cyclase-activating proteins (GCAPs) in teleost fish: characterization of three novel GCAPs (GCAP4, GCAP5, GCAP7) from zebrafish (Danio rerio) and prediction of eight GCAPs (GCAP1-8) in pufferfish (Fugu rubripes). *J. Mol. Evol.* 59, 204–217. doi: 10.1007/s00239-004-2614-y

Jacobson, S. G., Aleman, T. S., Cideciyan, A. V., Roman, A. J., Sumaroka, A., Windsor, E. A., et al. (2009a). Defining the residual vision in leber congenital amaurosis

caused by RPE65 mutations. *Invest. Ophthalmol. Vis. Sci.* 50, 2368–2375. doi: 10.1167/iovs.08-2696

Jacobson, S. G., Aleman, T. S., Cideciyan, A. V., Sumaroka, A., Schwartz, S. B., Windsor, E. A., et al. (2009b). Leber congenital amaurosis caused by Lebercilin (LCA5) mutation: retained photoreceptors adjacent to retinal disorganization. *Mol. Vis.* 15, 1098–1106.

Jacobson, S. G., Aleman, T. S., Cideciyan, A. V., Sumaroka, A., Schwartz, S. B., Windsor, E. A., et al. (2005). Identifying photoreceptors in blind eyes caused by RPE65 mutations: prerequisite for human gene therapy success. *Proc. Natl. Acad. Sci. U.S.A.* 102, 6177–6182. doi: 10.1073/pnas.0500646102

Jacobson, S. G., Cideciyan, A. V., Aleman, T. S., Pianta, M. J., Sumaroka, A., Schwartz, S. B., et al. (2003). Crumbs homolog 1 (CRB1) mutations result in a thick human retina with abnormal lamination. *Hum. Mol. Genet.* 12, 1073–1078. doi: 10.1093/hmg/ddg117

Jacobson, S. G., Cideciyan, A. V., Aleman, T. S., Sumaroka, A., Roman, A. J., Swider, M., et al. (2011). Human retinal disease from AIPL1 gene mutations: foveal cone loss with minimal macular photoreceptors and rod function remaining. *Invest. Ophthalmol. Vis. Sci.* 52, 70–79. doi: 10.1167/iovs.10-6127

Jacobson, S. G., Cideciyan, A. V., Aleman, T. S., Sumaroka, A., Schwartz, S. B., Roman, A. J., et al. (2007a). Leber's congenital amaurosis caused by an RPGRIP1 mutation shows treatment potential. *Ophthalmology* 114, 895–898. doi: 10.1016/j.ophtha.2006.10.028

Jacobson, S. G., Cideciyan, A. V., Aleman, T. S., Sumaroka, A., Schwartz, S. B., Windsor, E. A., et al. (2007b). RDH12 and RPE65, visual cycle genes causing leber congenital amaurosis, differ in disease expression. *Invest. Ophthalmol. Vis. Sci.* 48, 332–338. doi: 10.1167/iovs.06-0599

Jacobson, S. G., Cideciyan, A. V., Huang, Y., Hanna, D. B., Freund, C. L., Affatigato, L. M., et al. (1998). Retinal degenerations with truncation mutations in the cone-rod homeobox (CRX) gene. *Invest. Ophthalmol. Vis. Sci.* 39, 2417–2426.

Jacobson, S. G., Cideciyan, A. V., Peshenko, I. V., Sumaroka, A., Olshevskaya, E. V., Cao, L., et al. (2013). Determining consequences of retinal membrane guanylyl cyclase (RetGC1) deficiency in human Leber congenital amaurosis en route to therapy: residual cone-photoreceptor vision correlates with biochemical properties of the mutants. *Hum. Mol. Genet.* 22, 168–183. doi: 10.1093/hmg/dds421

Jacobson, S. G., Cideciyan, A. V., Ratnakaram, R., Heon, E., Schwartz, S. B., Roman, A. J., et al. (2012). Gene therapy for leber congenital amaurosis caused by RPE65 mutations: safety and efficacy in 15 children and adults followed up to 3 years. *Arch. Ophthalmol.* 130, 9–24. doi: 10.1001/archophthalmol.2011.298

Karan, S., Frederick, J. M., and Baehr, W. (2010). Novel functions of photoreceptor guanylate cyclases revealed by targeted deletion. *Mol. Cell. Biochem.* 334, 141–155. doi: 10.1007/s11010-009-0322-z

Khani, S. C., Pawlyk, B. S., Bulgakov, O. V., Kasperek, E., Young, J. E., Adamian, M., et al. (2007). AAV-mediated expression targeting of rod and cone photoreceptors with a human rhodopsin kinase promoter. *Invest. Ophthalmol. Vis. Sci.* 48, 3954–3961. doi: 10.1167/iovs.07-0257

Koch, K. W., and Stryer, L. (1988). Highly cooperative feedback control of retinal rod guanylate cyclase by calcium ions. *Nature* 334, 64–66. doi: 10.1038/334064a0

Komaromy, A. M., Alexander, J. J., Rowlan, J. S., Garcia, M. M., Chiodo, V. A., Kaya, A., et al. (2010). Gene therapy rescues cone function in congenital achromatopsia. *Hum. Mol. Genet.* 19, 2581–2593. doi: 10.1093/hmg/ddq136

Lheriteau, E., Petit, L., Weber, M., Le Meur, G., Deschamps, J.-Y., Libeau, L., et al. (2014). Successful gene therapy in the RPGRIP1-deficient dog: a large model of cone-rod dystrophy. *Mol. Ther.* 22, 265–277. doi: 10.1038/mt.2013.232

Lipinski, D. M., Barnard, A. R., Charbel Issa, P., Singh, M. S., De Silva, S. R., Trabalza, A., et al. (2014). Vesicular stomatitis virus glycoprotein- and venezuelan equine encephalitis virus-derived glycoprotein-pseudotyped lentivirus vectors differentially transduce corneal endothelium, trabecular meshwork, and human photoreceptors. *Hum. Gene Ther.* 25, 50–62. doi: 10.1089/hum.2013.009

Lowe, D. G., Dizhoor, A. M., Liu, K., Gu, Q., Spencer, M. R., Laura, L., et al. (1995). Cloning and expression of a second photoreceptor-specific membrane retina guanylyl cyclase (RetGC), RetGC-2. *Proc. Natl. Acad. Sci. U.S.A.* 92, 5535–5539. doi: 10.1073/pnas.92.12.5535

Mao, H., James, T. Jr., Schwein, A., Shabashvili, A. E., Hauswirth, W. W., Gorbatyuk, M. S., et al. (2011). AAV delivery of wild-type rhodopsin preserves retinal function in a mouse model of autosomal dominant retinitis pigmentosa. *Hum. Gene Ther.* 22, 567–575. doi: 10.1089/hum.2010.140

Margulis, A., Goraczniak, R. M., Duda, T., Sharma, R. K., and Sitaramayya, A. (1993). Structural and biochemical identity of retinal rod outer segment membrane guanylate cyclase. *Biochem. Biophys. Res. Commun.* 194, 855–861. doi: 10.1006/bbrc.1993.1900

Mihelec, M., Pearson, R. A., Robbie, S. J., Buch, P. K., Azam, S. A., Bainbridge, J. W., et al. (2011). Long-term preservation of cones and improvement in visual function following gene therapy in a mouse model of leber congenital amaurosis caused by guanylate cyclase-1 deficiency. *Hum. Gene Ther.* 22, 1179–1190. doi: 10.1089/hum.2011.069

Milam, A. H., Barakat, M. R., Gupta, N., Rose, L., Aleman, T. S., Pianta, M. J., et al. (2003). Clinicopathologic effects of mutant GUCY2D in Leber congenital amaurosis. *Ophthalmology* 110, 549–558. doi: 10.1016/S0161-6420(02)01757-8

Min, S. H., Molday, L. L., Seeliger, M. W., Dinculescu, A., Timmers, A. M., Janssen, A., et al. (2005). Prolonged recovery of retinal structure/function after gene therapy in an Rs1h-deficient mouse model of x-linked juvenile retinoschisis. *Mol. Ther.* 12, 644–651. doi: 10.1016/j.ymthe.2005.06.002

Miyoshi, H., Takahashi, M., Gage, F. H., and Verma, I. M. (1997). Stable and efficient gene transfer into the retina using an HIV-based lentiviral vector. *Proc. Natl. Acad. Sci. U.S.A.* 94, 10319–10323. doi: 10.1073/pnas.94.19.10319

Olshevskaya, E. V., Calvert, P. D., Woodruff, M. L., Peshenko, I. V., Savchenko, A. B., Makino, C. L., et al. (2004). The Y99C mutation in guanylyl cyclase-activating protein 1 increases intracellular Ca^{2+} and causes photoreceptor degeneration in transgenic mice. *J. Neurosci.* 24, 6078–6085. doi: 10.1523/JNEUROSCI.0963-04.2004

Olshevskaya, E. V., Peshenko, I. V., Savchenko, A. B., and Dizhoor, A. M. (2012). Retinal guanylyl cyclase isozyme 1 is the preferential in vivo target for constitutively active GCAP1 mutants causing congenital degeneration of photoreceptors. *J. Neurosci.* 32, 7208–7217. doi: 10.1523/JNEUROSCI.0976-12.2012

Palczewski, K., Subbaraya, I., Gorczyca, W. A., Helekar, B. S., Ruiz, C. C., Ohguro, H., et al. (1994). Molecular cloning and characterization of retinal photoreceptor guanylyl cyclase-activating protein. *Neuron* 13, 395–404. doi: 10.1016/0896-6273(94)90355-7

Pang, J., Cheng, M., Haire, S. E., Barker, E., Planelles, V., and Blanks, J. C. (2006). Efficiency of lentiviral transduction during development in normal and rd mice. *Mol. Vis.* 12, 756–767.

Pang, J. J., Dai, X., Boye, S. E., Barone, I., Boye, S. L., Mao, S., et al. (2011). Long-term retinal function and structure rescue using capsid mutant AAV8 vector in the rd10 mouse, a model of recessive retinitis pigmentosa. *Mol. Ther.* 19, 234–242. doi: 10.1038/mt.2010.273

Pang, J. J., Deng, W. T., Dai, X., Lei, B., Everhart, D., Umino, Y., et al. (2012). AAV-mediated cone rescue in a naturally occurring mouse model of CNGA3-achromatopsia. *PLoS ONE* 7:e35250. doi: 10.1371/journal.pone.0035250

Pasadhika, S., Fishman, G. A., Stone, E. M., Lindeman, M., Zelkha, R., Lopez, I., et al. (2010). Differential macular morphology in patients with RPE65-, CEP290-, GUCY2D-, and AIPL1-related Leber congenital amaurosis. *Invest. Ophthalmol. Vis. Sci.* 51, 2608–2614. doi: 10.1167/iovs.09-3734

Pawlyk, B. S., Bulgakov, O. V., Liu, X., Xu, X., Adamian, M., Sun, X., et al. (2010). Replacement gene therapy with a human RPGRIP1 sequence slows photoreceptor degeneration in a murine model of Leber congenital amaurosis. *Hum. Gene Ther.* 21, 993–1004. doi: 10.1089/hum.2009.218

Perrault, I., Rozet, J. M., Calvas, P., Gerber, S., Camuzat, A., Dollfus, H., et al. (1996). Retinal-specific guanylate cyclase gene mutations in Leber's congenital amaurosis. *Nat. Genet.* 14, 461–464. doi: 10.1038/ng1296-461

Perrault, I., Rozet, J. M., Gerber, S., Ghazi, I., Ducroq, D., Souied, E., et al. (2000). Spectrum of retGC1 mutations in Leber's congenital amaurosis. *Eur. J. Hum. Genet.* 8, 578–582. doi: 10.1038/sj.ejhg.5200503

Perrault, I., Rozet, J. M., Gerber, S., Ghazi, I., Leowski, C., Ducroq, D., et al. (1999a). Leber congenital amaurosis. *Mol. Genet. Metab.* 68, 200–208. doi: 10.1006/mgme.1999.2906

Perrault, I., Rozet, J. M., Ghazi, I., Leowski, C., Bonnemaison, M., Gerber, S., et al. (1999b). Different functional outcome of RetGC1 and RPE65 gene mutations in Leber congenital amaurosis. *Am. J. Hum. Genet.* 64, 1225–1228. doi: 10.1086/302335

Peshenko, I. V., and Dizhoor, A. M. (2004). Guanylyl cyclase-activating proteins (GCAPs) are Ca^{2+}/Mg^{2+} sensors: implications for photoreceptor guanylyl cyclase (RetGC) regulation in mammalian photoreceptors. *J. Biol. Chem.* 279, 16903–16906. doi: 10.1074/jbc.C400065200

Peshenko, I. V., and Dizhoor, A. M. (2006). Ca^{2+} and Mg^{2+} binding properties of GCAP-1. Evidence that Mg^{2+}-bound form is the physiological activator of photoreceptor guanylyl cyclase. *J. Biol. Chem.* 281, 23830–23841. doi: 10.1074/jbc.M600257200

Peshenko, I. V., Olshevskaya, E. V., Savchenko, A. B., Karan, S., Palczewski, K., Baehr, W., et al. (2011). Enzymatic properties and regulation of the native isozymes of retinal membrane guanylyl cyclase (RetGC) from mouse photoreceptors. *Biochemistry* 50, 5590–5600. doi: 10.1021/bi200491b

Petit, L., Lhériteau, E., Weber, M., Le Meur, G., Deschamps, J.-Y., Provost, N., et al. (2012). Restoration of vision in the pde6beta-deficient dog, a large animal model of rod-cone dystrophy. *Mol. Ther.* 20, 2019–2030. doi: 10.1038/mt.2012.134

Polans, A., Baehr, W., and Palczewski, K. (1996). Turned on by Ca^{2+}! The physiology and pathology of Ca(2+)-binding proteins in the retina. *Trends Neurosci.* 19, 547–554. doi: 10.1016/S0166-2236(96)10059-X

Porto, F. B., Perrault, I., Hicks, D., Rozet, J. M., Hanoteau, N., Hanein, S., et al. (2003). Prenatal human ocular degeneration occurs in Leber's Congenital Amaurosis (LCA1 and 2). *Adv. Exp. Med. Biol.* 533, 59–68. doi: 10.1007/978-1-4615-0067-4_8

Pugh, E. N. Jr., Duda, T., Sitaramayya, A., and Sharma, R. K. (1997). Photoreceptor guanylate cyclases: a review. *Biosci. Rep.* 17, 429–473. doi: 10.1023/A:1027365520442

Roman, A. J., Cideciyan, A. V., Aleman, T. S., and Jacobson, S. G. (2007). Full-field stimulus testing (FST) to quantify visual perception in severely blind candidates for treatment trials. *Physiol. Meas.* 28, N51–N56. doi: 10.1088/0967-3334/28/8/N02

Roman, A. J., Schwartz, S. B., Aleman, T. S., Cideciyan, A. V., Chico, J. D., Windsor, E. A., et al. (2005). Quantifying rod photoreceptor-mediated vision in retinal degenerations: dark-adapted thresholds as outcome measures. *Exp. Eye Res.* 80, 259–272. doi: 10.1016/j.exer.2004.09.008

Semple-Rowland, S. L., Lee, N. R., Van Hooser, J. P., Palczewski, K., and Baehr, W. (1998). A null mutation in the photoreceptor guanylate cyclase gene causes the retinal degeneration chicken phenotype. *Proc. Natl. Acad. Sci. U.S.A.* 95, 1271–1276. doi: 10.1073/pnas.95.3.1271

Sergouniotis, P. I., Davidson, A. E., Mackay, D. S., Li, Z., Yang, X., Plagnol, V., et al. (2011). Recessive mutations in KCNJ13, encoding an inwardly rectifying potassium channel subunit, cause leber congenital amaurosis. *Am. J. Hum. Genet.* 89, 183–190. doi: 10.1016/j.ajhg.2011.06.002

Shyjan, A. W., de Sauvage, F. J., Gillett, N. A., Goeddel, D. V., and Lowe, D. G. (1992). Molecular cloning of a retina-specific membrane guanylyl cyclase. *Neuron* 9, 727–737. doi: 10.1016/0896-6273(92)90035-C

Simonelli, F., Ziviello, C., Testa, F., Rossi, S., Fazzi, E., Bianchi, P. E., et al. (2007). Clinical and molecular genetics of Leber's congenital amaurosis: a multicenter study of Italian patients. *Invest. Ophthalmol. Vis. Sci.* 48, 4284–4290. doi: 10.1167/iovs.07-0068

Sun, X., Pawlyk, B., Xu, X., Liu, X., Bulgakov, O. V., Adamian, M., et al. (2010). Gene therapy with a promoter targeting both rods and cones rescues retinal degeneration caused by AIPL1 mutations. *Gene Ther.* 17, 117–131. doi: 10.1038/gt.2009.104

Tan, M. H., Smith, A. J., Pawlyk, B., Xu, X., Liu, X., Bainbridge, J. B., et al. (2009). Gene therapy for retinitis pigmentosa and Leber congenital amaurosis caused by defects in AIPL1: effective rescue of mouse models of partial and complete Aipl1 deficiency using AAV2/2 and AAV2/8 vectors. *Hum. Mol. Genet.* 18, 2099–2114. doi: 10.1093/hmg/ddp133

Timmers, A. M., Zhang, H., Squitieri, A., and Gonzalez-Pola, C. (2001). Subretinal injections in rodent eyes: effects on electrophysiology and histology of rat retina. *Mol. Vis.* 7, 131–137.

Ulshafer, R. J., and Allen, C. B. (1985a). Hereditary retinal degeneration in the Rhode Island Red chicken: ultrastructural analysis. *Exp. Eye Res.* 40, 865–877. doi: 10.1016/0014-4835(85)90131-9

Ulshafer, R. J., and Allen, C. B. (1985b). Ultrastructural changes in the retinal pigment epithelium of congenitally blind chickens. *Curr. Eye Res.* 4, 1009–1021. doi: 10.3109/02713688509003346

Ulshafer, R. J., Allen, C., Dawson, W. W., and Wolf, E. D. (1984). Hereditary retinal degeneration in the Rhode Island Red chicken. I. Histology and ERG. *Exp. Eye Res.* 39, 125–135. doi: 10.1016/0014-4835(84)90003-4

Vandenberghe, L. H., Bell, P., Maguire, A. M., Cearley, C. N., Xiao, R., Calcedo, R., et al. (2011). Dosage thresholds for AAV2 and AAV8 photoreceptor gene therapy in monkey. *Sci. Transl. Med.* 3:88ra54. doi: 10.1126/scitranslmed.3002103

Vandenberghe, L. H., Bell, P., Maguire, A. M., Xiao, R., Hopkins, T. B., Grant, R., et al. (2013). AAV9 targets cone photoreceptors in the nonhuman primate retina. *PLoS ONE* 8:e53463. doi: 10.1371/journal.pone.0053463

Verrier, J. D., Madorsky, I., Coggin, W. E., Geesey, M., Hochman, M., Walling, E., et al. (2011). Bicistronic lentiviruses containing a viral 2A cleavage sequence reliably co-express two proteins and restore vision to an animal model of LCA1. *PLoS ONE* 6:e20553. doi: 10.1371/journal.pone.0020553

Wallman, J., and Velez, J. (1985). Directional asymmetries of optokinetic nystagmus: developmental changes and relation to the accessory optic system and to the vestibular system. *J. Neurosci.* 5, 317–329.

Wang, H., den Hollander, A. I., Moayedi, Y., Abulimiti, A., Li, Y., Collin, R. W., et al. (2009). Mutations in SPATA7 cause Leber congenital amaurosis and juvenile retinitis pigmentosa. *Am. J. Hum. Genet.* 84, 380–387. doi: 10.1016/j.ajhg.2009.02.005

Williams, G. A., and Jacobs, G. H. (2007). Cone-based vision in the aging mouse. *Vision Res.* 47, 2037–2046. doi: 10.1016/j.visres.2007.03.023

Williams, M. L., Coleman, J. E., Haire, S. E., Aleman, T. S., Cideciyan, A. V., Sokal, I., et al. (2006). Lentiviral expression of retinal guanylate cyclase-1 (RetGC1) restores vision in an avian model of childhood blindness. *PLoS Med.* 3:e30201. doi: 10.1371/journal.pmed.0030201

Wright, A. F., Chakarova, C. F., Abd El-Aziz, M. M., and Bhattacharya, S. S. (2010). Photoreceptor degeneration: genetic and mechanistic dissection of a complex trait. *Nat. Rev. Genet.* 11, 273–284. doi: 10.1038/nrg2717

Yang, G. S., Schmidt, M., Yan, Z., Lindbloom, J. D., Harding, T. C., Donahue, B. A., et al. (2002). Virus-mediated transduction of murine retina with adeno-associated virus: effects of viral capsid and genome size. *J. Virol.* 76, 7651–7660. doi: 10.1128/JVI.76.15.7651-7660.2002

Yang, R. B., Foster, D. C., Garbers, D. L., and Fulle, H. J. (1995). Two membrane forms of guanylyl cyclase found in the eye. *Proc. Natl. Acad. Sci. U.S.A.* 92, 602–606. doi: 10.1073/pnas.92.2.602

Yang, R. B., Robinson, S. W., Xiong, W. H., Yau, K. W., Birch, D. G., and Garbers, D. L. (1999). Disruption of a retinal guanylyl cyclase gene leads to cone-specific dystrophy and paradoxical rod behavior. *J. Neurosci.* 19, 5889–5897.

Yao, J., Feathers, K. L., Khanna, H., Thompson, D., Tsilfidis, C., Hauswirth, W. W., et al. (2011). XIAP therapy increases survival of transplanted rod precursors in a degenerating host retina. *Invest. Ophthalmol. Vis. Sci.* 52, 1567–1572. doi: 10.1167/iovs.10-5998

Yzer, S., Leroy, B. P., De Baere, E., de Ravel, T. J., Zonneveld, M. N., Voesenek, K., et al. (2006). Microarray-based mutation detection and phenotypic characterization of patients with Leber congenital amaurosis. *Invest. Ophthalmol. Vis. Sci.* 47, 1167–1176. doi: 10.1167/iovs.05-0848

Conflict of Interest Statement: Shannon E. Boye is a co-inventor on US patent # 61/327,521 which covers some aspects of the material discussed within.

Received: 30 January 2014; accepted: 26 April 2014; published online: 14 May 2014.
*Citation: Boye SE (2014) Insights gained from gene therapy in animal models of retGC1 deficiency. Front. Mol. Neurosci. **7**:43. doi: 10.3389/fnmol.2014.00043*
This article was submitted to the journal Frontiers in Molecular Neuroscience.

frontiers in
MOLECULAR NEUROSCIENCE

REVIEW ARTICLE
published: 07 April 2014
doi: 10.3389/fnmol.2014.00025

RNA interference gene therapy in dominant retinitis pigmentosa and cone-rod dystrophy mouse models caused by GCAP1 mutations

***Li Jiang*[1] *, *Jeanne M. Frederick*[1] *and Wolfgang Baehr*[1,2,3] ***

[1] Department of Ophthalmology and Visual Sciences, John A. Moran Eye Center, University of Utah Health Science Center, Salt Lake City, UT, USA
[2] Department of Biology, University of Utah, Salt Lake City, UT, USA
[3] Department of Neurobiology and Anatomy, University of Utah Health Science Center, Salt Lake City, UT, USA

Edited by:
Rameshwar K. Sharma, Salus University, USA

Reviewed by:
Karl-Wilhelm Koch, Carl von Ossietzky University Oldenburg, Germany
James Ames, University of California, Davis, USA
Alexander Dizhoor, Salus University, USA

***Correspondence:**
Li Jiang and Wolfgang Baehr, Department of Ophthalmology and Visual Sciences, John A. Moran Eye Center, University of Utah Health Science Center, 65 Mario Capecchi Drive, Salt Lake City, UT 84132, USA
e-mail: li.jiang@hsc.utah.edu; wbaehr@hsc.utah.edu

RNA interference (RNAi) knockdown is an efficacious therapeutic strategy for silencing genes causative for dominant retinal dystrophies. To test this, we used self-complementary (sc) AAV2/8 vector to develop an RNAi-based therapy in two dominant retinal degeneration mouse models. The allele-specific model expresses transgenic bovine GCAP1(Y99C) establishing a rapid RP-like phenotype, whereas the nonallele-specific model expresses mouse GCAP1(L151F) producing a slowly progressing cone-rod dystrophy (CORD). The late onset GCAP1(L151F)-CORD mimics the dystrophy observed in human GCAP1-CORD patients. Subretinal injection of scAAV2/8 carrying shRNA expression cassettes specific for bovine or mouse guanylate cyclase-activating protein 1 (GCAP1) showed strong expression at 1 week post-injection. In both allele-specific [GCAP1(Y99C)-RP] and nonallele-specific [GCAP1(L151F)-CORD] models of dominant retinal dystrophy, RNAi-mediated gene silencing enhanced photoreceptor survival, delayed onset of degeneration and improved visual function. Such results provide a "proof of concept" toward effective RNAi-based gene therapy mediated by scAAV2/8 for dominant retinal disease based on GCAP1 mutation. Further, nonallele-specific RNAi knockdown of GCAP1 may prove generally applicable toward the rescue of any human GCAP1-based dominant cone-rod dystrophy.

Keywords: photoreceptor guanylate cyclase, guanylate cyclase-activating protein 1, short-hairpin RNA, RNA interference, self-complementary adeno-associated virus, cone-rod dystrophy, *retinitis pigmentosa*

INTRODUCTION

Cone-rod dystrophies constitute a rare (1/40,000 prevalence) and heterogeneous class of hereditary retinal disease (Hamel, 2007). Symptoms of cone-rod dystrophy (CORD) may include photoaversion, attenuation of central visual acuity, achromatopsia, and eventually, extinction of peripheral vision. To date, ten genes are associated with dominant CORD: *PROM1* (Prominin-1), *PRPH2* (Peripherin/rds), *GUCA1A* (GCAP1), *RIMS1* (Regulating Synaptic Membrane Exocytosis), *GUCY2D* (Guanylate Cyclase 1), *AIPL1* (Arylhydrocarbon-Interacting receptor Protein-Like 1), *PITPNM3* (Phosphatidyl Inositol Transfer Membrane-associated family member 3), *UNC119* (Uncoordinated 119 or HRG4), *CRX* (Cone-Rod otX-like photoreceptor homeobox transcription factor), *and SEMA4A* (Semaphorin 4A; RETNET at https://sph.uth.edu/retnet/disease.htm). *GUCA1A*, encoding guanylate cyclase-activating protein 1 (GCAP1), is one of the most fully-characterized dominant CORD genes (Baehr and Palczewski, 2009) and involves about one dozen families with >100 affected members harboring various *GUCA1A* mutations (Jiang et al., 2011).

Guanylate cyclase-activating protein 1 plays a key role in inhibiting photoreceptor guanylate cyclase activity at high free Ca^{2+}, and accelerating guanylate cyclase activity in low free Ca^{2+}. Hydrolysis of cyclic guanosine monophosphate (cGMP) by the phototransduction cascade closes cGMP-gated channels, reducing influx of Ca^{2+} ions (**Figure 1**). Continuous extrusion of Ca^{2+} by the light-insensitive NCKX exchanger lowers cytoplasmic Ca^{2+}, thereby activating GCAP1, and GC and re-establishing dark cGMP levels. In rods, cGMP levels are regulated by two guanylate cyclases (GC1 and GC2; Goraczniak et al., 1994, 1997; Lowe et al., 1995; Duda et al., 1996) and two GCAPs (GCAP1 and GCAP2; Dizhoor et al., 1994, 1995; Palczewski et al., 1994; Gorczyca et al., 1995), while cone phototransduction relies on GC1 and GCAP1 exclusively. The two GCAPs overlap partially in regulating the GCs of rods (Makino et al., 2008; Dizhoor et al., 2010; Peshenko et al., 2011), but with differential signaling modes (Duda et al., 2005, 2012). Both GCAPs contribute to rod recovery after photolysis (Mendez et al., 2001; Howes et al., 2002; Makino et al., 2008, 2012). Germline deletion of both GCAPs renders GC activity in rods and cones Ca^{2+}-insensitive (Mendez et al., 2001). Transgenic GCAP1 could restore normal rod and cone response recovery (Howes et al., 2002; Pennesi et al., 2003).

GCAPs feature four EF hand motifs, of which three (EF2-4) are high-affinity Ca^{2+} binding sites and one (EF1) is inactive (Palczewski et al., 2004; Baehr and Palczewski, 2009). Six missense mutations in GCAP1 associated with autosomal dominant CORD3 are found in EF3 (E89K, Y99C, D100E, D100G, N104K, I107T; Dizhoor et al., 1998; Payne et al., 1998; Sokal et al., 1998; Jiang et al., 2008; Kitiratschky et al., 2009; Kamenarova et al., 2013; Nong et al., 2014). In EF4, only four missense

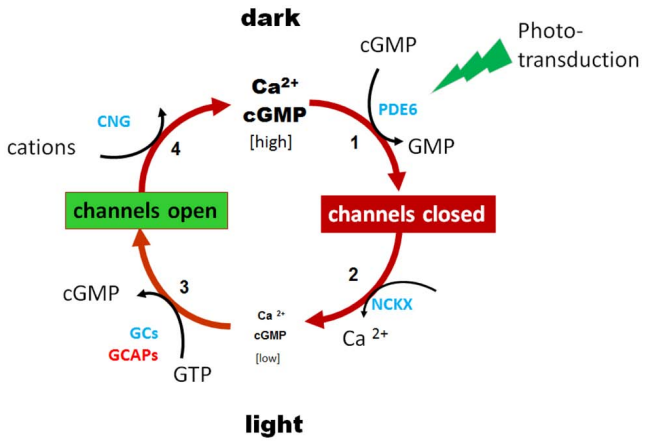

FIGURE 1 | Phototransduction feedback loop regulates levels of cGMP and Ca^{2+}. Dark levels of cGMP and Ca^{2+} are high in rod and cone photoreceptors. Light activation of rhodopsin initiates rod phototransduction, activated PDE6 rapidly hydrolyzes cytoplasmic cGMP, and cGMP-gated cation channels close. Continued extrusion of Ca^{2+} by the light-insensitive Na^{+}-K^{+}/Ca^{2+} exchanger (NCKX) lowers free Ca^{2+} which activates guanylate cyclase-activating proteins (GCAPs) and guanylate cyclases (GCs). Restoration of cGMP dark levels re-opens cation channels and Ca^{2+} levels equilibrate to dark levels.

mutations have been identified (I143NT, L151F, E155G, E155A, G159V; Wilkie et al., 2001; Nishiguchi et al., 2004; Jiang et al., 2005; Sokal et al., 2005; Huang et al., 2013; **Figure 2**). These dominant GCAP1 mutations alter Ca^{2+}-association, decrease Ca^{2+} sensitivity, and produce constitutive activity of photoreceptor GC1 at normal "dark" Ca^{2+} levels. Persistent stimulation of GC1 in the dark increases cGMP to toxic levels. (Dizhoor et al., 1998; Sokal et al., 1998; Woodruff et al., 2007). Elevated

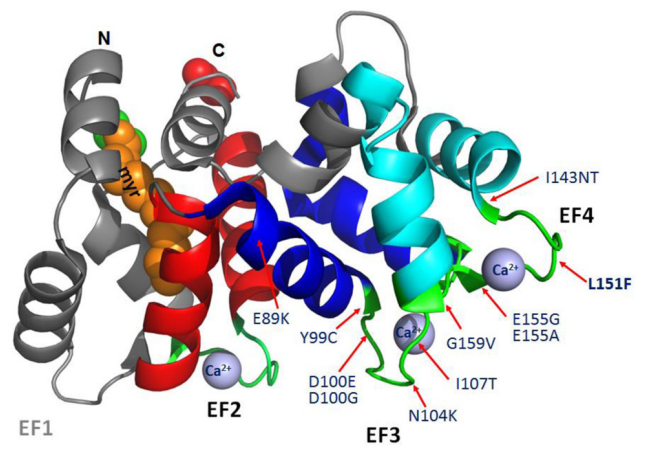

FIGURE 2 | Structure of myristoylated GCAP1 (PDB 2R2I; Baehr and Palczewski, 2009). N, N-terminal. C, C-terminal. EF hand helix-loop-helix structures are shown: EF1 (inactive and gray), EF2 (red), EF3 (dark blue), and EF4 (turquoise). Ca^{2+}-binding loops (green) and approximate positions of relevant missense mutations associated with adCORD (red arrows) are indicated. The N-terminal myristoyl group (orange–brown) is buried and nearly invisible.

levels of cGMP open more CNG channels, elevate free Ca^{2+} in outer segments, and trigger cell death by unknown mechanisms. Elevated Ca^{2+} levels have been suspected to trigger cell death, however a massive accumulation of cGMP in *Cnga3*$^{-/-}$;*Nrl*$^{-/-}$ mice lacking cation channels and elevated Ca^{2+} also correlated with photoreceptor apoptotic death. This result excludes Ca^{2+} as a death trigger and supports a role of cGMP accumulation as the major contributor to cone death and a role cGMP-dependent protein kinase G (PKG) regulation in cell death (Xu et al., 2013).

In a four-generation British family, CORD was mapped to chromosome 6p21.1 (Payne et al., 1998). The disease-causing mutation was identified as Y99C, a change that was absent in over 200 unrelated controls. The same mutation was later identified independently in two ancestrally related families (Downes et al., 2001). The Y99C mutation in GCAP1 has also been reported to cause isolated macular dysfunction (Michaelides et al., 2005). Thus far, families presenting with cone and CORD have been independently linked to a GCAP1(L151F) mutation. In the first family (Sokal et al., 2005), hemeralopia, dyschromatopsia and reduced visual acuity became evident by the second-to-third decades of life with non-recordable photopic ERG responses. In the second pedigree spanning five-generations (Jiang et al., 2005), 11 of 24 individuals displayed photoaversion, color vision defects, and central acuity loss with onset of legal blindness during the second-to-third decades of life. The GCAP1(L151F) gene product, known to disrupt Ca^{2+} coordination at EF-hand four, and alter Ca^{2+} sensitivity (Sokal et al., 2005), represents a conservative substitution.

GCAP1 MUTANT MOUSE MODELS

To study GCAP1-associated retinal degeneration disease, several GCAP1 mouse models have been generated, expressing different GCAP1 mutants. The first generated GCAP1 transgenic mice expressing bovine GCAP1(Y99C) mutant gene displayed severe *retinitis pigmentosa*-like phenotypes as the mutant transgene was specifically expressed in rod photoreceptors under control of a rhodopsin promoter (Olshevskaya et al., 2004). A GCAP1(E155G) knock-in mouse could mimick human patients and presented late-onset and slowly progressive cone-rod photoreceptor degeneration (Buch et al., 2011). Expressing GCAP1(E155G) in mouse rods also caused severe early-onset rod-cone degeneration (Woodruff et al., 2007). Our laboratory generated three transgenic mouse lines expressing wild-type GCAP1-EGFP, as well as mutant GCAP1(L151F), and GCAP1(L151F)-EGFP (Jiang et al., 2013; **Figure 3**). The three transgenes were modified from mouse genomic *Guca1a* gene fragment, containing its native regulatory elements. They are expressed at a level comparable with endogenous GCAP1 in the transgenic mice, and the mutant transgenic mice develop retina pathology slowly and recapitulate features of human CORD (Jiang et al., 2013).

Our aim was to develop first a self-complementary AAV2/8 (scAAV2/8) knockdown virus that expresses an allele-specific short hairpin RNA (shRNA) targeting the mutant *Guca1a* gene in the GCAP1(Y99C) transgenic mice. Further, we intended to target both mutant and native *Guca1a* in GCAP1(L151F)-EGFP transgenic mice (nonallele-specific shRNA targeting). In

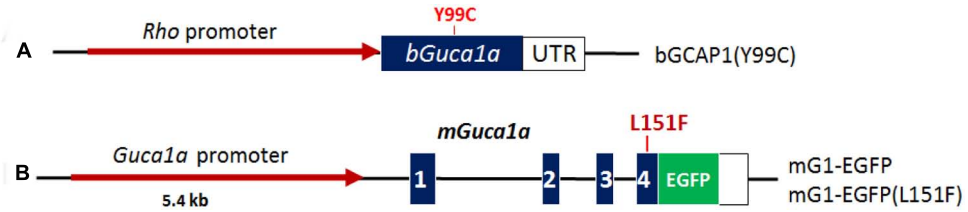

FIGURE 3 | Schematic representation of GCAP1 transgenes used to generate RP and CORD mouse models. (A), bovine GCAP1(Y99C) transgene. Bovine *Guca1a* cDNA (blue) is expressed under the control of the Rho promoter (red). Approximate position of the Y99C mutation in EF3 is indicated (Jiang et al., 2011). **(B)**, mouse GCAP1 transgene under the control of its native promoter (red). Exons (blue) are numbered; the L151F mutation is located in exon 4 and EGFP is fused in-frame to the GCAP1 C-terminus [see **Figure 2** (Jiang et al., 2013)].

the first set, we used two transgenic mouse lines expressing bGCAP1(Y99C) cDNA under the control of the rhodopsin promoter (**Figure 3**). One line expressed GCAP1 at near normal levels and the second line overexpressed GCAP1 (3–4X; Olshevskaya et al., 2004). These lines are models for dominant *retinitis pigmentosa* representing moderate (line L52H) or severe (line L53) retinal degeneration phenotypes (Olshevskaya et al., 2004). An allele-specific knockdown bGCAP1(Y99C) is expected to significantly slow down the dystrophy and even delay onset of degeneration.

The second set of transgenic mice contained the L151F mutation introduced in exon 4 of the *Guca1a* gene. We employed the entire *Guca1a* gene including promoter, all exons and introns, and the 3′-UTR containing the polyadenylation signals. We established two mutant GCAP1 mouse lines, GCAP1(L151F), and GCAP1(L151F)-GFP (**Figure 3**). A third line expressing a GCAP1-EGFP fusion protein (no L151 mutation) served as a WT control (**Figure 3**). The EGFP tag allowed detection of transgene expression by live fluorescence microscopy, and distinction of transgenic GCAP1-EGFP (50 kDa) from native GCAP1 (23 kDa). We

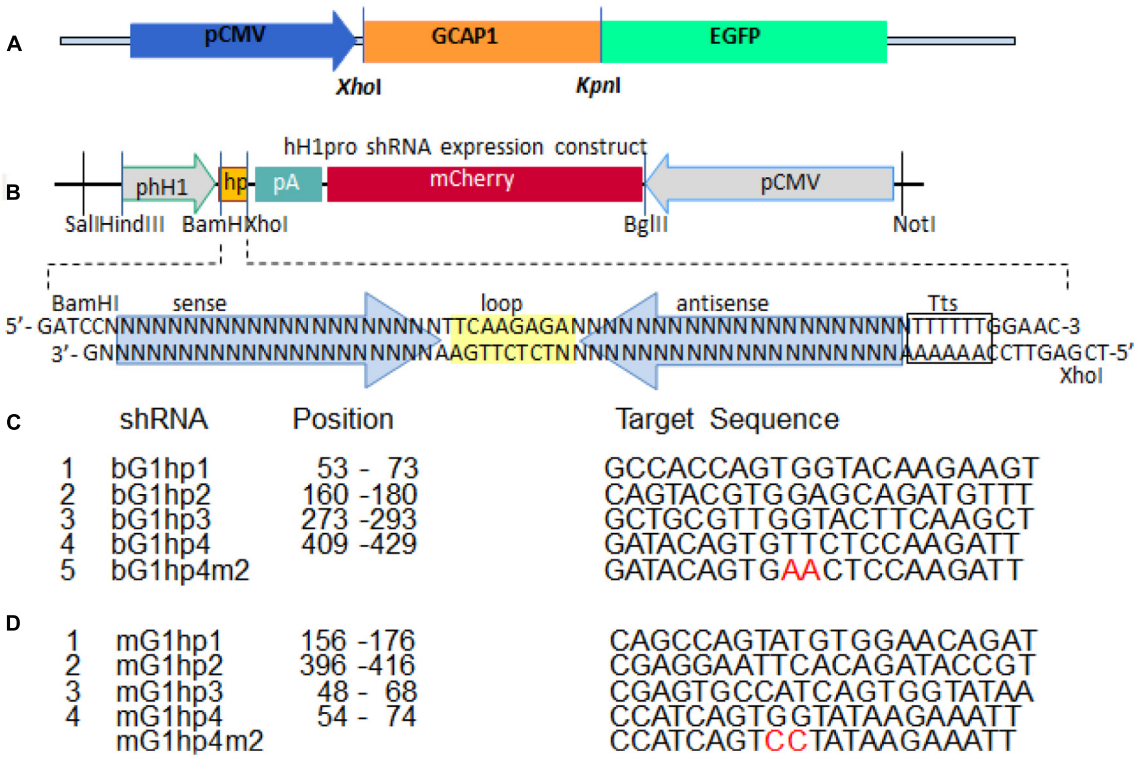

FIGURE 4 | *In vitro* screening strategy to identify a potent shRNA knockdown sequence. (A), a construct expressing the GCAP1-EGFP fusion protein under the control of the CMV promoter. **(B)**, the shRNA expression construct. shRNA (hp yellow box) is under the control of the H1 promoter, and the reporter gene mCherry is under the control of the CMV promoter. Hp consists of a sense-loop-antisense construct (the hairpin). Tts, transcription terminator signal. **(C)**, four candidate shRNAs for suppression of bovine GCAP1, and a 2-nucleotide mismatch control. **(D)**, four candidate shRNAs for suppression of both wild-type and mutant mouse Guca1a mRNA, and a 2-nucleotide mismatch control. See also **Figure 1** (Jiang et al., 2011), and **Figure 6** (Jiang et al., 2013).

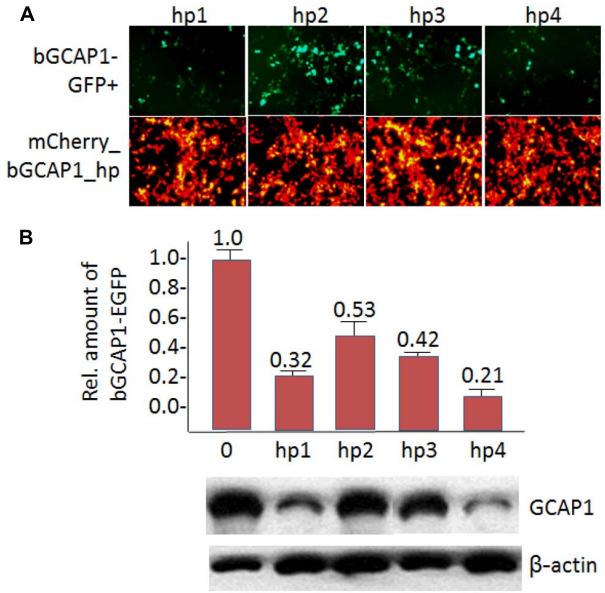

FIGURE 5 | *In vitro* knockdown of bGCAP1-EGFP. (A), *In vitro* transfection of HEK cells expressing bGCAP1-GFP (top) with bG1hp1-4 (bottom). Top panels show that hp1 and hp4 are highly effective. Bottom panels demonstrate fairly uniform transfection of four shRNA expression plasmids. **(B)**, Representative semi-quantitative immunoblot of GCAP1 knockdown. Bar graph (top, $n = 3$) identifies hp4 as the most potent shRNA. See also **Figure 2** (Jiang et al., 2011), and **Figure 7** (Jiang et al., 2013).

intended to knockdown both WT and mutant GCAP1s as removal of photoreceptor GCAP1 does not affect retina development or morphology, and GCAP1/2 double knockout mice do not exhibit retina degeneration.

IN VITRO SCREENING FOR POTENT shRNA SEQUENCES

For successful knockdown via shRNA, it is essential to screen candidate knockdown sequences for specificity and efficacy. We developed an *in vitro* screening strategy consisting of a shRNA expression vector with reporter gene, to be co-expressed with a second vector expressing GCAP1-GFP as a prey (**Figures 4A,B**). This *in vitro* screening system permits the testing of a number of candidates and eventual identification of the most powerful shRNA. The shRNA vector, hH1pro, contained an shRNA expression cassette driven by a human H1 pol-III promoter, and a CMV-driven mCherry reporter gene arranged in a tail-to-tail array (**Figure 4B**). For allele-specific targeting we generated four shRNA constructs, bovine (b) G1hp1-4, expressing four candidate anti-bovine GCAP1 shRNAs specifically targeting b*Guca1a* mRNA (**Figure 4C**). Similarly, we generated four anti-mouse GCAP1 shRNA expression constructs, mG1hp1-4, for nonallele-specific targeting of both transgenic and endogenous mouse GCAP1 mRNAs. (**Figure 4D**).

In HEK293 cell culture, we tested the knockdown efficiencies of four putative bGCAP1 shRNA by cotransfection of each expression construct (bG1hp1-4) with the target bGCAP1-EGFP (**Figure 5A**). The expression levels of bGCAP1-EGFP in the transfected cells were detected by live cell fluorescence microscopy and immunoblotting assay 48–50 h after cotransfection. Under a similar expression level indicating by the mCherry reporter (**Figure 5A**, lower panel), four bGCAP1 shRNA candidates suppressed GCAP1-GFP expression at different efficiencies (**Figure 5A**, upper panel). Among them, bG1hp4 was shown the highest knockdown efficiency, presented by the lowest GFP fluorescence in the cotransfected cell cultures, and 79% reduction of GCAP1-GFP compared to 68, 47, and 58% for other three shRNAs in semi-quantitative immunochemistry assay (**Figure 5B**). By using the same *in vitro*

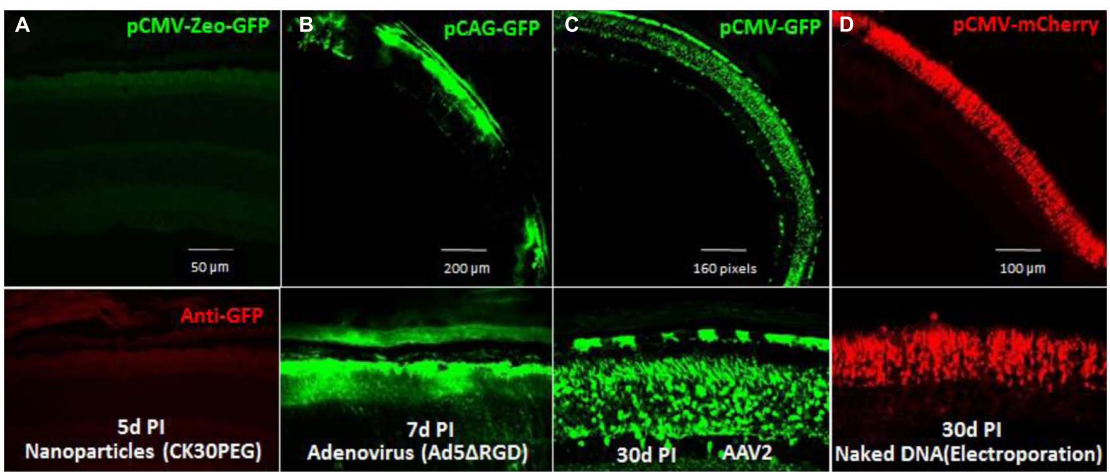

FIGURE 6 | Transduction efficiencies of four gene delivery methods for mouse photoreceptors tested by expression of fluorescent protein reporter. (A), Fluorescence microscopy of retina transverse-sections of mice injected subretinally with pCMV-Zeo-GFP, peptide/polymer nanoparticles. Below, retina section probed with anti-GFP antibody. **(B)**, Fluorescence microscopy of retina transfected with pCAG-GFP using recombinant adenovirus 5, Ad5ΔRGD. Below, section at higher magnification. **(C)**, pCMV-GFP-transfected retina using recombinant AAV vector, AAV2. Underneath, section at higher magnification. **(D)**, pCMV-mCherry-transfected retina using electroporation. Micrographs were recorded at various days post-injection (PI).

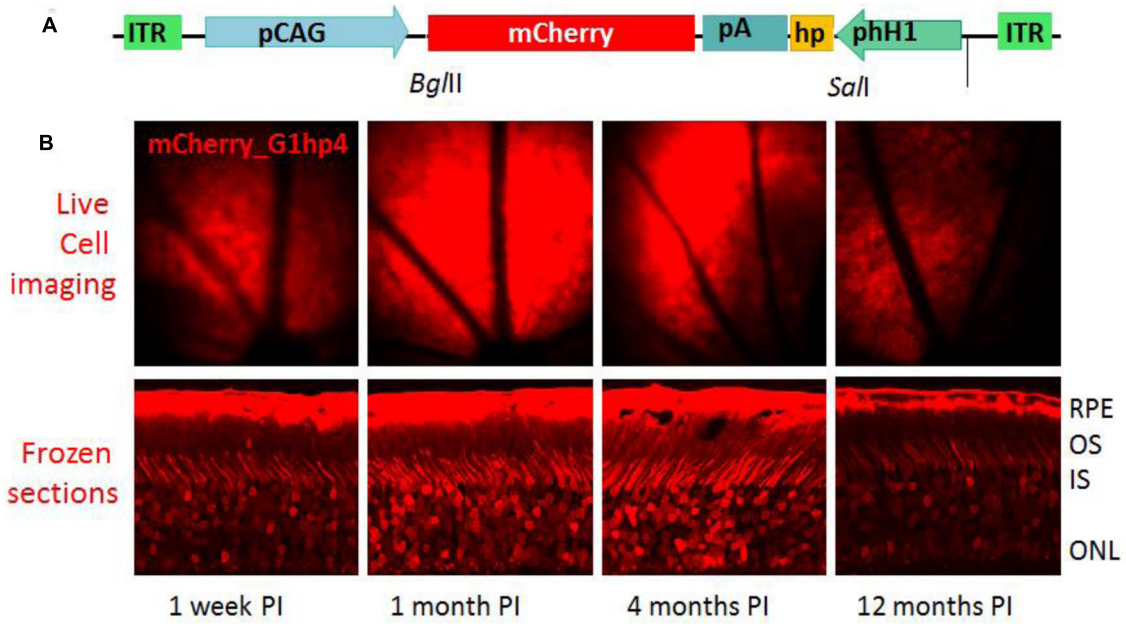

FIGURE 7 | Long-term expression of shRNA *in vivo*. (A), Schematic of scAAV2/8 shuttle vector for anti-bGCAP1 shRNA. ITR, inverted terminal repeats; hH1, human H1 promoter; hp, shRNA cassette; pCAG, chicken actin promoter driving mCherry. **(B)**, Upper panel, *in vivo* fluorescence fundus images of wild-type mice at 1 week and months (indicated) post-subretinal injection of scAAVhp4 viral particles. Lower panel, fluorescence microscopy of corresponding mouse retina transverse cryosections (Jiang et al., 2011). RPE, retinal pigmented epithelium; OS, outer segments; IS, inner segments; ONL, outer nuclear layer.

screening experiment, we demonstrated that among four anti-mouse GCAP1 shRNAs (mG1hp1-4), mG1hp4 is the most efficient, as it deceased mGCAP1-GFP expression by more than 70% in cell culture. Knockdown specificities of bG1hp4 and mG1hp4 were tested with their 2-nucleotide mismatch shRNA controls, bG1hp4m2 and mG1hp4m2. Compared to bG1hp4 and mG1hp4, the respective mismatch controls were unable to suppress expression of co-transfected bGCAP1-GFP and mGCAP1-GFP (**Figure 4**).

GENERATION OF SELF-COMPLEMENTARY ADENO-ASSOCIATED VIRUS

To efficiently express the shRNAs in mouse photoreceptors, we tested four currently used gene delivery vectors: a peptide/polymer nanoparticle (CK30PEG; Farjo et al., 2006), recombinant adenovirus (Ad5ΔRGD; Cashman et al., 2007; Sweigard et al., 2010), recombinant AAV2 (Wu et al., 2006), and electroporation with naked DNA. No GFP reporter gene expression was detected in the CK30PEG-transduced retina (**Figure 6A**), and the Ad5ΔRGD-transduced retina had much more robust GFP expression in RPE cells than in photoreceptors (**Figure 6B**). The AAV2-transduced retina showed the most robust GFP expression in photoreceptors (**Figure 6C**), suggesting AAV vector is a highly efficient gene vector for shRNA delivery to mouse photoreceptors. Although neonatal electroporation of subretinally injected plasmid DNA showed specific and efficient photoreceptor transfection (**Figure 6D**), this method is only useful for undifferentiated and mitotic photoreceptors and is therefore, not applicable for human gene therapy.

Among currently available AAV vectors, the scAAV vector, scAAV2/8, shows the most effective and stable transgene expression in mouse photoreceptors (Natkunarajah et al., 2008). We packaged the shRNA expression cassette with an mCherry reporter into the recombinant viral vector to generate two scAAV2/8 viral constructs expressing shRNAs targeting bovine and mouse GCAP1s, respectively, scAAVbG1hp4 and scAAVmG1hp4. By examining the mCherry reporter expressed in the scAAVbG1hp4-transduced mouse retinas, we demonstrated that scAAV2/8 vector could generate a long-term transgene expression lasting to 1 year (**Figure 7**).

THERAPEUTIC EFFECTS OF KNOCKDOWN VIRUS

To test allele-specific knockdown of GCAP1 *in vivo*, we injected the scAAVbG1hp4 virus into the mouse subretinal space using two different bGCAP1(Y99C) transgenic mouse lines, L53, and L52H. Expression of the mutant bGCAP1(Y99C), but not that of endogenous mouse GCAP1, was significantly suppressed by scAAV2/8-mediated bG1hp4 expression in the retinas of transgenic mice. In the severe and rapid retinal degeneration mouse line L53, bG1hp4 significantly delayed photoreceptor cell death, which was observed at 30 and 45 days post-injection. With the moderate retinal degeneration line L52H, we demonstrated a long-term therapeutic effect of scAAVbG1hp4 virus from 1 month up to 11 months post-injection, assayed by retinal morphology (**Figure 8A**) and function (**Figures 8B,C**).

As deletion of GCAPs in mouse apparently has no detrimental morphological nor disease-causing defect, except for increased sensitivity and delayed recovery from the dark state (Mendez

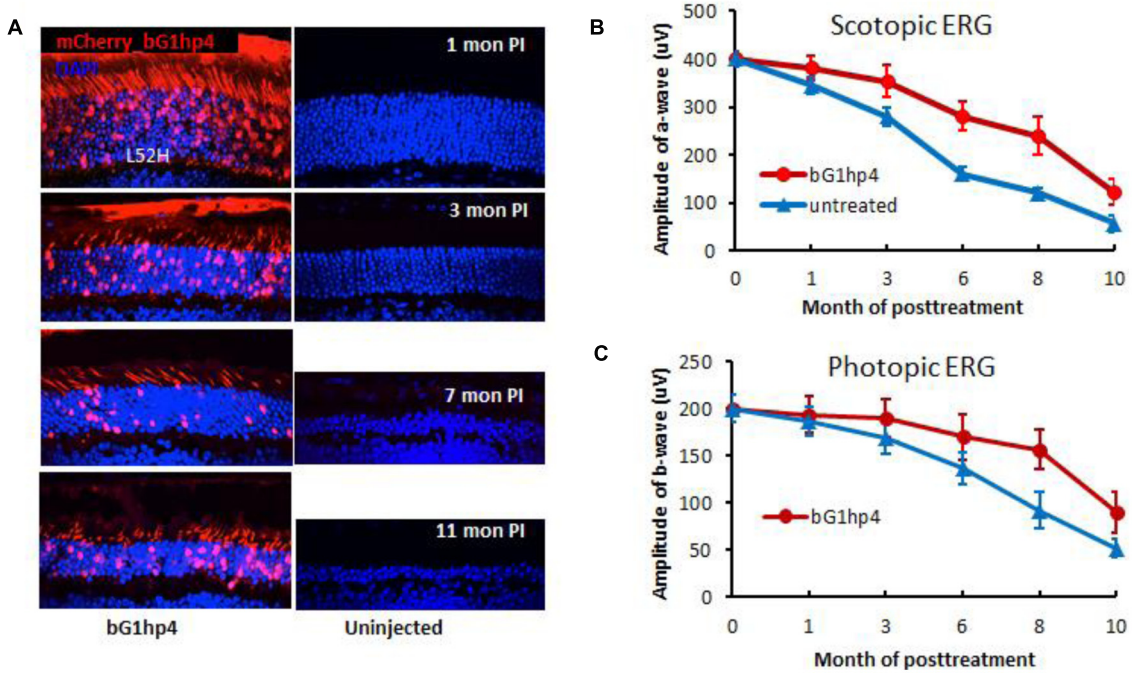

FIGURE 8 | Long-term therapeutic efficiency of allele-specific shRNA vector, scAAV2/8-bG1hp4. (A), Direct fluorescence microscopy of retinal cross-sections examines retinal morphology of the bG1hp4 treated and untreated L52H transgenic mice. Viral vectors were injected subretinally at mouse ages P21–P30. Both treated and untreated eyes were harvested at four representative times from 1–11 months post-injection. Red, mCherry expression demonstrating scAAV2/8 virus transduction. Blue, DAPI staining of nuclei. Note significant preservation of ONL thickness at 11 months post-treatment (~12 months of age) compared to non-treated controls. **(B,C)**. Scotopic and photopic ERG amplitudes recorded from bG1hp4-treated (red) and untreated (blue) L52H transgenic mice (Jiang et al., 2011). Subretinal injection of scAAV2/8-bG1hp4 in the transgenic mouse models delayed progression of both rod and cone dysfunction significantly.

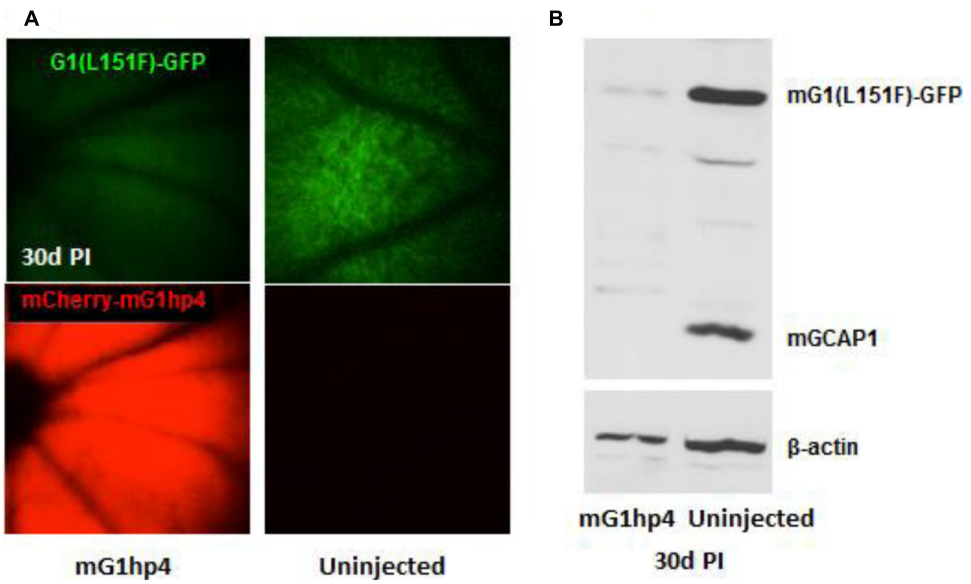

FIGURE 9 | Knockdown of mGCAP1 by nonallele-specific shRNA vector, scAAV2/8-mG1hp4. (A), Fluorescence fundus images of mG1(L151F)-GFP transgenic mice with subretinal injection of the virus vectors at P21–P30 (left) and non-injected control (right). GFP signal (top) represents the mG1(L151F)-GFP expression level in photoreceptors, and mCherry (bottom) signal indicates scAAV2/8 virus transduction. **(B)**, Immunoblot of the transgenic mG1(L151F)-GFP and endogenous GCAP1 protein levels in the injected and the non-injected retinas at 30 days PI. Transgenic mG1(L151F)-GFP (~50 kD) and endogenous GCAP1 (~25 kD) proteins were detected by UW101 antibody directed against GCAP1. -actin served as endogenous loading control. See also **Figure 9** (Jiang et al., 2013).

et al., 2001), we assumed that nonallele-specific shRNA knockdown of both wild-type and mutant GCAP1s may be a general therapeutic strategy to treat retinal degeneration in patients carrying GCAP1 mutations. We tested *in vivo* knockdown efficiency of scAAV2/8-mediated mG1hp4 in the mGCAP1(L151F)-GFP transgenic mice. Fluorescence fundus imaging indicated significant suppression of the mGCAP1(L151F)-GFP mutant transgene, but not in uninjected eyes (**Figure 9A**). Broad and robust mCherry reporter gene expression in scAAVmG1hp4-treated mouse retinas signaled even expression levels of the virus. Semi-quantitative analysis of GCAP1 levels in treated retinas revealed that mG1hp4 simultaneously knocked down *in vivo* expression of the mutant mGCAP1(L151F)-GFP transgene by 70% and endogenous wild-type GCAP1 by 90% (**Figure 9B**). Thus our experiment provides "proof of principle" that nonallele-specific RNA interference (RNAi) knockdown may be a strategy applicable to all GCAP1 mutations.

CONCLUSION

The experimental goal was to test whether allele-specific or nonallele-specific knockdown of a dominant GCAP1 mutant is able to ameliorate photoreceptor dystrophy. We demonstrated the feasibility of shRNA knockdown first with an allele-specific approach in a *retinitis pigmentosa* mouse model expressing GCAP1(Y99C). A scAAV robustly expressed shRNAs in photoreceptors at 1 week post-injection and gene silencing activity persisted as long as 1 year without any apparent off-target interference. Delayed disease onset, significantly improved rod photoreceptor survival and increased visual function support that the methodology can be useful for human gene therapy.

For nonallele-specific knockdown, we generated a sophisticated set of transgenic mouse models expressing GCAP1-EGFP fusion proteins with and without L151F mutation. The L151F mutation, discovered in our lab, was shown to cause dystrophy in two unrelated families. Nonallele-specific shRNA knockdown of both wild-type and mutant GCAP1s may serve as a therapeutic strategy to rescue the dominant degeneration caused by any of the eleven known EF-hand GCAP1 mutations. An advantage of dominant GCAP1 mutations is that a nonalle-specific approach promises to be successful, while mutations in other CORD genes require gene replacement to rescue the disease. Successful knockdown by RNAi suppression of both wild-type and mutant GCAP1s may be a potent therapeutic strategy, applicable to all affected family members with CORD based on GCAP1 mutations in EF3 and EF4, as long as the shRNA guide strand is located external to the disease-causing mutations.

REFERENCES

Baehr, W., and Palczewski, K. (2009). Focus on molecules: guanylate cyclase-activating proteins (GCAPs). *Exp. Eye Res.* 89, 2–3. doi: 10.1016/j.exer.2008.12.016

Buch, P. K., Mihelec, M., Cottrill, P., Wilkie, S. E., Pearson, R. A., Duran, Y., et al. (2011). Dominant cone-rod dystrophy: a mouse model generated by gene targeting of the GCAP1/Guca1a gene. *PLoS ONE* 6:e18089. doi: 10.1371/journal.pone.0018089

Cashman, S. M., McCullough, L., and Kumar-Singh, R. (2007). Improved retinal transduction *in vivo* and photoreceptor-specific transgene expression using adenovirus vectors with modified penton base. *Mol. Ther.* 15, 1640–1646. doi: 10.1038/sj.mt.6300203

Dizhoor, A. M., Boikov, S. G., and Olshevskaya, E. V. (1998). Constitutive activation of photoreceptor guanylate cyclase by Y99C mutant of GCAP-1. Possible role in causing human autosomal dominant cone degeneration. *J. Biol. Chem.* 273, 17311–17314. doi: 10.1074/jbc.273.28.17311

Dizhoor, A. M., Lowe, D. G., Olshevskaya, E. V., Laura, R. P., and Hurley, J. B. (1994). The human photoreceptor membrane guanylyl cyclase, RetGC, is present in outer segments and is regulated by Calcium and a soluble activator. *Neuron* 12, 1345–1352. doi: 10.1016/0896-6273(94)90449-9

Dizhoor, A. M., Olshevskaya, E. V., Henzel, W. J., Wong, S. C., Stults, J. T., Ankoudinova, I., et al. (1995). Cloning, sequencing, and expression of a 24-kDa Ca2+-binding protein activating photoreceptor guanylyl cyclase. *J. Biol. Chem.* 270, 25200–25206. doi: 10.1074/jbc.270.42.25200

Dizhoor, A. M., Olshevskaya, E. V., and Peshenko, I. V. (2010). Mg2+/Ca2+ cation binding cycle of guanylyl cyclase activating proteins (GCAPs): role in regulation of photoreceptor guanylyl cyclase. *Mol. Cell. Biochem.* 334, 117–124. doi: 10.1007/s11010-009-0328-6

Downes, S. M., Holder, G. E., Fitzke, F. W., Payne, A. M., Warren, M. J., Bhattacharya, S. S., et al. (2001). Autosomal dominant cone and cone-rod dystrophy with mutations in the guanylate cyclase activator 1A gene-encoding guanylate cyclase activating protein-1. *Arch. Ophthalmol.* 119, 96–105. doi: 10.1001/archopht.119.11.1667

Duda, T., Fik-Rymarkiewicz, E., Venkataraman, V., Krishnan, R., Koch, K. W., and Sharma, R. K. (2005). The calcium-sensor guanylate cyclase activating protein type 2 specific site in rod outer segment membrane guanylate cyclase type 1. *Biochemistry* 44, 7336–7345. doi: 10.1021/bi050068x

Duda, T., Goraczniak, R. M., Surgucheva, I., Rudnicka-Nawrot, M., Gorczyca, W. A., Palczewski, K., et al. (1996). Calcium modulation of bovine photoreceptor guanylate cyclase. *Biochemistry* 35, 8478–8482. doi: 10.1021/bi960752z

Duda, T., Pertzev, A., and Sharma, R. K. (2012). Differential Ca^{2+} sensor guanylate cyclase activating protein modes of photoreceptor rod outer segment membrane guanylate cyclase signaling. *Biochemistry* 51, 4650–4657. doi: 10.1021/bi300572w

Farjo, R., Skaggs, J., Quiambao, A. B., Cooper, M. J., and Naash, M. I. (2006). Efficient non-viral ocular gene transfer with compacted DNA nanoparticles. *PLoS ONE* 1:e38. doi: 10.1371/journal.pone.0000038

Goraczniak, R., Duda, T., and Sharma, R. K. (1997). Structural and functional characterization of a second subfamily member of the calcium-modulated bovine rod outer segment membrane guanylate cyclase, ROS-GC2. *Biochem. Biophys. Res. Commun.* 234, 666–670. doi: 10.1006/bbrc.1997.6579

Goraczniak, R. M., Duda, T., Sitaramayya, A., and Sharma, R. K. (1994). Structural and functional characterization of the rod outer segment membrane guanylate cyclase. *Biochem. J.* 302, 455–461.

Gorczyca, W. A., Polans, A. S., Surgucheva, I., Subbaraya, I., Baehr, W., and Palczewski, K. (1995). Guanylyl cyclase activating protein: a calcium-sensitive regulator of phototransduction. *J. Biol. Chem.* 270, 22029–22036. doi: 10.1074/jbc.270.37.22029

Hamel, C. P. (2007). Cone rod dystrophies. *Orphanet J. Rare Dis.* 2, 7. doi: 10.1186/1750-1172-2-7

Howes, K. A., Pennesi, M. E., Sokal, I., Church-Kopish, J., Schmidt, B., Margolis, D., et al. (2002). GCAP1 rescues rod photoreceptor response in GCAP1/GCAP2 knockout mice. *EMBO J.* 21, 1545–1554. doi: 10.1093/emboj/21.7.1545

Huang, L., Li, S., Xiao, X., Jia, X., Sun, W., Gao, Y., et al. (2013). Novel GUCA1A mutation identified in a Chinese family with cone-rod dystrophy. *Neurosci. Lett.* 541, 179–183. doi: 10.1016/j.neulet.2013.02.013

Jiang, L., Katz, B. J., Yang, Z., Zhao, Y., Faulkner, N., Hu, J., et al. (2005). Autosomal dominant cone dystrophy caused by a novel mutation in the GCAP1 gene (GUCA1A). *Mol. Vis.* 11, 143–151.

Jiang, L., Li, T. Z., Boye, S. E., Hauswirth, W. W., Frederick, J. M., and Baehr, W. (2013). RNAi-mediated gene suppression in a GCAP1(L151F) cone-rod dystrophy mouse model. *PLoS ONE* 8:e57676. doi: 10.1371/journal.pone.0057676

Jiang, L., Wheaton, D., Bereta, G., Zhang, K., Palczewski, K., Birch, D. G., et al. (2008). A novel GCAP1(N104K) mutation in EF-hand 3 (EF3) linked to autosomal dominant cone dystrophy. *Vision Res.* 48, 2425–2432. doi: 10.1016/j.visres.2008.07.016

Jiang, L., Zhang, H., Dizhoor, A. M., Boye, S. E., Hauswirth, W. W., Frederick, J. M., et al. (2011). Long-term RNA interference gene therapy in a dominant retinitis

pigmentosa mouse model. *Proc. Natl. Acad. Sci. U.S.A.* 108, 18476–18481. doi: 10.1073/pnas.1112758108

Kamenarova, K., Corton, M., Garcia-Sandoval, B., Fernandez-San, J. P., Panchev, V., Avila-Fernandez, A., et al. (2013). Novel GUCA1A mutations suggesting possible mechanisms of pathogenesis in cone, cone-rod, and macular dystrophy patients. *Biomed. Res. Int.* 2013, 517570. doi: 10.1155/2013/517570

Kitiratschky, V. B., Behnen, P., Kellner, U., Heckenlively, J. R., Zrenner, E., Jagle, H., et al. (2009). Mutations in the GUCA1A gene involved in hereditary cone dystrophies impair calcium-mediated regulation of guanylate cyclase. *Hum. Mutat.* 30, E782–E796. doi: 10.1002/humu.21055

Lowe, D. G., Dizhoor, A. M., Liu, K., Gu, Q., Spencer, M., Laura, R., et al. (1995). Cloning and expression of a second photoreceptor-specific membrane retina guanylyl cyclase (RetGC), RetGC-2. *Proc. Natl. Acad. Sci. U.S.A.* 92, 5535–5539. doi: 10.1073/pnas.92.12.5535

Makino, C. L., Peshenko, I. V., Wen, X. H., Olshevskaya, E. V., Barrett, R., and Dizhoor, A. M. (2008). A role for GCAP2 in regulating the photoresponse. Guanylyl cyclase activation and rod electrophysiology in GUCA1B knock-out mice. *J. Biol. Chem.* 283, 29135–29143. doi: 10.1074/jbc.M804445200

Makino, C. L., Wen, X. H., Olshevskaya, E. V., Peshenko, I. V., Savchenko, A. B., and Dizhoor, A. M. (2012). Enzymatic relay mechanism stimulates cyclic GMP synthesis in rod photoresponse: biochemical and physiological study in guanylyl cyclase activating protein 1 knockout mice. *PLoS ONE* 7:e47637. doi: 10.1371/journal.pone.0047637

Mendez, A., Burns, M. E., Sokal, I., Dizhoor, A. M., Baehr, W., Palczewski, K., et al. (2001). Role of guanylate cyclase-activating proteins (GCAPs) in setting the flash sensitivity of rod photoreceptors. *Proc. Natl. Acad. Sci. U.S.A.* 98, 9948–9953. doi: 10.1073/pnas.171308998

Michaelides, M., Wilkie, S. E., Jenkins, S., Holder, G. E., Hunt, D. M., Moore, A. T., et al. (2005). Mutation in the gene GUCA1A, encoding guanylate cyclase-activating protein 1, causes cone, cone-rod, and macular dystrophy. *Ophthalmology* 112, 1442–1447. doi: 10.1016/j.ophtha.2005.02.024

Natkunarajah, M., Trittibach, P., McIntosh, J., Duran, Y., Barker, S. E., Smith, A. J., et al. (2008). Assessment of ocular transduction using single-stranded and self-complementary recombinant adeno-associated virus serotype 2/8. *Gene Ther.* 15, 463–467. doi: 10.1038/sj.gt.3303074

Nishiguchi, K. M., Sokal, I., Yang, L., Roychowdhury, N., Palczewski, K., Berson, E. L., et al. (2004). A novel mutation (I143NT) in guanylate cyclase-activating protein 1 (GCAP1) associated with autosomal dominant cone degeneration. *Invest. Ophthalmol. Vis. Sci.* 45, 3863–3870. doi: 10.1167/iovs.04-0590

Nong, E., Lee, W., Merriam, J. E., Allikmets, R., and Tsang, S. H. (2014). Disease progression in autosomal dominant cone-rod dystrophy caused by a novel mutation (D100G) in the GUCA1A gene. *Doc. Ophthalmol.* 128, 59–67. doi: 10.1007/s10633-013-9420-z

Olshevskaya, E. V., Calvert, P. D., Woodruff, M. L., Peshenko, I. V., Savchenko, A. B., Makino, C. L., et al. (2004). The Y99C mutation in guanylyl cyclase-activating protein 1 increases intracellular Ca^{2+} and causes photoreceptor degeneration in transgenic mice. *J. Neurosci.* 24, 6078–6085. doi: 10.1523/JNEUROSCI.0963-04.2004

Palczewski, K., Sokal, I., and Baehr, W. (2004). Guanylate cyclase-activating proteins: structure, function, and diversity. *Biochem. Biophys. Res. Commun.* 322, 1123–1130. doi: 10.1016/j.bbrc.2004.07.122

Palczewski, K., Subbaraya, I., Gorczyca, W. A., Helekar, B. S., Ruiz, C. C., Ohguro, H., et al. (1994). Molecular cloning and characterization of retinal photoreceptor guanylyl cyclase activating protein (GCAP). *Neuron* 13, 395–404. doi: 10.1016/0896-6273(94)90355-7

Payne, A. M., Downes, S. M., Bessant, D. A., Taylor, R., Holder, G. E., Warren, M. J., et al. (1998). A mutation in guanylate cyclase activator 1A (GUCA1A) in an autosomal dominant cone dystrophy pedigree mapping to a new locus on chromosome 6p21.1. *Hum. Mol. Genet.* 7, 273–277. doi: 10.1093/hmg/7.2.273

Pennesi, M. E., Howes, K. A., Baehr, W., and Wu, S. M. (2003). Guanylate cyclase-activating protein (GCAP) 1 rescues cone recovery kinetics in GCAP1/GCAP2 knockout mice. *Proc. Natl. Acad. Sci U.S.A.* 100, 6783–6788. doi: 10.1073/pnas.1130102100

Peshenko, I. V., Olshevskaya, E. V., Savchenko, A. B., Karan, S., Palczewski, K., Baehr, W., et al. (2011). Enzymatic properties and regulation of the native isozymes of retinal membrane guanylyl cyclase (RetGC) from mouse photoreceptors. *Biochemistry* 50, 5590–5600. doi: 10.1021/bi200491b

Sokal, I., Dupps, W. J., Grassi, M. A., Brown, J. Jr., Affatigato, L. M., Roychowdhury, N., et al. (2005). A GCAP1 missense mutation (L151F) in a large family with autosomal dominant cone-rod dystrophy (adCORD). *Invest. Ophthalmol. Vis. Sci.* 46, 1124–1132. doi: 10.1167/iovs.04-1431

Sokal, I., Li, N., Surgucheva, I., Warren, M. J., Payne, A. M., Bhattacharya, S. S., et al. (1998). GCAP1(Y99C) mutant is constitutively active in autosomal dominant cone dystrophy. *Mol. Cell* 2, 129–133. doi: 10.1016/S1097-2765(00)80121-5

Sweigard, J. H., Cashman, S. M., and Kumar-Singh, R. (2010). Adenovirus vectors targeting distinct cell types in the retina. *Invest. Ophthalmol. Vis. Sci.* 51, 2219–2228. doi: 10.1167/iovs.09-4367

Wilkie, S. E., Li, Y., Deery, E. C., Newbold, R. J., Garibaldi, D., Bateman, J. B., et al. (2001). Identification and functional consequences of a new mutation (E155G) in the gene for GCAP1 that causes autosomal dominant cone dystrophy. *Am. J. Hum. Genet.* 69, 471–480. doi: 10.1086/323265

Woodruff, M. L., Olshevskaya, E. V., Savchenko, A. B., Peshenko, I. V., Barrett, R., Bush, R. A., et al. (2007). Constitutive excitation by Gly90Asp rhodopsin rescues rods from degeneration caused by elevated production of cGMP in the dark. *J. Neurosci.* 27, 8805–8815. doi: 10.1523/JNEUROSCI.2751-07.2007

Wu, Z., Asokan, A., and Samulski, R. J. (2006). Adeno-associated virus serotypes: vector toolkit for human gene therapy. *Mol. Ther.* 14, 316–327. doi: 10.1016/j.ymthe.2006.05.009

Xu, J., Morris, L., Thapa, A., Ma, H., Michalakis, S., Biel, M., et al. (2013). cGMP accumulation causes photoreceptor degeneration in CNG channel deficiency: evidence of cGMP cytotoxicity independently of enhanced CNG channel function. *J. Neurosci.* 33, 14939–14948. doi: 10.1523/JNEUROSCI.0909-13.2013

Conflict of Interest Statement: The authors declare that the research was conducted in the absence of any commercial or financial relationships that could be construed as a potential conflict of interest.

Received: 21 January 2014; accepted: 19 March 2014; published online: 07 April 2014.
*Citation: Jiang L, Frederick JM and Baehr W (2014) RNA interference gene therapy in dominant retinitis pigmentosa and cone-rod dystrophy mouse models caused by GCAP1 mutations. Front. Mol. Neurosci. **7**:25. doi: 10.3389/fnmol.2014.00025*
This article was submitted to the journal Frontiers in Molecular Neuroscience.

frontiers in
MOLECULAR NEUROSCIENCE

REVIEW ARTICLE
published: 19 May 2014
doi: 10.3389/fnmol.2014.00038

Regulation of intraocular pressure by soluble and membrane guanylate cyclases and their role in glaucoma

Emmanuel S. Buys[1]*, Lincoln R. Potter[2], Louis R. Pasquale[3] and Bruce R. Ksander[4]

[1] *Department of Anesthesia, Critical Care, and Pain Medicine, Anesthesia Center for Critical Care Research, Harvard Medical School, Massachusetts General Hospital, Boston, MA, USA*
[2] *Department of Pharmacology, University of Minnesota Medical School, Minneapolis, MN, USA*
[3] *Department of Ophthalmology, Glaucoma Service Mass Eye and Ear Infirmary and Channing Division of Network Medicine, Harvard Medical School, Brigham and Women's Hospital, Boston, MA, USA*
[4] *Department of Ophthalmology, Massachusetts Eye and Ear Infirmary, Schepens Eye Research Institute, Harvard Medical School, Boston, MA, USA*

Edited by:
Clint Lawrence Makino, Harvard Medical School, USA

Reviewed by:
Bin-Nan Wu, Kaohsiung Medical University, Taiwan
Alan Marmorstein, Mayo Clinic, USA

****Correspondence:***
Emmanuel S. Buys, Department of Anesthesia, Critical Care, and Pain Medicine, Anesthesia Center for Critical Care Research, Harvard Medical School, Massachusetts General Hospital, 55 Fruit Street, Thier 511B, Boston, MA 02114, USA
e-mail: ebuys@mgh.harvard.edu

Glaucoma is a progressive optic neuropathy characterized by visual field defects that ultimately lead to irreversible blindness (Alward, 2000; Anderson et al., 2006). By the year 2020, an estimated 80 million people will have glaucoma, 11 million of which will be bilaterally blind. Primary open-angle glaucoma (POAG) is the most common type of glaucoma. Elevated intraocular pressure (IOP) is currently the only risk factor amenable to treatment. How IOP is regulated and can be modulated remains a topic of active investigation. Available therapies, mostly geared toward lowering IOP, offer incomplete protection, and POAG often goes undetected until irreparable damage has been done, highlighting the need for novel therapeutic approaches, drug targets, and biomarkers (Heijl et al., 2002; Quigley, 2011). In this review, the role of soluble (nitric oxide (NO)-activated) and membrane-bound, natriuretic peptide (NP)-activated guanylate cyclases that generate the secondary signaling molecule cyclic guanosine monophosphate (cGMP) in the regulation of IOP and in the pathophysiology of POAG will be discussed.

Keywords: guanylate cyclase, nitric oxide, natriuretic peptides, glaucoma, open-angle, intraocular pressure

PRIMARY OPEN ANGLE GLAUCOMA

Primary open-angle glaucoma (POAG) is a leading cause of blindness, affecting over 2.2 million patients in the US alone, and is associated with an estimated health care cost upwards of $1.5 billion/year. Vision loss, occurring due to loss of retinal ganglion cells (RGCs) and degeneration of the optic nerve, has far-reaching effects on the patient's ability to function independently, dramatically affecting quality of life from a physical, mental and social well-being perspective. Currently, there is no definitive cure for POAG and although multiple risk factors for POAG have been identified [including intra-ocular pressure (IOP), race, age, and genetic factors], the molecular signaling involved in POAG pathogenesis remains largely unknown.

Although multiple POAG risk factors have been identified, the etiology of POAG remains to be elucidated, likely because the disease can be stratified into various subtypes defined by discrete but yet unknown biochemical pathways. Two major pathophysiologic mechanisms for POAG have been proposed. In the "mechanical theory" optic neuropathy is caused by increased IOP (see "Intraocular pressure: a risk factor for POAG" below). Alternatively, a vascular component has been hypothesized to contribute to POAG pathophysiology (see "Glaucoma and vascular dysfunction" below). However, the extent to which vascular dysfunction contributes to glaucomatous optic neuropathy remains to be elucidated and is controversial (Vajaranant and Pasquale, 2012).

INTRAOCULAR PRESSURE: A RISK FACTOR FOR POAG

POAG is often associated with elevated IOP. Measurement of IOP typically requires an anesthetized ocular surface and a cooperative patient, as corneal applanation is needed for accurate measurement of this ophthalmic vital sign. While POAG is a strongly age related disease (Sommer et al., 1991; Mukesh et al., 2002) and elevated IOP is a major risk factor for this condition, IOP does not necessarily increase with age. One longitudinal analysis found that among people aged 50–59, IOP increased after 9 years of follow-up but among subjects 60 and older, a slight decrease in IOP was noted in the same time period (Wu et al., 2006). Furthermore while African heritage is an undisputed risk factor for POAG, people of African heritage do not necessarily have higher IOP than Caucasian subjects drawn from the same population (Sommer et al., 1991). While the heritability of IOP is relative highly (56–64%) (Carbonaro et al., 2009) very few common loci for this trait have been discovered thus far (Van Koolwijk et al., 2012; Ozel et al., 2014). Other factors such as body mass index (Klein et al., 1992; Wu and Leske, 1997; Oh et al., 2005), blood pressure (Klein et al., 2005), and diabetes (Wu et al., 2006) have only modest positive associations with IOP. Data regarding how IOP might change while blood pressure varies in an individual patient are lacking. When a patient (regardless of glaucoma status) transitions between a seated to supine position there is a predictable increase in IOP of ∼3 mm Hg (Lee et al., 2012, 2013). Only a few medical conditions impact the level of IOP (Arevalo et al., 1996; Garcia Filho et al., 2011) but steroid exposure is notorious for leading to elevated IOP via

changes in trabecular meshwork permeability (Clark et al., 1995). It is thought that IOP fluctuates more in POAG patients than controls (Sacca et al., 1998) but the literature is conflicting regarding the role of IOP fluctuation on open-angle glaucoma disease progression (Nouri-Mahdavi et al., 2004; Bengtsson et al., 2007).

IOP is determined by the balance between the production/secretion of aqueous humor (AqH) by the ciliary processes and by the drainage of AqH via the iridocorneal angle. AqH can exit the eye through various routes: the conventional, the uveoscleral, and the uveolymphatic pathways. The conventional pathway consists of the trabecular meshwork (TM), Schlemm's canal, collecting channels, and the episcleral venous system. It is generally accepted that IOP reflects the pressure necessary to overcome the intrinsic resistance to aqueous outflow that occurs at the junction where the juxtacanalicular part of the TM meets the inner wall of Schlemm's canal (Ethier et al., 1986). In uveoscleral outflow, AqH drains through the ciliary muscle (CM) and exits through the supraciliary space and across the anterior or posterior sclera, into choroidal vessels (Fautsch and Johnson, 2006). Uveoscleral outflow, accounting for anywhere between 3% and 80% of outflow depending on the species studied (4–60% in humans) (Fautsch and Johnson, 2006), is particularly impacted by age, an important observation considering the age-dependency of POAG in both patients (Kass et al., 2002, 2010; Mukesh et al., 2002; De Voogd et al., 2005; Rudnicka et al., 2006; Leske et al., 2008) and animal models (Buys et al., 2013). Incidentally, also in animal models of secondary angle-closure glaucoma, IOP and prevalence of optic neuropathy and retinal lesions increased with age (John et al., 1998; Saleh et al., 2007). More recently, the existence of a third outflow route was postulated: lymphatic channels in the stroma of the ciliary body and interstitial spaces between CM muscle bundles may function as a backup outflow system (Yucel et al., 2009). The relevance of this uveolymphatic pathway and whether NO-cGMP signaling (see "NO-cGMP signaling in the eye" below) modulates contractility of ocular lymphatic vessels remains to be determined. Importantly, a central role for NO in lymphatic function was recently identified (Liao et al., 2011). Whether the effect of NO on lymphatic contractions is mediated by cGMP remains unknown.

In contrast to what is observed in angle closure glaucoma, POAG is not associated with apparent blockage of the anterior chamber angle. In POAG, there is variable elevation of IOP associated with impaired AqH outflow that occurs despite apparently normal anterior segment anatomy and an open iridocorneal angle (Weinreb and Khaw, 2004). IOP rises gradually over time, likely as a consequence of decreased drainage of AqH. IOP-lowering treatment significantly cuts the risk of developing glaucoma in ocular hypertensives (Kass et al., 2002, 2010).

GLAUCOMA AND VASCULAR DYSFUNCTION

While IOP reduction continues to be a successful treatment to reduce the progression of POAG (Leske et al., 2003; Kass et al., 2010), the pathogenesis of POAG seemingly also depends on factors other than increased IOP. Compounds that do not lower IOP dramatically may have properties that address the underlying glaucomatous disease process and therefore could be suitable therapeutic agents (Weinreb and Kaufman, 2009; Chen et al., 2011). For example, brimonidine was superior to timolol in stabilizing visual field deterioration, despite producing a similar IOP-lowering effect (Krupin et al., 2011). Also, ocular hypertension does not necessarily lead to POAG and ocular normotension does not preclude the development of POAG (Leske et al., 2001), suggesting that other pathologies, including neurologic (similar to other chronic central nervous system diseases such as Alzheimer's diseases or Multiple Sclerosis Quigley, 2011) or vascular dysfunction [e.g., as characterized by impaired retinovascular autoregulation (Feke and Pasquale, 2008) or peripheral vascular endothelial dysfunction (Henry et al., 1999; Su et al., 2008)], may contribute to the etiology of POAG. Vascular dysfunction contributes to the development of systemic hypertension (Mendelsohn, 2005; Michael et al., 2008) and several studies have provided evidence that blood pressure affects POAG risk (Kaiser and Flammer, 1991; Tielsch et al., 1995; Hulsman et al., 2007; Leske et al., 2008; Memarzadeh et al., 2010; Cherecheanu et al., 2013). In addition, the idea that vascular dysfunction contributes to the pathogenesis of POAG is based on the hypothesis that decreased perfusion of the optic nerve leads to neurodegeneration (Harris et al., 2005; Vajaranant and Pasquale, 2012).

Both impaired blood flow and impaired vascular autoregulation have been described in glaucoma patients (Flammer et al., 2002; Feke and Pasquale, 2008; Moore et al., 2008; Feke et al., 2011). Large epidemiologic studies have found adverse associations between POAG and low ocular perfusion pressure (OPP) (Hulsman et al., 2007; Leske, 2009) or low systemic blood pressure (Bonomi et al., 2000). In addition, the Early Manifest Glaucoma Trial observed that predictors of POAG disease progression included lower systolic blood and perfusion pressure (Leske et al., 2007). Especially in normal tension glaucoma patients, systemic vascular abnormalities have been described, including impaired flow- or acetylcholine-mediated vasodilation (Gasser and Flammer, 1991; Henry et al., 1999; Su et al., 2008). Also POAG patients with early paracentral visual field loss are more likely to have systemic vascular risk factors such as hypotension and migraines (Park et al., 2011, 2012). It is important to note that blood flow regulation in the optic nerve head seems to be strongly dependent on IOP and OPP (Schmidl et al., 2011). The interaction between systemic blood pressure and IOP (defining OPP) (Tielsch et al., 1995; He et al., 2011) is particularly relevant for this review, given the role of NO-cGMP signaling (see "NO-cGMP signaling in the eye" below) in both the regulation of IOP and systemic blood pressure.

NO-cGMP SIGNALING IN THE EYE

NO is an exceptionally well-characterized signaling molecule, with important roles in a wide variety of physiological and pathophysiological processes, including cardiovascular homeostasis, neuronal function, and inflammation. NO is synthesized from L-arginine by a family of three enzymes referred to as NO synthases (NOSs) (**Figure 1**) (Moncada and Higgs, 1993). NOS2, or inducible NOS, was first identified in macrophages but has since been detected in a wide variety of cells exposed to endotoxin and cytokines. Following bacterial infection, especially with gram-negative organisms, high levels of NO are produced by NOS2. NOS1 and NOS3 were initially described to be constitutively expressed in neuronal cells and endothelial cells, respectively

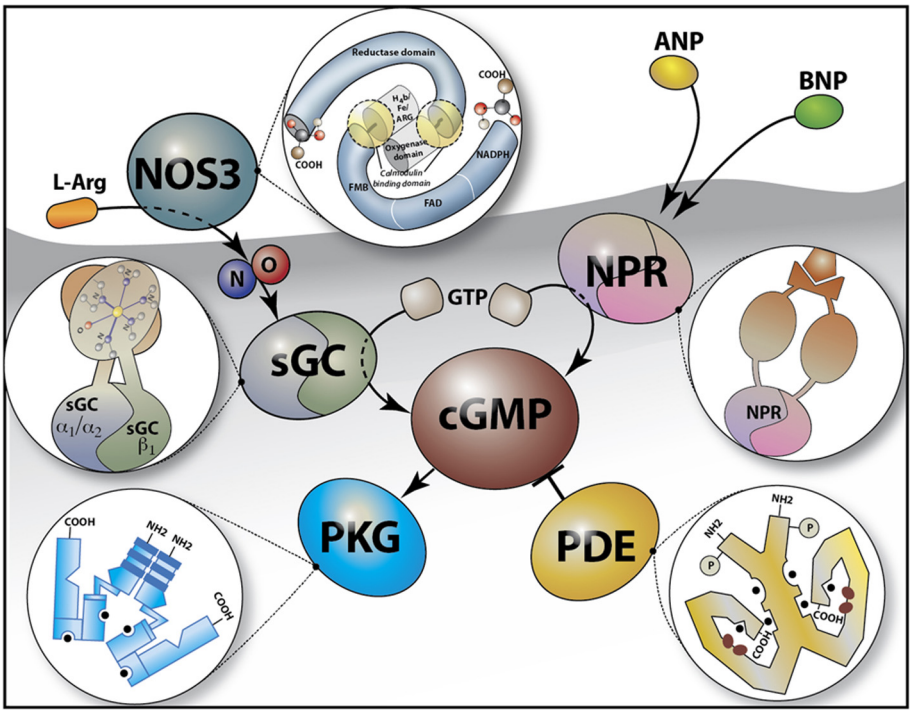

FIGURE 1 | Schematic of the Cyclic GMP (cGMP) signaling pathway. cGMP is synthesized from GTP by soluble guanylate cyclases (sGC$\alpha_1\beta_1$ or sGC$\alpha_2\beta_1$) in response to nitric oxide (NO) e.g., as generated by the conversion of L-arginine (L-Arg) by NO synthase 3 (NOS3), or by the membrane guanylate cyclase (natriuretic peptide) receptors (NPR) which are activated by peptide hormones [e.g., atrial natriuretic peptide (ANP) and B-type natriuretic peptide (BNP)]. cGMP binds to and activates cGMP-dependent protein kinase G (PKG) and is hydrolyzed by phosphodiesterases (such as PDE5, the target for sildenafil). The insets depict a schematic overview of the structure of NOS3, NPR, PKG, PDE, and sGC.

(Moncada and Higgs, 1993). Under physiological conditions, the low levels of NO produced by the two constitutive Ca^{2+}-dependent enzymes NOS1 and NOS3 have diverse functions ranging from neurotransmission and vasodilatation to inhibition of platelet adhesion and aggregation. NO, is an important modulator of smooth muscle function and all three NOS isoforms are expressed in the eye (**Table 1**). Multiple studies have reported on the ability of NO to modulate resistance in the AqH outflow pathway and IOP (see "NO-cGMP-mediated regulation of IOP: implications for POAG" below). Therefore, NO is an attractive candidate as a factor that could modify both mechanical and vascular events in POAG pathogenesis.

NO has numerous targets, reacting with a variety of intracellular and extracellular molecules typically via thiol groups or transition metal centers (Chiamvimonvat et al., 1995; Torres et al., 1995; Davis et al., 2001; Jaffrey et al., 2001; Stamler et al., 2001). A major target of NO is the obligate heterodimer soluble guanylate cyclase (sGC) (Mergia et al., 2003, 2006; Nimmegeers et al., 2007; Vermeersch et al., 2007; Buys et al., 2008), a heme-containing heterodimeric enzyme, consisting of one α and one β subunit (**Figure 1**). cGMP interacts with a variety of effector proteins including cGMP-dependent protein kinases (PKGs), cGMP-regulated phosphodiesterases (PDE's), and ion channels. cGMP is also synthesized by receptor guanylate cyclases that are activated by NPs (NPRs, **Figure 1**). However, cGMP produced by NPRs and sGC may have differential effects, possibly due to differential spatiotemporal distributions of cGMP produced by the two guanylate cyclase families (Su et al., 2005; Castro et al., 2006; Piggott et al., 2006).

Two functional isoforms of sGC exist: sGC$\alpha_1\beta_1$, the predominant isoform in most tissues (Mergia et al., 2003), and sGC$\alpha_2\beta_1$ (Hobbs, 1997; Russwurm et al., 1998; Bamberger et al., 2001). sGCα and β subunits were shown to be expressed in several anatomical sites relevant for glaucoma (**Table 1** and **Figure 2**). sGC activity was detected in rabbit (Haberecht et al., 1998), rat (Kajimura et al., 2003), turtle (Blute et al., 1998), and mouse retina (Blom et al., 2012; Buys et al., 2013). sGC is expressed both in retinal ganglion cells and photoreceptors and in the vascular smooth muscle layer of retinal arterioles. Finally, and most relevant to the potential ability of NO-sGC to modulate AqH outflow, sGC is abundantly expressed in isolated human TM cells (Ellis et al., 2009) and in both human and mouse CM (Buys et al., 2013). Also NP-activated membrane bound guanylate cyclase are expressed in various ocular tissues (see "NP receptors and their effects on IOP" below and **Table 1**).

NO-cGMP-MEDIATED REGULATION OF IOP: IMPLICATIONS FOR POAG

Multiple studies have yielded evidence suggesting that NO-cGMP signaling regulates AqH outflow and IOP. For example, both an NO donor and a cGMP-analog decreased IOP (Kotikoski et al., 2002) and increased outflow facility in rabbits (Kotikoski

Table 1 | Ocular localization of nitric oxide synthase (NOS), soluble guanylate cyclase (sGC), and NP receptors (NPR).

Gene	Species	Cell- or tissue type	References
NOS1	Human	Ciliary non-pigmented epithelium	Nathanson and Mckee, 1995a
	Human	ONH astrocytes, lamina cribrosa	Neufeld et al., 1997
	Monkey	Amacrine cells, rod and cone photoreceptors, RGC	Haberecht et al., 1998
	Canine	RGC	Franco-Bourland et al., 1998
	Rabbit	Amacrine cells, rod and cone photoreceptors, RGC	Haberecht et al., 1998
	Rat	Ciliary process epithelium	Yamamoto et al., 1993
	Murine	Retinal amacrine cells	May and Mittag, 2004
	Murine	Retinal amacrine cells, RGC layer somata; IPL puncta	Blom et al., 2012
	Murine	Müller cells	Chen et al., 2013
NOS2	Human	Macrophages in stroma and ciliary processes	Nathanson and Mckee, 1995a
	Human	Astrocytes	Liu and Neufeld, 2001
NOS3	Human	Longitudinal CM fibers, TM, SC	Nathanson and Mckee, 1995b
	Human	Retinal vasculature	Neufeld et al., 1997
	Human	TM	Fernandez-Durango et al., 2008
sGC	Human	RGC, IPL, ONL	Buys et al., 2013
	Human	TM cells	Ellis et al., 2009
	Rabbit	Amacrine cells, bipolar cells, cone photoreceptors, RGC	Haberecht et al., 1998
	Murine	Somata in the INL, ONL, IPL, and OPL.	Blom et al., 2012
	Murine	RGC, IPL, ONL	Buys et al., 2013
	Turtle	Amacrine cells; bipolar cells, RGC layer, IPL	Blute et al., 1998
NPR	Rabbit	Ciliary processes	Mittag et al., 1987
	Rabbit/bovine/human	Corneal endothelium	Walkenbach et al., 1993
	Rabbit/rat	Retina, choroid and ciliary process	Fernandez-Durango et al., 1995
	Human	Retina	Rollin et al., 2004
	Bovine	Choroid	Schmidt et al., 2004

ONH, optic nerve head; RGC, retinal ganglion cell; IPL, inner plexiform layer; CM, ciliary muscle; TM, trabecular meshwork; SC, Schlemm's canal; ONL, outer nuclear layer; INL, inner nuclear layer; OPL, outer plexiform layer.

et al., 2003). The NO-induced increase in outflow facility was impaired by treating perfused porcine eyes with the sGC inhibitor 1H-[1,2,4]oxadiazolo[4,3-a]quinoxalin-1-1 (ODQ), suggesting that the effects of NO on outflow are cGMP-dependent (Ellis et al., 2009). The non-isoform specific NOS-inhibitor L-NG-Nitroarginine methyl ester (L-NAME) decreased and an NO-donor compound increased AqH flow rate in perfused human donor eyes. This increase in flow was associated with an increase in cGMP levels measured in the perfusate, again suggesting a central role for sGC and cGMP in the ability of NO to modulate outflow (Schneemann et al., 2002). Accordingly, NO-donor compounds lower IOP (Nathanson, 1988, 1992; Schuman et al., 1994; Behar-Cohen et al., 1996; Krauss et al., 2011) and enhance tissue oxygenation of the optic nerve head in preclinical animal models (Khoobehi et al., 2011). Overexpressing NOS3 in mice lowers IOP by increasing pressure-dependent drainage (Stamer et al., 2011), confirming previous reports suggesting that the ability of NO to lower IOP is mediated by a decrease in the AqH resistance rather than a change in the rate of AqH secretion (Nathanson and Mckee, 1995b). Other possible mechanisms by which NO and cGMP can modulate outflow include regulation of Schlemm's canal cell volume (Dismuke et al., 2008; Ellis et al., 2010) and TM cell volume (Dismuke et al., 2009).

Impaired NO-cGMP signaling has been implicated in POAG. For example, NO metabolites and cGMP levels were lower in both plasma and AqH samples from POAG patients than in those from individuals without POAG (Galassi et al., 2000, 2004; Doganay et al., 2002). Also, NADPH-diaphorase (NADPH-d) reactivity, a marker for NO production, was decreased in TM, SC, and anterior longitudinal CM fibers isolated from POAG eyes (Nathanson and Mckee, 1995a) and serum levels of L-arginine analogs (endogenous NOS inhibitors) were found to be elevated in patients with advanced glaucoma (Javadiyan et al., 2012). In addition, NOS3 gene variants were associated with POAG in women (see "Genetics of POAG" below Kang et al., 2010; Magalhaes Da Silva et al., 2012). Together, these studies suggest that impaired NO-cGMP signaling can contribute to the etiology of POAG, identifying the NO-cGMP signaling pathway as a potential therapeutic target for POAG. However, the molecular mechanisms mediating cGMP's effects in the eye, and exactly how NO-cGMP signaling regulates IOP or impacts optic neuropathy remain unclear.

It is important to recognize that the role of NO-cGMP signaling in the eye is likely complex with physiological and pathophysiological effects. For example, contrary to the observations described above that NO lowers IOP, topical application of the

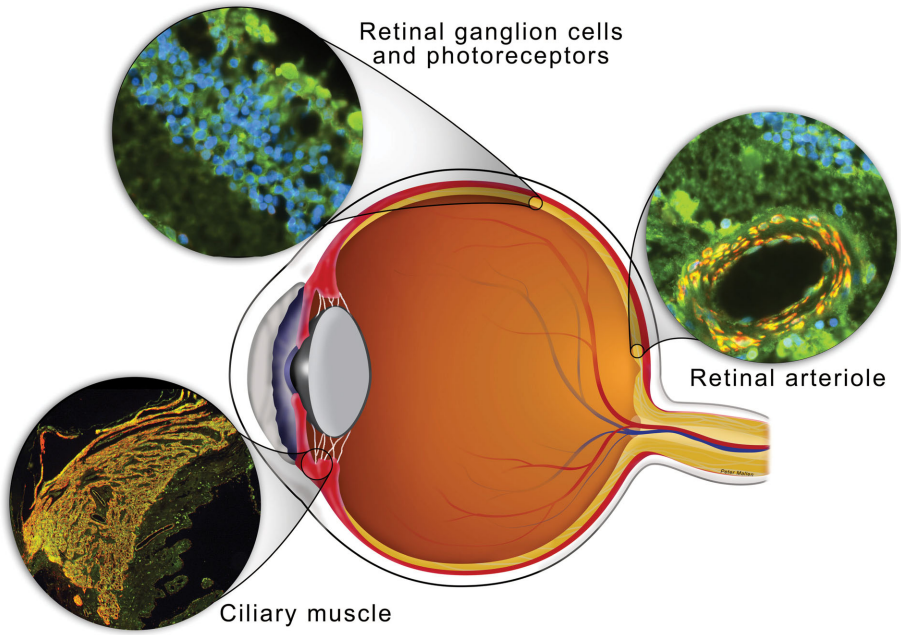

FIGURE 2 | Schematic of the eye with anatomical sites relevant for the development of POAG in which sGC is expressed indicated. Sections through retinal ganglion cells, ciliary muscle and a retinal arteriole from a human eye were stained for $sGC\alpha_1$ (green), α-smooth muscle actin (red), and/or DAPI nucleic acid stain (blue). Both $sGC\alpha_1$ and $sGC\beta_1$ (not shown) co-localized with a-smooth muscle actin in ciliary muscle and the smooth muscle cell layer of a retinal arteriole (yellow in merged images). In addition, $sGC\alpha_1$ and $sGC\beta_1$ (not shown) expression was detected histologically in the outer nuclear layer, inner nuclear layer, and ganglion cell layer of the retina.

NOS-inhibitor L-NAME reduced IOP in a rabbit model of ocular hypertension (Giuffrida et al., 2003). This reduction of IOP, observed only in hypertensive eyes and not normotensive controls, was suggested to be associated with a decreased formation of AqH production (Giuffrida et al., 2003). Opposing effects of cGMP itself on AqH dynamics have been reported: AqH flow rate decreased after intravitreal administration of the cell permeable cGMP analog 8-Br-cGMP but increased after intra-cameral administration of 8-Br-cGMP, underscoring that the route of administration of any drug aimed at lowering IOP or preventing POAG progression may significantly determines its therapeutic efficacy (Kee et al., 1994).

NO MODULATES RGC VIABILITY

NO can also exert a direct neurotoxic effect on RGC's (Morgan et al., 1999; Takahata et al., 2003). For example, in acute angle-closure glaucoma patients, higher levels of NO in AqH were postulated to contribute to RGC and optic nerve damage (Chang et al., 2000; Chiou et al., 2001). Similarly, in a rat model of chronic glaucoma, elevated retinal NOS1 expression was suggested to contribute to cytotoxicity and selective RGC loss (Park et al., 2007). Furthermore, NO generated by NOS2 can contribute to RGC death seen in response to increased IOP: treatment of rats with chronically elevated IOP with an inhibitor of NOS2 prevented RGC loss (Neufeld et al., 1999, 2002). More clinically relevant, expression of NOS2 was increased in the TM of POAG patients and activity of NOS2 in the TM of patients with POAG was reported to be proportional to the observed visual field defects (Fernandez-Durango et al., 2008). Together, these data could be interpreted to suggest that inhibiting NOS activity may be useful for the treatment of glaucoma by protecting RGCs from stress (e.g., as associated with elevated IOP). However, as described in the studies referred to above, there is ample evidence that impaired NO-cGMP signaling contributes to the pathogenesis of POAG. Together with the fact that NO has multiple downstream targets, of which sGC is arguably a predominant one, these observations support focusing on sGC and cGMP as therapeutic targets in POAG (see "The NO-cGMP pathway as a therapeutic target for POAG" below).

MODULATION OF TM AND CM CONTRACTILITY BY NO-cGMP AND ITS RELEVANCE IN IOP REGULATION

It is generally accepted that the TM and CM are active structures rather than passive filters. The CM is a smooth-muscle like structure and the TM contains contractile smooth-muscle-specific alpha-actin filaments. Both are involved in fine-tuning the regulation of AqH outflow (Erickson-Lamy et al., 1991; Wiederholt, 1998; Wiederholt et al., 2000). Several studies (reviewed in Wiederholt et al., 2000) have suggested the existence of a functional antagonism between the TM and the CM, and TM resistance may be regulated by contractile state of CM (Nathanson and Mckee, 1995b): contraction of the CM would decrease TM resistance, increase AqH outflow and decrease IOP.

Alterations in smooth muscle contractility have previously been implicated in glaucoma. For example, RhoA-Rho kinase-mediated signaling, which regulates the phosphorylation

status of myosin light chain, thereby directly influencing TM contraction, was reported to influence AqH drainage (Russ et al., 2010). Inhibiting Rho kinase, an enzyme that plays a critical role in regulating the contractile tone of smooth muscle tissues, increased AqH outflow in various animal models (Honjo et al., 2001; Rao and Epstein, 2007; Lu et al., 2008). The ability of Rho-kinase inhibitors to lower IOP is currently being tested in clinical trials (Chen et al., 2011; Tanihara et al., 2013).

The presence of NOS3 and sGC in the CM and TM (**Table 1**) suggest that the NO-sGC pathway may modulate outflow resistance by regulating CM and TM contractility. In fact, both NO-donor compounds and a cGMP analog were previously demonstrated to regulate the contractile state of bovine CM and TM in organ bath experiments (Wiederholt et al., 1994; Masuda et al., 1997; Kamikawatoko et al., 1998). The ability of NO-cGMP to regulate smooth muscle cell relaxation is well known. For example, vascular reactivity was attenuated in NOS3 mutant mice (Atochin et al., 2007) and in $sGC\alpha_1^{-/-}$ mice (Mergia et al., 2006; Nimmegeers et al., 2007). NO-cGMP signaling (facilitating smooth muscle relaxation Surks et al., 1999) and RhoA-Rho kinase signaling (causing smooth muscle contraction Bennett et al., 1988) have opposing effects on smooth muscle function and NO-cGMP signaling controls activity of the RhoA-Rho kinase pathway (Sauzeau et al., 2003). Together, these findings raise the possibility that impaired NO-cGMP signaling, previously suggested to participate in the regulation of AqH outflow and IOP (see "NO-cGMP-mediated regulation of IOP: implications for POAG" above) has a similar impact on AqH drainage as does increased RhoA-signaling: both could result in augmented contractility of the smooth muscle-like CM, thereby potentially decreasing AqH drainage and increasing IOP (Honjo et al., 2001).

There is, however, an apparent paradox in the dynamic regulation of IOP by the CM and the role of NO-cGMP therein: impaired NO-cGMP signaling would be expected to result in a decreased ability of the SMC-like CM to relax, just as it does in other SMC-like structures (Mergia et al., 2006; Friebe et al., 2007; Nimmegeers et al., 2007; Vanneste et al., 2007; Decaluwe et al., 2010), and hence decrease TM resistance. Importantly, there are two types of CM in humans: circular, involved in accommodation, and longitudinal (Flugel et al., 1990; Sharif et al., 2004). The effect of CM contraction and relaxation on IOP is not uniform: the circular and longitudinal components of the CM appear to have opposite roles in controlling IOP. Contraction of the circular muscle via muscarinic stimulation (e.g., in response to pilocarpine) causes tightening of the trabecular ring leading to an opening of the trabecular juxtacanalicular tissue, decreased resistance, and increased outflow facility, ultimately lowering IOP (Kaufman, 2008). On the other hand, there is evidence that contraction of the longitudinal muscle can impair outflow and increase IOP. The latter was demonstrated in patients that suffered significant blunt trauma where the circular CM is disabled without affecting the longitudinal muscle. When these patients were treated with pilocarpine, the contraction of the longitudinal muscle paradoxically increased IOP (Bleiman and Schwartz, 1979). Therefore, relaxation of the posterior longitudinal muscle in the CM (e.g., with Rho-kinase inhibitors Honjo et al., 2001) likely has an outflow enhancing effect, lowering IOP. On the other hand, decreased relaxation of longitudinal CM fibers associated with impaired NO-cGMP signaling (e.g., in $sGC\alpha_1^{-/-}$ mice, see "sGC-deficient mice: a model of elevated IOP and POAG" below), would result in increased IOP. In addition, repeated contraction and NO-mediated relaxation of any CM component may decreases outflow resistance and lower IOP, likely due to a direct mechanical effect on the TM. Lack of NO-sGC-cGMP signaling in the CM may prevent flushing of the TM, possibly resulting in altered (increased) outflow resistance.

THE NO-cGMP PATHWAY AS A THERAPEUTIC TARGET FOR POAG

The NO-cGMP pathway can be perturbed by a variety of mechanisms. Decreases in NOS3 expression or uncoupling of NOS3 result in lower NO levels (Takimoto et al., 2005). Alternatively, NO bioavailability can be reduced by interaction of NO with reactive oxygen species (ROS) (Munzel et al., 2010). sGC itself can be converted to an NO-insensitive state as a consequence of increased oxidative stress: it is conceivable that the mechanism by which increased oxidative stress results in POAG (Majsterek et al., 2011a) may involve direct oxidation and inactivation of sGC (Stasch et al., 2006). Also, sGC expression can be repressed under pro-inflammatory conditions (Marro et al., 2008). The latter is relevant based on the hypothesis that inflammation contributes to the development of glaucoma (Vohra et al., 2013). Lastly, NO-cGMP signaling can be modulated by genetic variation (see "Genetics of POAG" below) (Kang et al., 2010, 2011; Ehret et al., 2011; Buys et al., 2013). Whether any of the mechanisms that alter activity of the NO-cGMP pathway contribute to the etiology of POAG remains a matter of active investigation. Nonetheless, the studies described here and in the "Modulation of TM and CM contractility by NO-cGMP and its relevance in IOP regulation" section certainly imply the potential usefulness of focusing on NO-cGMP signaling as a therapeutic approach to the treatment of POAG.

Various therapeutic agents have been and are being developed to enhance NO-sGC-cGMP signaling. NO-independent sGC stimulators are already being clinically tested and have been approved for treating cardiovascular disease (Ghofrani et al., 2013). These compounds could conceivably be developed to treat POAG. NO-independent and heme-independent sGC activators preferentially activate sGC when the heme is oxidized or missing (Stasch et al., 2006). The selectivity of sGC activators for oxidized/heme-free sGC could be exploited therapeutically to preferentially target diseased tissue (Boerrigter et al., 2007), especially since oxidative stress may have a pathogenic role in POAG (Majsterek et al., 2011a). Another advantage of specifically activating sGC is that it bypasses any toxicity associated with activating NOS (see "NO-cGMP-mediated regulation of IOP: implications for POAG" above). In addition, targeting sGC rather than NOS circumvents concerns related with reduced NO bioavailability (e.g., in a setting of increased oxidative stress) and allows for a more specific approach since the biological actions of NO are not only mediated by cGMP but also by cGMP-independent mechanisms.

Other potential therapeutic approaches specifically aimed at cGMP signaling that may be developed for treatment of POAG include targeting other enzymes that control GMP levels and which are abundantly present in the eye, including cGMP-catabolizing PDE's (Francis et al., 2011) and NP activated membrane bound guanylate cyclades (see "NP receptors and their effects on IOP" below, Mckie et al., 2010). Pilot studies testing the ability of the PDE5 inhibitor sildenafil to lower IOP were not successful. A single oral dose of 50–100 mg sildenafil failed to impact IOP in POAG patients (Grunwald et al., 2001) and healthy volunteers (Vobig et al., 1999; Sponsel et al., 2000), but did increase blood flow in both healthy subjects (Sponsel et al., 2000; Foresta et al., 2008) and patients with systemic vascular dysfunction (Koksal et al., 2005). Also chronic treatment with sildenafil (twice per week for 3 months) failed to impact IOP (Dundar et al., 2006). It is noteworthy that the cohorts in which the effect of sildenafil on IOP was studied were of limited size (5–15 subjects). It is conceivable that these studies were underpowered to detect small decreases in IOP associated with sildenafil treatment. This is a relevant concern since modest changes in IOP have been reported to impact POAG risk in humans. For example, a 2-mmHg difference in IOP distinguished between progression and non-progression in POAG patients (Leske et al., 2007; Konstas et al., 2012). Also, most of the cohorts studied consisted of men only. In light of a possible gender-specificity of POAG (Vajaranant et al., 2010; Pasquale and Kang, 2011; Tsai et al., 2012) and the role of NO-cGMP signaling therein (Kang et al., 2010), it would be of interest to see whether preventing cGMP catabolism by PDE5 would impact IOP in women. Finally, the half-life of sildenafil is rather limited (∼4 h) (Smith et al., 2013). It may be worthwhile testing the effect on IOP of other PDE5 inhibitors with longer half-lives (e.g., tadalafil with a half-life of ∼17 h Smith et al., 2013) and/or performing a carefully controlled dose response experiment. Finally, various methods to deliver the drug should be tested. Whether pharmacological modulation of the activity of enzymes that ultimately modulate cGMP levels may prevent POAG progression remains to be determined.

sGC-DEFICIENT MICE: A MODEL OF ELEVATED IOP AND POAG

Mice lacking the α_1 subunit of the NO receptor soluble guanylate cyclase ($sGC\alpha_1^{-/-}$ mice) were recently reported to represent a novel and translatable animal model of POAG, characterized by thinning of the retinal nerve fiber layer (RNFL) and loss of optic nerve axons (Buys et al., 2013). The optic neuropathy associated with $sGC\alpha_1$—deficiency was accompanied by modestly increased IOP, on average 2 mmHg higher in 39 ± 14 weeks old female $sGC\alpha_1^{-/-}$ mice than in age-matched female wild-type (WT) mice. No IOP difference was detected between age-matched 15 ± 6 weeks old female $sGC\alpha_1^{-/-}$ and age-matched WT mice: age was a predictor of elevated IOP in female $sGC\alpha_1^{-/-}$ but not in WT mice. The increase in IOP was accompanied by a decrease in AqH turnover in the context of an open iridocorneal angle: $sGC\alpha_1^{-/-}$ mice presented with a normal ciliary body, a well-defined TM, and a patent Schlemm's canal. In addition, spectral domain optical coherence tomography analysis of the iridocorneal angle did not reveal any evidence for angle-closure in $sGC\alpha_1^{-/-}$ mice. Similarly, biomicroscopy did not reveal any evidence of exfoliation syndrome, pigment dispersion syndrome, or other conditions that could produce elevated IOP.

Highlighting the multi-faceted role of NO-cGMP signaling in ocular (patho)physiology, retinal vascular dysfunction was observed in $sGC\alpha_1^{-/-}$ mice. Other studies had postulated that vascular dysfunction contributes to the etiology of POAG (Henry et al., 1999; Feke and Pasquale, 2008; Su et al., 2008) and systemic vascular dysfunction had been previously reported in $sGC\alpha_1^{-/-}$ mice (Nimmegeers et al., 2007; Atochin et al., 2010; Buys et al., 2012). Whether retinal vascular dysfunction underlies the retinal degeneration and optic neuropathy in $sGC\alpha_1^{-/-}$ mice remains to be determined. Vascular dysfunction may also contribute to the observed increases in IOP in $sGC\alpha_1^{-/-}$ mice, possibly by impairing uveolymphatic outflow (see "Intraocular pressure: a risk factor for POAG" above). Finally, it cannot be excluded that loss of RGCs in $sGC\alpha_1^{-/-}$ mice is caused by a direct effect of sGC-deficiency on RGCs, possibly modulating the susceptibility of RGCs to stress imposed by increased IOP or vascular dysfunction. Taken together, targeting sGC may represent a multi-pronged approach, aimed at lowering IOP, ameliorating vascular function, and protecting RGCs from stress-induced dysfunction and death. To test this hypothesis, additional studies, including in animal models of POAG, such as the $sGC\alpha_1^{-/-}$ mouse model, are required.

GENETICS OF POAG

First-degree relatives of glaucoma patients have a 22% risk of developing glaucoma versus a 2% lifetime risk of relatives of controls (Wolfs et al., 1998). In recent years, familial aggregation, genome wide and candidate gene association studies have uncovered an important genetic component to POAG (**Table 2**). Several dozen genetic loci have been linked to POAG (Fan et al., 2006). The role of many of the identified genes in the etiology of POAG, some of which were identified in single studies that need to be replicated, remains controversial. Among the genes identified to date, three are involved in the nitric oxide (NO)-cGMP system, highlighting a central role of this signaling pathway in the development of POAG. First, variants were identified in or near the genes encoding caveolin 1 and 2 (*CAV1/CAV2*) (Thorleifsson et al., 2010; Wiggs et al., 2011). Caveolins modulate the ability of NOS3 to generate NO (Mineo and Shaul, 2012). At least one variant in the *CAV1/CAV2* locus was subsequently found to be associated with increased IOP (Van Koolwijk et al., 2012; Ozel et al., 2014). Second, A candidate gene association study in 527 incident cases and 1543 controls revealed interactions between *NOS3* gene variants, potentially affecting expression and/or activity of NOS3, and high tension POAG in females (Kang et al., 2010). In addition, a functional NOS3 polymorphism (T-786C) was associated with POAG and appears to interact with gender and age in modulating the risk of POAG (Magalhaes Da Silva et al., 2012). The same variant also affects the interaction of systemic hypertension and cigarette smoking with POAG risk, highlighting the complex gene-environment interactions that impact the etiology of POAG (Kang et al., 2011). And

Table 2 | POAG-associated genes.

Gene	Association	References	Remarks
AGTR2	NTG	Hashizume et al., 2005	CGAS, interaction with gender
APOE	POAG	Copin et al., 2002	CGAS
ASB10	POAG	Pasutto et al., 2012	Family-based linkage study
ATOH7	POAG	Ramdas et al., 2011; Chen et al., 2012	CGAS, interactive effect with RFTN1
C7	POAG	Scheetz et al., 2013	GWAS
CAV1/CAV2	POAG	Thorleifsson et al., 2010	GWAS, also associated with IOP (Ozel et al., 2014)
	POAG	Wiggs et al., 2011	CGAS, interaction with gender, also associated with IOP (Ozel et al., 2014)
CDKN1A	POAG	Tsai et al., 2004	CGAS
CDKN2B-AS1	POAG	Ramdas et al., 2011	CGAS
	POAG	Burdon et al., 2011	GWAS, also associated with IOP (Ozel et al., 2014)
	POAG	Nakano et al., 2012	GWAS, also associated with IOP (Ozel et al., 2014)
	POAG, NTG, XFG	Wiggs et al., 2012	GWAS, also associated with IOP (Ozel et al., 2014)
CYP1B1	JOAG	Vincent et al., 2002	CGAS
EDNRA	NTG	Ishikawa et al., 2005	CGAS
ELOVL5	NTG	Meguro et al., 2010	GWAS
GAS7	POAG	Van Koolwijk et al., 2012	CGAS, SNP identified in IOP GWAS
GLC1B	POAG	Stoilova et al., 1996	Family-based linkage study
GSTM1	POAG	Juronen et al., 2000	CGAS
HK2	POAG and NTG	Shi et al., 2013	CGAS
IGF2	POAG	Tsai et al., 2003	CGAS
IL1B	POAG	Lin et al., 2003b	CGAS
LOXL1	XFG	Thorleifsson et al., 2007	GWAS, not associated with POAG
MMP1	POAG	Majsterek et al., 2011b	CGAS
MTHFR	POAG	Junemann et al., 2005	CGAS
MYOC	JOAG	Sheffield et al., 1993; Stone et al., 1997	Family-based linkage study
NCK2	NTG	Shi et al., 2013	CGAS
NOS3	POAG	Tunny et al., 1998	CGAS
	HTG	Kang et al., 2010	CGAS, interaction with gender and hormone use
	POAG	Kang et al., 2011	CGAS, interaction with hypertension and smoking
NPPA	POAG	Tunny et al., 1996	CGAS
OCLM	POAG	Fujiwara et al., 2003	CGAS
OPA1	NTG	Aung et al., 2002	CGAS
OPTN	NTG	Sarfarazi et al., 1998; Rezaie et al., 2002	Family-based linkage study
Six1/Six6	POAG	Ramdas et al., 2011	CGAS
	POAG	Wiggs et al., 2012	GWAS, also associated with IOP (Ozel et al., 2014)
SRBD1	NTG	Meguro et al., 2010	GWAS
TAP1	POAG	Lin et al., 2004	CGAS
TMCO1	POAG	Burdon et al., 2011	GWAS, also associated with IOP (Van Koolwijk et al., 2012; Ozel et al., 2014)
TNF	POAG	Lin et al., 2003a	CGAS
TP53	POAG	Lin et al., 2002	CGAS
WDR36	POAG	Monemi et al., 2005	CGAS

AGTR2, Angiotensin II receptor type 2; APOE, Apolipoprotein E; ASB10, ankyrin repeat and SOCS box-containing 1; ATOH7, atonal homolog 7; C7, complement component 7; CAV1, caveolin 1; CAV2, caveolin 2; CDKN1A, cyclin-dependent kinase inhibitor 1A; CDKN2B-AS1, CDKN2B antisense RNA 1; CGAS, candidate gene association study; CYP1B1, cytochrome P450 subfamily I polypeptide 1; EDNRA, endothelin receptor type A; ELOVL1, elongation of very-long-chain-fatty acids 1; GAS7, growth arrest-specific protein 7; GLC1B, glaucoma 1, open angle, B; GSTM1, glutathione S-transferase mu-1; GWAS, genome-wide association study; HK2, hexokinase 2; HTG, high-tension glaucoma; IGF2, insulin-like growth factor II; IL1B, interleukin 1-beta; IOP, intra-ocular pressure; JOAG, juvenile open angle glaucoma; LOXL1, lysyl oxidase-like 1; MMP1, matrix metalloproteinase 1; MTHFR, 5,10-methylenetetrahydrofolate reductase; MYOC, myocilin; NCK2, NCK adaptor protein 2; NOS3, nitric oxide synthase 3; NPPA, natriuretic peptide precursor; NTG, normal-tension glaucoma; OCLM, oculomedin; OPA1, optic atrophy 1; OPTN, optineurin; POAG, primary open angle glaucoma; RFTN1, raftlin lipid raft linker 1; Six1/Six6, six homeobox1/6; SRBD1, S1 RNA-Binding Domain-Containing Protein 1; TAP1, transporter ATP-binding cassette major histocompatibility complex 1; TMCO1, transmembrane and coiled-coil domains 1; TNF, tumor necrosis factor; TP53, tumor protein p53; WDR36, WD repeat domain 36; XFG, exfoliation glaucoma.

thirdly, in a recent candidate gene association study in POAG patients from the GLAUGEN cohort (Wiggs et al., 2011), a variant (rs11722059) was identified in the *GUCY1A3/GUCY1B3* locus (containing the genes encoding the α_1 and β_1 subunits of sGC, arranged in tandem) (Wiggs et al., 2011). Intriguingly, the association was only present in POAG characterized by early paracentral visual field loss (Buys et al., 2013). Early paracentral visual field loss is a subtype of POAG previously postulated to be associated with ocular vascular dysregulation (Park et al., 2011). This was a particularly interesting finding in light of the identification of $sGC\alpha_1^{-/-}$ mice with systemic and retinal vascular dysfunction, as a model of POAG with moderately elevated IOP: as described above, POAG patients with early paracentral visual field loss tend to have more frequent systemic vascular risk factors (Park et al., 2011, 2012), and low OPP is a risk factor for POAG (Leske, 2009; Cherecheanu et al., 2013). In addition, rs11722059 is in linkage disequilibrium with a *GUCY1A3/GUCY1B3* variant associated with blood pressure in a large genome wide association study (GWAS) (Ehret et al., 2011). However, the extent to which vascular dysfunction contributes to glaucomatous optic neuropathy remains to be elucidated (Flammer et al., 2002; Vajaranant and Pasquale, 2012).

For neither the *NOS3* or *GUCY1A3/GUCY1B3* variants, an association with IOP was detected. Whether this truly means that there is no association with the identified variants remains unsure: it is conceivable that the GWAS and candidate gene association studies discussed were underpowered to detect small effect on IOP. For example, the GWAS in which the sGC blood pressure variant was identified included 200,000 subjects (Ehret et al., 2011). In contrast, the studies aimed at identifying associations with POAG and IOP (like systemic blood pressure a continuous variable) were much smaller in scope (hundreds to several thousand subjects).

NP RECEPTORS AND THEIR EFFECTS ON IOP

There are three NPs in mammals: atrial NP, B-type NP and C-type NP (Potter et al., 2009). A separate gene encodes each NP, and mouse "knock out" experiments have shown that each NP has unique functions, although all members stimulate vasorelaxation. ANP and BNP are cardiac endocrine hormones that decrease blood pressure and volume. CNP is a paracrine-signaling molecule that stimulates long bone growth, causes bifurcation of neurons in the spinal cord and inhibits meiosis in the oocyte.

There are also three known NP peptide receptors (Potter, 2011a,b,c). The natriuretic clearance receptor (NPR-C) controls the local concentration of all three natriuretic peptides through an undefined receptor-mediated internalization and degradation process, but it has also been reported to signal through a G-protein-dependent pathway. The primary signaling receptor for ANP and BNP is guanylate cyclase-A (GC-A), which is also known as natriuretic peptide receptor-A or NPR1. It consists of an extracellular ligand-binding domain, a single membrane-spanning region and intracellular guanylate cyclase domain. GC-B, also known at NPR-B or NPR2, is the primary signaling receptor for CNP and it is topologically and structurally similar to GC-A. The vast majority of NPs functions are mediated through elevation of intracellular cGMP concentrations synthesized by the guanylate cyclase domains of GC-A or GC-B.

Early studies reported that binding sites for ^{125}I-ANP were found in rat and rabbit ciliary processes (Bianchi et al., 1986). Shortly thereafter, topical, intracameral and intravitreal application of ANP was shown to decrease IOP in rabbits (Sugrue and Viader, 1986). The pressure reductions were longer lasting with the intravitreal treatments but even the topical application reduced IOP. Additional studies found that ANP stimulated guanylate cyclase activity in ciliary processes of the rabbit eye and that intravitreous injection of ANP decreased IOP in the rabbit eye for up to 24 h (Mittag et al., 1987). The reduction of IOP by intravitreal ANP was later correlated to a decrease in AqH flow in the rabbit eye (Korenfeld and Becker, 1989).

Relatively low concentrations of CNP (∼2 nmol/L) were also shown to increase cGMP concentrations in the AqH of the rabbit eye and reduce IOP in rabbit eyes by a process associated with an increase in total outflow facility (Takashima et al., 1998). In the same study, CNP-like immunoreactivity was detected in rabbit and porcine AqH at about two-fold higher concentrations than that found in plasma. In a more recent study, CNP was shown to be a more potent reducer of IOP than ANP in rabbit eyes, and a ring-deleted analog of ANP that blocked binding to NPR-C and increased the concentration of all endogenous natriuretic peptides, maintained IOP reductions longer that other natriuretic peptides (Fernandez-Durango et al., 1999). Thus, whether the reductions in IOP observed by early investigators were due to cross-activation of GC-B or whether activation of GC-B and GC-A leads to decreased IOP is not known. Regardless, CNP is the most potent natriuretic peptide for reducing IOP in mammals, which suggests that the degradation resistant CNP analog developed for the treatment of achondroplasia may be an ideal peptide-based molecule to reduce IOP in the clinic (Lorget et al., 2012).

CONCLUSION

In conclusion, POAG remains a major cause of blindness in the USA and worldwide. The identification of new therapeutic targets for the treatment of POAG has been hampered by lack of understanding of the etiology of POAG and the limited number of animal models available that likely represent only a small subset of human POAG cases. There continues to be an urgent need for biomarkers that allow to detect/diagnose/track POAG progression and treatment efficacy. Also, the lack of a definitive cure underscores the need to develop novel therapeutic approaches for POAG.

Evidence obtained from animal models indicates that cGMP signaling plays an important role in POAG pathogenesis. These findings are supported by genetic studies of IOP and POAG risk in human subjects, highlighting the relevance of cGMP signaling in the development of POAG. Strategies aimed at modulating cGMP levels may constitute a pharmacological approach for a disease for which no definitive cure is currently available. However, additional studies are required to unequivocally determine the role of impaired cGMP signaling in POAG and to advance bench-to-bedside translation of available cGMP-enhancing reagents.

ACKNOWLEDGMENTS

The authors thank Peter Mallen for generating the figures. Dr. Buys was supported by NIH/NEI 1R01EY022746-01. Dr. Pasquale was supported by a Harvard Medical School

Distinguished Ophthalmology Scholar Award and by NIH/NEI RO1EY015473-10.

REFERENCES

Alward, W. L. (2000). The genetics of open-angle glaucoma: the story of GLC1A and myocilin. *Eye* 14 (Pt 3B), 429–436. doi: 10.1038/eye.2000.127

Anderson, M. G., Libby, R. T., Mao, M., Cosma, I. M., Wilson, L. A., Smith, R. S., et al. (2006). Genetic context determines susceptibility to intraocular pressure elevation in a mouse pigmentary glaucoma. *BMC Biol.* 4, 20. doi: 10.1186/1741-7007-4-20

Arevalo, J. F., Munguia, D., Faber, D., Friedlander, S. M., Quiceno, J. I., Rahhal, F. M., et al. (1996). Correlation between intraocular pressure and CD4+ T-lymphocyte counts in patients with human immunodeficiency virus with and without cytomegalovirus retinitis. *Am. J. Ophthalmol.* 122, 91–96.

Atochin, D. N., Wang, A., Liu, V. W., Critchlow, J. D., Dantas, A. P., Looft-Wilson, R., et al. (2007). The phosphorylation state of eNOS modulates vascular reactivity and outcome of cerebral ischemia *in vivo*. *J. Clin. Invest.* 117, 1961–1967. doi: 10.1172/JCI29877

Atochin, D. N., Yuzawa, I., Li, Q., Rauwerdink, K. M., Malhotra, R., Chang, J., et al. (2010). Soluble guanylate cyclase alpha1beta1 limits stroke size and attenuates neurological injury. *Stroke* 41, 1815–1819. doi: 10.1161/STROKEAHA.109.577635

Aung, T., Ocaka, L., Ebenezer, N. D., Morris, A. G., Krawczak, M., Thiselton, D. L., et al. (2002). A major marker for normal tension glaucoma: association with polymorphisms in the OPA1 gene. *Hum. Genet.* 110, 52–56. doi: 10.1007/s00439-001-0645-7

Bamberger, A. M., Koglin, M., Kempfert, J., Loning, T., Scholz, H., and Behrends, S. (2001). Expression and tissue localization of soluble guanylyl cyclase in the human placenta using novel antibodies directed against the alpha(2) subunit. *J. Clin. Endocrinol. Metab.* 86, 909–912. doi: 10.1210/jcem.86.2.7409

Behar-Cohen, F. F., Goureau, O., D'hermies, F., and Courtois, Y. (1996). Decreased intraocular pressure induced by nitric oxide donors is correlated to nitrite production in the rabbit eye. *Invest. Ophthalmol. Vis. Sci.* 37, 1711–1715.

Bengtsson, B., Leske, M. C., Hyman, L., and Heijl, A. (2007). Fluctuation of intraocular pressure and glaucoma progression in the early manifest glaucoma trial. *Ophthalmology* 114, 205–209. doi: 10.1016/j.ophtha.2006.07.060

Bennett, J. P., Cross, R. A., Kendrick-Jones, J., and Weeds, A. G. (1988). Spatial pattern of myosin phosphorylation in contracting smooth muscle cells: evidence for contractile zones. *J. Cell Biol.* 107, 2623–2629. doi: 10.1083/jcb.107.6.2623

Bianchi, C., Anand-Srivastava, M. B., De Lean, A., Gutkowska, J., Forthomme, D., Genest, J., et al. (1986). Localization and characterization of specific receptors for atrial natriuretic factor in the ciliary processes of the eye. *Curr. Eye Res.* 5, 283–293. doi: 10.3109/02713688609020054

Bleiman, B. S., and Schwartz, A. L. (1979). Paradoxical intraocular pressure response to pilocarpine. A proposed mechanism and treatment. *Arch. Ophthalmol.* 97, 1305–1306. doi: 10.1001/archopht.1979.01020020047010

Blom, J., Giove, T., Deshpande, M., and Eldred, W. D. (2012). Characterization of nitric oxide signaling pathways in the mouse retina. *J. Comp. Neurol.* 520, 4204–4217. doi: 10.1002/cne.23148

Blute, T. A., Velasco, P., and Eldred, W. D. (1998). Functional localization of soluble guanylate cyclase in turtle retina: modulation of cGMP by nitric oxide donors. *Vis. Neurosci.* 15, 485–498. doi: 10.1017/S0952523898153075

Boerrigter, G., Costello-Boerrigter, L. C., Cataliotti, A., Lapp, H., Stasch, J. P., and Burnett, J. C., Jr. (2007). Targeting heme-oxidized soluble guanylate cyclase in experimental heart failure. *Hypertension* 49, 1128–1133. doi: 10.1161/HYPERTENSIONAHA.106.083832

Bonomi, L., Marchini, G., Marraffa, M., Bernardi, P., Morbio, R., and Varotto, A. (2000). Vascular risk factors for primary open angle glaucoma: the Egna-Neumarkt Study. *Ophthalmology* 107, 1287–1293. doi: 10.1016/S0161-6420(00)00138-X

Burdon, K. P., Macgregor, S., Hewitt, A. W., Sharma, S., Chidlow, G., Mills, R. A., et al. (2011). Genome-wide association study identifies susceptibility loci for open angle glaucoma at TMCO1 and CDKN2B-AS1. *Nat. Genet.* 43, 574–578. doi: 10.1038/ng.824

Buys, E. S., Ko, Y. C., Alt, C., Hayton, S. R., Jones, A., Tainsh, L. T., et al. (2013). Soluble guanylate cyclase alpha1-deficient mice: a novel murine model for primary open angle glaucoma. *PLoS ONE* 8:e60156. doi: 10.1371/journal.pone.0060156

Buys, E. S., Raher, M. J., Kirby, A., Mohd, S., Baron, D. M., Hayton, S. R., et al. (2012). Genetic modifiers of hypertension in soluble guanylate cyclase alpha1-deficient mice. *J. Clin. Invest.* 122, 2316–2325. doi: 10.1172/JCI60119

Buys, E. S., Sips, P., Vermeersch, P., Raher, M. J., Rogge, E., Ichinose, F., et al. (2008). Gender-specific hypertension and responsiveness to nitric oxide in sGC{alpha}1 knockout mice. *Cardiovasc. Res.* 79, 179–186. doi: 10.1093/cvr/cvn068

Carbonaro, F., Andrew, T., Mackey, D. A., Young, T. L., Spector, T. D., and Hammond, C. J. (2009). Repeated measures of intraocular pressure result in higher heritability and greater power in genetic linkage studies. *Invest. Ophthalmol. Vis. Sci.* 50, 5115–5119. doi: 10.1167/iovs.09-3577

Castro, L. R., Verde, I., Cooper, D. M., and Fischmeister, R. (2006). Cyclic guanosine monophosphate compartmentation in rat cardiac myocytes. *Circulation* 113, 2221–2228. doi: 10.1161/CIRCULATIONAHA.105.599241

Chang, C. J., Chiang, C. H., Chow, J. C., and Lu, D. W. (2000). Aqueous humor nitric oxide levels differ in patients with different types of glaucoma. *J. Ocul. Pharmacol. Ther.* 16, 399–406. doi: 10.1089/jop.2000.16.399

Chen, C., Xu, Y., Zhang, J., Zhu, J., Hu, N., and Guan, H. (2013). Altered expression of nNOS/NIDD in the retina of a glaucoma model of DBA/2J mice and the intervention by nNOS inhibition. *J. Mol. Neurosci.* 51, 47–56. doi: 10.1007/s12031-012-9943-x

Chen, J. H., Wang, D., Huang, C., Zheng, Y., Chen, H., Pang, C. P., et al. (2012). Interactive effects of ATOH7 and RFTN1 in association with adult-onset primary open-angle glaucoma. *Invest. Ophthalmol. Vis. Sci.* 53, 779–785. doi: 10.1167/iovs.11-8277

Chen, J., Runyan, S. A., and Robinson, M. R. (2011). Novel ocular antihypertensive compounds in clinical trials. *Clin. Ophthalmol.* 5, 667–677. doi: 10.2147/OPTH.S15971

Cherecheanu, A. P., Garhofer, G., Schmidl, D., Werkmeister, R., and Schmetterer, L. (2013). Ocular perfusion pressure and ocular blood flow in glaucoma. *Curr. Opin. Pharmacol.* 13, 36–42. doi: 10.1016/j.coph.2012.09.003

Chiamvimonvat, N., O'Rourke, B., Kamp, T. J., Kallen, R. G., Hofmann, F., Flockerzi, V., et al. (1995). Functional consequences of sulfhydryl modification in the pore-forming subunits of cardiovascular Ca2+ and Na+ channels. *Circ. Res.* 76, 325–334. doi: 10.1161/01.RES.76.3.325

Chiou, S. H., Chang, C. J., Hsu, W. M., Kao, C. L., Liu, J. H., Chen, W. L., et al. (2001). Elevated nitric oxide level in aqueous humor of patients with acute angle-closure glaucoma. *Ophthalmologica* 215, 113–116. doi: 10.1159/000050840

Clark, A. F., Wilson, K., De Kater, A. W., Allingham, R. R., and Mccartney, M. D. (1995). Dexamethasone-induced ocular hypertension in perfusion-cultured human eyes. *Invest. Ophthalmol. Vis. Sci.* 36, 478–489.

Copin, B., Brezin, A. P., Valtot, F., Dascotte, J. C., Bechetoille, A., and Garchon, H. J. (2002). Apolipoprotein E-promoter single-nucleotide polymorphisms affect the phenotype of primary open-angle glaucoma and demonstrate interaction with the myocilin gene. *Am. J. Hum. Genet.* 70, 1575–1581. doi: 10.1086/340733

Davis, K. L., Martin, E., Turko, I. V., and Murad, F. (2001). Novel effects of nitric oxide. *Annu. Rev. Pharmacol. Toxicol.* 41, 203–236. doi: 10.1146/annurev.pharmtox.41.1.203

Decaluwe, K., Nimmegeers, S., Thoonen, R., Buys, E., Brouckaert, P., and Van De Voorde, J. (2010). *In vitro* and *in vivo* studies on the importance of the soluble guanylyl cyclase alpha1 subunit in penile erection. *World J. Urol.* 28, 643–650. doi: 10.1007/s00345-010-0509-7

De Voogd, S., Ikram, M. K., Wolfs, R. C., Jansonius, N. M., Hofman, A., and De Jong, P. T. (2005). Incidence of open-angle glaucoma in a general elderly population: the Rotterdam Study. *Ophthalmology* 112, 1487–1493. doi: 10.1016/j.ophtha.2005.04.018

Dismuke, W. M., Mbadugha, C. C., and Ellis, D. Z. (2008). NO-induced regulation of human trabecular meshwork cell volume and aqueous humor outflow facility involve the BKCa ion channel. *Am. J. Physiol. Cell Physiol.* 294, C1378–C1386. doi: 10.1152/ajpcell.00363.2007

Dismuke, W. M., Sharif, N. A., and Ellis, D. Z. (2009). Human trabecular meshwork cell volume decrease by NO-independent soluble guanylate cyclase activators YC-1 and BAY-58-2667 involves the BKCa ion channel. *Invest. Ophthalmol. Vis. Sci.* 50, 3353–3359. doi: 10.1167/iovs.08-3127

Doganay, S., Evereklioglu, C., Turkoz, Y., and Er, H. (2002). Decreased nitric oxide production in primary open-angle glaucoma. *Eur. J. Ophthalmol.* 12, 44–48.

Dundar, S. O., Dayanir, Y., Topaloglu, A., Dundar, M., and Kocak, I. (2006). Effect of sildenafil on ocular hemodynamics in 3 months regular use. *Int. J. Impot. Res.* 18, 282–286. doi: 10.1038/sj.ijir.3901416

Ehret, G. B., Munroe, P. B., Rice, K. M., Bochud, M., Johnson, A. D., Chasman, D. I., et al. (2011). Genetic variants in novel pathways influence blood pressure and cardiovascular disease risk. *Nature* 478, 103–109. doi: 10.1038/nature10405

Ellis, D. Z., Dismuke, W. M., and Chokshi, B. M. (2009). Characterization of soluble guanylate cyclase in NO-induced increases in aqueous humor outflow facility and in the trabecular meshwork. *Invest. Ophthalmol. Vis. Sci.* 50, 1808–1813. doi: 10.1167/iovs.08-2750

Ellis, D. Z., Sharif, N. A., and Dismuke, W. M. (2010). Endogenous regulation of human Schlemm's canal cell volume by nitric oxide signaling. *Invest. Ophthalmol. Vis. Sci.* 51, 5817–5824. doi: 10.1167/iovs.09-5072

Erickson-Lamy, K., Rohen, J. W., and Grant, W. M. (1991). Outflow facility studies in the perfused human ocular anterior segment. *Exp. Eye Res.* 52, 723–731. doi: 10.1016/0014-4835(91)90024-9

Ethier, C. R., Kamm, R. D., Palaszewski, B. A., Johnson, M. C., and Richardson, T. M. (1986). Calculations of flow resistance in the juxtacanalicular meshwork. *Invest. Ophthalmol. Vis. Sci.* 27, 1741–1750.

Fan, B. J., Wang, D. Y., Lam, D. S., and Pang, C. P. (2006). Gene mapping for primary open angle glaucoma. *Clin. Biochem.* 39, 249–258. doi: 10.1016/j.clinbiochem.2005.11.001

Fautsch, M. P., and Johnson, D. H. (2006). Aqueous humor outflow: what do we know? Where will it lead us? *Invest. Ophthalmol. Vis. Sci.* 47, 4181–4187. doi: 10.1167/iovs.06-0830

Feke, G. T., Hazin, R., Grosskreutz, C. L., and Pasquale, L. R. (2011). Effect of brimonidine on retinal blood flow autoregulation in primary open-angle glaucoma. *J. Ocul. Pharmacol.*7, 347–352. doi: 10.1089/jop.2011.0014

Feke, G. T., and Pasquale, L. R. (2008). Retinal blood flow response to posture change in glaucoma patients compared with healthy subjects. *Ophthalmology* 115, 246–252. doi: 10.1016/j.ophtha.2007.04.055

Fernandez-Durango, R., Fernandez-Martinez, A., Garcia-Feijoo, J., Castillo, A., De La Casa, J. M., Garcia-Bueno, B., et al. (2008). Expression of nitrotyrosine and oxidative consequences in the trabecular meshwork of patients with primary open-angle glaucoma. *Invest. Ophthalmol. Vis. Sci.* 49, 2506–2511. doi: 10.1167/iovs.07-1363

Fernandez-Durango, R., Moya, F. J., Ripodas, A., De Juan, J. A., Fernandez-Cruz, A., and Bernal, R. (1999). Type B and type C natriuretic peptide receptors modulate intraocular pressure in the rabbit eye. *Eur. J. Pharmacol.* 364, 107–113. doi: 10.1016/S0014-2999(98)00828-0

Fernandez-Durango, R., Nunez, D. J., and Brown, M. J. (1995). Messenger RNAs encoding the natriuretic peptides and their receptors are expressed in the eye. *Exp. Eye Res.* 61, 723–729. doi: 10.1016/S0014-4835(05)80023-5

Flammer, J., Orgul, S., Costa, V. P., Orzalesi, N., Krieglstein, G. K., Serra, L. M., et al. (2002). The impact of ocular blood flow in glaucoma. *Prog. Retin. Eye Res.* 21, 359–393. doi: 10.1016/S1350-9462(02)00008-3

Flugel, C., Barany, E. H., and Lutjen-Drecoll, E. (1990). Histochemical differences within the ciliary muscle and its function in accommodation. *Exp. Eye Res.* 50, 219–226. doi: 10.1016/0014-4835(90)90234-L

Foresta, C., Caretta, N., Zuccarello, D., Poletti, A., Biagioli, A., Caretti, L., et al. (2008). Expression of the PDE5 enzyme on human retinal tissue: new aspects of PDE5 inhibitors ocular side effects. *Eye* 22, 144–149. doi: 10.1038/sj.eye.6702908

Francis, S. H., Blount, M. A., and Corbin, J. D. (2011). Mammalian cyclic nucleotide phosphodiesterases: molecular mechanisms and physiological functions. *Physiol. Rev.* 91, 651–690. doi: 10.1152/physrev.00030.2010

Franco-Bourland, R. E., Guizar-Sahagun, G., Garcia, G. A., Odor-Morales, A., Alvarez, A., Esquivel, F., et al. (1998). Retinal vulnerability to glutamate excitotoxicity in canine glaucoma: induction of neuronal nitric oxide synthase in retinal ganglion cells. *Proc. West. Pharmacol. Soc.* 41, 201–204.

Friebe, A., Mergia, E., Dangel, O., Lange, A., and Koesling, D. (2007). Fatal gastrointestinal obstruction and hypertension in mice lacking nitric oxide-sensitive guanylyl cyclase. *Proc. Natl. Acad. Sci. U.S.A.* 104, 7699–7704. doi: 10.1073/pnas.0609778104

Fujiwara, N., Matsuo, T., and Ohtsuki, H. (2003). Protein expression, genomic structure, and polymorphisms of oculomedin. *Ophthal. Genet.* 24, 141–151. doi: 10.1076/opge.24.3.141.15604

Galassi, F., Renieri, G., Sodi, A., Ucci, F., Vannozzi, L., and Masini, E. (2004). Nitric oxide proxies and ocular perfusion pressure in primary open angle glaucoma. *Br. J. Ophthalmol.* 88, 757–760. doi: 10.1136/bjo.2003.028357

Galassi, F., Sodi, A., Ucci, F., Renieri, G., Pieri, B., and Masini, E. (2000). Ocular haemodynamics and nitric oxide in normal pressure glaucoma. *Acta. Ophthalmol. Scand. Suppl.* 78, 37–38. doi: 10.1111/j.1600-0420.2000.tb01093.x

Garcia Filho, C. A., Prata, T. S., Sousa, A. K., Doi, L. M., and Melo, L. A. Jr. (2011). Intraocular pressure, corneal thickness, and corneal hysteresis in Steinert's myotonic dystrophy. *Arq. Bras. Oftalmol.* 74, 161–162. doi: 10.1590/S0004-27492011000300002

Gasser, P., and Flammer, J. (1991). Blood-cell velocity in the nailfold capillaries of patients with normal-tension and high-tension glaucoma. *Am. J. Ophthalmol.* 111, 585–588.

Ghofrani, H. A., Galie, N., Grimminger, F., Grunig, E., Humbert, M., Jing, Z. C., et al. (2013). Riociguat for the treatment of pulmonary arterial hypertension. *New Engl. J. Med.* 369, 330–340. doi: 10.1056/NEJMoa1209655

Giuffrida, S., Bucolo, C., and Drago, F. (2003). Topical application of a nitric oxide synthase inhibitor reduces intraocular pressure in rabbits with experimental glaucoma. *J. Ocul. Pharmacol. Ther.* 19, 527–534. doi: 10.1089/108076803322660440

Grunwald, J. E., Jacob, S. S., Siu, K., Piltz, J., and Dupont, J. (2001). Acute effects of sldenafil ctrate (Viagra) on intraocular pressure in open-angle glaucoma. *Am. J. Ophthalmol.* 132, 872–874. doi: 10.1016/S0002-9394(01)01268-5

Haberecht, M. F., Schmidt, H. H., Mills, S. L., Massey, S. C., Nakane, M., and Redburn-Johnson, D. A. (1998). Localization of nitric oxide synthase, NADPH diaphorase and soluble guanylyl cyclase in adult rabbit retina. *Vis. Neurosci.* 15, 881–890. doi: 10.1017/S0952523898155104

Harris, A., Rechtman, E., Siesky, B., Jonescu-Cuypers, C., Mccranor, L., and Garzozi, H. J. (2005). The role of optic nerve blood flow in the pathogenesis of glaucoma. *Ophthalmol. Clin. North Am.* 18, 345–353. doi: 10.1016/j.ohc.2005.04.001

Hashizume, K., Mashima, Y., Fumayama, T., Ohtake, Y., Kimura, I., Yoshida, K., et al. (2005). Genetic polymorphisms in the angiotensin II receptor gene and their association with open-angle glaucoma in a Japanese population. *Invest. Ophthalmol. Vis. Sci.* 46, 1993–2001. doi: 10.1167/iovs.04-1100

He, Z., Vingrys, A. J., Armitage, J. A., and Bui, B. V. (2011). The role of blood pressure in glaucoma. *Clin. Exp. Optom.* 94, 133–149. doi: 10.1111/j.1444-0938.2010.00564.x

Heijl, A., Leske, M. C., Bengtsson, B., Hyman, L., Bengtsson, B., and Hussein, M. (2002). Reduction of intraocular pressure and glaucoma progression: results from the Early Manifest Glaucoma Trial. *Arch. Ophthalmol.* 120, 1268–1279. doi: 10.1001/archopht.120.10.1268

Henry, E., Newby, D. E., Webb, D. J., and O'brien, C. (1999). Peripheral endothelial dysfunction in normal pressure glaucoma. *Invest. Ophthalmol. Vis. Sci.* 40, 1710–1714.

Hobbs, A. J. (1997). Soluble guanylate cyclase: the forgotten sibling. *Trends Pharmacol. Sci.* 18, 484–491. doi: 10.1016/S0165-6147(97)01137-1

Honjo, M., Tanihara, H., Inatani, M., Kido, N., Sawamura, T., Yue, B. Y., et al. (2001). Effects of rho-associated protein kinase inhibitor Y-27632 on intraocular pressure and outflow facility. *Invest. Ophthalmol. Vis. Sci.* 42, 137–144.

Hulsman, C. A., Vingerling, J. R., Hofman, A., Witteman, J. C., and De Jong, P. T. (2007). Blood pressure, arterial stiffness, and open-angle glaucoma: the Rotterdam study. *Arch. Ophthalmol.* 125, 805–812. doi: 10.1001/archopht.125.6.805

Ishikawa, K., Funayama, T., Ohtake, Y., Kimura, I., Ideta, H., Nakamoto, K., et al. (2005). Association between glaucoma and gene polymorphism of endothelin type A receptor. *Mol. Vis.* 11, 431–437.

Jaffrey, S. R., Erdjument-Bromage, H., Ferris, C. D., Tempst, P., and Snyder, S. H. (2001). Protein S-nitrosylation: a physiological signal for neuronal nitric oxide. *Nat. Cell Biol.* 3, 193–197. doi: 10.1038/35055104

Javadiyan, S., Burdon, K. P., Whiting, M. J., Abhary, S., Straga, T., Hewitt, A. W., et al. (2012). Elevation of serum asymmetrical and symmetrical dimethylarginine in patients with advanced glaucoma. *Invest. Ophthalmol. Vis. Sci.* 53, 1923–1927. doi: 10.1167/iovs.11-8420

John, S. W., Smith, R. S., Savinova, O. V., Hawes, N. L., Chang, B., Turnbull, D., et al. (1998). Essential iris atrophy, pigment dispersion, and glaucoma in DBA/2J mice. *Invest. Ophthalmol. Vis. Sci.* 39, 951–962.

Junemann, A. G., Von Ahsen, N., Reulbach, U., Roedl, J., Bonsch, D., Kornhuber, J., et al. (2005). C677T variant in the methylentetrahydrofolate reductase gene is a genetic risk factor for primary open-angle glaucoma. *Am. J. Ophthalmol.* 139, 721–723. doi: 10.1016/j.ajo.2004.09.081

Juronen, E., Tasa, G., Veromann, S., Parts, L., Tiidla, A., Pulges, R., et al. (2000). Polymorphic glutathione S-transferase M1 is a risk factor of primary open-angle glaucoma among Estonians. *Exp. Eye Res.* 71, 447–452. doi: 10.1006/exer.2000.0899

Kaiser, H. J., and Flammer, J. (1991). Systemic hypotension: a risk factor for glaucomatous damage? *Ophthalmologica* 203, 105–108.

Kajimura, M., Shimoyama, M., Tsuyama, S., Suzuki, T., Kozaki, S., Takenaka, S., et al. (2003). Visualization of gaseous monoxide reception by soluble guanylate cyclase in the rat retina. *FASEB J.* 17, 506–508. doi: 10.1096/fj.02-0359fje

Kamikawatoko, S., Tokoro, T., Ishida, A., Masuda, H., Hamasaki, H., Sato, J., et al. (1998). Nitric oxide relaxes bovine ciliary muscle contracted by carbachol through elevation of cyclic GMP. *Exp. Eye Res.* 66, 1–7. doi: 10.1006/exer.1997.0408

Kang, J. H., Wiggs, J. L., Rosner, B. A., Haines, J., Abdrabou, W., and Pasquale, L. R. (2011). Endothelial nitric oxide synthase gene variants and primary open-angle glaucoma: interactions with hypertension, alcohol intake, and cigarette smoking. *Arch. Ophthalmol.* 129, 773–780. doi: 10.1001/archophthalmol.2011.118

Kang, J. H., Wiggs, J. L., Rosner, B. A., Hankinson, S. E., Abdrabou, W., Fan, B. J., et al. (2010). Endothelial nitric oxide synthase gene variants and primary open-angle glaucoma: interactions with sex and postmenopausal hormone use. *Invest. Ophthalmol. Vis. Sci.* 51, 971–979. doi: 10.1167/iovs.09-4266

Kass, M. A., Gordon, M. O., Gao, F., Heuer, D. K., Higginbotham, E. J., Johnson, C. A., et al. (2010). Delaying treatment of ocular hypertension: the ocular hypertension treatment study. *Arch. Ophthalmol.* 128, 276–287. doi: 10.1001/archophthalmol.2010.20

Kass, M. A., Heuer, D. K., Higginbotham, E. J., Johnson, C. A., Keltner, J. L., Miller, J. P., et al. (2002). The ocular hypertension treatment study: a randomized trial determines that topical ocular hypotensive medication delays or prevents the onset of primary open-angle glaucoma. *Arch. Ophthalmol.* 120, 701–713; discussion 829-730. doi: 10.1001/archopht.120.6.701

Kaufman, P. L. (2008). Enhancing trabecular outflow by disrupting the actin cytoskeleton, increasing uveoscleral outflow with prostaglandins, and understanding the pathophysiology of presbyopia interrogating Mother Nature: asking why, asking how, recognizing the signs, following the trail. *Exp. Eye Res.* 86, 3–17. doi: 10.1016/j.exer.2007.10.007

Kee, C., Kaufman, P. L., and Gabelt, B. T. (1994). Effect of 8-Br cGMP on aqueous humor dynamics in monkeys. *Invest. Ophthalmol. Vis. Sci.* 35, 2769–2773.

Khoobehi, B., Chiroli, V., Ronchetti, D., Miglietta, D., Thompson, H., Ongini, E., et al. (2011). Enhanced oxygen saturation in optic nerve head of non-human primate eyes following the intravitreal injection of NCX 434, an innovative nitric oxide-donating glucocorticoid. *J. Ocul. Pharmacol. Ther.* 27, 115–121. doi: 10.1089/jop.2010.0150

Klein, B. E., Klein, R., and Knudtson, M. D. (2005). Intraocular pressure and systemic blood pressure: longitudinal perspective: the Beaver Dam Eye Study. *Br. J. Ophthalmol.* 89, 284–287. doi: 10.1136/bjo.2004.048710

Klein, B. E., Klein, R., and Linton, K. L. (1992). Intraocular pressure in an American community. the beaver dam eye study. *Invest. Ophthalmol. Vis. Sci.* 33, 2224–2228.

Koksal, M., Ozdemir, H., Kargi, S., Yesilli, C., Tomac, S., Mahmutyazicioglu, K., et al. (2005). The effects of sildenafil on ocular blood flow. *Acta. Ophthalmol. Scand.* 83, 355–359. doi: 10.1111/j.1600-0420.2005.00422.x

Konstas, A. G., Quaranta, L., Mikropoulos, D. G., Nasr, M. B., Russo, A., Jaffee, H. A., et al. (2012). Peak intraocular pressure and glaucomatous progression in primary open-angle glaucoma. *J. Ocul. Pharmacol. Ther.* 28, 26–32. doi: 10.1089/jop.2011.0081

Korenfeld, M. S., and Becker, B. (1989). Atrial natriuretic peptides. Effects on intraocular pressure, cGMP, and aqueous flow. *Invest. Ophthalmol. Vis. Sci.* 30, 2385–2392.

Kotikoski, H., Alajuuma, P., Moilanen, E., Salmenpera, P., Oksala, O., Laippala, P., et al. (2002). Comparison of nitric oxide donors in lowering intraocular pressure in rabbits: role of cyclic GMP. *J. Ocul. Pharmacol. Ther.* 18, 11–23. doi: 10.1089/108076802317233171

Kotikoski, H., Vapaatalo, H., and Oksala, O. (2003). Nitric oxide and cyclic GMP enhance aqueous humor outflow facility in rabbits. *Curr. Eye Res.* 26, 119–123. doi: 10.1076/ceyr.26.2.119.14511

Krauss, A. H., Impagnatiello, F., Toris, C. B., Gale, D. C., Prasanna, G., Borghi, V., et al. (2011). Ocular hypotensive activity of BOL-303259-X, a nitric oxide donating prostaglandin F2alpha agonist, in preclinical models. *Exp. Eye Res.* 93, 250–255. doi: 10.1016/j.exer.2011.03.001

Krupin, T., Liebmann, J. M., Greenfield, D. S., Ritch, R., and Gardiner, S. (2011). A randomized trial of brimonidine versus timolol in preserving visual function: results from the Low-Pressure Glaucoma Treatment Study. *Am. J. Ophthalmol.* 151, 671–681. doi: 10.1016/j.ajo.2010.09.026

Lee, J. Y., Yoo, C., Jung, J. H., Hwang, Y. H., and Kim, Y. Y. (2012). The effect of lateral decubitus position on intraocular pressure in healthy young subjects. *Acta. Ophthalmol.* 90, e68–e72. doi: 10.1111/j.1755-3768.2011.02208.x

Lee, J. Y., Yoo, C., and Kim, Y. Y. (2013). The effect of lateral decubitus position on intraocular pressure in patients with untreated open-angle glaucoma. *Am. J. Ophthalmol.* 155, 329–335.e322. doi: 10.1016/j.ajo.2012.08.003

Leske, M. C. (2009). Ocular perfusion pressure and glaucoma: clinical trial and epidemiologic findings. *Curr. Opin. Ophthalmol.* 20, 73–78. doi: 10.1097/ICU.0b013e32831eef82

Leske, M. C., Connell, A. M., Wu, S. Y., Nemesure, B., Li, X., Schachat, A., et al. (2001). Incidence of open-angle glaucoma: the Barbados eye studies. the Barbados eye studies group. *Arch. Ophthalmol.* 119, 89–95.

Leske, M. C., Heijl, A., Hussein, M., Bengtsson, B., Hyman, L., and Komaroff, E. (2003). Factors for glaucoma progression and the effect of treatment: the early manifest glaucoma trial. *Arch. Ophthalmol.* 121, 48–56. doi: 10.1001/archopht.121.1.48

Leske, M. C., Heijl, A., Hyman, L., Bengtsson, B., Dong, L., and Yang, Z. (2007). Predictors of long-term progression in the early manifest glaucoma trial. *Ophthalmology* 114, 1965–1972. doi: 10.1016/j.ophtha.2007.03.016

Leske, M. C., Wu, S. Y., Hennis, A., Honkanen, R., and Nemesure, B. (2008). Risk factors for incident open-angle glaucoma: the Barbados Eye Studies. *Ophthalmology* 115, 85–93. doi: 10.1016/j.ophtha.2007.03.017

Liao, S., Cheng, G., Conner, D. A., Huang, Y., Kucherlapati, R. S., Munn, L. L., et al. (2011). Impaired lymphatic contraction associated with immunosuppression. *Proc. Natl. Acad. Sci. U.S.A.* 108, 18784–18789. doi: 10.1073/pnas.1116152108

Lin, H. J., Chen, W. C., Tsai, F. J., and Tsai, S. W. (2002). Distributions of p53 codon 72 polymorphism in primary open angle glaucoma. *Br. J. Ophthalmol.* 86, 767–770. doi: 10.1136/bjo.86.7.767

Lin, H. J., Tsai, C. H., Tsai, F. J., Chen, W. C., Chen, H. Y., and Fan, S. S. (2004). Transporter associated with antigen processing gene 1 codon 333 and codon 637 polymorphisms are associated with primary open-angle glaucoma. *Mol. Diagn.* 8, 245–252. doi: 10.1007/BF03260069

Lin, H. J., Tsai, F. J., Chen, W. C., Shi, Y. R., Hsu, Y., and Tsai, S. W. (2003a). Association of tumour necrosis factor alpha -308 gene polymorphism with primary open-angle glaucoma in Chinese. *Eye* 17, 31–34. doi: 10.1038/sj.eye.6700227

Lin, H. J., Tsai, S. C., Tsai, F. J., Chen, W. C., Tsai, J. J., and Hsu, C. D. (2003b). Association of interleukin 1beta and receptor antagonist gene polymorphisms with primary open-angle glaucoma. *Ophthalmologica* 217, 358–364. doi: 10.1159/000071352

Liu, B., and Neufeld, A. H. (2001). Nitric oxide synthase-2 in human optic nerve head astrocytes induced by elevated pressure *in vitro*. *Arch. Ophthalmol.* 119, 240–245.

Lorget, F., Kaci, N., Peng, J., Benoist-Lasselin, C., Mugniery, E., Oppeneer, T., et al. (2012). Evaluation of the therapeutic potential of a CNP analog in a Fgfr3 mouse model recapitulating achondroplasia. *Am. J. Hum. Genet.* 91, 1108–1114. doi: 10.1016/j.ajhg.2012.10.014

Lu, Z., Overby, D. R., Scott, P. A., Freddo, T. F., and Gong, H. (2008). The mechanism of increasing outflow facility by rho-kinase inhibition with Y-27632 in bovine eyes. *Exp. Eye Res.* 86, 271–281. doi: 10.1016/j.exer.2007.10.018

Magalhaes Da Silva, T., Rocha, A. V., Lacchini, R., Marques, C. R., Silva, E. S., Tanus-Santos, J. E., et al. (2012). Association of polymorphisms of endothelial nitric oxide synthase (eNOS) gene with the risk of primary open angle glaucoma in a Brazilian population. *Gene* 502, 142–146. doi: 10.1016/j.gene.2012.04.047

Majsterek, I., Malinowska, K., Stanczyk, M., Kowalski, M., Blaszczyk, J., Kurowska, A. K., et al. (2011a). Evaluation of oxidative stress markers in pathogenesis of primary open-angle glaucoma. *Exp. Mol. Pathol.* 90, 231–237. doi: 10.1016/j.yexmp.2011.01.001

Majsterek, I., Markiewicz, L., Przybylowska, K., Gacek, M., Kurowska, A. K., Kaminska, A., et al. (2011b). Association of MMP1-1607 1G/2G and TIMP1 372 T/C gene polymorphisms with risk of primary open angle glaucoma in a Polish population. *Med. Sci. Monit.* 17, CR417–421. doi: 10.12659/MSM.881854

Marro, M. L., Peiro, C., Panayiotou, C. M., Baliga, R. S., Meurer, S., Schmidt, H. H., et al. (2008). Characterization of the human alpha1 beta1 soluble guanylyl cyclase promoter: key role for NF-kappaB(p50) and CCAAT-binding

factors in regulating expression of the nitric oxide receptor. *J. Biol. Chem.* 283, 20027–20036. doi: 10.1074/jbc.M801223200

Masuda, H., Tamaoki, S., Goto, M., Ishida, A., Kamikawatoko, S., Tokoro, T., et al. (1997). Nitric oxide-induced ciliary muscle relaxation during contraction with endothelin-1 is mediated through elevation of cyclic GMP. *Curr. Eye Res.* 16, 1245–1251. doi: 10.1076/ceyr.16.12.1245.5025

May, C. A., and Mittag, T. (2004). Neuronal nitric oxide synthase (nNOS) positive retinal amacrine cells are altered in the DBA/2NNia mouse, a murine model for angle-closure glaucoma. *J. Glaucoma* 13, 496–499. doi: 10.1097/01.ijg.0000137435.83307.fd

Mckie, P. M., Sangaralingham, S. J., and Burnett, J. C., Jr. (2010). CD-NP: an innovative designer natriuretic peptide activator of particulate guanylyl cyclase receptors for cardiorenal disease. *Curr. Heart Fail. Rep.* 7, 93–99. doi: 10.1007/s11897-010-0016-6

Meguro, A., Inoko, H., Ota, M., Mizuki, N., and Bahram, S. (2010). Genome-wide association study of normal tension glaucoma: common variants in SRBD1 and ELOVL5 contribute to disease susceptibility. *Ophthalmology* 117, 1331–1338. e1335. doi: 10.1016/j.ophtha.2009.12.001

Memarzadeh, F., Ying-Lai, M., Chung, J., Azen, S. P., and Varma, R. (2010). Blood pressure, perfusion pressure, and open-angle glaucoma: the Los Angeles Latino Eye Study. *Invest. Ophthalmol. Vis. Sci.* 51, 2872–2877. doi: 10.1167/iovs.08-2956

Mendelsohn, M. E. (2005). In hypertension, the kidney is not always the heart of the matter. *J. Clin. Invest.* 115, 840–844. doi: 10.1172/JCI200524806

Mergia, E., Friebe, A., Dangel, O., Russwurm, M., and Koesling, D. (2006). Spare guanylyl cyclase NO receptors ensure high NO sensitivity in the vascular system. *J. Clin. Invest.* 116, 1731–1737. doi: 10.1172/JCI27657

Mergia, E., Russwurm, M., Zoidl, G., and Koesling, D. (2003). Major occurrence of the new alpha(2)beta(1) isoform of NO-sensitive guanylyl cyclase in brain. *Cell. Signall.* 15, 189–195. doi: 10.1016/S0898-6568(02)00078-5

Michael, S. K., Surks, H. K., Wang, Y., Zhu, Y., Blanton, R., Jamnongjit, M., et al. (2008). High blood pressure arising from a defect in vascular function. *Proc. Natl. Acad. Sci. U.S.A.* 105, 6702–6707. doi: 10.1073/pnas.0802128105

Mineo, C., and Shaul, P. W. (2012). Regulation of eNOS in caveolae. *Adv. Exp. Med. Biol.* 729, 51–62. doi: 10.1007/978-1-4614-1222-9_4

Mittag, T. W., Tormay, A., Ortega, M., and Severin, C. (1987). Atrial natriuretic peptide (ANP), guanylate cyclase, and intraocular pressure in the rabbit eye. *Curr. Eye Res.* 6, 1189–1196. doi: 10.3109/02713688709025228

Moncada, S., and Higgs, A. (1993). The L-arginine-nitric oxide pathway. *New Engl. J. Med.* 329, 2002–2012. doi: 10.1056/NEJM199312303292706

Monemi, S., Spaeth, G., Dasilva, A., Popinchalk, S., Ilitchev, E., Liebmann, J., et al. (2005). Identification of a novel adult-onset primary open-angle glaucoma (POAG) gene on 5q22.1. *Hum. Mol. Genet.* 14, 725–733. doi: 10.1093/hmg/ddi068

Moore, D., Harris, A., Wudunn, D., Kheradiya, N., and Siesky, B. (2008). Dysfunctional regulation of ocular blood flow: a risk factor for glaucoma? *Clin. Ophthalmol.* 2, 849–861.

Morgan, J., Caprioli, J., and Koseki, Y. (1999). Nitric oxide mediates excitotoxic and anoxic damage in rat retinal ganglion cells cocultured with astroglia. *Arch. Ophthalmol.* 117, 1524–1529. doi: 10.1001/archopht.117.11.1524

Mukesh, B. N., Mccarty, C. A., Rait, J. L., and Taylor, H. R. (2002). Five-year incidence of open-angle glaucoma: the visual impairment project. *Ophthalmology* 109, 1047–1051. doi: 10.1016/S0161-6420(02)01040-0

Munzel, T., Gori, T., Bruno, R. M., and Taddei, S. (2010). Is oxidative stress a therapeutic target in cardiovascular disease? *Eur. Heart J.* 31, 2741–2748. doi: 10.1093/eurheartj/ehq396

Nakano, M., Ikeda, Y., Tokuda, Y., Fuwa, M., Omi, N., Ueno, M., et al. (2012). Common variants in CDKN2B-AS1 associated with optic-nerve vulnerability of glaucoma identified by genome-wide association studies in Japanese. *PLoS ONE* 7:e33389. doi: 10.1371/journal.pone.0033389

Nathanson, J. A. (1988). Direct application of a guanylate cyclase activator lowers intraocular pressure. *Eur. J. Pharmacol.* 147, 155–156. doi: 10.1016/0014-2999(88)90648-6

Nathanson, J. A. (1992). Nitrovasodilators as a new class of ocular hypotensive agents. *J. Pharmacol. Exp. Ther.* 260, 956–965.

Nathanson, J. A., and Mckee, M. (1995a). Alterations of ocular nitric oxide synthase in human glaucoma. *Invest. Ophthalmol. Vis. Sci.* 36, 1774–1784.

Nathanson, J. A., and Mckee, M. (1995b). Identification of an extensive system of nitric oxide-producing cells in the ciliary muscle and outflow pathway of the human eye. *Invest. Ophthalmol. Vis. Sci.* 36, 1765–1773.

Neufeld, A. H., Das, S., Vora, S., Gachie, E., Kawai, S., Manning, P. T., et al. (2002). A prodrug of a selective inhibitor of inducible nitric oxide synthase is neuroprotective in the rat model of glaucoma. *J. Glaucoma* 11, 221–225. doi: 10.1097/00061198-200206000-00010

Neufeld, A. H., Hernandez, M. R., and Gonzalez, M. (1997). Nitric oxide synthase in the human glaucomatous optic nerve head. *Arch. Ophthalmol.* 115, 497–503. doi: 10.1001/archopht.1997.01100150499009

Neufeld, A. H., Sawada, A., and Becker, B. (1999). Inhibition of nitric-oxide synthase 2 by aminoguanidine provides neuroprotection of retinal ganglion cells in a rat model of chronic glaucoma. *Proc. Natl. Acad. Sci. U.S.A.* 96, 9944–9948. doi: 10.1073/pnas.96.17.9944

Nimmegeers, S., Sips, P., Buys, E., Brouckaert, P., and Van De Voorde, J. (2007). Functional role of the soluble guanylyl cyclase alpha(1) subunit in vascular smooth muscle relaxation. *Cardiovasc. Res.* 76, 149–159. doi: 10.1016/j.cardiores.2007.06.002

Nouri-Mahdavi, K., Hoffman, D., Coleman, A. L., Liu, G., Li, G., Gaasterland, D., et al. (2004). Predictive factors for glaucomatous visual field progression in the advanced Glaucoma intervention study. *Ophthalmology* 111, 1627–1635. doi: 10.1016/j.ophtha.2004.02.017

Oh, S. W., Lee, S., Park, C., and Kim, D. J. (2005). Elevated intraocular pressure is associated with insulin resistance and metabolic syndrome. *Diabetes Metab. Res. Rev.* 21, 434–440. doi: 10.1002/dmrr.529

Ozel, A. B., Moroi, S. E., Reed, D. M., Nika, M., Schmidt, C. M., Akbari, S., et al. (2014). Genome-wide association study and meta-analysis of intraocular pressure. *Hum. Genet.* 133, 41–57. doi: 10.1007/s00439-013-1349-5

Park, H. Y., Jung, K. I., Na, K. S., Park, S. H., and Park, C. K. (2012). Visual field characteristics in normal-tension glaucoma patients with autonomic dysfunction and abnormal peripheral microcirculation. *Am. J. Ophthalmol.* 154, 466–475 e461. doi: 10.1016/j.ajo.2012.03.028

Park, S. C., De Moraes, C. G., Teng, C. C., Tello, C., Liebmann, J. M., and Ritch, R. (2011). Initial parafoveal versus peripheral scotomas in glaucoma: risk factors and visual field characteristics. *Ophthalmology* 118, 1782–1789. doi: 10.1016/j.ophtha.2011.02.013

Park, S. H., Kim, J. H., Kim, Y. H., and Park, C. K. (2007). Expression of neuronal nitric oxide synthase in the retina of a rat model of chronic glaucoma. *Vis. Res.* 47, 2732–2740. doi: 10.1016/j.visres.2007.07.011

Pasquale, L. R., and Kang, J. H. (2011). Female reproductive factors and primary open-angle glaucoma in the nurses' health study. *Eye* 25, 633–641. doi: 10.1038/eye.2011.34

Pasutto, F., Keller, K. E., Weisschuh, N., Sticht, H., Samples, J. R., Yang, Y. F., et al. (2012). Variants in ASB10 are associated with open-angle glaucoma. *Hum. Mol. Genet.* 21, 1336–1349. doi: 10.1093/hmg/ddr572

Piggott, L. A., Hassell, K. A., Berkova, Z., Morris, A. P., Silberbach, M., and Rich, T. C. (2006). Natriuretic peptides and nitric oxide stimulate cGMP synthesis in different cellular compartments. *J. Gen. Physiol.* 128, 3–14. doi: 10.1085/jgp.200509403

Potter, L. R. (2011a). Guanylyl cyclase structure, function and regulation. *Cell. Signal.* 23, 1921–1926. doi: 10.1016/j.cellsig.2011.09.001

Potter, L. R. (2011b). Natriuretic peptide metabolism, clearance and degradation. *FEBS J.* 278, 1808–1817. doi: 10.1111/j.1742-4658.2011.08082.x

Potter, L. R. (2011c). Regulation and therapeutic targeting of peptide-activated receptor guanylyl cyclases. *Pharmacol. Ther.* 130, 71–82. doi: 10.1016/j.pharmthera.2010.12.005

Potter, L. R., Yoder, A. R., Flora, D. R., Antos, L. K., and Dickey, D. M. (2009). Natriuretic peptides: their structures, receptors, physiologic functions and therapeutic applications. *Handb. Exp. Pharmacol.* 341–366. doi: 10.1007/978-3-540-68964-5_15

Quigley, H. A. (2011). Glaucoma. *Lancet* 377, 1367–1377. doi: 10.1016/S0140-6736(10)61423-7

Ramdas, W. D., Van Koolwijk, L. M., Lemij, H. G., Pasutto, F., Cree, A. J., Thorleifsson, G., et al. (2011). Common genetic variants associated with open-angle glaucoma. *Hum. Mol. Genet.* 20, 2464–2471. doi: 10.1093/hmg/ddr120

Rao, V. P., and Epstein, D. L. (2007). Rho GTPase/Rho kinase inhibition as a novel target for the treatment of glaucoma. *BioDrugs* 21, 167–177. doi: 10.2165/00063030-200721030-00004

Rezaie, T., Child, A., Hitchings, R., Brice, G., Miller, L., Coca-Prados, M., et al. (2002). Adult-onset primary open-angle glaucoma caused by mutations in optineurin. *Science* 295, 1077–1079. doi: 10.1126/science.1066901

Rollin, R., Mediero, A., Roldan-Pallares, M., Fernandez-Cruz, A., and Fernandez-Durango, R. (2004). Natriuretic peptide system in the human retina. *Mol. Vis.* 10, 15–22.

Rudnicka, A. R., Mt-Isa, S., Owen, C. G., Cook, D. G., and Ashby, D. (2006). Variations in primary open-angle glaucoma prevalence by age, gender, and race: a Bayesian meta-analysis. *Invest. Ophthalmol. Vis. Sci.* 47, 4254–4261. doi: 10.1167/iovs.06-0299

Russ, P. K., Kupperman, A. I., Presley, S. H., Haselton, F. R., and Chang, M. S. (2010). Inhibition of RhoA signaling with increased Bves in trabecular meshwork cells. *Invest. Ophthalmol. Vis. Sci.* 51, 223–230. doi: 10.1167/iovs.09-3539

Russwurm, M., Behrends, S., Harteneck, C., and Koesling, D. (1998). Functional properties of a naturally occurring isoform of soluble guanylyl cyclase. *Biochem. J.* 335, 125–130.

Sacca, S. C., Rolando, M., Marletta, A., Macri, A., Cerqueti, P., and Ciurlo, G. (1998). Fluctuations of intraocular pressure during the day in open-angle glaucoma, normal-tension glaucoma and normal subjects. *Ophthalmologica* 212, 115–119. doi: 10.1159/000027290

Saleh, M., Nagaraju, M., and Porciatti, V. (2007). Longitudinal evaluation of retinal ganglion cell function and IOP in the DBA/2J mouse model of glaucoma. *Invest. Ophthalmol. Vis. Sci.* 48, 4564–4572. doi: 10.1167/iovs.07-0483

Sarfarazi, M., Child, A., Stoilova, D., Brice, G., Desai, T., Trifan, O. C., et al. (1998). Localization of the fourth locus (GLC1E) for adult-onset primary open-angle glaucoma to the 10p15-p14 region. *Am. J. Hum. Genet.* 62, 641–652. doi: 10.1086/301767

Sauzeau, V., Rolli-Derkinderen, M., Marionneau, C., Loirand, G., and Pacaud, P. (2003). RhoA expression is controlled by nitric oxide through cGMP-dependent protein kinase activation. *J. Biol. Chem.* 278, 9472–9480. doi: 10.1074/jbc.M212776200

Scheetz, T. E., Fingert, J. H., Wang, K., Kuehn, M. H., Knudtson, K. L., Alward, W. L., et al. (2013). A genome-wide association study for primary open angle glaucoma and macular degeneration reveals novel Loci. *PLoS ONE* 8:e58657. doi: 10.1371/journal.pone.0058657

Schmidl, D., Garhofer, G., and Schmetterer, L. (2011). The complex interaction between ocular perfusion pressure and ocular blood flow - relevance for glaucoma. *Exp. Eye Res.* 93, 141–155. doi: 10.1016/j.exer.2010.09.002

Schmidt, K. G., Geyer, O., and Mittag, T. W. (2004). Adenylyl and guanylyl cyclase activity in the choroid. *Exp. Eye Res.* 78, 901–907. doi: 10.1016/j.exer.2004.01.008

Schneemann, A., Dijkstra, B. G., Van Den Berg, T. J., Kamphuis, W., and Hoyng, P. F. (2002). Nitric oxide/guanylate cyclase pathways and flow in anterior segment perfusion. *Graefe's Arch. Clin. Exp. Ophthalmol.* 240, 936–941. doi: 10.1007/s00417-002-0559-7

Schuman, J. S., Erickson, K., and Nathanson, J. A. (1994). Nitrovasodilator effects on intraocular pressure and outflow facility in monkeys. *Exp. Eye Res.* 58, 99–105. doi: 10.1006/exer.1994.1199

Sharif, N. A., Williams, G. W., Crider, J. Y., Xu, S. X., and Davis, T. L. (2004). Molecular pharmacology of the DP/EP2 class prostaglandin AL-6598 and quantitative autoradiographic visualization of DP and EP2 receptor sites in human eyes. *J. Ocul. Pharmacol. Ther.* 20, 489–508. doi: 10.1089/jop.2004.20.489

Sheffield, V. C., Stone, E. M., Alward, W. L., Drack, A. V., Johnson, A. T., Streb, L. M., et al. (1993). Genetic linkage of familial open angle glaucoma to chromosome 1q21-q31. *Nat. Genet.* 4, 47–50. doi: 10.1038/ng0593-47

Shi, D., Funayama, T., Mashima, Y., Takano, Y., Shimizu, A., Yamamoto, K., et al. (2013). Association of HK2 and NCK2 with normal tension glaucoma in the Japanese population. *PLoS ONE* 8:e54115. doi: 10.1371/journal.pone.0054115

Smith, W. B., 2nd, Mccaslin, I. R., Gokce, A., Mandava, S. H., Trost, L., and Hellstrom, W. J. (2013). PDE5 inhibitors: considerations for preference and long-term adherence. *Int. J. Clin. Pract.* 67, 768–780. doi: 10.1111/ijcp.12074

Sommer, A., Tielsch, J. M., Katz, J., Quigley, H. A., Gottsch, J. D., Javitt, J., et al. (1991). Relationship between intraocular pressure and primary open angle glaucoma among white and black Americans. The Baltimore Eye Survey. *Arch. Ophthalmol.* 109, 1090–1095. doi: 10.1001/archopht.1991.01080080050026

Sponsel, W. E., Paris, G., Sandoval, S. S., Sanford, D. K., Harrison, J. M., Elliott, W. R., et al. (2000). Sildenafil and ocular perfusion. *New Engl. J. Med.* 342, 1680. doi: 10.1056/NEJM200006013422218

Stamer, W. D., Lei, Y., Boussommier-Calleja, A., Overby, D. R., and Ethier, C. R. (2011). eNOS, a pressure-dependent regulator of intraocular pressure. *Invest. Ophthalmol. Vis. Sci.* 52, 9438–9444. doi: 10.1167/iovs.11-7839

Stamler, J. S., Lamas, S., and Fang, F. C. (2001). Nitrosylation. the prototypic redox-based signaling mechanism. *Cell* 106, 675–683. doi: 10.1016/S0092-8674(01)00495-0

Stasch, J. P., Schmidt, P. M., Nedvetsky, P. I., Nedvetskaya, T. Y., HS, A. K., Meurer, S., et al. (2006). Targeting the heme-oxidized nitric oxide receptor for selective vasodilatation of diseased blood vessels. *J. Clin. Invest.* 116, 2552–2561. doi: 10.1172/JCI28371

Stoilova, D., Child, A., Trifan, O. C., Crick, R. P., Coakes, R. L., and Sarfarazi, M. (1996). Localization of a locus (GLC1B) for adult-onset primary open angle glaucoma to the 2cen-q13 region. *Genomics* 36, 142–150. doi: 10.1006/geno.1996.0434

Stone, E. M., Fingert, J. H., Alward, W. L., Nguyen, T. D., Polansky, J. R., Sunden, S. L., et al. (1997). Identification of a gene that causes primary open angle glaucoma. *Science* 275, 668–670. doi: 10.1126/science.275.[]5300.668

Su, J., Scholz, P. M., and Weiss, H. R. (2005). Differential effects of cGMP produced by soluble and particulate guanylyl cyclase on mouse ventricular myocytes. *Exp. Biol. Med. (Maywood)* 230, 242–250.

Su, W. W., Cheng, S. T., Ho, W. J., Tsay, P. K., Wu, S. C., and Chang, S. H. (2008). Glaucoma is associated with peripheral vascular endothelial dysfunction. *Ophthalmology* 115, 1173–1178.e1171.

Sugrue, M. F., and Viader, M. P. (1986). Synthetic atrial natriuretic factor lowers rabbit intraocular pressure. *Eur. J. Pharmacol.* 130, 349–350. doi: 10.1016/0014-2999(86)90292-X

Surks, H. K., Mochizuki, N., Kasai, Y., Georgescu, S. P., Tang, K. M., Ito, M., et al. (1999). Regulation of myosin phosphatase by a specific interaction with cGMP- dependent protein kinase Ialpha. *Science* 286, 1583–1587. doi: 10.1126/science.286.5444.1583

Takahata, K., Katsuki, H., Kume, T., Nakata, D., Ito, K., Muraoka, S., et al. (2003). Retinal neuronal death induced by intraocular administration of a nitric oxide donor and its rescue by neurotrophic factors in rats. *Invest. Ophthalmol. Vis. Sci.* 44, 1760–1766. doi: 10.1167/iovs.02-0471

Takashima, Y., Taniguchi, T., Yoshida, M., Haque, M. S., Igaki, T., Itoh, H., et al. (1998). Ocular hypotension induced by intravitreally injected C-type natriuretic peptide. *Exp. Eye Res.* 66, 89–96. doi: 10.1006/exer.1997.0403

Takimoto, E., Champion, H. C., Li, M., Ren, S., Rodriguez, E. R., Tavazzi, B., et al. (2005). Oxidant stress from nitric oxide synthase-3 uncoupling stimulates cardiac pathologic remodeling from chronic pressure load. *J. Clin. Invest.* 115, 1221–1231. doi: 10.1172/JCI21968

Tanihara, H., Inoue, T., Yamamoto, T., Kuwayama, Y., Abe, H., and Araie, M. (2013). Phase 2 randomized clinical study of a Rho kinase inhibitor, K-115, in primary open-angle glaucoma and ocular hypertension. *Am. J. Ophthalmol.* 156, 731–736. doi: 10.1016/j.ajo.2013.05.016

Thorleifsson, G., Magnusson, K. P., Sulem, P., Walters, G. B., Gudbjartsson, D. F., Stefansson, H., et al. (2007). Common sequence variants in the LOXL1 gene confer susceptibility to exfoliation glaucoma. *Science* 317, 1397–1400. doi: 10.1126/science.1146554

Thorleifsson, G., Walters, G. B., Hewitt, A. W., Masson, G., Helgason, A., Dewan, A., et al. (2010). Common variants near CAV1 and CAV2 are associated with primary open-angle glaucoma. *Nat. Genet.* 42, 906–909. doi: 10.1038/ng.661

Tielsch, J. M., Katz, J., Sommer, A., Quigley, H. A., and Javitt, J. C. (1995). Hypertension, perfusion pressure, and primary open-angle glaucoma. A population-based assessment. *Arch. Ophthalmol.* 113, 216–221. doi: 10.1001/archopht.1995.01100020100038

Torres, J., Darley-Usmar, V., and Wilson, M. T. (1995). Inhibition of cytochrome c oxidase in turnover by nitric oxide: mechanism and implications for control of respiration. *Biochem. J.* 312(Pt 1), 169–173.

Tsai, F. J., Lin, H. J., Chen, W. C., Chen, H. Y., and Fan, S. S. (2003). Insulin-like growth factor-II gene polymorphism is associated with primary open angle glaucoma. *J. Clin. Lab. Anal.* 17, 259–263. doi: 10.1002/jcla.10106

Tsai, F. J., Lin, H. J., Chen, W. C., Tsai, C. H., and Tsai, S. W. (2004). A codon 31ser-arg polymorphism of the WAF-1/CIP-1/p21/tumour suppressor gene in Chinese primary open-angle glaucoma. *Acta. Ophthalmol. Scand.* 82, 76–80. doi: 10.1111/j.1395-3907.2004.0180.x

Tsai, S., Bentley, E., Miller, P. E., Gomes, F. E., Vangyi, C., Wiese, A., et al. (2012). Gender differences in iridocorneal angle morphology: a potential explanation for the female predisposition to primary angle closure glaucoma in

dogs. *Vet. Ophthalmol.* 15(Suppl. 1), 60–63. doi: 10.1111/j.1463-5224.2011.00956.x

Tunny, T. J., Richardson, K. A., and Clark, C. V. (1998). Association study of the 5′ flanking regions of endothelial-nitric oxide synthase and endothelin-1 genes in familial primary open-angle glaucoma. *Clin. Exp. Pharmacol. Physiol.* 25, 26–29. doi: 10.1111/j.1440-1681.1998.tb02138.x

Tunny, T. J., Richardson, K. A., Clark, C. V., and Gordon, R. D. (1996). The atrial natriuretic peptide gene in patients with familial primary open-angle glaucoma. *Biochem. Biophys. Res. Commun.* 223, 221–225. doi: 10.1006/bbrc.1996.0874

Vajaranant, T. S., Nayak, S., Wilensky, J. T., and Joslin, C. E. (2010). Gender and glaucoma: what we know and what we need to know. *Curr. Opin. Ophthalmol.* 21, 91–99. doi: 10.1097/ICU.0b013e3283360b7e

Vajaranant, T. S., and Pasquale, L. R. (2012). Estrogen deficiency accelerates aging of the optic nerve. *Menopause* 19, 942–947. doi: 10.1097/gme.0b013e3182443137

Van Koolwijk, L. M., Ramdas, W. D., Ikram, M. K., Jansonius, N. M., Pasutto, F., Hysi, P. G., et al. (2012). Common genetic determinants of intraocular pressure and primary open-angle glaucoma. *PLoS Genet.* 8:e1002611. doi: 10.1371/journal.pgen.1002611

Vanneste, G., Dhaese, I., Sips, P., Buys, E., Brouckaert, P., and Lefebvre, R. A. (2007). Gastric motility in soluble guanylate cyclase alpha 1 knock-out mice. *J. Physiol.* 584, 907–920. doi: 10.1113/jphysiol.2007.140608

Vermeersch, P., Buys, E., Pokreisz, P., Marsboom, G., Ichinose, F., Sips, P., et al. (2007). Soluble guanylate cyclase-alpha1 deficiency selectively inhibits the pulmonary vasodilator response to nitric oxide and increases the pulmonary vascular remodeling response to chronic hypoxia. *Circulation* 116, 936–943. doi: 10.1161/CIRCULATIONAHA.106.677245

Vincent, A. L., Billingsley, G., Buys, Y., Levin, A. V., Priston, M., Trope, G., et al. (2002). Digenic inheritance of early-onset glaucoma: CYP1B1, a potential modifier gene. *Am. J. Hum. Genet.* 70, 448–460. doi: 10.1086/338709

Vobig, M. A., Klotz, T., Staak, M., Bartz-Schmidt, K. U., Engelmann, U., and Walter, P. (1999). Retinal side-effects of sildenafil. *Lancet* 353, 375. doi: 10.1016/S0140-6736(98)05473-7

Vohra, R., Tsai, J. C., and Kolko, M. (2013). The role of inflammation in the pathogenesis of glaucoma. *Surv. Ophthalmol.* 58, 311–320. doi: 10.1016/j.survophthal.2012.08.010

Walkenbach, R. J., Ye, G. S., Korenfeld, M. S., and Boney, F. (1993). Atrial natriuretic peptide receptors on the corneal endothelium. *Invest. Ophthalmol. Vis. Sci.* 34, 2538–2543.

Weinreb, R. N., and Kaufman, P. L. (2009). The glaucoma research community and FDA look to the future: a report from the NEI/FDA CDER glaucoma clinical trial design and endpoints symposium. *Invest. Ophthalmol. Vis. Sci.* 50, 1497–1505. doi: 10.1167/iovs.08–2843

Weinreb, R. N., and Khaw, P. T. (2004). Primary open-angle glaucoma. *Lancet* 363, 1711–1720. doi: 10.1016/S0140-6736(04)16257-0

Wiederholt, M. (1998). Direct involvement of trabecular meshwork in the regulation of aqueous humor outflow. *Curr. Opin. Ophthalmol.* 9, 46–49. doi: 10.1097/00055735-199804000-00009

Wiederholt, M., Sturm, A., and Lepple-Wienhues, A. (1994). Relaxation of trabecular meshwork and ciliary muscle by release of nitric oxide. *Invest. Ophthalmol. Vis. Sci.* 35, 2515–2520.

Wiederholt, M., Thieme, H., and Stumpff, F. (2000). The regulation of trabecular meshwork and ciliary muscle contractility. *Prog. Retin. Eye Res.* 19, 271–295. doi: 10.1016/S1350-9462(99)00015-4

Wiggs, J. L., Kang, J. H., Yaspan, B. L., Mirel, D. B., Laurie, C., Crenshaw, A., et al. (2011). Common variants near CAV1 and CAV2 are associated with primary open-angle glaucoma in Caucasians from the USA. *Hum. Mol. Genet.* 20, 4707–4713. doi: 10.1093/hmg/ddr382

Wiggs, J. L., Yaspan, B. L., Hauser, M. A., Kang, J. H., Allingham, R. R., Olson, L. M., et al. (2012). Common variants at 9p21 and 8q22 are associated with increased susceptibility to optic nerve degeneration in glaucoma. *PLoS Genet.* 8:e1002654. doi: 10.1371/journal.pgen.1002654

Wolfs, R. C., Klaver, C. C., Ramrattan, R. S., Van Duijn, C. M., Hofman, A., and De Jong, P. T. (1998). Genetic risk of primary open-angle glaucoma. Population-based familial aggregation study. *Arch. Ophthalmol.* 116, 1640–1645. doi: 10.1001/archopht.116.12.1640

Wu, S. Y., and Leske, M. C. (1997). Associations with intraocular pressure in the Barbados Eye Study. *Arch. Ophthalmol.* 115, 1572–1576. doi: 10.1001/archopht.1997.01100160742012

Wu, S. Y., Nemesure, B., Hennis, A., and Leske, M. C. (2006). Nine-year changes in intraocular pressure: the Barbados Eye Studies. *Arch. Ophthalmol.* 124, 1631–1636. doi: 10.1001/archopht.124.11.1631

Yamamoto, R., Bredt, D. S., Snyder, S. H., and Stone, R. A. (1993). The localization of nitric oxide synthase in the rat eye and related cranial ganglia. *Neuroscience* 54, 189–200. doi: 10.1016/0306-4522(93)90393-T

Yucel, Y. H., Johnston, M. G., Ly, T., Patel, M., Drake, B., Gumus, E., et al. (2009). Identification of lymphatics in the ciliary body of the human eye: a novel "uveolymphatic" outflow pathway. *Exp. Eye Res.* 89, 810–819. doi: 10.1016/j.exer.2009.08.010

Conflict of Interest Statement: The authors declare that the research was conducted in the absence of any commercial or financial relationships that could be construed as a potential conflict of interest.

Received: 14 March 2014; paper pending published: 19 April 2014; accepted: 21 April 2014; published online: 19 May 2014.

Citation: Buys ES, Potter LR, Pasquale LR and Ksander BR (2014) Regulation of intraocular pressure by soluble and membrane guanylate cyclases and their role in glaucoma. Front. Mol. Neurosci. 7:38. doi: 10.3389/fnmol.2014.00038

This article was submitted to the journal Frontiers in Molecular Neuroscience.

frontiers in
MOLECULAR NEUROSCIENCE

MINI REVIEW ARTICLE
published: 16 April 2014
doi: 10.3389/fnmol.2014.00031

Guanylate cyclase-C/cGMP: an emerging pathway in the regulation of visceral pain

Gerhard Hannig, Boris Tchernychev, Caroline B. Kurtz, Alexander P. Bryant, Mark G. Currie and Inmaculada Silos-Santiago*

Department of Discovery Pharmacology, Ironwood Pharmaceuticals, Inc., Cambridge, MA, USA

Edited by:
Clint Lawrence Makino, Massachusetts Eye and Ear Infirmary and Harvard Medical School, USA

Reviewed by:
Jakub Fichna, Medical University of Lodz, Poland
Scott Waldman, Thomas Jefferson University, USA

***Correspondence:**
Inmaculada Silos-Santiago, Department of Discovery Pharmacology, Ironwood Pharmaceuticals, Inc., 301 Binney Street, Cambridge, MA 02142, USA
e-mail: isilos-santiago@ironwoodpharma.com

Activation of guanylate cyclase-C (GC-C) expressed predominantly on intestinal epithelial cells by guanylin, uroguanylin or the closely related GC-C agonist peptide, linaclotide, stimulates generation, and release of cyclic guanosine-3′,5′-monophosphate (cGMP). Evidence that the visceral analgesic effects of linaclotide are mediated by a novel, GC-C-dependent peripheral sensory mechanism was first demonstrated in animal models of visceral pain. Subsequent studies with uroguanylin or linaclotide have confirmed the activation of a GC-C/cGMP pathway leading to increased submucosal cGMP mediated by cGMP efflux pumps, which modulates intestinal nociceptor function resulting in peripheral analgesia. These effects can be reproduced by the addition of exogenous cGMP and support a role for GC-C/cGMP signaling in the regulation of visceral sensation, a physiological function that has not previously been linked to the GC-C/cGMP pathway. Notably, targeting the GC-C/cGMP pathway for treatment of gastrointestinal pain and abdominal sensory symptoms has now been validated in the clinic. In 2012, linaclotide was approved in the United States and European Union for the treatment of adult patients with irritable bowel syndrome with constipation.

Keywords: abdominal pain, colonic nociceptor, cyclic guanosine monophosphate, guanylate cyclase-C, irritable bowel syndrome with constipation, linaclotide, uroguanylin, visceral analgesia

INTRODUCTION

Guanylate cyclase-C (GC-C) is a type I transmembrane receptor with intrinsic guanylate cyclase activity, belonging to a larger family of enzymes comprising both soluble and receptor guanylate cyclases that respond to a diverse range of signals by catalyzing the conversion of guanosine triphosphate to cyclic guanosine-3′,5′ monophosphate (cGMP; Lucas et al., 2000; Vaandrager, 2002). This receptor is expressed predominantly on the apical surface of intestinal epithelial cells (IEC), and its important role in the regulation of intestinal electrolyte and fluid homeostasis is firmly established (Schulz et al., 1990; Carrithers et al., 1996; Castro et al., 2013; Silos-Santiago et al., 2013). The endogenous hormones guanylin and uroguanylin, cognate ligands of GC-C, are expressed in a distinct but overlapping regional pattern in enteroendocrine cells along the longitudinal axis of the gastrointestinal (GI) tract and released into the intestinal lumen (Currie et al., 1992; Kita et al., 1994; Perkins et al., 1997; Qian et al., 2000; Silos-Santiago et al., 2013). Activation of GC-C by either guanylin or uroguanylin results in cGMP accumulation in IEC. Cyclic GMP is the sole second messenger generated by GC-C and is known to regulate several canonical intracellular signaling pathways mediated primarily through direct interaction with three groups of target proteins: cGMP-dependent protein kinases, cyclic nucleotide-gated ion channels, and cGMP-regulated phosphodiesterases (Pfeifer et al., 1996; Schlossman et al., 2005). Cyclic GMP regulation of intestinal electrolyte and fluid homeostasis is dependent on protein kinase II (PKG-II) phosphorylation and activation of the cystic fibrosis transmembrane conductance regulator (CFTR) ion channel, stimulating transepithelial secretion of chloride and bicarbonate ions and concomitant inhibition of sodium absorption by the sodium/hydrogen exchanger 3 (NHE3), resulting in the net efflux of ions and water into the lumen (Forte, 1999; Vaandrager, 2002; Sindic and Schlatter, 2006). Studies in GC-C null (*Gucy2c*$^{-/-}$) mice have confirmed the central role of GC-C in the control of electrolyte and fluid homeostasis (Mann et al., 1997; Schulz et al., 1997).

Our understanding of cellular processes regulated by activation of the GC-C/cGMP pathway has markedly evolved over the past two decades. Importantly, this knowledge has guided the development of novel therapeutic paradigms targeting the GC-C/cGMP pathway that have successfully translated into the clinic.

LINACLOTIDE IS A POTENT AND SELECTIVE GUANYLATE CYCLASE-C AGONIST

Linaclotide, a synthetic 14-amino acid peptide composed of naturally occurring amino acids (N-CCEYCCNPACTGCY-C; molecular weight: 1524.2 Dalton), is a potent and selective agonist of GC-C. This orally administered, minimally absorbed peptide ($\leq$0.1% in all non-clinical species) is a member of the guanylin family of cGMP-regulating peptides that includes the natural hormones guanylin and uroguanylin (Bryant et al., 2010; Busby et al., 2010). Linaclotide is stabilized by three intramolecular disulfide bonds (Cys^1-Cys^6, Cys^2-Cys^{10}, Cys^5-Cys^{13}), locking this peptide into a single conformation similar in structure to guanylin and uroguanylin, with the distinct difference that the biologically active conformation (A-isoform) of these peptides contains only two

disulfide bonds (Skelton et al., 1994; Marx et al., 1998; Busby et al., 2010). Linaclotide exhibited high-affinity and pH-independent binding to GC-C on human colon carcinoma T84 cells and concomitantly stimulated a significant and concentration-dependent accumulation of intracellular cGMP, with greater potency than guanylin or uroguanylin. In standard rodent models of GI function, orally administered linaclotide elicited significant *in vivo* pharmacological effects, stimulating fluid secretion and accelerating transit (Bryant et al., 2010; Busby et al., 2010). The lack of such effects in *Gucy2c*$^{-/-}$mice further confirmed GC-C as the molecular target of linaclotide and supported an underlying mechanism linking the effects of linaclotide in these models to local activation of GC-C in the intestine. The single pharmacologically active metabolite of linaclotide, MM-419447 (Des-Tyr^{14}) mirrors the effects of linaclotide *in vitro* and *in vivo*, providing evidence that this active metabolite contributes to the pharmacology associated with oral administration of linaclotide (Busby et al., 2013).

The potent pharmacological effects of linaclotide in nonclinical models provided the rationale for development of this peptide as a novel therapeutic for the treatment of functional GI disorders associated with constipation, such as chronic idiopathic constipation (CIC), and irritable bowel syndrome with constipation (IBS-C). However, no reports had previously linked local activation of the intestinal GC-C pathway to the regulation of abdominal pain.

LINACLOTIDE ACTIVATION OF GUANYLATE CYCLASE-C ELICITS ANALGESIC EFFECTS IN VISCERAL PAIN MODELS

Abdominal pain or discomfort (associated with a change in bowel function) is a defining symptom of the diagnostic criteria for IBS and is hypothesized to originate from hypersensitivity of the colon to mechanical stimuli (Drossman, 2006; Tack et al., 2006; Videlock and Chang, 2007). In clinical studies, IBS patients have shown lowered colorectal pain thresholds and increased sensory ratings, further consistent with persistent enhanced perception and responsiveness to visceral stimuli (= visceral hyperalgesia; Mertz et al., 1995; Bouin et al., 2002).

Antinociceptive effects of an orally administered GC-C agonist, linaclotide, were first demonstrated by Eutamene et al. (2010), using rodent models of visceral hypersensitivity associated with inflammation produced by trinitrobenzene sulfonic acid (TNBS) or stress models (following acute water avoidance or partial restraint) that induce this condition. In these models, visceral pain is measured using colorectal balloon distension. This well-characterized method evokes contractions of the abdominal musculature (visceromotor response) to graded distension pressures. It differs from measurements of visceral sensitivity in humans, which is primarily based on conscious perception of controlled colon distension. Orally administered linaclotide elicited significant analgesic effects during colonic distension in all models tested, without affecting basal sensitivity. Notably, the specificity of linaclotide-mediated analgesic effects was mechanistically linked to the activation of intestinal GC-C, confirmed in studies that assessed the effects of linaclotide on TNBS-induced colonic hypersensitivity in *Gucy2c* wild-type and *Gucy2c*$^{-/-}$ mice. In these studies, linaclotide reversed colonic hypersensitivity only in *Gucy2c* wild-type, but not *Gucy2c*$^{-/-}$ mice. The analgesic effects of linaclotide were also reproduced by the endogenous GC-C ligand, uroguanylin, a finding not previously attributed to the endogenous hormones. The analgesic effects of linaclotide and uroguanylin in these models were not associated with changes in colonic pressure-volume relationships, further suggesting that the antinociceptive effects are linked specifically to GC-C activation and are not associated with altered colonic compliance (Eutamene et al., 2010; Silos-Santiago et al., 2013). These findings raised the intriguing question of whether activation of an intestinal GC-C pathway had emerged as a novel physiological pathway regulating visceral pain.

LINACLOTIDE INDUCES PERIPHERAL VISCERAL ANALGESIA BY ACTIVATION OF A GUANYLATE CYCLASE-C/EXTRACELLULAR cGMP PATHWAY

Hallmarks of IBS include allodynia (persistent response to normally non-noxious stimuli) and hyperalgesia (persistent enhanced perception and responsiveness to noxious stimuli) to mechanical stimuli within the intestine, mediated by chronic changes in afferent pathways (sensitization). High-threshold colonic nociceptive sensory afferents (mesenteric, serosal afferents) that only respond at sufficiently high levels to mechanical stimulation are predominantly found in the splanchnic nerve pathway, while low-threshold stretch receptors [muscular/mucosal (M/M), muscular afferents] are predominantly found in the pelvic pathway (Hughes et al., 2009; Feng and Gebhart, 2011; Blackshaw and Brierley, 2013).

In a mouse model of chronic post-inflammatory visceral hypersensitivity (CVH) in which colonic mechanical hyperalgesia and allodynia are evident long after resolution of TNBS-induced colitis, linaclotide, and uroguanylin reversed chronic mechanical hypersensitivity in CVH colonic high-threshold splanchnic serosal nociceptors, and also inhibited mechanical hypersensitivity of healthy nociceptors. Inhibition of CVH colonic nociceptors by either peptide was greater than their inhibition of control nociceptors from healthy animals, and linaclotide-induced inhibition was more potent than that produced by uroguanylin. Importantly, *in vitro* inhibition of colonic nociceptors correlated with *in vivo* findings in which linaclotide decreased the processing of noxious colorectal distension stimuli in the thoracolumbar spinal cord indicated by a lower number of activated dorsal horn (DH) neurons within the thoracolumbar spinal cord, specifically the superficial lamina of the DH, recognized as the major termination zone for nociceptive afferents (Castro et al., 2013). Further evidence supporting a mechanism in which linaclotide inhibition of colonic nociceptors is dependent on local activation of GC-C in IEC rather than direct effects on colonic nociceptors was derived from expression studies using *in situ* hybridization in whole adult mouse, colonic segments, and spinal cord and dorsal root ganglion (DRG) sections, and studies assessing linaclotide inhibition of colonic nociceptors in *Gucy2c*$^{-/-}$ mice. While abundant GC-C expression was found in the intestine, no expression was detected in key sensory structures, such as DRG and spinal cord neurons. Furthermore, while mechanosensory responses of colonic nociceptors at baseline were similar in control and *Gucy2*$^{-/-}$ mice, linaclotide-induced inhibition was completely lost in *Gucy2c*$^{-/-}$ mice. This was further corroborated by findings that prior removal of the mucosa,

the source of GC-C, in healthy and CVH states significantly attenuated linaclotide inhibition of colonic nociceptors (Castro et al., 2013). Finally, electric field stimulation-induced contractions of colonic tissues were not affected by linaclotide, which confirmed that antinociceptive effects of linaclotide were not linked to altered smooth muscle cell contractility, consistent with the absence of GC-C expression on colonic smooth muscle cells (Castro et al., 2013).

While these findings indicate that the analgesic effects of linaclotide are mediated entirely by peripheral expression of GC-C on the apical surface of IEC, a direct inhibitory effect of linaclotide on colonic nociceptors was further considered unlikely because of minimal absorption of this peptide, and the location of peripheral endings of colonic nociceptors in the submucosa. This provoked studies that investigated the potential role of cGMP, the common primary downstream effector of linaclotide and uroguanylin, in altered intestinal nociceptor function and peripheral analgesia. The involvement of an intracellular GC-C/cGMP pathway in the regulation of intestinal fluid and electrolyte homeostasis is firmly established; however, the effects of extracellular cGMP transported out of IEC following local GC-C activation have remained elusive. Precedence that extracellular cGMP is involved in the modulation of neuronal activity was obtained from studies that showed direct inhibitory effects of extracellular cGMP on CNS neurons, resulting in reduced excitability and inhibition of neurotransmitter release (Linden et al., 1995; Poupoloupou and Nowak, 1998; Cervetto et al., 2010). When assessed in rat models of colonic hypersensitivity, orally administered cGMP elicited significant analgesic effects, in a dose-dependent manner, reproducing the effects of linaclotide and uroguanylin in these models (Silos-Santiago et al., 2013). There is now compelling evidence supporting a model in which the potent analgesic effects of cGMP *in vivo* are mediated by a pathway linking extracellular cGMP, secreted from IEC into the submucosa following activation of the GC-C/cGMP pathway by linaclotide or uroguanylin, to altered function of colonic nociceptors resulting in peripheral analgesia. *In vitro* exposure of human intestinal Caco-2 cells to linaclotide or uroguanylin stimulated extracellular transport of cGMP into the apical and basolateral spaces, which was inhibited by the cGMP efflux pump inhibitor probenecid in a concentration-dependent manner (Castro et al., 2013; Silos-Santiago et al., 2013). This provided evidence implicating energy-dependent transport of cGMP by the cGMP efflux pumps multidrug-resistance protein (MRP) 4 and 5 (Sager, 2004). While cGMP-binding phosphodiesterases are generally recognized as the major elimination pathway for intracellular cGMP, MRP4/5-mediated extracellular transport of cGMP is consistent with their function as overflow pumps, decreasing intracellular cGMP levels under conditions when cGMP production is strongly induced and importantly, providing extracellular cGMP for paracrine actions (Ritter et al., 2005; Zimmermann et al., 2005). Further evidence supporting a role of extracellular cGMP in the regulation of colonic afferent activity was obtained from *ex vivo* Ussing chamber assays, in which exposure of rat colonic tissue (luminal side) to uroguanylin stimulated secretion of cGMP into the submucosal space (Silos-Santiago et al., 2013). Moreover, in a rat model of TNBS-induced colonic afferent sensitization, exogenous cGMP significantly decreased pelvic afferent firing rates in response to colonic distension, and in CVH mice colonic nociceptors were significantly inhibited by application of exogenous cGMP to the mucosal epithelium, to a greater extent than those from healthy mice (Castro et al., 2013; Silos-Santiago et al., 2013). While cGMP dose levels required for inhibition of colonic nociceptors exceeded those for linaclotide and uroguanylin, facilitating access of cGMP to colonic nociceptors by removal of the mucosa significantly increased its potency, confirming the barrier function of the epithelium for luminal cGMP to diffuse across the mucosa (Castro et al., 2013). Furthermore, direct application of cGMP to mouse colorectal receptive endings significantly decreased the response of control pelvic muscular and M/M afferents to circumferential stretch, and sensitized responses of muscular and M/M afferents to stretch were reversed (Feng et al., 2013). Similar to findings with linaclotide and uroguanylin, antinociceptive effects of extracellular cGMP were not associated with altered smooth muscle contractility (Castro et al., 2013; Silos-Santiago et al., 2013).

In conclusion, accumulating evidence now strongly supports a direct peripherally acting analgesic mechanism that, following activation of a GC-C/extracellular cGMP pathway by selective GC-C agonists, mediates inhibition of colonic nociception and decreases visceral pain (**Figure 1**). This mechanism suggests that the regulation of colonic sensation may have evolved as an effect of GC-C agonism by the endogenous hormones guanylin and uroguanylin in IEC (Castro et al., 2013; Silos-Santiago et al., 2013).

LINACLOTIDE DECREASES ABDOMINAL PAIN AND DISCOMFORT IN PATIENTS WITH IRRITABLE BOWEL SYNDROME WITH CONSTIPATION

Results from two pivotal phase 3 clinical trials with linaclotide in adult patients with IBS-C have validated the approach of therapeutically targeting the GC-C/cGMP pathway for treatment of abdominal pain in this disorder (Chey et al., 2012; Rao et al., 2012). The efficacy and safety of linaclotide were assessed in a 26 week, double-blind, parallel-group, placebo-controlled, randomized trial, and a 12 week, double-blind, parallel-group, placebo-controlled, randomized trial, with a 4 week randomized withdrawal period. In both trials, four prespecified primary endpoints were evaluated, based on the FDA primary endpoint for IBS-C [responder: improvement $\geq$30% from baseline in average daily worst abdominal pain score and increase by $\geq$1 complete spontaneous bowel movement (CSBM) from baseline (same week) for at least 50% of weeks assessed], and three other primary endpoints, based on improvements in abdominal pain and CSBM for 9/12 weeks. Notably, a 30% reduction in the pain score has previously been shown of clinical importance in IBS patients and in patients reporting pain relief in general (Farrar et al., 2001; Spiegel et al., 2009).

In the 26 week trial, 804 IBS-C patients randomized (1:1) to linaclotide or placebo, received oral linaclotide (290 μg, once daily) during the 26 week treatment period (primary and secondary efficacy assessments were evaluated over the first 12 weeks of treatment; Chey et al., 2012). For the rigorous, combined IBS-C endpoint recommended in the recent *Guidance for IBS Clinical Trials* (Food and Drug Administration, 2010), 33.7% of IBS-C patients in the linaclotide group were endpoint responders,

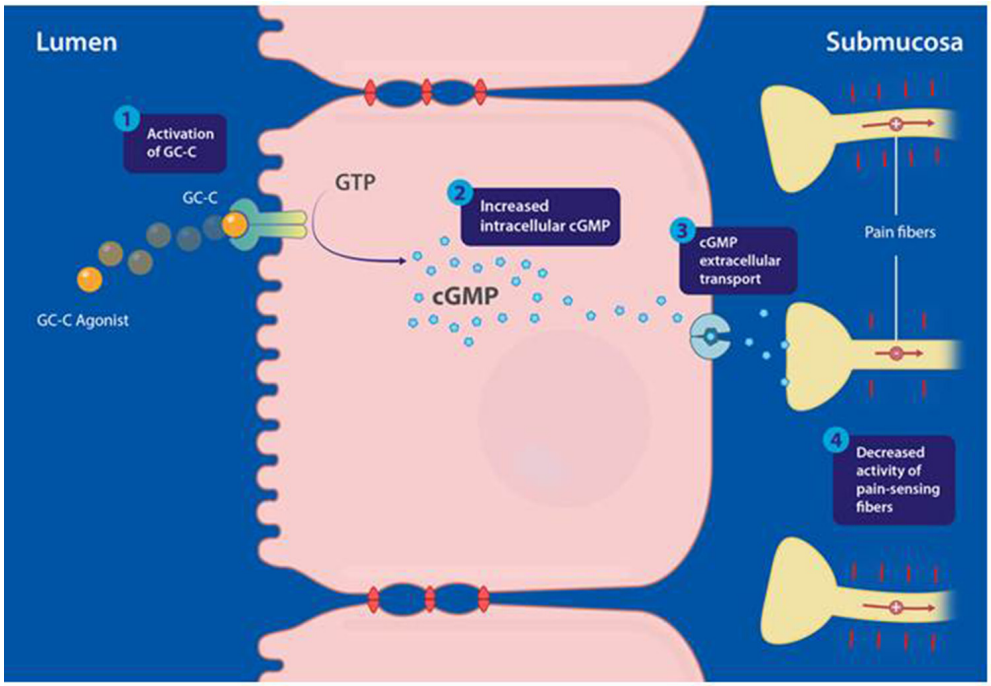

FIGURE 1 | Proposed mechanism of action of guanylate cyclase-C (GC-C) agonists modulating visceral pain, mediated through activation of the GC-C/cyclic guanosine-3′,5′-monophosphate (cGMP) pathway. (1) Linaclotide binds and activates GC-C, expressed at the apical surface of intestinal epithelial cells. (2) Activation of GC-C results in hydrolysis of guanosine triphosphate (GTP) and production of cGMP inside intestinal epithelial cells. (3) Intracellular cGMP is actively transported out of intestinal epithelial cells by efflux pumps into the submucosa. (4) Extracellular cGMP is proposed to inhibit colonic nociceptors. Adapted from Silos-Santiago et al. (2013); the figure has been reproduced with permission of the International Association for the Study of Pain® (IASP).

compared with 13.9% in the placebo group ($P < 0.0001$). The FDA pain responder criterion was met by 48.9% of linaclotide-treated patients, compared to 34.5% in the placebo group ($P < 0.0001$) and similarly, 49.1% of linaclotide-treated patients met the abdominal pain endpoint for at least 13/26 weeks, compared to the placebo group ($P < 0.0001$). Furthermore, improvement in abdominal pain compared to placebo, was significant starting from the first week of therapy and continuing throughout the 26 week treatment period.

In the 12 week randomized trial, followed by a 4 week randomized withdrawal period, 800 patients (1:1, linaclotide or placebo) received oral linaclotide (290 μg, once daily) during the 12 week treatment period (Rao et al., 2012). Patients who had completed all 12 weeks of the double-blind treatment period were eligible to enter the double-blind 4 week randomized withdrawal period, in which patients initially randomized to linaclotide were re-randomized (1:1) to oral linaclotide (290 μg, once daily) or placebo, and patients previously randomized to placebo were assigned to receive oral linaclotide (290 μg) once a day. The combined FDA-recommended IBS-C responder endpoint was met by 33.6%, compared to 21% in the placebo group ($P < 0.0001$), and similarly a larger number of linaclotide-treated patients (50.1%) reported a reduction of ≥30% in abdominal pain, compared to the placebo group (37.5%; $P = 0.0003$). As in the 26 week clinical trial with linaclotide, improvement in abdominal pain was recorded within the first week of therapy and sustained throughout the treatment period. During the 4 week randomized withdrawal period, patients on linaclotide had continued relief of abdominal pain, while patients re-randomized to placebo showed a gradual worsening of abdominal pain symptoms to the level experienced by patients receiving placebo during the treatment period, however, without worsening of symptoms relative to baseline.

Finally, results from several pooled *post hoc* analyses of these two phase 3 trials further confirmed the efficacy of linaclotide treatment on symptoms of abdominal pain and discomfort in patients with IBS-C (Johnston et al., 2013). Importantly, it was shown in a *post hoc* longitudinal responder analysis using the FDA responder criterion that at week 3, more than 50% of linaclotide-treated patients reported >30% reduction in abdominal pain, and that this analgesic effect increased to greater than 60% of linaclotide-treated patients at week 7 and was sustained at approximately 70% of linaclotide-treated patients for the duration of the 26 week study (Castro et al., 2013).

Based on results from these two phase 3 pivotal trials, linaclotide received FDA approval in 2012 as a first-in-class drug for the treatment of adult patients with IBS-C, and by the European Medicines Agency for the symptomatic treatment of moderate to severe IBS-C in adult patients. Linaclotide was also approved in the US for the treatment of CIC (2012) and in Canada for the treatment of both IBS-C and CIC (2013). Today, linaclotide is in worldwide development for the treatment of IBS-C.

SUMMARY AND PERSPECTIVE

This review offers a new perspective and understanding of endogenous mechanisms involved in the regulation of visceral pain. The intestinal GC-C/extracellular cGMP pathway is emerging as a novel pathway that regulates peripheral analgesia via inhibition of primary colonic afferents, which results in decreased visceral pain. Findings from both non-clinical models and clinical studies have confirmed that the analgesic effects of linaclotide are mediated by a distinct pain-regulating pathway that operates independently from improvements in bowel function. In order to maximize the benefits of these novel findings for patients work is ongoing to fully elucidate the underlying mechanisms of this pathway, such as the identification and characterization of the molecular target(s) on colonic afferents and secondly, to more broadly assess the significant therapeutic potential of targeting the GC-C/cGMP pathway in GI disorders associated with visceral pain. The efficacy of linaclotide on abdominal pain demonstrated in the phase 3 IBS-C clinical trials translates the targeting of the GC-C/cGMP pain pathway into the clinic. This pathway continues to emerge as a novel therapeutic target for GI dysfunction with the potential for broader utility in treating visceral pain.

AUTHOR CONTRIBUTIONS

Alexander P. Bryant, Mark G. Currie, Gerhard Hannig, Caroline B. Kurtz, Inmaculada Silos-Santiago, and Boris Tchernychev contributed to writing and critical revisions of the manuscript.

REFERENCES

Bouin, M., Plourde, V., Boivin, M., Riberdy, M., Lupien, F., Laganiere, M., et al. (2002). Rectal distention testing in patients with irritable bowel syndrome: sensitivity, specificity, and predictive values of pain sensory thresholds. *Gastroenterology* 122, 1771–1777. doi: 10.1053/gast.2002.33601

Blackshaw, L. A., and Brierley, S. M. (2013). Emerging receptor target in the pharmacotherapy of irritable bowel syndrome with constipation. *Expert Rev. Gastroenterol. Hepatol.* 7(Suppl.1), 15–19. doi: 10.1586/17474124.2013.820045

Bryant, A. P., Busby, R. W., Bartolini, W. P., Cordero, E. A., Hannig, G., Kessler, M. M., et al. (2010). Linaclotide is a potent and selective guanylate cyclase C agonist that elicits pharmacological effects locally in the gastrointestinal tract. *Life Sci.* 86, 760–765. doi: 10.1016/j.lfs.2010.03.015

Busby, R. W., Bryant, A. P., Bartolini, W. P., Cordero, E. A., Hannig, G., Kessler, M. M., et al. (2010). Linaclotide, through activation of guanylate cyclase C, acts locally in the gastrointestinal tract to elicit enhanced intestinal secretion and transit. *Eur. J. Pharmacol.* 649, 328–335. doi: 10.1016/j.ejphar.2010.09.019

Busby, R. W., Kessler, M. M., Bartolini, W. P., Bryant, A. P., Hannig, G., Higgins, C. S., et al. (2013). Pharmacologic properties, metabolism, and disposition of linaclotide, a novel therapeutic peptide approved for the treatment of irritable bowel syndrome with constipation and chronic idiopathic constipation. *J. Pharmacol. Exp. Ther.* 344, 196–206. doi: 10.1124/jpet.112.199430

Carrithers, S. L., Barber, M. T., Biswas, S., Parkinson, S. J., Park, P. K., Goldstein, S. D., et al. (1996). Guanylyl cyclase C is a selective marker for metastatic colorectal tumors in human extraintestinal tissues. *Proc. Natl. Acad. Sci. U.S.A.* 93, 14827–14832. doi: 10.1073/pnas.93.25.14827

Castro, J., Harrington, A. M., Hughes, P. A., Martin, C. M., Ge, P., Shea, C. M., et al. (2013). Linaclotide inhibits colonic nociceptors and relieves abdominal pain via guanylate cyclase-C and extracellular cyclic GMP. *Gastroenterology* 145, 1334–1346. doi: 10.1053/j.gastro.2013.08.017

Cervetto, C., Maura, G., and Marcoli, M. (2010). Inhibition of presynaptic release-facilitatory kainate autoreceptors by extracellular cyclic GMP. *J. Pharmacol. Exp. Ther.* 332, 210–219. doi: 10.1124/jpet.109.154955

Chey, W. D., Lembo, A. J., Lavins, B. J., Shiff, S. J., Kurtz, C. B., Currie, M. G., et al. (2012). Linaclotide for irritable bowel syndrome with constipation: a 26-week, randomized, double-blind, placebo-controlled trial to evaluate efficacy and safety. *Am. J. Gastroenterol.* 107, 1702–1712. doi: 10.1038/ajg.2012.254

Currie, M. G., Fok, K. F., Kato, J., Moore, R. J., Hamra, F. K., Duffin, K. L., et al. (1992). Guanylin: an endogenous activator of intestinal guanylate cyclase. *Proc. Natl. Acad. Sci. U.S.A.* 89, 947–951. doi: 10.1073/pnas.89.3.947

Drossman, D. A. (2006). The functional gastrointestinal disorders and the Rome III process. *Gastroenterology* 130, 1377–1390. doi: 10.1053/j.gastro.2006.03.008

Eutamene, H., Bradesi, S., Larauche, M., Theodorou, V., Beaufrand, C., Ohning, G., et al. (2010). Guanylate cyclase C-mediated antinociceptive effects of linaclotide in rodent models of visceral pain. *Neurogastroenterol. Motil.* 22, 312–e84. doi: 10.1111/j.1365-2982.2009.01385.x

Farrar, J. T., Young, J. P., LaMoreaux, L., Werth, J. L., and Poole, R. M. (2001). Clinical importance of changes in chronic pain intensity measured on an 11-point numerical pain rating scale. *Pain* 94, 149–158. doi: 10.1016/S0304-3959(01)00349-9

Feng, B., and Gebhart, G. F. (2011). Characterization of silent afferents in the pelvic and splanchnic innervations of the mouse colorectum. *Am. J. Physiol. Gastrointest. Liver Physiol.* 300, G170–G180. doi: 10.1152/ajpgi.00406.2010

Feng, B., Kiyatkin, M. E., La, J.-H., Ge, P., Solinga, R., Silos-Santiago, I., et al. (2013). Activation of guanylate cyclase-C attenuates stretch responses and sensitization of mouse colorectal afferents. *J. Neurosci.* 33, 9831–9839. doi: 10.1523/JNEUROSCI.5114-12.2013

Food and Drug Administration. (2010). Guidance for industry. Irritable bowel syndrome – clinical evaluation of products for treatment. Available at: http://www.fda.gov/Drugs/GuidanceComplianceRegulatoryInformation/Guidances/default.htm (accessed August 1, 2012).

Forte, L. R. (1999). Guanylin regulatory peptides: structures, biological activities mediated by cyclic GMP and pathobiology. *Regul. Pept.* 81, 25–39. doi: 10.1016/S0167-0115(99)00033-6

Hughes, P. A., Brierley, S. M., Martin, C. M., Brookes, S. J., Linden, D. R., and Blackshaw, L. A. (2009). Post-inflammatory colonic afferent sensitization: different subtypes, different pathways and different time courses. *Gut* 58, 1333–1341. doi: 10.1136/gut.2008.170811

Johnston, J. M., Shiff, S. J., and Quigley, E. M. M. (2013). A review of the clinical efficacy of linaclotide in irritable bowel syndrome with constipation. *Curr. Med. Res. Opin.* 29, 149–160. doi: 10.1185/03007995.2012.754743

Kita, T., Smith, C. E., Fok, K. F., Duffin, K. L., Moore, W. M., Karabatsos, P. J., et al. (1994). Characterization of human uroguanylin: a member of the guanylin peptide family. *Am. J. Physiol.* 266, F342–F348.

Linden, D. J., Dawson, T. M., and Dawson, V. L. (1995). An evaluation of the nitric oxide/cGMP/cGMP-dependent protein kinase cascade in the induction of cerebellar long- term depression in culture. *J. Neurosci.* 15, 5098–5105.

Lucas, K. A., Pitari, G. M., Kazerounian, S., Ruiz-Stewart, I., Park, J., Schulz, S., et al. (2000). Guanylyl cyclases and signaling by cyclic GMP. *Pharmacol. Rev.* 52, 375–413.

Mann, E. A., Jump, M. L., Wu, J., Yee, E., and Giannella, R. A. (1997). Mice lacking the guanylate cyclase C receptor are resistant to STa-induced intestinal secretion. *Biochem. Biophys. Res. Commun.* 239, 463–466. doi: 10.1006/bbrc.1997.7487

Marx, U. C., Klodt, J., Meyer, M., Gerlach, H., Roesch, P., Forssmann, W. G., et al. (1998). One peptide, two topologies: structure and interconversion dynamics of human uroguanylin isomers. *J. Pept. Res.* 52, 229–240. doi: 10.1111/j.1399-3011.1998.tb01480.x

Mertz, H., Naliboff, B., Munakata, J., Niazi, N., and Mayer, E. A. (1995). Altered rectal perception is a biological marker of patients with irritable bowel syndrome. *Gastroenterology* 109, 40–52. doi: 10.1016/0016-5085(95)90267-8

Perkins, A., Goy, M. F., and Li, Z. (1997). Uroguanylin is expressed by enterochromaffin cells in the rat gastrointestinal tract. *Gastroenterology* 113, 1007–1014. doi: 10.1016/S0016-5085(97)70198-7

Pfeifer, A., Aszodi, A., Seidler, U., Ruth, P., Hofmann, F., and Faessler, R. (1996). Intestinal secretory defects and dwarfism in mice lacking cGMP-dependent protein kinase II. *Science* 274, 2082–2085. doi: 10.1126/science.274.5295.2082

Poupoloupou, C., and Nowak, L. M. (1998). Extracellular 3′,5′ cyclic guanosine monophosphate inhibits kainate-activated responses in cultured mouse cerebellar neurons. *J. Pharmacol. Exp. Ther.* 286, 99–109.

Qian, X., Prabhakar, S., Nandi, A., Visweswariah, S. S., and Goy, M. F. (2000). Expression of GC-C, a receptor-guanylate cyclase, and its endogenous ligands uroguanylin and guanylin along the rostrocaudal axis of the intestine. *Endocrinology* 141, 3210–3224.

Rao, S., Lembo, A. J., Shiff, S. J., Lavins, B. J., Currie, M. G., Jia, X. D., et al. (2012). A 12-week, randomized, controlled trial with a 4-week randomized withdrawal period to evaluate the efficacy and safety of linaclotide in irritable

bowel syndrome with constipation. *Am. J. Gastroenterol.* 107, 1714–1724. doi: 10.1038/ajg.2012.255

Ritter, C. A., Jedlitschky, G., Meyer zu Schwabedissen, H., Grube, M., Köck, K., and Kroemer, H. K. (2005). Cellular export of drugs and signaling molecules by the ATP-binding cassette transporters MRP4 (ABCC4) and MRP5 (ABCC5). *Drug Metab. Rev.* 37, 253–278. doi: 10.1081/DMR-200047984

Sager, G. (2004). Cyclic GMP transporters. *Neurochem. Int.* 45, 865–873. doi: 10.1016/j.neuint.2004.03.017

Schlossman, J., Feil, R., and Hofmann, F. (2005). Insights into cGMP signaling derived from cGMP kinase knockout mice. *Front. Biosci.* 10:1279–1289. doi: 10.2741/1618

Schulz, S., Green, C. K., Yuen, P. S., and Garbers, D. L. (1990). Guanylyl cyclase is a heat- stable enterotoxin receptor. *Cell* 63, 941–948. doi: 10.1016/0092-8674(90)90497-3

Schulz, S., Lopez, M. J., Kuhn, M., and Garbers, D. L. (1997). Disruption of the guanylyl cyclase-C gene leads to a paradoxical phenotype of viable but heat-stable enterotoxin- resistant mice. *J. Clin. Invest.* 100, 1590–1595. doi: 10.1172/JCI119683

Silos-Santiago, I., Hannig, G., Eutamene, H., Ustinova, E. E., Bernier, S. G., Ge, P., et al. (2013). Gastrointestinal pain: Unraveling a novel endogenous pathway through uroguanylin/guanylate cyclase-C/cGMP activation. *Pain* 154, 1820–1830. doi: 10.1016/j.pain.2013.05.044

Sindic, A., and Schlatter, E. (2006). Cellular effects of guanylin and uroguanylin. *J. Am. Soc. Nephrol.* 17, 607–616. doi: 10.1681/ASN.2005080818

Skelton, N. J., Garcia, K. C., Goeddel, D. V., Quan, C., and Burnier, J. P. (1994). Determination of the solution structure of the peptide hormone guanylin: observation of a novel form of topological stereoisomerism. *Biochemistry* 33, 13581–13592. doi: 10.1021/bi00250a010

Spiegel, B., Bolus, R., Harris, L. A., Lucak, S., Naliboff, B., Esrailian, E., et al. (2009). Measuring irritable bowel syndrome patient-reported outcomes with an abdominal pain numeric rating scale. *Aliment. Pharmacol. Ther.* 30, 1159–1170. doi: 10.1111/j.1365-2036.2009.04144.x

Tack, J., Talley, N. J., Camilleri, M., Holtmann, G., Hu, P., Malagelada, J. R., et al. (2006). Functional gastroduodenal disorders. *Gastroenterology* 130, 1466–1479. doi: 10.1053/j.gastro.2005.11.059

Vaandrager, A. B. (2002). Structure and function of the heat-stable enterotoxin receptor/guanylyl cyclase C. *Mol. Cell. Biochem.* 230, 73–83. doi: 10.1023/A:1014231722696

Videlock, E. J., and Chang, L. (2007). Irritable bowel syndrome: current approach to symptoms, evaluation, and treatment. *Gastroenterol. Clin. North Am.* 36, 665–685. doi: 10.1016/j.gtc.2007.07.002

Zimmermann, C., Gutmann, H., Hruz, P., Gutzwiller, J. P., Beglinger, C., and Drewe, J. (2005). Mapping of multidrug resistance gene 1 and multidrug resistance-associated protein isoform 1 and 5 mRNA expression along the human intestinal tract. *Drug Metab. Dispos.* 33, 219–224. doi: 10.1124/dmd.104.001354

Conflict of Interest Statement: Alexander P. Bryant, Mark G. Currie, Gerhard Hannig, Caroline B. Kurtz, Inmaculada Silos-Santiago and Boris Tchernychev are employees and stock/stock option holders in Ironwood Pharmaceuticals, Inc.

Received: 30 January 2014; paper pending published: 19 March 2014; accepted: 01 April 2014; published online: 16 April 2014.

Citation: Hannig G, Tchernychev B, Kurtz CB, Bryant AP, Currie MG and Silos-Santiago I (2014) Guanylate cyclase-C/cGMP: an emerging pathway in the regulation of visceral pain. Front. Mol. Neurosci. 7:31. doi: 10.3389/fnmol.2014.00031

This article was submitted to the journal Frontiers in Molecular Neuroscience.